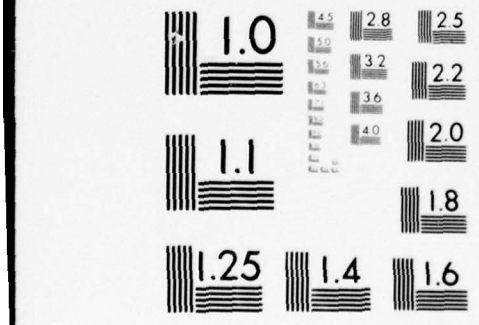
AD-A053 427 STATE UNIV OF NEW YORK AT STONY BROOK MARINE SCIENCES--ETC F/G 13/2
AQUATIC DISPOSAL FIELD INVESTIGATIONS, EATONS NECK DISPOSAL SIT--ETC(U)
JAN 78 DACW51-75-C-0016

UNCLASSIFIED WES-TR-D-77-6-APP-B NL

1 OF 5
AD A053427



05342




MICROCOPY RESOLUTION TEST CHART
NATIONAL BUREAU OF STANDARDS-1963-A

AD A053427

(12)

# DREDGED MATERIAL RESEARCH PROGRAM

TECHNICAL REPORT D-77-6

# AQUATIC DISPOSAL FIELD INVESTIGATIONS EATONS NECK DISPOSAL SITE LONG ISLAND SOUND

## APPENDIX B: WATER-QUALITY PARAMETERS AND PHYSICOCHEMICAL SEDIMENT PARAMETERS

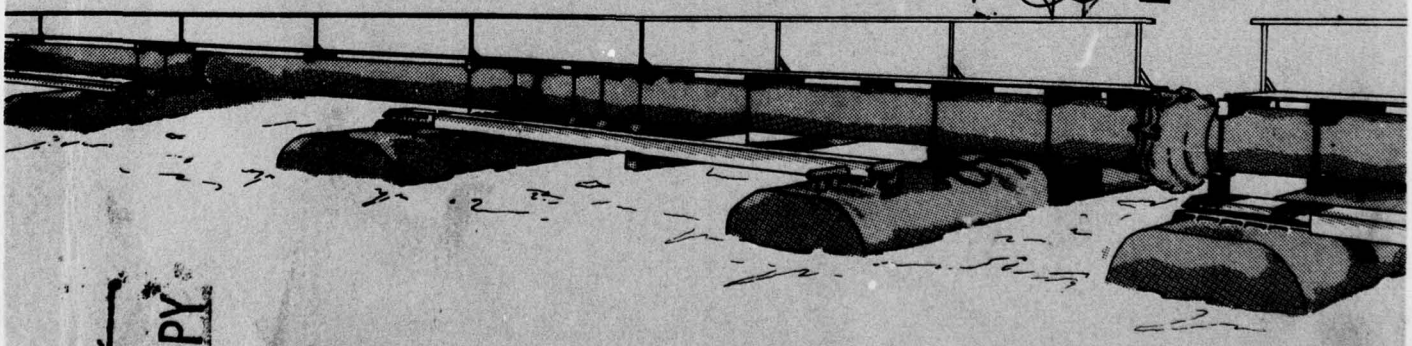
by

Marine Sciences Research Center
State University of New York
Stony Brook, New York 11794

DDC
RECEIVED
NOV 3 1978
E

January 1978
Final Report

Approved For Public Release; Distribution Unlimited



Prepared for Office, Chief of Engineers, U. S. Army
Washington, D. C. 20314

Under Contract No. DACW51-75-C-0016
(DMRP Work Unit No. 1A06B)

Monitored by Environmental Effects Laboratory
U. S. Army Engineer Waterways Experiment Station
P. O. Box 631, Vicksburg, Miss. 39180

AD No.
DDC FILE COPY

AQUATIC DISPOSAL FIELD INVESTIGATIONS
EATONS NECK DISPOSAL SITE
LONG ISLAND SOUND

Appendix A: Investigation of the Hydraulic Regime and the Physical Characteristics of Bottom Sedimentation

Appendix B: Water-Quality Parameters and Physicochemical Sediment Parameters

Appendix C: Predisposal Baseline Conditions of Benthic Assemblages

Appendix D: Predisposal Baseline Conditions of Demersal Fish Assemblages

Appendix E: Predisposal Baseline Conditions of Zooplankton Assemblages

Appendix F: Predisposal Baseline Conditions of Phytoplankton Assemblages

Destroy this report when no longer needed. Do not return
it to the originator.

DEPARTMENT OF THE ARMY
WATERWAYS EXPERIMENT STATION, CORPS OF ENGINEERS
P. O. BOX 631
VICKSBURG, MISSISSIPPI 39180

IN REPLY REFER TO: WESYV

1 May 1978

SUBJECT: Transmittal of Technical Report D-77-6 (Appendix B)

TO: All Report Recipients

1. The technical report transmitted herewith represents the results of one of several research efforts (work units) undertaken as part of Task 1A, Aquatic Disposal Field Investigations, of the Corps of Engineers' Dredged Material Research Program. Task 1A is a part of the Environmental Impacts and Criteria Development Project (EICDP), which has as a general objective determination of the magnitude and extent of effects of disposal sites on organisms and the quality of surrounding water, and the rate, diversity, and extent such sites are recolonized by benthic flora and fauna. The study reported on herein was an integral part of a series of research contracts jointly developed to achieve the EICDP general objective at the Eatons Neck Disposal Site, one of five sites located in several geographical regions of the United States. Consequently, this report presents results and interpretations of but one of several closely interrelated efforts and should be used only in conjunction with and consideration of the other related reports for this site.

2. This report, Appendix B: Water-Quality Parameters and Physicochemical Sediment Parameters, is one of six contractor-prepared appendices published relative to the Waterways Experiment Station Technical Report D-77-6 entitled: Aquatic Disposal Field Investigations, Eatons Neck Disposal Site, Long Island Sound. The titles of all appendices of this series are listed on the inside front cover of this report. The main report will provide additional results, interpretations, and conclusions not found in the individual appendices and will provide a comprehensive summary and synthesis overview of the entire project.

3. The purpose of this study, conducted as Work Unit 1A06B, was to determine the baseline water column and sediment water quality and the physicochemical properties of the Eatons Neck Disposal Site, located at the western end of Long Island Sound. The report includes a discussion of the water-column distribution of dissolved and particulate metals

and nutrients and other water-column properties within and in the vicinity of the disposal site. Water-column properties were determined through seven oceanographic cruises during fall, winter, and spring seasons. Sediment physicochemical conditions as related to past dumping at the site were evaluated through three sediment-coring cruises. Bulk and soluble sediment concentrations of metals and nutrients in the dump site are contrasted to reference sites out of the influence of the dumping area. Sediment textural, mineralogical, and other physico-chemical properties are also evaluated.

4. Water-column studies showed no effect of past dumping at this site and any variation in water-column parameters could be explained by factors other than the presence of dredged material. There were no significant differences between reference stations and the disposal site for sediment mineralogy, bulk metal concentrations, soluble metals, oil and grease, and cation exchange capacity. Sediment ammonia, organic carbon, organic nitrogen, and pH were higher at the dump site relating to higher organic matter content and resultant degradation products of the dump site. Effects of past dredged material disposal on nutrients, metals, and related parameters in the Sound are minimal and are for the most part overshadowed by the effects of sewage effluents and other inputs from river discharge.

5. The baseline evaluations at all of the EICDP field sites were developed to determine the base or ambient physical, chemical, and biological conditions at the respective sites from which to determine impacts due to the subsequent disposal operations. Where the dump site had historical usage, the long-term impacts of dumping at these sites could also be ascertained. Controlled disposal operations at the Eatons Neck Disposal Site, however, did not occur due to local opposition to research activities and even though the Eatons Neck project was terminate after completion of the baseline evaluation, this information will be useful in evaluating the impacts of past disposal at this site. The results of this study are particularly important in determining placement of dredged material for open-water disposal. Referenced studies, as well as the ones summarized in this report, will aid in determining the optimum disposal conditions and site selection in relation to the water and sediment quality of the historical dump site and surrounding areas.

JOHN L. CANNON
Colonel, Corps of Engineers
Commander and Director

Unclassified

SECURITY CLASSIFICATION OF THIS PAGE (When Data Entered)

| REPORT DOCUMENTATION PAGE | | READ INSTRUCTIONS BEFORE COMPLETING FORM |
|---|---|---|
| 1. REPORT NUMBER<br>Technical Report D-77-6 | 2. GOVT ACCESSION NO. | 3. RECIPIENT'S CATALOG NUMBER |
| 4. TITLE (and Subtitle)<br>AQUATIC DISPOSAL FIELD INVESTIGATIONS, EATONS NECK DISPOSAL SITE, LONG ISLAND SOUND; APPENDIX B: WATER-QUALITY PARAMETERS AND PHYSICOCHEMICAL SEDIMENT PARAMETERS. | | 5. TYPE OF REPORT & PERIOD COVERED<br>Final report.<br>30 Oct 74 - 29 May 75 |
| | | 6. PERFORMING ORG. REPORT NUMBER |
| 7. AUTHOR(a) | | 8. CONTRACT OR GRANT NUMBER(a)<br>Contract No.<br>DACW51-75-C-0016 |
| 9. PERFORMING ORGANIZATION NAME AND ADDRESS<br>Marine Sciences Research Center<br>State University of New York<br>Stony Brook, New York 11794 | | 10. PROGRAM ELEMENT, PROJECT, TASK AREA & WORK UNIT NUMBERS<br>DMRP Work Unit No.<br>1A06B |
| 11. CONTROLLING OFFICE NAME AND ADDRESS<br>Office, Chief of Engineers, U. S. Army<br>Washington, D. C. 20314 | | 12. REPORT DATE<br>Jan 1978<br>13. NUMBER OF PAGES<br>329 (12) 336 p. |
| 14. MONITORING AGENCY NAME & ADDRESS(if different from Controlling Office)<br>U. S. Army Engineer Waterways Experiment Station<br>Environmental Effects Laboratory<br>P. O. Box 631, Vicksburg Miss. 39180 | | 15. SECURITY CLASS. (of this report)<br>Unclassified<br>15a. DECLASSIFICATION/DOWNGRADING SCHEDULE |

16. DISTRIBUTION STATEMENT (of this Report)

Approved for public release; distribution unlimited.

(19)

17. DISTRIBUTION STATEMENT (of the abstract entered in Block 20, if different from Report)

(18) WES/TR-D-77-6-APP-B

18. SUPPLEMENTARY NOTES

DDC
RECEIVED
MAY 3 1978
A

19. KEY WORDS (Continue on reverse side if necessary and identify by block number)

Dredged material disposal
Eatons Neck Disposal Site
Field investigations
Long Island Sound
Sediment sampling
Water quality

20. ABSTRACT (Continue on reverse side if necessary and identify by block number)

Seven oceanographic cruises and three sediment coring cruises, which took place between October 30, 1974 and May 29, 1975, were conducted in western Long Island Sound to assess the baseline water column and sediment properties near the Eatons Neck disposal site. The following points summarize our main findings:

1. Seasonal spatial distributions of $NH_4^+$ and $NO_3^-$ show that both the East River as well as the lateral embayments (Continued)

DD FORM 1 JAN 73 1473 EDITION OF 1 NOV 65 IS OBSOLETE

Unclassified

SECURITY CLASSIFICATION OF THIS PAGE (When Data Entered)

AD A045310
A - AD47421
B - 053427
C - 050046
E - 045310
F - AD45313
H06 652

20. ABSTRACT (Continued).

are important nitrogen sources to the western portion of Long Island Sound.

2. Increased water column stability coincided with increased chlorophyll a concentration.
3. Seasonal depth and water column averages of $NH_4^+$ and $NO_3^-$ showed nitrogen depletion in the surface layer.
4. Observed seasonal concentrations of $NO_3^-$ were similar to those measured by Gordon Riley (1955), but higher concentrations occurred later in the year, as did the phytoplankton bloom.
5. Observed $PO_4^{3-}$ concentrations were seasonally elevated over those determined by Gordon Riley (1955) by about 1 μM.
6. Depletion of $Si(OH)_4$ coincided with that of $NO_3^-$.
7. Maximum concentrations of particulate Cu, Fe, and Zn occurred with high chlorphyll a concentrations.
8. Maximum concentrations of particulate Mn and Pb occurred with the maximum concentration of particulate carbon and nitrogen.
9. The Eatons Neck region of Long Island Sound is an area of strong seasonal gradients of S°/$_{oo}$, $NH_4^+$, particulate carbon, suspended solids, particulate Pb, Ag, and chlorophyll a.
10. The sediments in the Eatons Neck area of Long Island Sound are generally silty with pockets of high sand and clay concentrations.
11. Fine-fraction mineralogy consists of illite, chlorite, kaolinite, and montmorillonite with minor amounts of feldspars and quartz.
12. No significant mineralogical variations were observed with increasing depth of burial.
13. For most sediment cores, the concentrations of Pb, Cu, Zn, Cd, and Hg exhibit a stepwise decrease with increasing depth of sediment burial. Fe, Mn, and Ni, however, show irregular vertical distribution patterns.
14. Sediment interstitial metal data indicate that the vertical distribution patterns of Pb, Cu, and Zn in sediments may not be controlled by precipitation of their respective sulphide phases.
15. Total concentrations of metals show a positive correlation with the organic fraction of sediment.
16. Pb, Cu, Zn, Ni, and Mn show association with total iron content of sediment.

THE CONTENTS OF THIS REPORT ARE NOT TO BE USED FOR ADVERTISING, PUBLICATION, OR PROMOTIONAL PURPOSES. CITATION OF TRADE NAMES DOES NOT CONSTITUTE AN OFFICIAL ENDORSEMENT OR APPROVAL OF THE USE OF SUCH COMMERCIAL PRODUCTS.

DDC
RECEIVED
MAY 3 1978
E

# PREFACE

This report presents the results of an investigation to determine the baseline conditions of the macrofauna and meiofauna at an established disposal site off Eatons Neck, Long Island, New York.

The study was supported by the U. S. Army Engineer Waterways Experiment Station (WES), Environmental Effects Laboratory (EEL), Vicksburg, Mississippi, under Contract No. DACW51-75-C-0016 with the Marine Sciences Research Center, State University of New York, Stony Brook, New York. The report forms part of the Dredged Material Research Program, which is sponsored by the Office, Chief of Engineers. Contracting was handled by the New York District (NYD); COL Thomas C. Hunter, CE, NYD, was contracting officer.

The following New York Ocean Science Laboratory personnel assisted in all phases of the research project: G. E. Carroll, R. Dayal, I. W. Duedall, M. T. Eisel, G. S. Grunseich, G. L. Hulse, A. D. Hamilton, P. J. Harder, K. Henrickson, D. J. Hirschberg, J. F. Lekan, G. L. Lynch, C. J. Marks, W. A. Miloski, J. W. Moren, H. B. O'Connors, Jr., S. A. Oakley, R. A. Olson, J. H. Parker, J. M. Restivo, A. S. Robbins, J. R. Schubel, H. C. Stuebe, G. M. Weik, W. M. Wise, and C. R. Zeppie.

The study was conducted under the direction of the following EEL personnel: Dr. R. M. Engler, Environmental Impacts and Criteria Development Manager, and James Reese, Site Manager. The study was under the general supervision of Dr. John Harrison, Chief, EEL.

Directors of WES during the study and the preparation of this report were COL G. H. Hilt, CE, and COL J. L. Cannon, CE. Technical Director was Mr. F. R. Brown.

## CONCENTRATION UNITS, CONVERSION FACTORS, U. S. CUSTOMARY TO METRIC (SI) UNITS OF MEASUREMENT

Concentration units in this work are the following:

| Water Column Properties | Units |
|---|---|
| Nutrients (ammonium, nitrite, nitrate, phosphate, silicic acid)* | µM |
| Urea* | µM |
| Dissolved organic carbon | mg/l |
| Dissolved metals | µg/l |
| Particulate metals | µg/l |
| Particulate organic carbon | µg/l |
| Particulate organic nitrogen | µg/l |
| Chlorophyll a | µg/l |
| Suspended solids | mg/l |

| Sediment Properties | |
|---|---|
| Nutrients (ammonium, nitrite, nitrate, phosphate, silicic acid)* | µM |
| Dissolved metals in pore waters | µg/l |
| Total dissolved organic carbon | mg/l |
| Total metals in sediment | µg/g |
| Total cation exchange capacity | meq/g of dry sediment |
| Particulate organic carbon | % (wt) |
| Particulate organic nitrogen | % (wt) |
| Oil and Grease | % (wt) |

---

Conversion factors

U. S. customary units of measurement used in this report can be converted to metric (SI) units as follows:

| Multiply | By | To Obtain |
|---|---|---|
| feet | 0.3048 | meters |
| ounces (mass) | 28.34952 | grams |
| pounds (force) per square inch | 6894.757 | pascals |

---

*1 µM ammonium = 14 µg N/l
1 µM nitrite = 14 µg N/l
1 µM nitrate = 14 µg N/l
1 µM phosphate = 31 µg P/l
1 µM silicic acid = 28 µg Si/l
1 µM urea = 14 µg N/l

## SUMMARY

Seven oceanographic cruises and three sediment coring cruises, which took place between October 30, 1974 and May 29, 1975, were conducted in western Long Island Sound to assess the baseline water column and sediment properties near the Eatons Neck disposal site. The following points summarize our main findings:

1. Seasonal spatial distributions of $NH_4^+$ and $NO_3^-$ show that both the East River as well as the lateral embayments are important nitrogen sources to the western portion of Long Island Sound.
2. Increased water column stability coincided with increased chlorophyll *a* concentration.
3. Seasonal depth and water column averages of $NH_4^+$ and $NO_3^-$ showed nitrogen depletion in the surface layer.
4. Observed seasonal concentrations of $NO_3^-$ were similar to those measured by Gordon Riley (1955), but higher concentrations occurred later in the year, as did the phytoplankton bloom.
5. Observed $PO_4^{3-}$ concentrations were seasonally elevated over those determined by Gordon Riley (1955) by about 1 μM.
6. Depletion of $Si(OH)_4$ coincided with that of $NO_3^-$.
7. Maximum concentrations of particulate Cu, Fe, and Zn occurred with high chlorophyll *a* concentrations.



NTIS White Section
DDC Buff Section
UNANNOUNCED
JUSTIFICATION
BY
DISTRIBUTION/AVAILABILITY CODES
DIST. AVAIL. and/or SPECIAL
A

8. Maximum concentrations of particulate Mn and Pb occurred with the maximum concentration of particulate carbon and nitrogen.
9. The Eatons Neck region of Long Island Sound is an area of strong seasonal gradients of S°/$_{oo}$, $NH_4^+$, particulate carbon, suspended solids, particulate Pb, Ag, and chlorophyll *a*.
10. The sediments in the Eatons Neck area of Long Island Sound are generally silty with pockets of high sand and clay concentrations.
11. Fine-fraction mineralogy consists of illite, chlorite, kaolinite, and montmorillonite with minor amounts of feldspars and quartz.
12. No significant mineralogical variations were observed with increasing depth of burial.
13. For most sediment cores, the concentrations of Pb, Cu, Zn, Cd and Hg exhibit a stepwise decrease with increasing depth of sediment burial. Fe, Mn and Ni, however, show irregular vertical distribution patterns.
14. Sediment interstitial metal data indicate that the vertical distribution patterns of Pb, Cu, and Zn in sediments may not be controlled by precipitation of their respective sulphide phases.
15. Total concentrations of metals show a positive correlation with the organic fraction of sediment.
16. Pb, Cu, Zn, Ni and Mn show association with total iron content of sediment.

CONTENTS


| | Page |
|---|---|
| PREFACE | i |
| CONCENTRATION UNITS, CONVERSION FACTORS, U. S. CUSTOMARY TO METRIC (SI) UNITS OF MEASUREMENT | ii |
| SUMMARY | iii |
| PART I: INTRODUCTION | 1 |
| Purpose and Scope | 1 |
| Literature Review | 1 |
| Hydrography and circulation | 1 |
| Nutrient and organic carbon distributions | 6 |
| Oxygen distribution | 9 |
| Heavy metal distribution | 10 |
| Sediments in Long Island Sound | 12 |
| Solid-waste disposal in Long Island Sound | 14 |
| PART II: SAMPLING AND ANALYTICAL METHODS | 16 |
| Sampling | 16 |
| Water column | 16 |
| Sediment | 16 |
| Shipboard Testing | 20 |
| Water Column Analyses | 25 |
| Nutrient analysis | 25 |
| Chlorophyll a extraction | 25 |
| Dissolved organic carbon | 25 |
| Particulate organic carbon and nitrogen | 26 |
| Dissolved and particulate metals | 26 |
| Suspended matter | 26 |
| Particulate size analysis | 26 |
| Sediment Analyses | 26 |
| Sediment coring | 26 |
| Pore water extraction | 27 |
| Interstitial metals | 27 |
| Interstitial nutrients | 28 |
| Sediment texture | 28 |
| Particulate C and N | 30 |
| Total Sulfides | 30 |
| Percent water | 31 |
| Clay-fraction mineralogy | 31 |
| Bulk mineralogy | 33 |
| Trace metal analysis of bulk samples | 34 |
| Total cation exchange capacity | 35 |
| Oil and grease | 35 |

PART III: RESULTS AND DISCUSSION. . . . . 37

Water Column Properties. . . . . 37

Precision and sampling variability. . . . . 37
Variability over a tidal cycle. . . . . 40

ACE 1. . . . . 40
ACE II-VII . . . . . 56

Horizontal and vertical distribution of water properties . . . . . 63

Temperature and salinity . . . . . 63
Percent dissolved oxygen saturation. . . . 70
Ammonium . . . . . 70
Nitrate. . . . . 76
Dissolved $PO_4^{3-}$ concentrations . . . . . 80
Silicic acid . . . . . 85
Particulate carbon . . . . . 89
Particulate nitrogen . . . . . 93
Chlorophyll a. . . . . 93
Suspended solids . . . . . 100
Suspended metals . . . . . 110

Sediment Geochemistry. . . . . 110

Water content . . . . . 110
Texture . . . . . 110
pH-Eh . . . . . 122
Mineralogy. . . . . 127
Particulate nitrogen and carbon . . . . . 128
Oil and Grease. . . . . 146
Cation exchange capacity. . . . . 146
Total and dissolved metals. . . . . 147

Sediment . . . . . 147

Interstitial nutrient concentrations. . . . . 187

PART IV: SUMMARY OF RESULTS . . . . . 189

Seasonal and Depth Distribution of the Important Water Column Data. . . . . 189
Evaluation of Proposed Disposal Site Relative to the Control Site in Terms of Sediment Properties . . . 196

Sediment texture and mineralogy . . . . . 196
Chemistry . . . . . 196

Summarized Interpretation of Sediment Geochemistry Data Based on Correlation Coefficient Matrix . . . 197

APPENDIX A': SAMPLING AND ANALYTICAL PROCEDURES USED FOR THE DETERMINATION OF TRACE HEAVY METALS. . . . . 208

APPENDIX B': WATER COLUMN OBSERVATIONS DURING CRUISES ACE II, ACE III, ACE IV, ACE V, ACE VI, AND ACE VII. . 240

REFERENCES . . . . . 313

# AQUATIC DISPOSAL FIELD INVESTIGATIONS
# EATONS NECK DISPOSAL SITE, LONG ISLAND SOUND
# APPENDIX B: WATER-QUALITY PARAMETERS AND PHYSICOCHEMICAL SEDIMENT PARAMETERS

## PART I: INTRODUCTION

### Purpose and Scope

1. This report presents the principal findings of the investigation of water column and sediment properties at the Eatons Neck disposal site, located at the western end of Long Island Sound (Figure 1). The investigation was primarily descriptive and was conducted to provide baseline properties from which the effects of future controlled dredged material disposal on the marine environmental quality of the western sound could be assessed.

2. This report includes: (1) a literature review of Long Island Sound, (2) the analytical methods used in the work, and (3) a description and discussion of general features observed in the study area.

### Literature Review

#### Hydrography and circulation

3. The growth of commerce and the need for adequate data for navigation as well as engineering and scientific work in Long Island Sound created an early need for up-to-date and comprehensive information on the sound's hydrography, tides and currents. LeLacheur and Sammons[1] collected tide and current data from as early as 1835 and used Coast and Geodetic Survey data from cruises conducted in 1929 and 1930 to publish a comprehensive work on the tides and currents of Long Island and Block Island Sounds.

4. Riley[2] reported temperature and salinity data collected on nine Woods Hole Oceanographic Institution

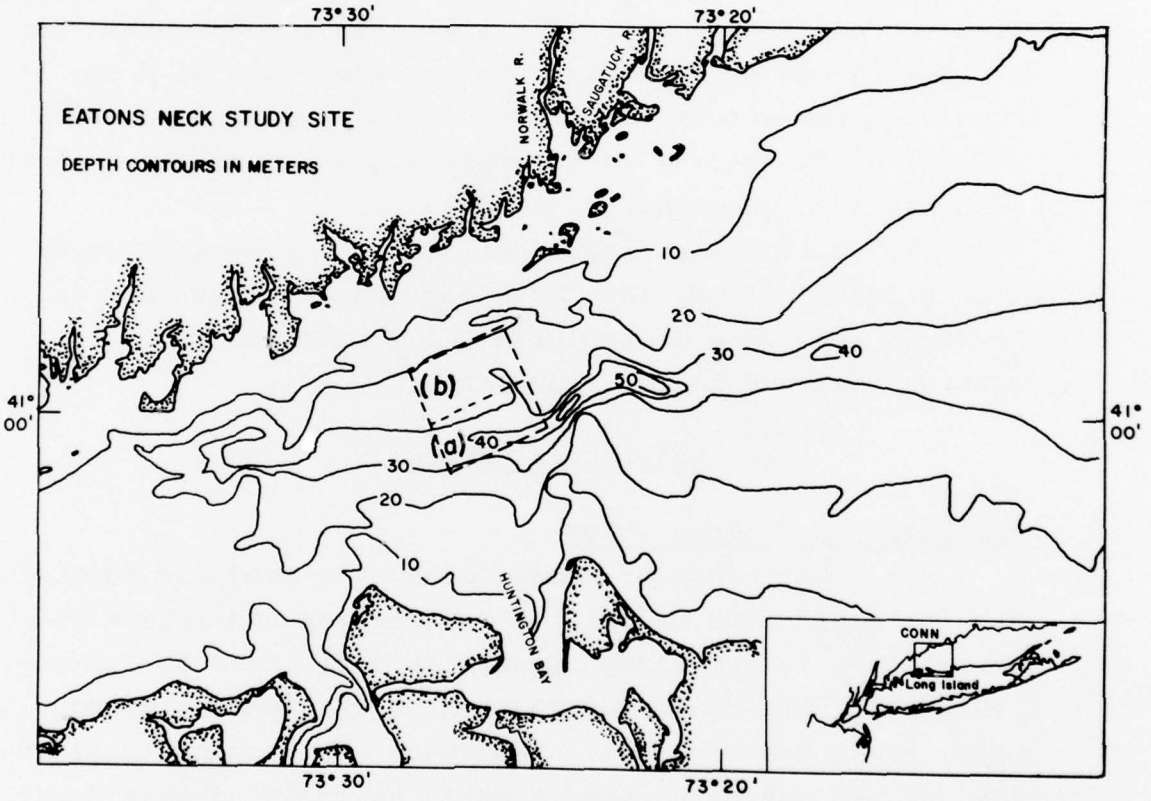



Figure 1. Eatons Neck disposal site study area: (a) existing disposal site, and (b) extended disposal site established for the controlled dredged material experiment.

cruises conducted between January 1946 and January 1947. Using these data and additional information from the U. S. Coast and Geodetic Survey (now the National Ocean Survey) concerning tidal currents and freshwater drainage, drift bottle data from Prytherch,[3] plus freshwater inflow data from Suttie,[4] Riley[2] was able to (1) show some seasonal temperature and salinity distributions, (2) calculate surface density distributions, and (3) infer tidal and nontidal surface current patterns. Riley[2] also computed water transport values, assuming the conservation of mass and salt within the sound, and discussed turbulent mixing and evaluated coefficients of lateral eddy diffusivity and vertical eddy conductivity. Expanding his sampling program, Riley[5,6] continued his investigation of the distribution of temperature and salinity as well as east-west mass transport, vertical eddy conductivity, and transparency in Long Island Sound. Riley[7] published a brief review of his findings and elaborated further on aspects of the oceanography of the sound, based on earlier investigations, especially water exchange as computed by the salt balance method. With respect to water properties and transport processes, Riley[7] emphasized the nontidal circulation which results in a two-layered system in which a freshened surface layer moves eastward out of the sound but is replaced by the input of higher salinity water along the bottom.

5. Hardy[8] and Hardy and Weyl[9] reported observations gathered in 1969 and 1970 on the hydrography and water quality of Long Island Sound. These two reports are essentially data reports containing very little interpretation. In April and August, 1971, Hardy[10] made further oceanographic observations in the sound and presented a detailed description of the distribution of dissolved oxygen, nutrients, and other water properties and their relation to wind, weather, circulation,

and bottom topography. Hardy found that winter-formed bottom water exhibited a seasonal lag in warming in the central basin of the sound and that the persistence into the summer of this colder, more dense bottom layer would indicate limited mixing. Additionally, Hardy suggested that the stagnation of this bottom water is promoted by: (1) the seasonal formation of a weak to moderate thermocline and (2) the inhibition of exchange with Block Island Sound due to the presence of the Mattituck sill which separates the central and eastern basins of Long Island Sound. Hardy observed maximum nutrient concentrations in the East River and western Long Island Sound and proposed a two layer transport system to explain how East River pollutants enter the sound.

6. Gross and Bumpus[11] released seabed drifters in eastern and western Long Island Sound in January, March, and October, 1969, and observed that in the eastern sound the residual drift of near-bottom waters was dominantly westward with a northerly component toward the Connecticut coast, the location of major freshwater sources. In the western sound, they also observed the drifters to move westward; this was attributed to an estuarine flow caused by inflow of low salinity water from the East River.

7. Paskausky and Murphy[12] also examined the residual drift in the sound based on the recovery of surface and bottom drifters released between March, 1973 and January, 1974. They observed an estuarine circulation in the eastern sound throughout the year although two periods of distinctly differing residual drift correlated with wind and freshwater discharge variation. Their results showed that during the summer period the westward flux of near-bottom water does not extend into the central sound past the Mattituck sill which separates the central and eastern basins of the sound.

However, during the winter season the near-bottom waters moved well into the central sound. They found little evidence to suggest a significant near bottom exchange between the western and central sound.

8. Wilson[13] calculated, based on the field work of Hardy[8,9], that longitudinal salinity and associated density gradients maintain a non-tidal two layer gravitational circulation which is well developed in the western and central sound and intensely developed in the eastern sound. Wilson calculated volume transports which varied from approximately 500 $m^3$ $sec^{-1}$ in the western sound, to 5,000 $m^3$/sec in the central basin, to approximately 30,000 $m^3$/sec in the eastern sound. The calculated transports were reported not to vary significantly with season, although Wilson found that circulation for 20-30 January, 1969, was least developed and that for 9-13 August, 1971, was most developed. Wilson concluded that gravitational circulation contributes to rapid exchange between waters of the eastern sound and those of the central and western sound.

9. Swanson[14] made current observations during a 15-32 day period in August-September, 1966 at four stations situated over a north-south cross section in the central sound. Three stations with concurrent 15-day records were selected for analysis of tidal constituents. The major currents were semi-diurnal, tidal flows and were reported to be greatly influenced by topography. The mid-channel flow was found to be rotary. The observations further indicated that maximum ebb occurs along the shore before it does in mid-channel. Swanson also observed a very pronounced lead in both the maximum ebb and flood along the Connecticut shoreline, as compared to the southern half of the sound in the cross section.

10. Gordon and Pilbeam[15] have measured, for periods as long as over one year between October, 1971 and September, 1973, the tidal and nontidal components of near bottom water

movements in central Long Island Sound. They found that higher salinity bottom waters at depths greater than 20 m flow upstream at a rate that decreases toward the head of the estuary. At depths shallower than 20 m, they observed a shoreward flow of bottom water toward a complex mixing zone whose origin seems to be associated with Six Mile Reef. They also observed a layer of less-saline surface water whose flow was generally to the southeast.

11. Recently Weyl[16] has reviewed the tides and tidal currents in Long Island Sound. Weyl reports that the tidal oscillation in the sound is approximately one-quarter of a standing wave with the node near the Race and the antinode near the western end of the sound. Weyl also reports that the tide is close to synchronous in the central and western portions of the sound but can be represented by a westerly progressive wave in the eastern portion. Using the amplitude and time relationship of the variation in tidal height, Weyl computed the mean east-west tidal water motion through north-south sections in the sound. Weyl found that during an average tide, about 5.5 $km^3$, or about 9% of the volume of the sound, is replaced. During spring and neap tides, 6.5 $km^3$ and 4.4 $km^3$ of water are exchanged, respectively.

Nutrient and organic carbon distributions

12. Riley and Conover[17] reported chemical oceanographic data in Long Island Sound during the period 1952-1954. Their investigations revealed the major features of the seasonal cycles in $NO_3^-$ and $PO_4^{3-}$ concentrations in the sound. During the spring phytoplankton blooms of 1953 and 1954, $NO_3^-$ was almost completely exhausted in about 3 weeks but about 0.5 µM of $PO_4^{3-}$ remained in the water. $NO_3^-$ remained low until September, while $PO_4^{3-}$ tended to increase gradually during the summer and then more rapidly in autumn. Both $PO_4^{3-}$ and $NO_3^-$ were observed to increase slightly from surface to bottom during most of the spring and summers of 1952 and 1953; slight and variable vertical gradients were observed in autumn and

winter seasons. In the autumn, 1952, an east-west gradient in both $NO_3^-$ and $PO_4^{3-}$ was observed in the surface. However, no discernible horizontal gradients were observed during the summer period, due to the nearly exhausted levels of these nutrients. Riley and Conover suggest that the presence of a two-layered transport system helps explain the nutrient distribution: a two-layered system gradually removes the nutrient-poor surface layer while it is the bottom water that brings in nutrients.

13. Riley[18] used observed distributions of oxygen and $PO_4^{3-}$ to calculate net biological rates of change of oxygen and phosphorous on a seasonal basis. These changes were then converted to estimates of total plant production and utilization of organic matter by marine organisms. Riley reports that the total annual fixation of carbon by photosynthesis is estimated to be about 470 $g/m^3$. Over half of this carbon is utilized in phytoplankton respiration; of the remainder, 26% was used by those zooplankton that pass through a No. 10 mesh net, 43% by microzooplankton and bacteria in the water column, and 31% by the benthic fauna and flora.

14. Harris and Riley[19] analyzed plankton samples collected in the sound during 1952-1954 for wet- and dry-weight, ash, chlorophyll, total phosphorous, and nitrogen. Riley reported that phytoplankton samples showed seasonal variations in ash content which could be explained by changes in the relative abundances of certain species. Chlorophyll also showed variations which were attributed to adaptation of the phytoplankton to seasonal changes in illumination.

15. Riley[20] made measurements of total organic matter in water samples collected in Long Island Sound during January-December, 1956. Concentrations of total organic matter ranged between 1.2 and 3.1 mg/l during the period of study. Riley suggested that a considerable fraction of the organic matter in the sound occurs as detritus or as organisms containing little or no chlorophyll.

16. Harris[21] made observations on the concentrations of $NH_4^+$, $NO_2^-$, and $NO_3^-$, plus particulate nitrogen and dissolved organic nitrogen in Long Island Sound from October 1954 to June 1955. He observed that the seasonal nitrogen cycle was qualitatively similar in different parts of the sound except for small differences associated with the time of the early phytoplankton bloom. He noted a strong horizontal total inorganic nitrogen gradient, with maximum concentrations of all fractions at the western end of the sound. Daily nitrogen enrichment, averaged for the entire sound, by freshwater drainage during the winter and spring was about 0.04 µmole N per $cm^2$. However, as Harris points out, 75% of the total input of freshwater is localized in the eastern sound and thus the effective enrichment elsewhere in the sound was estimated to be only about 0.01 µmole/$cm^2$. Nitrogen transport from New York harbor at the western end of the sound was considered important locally, but was found to be only one-tenth of that of the total river drainage.

17. Hardy[22] discussed the impact and seasonal variability of $NO_3^-$, $NO_2^-$, and $NH_4^+$, and seasonal concentrations of chlorophyll at the western end of the sound. During the winter, when phytoplankton production is least active, the rate of addition of nitrogenous wastes exceeds the rate of biological uptake which causes an accumulation of inorganic nitrogen, mainly in the form of $NH_4^+$, at the western end of the sound. Hardy reports winter $NH_4^+$ concentrations that exceed 10 µM near Hempstead Harbor; near the Throgs Neck Bridge, $NH_4^+$ concentrations are in excess of 20 µM. In the summer, however, the $NH_4^+$ concentrations are greatly reduced due to biological activity and typical $NH_4^+$ values near Hempstead Harbor are reported by Hardy to be in the 1-5 µM range.

18. Bowman[23] investigated the distributions and transport of $NH_4^+$, $NO_2^-$, and $NO_3^-$ in Long Island Sound for both

winter and summer conditions using a steady state, one dimensional mass balance model. The nutrient budgets were based on horizontal exchange, lateral input from sewage and agricultural sources, and first-order biochemical uptake (utilization minus regeneration). Bowman has shown that sewage effluents are the prime external source of nutrients for the sound and that there is a continual loss of nitrogen to the sediment in the sound via zooplankton grazing, excretion, and mortality.

Oxygen distribution

19. Hardy and Weyl[24] give the only detailed description of dissolved oxygen in Long Island Sound. Their investigation, based on surveys during the periods 7-15 August and 5 October 1970, covers the region between Brothers Island (East River) eastward through Long Island Sound to Port Jefferson (Long Island). During the August period, they observed a serious oxygen depletion, where the oxygen concentrations were less than 1.5 mg/l throughout the entire water column of the upper East River and also in the bottom waters of western Long Island Sound. In contrast, the surface waters of a considerable portion of western Long Island Sound were reported to be supersaturated with oxygen to a depth of 2 to 3 meters; oxygen supersaturation occasionally was over 200% of saturation. By October, the bottom oxygen concentrations in the sound (but not the East River) had increased to acceptable levels of 7-8 mg/l.

20. Weyl[16] describes the oxygen depletion in western Long Island Sound as primarily a summer problem. He gives the following reasons: "(1) in summer, the temperature is near its maximum and the solubility of oxygen in the water is therefore at its annual minimum; (2) in summer, vertical density stratification is also at its maximum, reducing vertical mixing; (3) the rate of respiration by bacteria and cold-blooded animals (e.g. fish) increases as the temperature

increases. Therefore the rate of respiration is at a maximum in summer. In addition, many species of fish migrate into the sound during warm months and further increase the summer respiration rate."

Heavy metal distribution

21. The concentration and distribution of heavy metals in Long Island Sound waters are probably influenced by anthropogenic inputs originating from (1) Connecticut and Long Island rivers and streams (Turekian[25]) and shore-based sewage treatment plants; (2) sewage and industrial effluents discharged into the East River and other waters adjacent to the New York metropolitan region (Mytelka et al.,[26] Klein et al.,[27] Interstate Sanitation Commission[28]); and (3) disposal of waste solids in Long Island Sound (Gross et al.[29]).

22. There has been no systematic study to determine the distribution of dissolved or particulate heavy metals in Long Island Sound. Turekian[25] has reviewed the concentrations of trace metals in the Connecticut and Housatonic Rivers and has discussed the fate of Co, Ni, and Ag in the western and central basin of Long Island Sound. Turekian reports that: "1. Trace elements injected into the streams in soluble form are adsorbed rapidly but on suspended particles. This is best seen in the case of the Naugatuck River where the high cobalt and silver concentration as the result of industrial injection north of Naugatuck diminishes downstream so that where the Naugatuck River joins the Housatonic River it is as low in trace-element concentration as the Housatonic.

2. Some trace elements seem to be injected by industry either directly into the Sound or through small streams before adsorption on suspended material takes place.

3. At the mouth of the Housatonic, as the salinity of the Sound is approached, the trace-element content increases dramatically. This may be interpreted to mean either that

there is release of the trace elements adsorbed by the suspended material on contact with seawater as shown by the experiments of Kharkar et al.[30] [see reference 25] discussed above or that there is peculiarly high release on these metals into the mouth of the Housatonic by local industry. Of the two explanations, the first seems more probable because the effect is seen by all the elements and industry is not uniquely associated with the mouth of this river.

4. A short distance away from the sources of injection of trace elements into the Sound, by whatever means, they are apparently removed from the dissolved state by planktonic organisms.

5. Some of the plankton undoubtedly disintegrates on the bottom or on the way to the bottom, and local pockets of high trace-element concentrations in the water are encountered at depth on the western side of the Sound.

6. Most of the trace elements, however, are removed and retained in the reducing sediments of the Sound since the solubility of the sulfides of the metals would be exceeded in the sediments of the Sound with the production of $H_2S$. The sediments of Long Island Sound are very high in silt, yet the silver content is about 1 µg/g which implies some concentration above average shales (0.1 µg/g).

7. The water leaving Long Island Sound (that above 20 ft for a large part of the Sound, Riley, 1956 [see reference 5 ] is less than or equal to the concentration of trace elements in the deeper water entering the Sound from the ocean indicating that little or none of the trace-element load supplied by streams (reinforced by the strong contribution from industry) leaves the Sound but is trapped in the sediments depositing there."

23. Fitzgerald et al.[31] have determined the concentrations of Cu, Zn, Ni, and Cd in eastern Long Island Sound.

They have also developed a preliminary mass balance model for Cu and Zn for the sound; the model shows good agreement between input and output of these metals, suggesting a steady-state for the amounts of these metals in the water column. Significant removal of the metals was reported to occur through biological and geochemical processes and by rapid water renewal in the eastern sound. Additionally, they report that a large fraction of Cu and possibly other metals, including Hg, brought into the sound from the Connecticut River appear to be bound to organic matter.

Sediments in Long Island Sound

24. A general description of sediment distribution in Long Island Sound has been reported by McCrone et al.[32] and Buzas[33]. McCrone[34] published a brief review of the physical and chemical properties of these sediments. He reported that silts prevail in the sediments from western Long Island Sound, with the fine-fraction mineralogy dominated by illite and chlorite.

25. Bokuniewicz et al.[35] used sonic reflection profiling and bottom sampling to measure the volume of sediments accumulated in Long Island Sound. Their sediment mass balance calculations show that this volume of sediment consists of marine mud, sediment of premarine, lacustrine origin and reworked sand derived from glacial drift. They reported that Long Island Sound acts as a trap, not only for material carried by rivers but for suspended material in the water on the continental shelf. Inward transport of mud from outside of the sound has been proposed as the principal source of the muddy sediment presently accumulating in Long Island Sound. Deposits south of Marthas Vinyard and in the Gulf of Maine are believed to be the possible sources of the mud.

26. A recent study, covering a small area of investigation in eastern Long Island Sound, of the mineral

composition, sediment distribution, pathways of sediment movement, and sedimentation rate has been published by Akpati.[36] Of interest is the observation that the offshore sands in the area are characterized by quartz grains with ocherons hamatite stains, with stained quartz decreasing landward. The shoreward decrease in stained quartz has been attributed to a dilution effect by unstained quartz grains from land or may indicate an offshore contribution of this mineral, presumably transported in the sound by the prevalent landward bottom current.

27 . Thomson et al. (In Turekian[37]) studied the vertical distribution of $Pb^{210}$, $Ra^{226}$, $U^{234}$, $U^{238}$, $Th^{228}$, $Th^{230}$, and $Th^{232}$ as well as Pb, Zn, Cd, and Mn in sediment cores from central Long Island Sound. On the basis of their results, they were able to determine the modes and rates of accumulation of metals over time in sediments of central Long Island Sound and the patterns of their release. Their results also indicate that U, and possibly Mn, may be remobilized from sediments to the overlying water column.

28 . Fitzgerald et al.[31] in their model for the distribution and fluxes of Cu and Zn in Long Island Sound indicates that about 90% of the Cu and Zn entering the sound annually is removed to the sediments. They further report that more than 80% of the Cu and Zn input to the sound appears to be anthropogenic in origin.

29 . Martens and Berner[38] studied the relation between methane and dissolved sulphate distributions in the interstitial waters of organic-rich sediments in central Long Island Sound. They reported that in the interstitial waters of anoxic sediments from the sound methane does not reach appreciable concentrations until dissolved sulfate concentrations are considerably lowered.

30 . Aller and Cochran[39] used $^{234}Th/^{238}U$ disequilibrium

in sediment to evaluate short-term sediment reworking and diagenetic rates. Their results of seasonal measurement of $^{234}Th/^{238}U$ disequilibrium in central Long Island Sound sediment show rapid particle reworking in the upper 4 cm of sediment, with the rate varying seasonally and being highest in the fall.

Solid-waste disposal in Long Island Sound

31 . According to Gross[40] and Gross et al.,[41] thirteen offshore sites are actively used for disposal of solid wastes in Long Island Sound in which an average of $1.9 \times 10^6$ metric tons of waste solids are disposed in western Long Island Sound annually.

32 . Table 1 gives the volume of dredged material disposed at the Eatons Neck disposal site from 1954 to 1972.* Unfortunately, there are no available data on the composition of the dredged material.

33 . O'Connor[42] has reviewed the dredging and disposal activity in the shore zone of Nassau and Suffolk counties on Long Island. According to O'Connor, most of the activity has been conducted at the margins of Great South and Peconic Bays, principally for maintenance dredging of navigation channels and development of the shore zone for residential and commercial purposes; a marked reduction in dredge/spoil activity occurred in 1968.

34 . Gordon[43] has studied the dispersion of dredged material disposed in waters near New Haven Harbor. He found that 99% of non-cohesive spoil of high silt discharged from a skow in the presence of a tidal stream was transported to the bottom as a high speed turbulent jet. The thickness of the bottom cloud was about 5 m. After about 26 minutes, the turbidity of the water 5 m from the bottom site was nearly at background levels.

* D. Suszkowski, personal communication.

Table 1

Volume of Dredged Material Disposed
at Eatons Neck Disposal Site

| Year | Volume ($m^3$) |
|---|---|
| 1955 | 7,630 |
| 1956 | 84,400 |
| 1957 | 100,000 |
| 1958 | 98,000 |
| 1959 | 650,000 |
| 1960 | 266,000 |
| 1961 | 129,000 |
| 1962 | 192,000 |
| 1963 | 3,860,000 |
| 1964 | 2,100,000 |
| 1965 | 138,000 |
| 1966 | 999,000 |
| 1967 | 428,000 |
| 1968 | 446,000 |
| 1969 | 102,000 |
| 1970 | 38,000 |
| 1971 | 84,000 |

## PART II: SAMPLING AND ANALYTICAL METHODS

### Sampling

#### Water column

35 . The sampling grid (Figure 2) consisted of 26 stations and was designed to observe larger scale spatial and seasonal variations in the water properties in a broad region of western Long Island Sound surrounding the Eatons Neck disposal site.

36 . The following transects formed the station grid: Z-X; S-Q; K-G; P-L; and W-T. Transect K-G covered the proposed experimental disposal site, and station A was the control site. A transect consisting of the stations V, A, D, R, and Y provided a longitudinal section.

37 . Figure 3 shows continuous sounding records along each transect.

38 . The stations were sampled sequentially through any particular transect aboard the RV ONRUST. It usually took 2 days to sample the grid. The sampling depths were every 2 m for suspended solids and every 4-6 m for the other variables.

39 . In addition to the above sampling, another sampling procedure, used during the first 2 cruises, involved an intensive 24-hr study of stations, A, B, C, D, E, F, G, H, J, and K. Here the purpose was to obtain an estimate of variability in water column properties over a tidal cycle within the disposal site.

40 . Stations DSA and DSB were sampled during March, April, and May when it was learned that these two sites had been proposed for future dredged material disposal experiments.

41 . Table 2 is a summary of the water column cruises.

#### Sediment

42 . The sediment sampling consisted of 17 coring

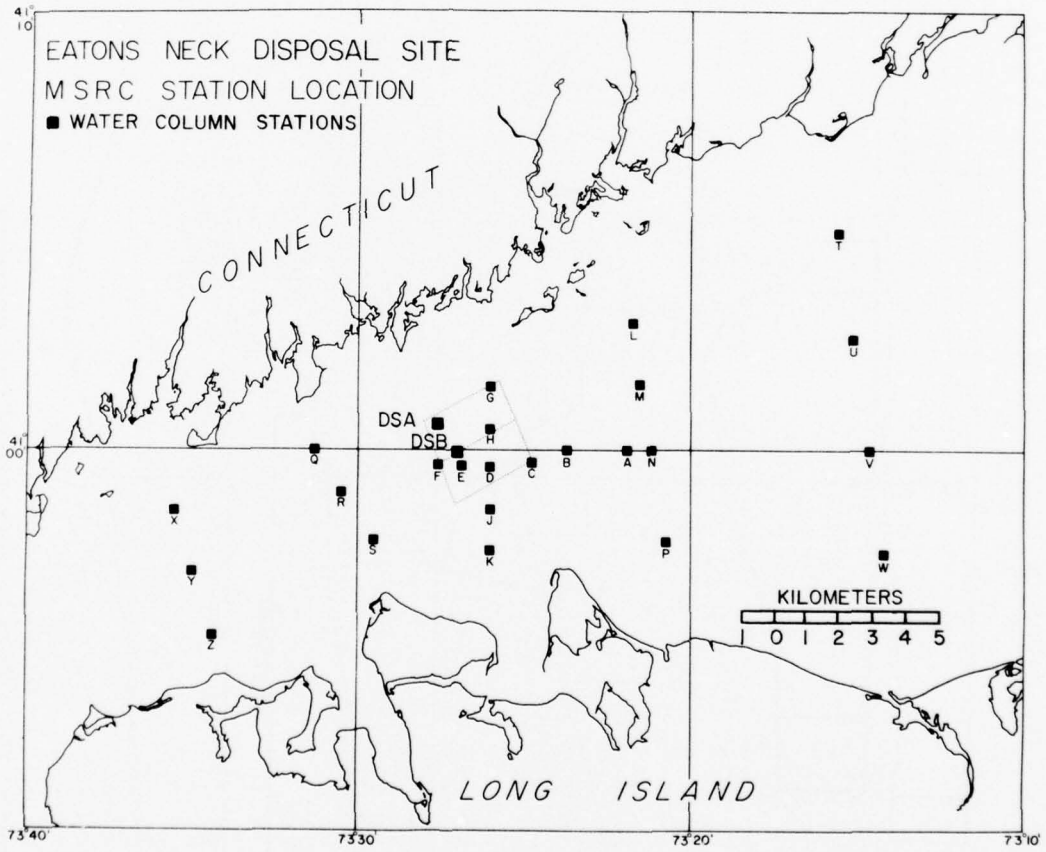



Figure 2. Location of water column stations

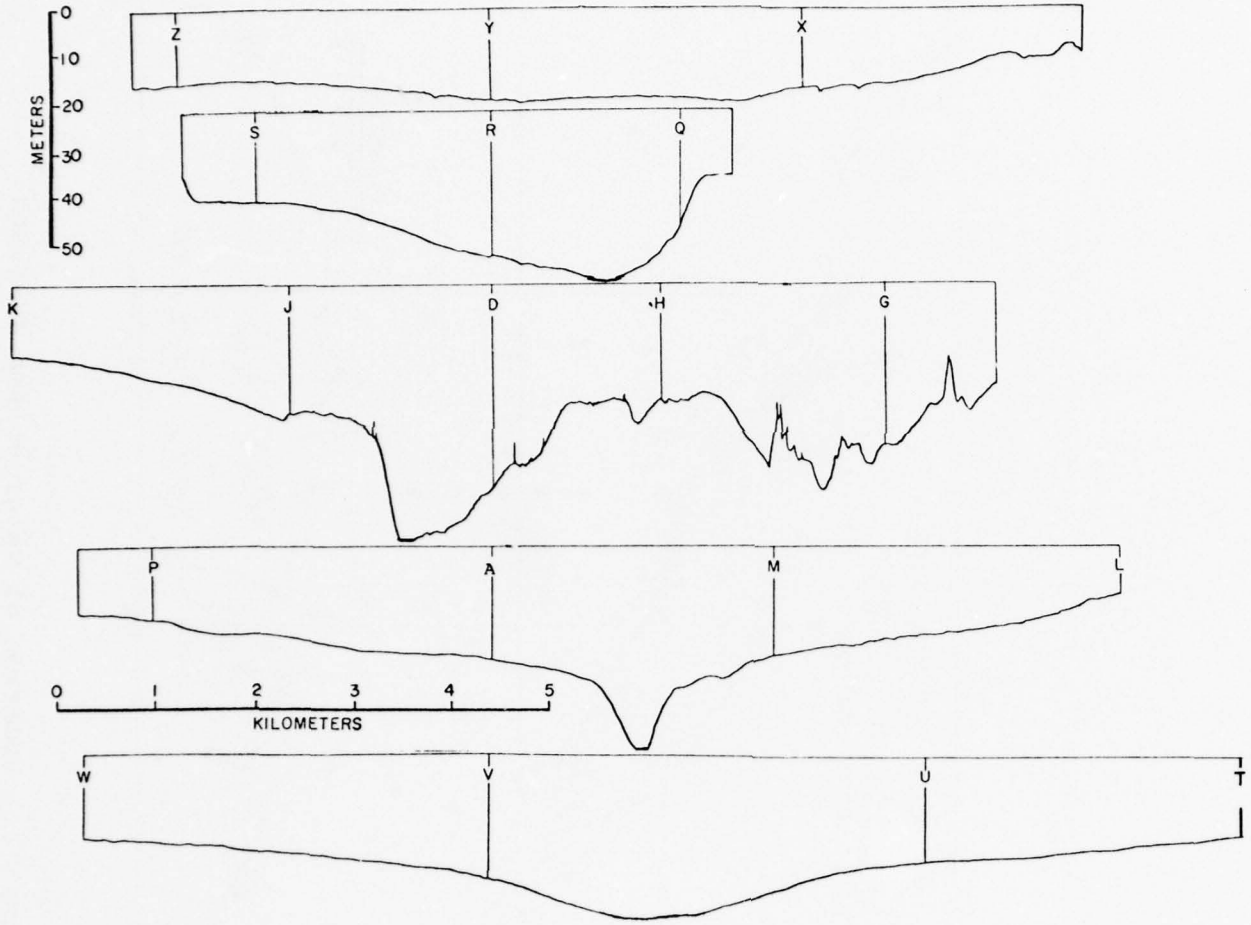



Figure 3. Continuous sounding records

Table 2

Water Column Cruises

| Cruise | Date | Stations Sampled, in Sequence |
|---|---|---|
| ACE I | 30-31 Oct 1974 | A, B, C, D, E, F, G, H, J, K, |
| | 1 Nov 1974 | L, M, N, P, Q, R, S |
| ACE II | 5 Dec 1974 | A, B, C, D, E, F, G, H, J, K |
| | 6 Dec 1974 | S, R, Q, L, M. N, P |
| ACE III | 13 Jan 1975 | X, Y, Z, S, R, Q, G, H, D, J, K |
| | 14 Jan 1975 | P, A, M, L, T, U, V, W |
| ACE IV | 19 Feb 1975 | X, Y, Z, S, R, Q, G, H, D, J, K |
| | 20 Feb 1975 | W, V, U, T, L, M, A, P |
| ACE V | 19 Mar 1975 | X, Y, Z, S, R, Q |
| | 20 Mar 1975 | DSB, DSA, G, H, D, J, K |
| | 21 Mar 1975 | P, A, M, L, T, U, V, W |
| ACE VI | 23 Apr 1975 | X, Y, Z, S, R, Q, DSA, DSB, G, H, D, J, K |
| | 24 Apr 1975 | P, A, M, L, T, U, V, W |
| ACE VII | 28 May 1975 | X, Y, Z, S, R, Q, DSA, DSB, G, H, D, J, K |
| | 29 May 1975 | P, A, M, L, T, U, V, W |

stations (Figure 4) in which 10 stations were located within the proposed experimental disposal site. The dense sampling grid in the experimental disposal site was chosen to give detailed information on the spatial variability of sediment properties. Stations were located by sextant and radar.

43. Table 3 gives the dates, station locations, and depth of water for each sampling station. On 22 April, cores at DSA-1, -2, -3, and -4 were taken on a circle of a radius of about 100 m from DSA. In addition, duplicate cores were collected at stations A (A-1 and A-2), O (O-1 and O-2), and DSA (DSA-A and DSA-B) [see Table 3].

## Shipboard Testing

44. The Hulse system (Plunket)[44] was used to measure temperature, salinity, oxygen, and in vivo chlorophyll a fluorescence. This system is a shipboard, semi-automated, data acquisition system in which seawater is continuously pumped from depth, via a submersible pump, to a manifold (located inside the ship) which directs water to various sensors (Figures 5 and 6 illustrate the Plunket).

45. The thermistor sensor, with a specified accuracy of $\pm$ 0.05°C, located near the submersible pump, permitted in situ temperature recording at each sample depth.

46. The salinity sensor was a Bisset-Berman Salinograph$^{R}$ having a specified accuracy of $\pm$ 0.01°/$_{oo}$.

47. Dissolved oxygen was measured with a YSI electrode which was calibrated according to the procedure outlined by Hulse.[44]

48. The in vivo chlorophyll fluorescence was measured with a Turner$^{R}$ (Model 110) fluorometer and was used primarily as a diagnostic indicator to locate chlorophyll maxima and minima in the water column.

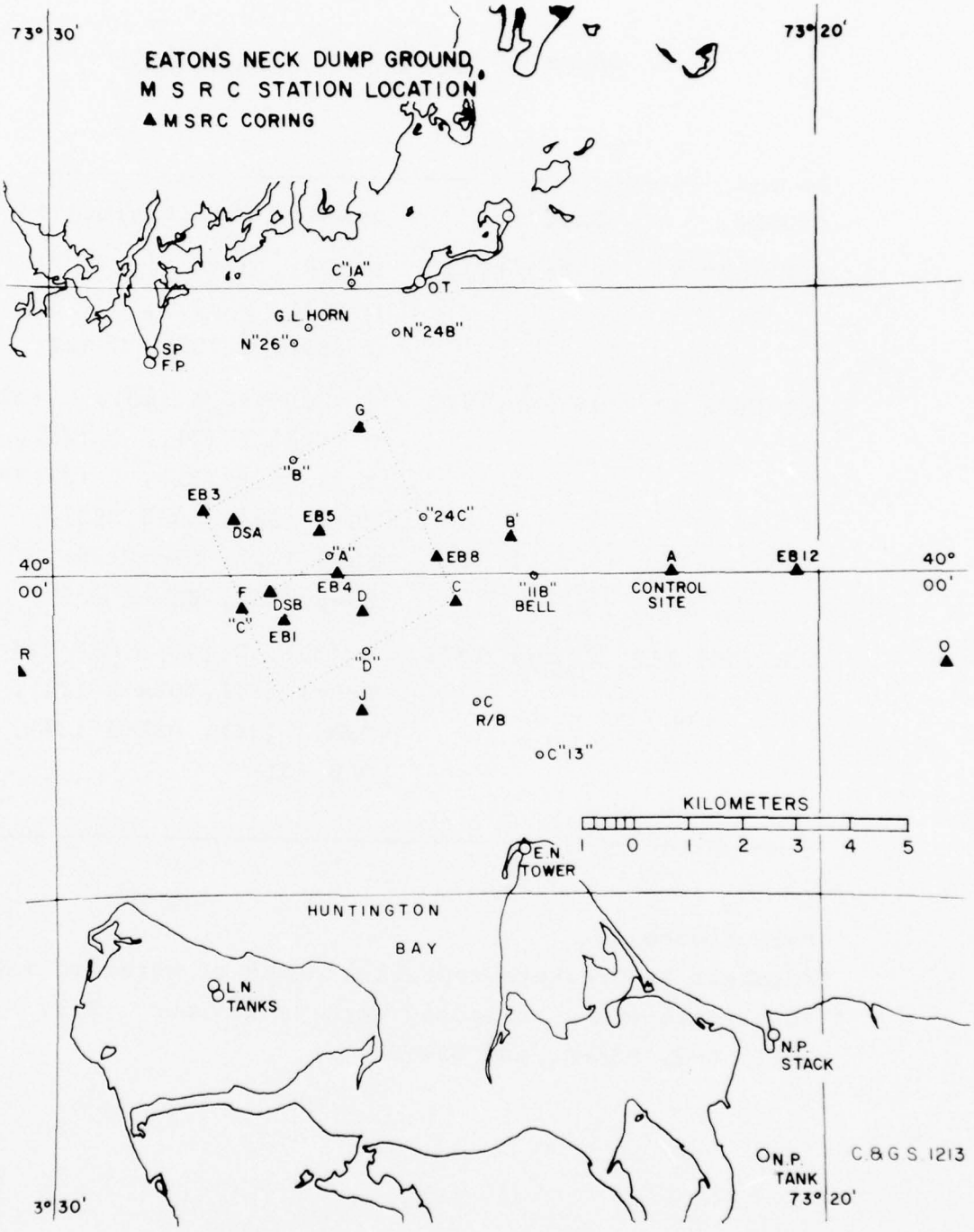



Figure 4. Location of coring stations.

TABLE 3

Dates of Sediment Coring Cruises

| Cruise | Date | Station Designation*,** |
|---|---|---|
| ACE CORE I | 4 Nov 1974 | A (26), B (63), C (37), D (41), F (31), G (25), J (23), R (30), O (22) |
| ACE CORE II | 15 Jan 1975 | A (26)***, B (63), C (37), D (41), F (31), G (25), J (23), R (31), O (22)***, EB-1 (39), EB-3 (23), EB-4 (32), EB-5 (26), EB-8 (26), EB-12 (25) |
| ACE CORE III | 22 Apr 1975 | A (26), D (41), DSA (24.1)***, DSA-1 (24), DSA-2 (24), DSA-3 (24), DSA-4 (24), DSB (31) |

*See Figure 4.

**Numbers in brackets represent depth of water in meters.

***Duplicate cores collected were as follows: A-1, A-2, O-1, O-2, DSA-A, and DSA-B.

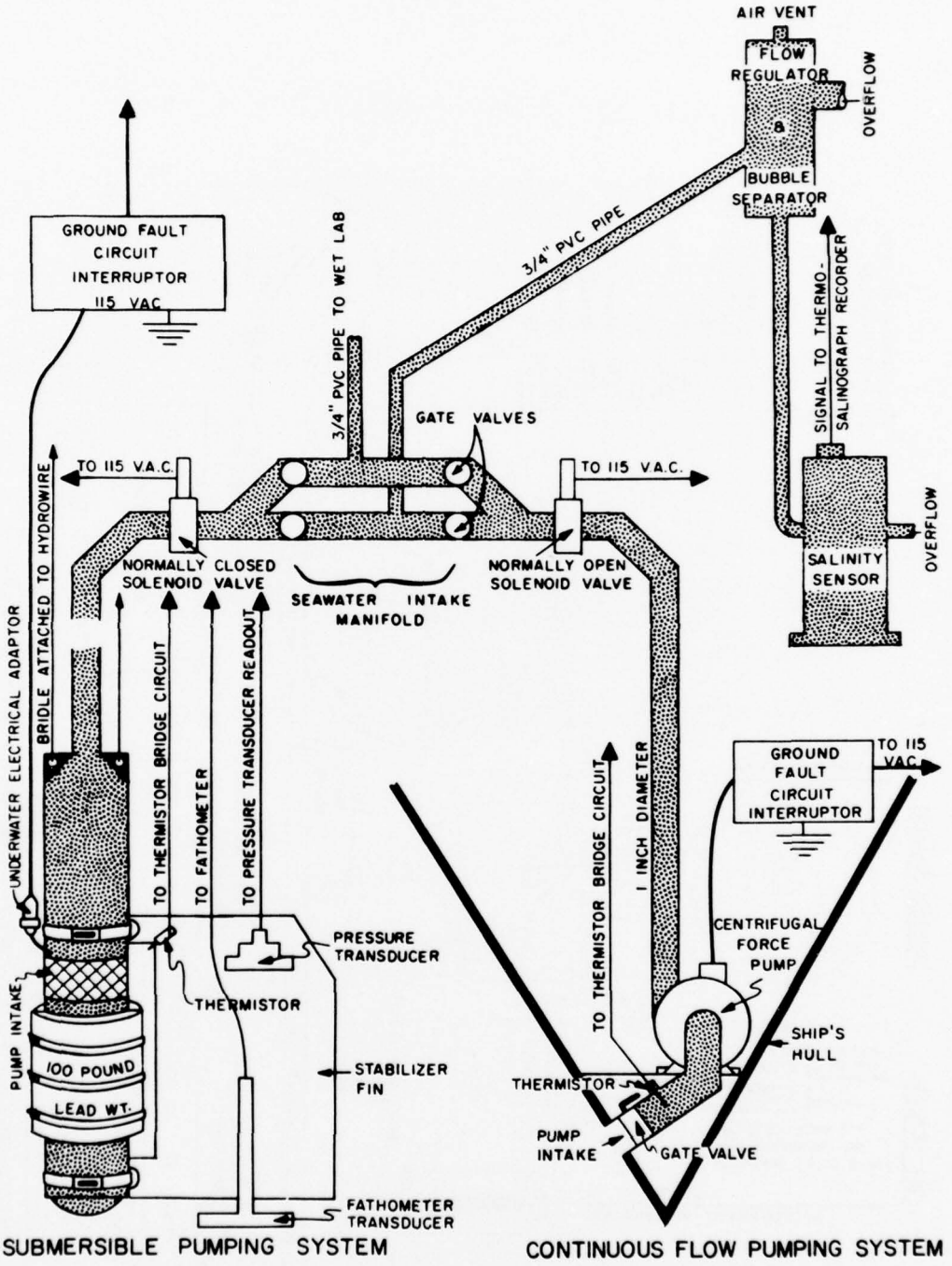



Figure 5. Submersible pumping system and continuous flow pumping system associated with the seawater sampling equipment.

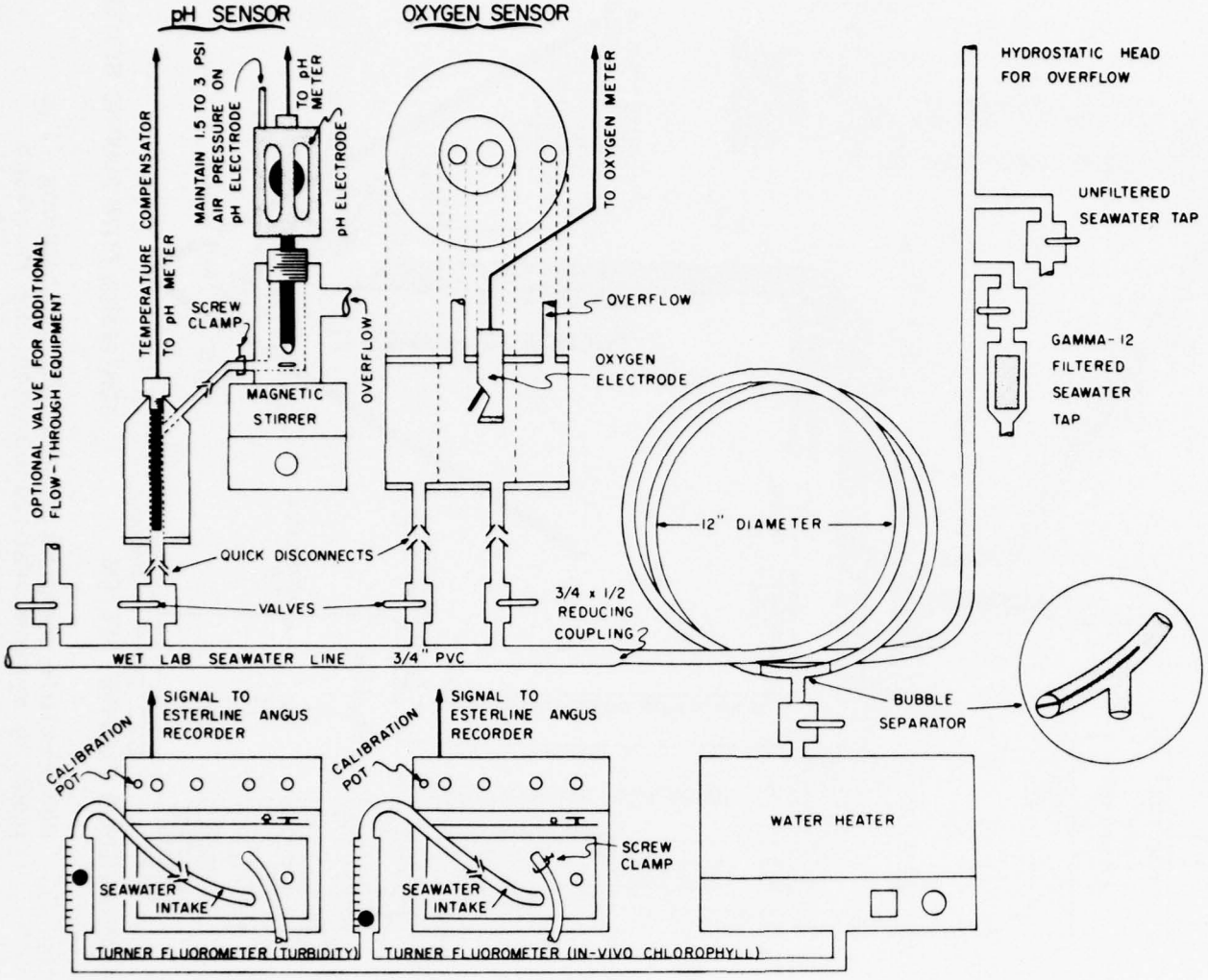



Figure 6. Wet lab sensors associated with the seawater sampling equipment.

## Water Column Analyses

### Nutrient analysis

49. Glass-fiber filtered (8-μm porosity) water samples for $NH_4^+$, $NO_2^-$, $NO_3^-$, $PO_4^{3-}$, and $Si(OH)_4$ were collected in 125-ml polyethylene bottles from the Plunket. Immediately after collection, these samples were stored under ice until they could be analyzed in the laboratory. Urea samples were collected in 250-ml glass bottles and immediately frozen.

50. $NH_4^+$, which includes about 5 percent by weight of dissolved $NH_3$,[45] was determined 20 to 30 hr after collection using a Technicon$^R$ Autoanalyzer II and an indophenol method.

51. $NO_2^-$, $NO_3^-$, $PO_4^{3-}$, and $Si(OH)_4$ were determined[46] from 2 to 3 days after each cruise using a Technicon$^R$ Autoanalyzer II system.

52. Because of the complexity of the urea analyses, all urea samples were analyzed in one batch run using a modification of the method by McCarthy.[47] A Technicon$^R$ Autoanalyzer II system was used to determine urea plus ammonia in ingested samples. The urea concentration was thus found by difference.

### Chlorophyll a extraction

53. The concentration of chlorophyll a was measured trichromatically and fluorometrically[46] using acetone extracts of the pigment. An ultrasonic probe was used in the extraction procedure in a darkened room to rupture the cells previously collected on the Millipore$^R$ filters.

### Dissolved organic carbon

54. Glass-fiber filtered (8-μm porosity) water samples for dissolved organic carbon (DOC) were collected in 250-ml glass bottles from the Plunket spigot. Immediately after

collection, each sample was frozen until the analysis could be performed in the laboratory. A Beckman organic carbon analyzer (Model 915) was used for the analysis. Weighed samples of potassium phthalate were used as the calibration standard. Each sample was acidified with HCl to pH 2-3 and then agitated to remove the dissolved inorganic carbon.

Particulate organic carbon and nitrogen

55. Samples for particulate carbon and nitrogen determination were collected on (0.8-µm nominal porosity) glass-fiber filters. The volume of water filtered varied from 50 to 100 ml. The filters were stored frozen until the analysis could be performed. A Hewlett-Packard CHN analyzer (Model 185) was used for the analysis. The combustion temperature was 1140°C, and acetanalide was used as the standard.

Dissolved and particulate metals

56. Samples for metals analysis were collected using 10-ℓ Niskin top-drop PVC samplers. Because of the complexity and the importance of the metal analyses, a complete description of the methods used is given in Appendix A'.

Suspended matter

57. Samples for gravimetric analysis of suspended matter were collected in 500-ml glass bottles from the Plunket spigot. These samples were filtered in the laboratory using pre-weighed 0.8-µm Nuclepore (47 mm diameter) filters; the filter was dried in a desiccator and then reweighed.

Particulate size analysis

58. Water samples for particulate-size analysis were collected from the Plunket spigot and immediately filtered onboard the research vessel.

## Sediment Analyses

Sediment coring

59. Sediment cores were obtained with a cellulose acetate butyrate core liner using a Benthos Model 2171

gravity corer. Any metal parts that could introduce contamination, such as core catcher and cutting nose cone of the corer, were not used. Immediately after recovery of the core, the core liner was sealed with end caps to prevent oxidation and allowed to stand in an upright position for half an hour. After draining the overlying water, the cores were extracted from the core liners by extruding the core with a plunger. Each core was cut into the top 10-cm and lower 20-cm sections. The pH of each core section was measured on shipboard. The core sections were stored in plastic bags at 5 $\pm$ 4°C for further sediment analysis.

Pore water extraction

60. Reeburgh[48] type squeezers were used to extract the pore water out of sediment samples. Subsamples from each core section were placed in the sediment holder of the squeezer and the pore water was extracted under a pressure of 10-150 psi using helium gas. In a period of 2 hr, about 40-120 ml of pore water was collected in acid-cleaned 180-ml polyethylene bottles. About 20 ml of the extracted pore water was frozen for the analysis of $NH_4^+$, $NO_3^-$, $NO_2^-$, $PO_4^{3-}$, $Si(OH)_4$, and DOC. The remaining pore water sample was acidified with concentrated HCl and stored at 4°C for the analysis of dissolved Pb, Zn, Cu, Fe, Mn, and Ni.

Interstitial metals

61. Pb, Cu, and Ni in extracted pore water samples were analyzed by flameless atomic absorption spectrophotometry following solvent extraction. Fe, Mn, and Zn were analyzed by directly aspirating the sample solution into the air-acetylene flame. The concentrations of these metals in pore water samples were high enough to be detected by the flame. The details of the method, the range of analytical precision, the limit of detection, and the sensitivity for each metal

analyzed using the air-acetylene flame method are given in Appendix A'.

Interstitial nutrients

62. The analysis of $NH_4^+$, $NO_3^-$, $PO_4^{3-}$, and $Si(OH)_4$ was carried out by the Autoanalyzer using conventional methods.[46] DOC was determined using a Beckman Carbon Analyzer.

Sediment texture

63. Analyses of grain-size distribution were performed on all sediment core sections by sieving and pipetting according to standard sample preparation and analytical techniques.[49] The limits and names of size grades used in this study are: gravel, for particles coarser than 2 mm; sand, for particle diameters between 2 and 0.063 mm. For material finer than 0.063 mm, the term mud is used. Mud is composed of silt particles ranging in size from 0.063 to 0.002 mm in diameter and clay particles finer than 0.002 mm in diameter. The nomenclatural system used to describe the texture of the sediment is similar to that of Folk.[50] Samples containing between 5 and 30 percent are indicated by an adjective (sandy) and those over 30 percent qualify as nouns (sand). If two components represent more than 30 percent, the finer-grained component is indicated by a noun, the other by an adjective with the adverb 'very'. The grain-size distribution data are presented on ternary plots with the sand, silt, and clay being the end components. In cases where appreciable amounts of gravel were present, the clay and silt were grouped together as mud, with the other two end components being gravel and sand on the ternary plots. The presentation of grain-size distribution data in this form enables one to identify the sediment texture immediately. An example of such a graphic presentation of grain-size data is shown in Figure 7.

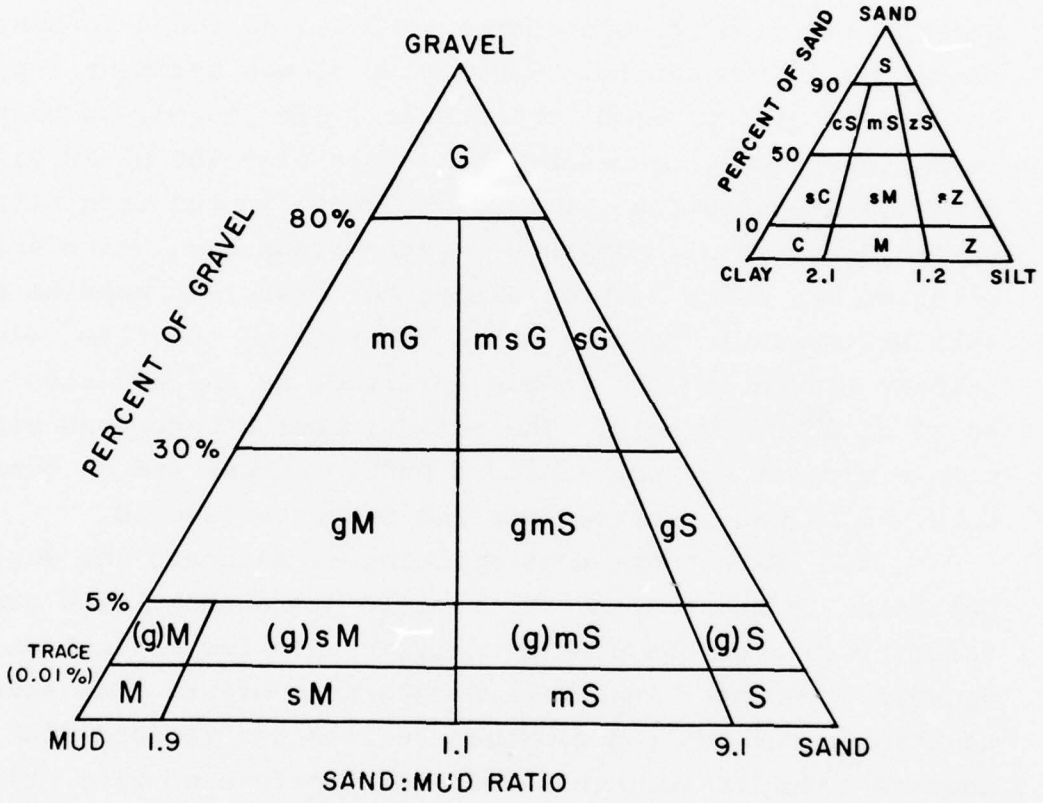



Figure 7. Ternary plot representing nomenclatural system describing sediment texture

Particulate C and N

64. Particulate C and N were determined on dried sediment subsamples using a CHN analyzer.

Total sulfides

65. Total sulfides consists of soluble sulfides in pore water and authigenic sulfide minerals. The sample storage and handling procedures were all designed to prevent oxidation of the sample. Subsamples of wet sediment (approximately 50 g) from each core section were placed, on shipboard, in a preweighed wide-mouth flask containing 150 ml of dilute zinc acetate solution. The flasks were flushed with nitrogen gas to displace air and then lightly stoppered. Zinc acetate solution was added to precipitate the dissolved sulfide phase into an insoluble form. In the laboratory, the flask was quickly opened and the sample acidified by the addition of 10 ml of sulfuric acid. The solid rubber stopper was replaced with a similar one containing a bubbler stone and an outlet tube, which was inserted into the suspended sample.

66. With continuous stirring to maintain the sediment particles in suspension, the evolved hydrogen sulfide gas was forced with a carbon dioxide carrier into two collection vessels, connected in series, containing dilute zinc acetate solution. The evolved hydrogen sulfide gas reacted with zinc acetate solution to form a white precipitate of zinc sulfide. After 1 hr, the contents of the two collection vessels were quantitatively transferred to a large flask. A solution of 0.025 N iodine solution was added in excess of the amount needed to react with the precipitated sulfide.

67. After acidifying the solution with HCl, the excess iodine was back titrated with standardized sodium thiosulfate solution using starch as an indicator. At the end point, the amount of thiosulfate added is equivalent to the amount of excess iodine in solution, and the quantity of iodine required

to react with the sulfide can be found by difference. Chemical yield of the system was checked by direct titration of an aliquot of zinc sulfide solution. It was found to be greater than 98 percent. Precision and chemical yield were monitored by running standards of dilute sodium sulfide solution after every 10 samples. The precision of the method was found to be better than ± 10 percent in terms of relative standard deviation for three replicate analyses on standards. Sulfides were determined on samples from the dredge spoil site only.

Percent water

68. The mass percent water of each core section was determined gravimetrically by drying at 70°C until the weight was constant.

Clay-fraction mineralogy

69. All top core sections were chosen for clay mineralogical analysis. In addition, the subsurface samples at stations A, D, and F were also analyzed to study possible diagenetic clay mineral transformation with increasing depth of sediment burial. Following grain-size analysis of these samples, the clay fraction (finer than 2 μm) was collected for x-ray diffraction analysis.

70. Gibbs[51] showed that of all the commonly used methods of preparing oriented mounts for quantitative clay mineral studies, only three were acceptable with regard to accuracy and precision. These three are smear-on-glass slide, suction-on-ceramic-plate, and powder-press techniques. This study used the suction-on-ceramic-plate method discussed by Carlton.[52] Porous unglazed ceramic tiles were purchased from Coors Porcelain Co., Golden, Colorado. The ceramic tile holder was similar in design to that described by Carlton.[52]

71. An aliquot of clay suspension was poured on the porous tile and the assembly fitted to a vacuum pump. The short time required for complete suction (5-10 min) did not

allow preferential settling of the clay particles according to their size. X-ray diffractograms were obtained from the oriented mounts of clay-size fraction treated in the following manner: (1) untreated and (2) solvated overnight in a dessicator with ethylene glycol vapour at 60°C.

72. The samples were run on a Picker diffractometer using Cu $k_\alpha$ radiation at 40 kV and 20 mA. A monochromator set was used to screen out the K-beta radiation. The untreated samples were scanned from 2° to 30°2θ also at fast scan conditions. Glycolated samples were scanned from 2° to 13° 2θ also at fast scan conditions. In order to resolve the (004) chlorite and (002) kaolinite doublet at 3.5 Å, the samples were scanned from 25.5° to 24.0°2θ at slow scan speed.

FAST SCAN CONDITIONS 2°2θ - 30°2θ
Scan Speed 1°2θ/min
Chart Speed 1"/min
Slit Width 0.02 mm
Diff. Time constant 2 μ sec
Range $1x10^3$ counts per second
Analyzer Baseline 1.31 V
Window 1.72 V

SLOW SCAN CONDITIONS 25.5°2θ - 24.0°2θ
Scan Speed 0.25°2θ/min
Chart Speed 1"/min
Slit Width 0.01 mm
Diff. Time constant 2 μ sec
Range $1x10^3$ counts per second
Analyzer Baseline 1.31 V
Window 1.72 V

73. Illite was identified by a strong 10 Å and a weak 5 Å reflection. Fe-chlorite was identified by weak first-(14 Å) and third-(4.7 Å) order basal reflections and strong second-(7 Å) and fourth-(3.5Å) order reflections.[53] Chlorite reflections were unaffected by glycolation. Glycolation of

the samples resulted in the appearance of a weak peak in the 17 Å region indicating the presence of montmorillonite. Presence of a 3.58 Å reflection on the slow scan diffractogram showed that kaolinite was present.[54] Minor amounts of quartz and feldspar were also detected in the clay fraction.

74. Quantitative estimates of clay mineral abundances were determined by measuring the peak areas of the 7 Å (chlorite + kaolinite), 10 Å (illite), and 17 Å (montmorillonite) reflections on the diffractogram of a glycolated sample. The abundance of each mineral was expressed with respect to the total mineral composition. The weighting factors used were 17 Å glycolated peak for montmorillonite, four times the 10 Å glycolated peak for illite, and twice the 7 Å glycolated peak for chlorite and kaolinite (Biscaye[54]). The Å peak, common to both kaolinite and chlorite, was divided between the two in proportion to the fraction of each mineral in the total area under the resolved 3.5 Å kaolinite-chlorite doublet on the slow scan diffractogram. The four weighted peak areas were added, and the weighted peak area of each mineral multiplied by 100 and divided by the sum of the areas to give the percentage of each mineral.

Bulk mineralogy

75. Ten cores were selected and their top 10-cm sections analyzed for bulk mineralogy. The subsamples were oven-dried and ground to a uniform fine powder in a ball mill. The interstitial salt was removed by mixing about 2 g of sample with 20 ml of distilled water in an Erlenmeyer flask, homogenizing the sample for 30 min on an automatic shaker, then centrifuging off the water.[55] Mineralogical analyses of bulk samples were performed by x-ray diffraction employing the same instrument settings described for clay mineral analysis, but using random mounts of the dry powders and scanning from 1° to

60°2θ at 2°2θ/min. The random mounts were prepared according to the method described by Carroll.[53] The following minerals were identified: quartz with all characteristic reflections from 4.26 Å (100) to 1.54 Å (211); orthoclase with major reflections at 3.79 Å (130), 3.28 Å (202), and 3.22 Å (002); plagioclase with reflections at 4.03 Å (201) and 3.20 Å (002); the (110) reflection of amphibole at 8.4 Å; (001) muscovite reflections at 10.0 Å, 4.99 Å, and 1.99 Å and (hkl) reflections at 4.49 Å, 2.98 Å, and 2.56 Å; chlorite (001) reflections at 14.2 Å, 7.1 Å, 4.75 Å, 3.56 Å,and 2.85 Å, and (hkl) reflection at 2.53 Å; and other clay minerals that have been previously described. Bulk samples are composed principally of quartz and feldspar with only minor amounts of amphiboles and clay minerals.

Trace metal analysis of bulk samples

76. A sample of 2.5 g of oven-dried, finely-ground bulk sediment was weighed in an acid-cleaned 4-oz polyethylene bottle. The sample was digested in 10 ml of concentrated nitric acid on a sand bath at 80°C for 2 hr. The warm sample was filtered using Millipore filtration apparatus and the sediment residue was washed three times with 10-ml aliquots of distilled water. The filtrate and wash solution were collected in a 50-ml volumetric flask and the total volume was brought to 50 ml with distilled water. The resulting solution was analyzed for Cd, Zn, Pb, Cu, Fe, Mn, and Ni by atomic absorption spectrophotometry. The method of analysis for Hg is discussed in Appendix A'. Also given in Appendix A' are the analytical precision, detection limit, and sensitivity for each metal.

Total cation exchange capacity

77. Total cation exchange capacity (TCEC) is expressed as the sum of major exchangeable cations ($Na^+ + K^+ + Mg^{2+} + Ca^{2+}$) in meq per 100 g of dry sediment. Determination of exchangeable cations was accomplished by replacing $Na^+$, $K^+$, $Ca^{2+}$, and $Mg^{2+}$ with $NH_4^+$. A subsample of 0.5 g of oven-dried sediment was placed on a 0.45-µm filter. The sample was then leached with three 10-ml aliquots of neutral 1 M ammonium acetate solution followed by two 10-ml washings with neutral distilled water. The leachate was diluted to 50 ml and analyzed for $Na^+$, $K^+$, $Ca^{2+}$, and $Mg^{2+}$ by atomic emission techniques. No suction was applied during filtration to ensure long leaching times and complete replacement of exchangeable cations. Leaching times were usually greater than 10 ml/hr, depending upon the grain size of the sample. The precision of the method was found to be better than ± 10 percent for four determinations.

Oil and grease

78. Oil and grease were determined using a simplified ether extraction method.[56] Approximately 10 g of oven-dried, finely-ground sediment subsample was weighed into a 125-ml screw-top flask. Ten ml of ethyl ether was added to the sample and the flask allowed to shake for 18 to 20 hr on a shaker table. The extracted hydrocarbons were collected in a preweighed aluminum dish. The sediment residue was rinsed several times with small aliquots of ethyl ether and the wash solution collected in the same aluminum dish. The extracted solution collected in the same aluminum dish was allowed to evaporate to dryness overnight and the aluminum dish containing the residue was reweighed. The difference between the initial and the final weights of the dish correspond to the amount of oil and grease present in the sediment sample. In order to

obtain some information on the precision of the method, three subsamples were taken from a homogenized core section and analyzed for the oil and grease content under identical experimental conditions. The precision of the method for three analyses was found to be 5.7 percent, in terms of relative standard deviation.

## PART III: RESULTS AND DISCUSSION

### Water Column Properties

#### Precision and sampling variability

79. Variation in replicates. Replicate samples (repeated sampling at depth) were collected as quickly as possible at a limited number of stations on each cruise. Different sets of replicates were used to compare the variability in our analytical procedures. The analysis of the replicate samples for the water constituents listed in Table 4 were used to compute an estimate of the measurements' variability; the estimate chosen was the coefficient of variation (CV). The results obtained from $n_r$ replicate samples (column 1, Table B4) were used to calculate the coefficient of variation ($CV_i$) and the standard error of coefficient of variation ($Scv_i$) for each set of $n_s$ sets (column 2) of replicates. These $CV_i$ and $Scv_i$ were then averaged ($\overline{CV}$, column 3 and $\overline{Scv}$, column 4).

80. The mean coefficient of variation ranged from a low of 4.1 percent for dissolved $PO_4^{3-}$ concentration up to 42.6 percent for urea concentration.

81. Analysis of variance. In addition to determining a replicate sample variability, based on the CV of the variables measured, a nested analysis of variance (anova) was calculated for each variable where sufficient replicate data exist. The objective of this analysis was to determine whether the observed sample differences were due to sampling at different depths, stations, or cruises, or whether sample differences were attributable to variation introduced from sample collecting methods and lab analyses.

82. Table 5 shows the data for a nested anova testing variances among stations and depths against the error variance estimated from replicate samples. The probability, P, that

TABLE 4

Replicate Sample Variability

| Variable | (1) | (2) | (3) | (4) |
|---|---|---|---|---|
| Particulate Constituents | $n_r$* | $n_s$** | $\overline{CV}$† % | $\overline{Scv}$†† |
| Suspended Solids | 5 | 3 | 10 | 3 |
| Total - P | 5 | 17 | 9.8 | 1.8 |
| Particulate - C | 3 | 9 | 32.2 | 5 |
| Particulate - N | 3 | 9 | 23.4 | 3.7 |
| Chlorophyll a | 3 | 31 | 5.5 | 0.7 |
| Dissolved Constituents | | | | |
| $NH_4^+$ | 5 | 13 | 26.1 | 7.2 |
| $NO_2^-$ | 5 | 12 | 22.8 | 6.6 |
| $NO_3^-$ | 5 | 13 | 6.5 | 1.2 |
| $PO_4^{3-}$ | 5 | 13 | 4.1 | 0.7 |
| $Si(OH)_4$ | 5 | 13 | 9.0 | 1.9 |
| Urea | 5 | 6 | 42.6 | 4.8 |
| TOC | 3 | 8 | 23.2 | 1.8 |

* $n_r$ = number of replicate samples per set.

** $n_s$ = number of sets containing $n_r$ samples each.

† $\overline{CV}$ mean coefficient of variation $(s/\bar{x})100$, computed from $CV_i$'s[57] calculated for each of $n_s$ sets

$$\overline{CV} = \sum_{i=1}^{n_s} (CV)_i / n_s$$

†† $\overline{Scv} = \frac{\Sigma Scv_i}{n_s}$ where $Scv_i$ is calculated for each $CV_i$ of the $n_s$ sets.

TABLE 5

Analysis of Variance (Nested Anova) --

Comparison of variances among subsamples, depths, and stations

| VARIABLE | SUBSAMPLE | | AMONG DEPTHS | | | AMONG STATIONS | | |
|---|---|---|---|---|---|---|---|---|
| | Degrees of Freedom | Mean Square | Degrees of Freedom | Mean Square | P | Degrees of Freedom | Mean Square | P |
| $NH_4^+$ | 24 | .0807 | 3 | .0607 | ns | 2 | .2410 | ns |
| $NO_3^-$ | 24 | .3599 | 3 | 2.418 | <.01 | 2 | 9.9845 | ns |
| $NO_2^-$ | 24 | .0099 | 3 | .0123 | ns | 2 | .3306 | <.05 |
| $PO_4^{3-}$ | 24 | .0036 | 3 | .0024 | ns | 2 | .1236 | <.05 |
| Total P | 24 | .0472 | 3 | .1600 | <.05 | 2 | .1432 | ns |
| $Si(OH)_4$ | 24 | .0228 | 3 | 9.444 | <.001 | 2 | 1.857 | ns |
| Chlorophyll a | 32 | .0091 | 16 | .7244 | <.001 | 15 | 8.7744 | <.001 |
| Suspended Solids | 30 | .1269 | 20 | 4.814 | <.001 | 9 | 111.2 | <.001 |
| Particulate Carbon | 16 | 3028 | - | - | - | 3 | 126308 | <.001 |
| Particulate Nitrogen | 16 | 90.75 | - | - | - | 3 | 1736 | <.001 |

all the values are actually from the same population for a particular variable is indicated in the table. An entry of ns indicates a nonsignificant difference between the variance due to depths or stations and the error variance.

83. Except for $NH_4^+$, all variables tested show significant variation due to either depths, stations, or both. The $NH_4^+$ data from ACE V (19-20 March) show that the $NH_4^+$ concentrations were uniformly low throughout the study area and sample variability due to depth or station could not be distinguished. Table 6 shows the data for an additional nested anova testing differences among stations and cruises for variables where sufficient replicate data exist. All variables tested show significant variation due to stations, cruises, or both.

Variability over a tidal cycle

84. ACE I. During ACE 1, a special experiment was conducted to determine the tidal variability of several water column variables (salinity, temperature, $NH_4^+$, $NO_2^-$, $NO_3^-$, dissolved $PO_4^{3-}$, total $PO_4^{3-}$, $Si(OH)_4$, particulate nitrogen, particulate carbon, and chlorophyll *a*) at a single station. Samples were collected eight times (about every 2-1/2 hr) over 1.5 tidal cycles (20-hr period) at station D during the 10-11 October cruise. The data taken at station D were a portion of a more complete study involving the sequential sampling of stations A, B, C, D, E, F, G, H, J, and K. All the data from the completed study are on file at WES on the data tape. Only results obtained from station D will be presented (Figures 8- 20) and discussed here.

85. At station D salinity (Figure 8) varied relatively little over the tidal cycle, especially at depth. Observed variations, especially at the surface, may be as much due to the sampling of randomly distributed salinity patches as to any tidally driven salinity fluctuations.

TABLE 6

Analysis of Variance (Nested Anova)--
Comparison of variances among subsamples, stations, and cruises

| VARIABLE | SUBSAMPLE | | AMONG STATIONS | | | AMONG CRUISES | | |
|---|---|---|---|---|---|---|---|---|
| | Degrees of Freedom | Mean Square | Degrees of Freedom | Mean Square | P | Degrees of Freedom | Mean Square | P |
| $NH_4^+$ | 48 | .1952 | 9 | 2.049 | <.01 | 2 | 34.23 | <.001 |
| $NO_3^-$ | 48 | .1176 | 9 | 3.612 | <.001 | 2 | 997.4 | <.001 |
| $NO_2^-$ | 48 | .0055 | 9 | .0725 | <.01 | 2 | .0996 | ns |
| Dissolved $PO_4^{3-}$ | 48 | .0037 | 9 | .0411 | <.001 | 2 | 5.242 | <.001 |
| Total P | 24 | .0394 | 9 | .1445 | <.05 | 2 | .5520 | ns |
| $Si(OH)_4$ | 48 | 3.331 | 9 | 6.309 | ns | 2 | 3751 | <.001 |
| Chlorophyll *a* | 30 | .7046 | 10 | 4.621 | <.001 | 4 | 332.8 | <.001 |

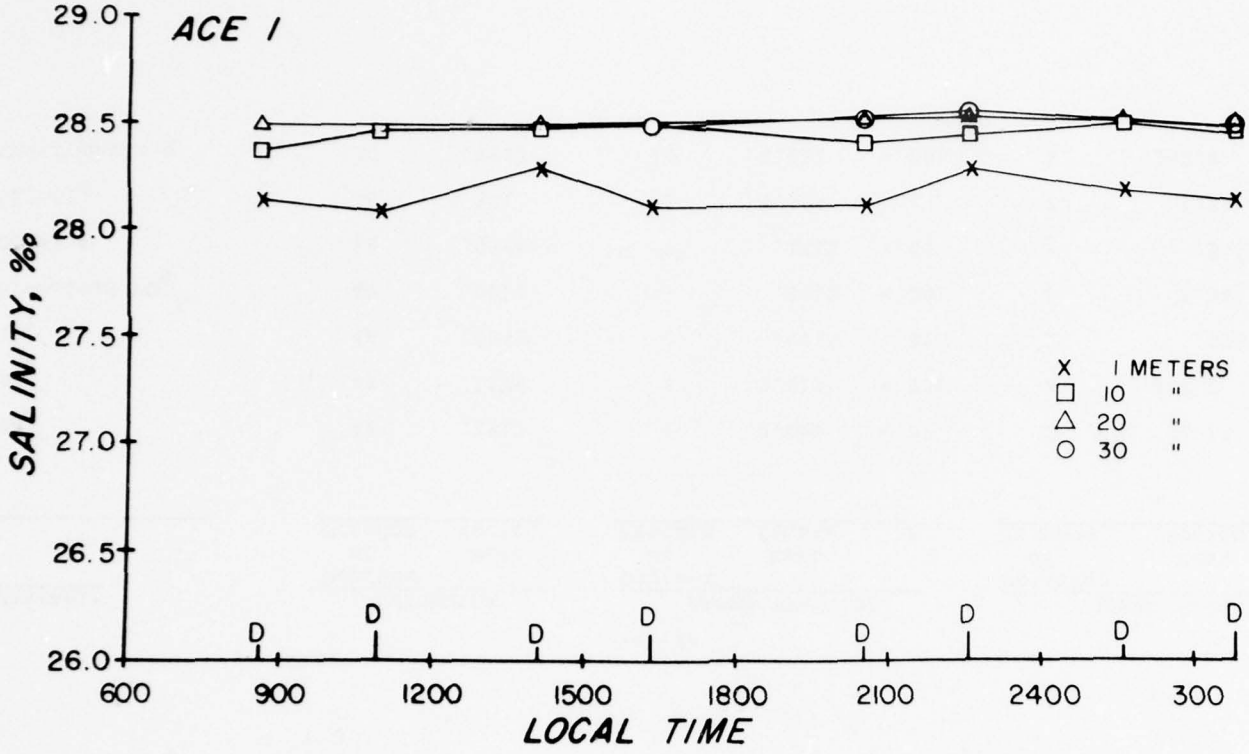



Figure 8. Tidal variation in salinity at station D.

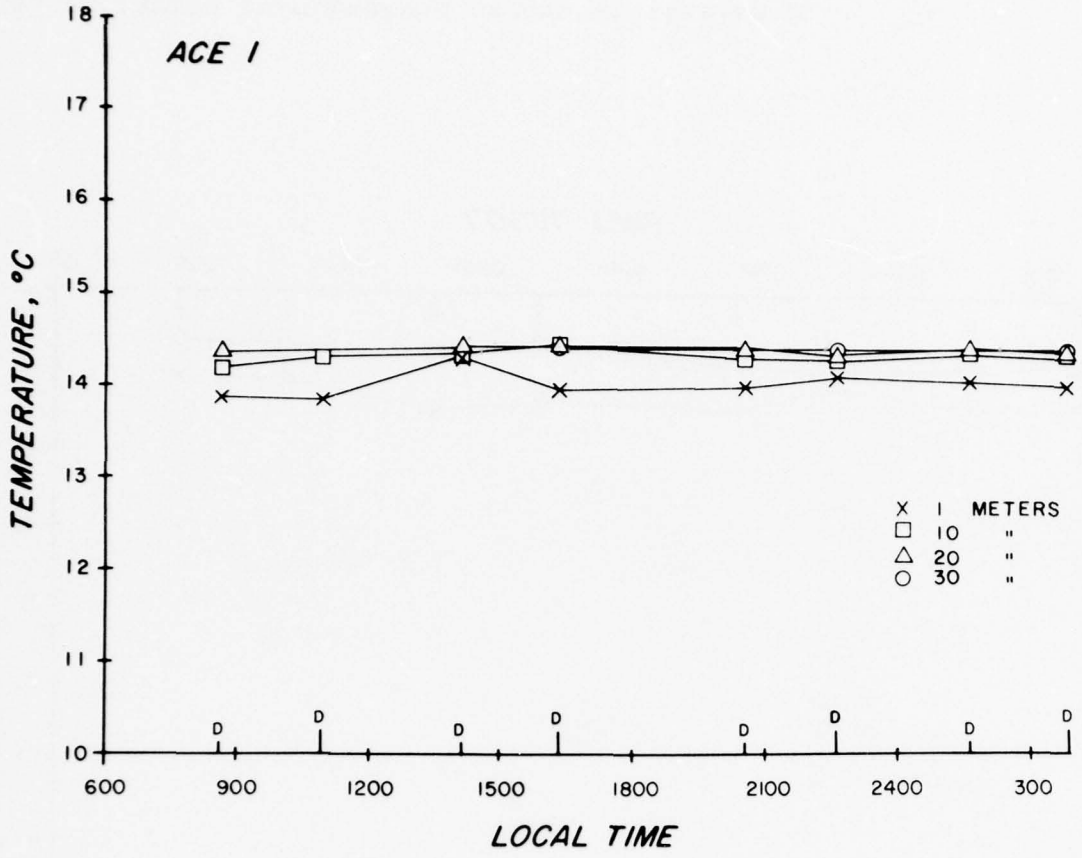



Figure 9. Tidal variation in temperature at station D.

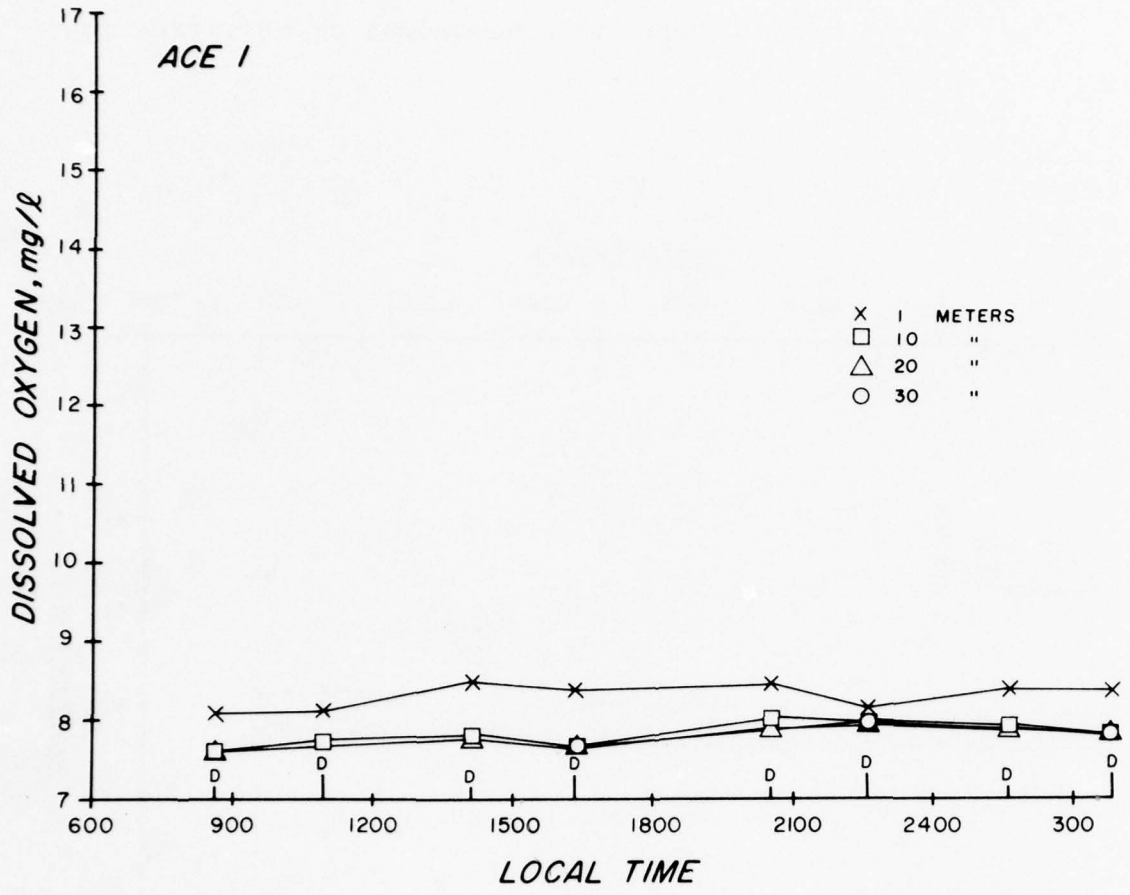



Figure 10. Tidal variation in dissolved oxygen at station D.

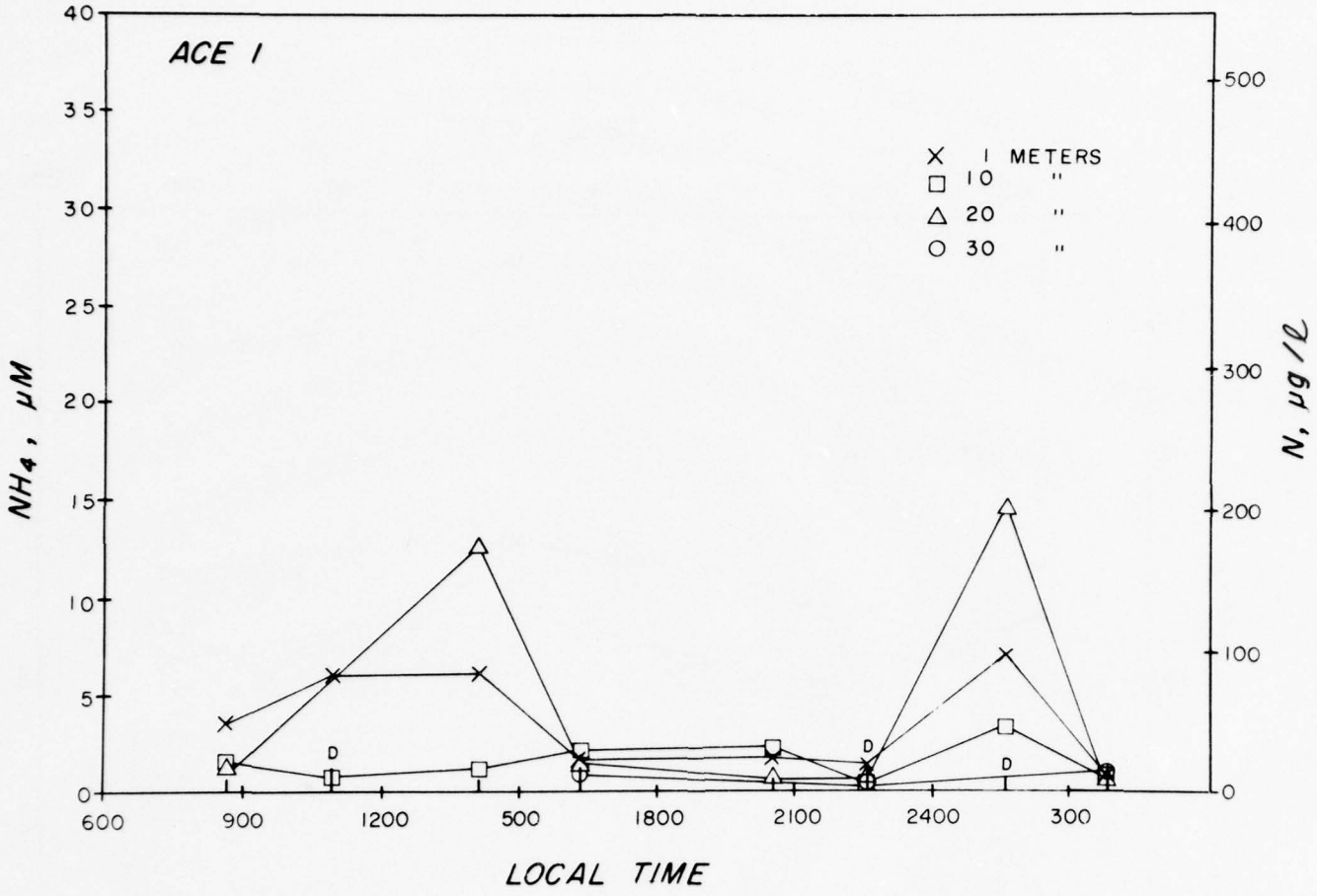



Figure 11. Tidal variation in ammonium concentration at station D.

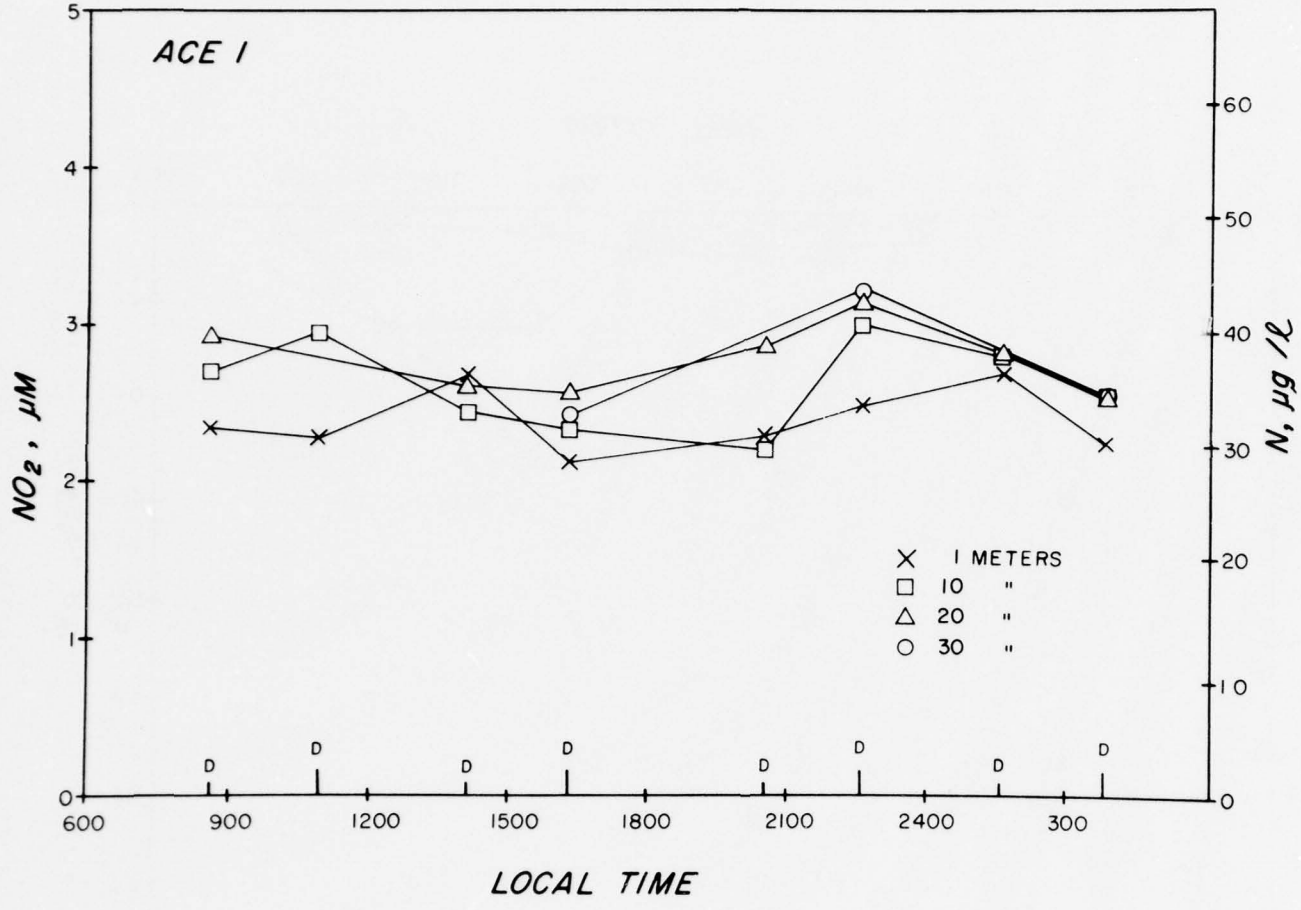



Figure 12. Tidal variation in nitrite concentration at station D.

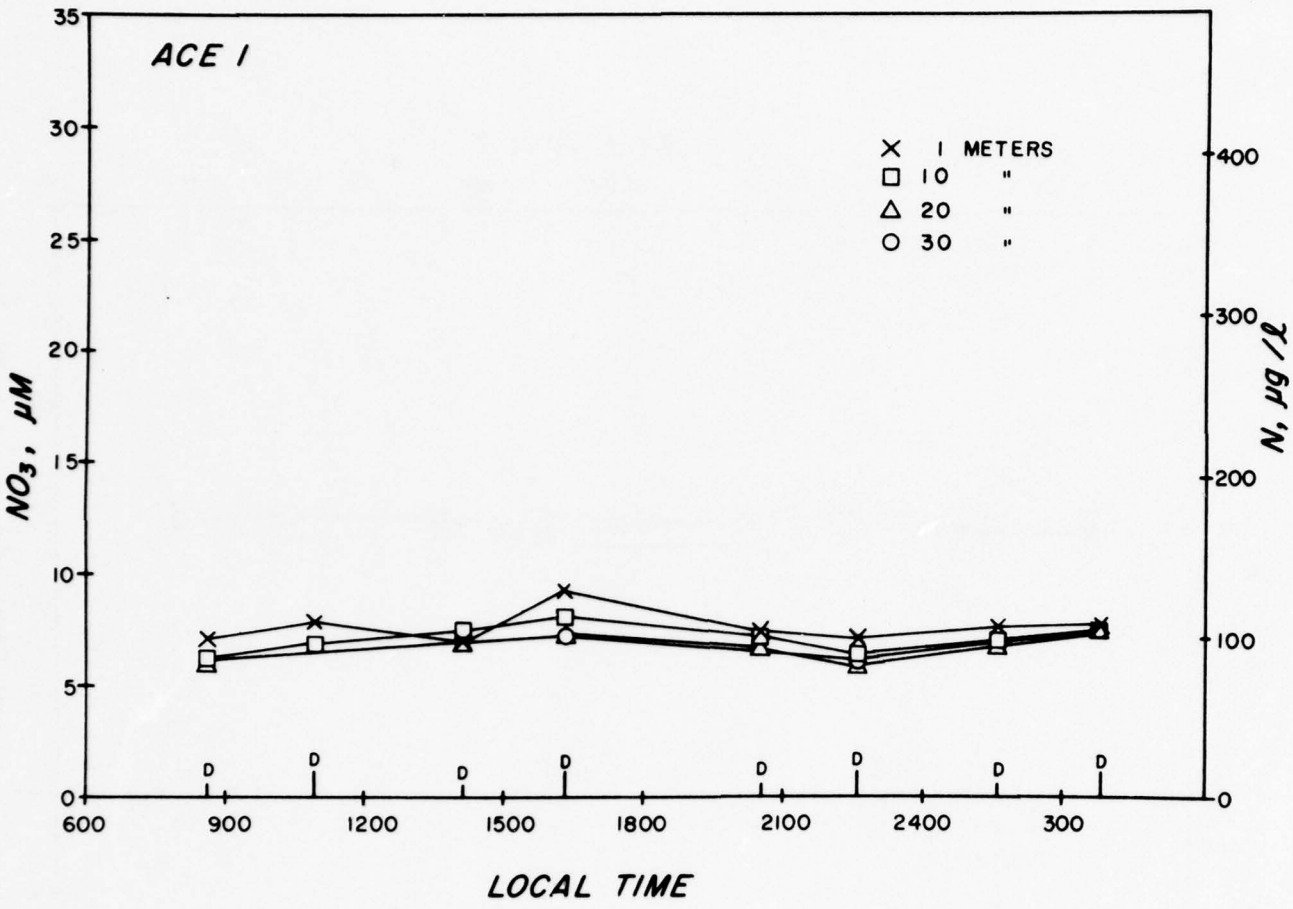



Figure 13. Tidal variation in nitrate concentration at station D.

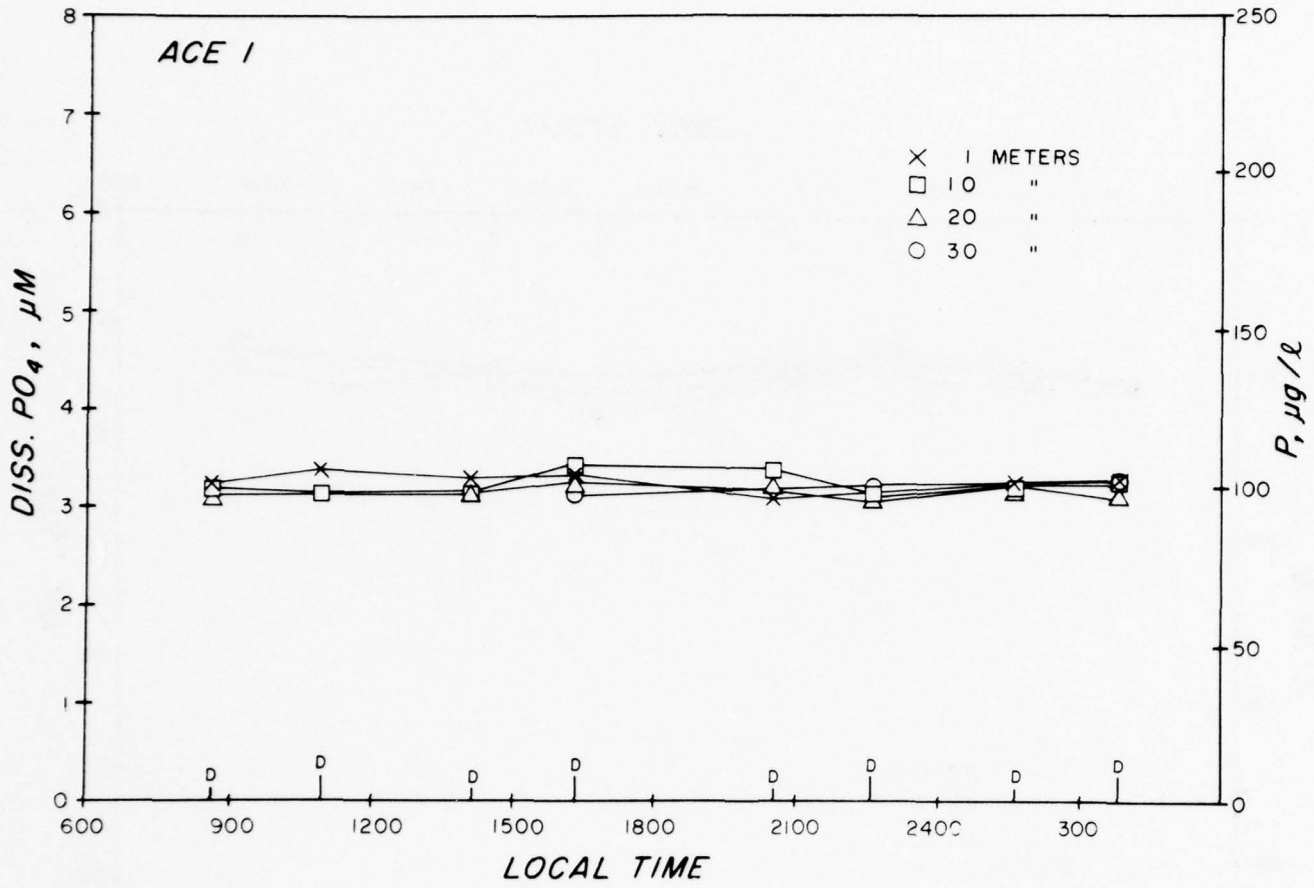



Figure 14. Tidal variation in dissolved $PO_4^{3-}$ concentration at station D.

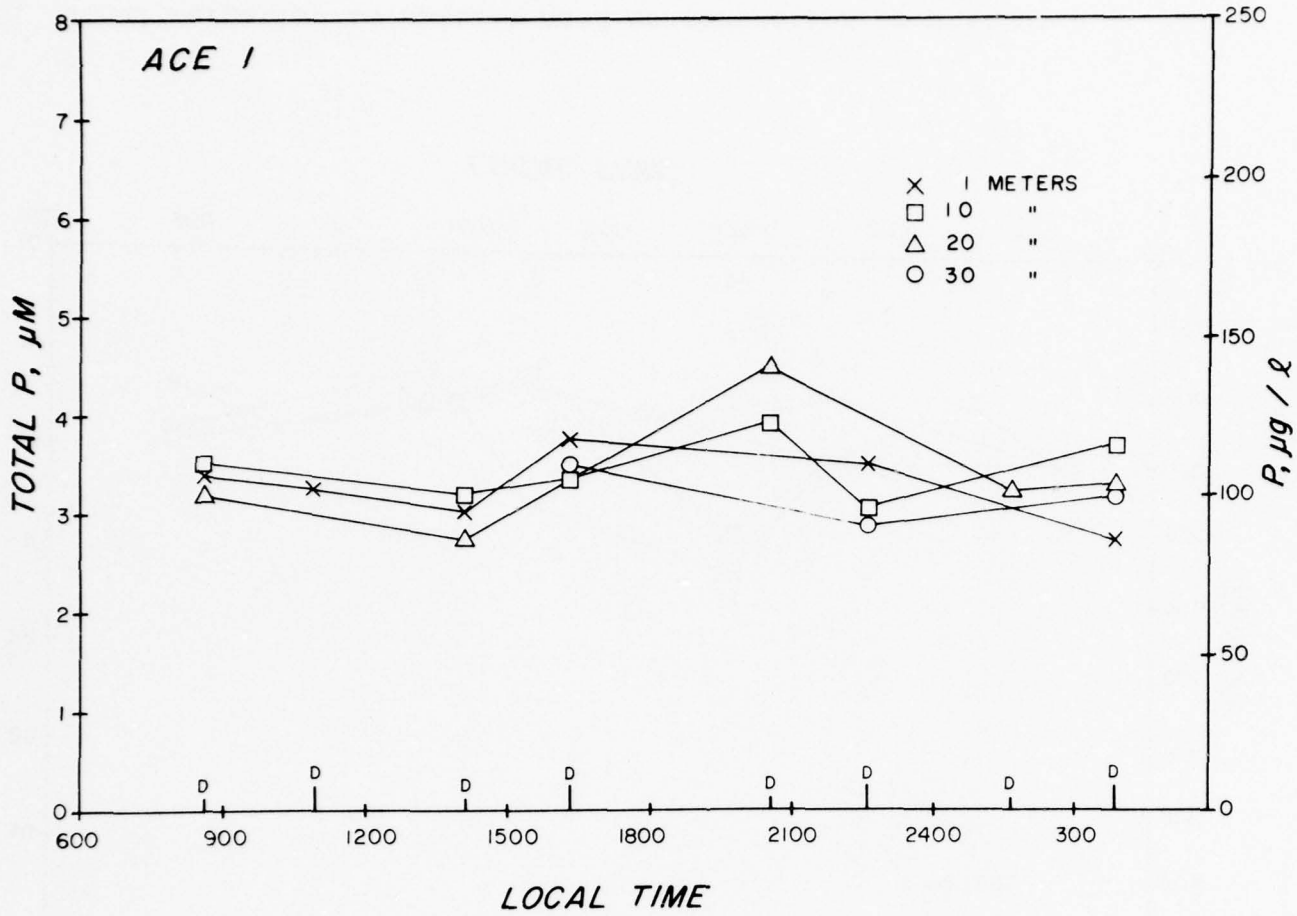



Figure 15. Tidal variation in total P concentration at station D.

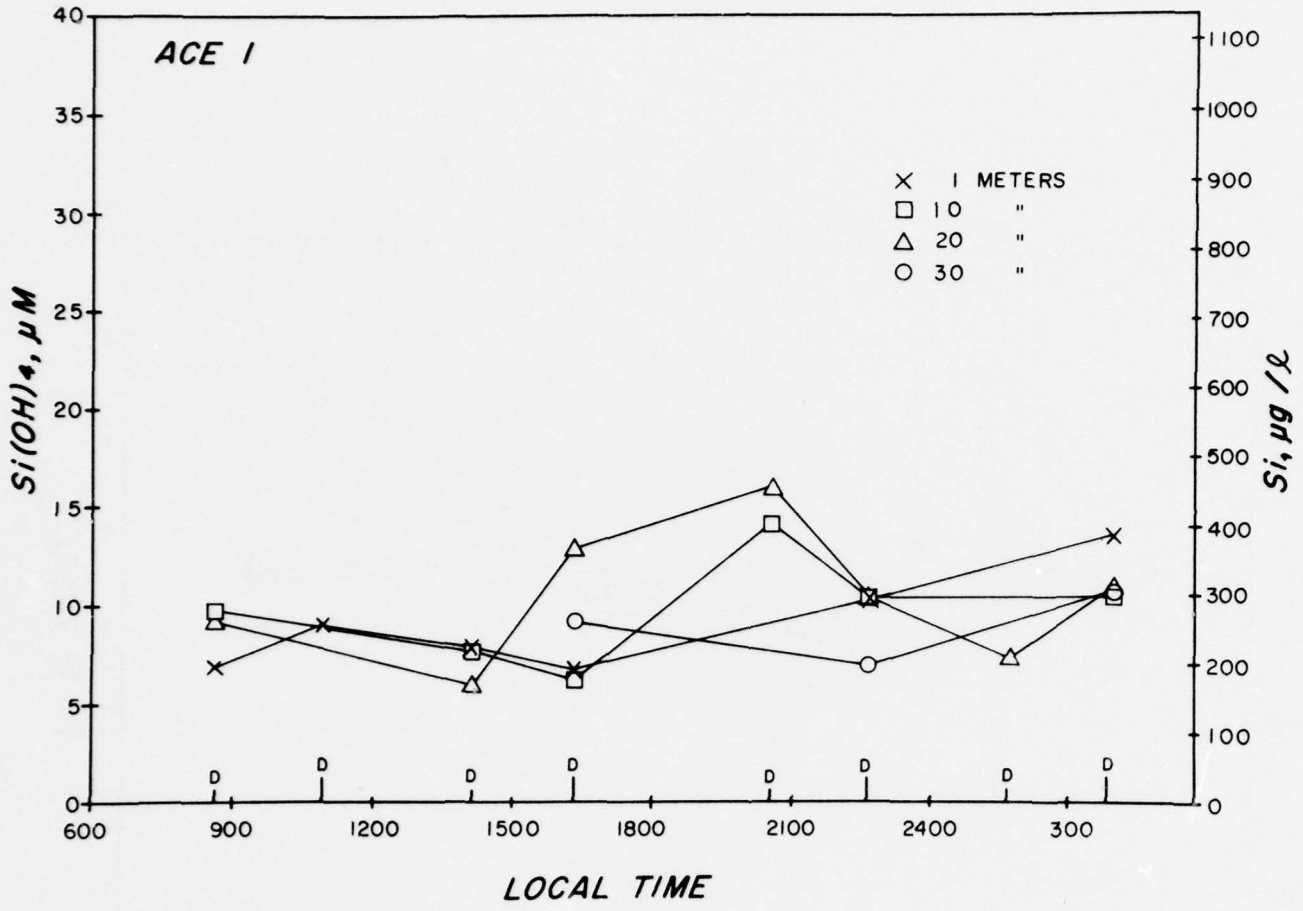



Figure 16. Tidal variation in silicic acid concentration at station D.

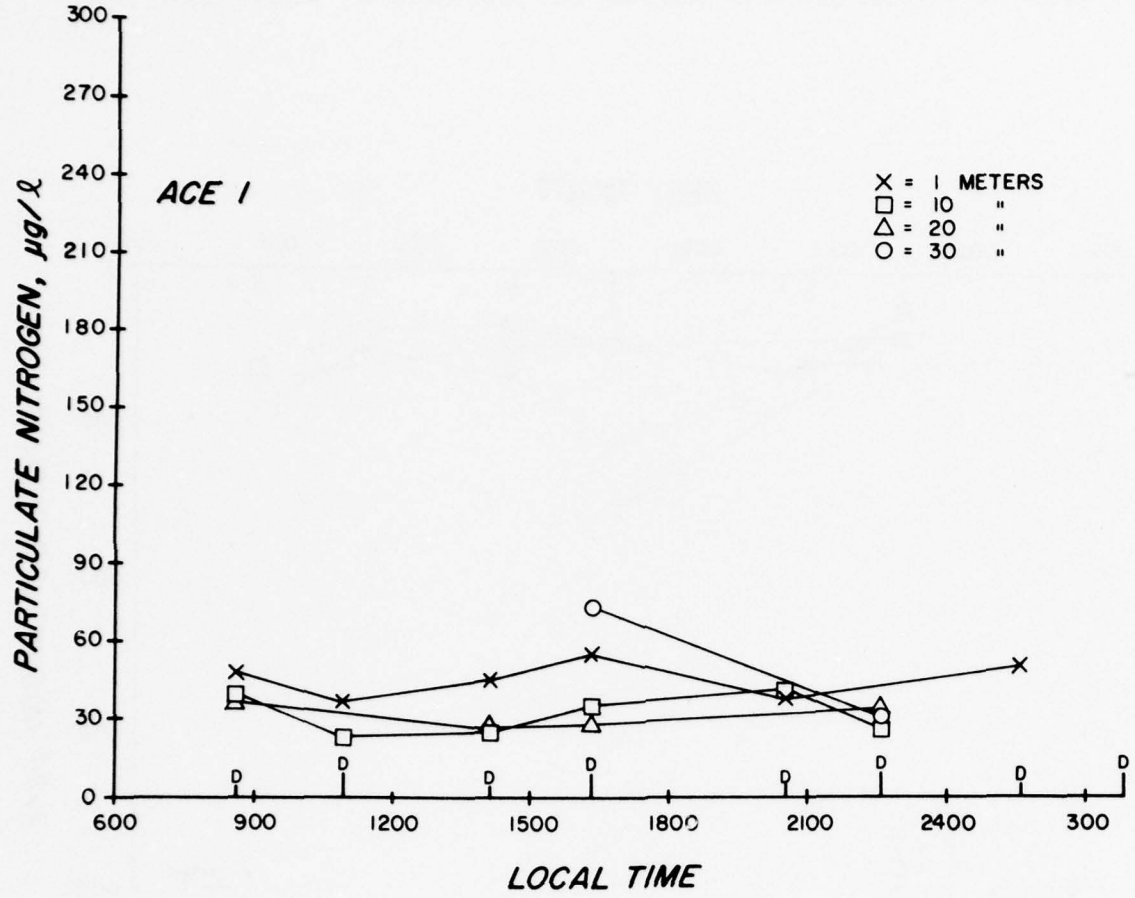



Figure 17. Tidal variation in particulate nitrogen concentration at station D.

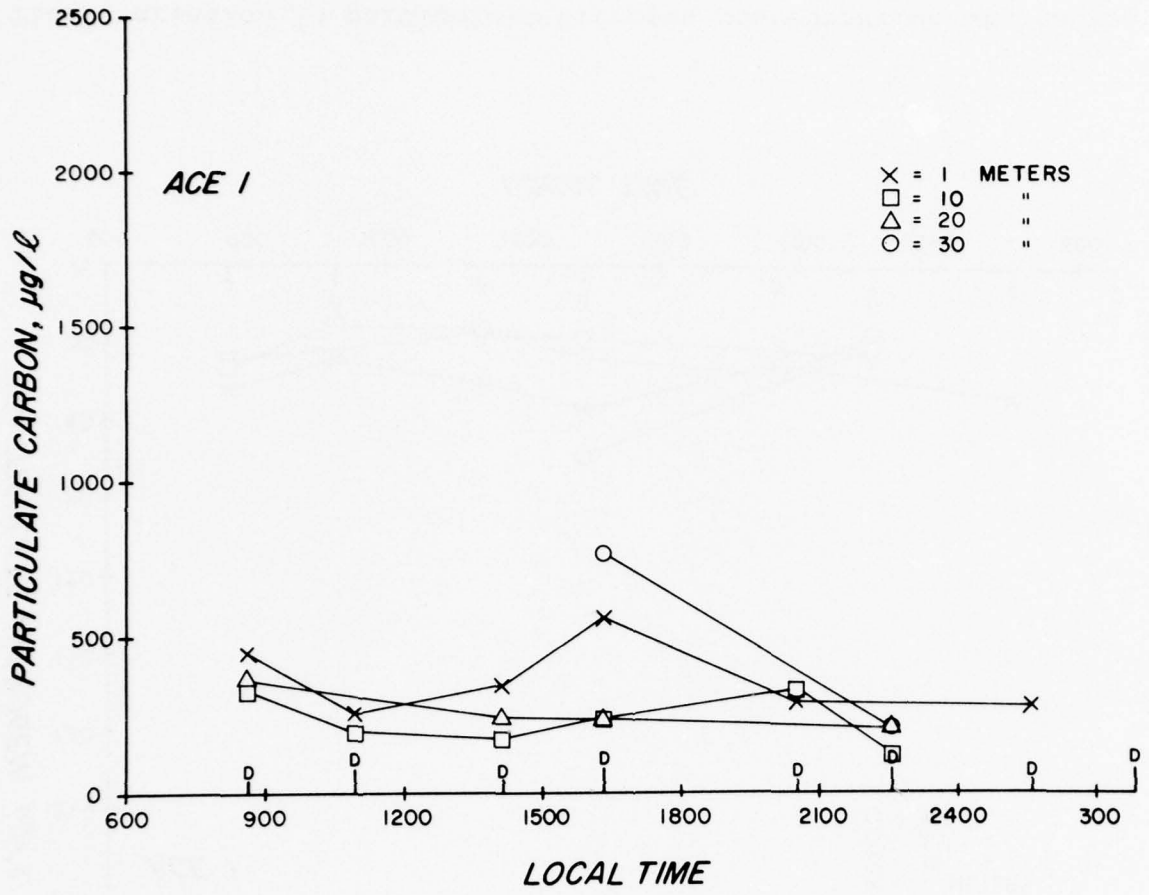



Figure 18. Tidal variation in particulate carbon concentration at station D.

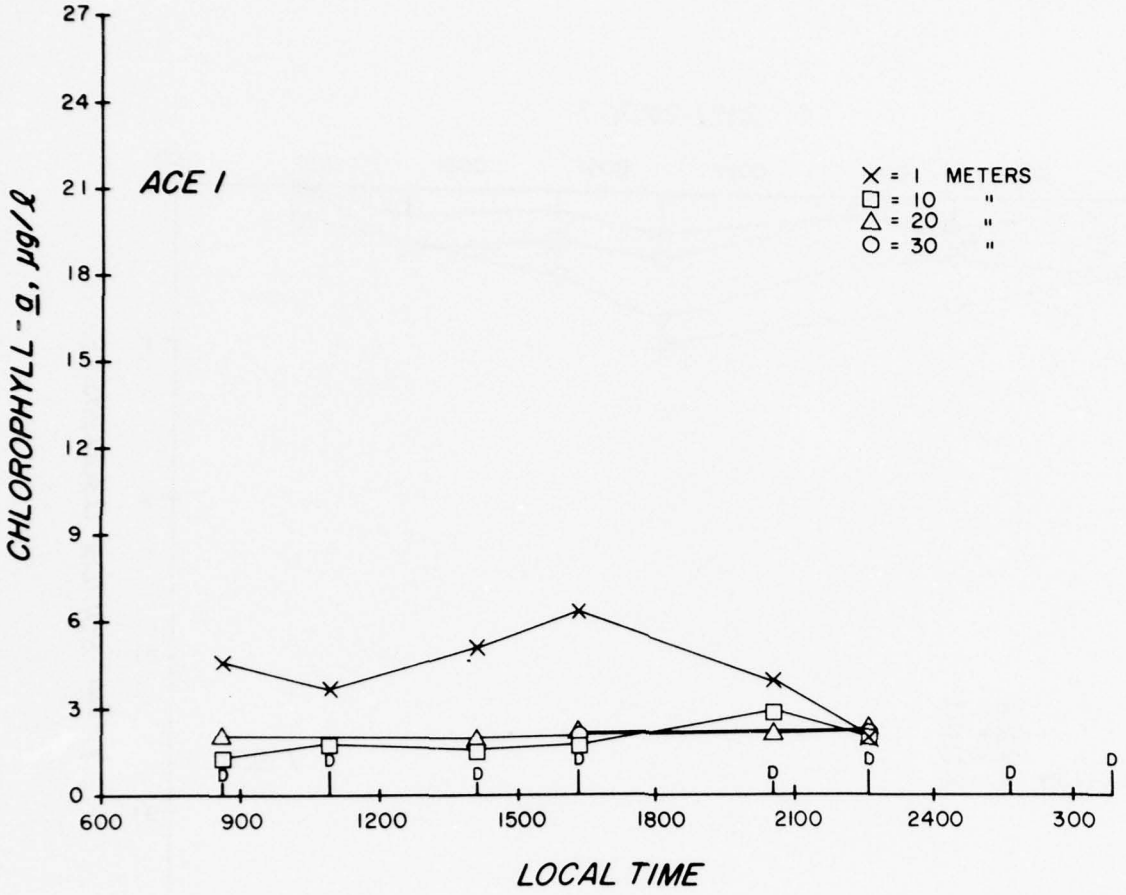



Figure 19. Tidal variation in chlorophyll a concentration at station D.

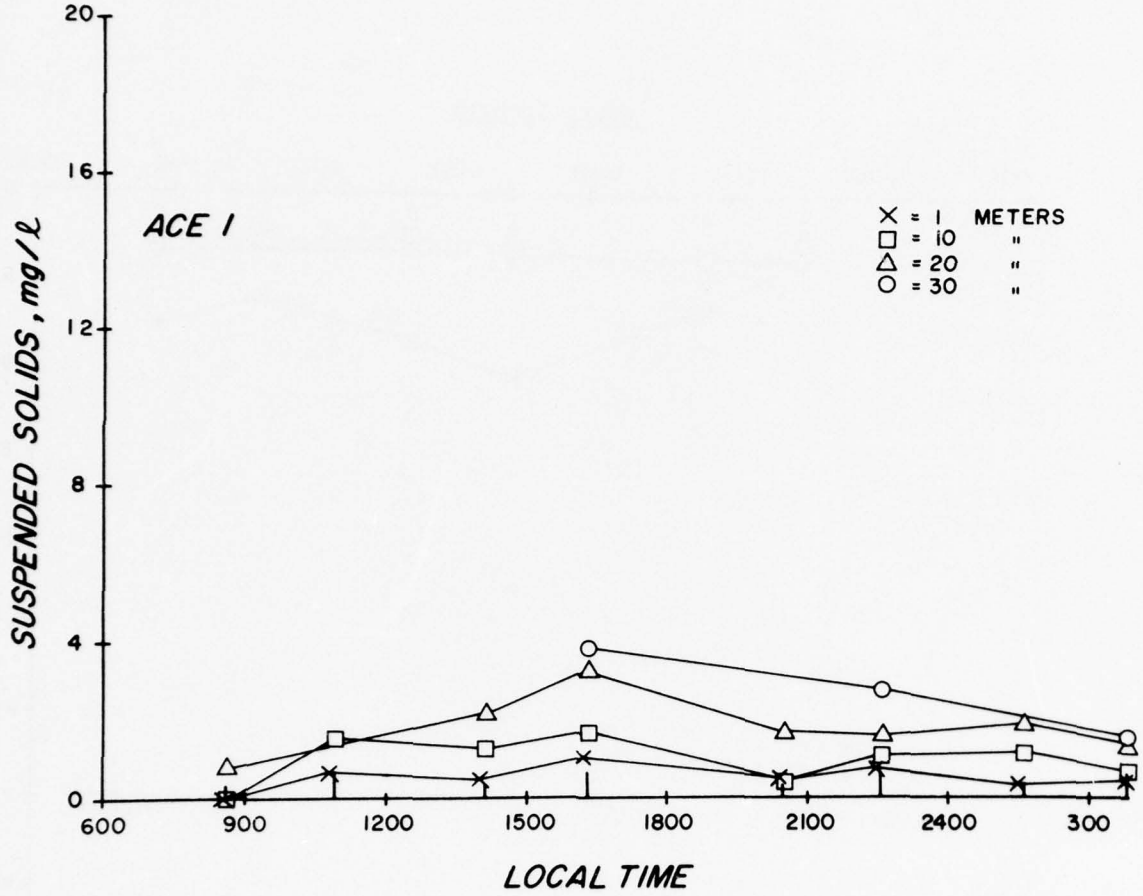



Figure 20. Tidal variation in suspended solids concentration at station D.

86. The water column was virtually isothermal (14-14.3°C) during this period and thus temperature (Figure 9) showed very little variation with tide. (Tide data were obtained from the Tidal Current Tables (National Ocean Survey, 1974) using the current differences reported for 0.5 mile north of Eatons Neck point.)

87. Dissolved oxygen (Figure 10) also varied little over the tidal cycle. As expected, highest concentrations were observed in the surface layer.

88. $NH_4^+$, $NO_2^-$, and $NO_3^-$ concentration values (Figures 11- 13) appeared highest during the ebbing portion of the tide. This pattern may be due to the influence of eutrophic waters from western Long Island Sound or from sewage-enriched harbors of Connecticut or Long Island. The high concentrations observed in Figure 11 was at the 20 m depth where one would not expect tidal variation.

89. Dissolved $PO_4^{3-}$ concentrations (Figure 14) at both stations were about 3 µM and varied relatively little over the sampling period. Total phosphorous concentrations were highest at slack after ebb (Figure 15).

90. $Si(OH)_4$ concentrations (Figure 16) showed some variability over the entire tidal cycle; especially at 20 m; the highest concentrations were observed at slack after ebb.

91. The highest concentrations of particulate nitrogen and particulate carbon (Figures 17 and 18) were observed at slack after ebb in the surface waters.

92. Surface chlorophyll *a* concentrations (Figure 19) were greatest on ebb tide. Subsurface concentrations were nearly constant over the tidal cycle.

93. Concentrations of suspended solids (Figure 20) were greatest in the bottom waters and at slack after flood.

94. ACE II-VII. Figures 21- 26 show the time variation in salinity at all stations for cruises ACE II thru VII (see Table 2). The plots illustrate the combined effects of tidal, spatial, and seasonal variability in salinity of similar plots for the other water properties, except for concentrations of dissolved and particulate metals for which we have insufficient data to demonstrate tidal variability, are given in Appendix B'.

95. When compared to Figure 8, one can see that most of the hourly and daily variability appears associated with where stations are located rather than tidal effects. For instance, Figure 21 shows the presence of a well-mixed water column during the 5-6 December cruise (ACE II). Lowest surface salinities were observed at stations K and L which were located near Huntington Bay and Norwalk Harbors, respectively, and thus are probably due to freshwater input either from sewage or river flow. The discharge of sewage[28] from the Huntington sewer district is 6,800 $m^3$/day. During the 13-14 January cruise period, when freshwater input was the greatest (Figure 27), low salinity water was distributed over a much wider area, as evidenced by the depressed salinities observed at stations Z, G, M, and L. Station Z is located more or less midway between Oyster Bay and Hempstead Harbor; stations G, M, and L are near the Connecticut shore and therefore surface salinities at these stations would be expected to be under the influence of the Norwalk and Saugatuck Rivers.[58,59]

96. For the sampling periods in March, April, and May, surface and 5 m salinity values were found to be consistently less than those observed at most of the other stations. The decreased surface, 5 and 9 m salinities observed during ACE IV at stations D, J, and, approximately 12 hours after station Z and S were sampled, K is probably more due to their nearness to Huntington Bay than due to tidal effects.

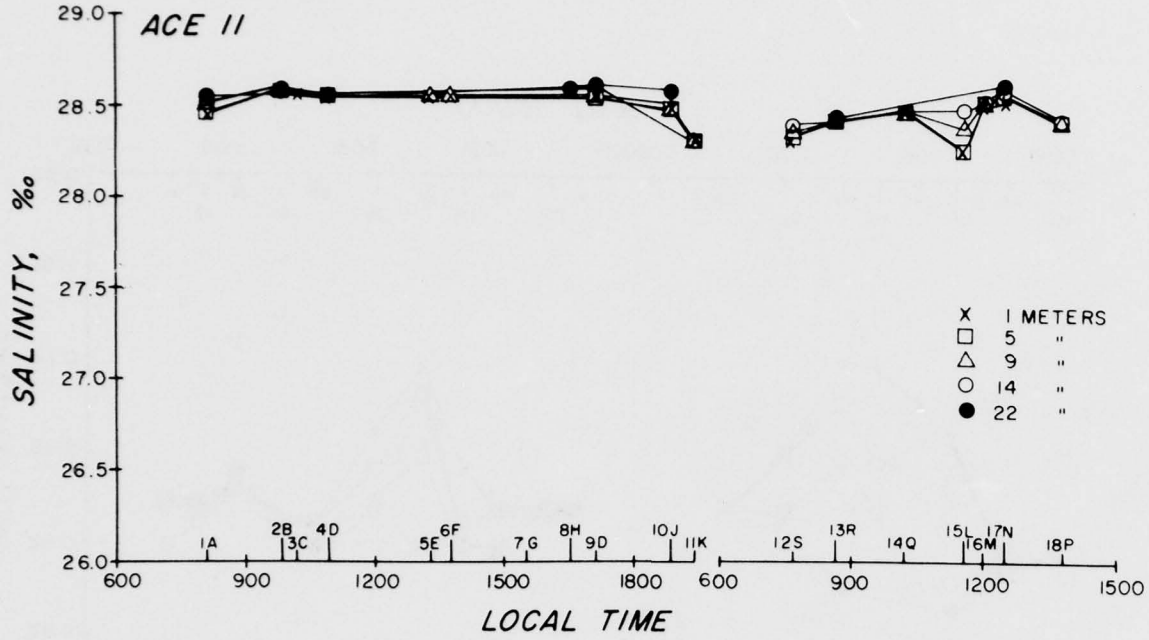



Figure 21. Salinity observations during ACE II.

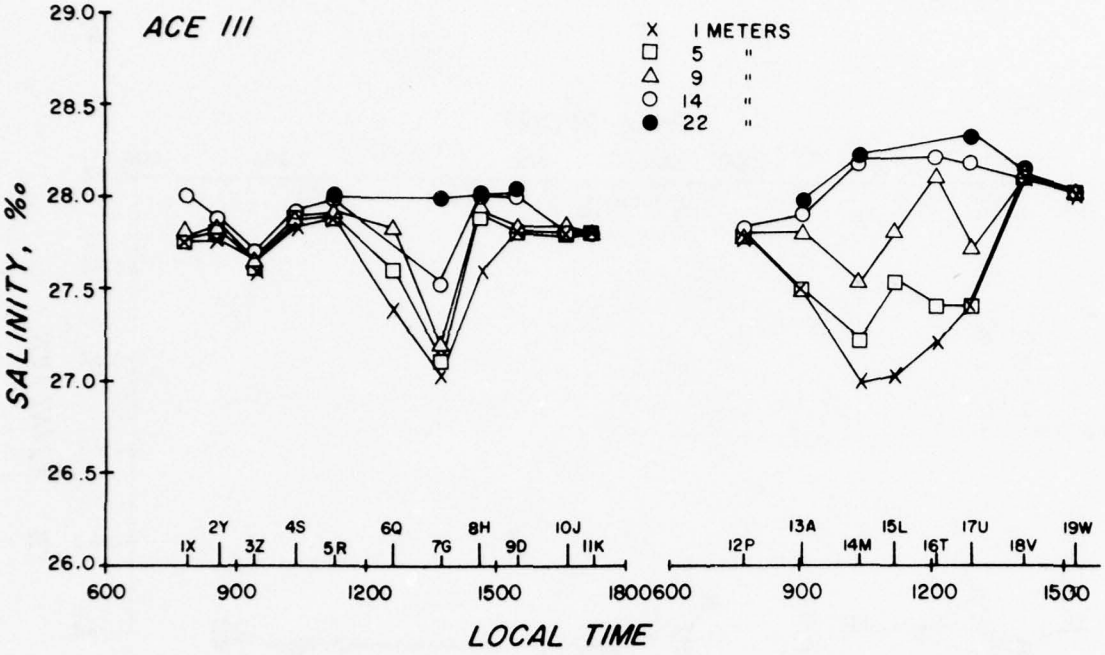



Figure 22. Salinity observations during ACE III.

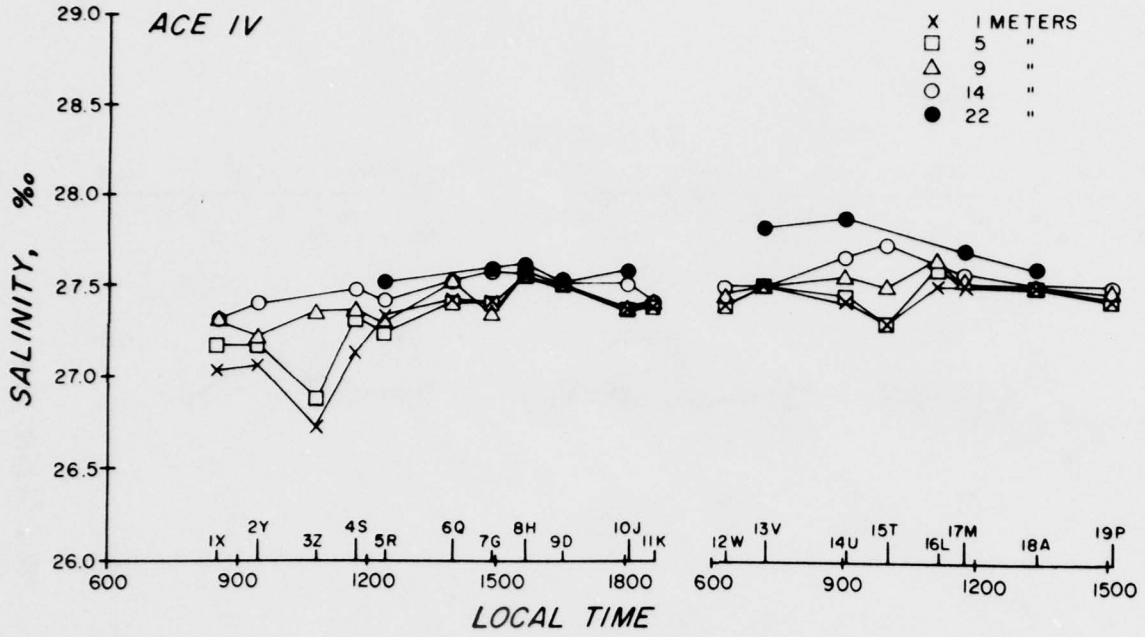



Figure 23. Salinity observations during ACE IV.

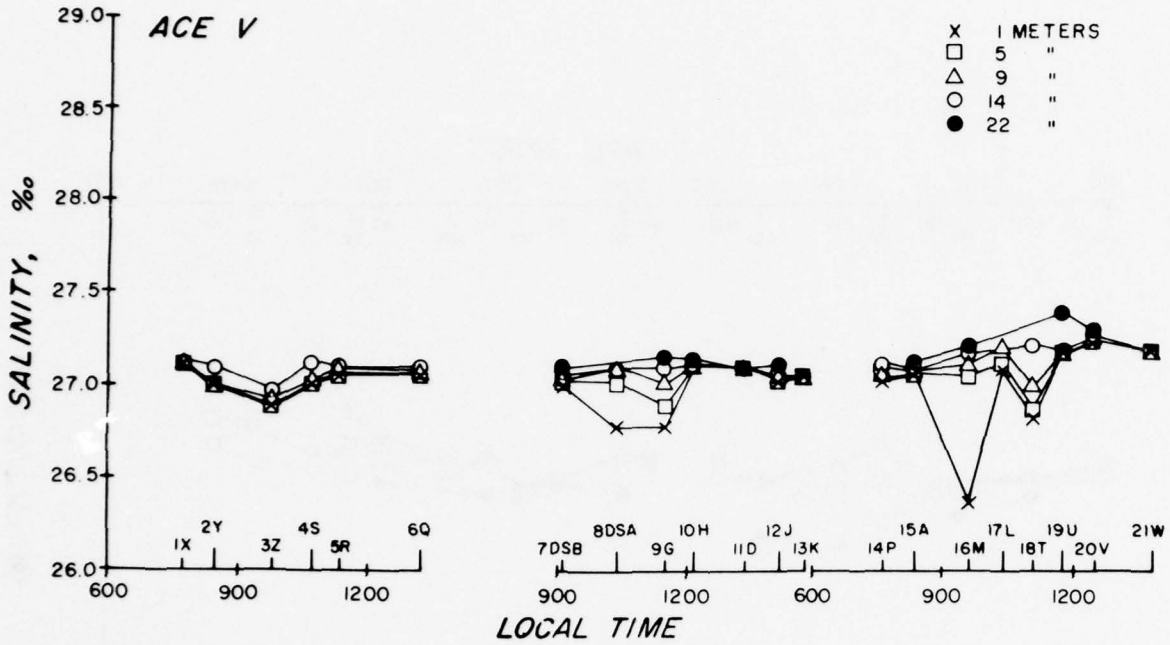



Figure 24. Salinity observations during ACE V.

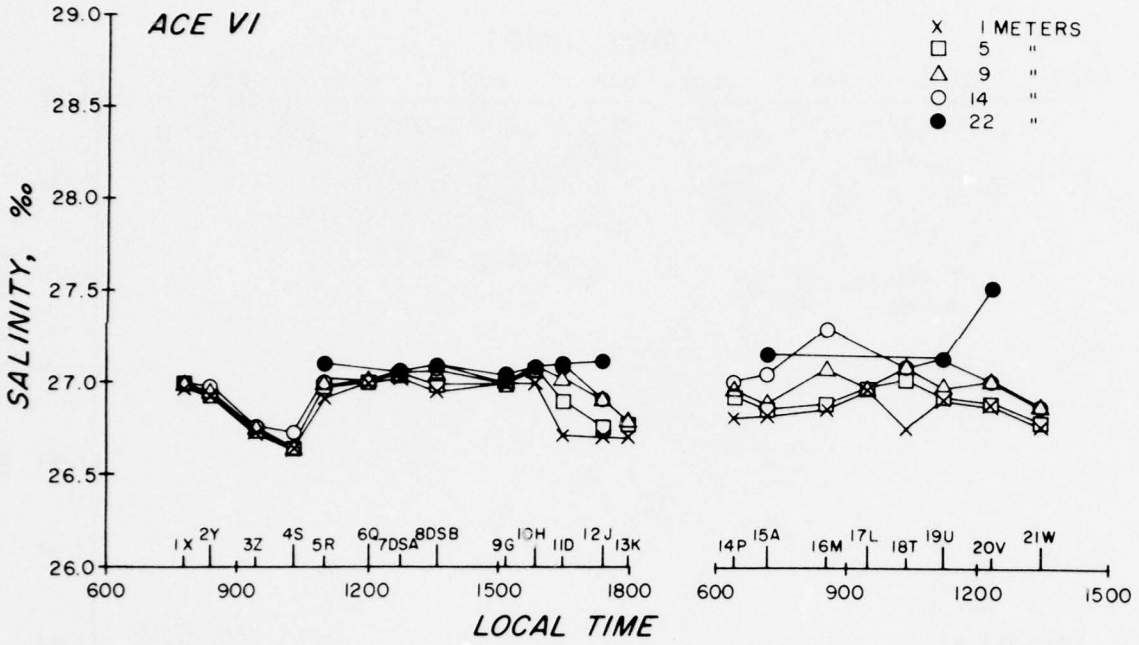



Figure 25. Salinity observations during ACE VI .

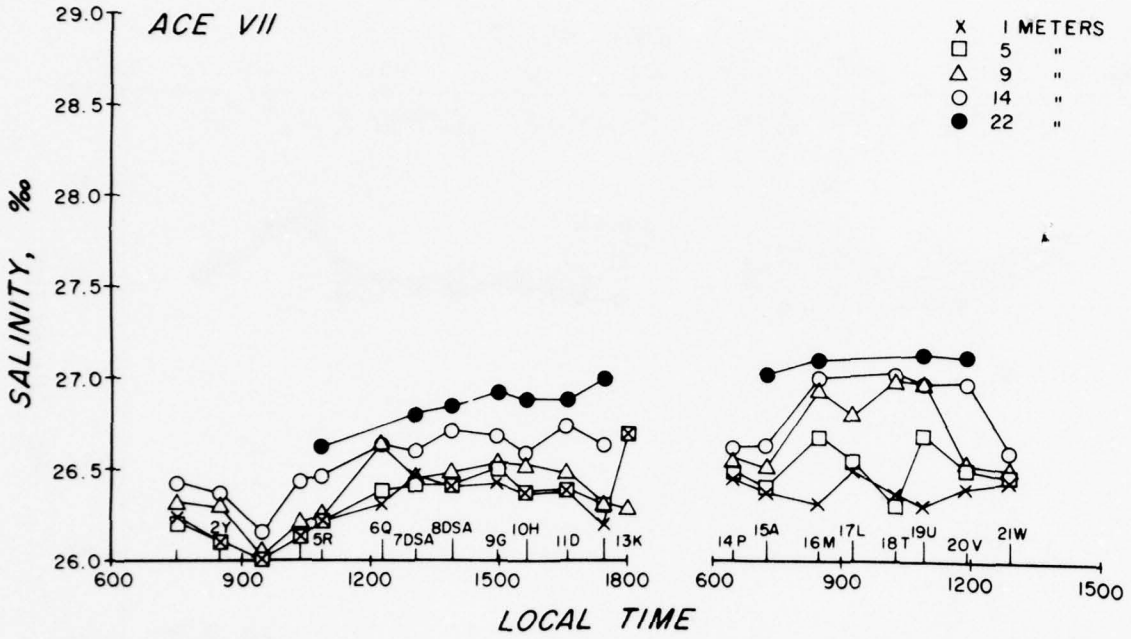



Figure 26. Salinity observations during ACE VII.

Horizontal and vertical distribution of water properties

97. The distribution of water properties is presented for the three cruises, 13-14 January (ACE III), 19-20 March (ACE V), and 28-29 May (ACE VII), by means of horizontal contoured maps plus longitudinal and transverse sections. The locations of the stations shown on the maps and sections are given in Figure 2. These three cruise periods occurred during pre-bloom, bloom, and secondary bloom periods and also during high and low river flows (Figure 27).

98. The seasonal cycle in averaged results for each variable for each of the seven sampling periods is presented in a figure following each set of the horizontal and transverse sections. For each variable, three types of averaged results are presented: (1) the mean of all surface values; (2) the mean of all bottom values; and (3) the mean of all values for all depths.

99. Temperature and salinity. Figures 28, 29, and 30 show the horizontal and vertical distribution of temperature and salinity for the January, March, and May sampling periods. Figures 31 and 32 show the seasonal cycles of temperature and salinity, respectively.

100. From October through March, the water was nearly isothermal (Figures 28 a,b,d,e, and 31) indicating a fairly well-mixed water column during this period. The coldest water temperature was observed in the February cruise (Figure 31). In April and May, surface water temperature had increased to about 8° and 15°C and bottom temperatures increased to 6° and 12°C, respectively (Figure 31). The presence of the May thermocline (Figure 28 c,f), combined with the halocline (Figure 30 c,f), produced a fairly well-stratified water column during these months.

101. Generally, surface salinities during the January, March, and May sampling periods were patchy and lower

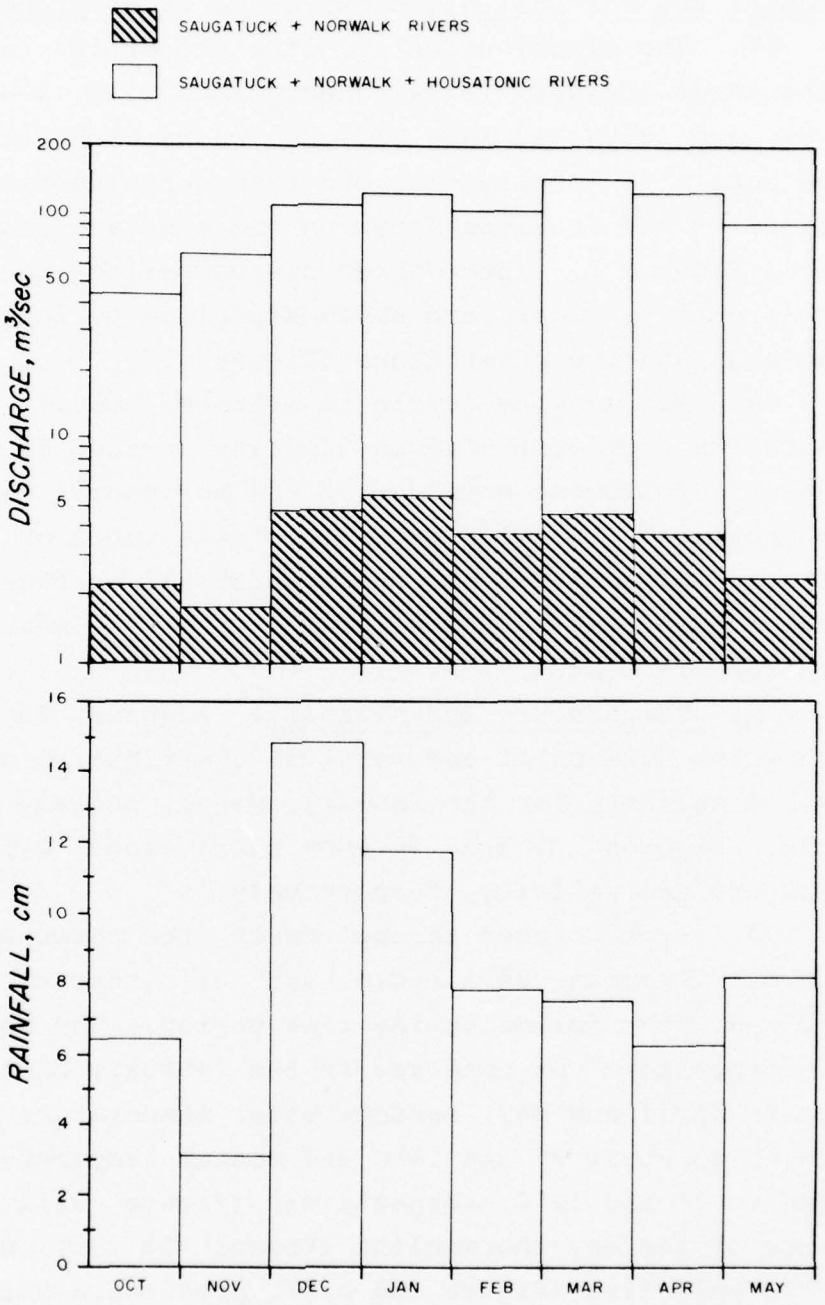



Figure 27. Rainfall[59] observed at Bridgeport, Connecticut and gauged river flow[58] for October 1974 through May 1975.

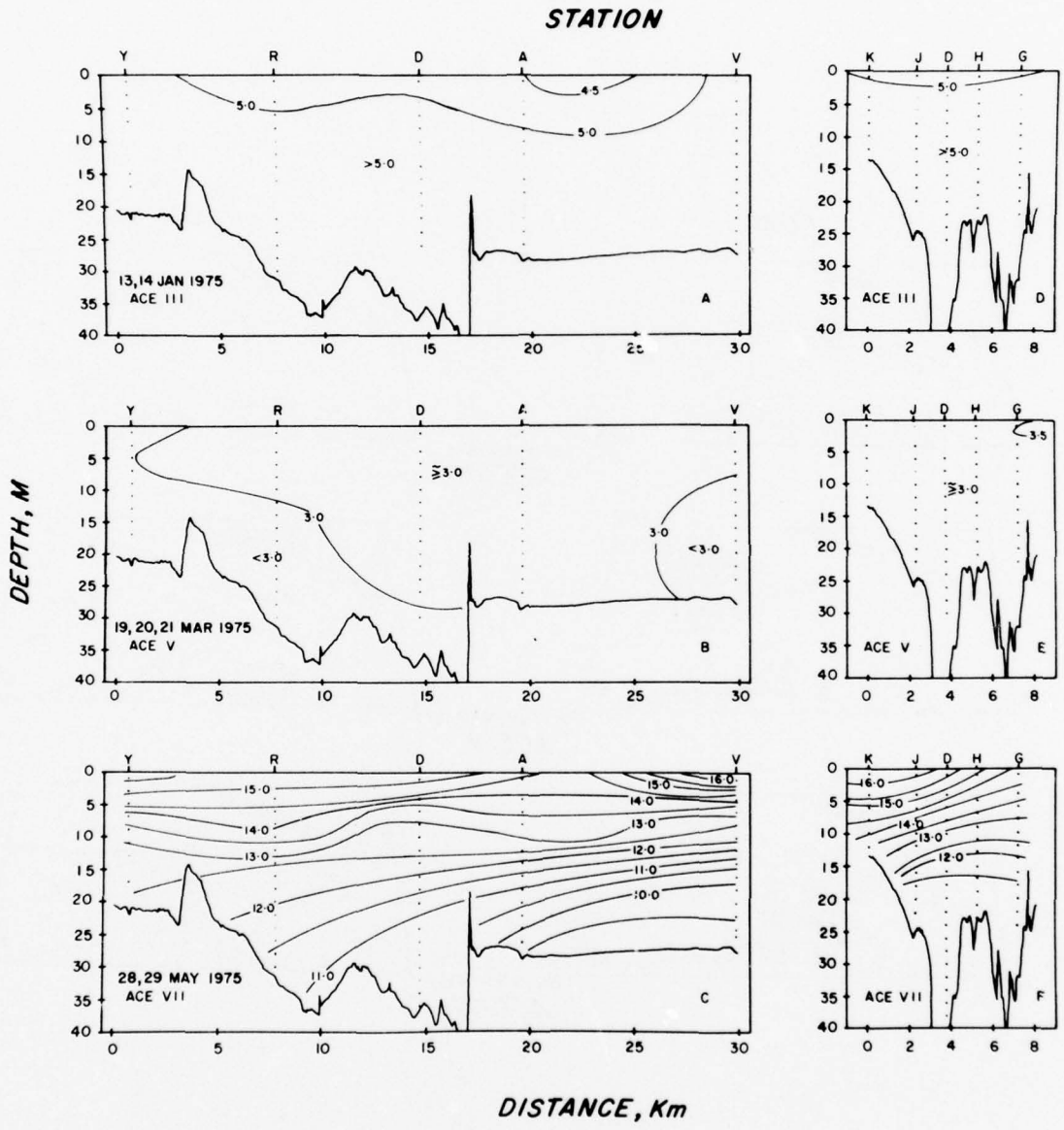



Figure 28. Vertical variation in temperature (°C).

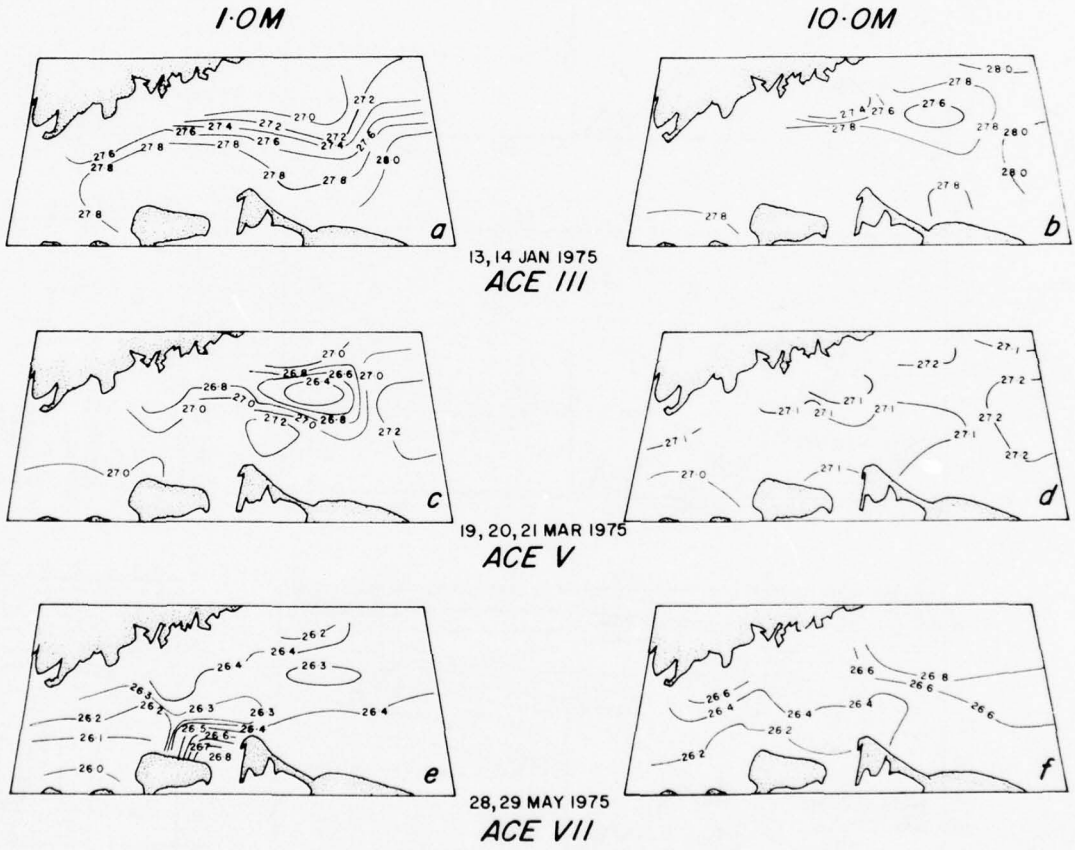



Figure 29. Horizontal distribution of salinity (°/₀₀).

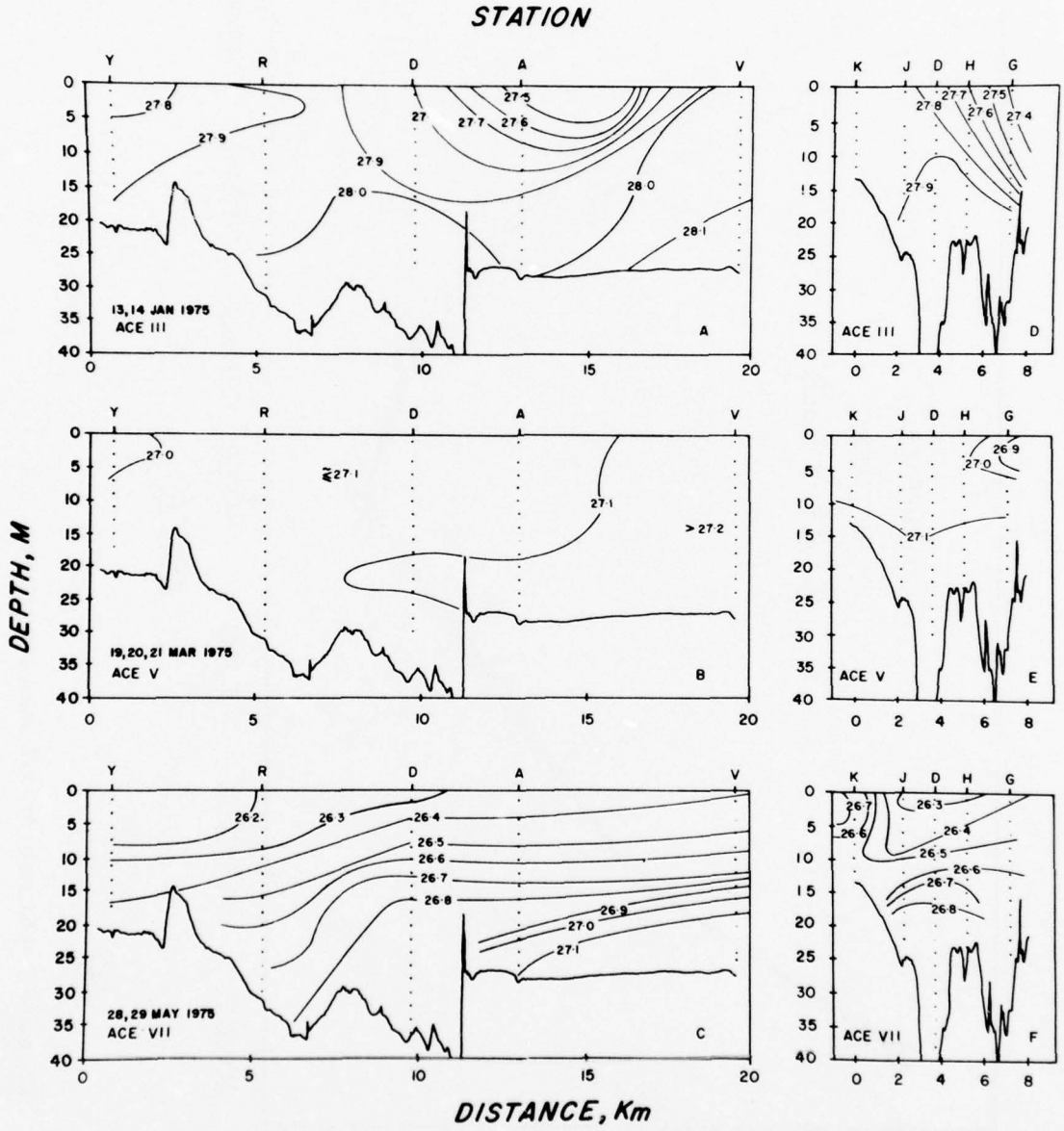



Figure 30. Vertical sections of salinity (°/₀₀).

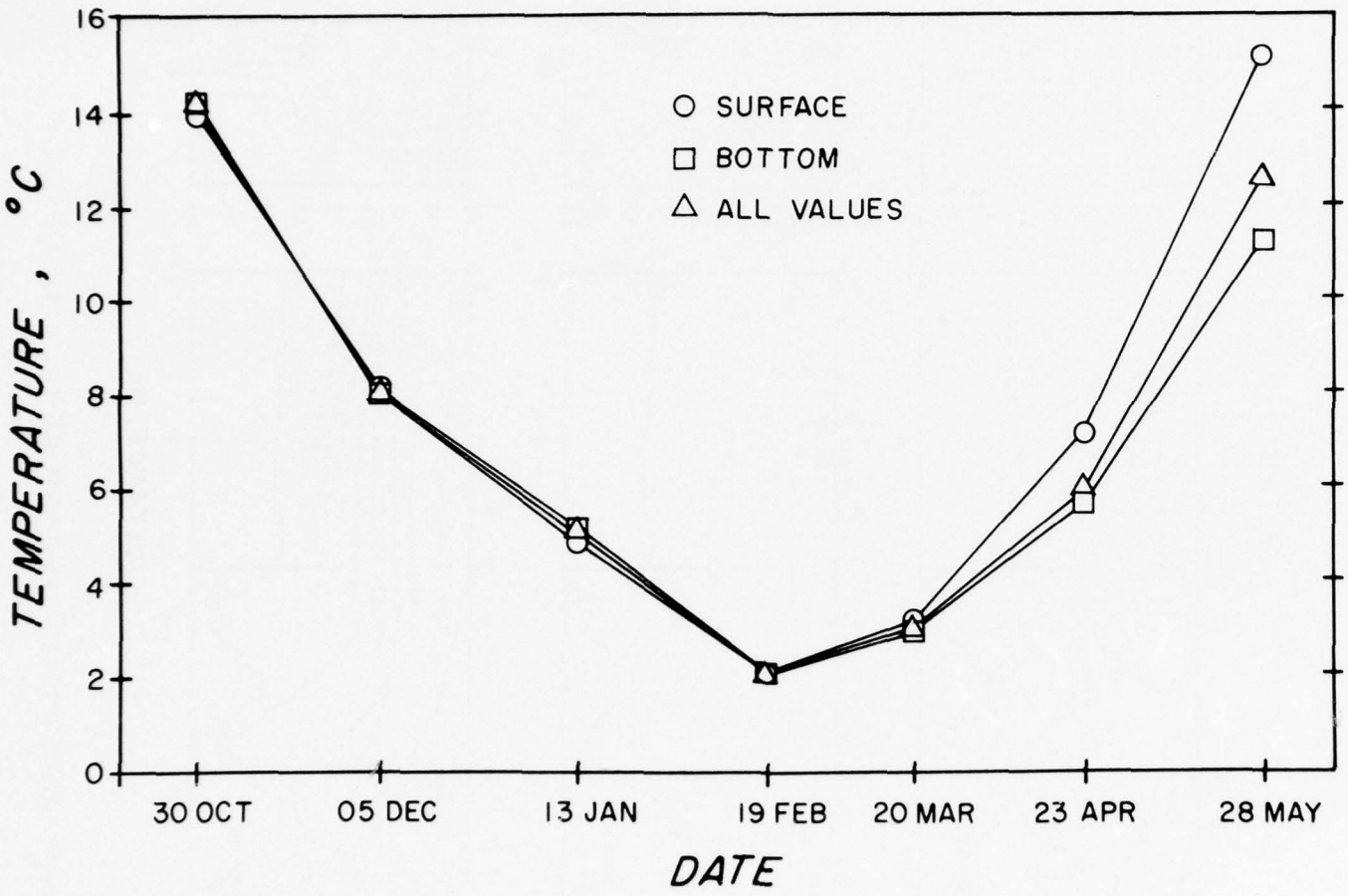



Figure 31. Seasonal variation of mean temperature.

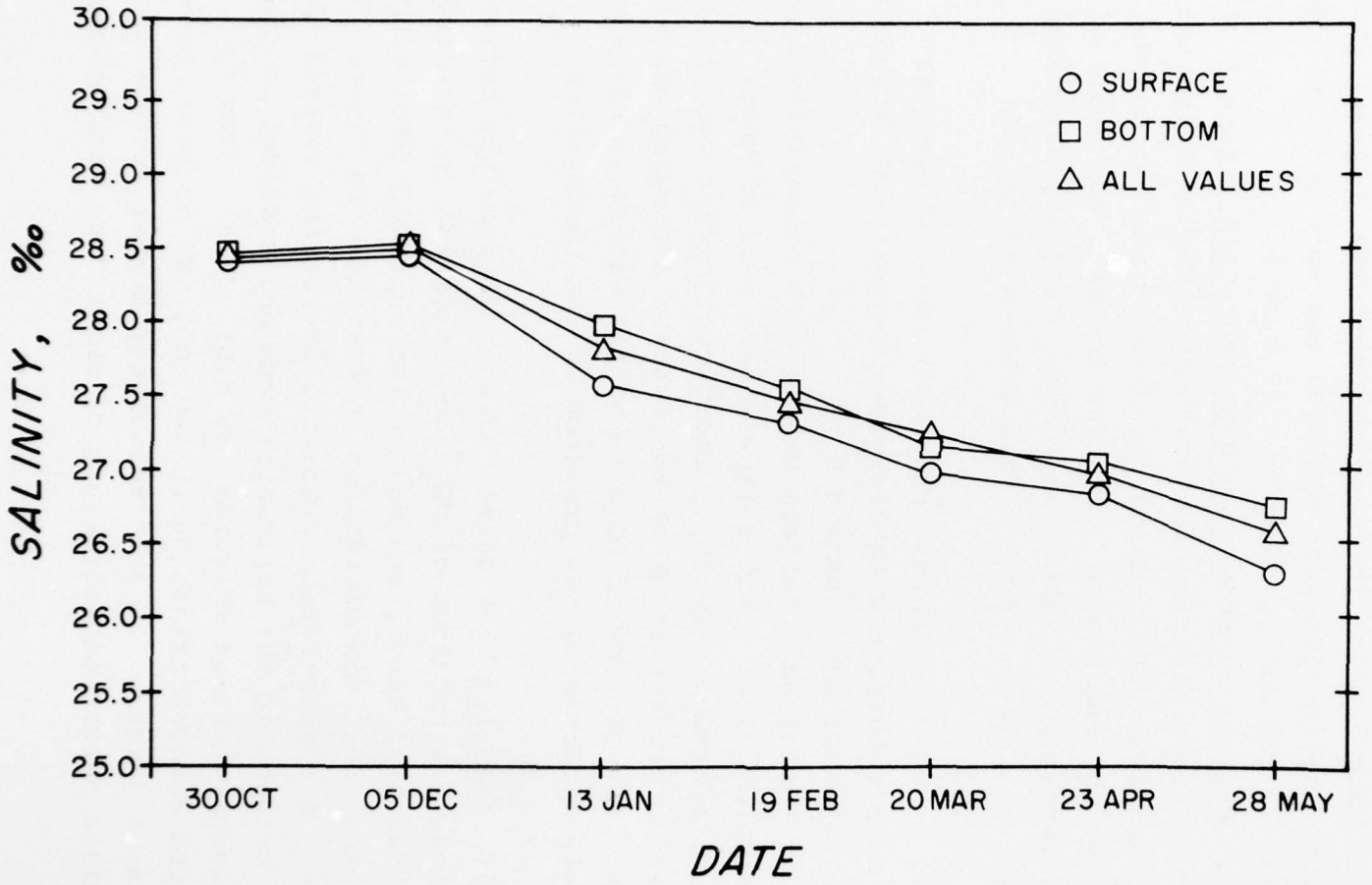



Figure 32. Seasonal variation of mean salinity.

(~26.3°/$_{oo}$) near the Connecticut shore where the presence of the Norwalk and Saugatuck Rivers (Figure 27) would be expected to have a major influence on salinity (Figure 29 a, c,e). Bottom salinities were elevated and more uniform, ranging between 27 and 28°/$_{oo}$ (Figure 30 a,b,c).

102. Percent dissolved oxygen saturation. Figure 33 shows the verticle distribution of the percent of dissolved oxygen saturation (PDOS) during the January, March, and May sampling periods and Figure 34 shows the seasonal cycle of PDOS. In January, the water was nearly uniformly saturated with dissolved oxygen. PDOS ranged between 93 and 95% (Figure 33 a,d).

103. During the March cruise, the water column was slightly supersaturated with dissolved oxygen; PDOS values of 115% were observed near station D.

104. During May, surface waters were excessively supersaturated (PDOS >130%), but bottom waters were slightly undersaturated (PDOS ~80-95%). The excess oxygen was probably due to oxygen production by photosynthesis exceeding oxidation processes. The decline of PDOS in bottom waters in May was most likely affected by the presence of the thermocline (Figure 28 c,f).

105. Ammonium . Figures 35 and 36 show the horizontal and vertical distribution of $NH_4^+$ concentration in the study area for January, March, and May cruise periods. The seasonal cycle of mean $NH_4^+$ concentrations is presented in Figure 37.

106. A concentration gradient, increasing towards the west, is evident in the horizontal maps and vertical sections for the January cruise (Figures 35 a,b; 36 a). During this period concentrations decreased to 1 µM, or less, east of station A (Figure 36 a). Relatively higher surface and intermediate depth concentrations of about 7 µM were observed

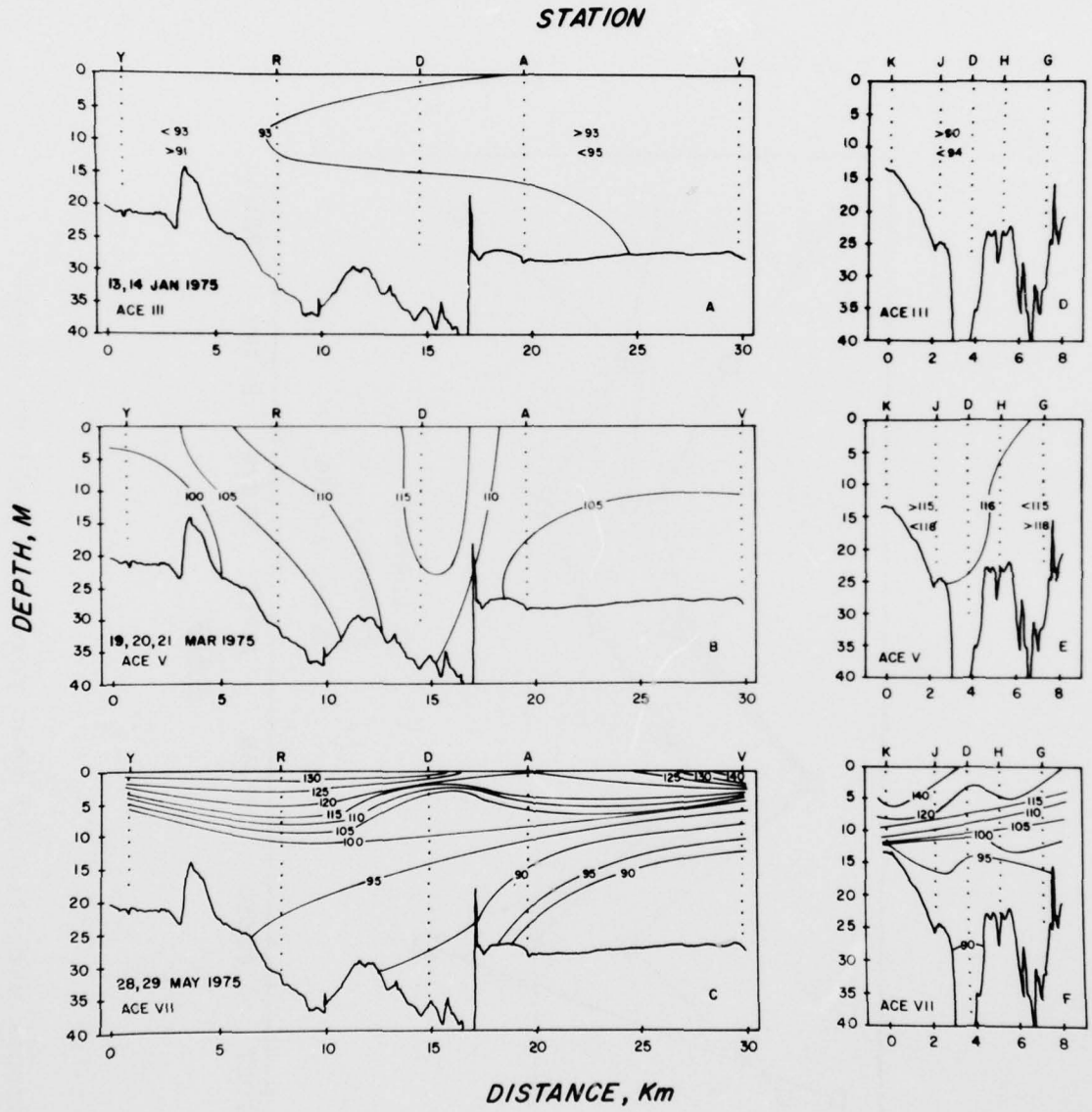



Figure 33. Vertical sections of percent dissolved oxygen saturation (PDOS).

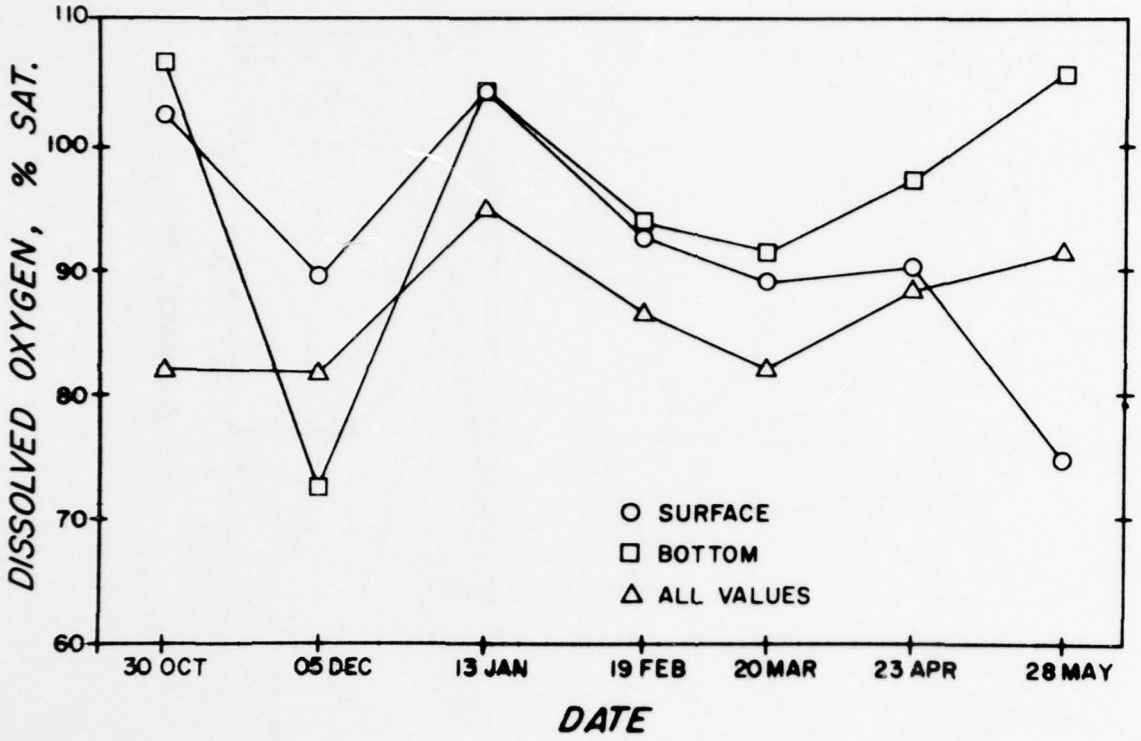



Figure 34. Seasonal variation of mean percent dissolved oxygen saturation (PDOS).

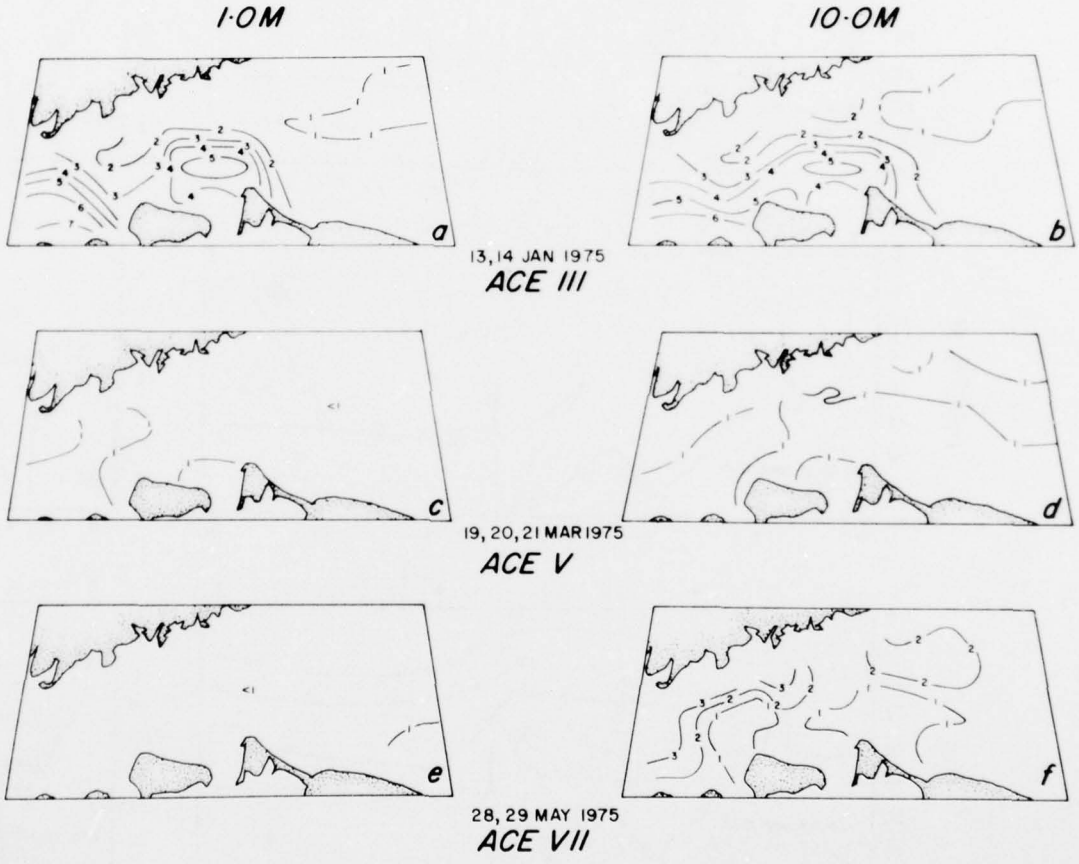



Figure 35. Horizontal distribution of ammonium concentration (μM) [1 μM $NH_4^+$ equals 14 μg/l N].

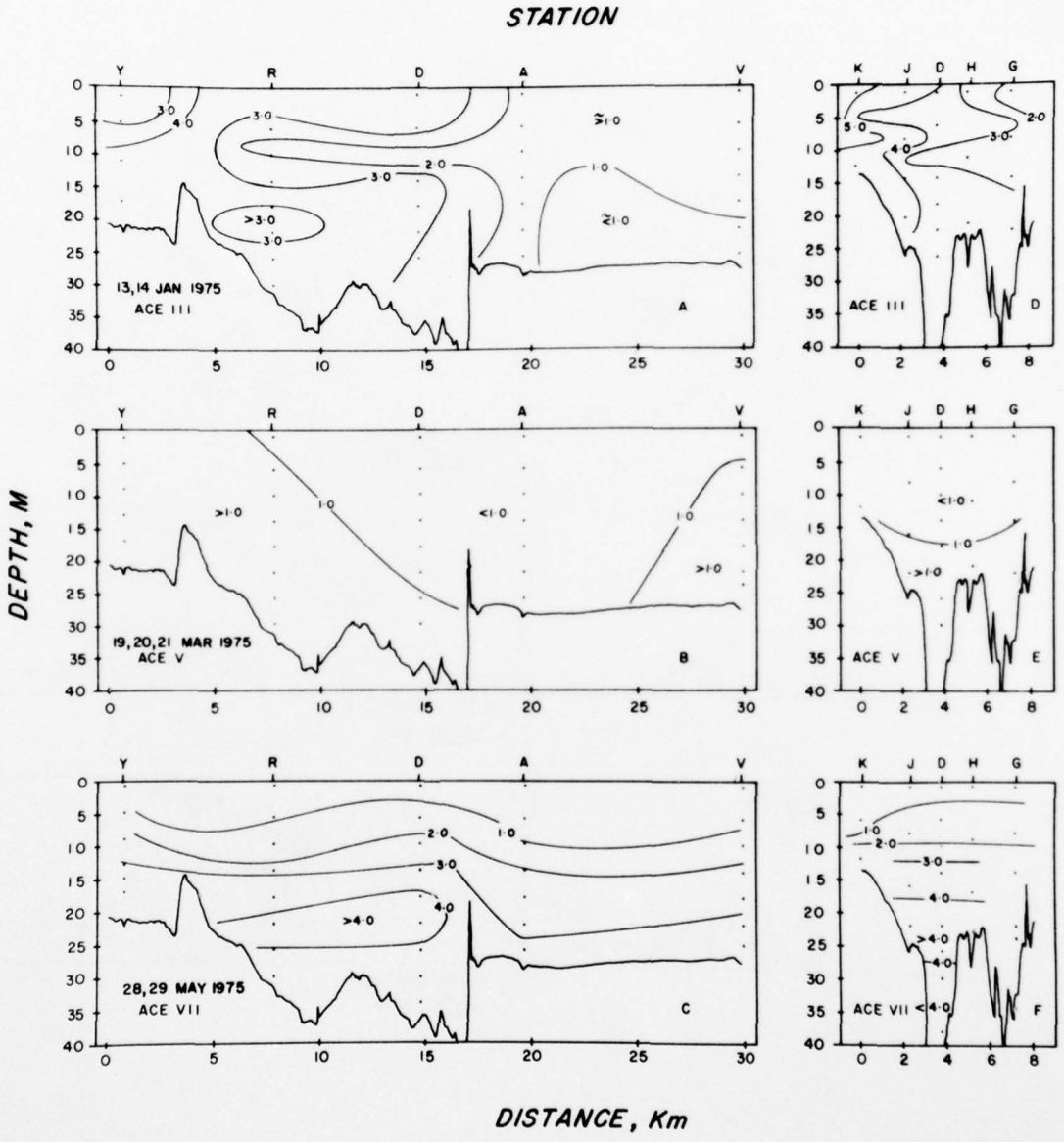



Figure 36. Vertical sections of ammonium concentration [μM $NH_4^+$ equals 14 μg/l N].

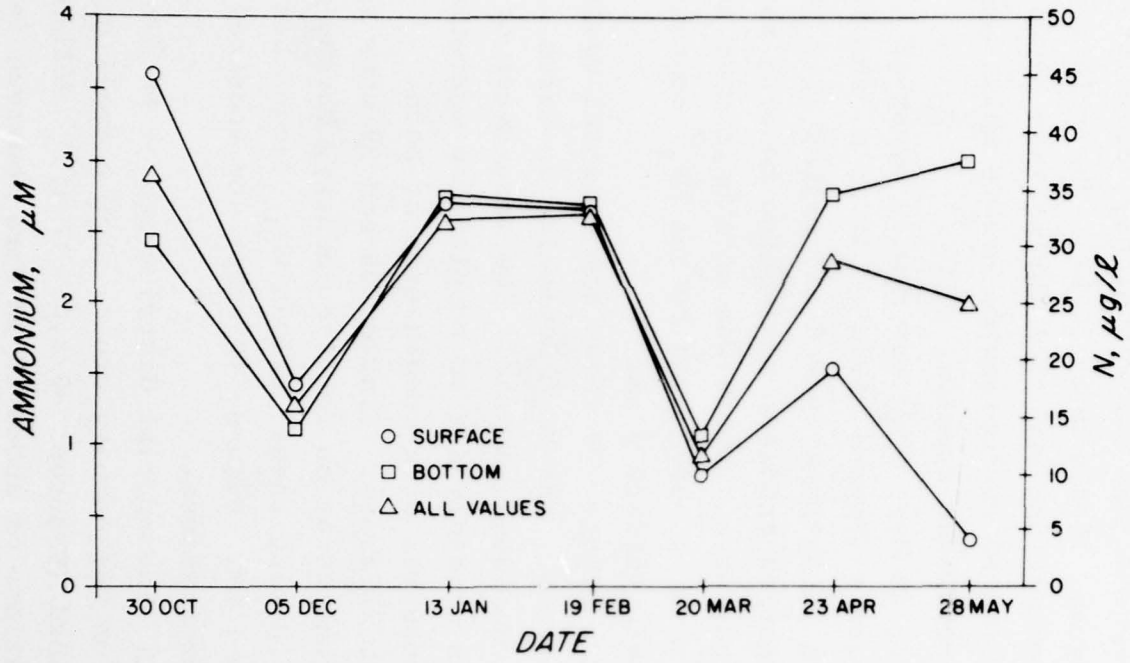



Figure 37. Seasonal variation of mean ammonium concentration.

at the western stations (Figures 35 a,b and 36 a). Elevated $NH_4^+$ concentrations were also observed at stations closest to the north shore of Long Island near Huntington Bay (Figures 35 b and 36 d; see also time series plots in Appendix B').

107. The data from the March cruise show more or less uniform vertical and horizontal $NH_4^+$ concentrations of about 1 µM (Figures 35 c,d and 36 b). The relatively decreased $NH_4^+$ concentrations observed during this period are probably due to increased phytoplankton growth which tends to deplete inorganic nitrogen species.

108. In May, $NH_4^+$ was nearly depleted (<1 µM) from the surface waters (Figure 35 e). At 10 m, the $NH_4^+$ concentrations were slightly elevated and patchy (1-3 µM) and exhibited a concentration gradient increasing towards the western end of the study area. There was no significant north-south gradient (Figure 36 f) and bottom $NH_4^+$ concentrations were a relatively uniform 4 µM.

109. Figure 37 shows the seasonal cycle of mean $NH_4^+$ concentrations. The $NH_4^+$ depletion in March is most likely due to phytoplankton uptake. The resurgence of $NH_4^+$ in April and May is probably due to zooplankton excretion or regeneration processes, or a combination of both.

110. Nitrate. Figures 38 and 39 show the distribution of $NO_3^-$ concentration for the January, March, and May sampling periods. During these periods, $NO_3^-$ ranged between 18 µM and less than 1 µM. Figure 40 shows the seasonal cycle of mean $NO_3^-$ concentrations.

111. The spatial distribution of $NO_3^-$ concentrations observed on the January cruise show a small gradient decreasing eastward (Figures 38 a,b; 39 a). Relatively high concentrations of about 18 µM were observed in the surface waters near Huntington Bay on the north shore on Long Island

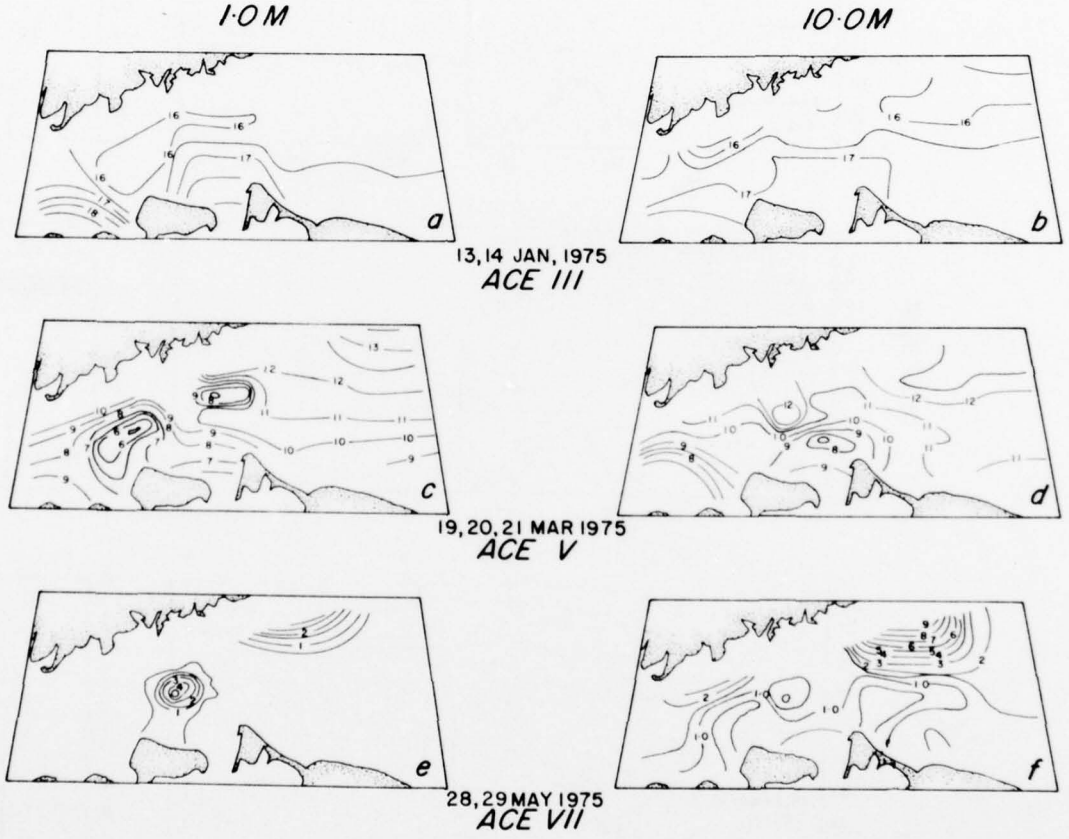



Figure 38. Horizontal distribution of nitrate concentration (μM) [1 μM $NO_3$ equals 14 μg/l N].

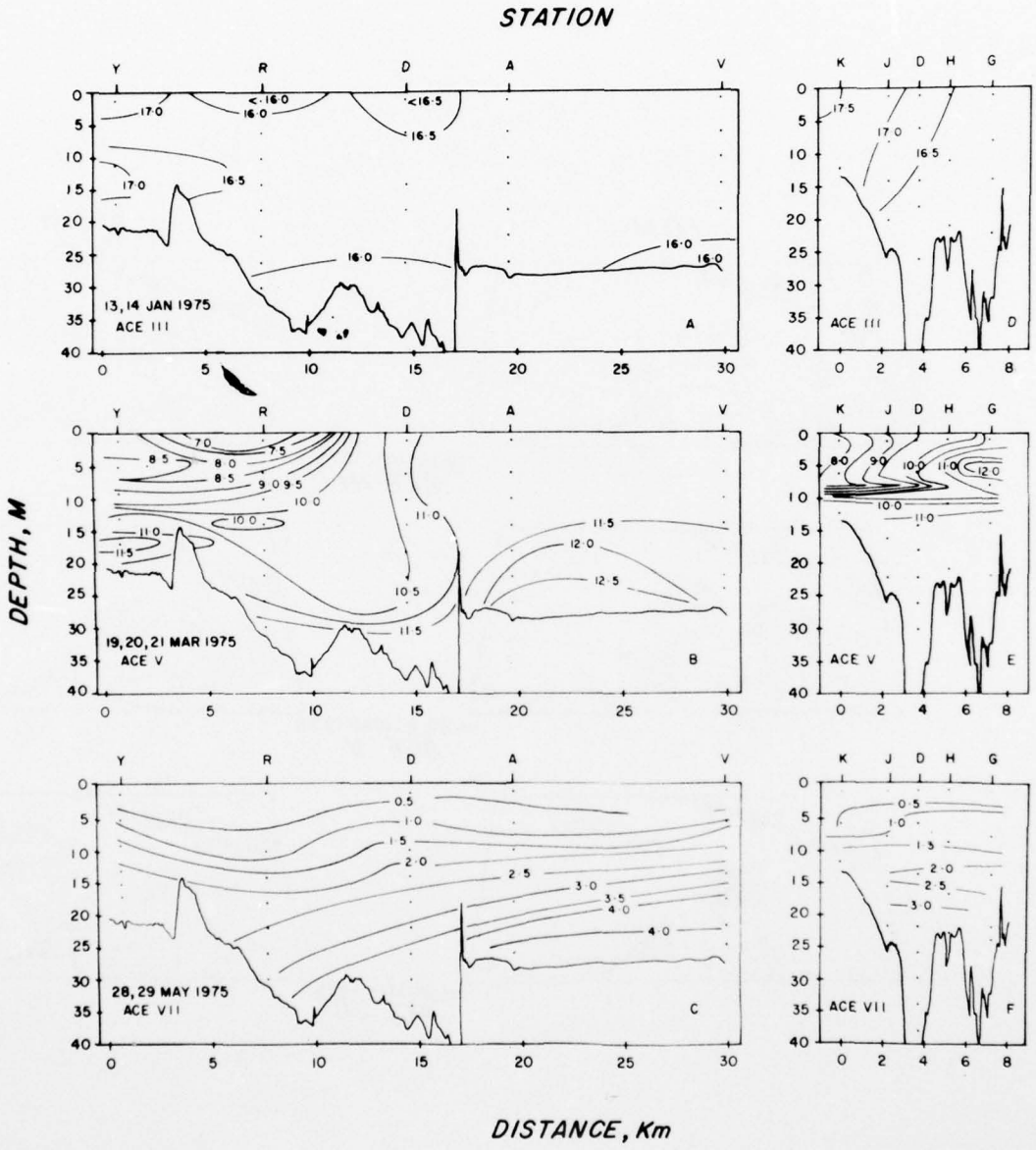



Figure 39. Vertical sections of nitrate concentration (μM) [1 μM $NO_3^-$ equals 14 μg/l N].

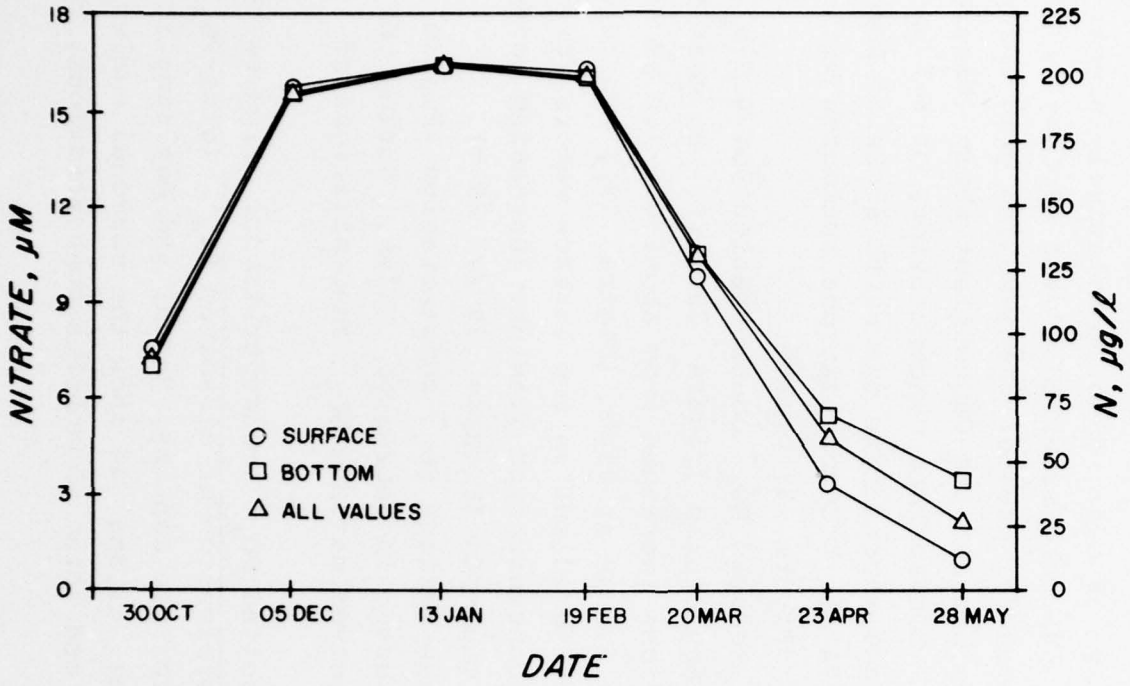



Figure 40. Seasonal variation of mean nitrate concentration.

(Figures 38 a,b; 39 d). Concentrations of $NO_3^-$ were nearly uniform with depth at each station but decreased to about 16 µM at the eastern stations (Figure 39 a).

112. $NO_3^-$ concentrations observed on the March cruise were lower (~7-12 µM) and exhibited a gradient increasing eastward (Figures 38 c,d; 39 b). Relatively higher concentrations (~11 µM) were observed in the surface layer at stations in the central part of the sampling grid and also at those stations nearest the Connecticut shore (Figures 38 c,d; 39 b). Low surface concentrations of 6-7 µM were observed in surface waters near the north shore of Long Island (Figure 38 d). Concentrations increased with depth at most stations (Figure 39 b,e).

113. Very reduced $NO_3^-$ concentrations of 0.5-5 µM were observed on the May cruise (Figure 39 c,f). At most stations concentrations increased from about 0.5-1.0 µM in the surface layer to 3.5 µM at depth (Figure 39). There was no apparent east-west gradient in the surface waters (Figure 38 e). However, a concentration gradient increasing eastward was observed at middepth (Figures 38 f; 39 c).

114. A mean maximum $NO_3^-$ concentration (Figure 40) of 17 µM was observed in February. Riley,[7] during the 1954-1955 season, observed maximum $NO_3^-$ concentrations of 16 µM in November.

115. Dissolved $PO_4^{3-}$ concentrations. Figures 41 and 42 show the distribution of dissolved $PO_4^{3-}$ (diss-$PO_4^{3-}$) in the study area for the January, March, and May sampling periods. Figures 43 and 44 show the seasonal cycles of mean diss-$PO_4^{3-}$ and total phosphorus concentrations, respectively.

116. In January, the vertical concentrations of diss-$PO_4^{3-}$ were nearly uniform at 3.2 µM throughout the sampling

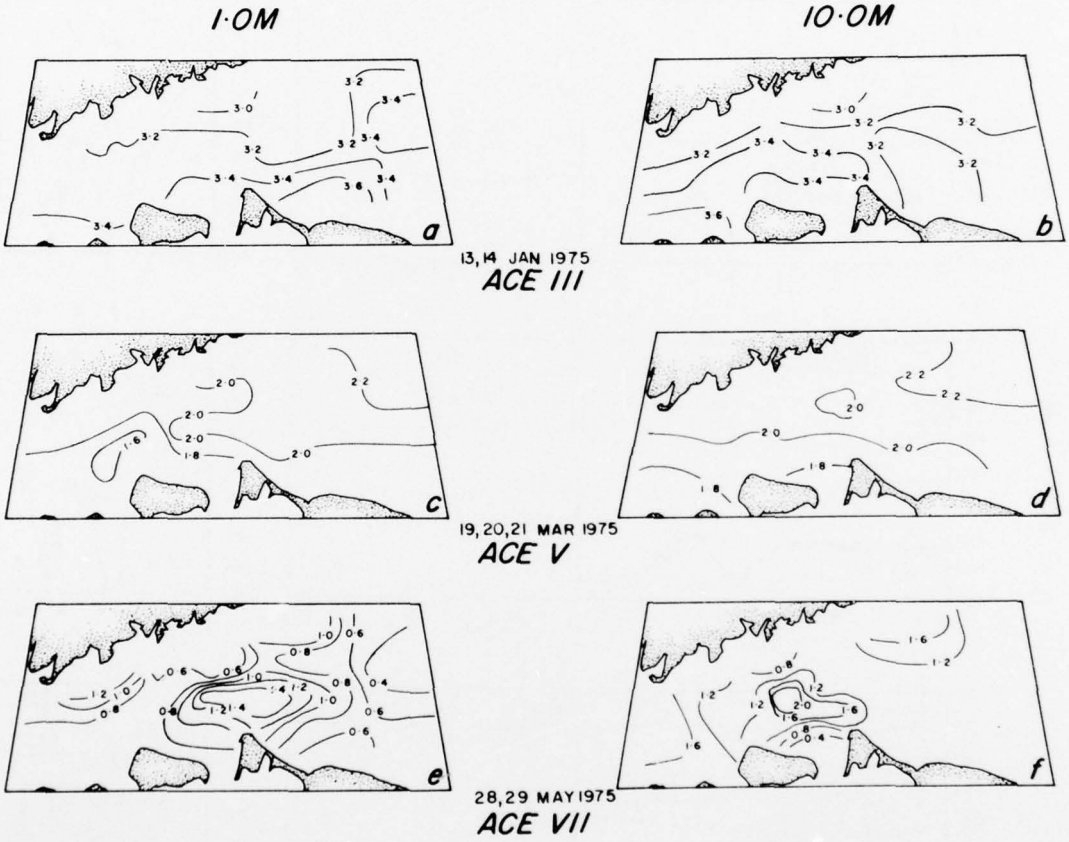



Figure 41. Horizontal distribution of mean dissolved phosphate concentrations (μM) [1 μM $PO_4^{3-}$ equals 31 μg/l P].

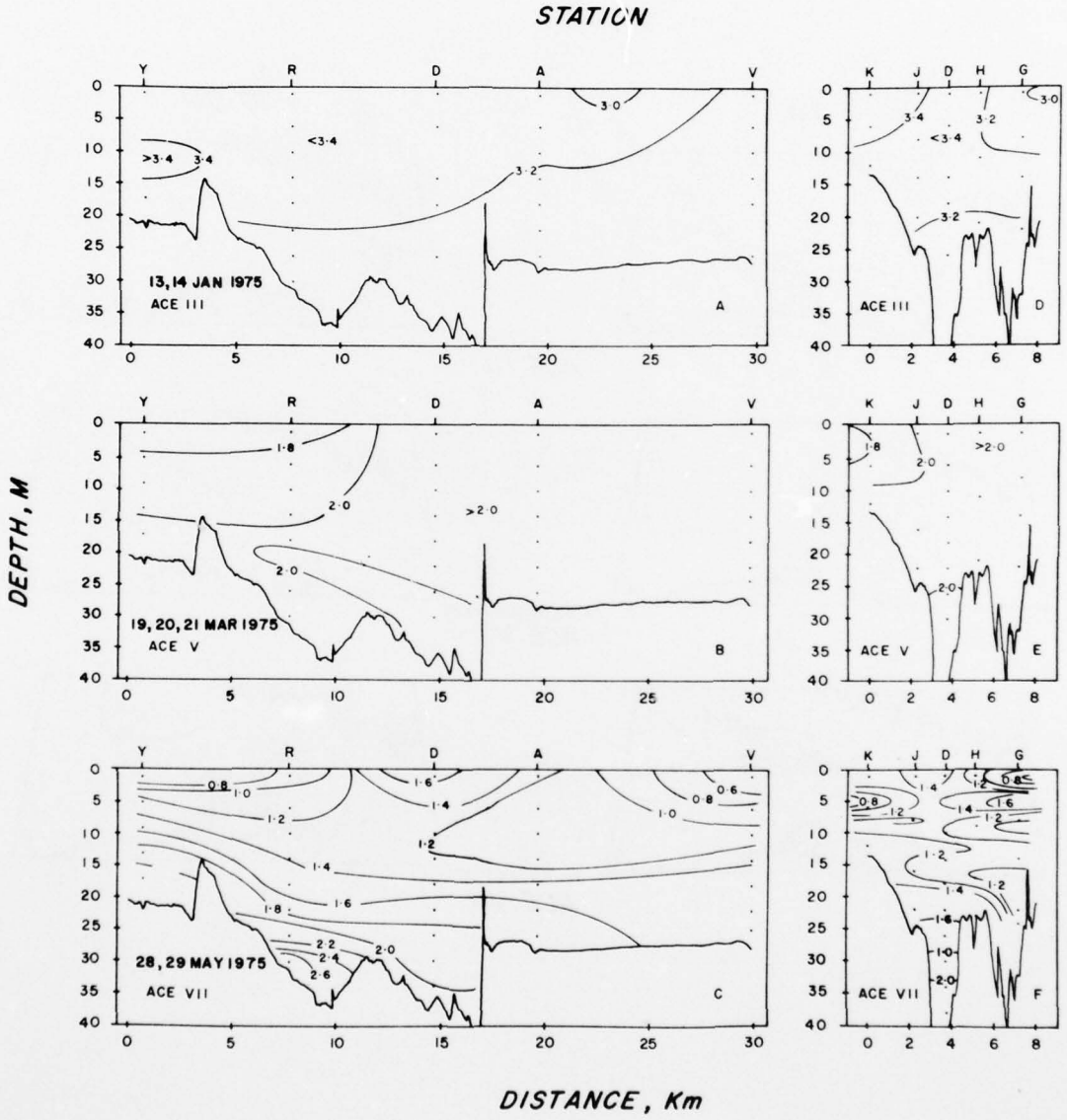



Figure 42. Vertical sections of dissolved phosphate concentration (μM) [1 μM $PO_4^{3-}$ equals 31 μg/l P].

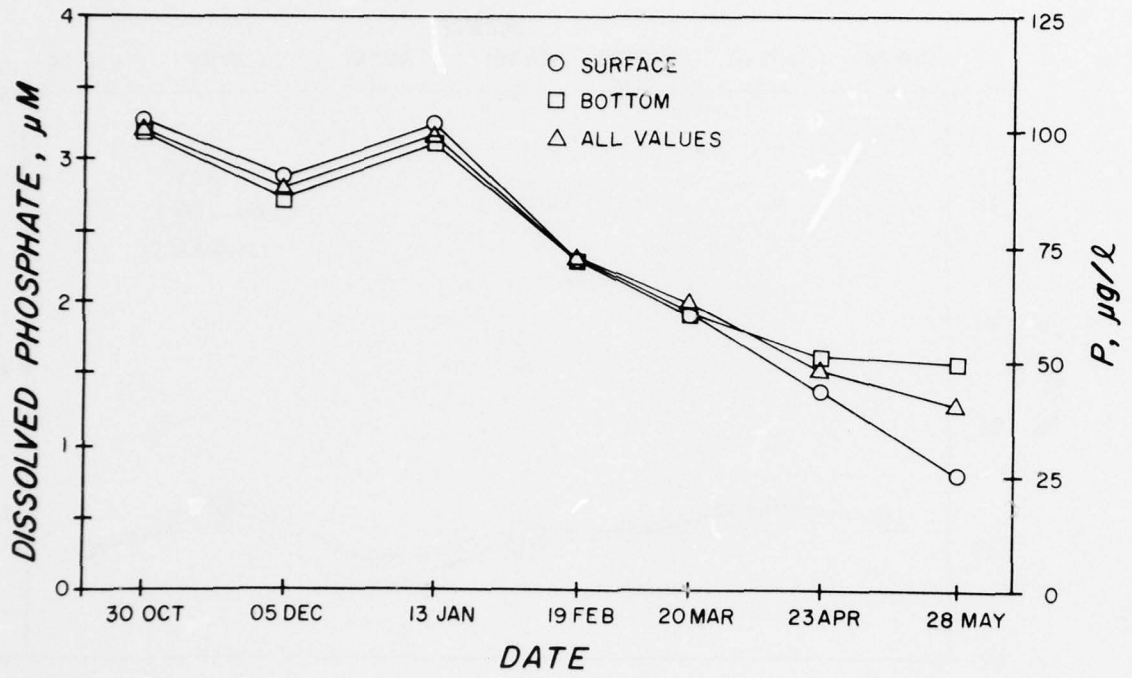



Figure 43. Seasonal variation of mean dissolved phosphate concentration.

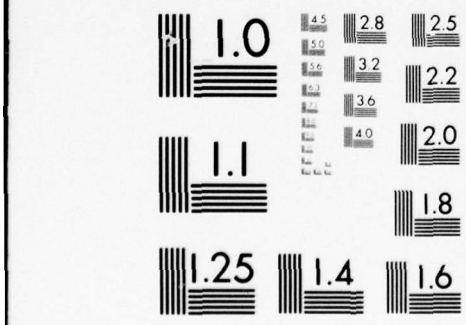
AD-A053 427 STATE UNIV OF NEW YORK AT STONY BROOK MARINE SCIENCES--ETC F/G 13/2
AQUATIC DISPOSAL FIELD INVESTIGATIONS, EATONS NECK DISPOSAL SIT--ETC(U)
JAN 78 DACW51-75-C-0016

UNCLASSIFIED WES-TR-D-77-6-APP-B NL

2 OF 5
AD A053427



05342




MICROCOPY RESOLUTION TEST CHART
NATIONAL BUREAU OF STANDARDS-1963-A

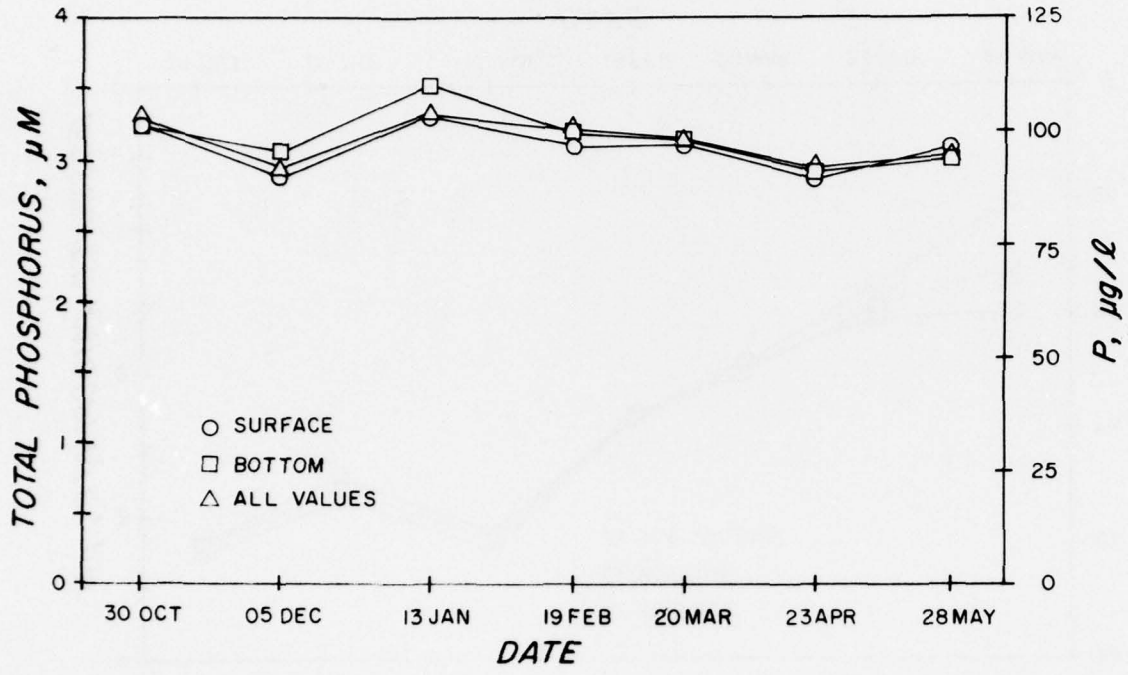



Figure 44. Seasonal variation of total phosphorus concentration.

area (Figures 41 a,b; 42 a). Concentrations were, however, slightly greater on the south side of the study area (Figures 41 a,b; 42 d) near the north shore of Long Island.

117. In March, dissolved-$PO_4^{3-}$ concentrations were reduced to levels ranging between 1.6 and 2.2 µM (Figures 41 c,d; 42 b,e). Concentration gradients increasing towards the north and also towards the east were evident in the deeper waters (Figures 41 c,d; 42 e).

118. During the May cruise, surface dissolved-$PO_4^{3-}$ concentrations were patchy, ranging between 0.4 and 1.6 µM. At 10 m, the concentrations near the central region of the sampling area were ~1.6 µM (Figure 41 e,f).

119. The seasonal cycle (Figure 43) of dissolved-$PO_4^{3-}$ was similar to that observed by Riley.[7] However, the dissolved-$PO_4^{3-}$ concentrations observed during the present study were consistently about 1 µM higher than those reported by Riley.[7] The increased $PO_4^{3-}$ in Figure 44 is most likely due to organic phosphorous bound to particulate matter.

120. Silicic acid. Figures 45 and 46 show the distribution of $Si(OH)_4$ concentrations for the January, March, and May sampling periods. Figure 47 shows the seasonal cycle of mean $Si(OH)_4$ concentrations.

121. In January, the $Si(OH)_4$ concentrations were nearly uniform (~28 µM) with depth (Figure 46 a,d). Concentration gradients increasing toward the west and north shore of Long Island were observed (Figures 45 a,b; 46 a,d).

122. During the March cruise, $Si(OH)_4$ concentrations decreased to 10-20 µM, with the higher concentrations found at depth (Figures 45 d; 46 b,e). Concentration gradients increasing towards the western and northern regions of the study area were observed during this period (Figure 45 c,d; 46 e).

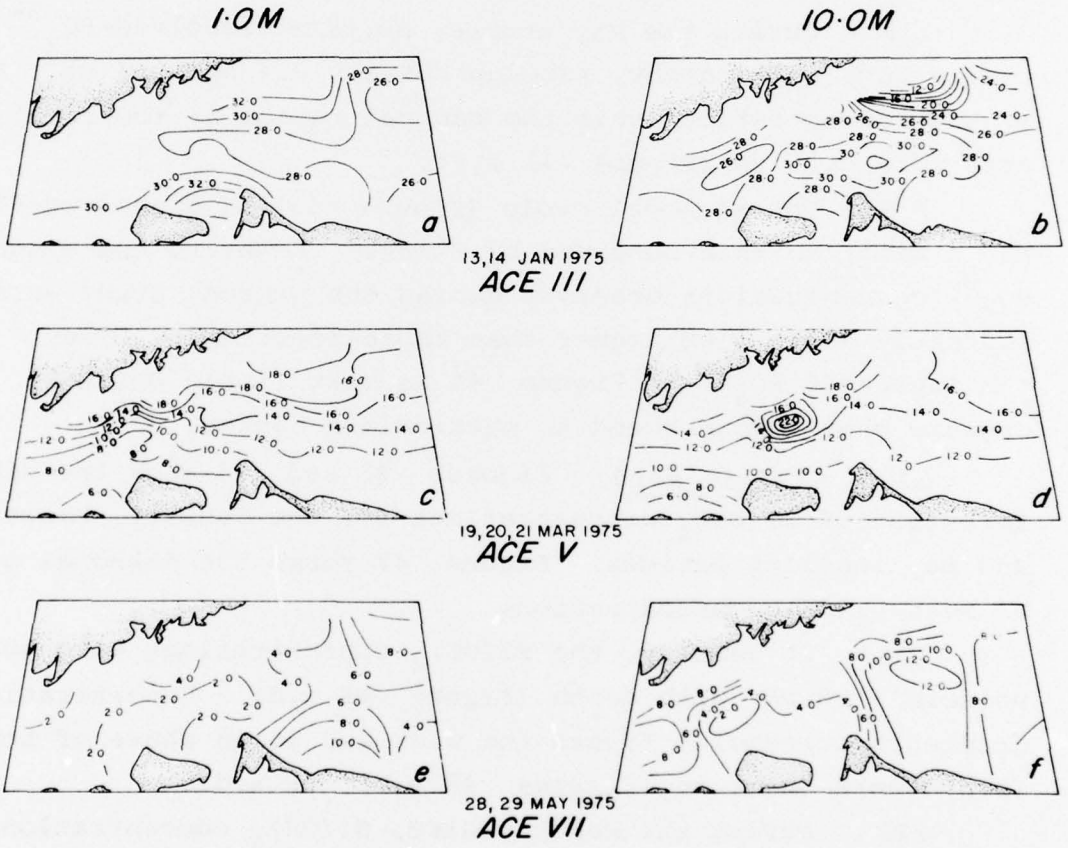



Figure 45. Horizontal distribution of silicic acid concentration (μM) [1 μM Si $(OH)_4$ equals 28 μg/l Si].

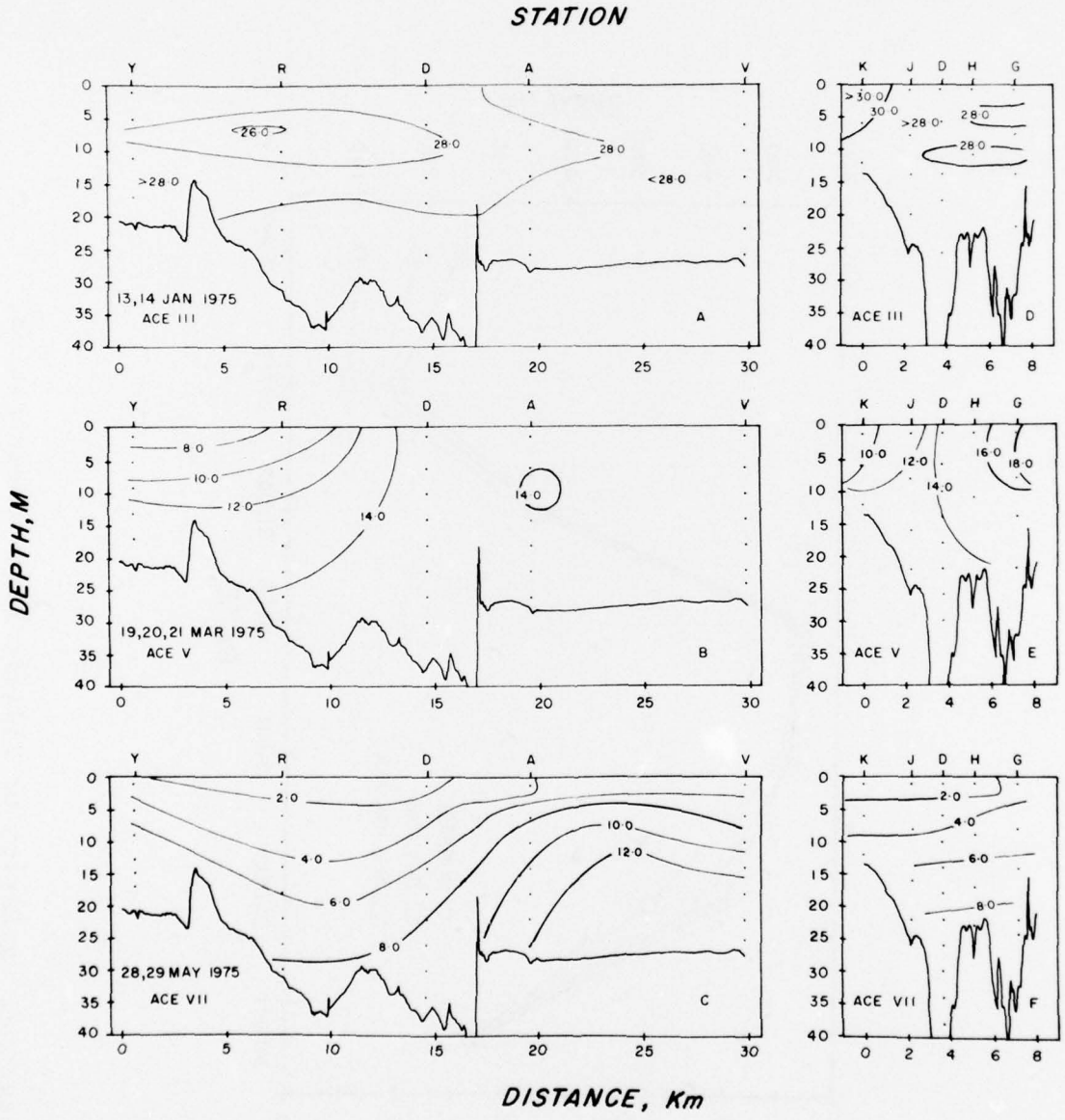



Figure 46. Vertical distribution of silicic acid concentration (μM) [1 μM $Si(OH)_4$ equals 28 μg/l Si].

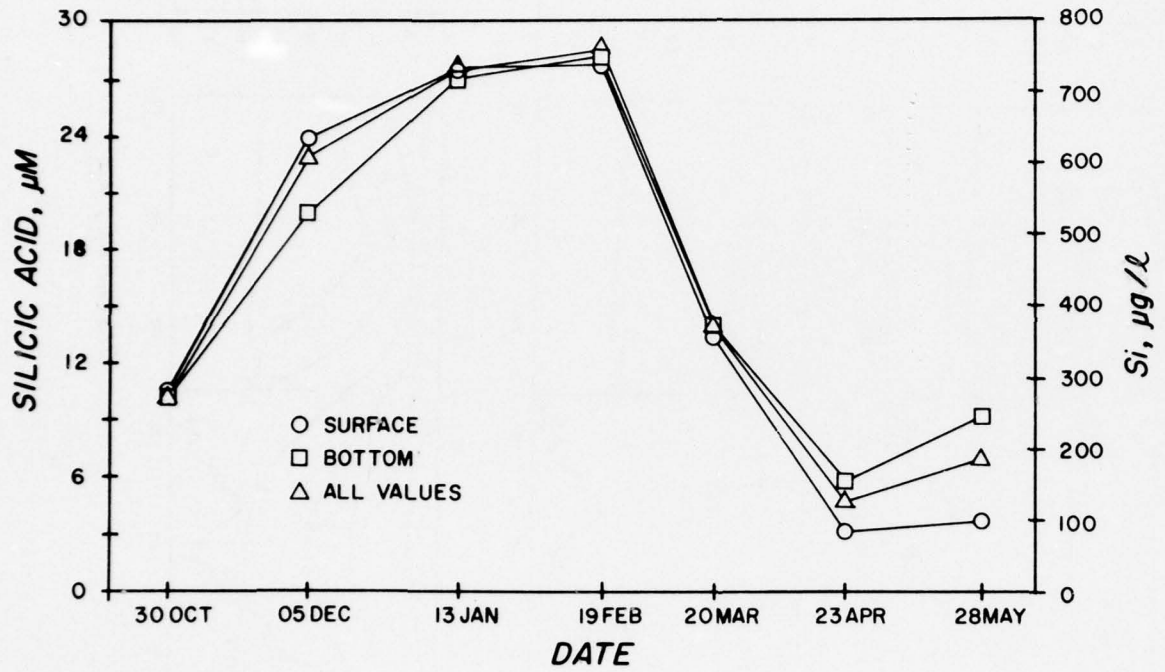



Figure 47. Seasonal variation of silicic acid concentration.

123. In May, $Si(OH)_4$ concentrations decreased further to 2-12 µM, with the higher concentrations observed at depth (Figures 45 f; 46 c,f). There were neither east-west nor north-south concentration gradients observed during this period (Figure 45 e,f).

124. The strong seasonal variation in $Si(OH)_4$ is evident from the results shown in Figure 47. The decreased $Si(OH)_4$ levels observed in the surface waters in April and May are probably due to phytoplankton uptake.

125. Particulate carbon. The particulate organic carbon (POC) concentrations observed during the January, March, and May periods are presented in Figures 48 and 49. During these periods, the concentrations varied from a low of less than 200 ug/l for January to a high of over 2000 ug/l for May. The seasonal cycle of mean of POC concentrations is shown in Figure 50.

126. In January, the distribution of POC was nearly unfirom at ~200 ug/l (Figure 48 a,b). In March, POC concentrations showed a marked increase, with the highest concentrations observed in the western portion of the study area (Figures 48 c,d; Figure 49 b) near the north shore of Long Island. Concentrations decreased with depth at most stations (Figure 49 b,e).

127. The POC concentrations observed in May were characterized by a very patchy distribution; concentrations ranged between 600 and 2000 ug/l (Figure 48 e,f). Generally, the concentrations decreased with depth (Figure 49 c,f). At some stations, the POC tended to increase near the bottom. Disturbed bottom sediments due to the Plunket sampling procedure may have produced the elevated concentrations shown at stations R and D in Figure 49 c.

128. The measured mean POC concentrations (Figure 50)

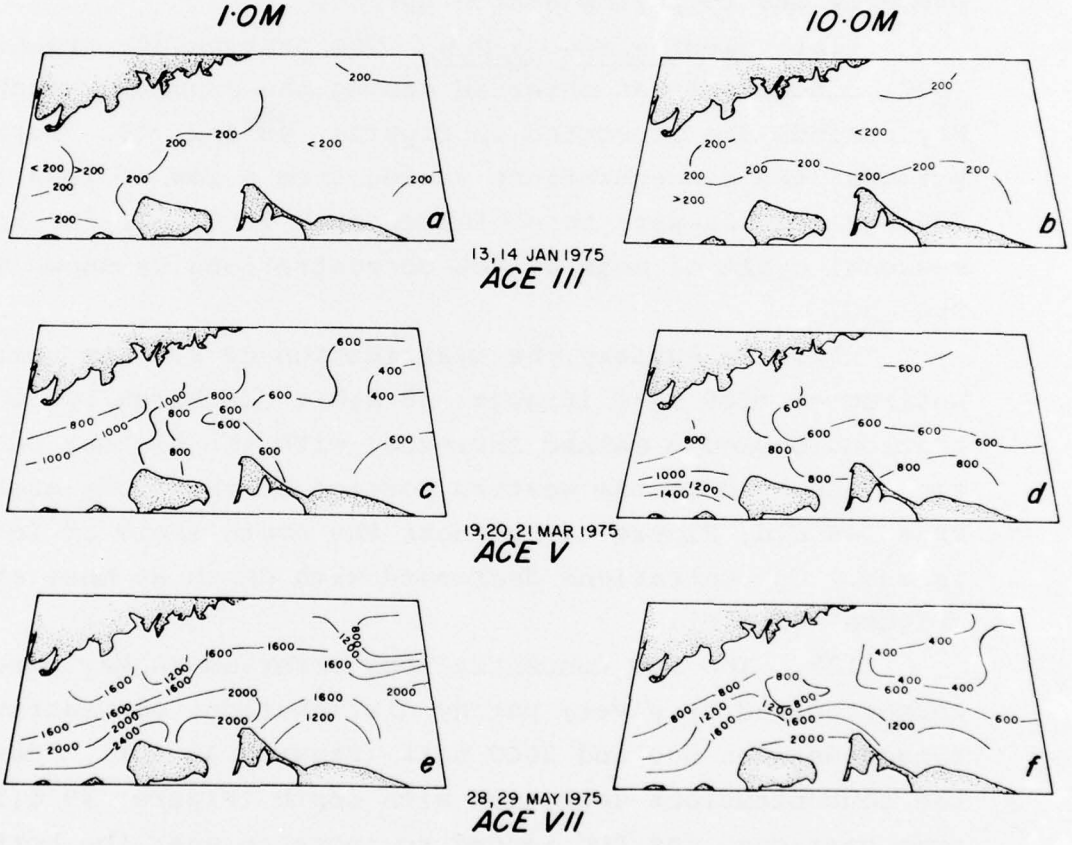



Figure 48. Horizontal distribution of particulate carbon concentration (μg/l).

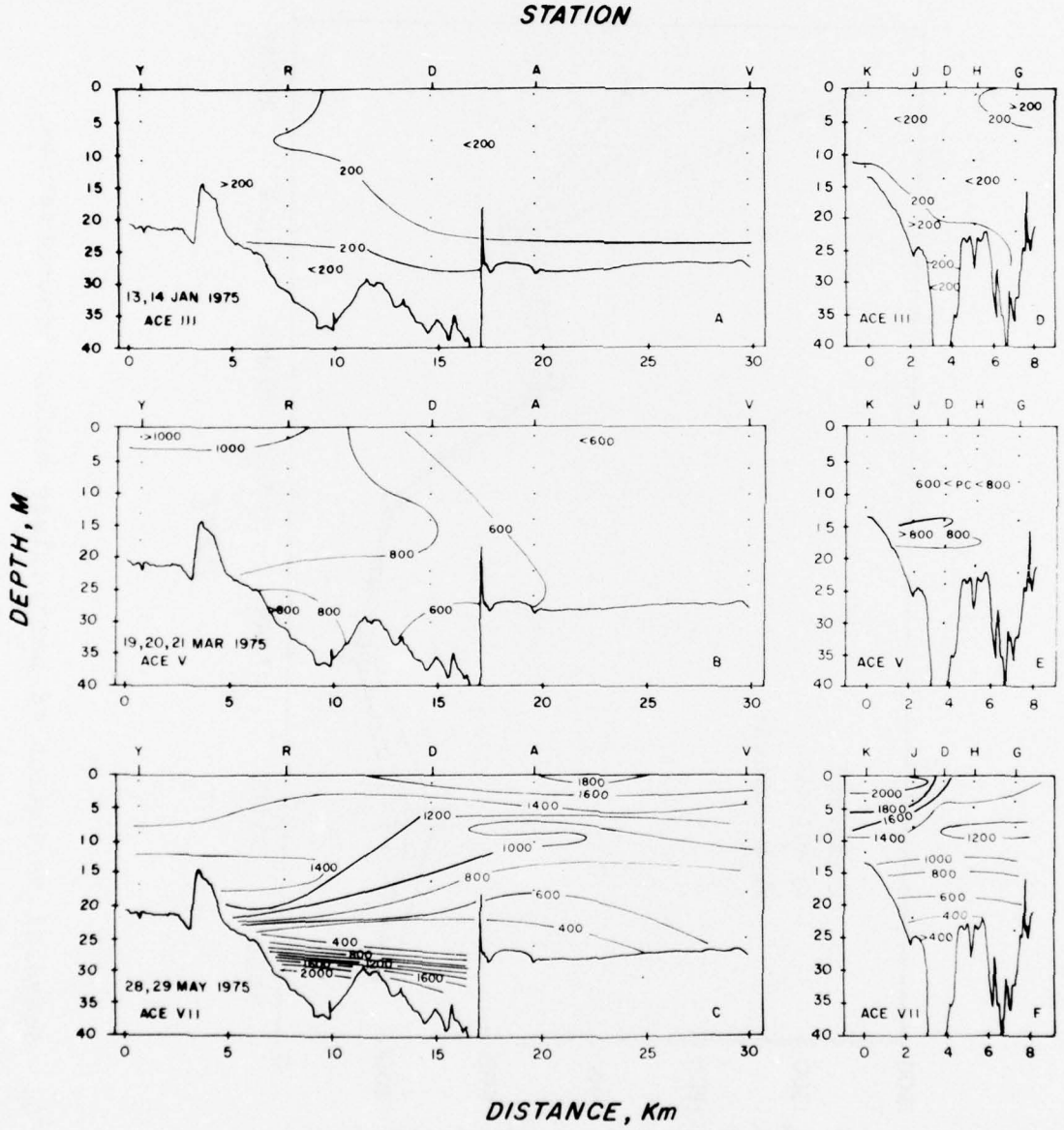



Figure 49. Vertical section of particulate carbon concentration (µg/l).

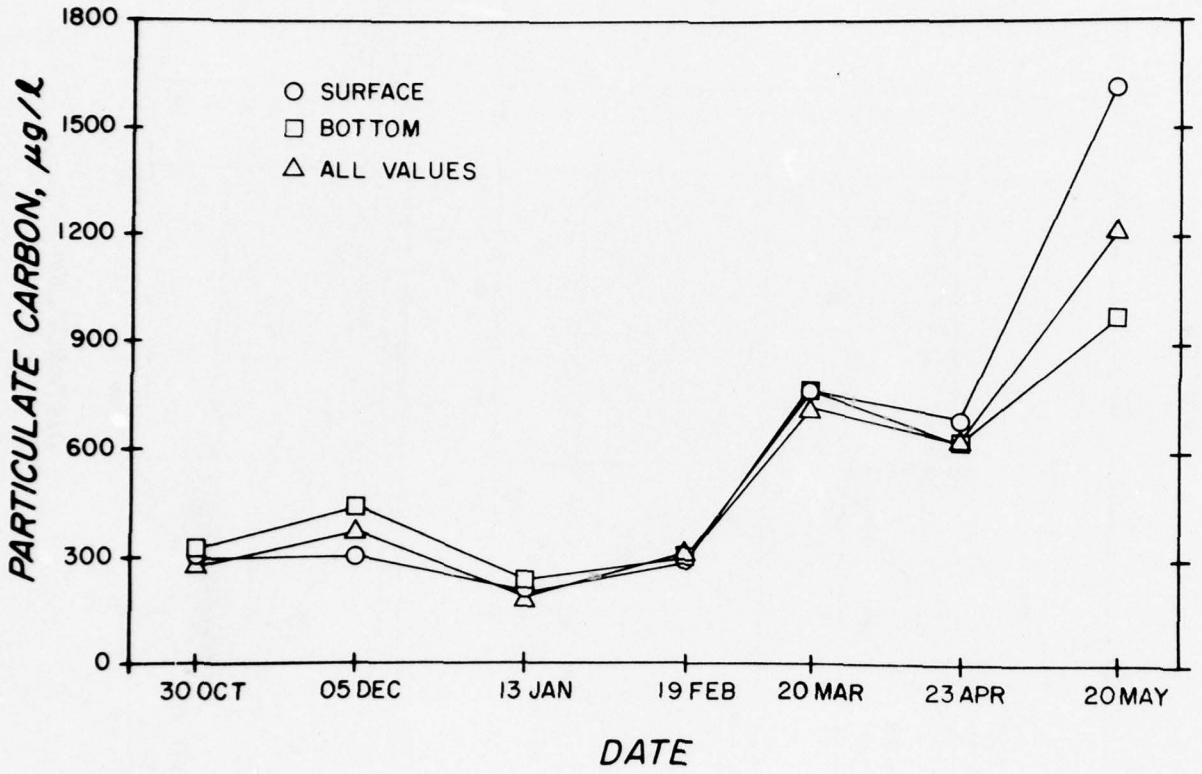



Figure 50. Seasonal variation of particulate carbon concentration.

observed during March, April, and May are due to increased biological production during these periods.

129. Particulate nitrogen. Figures 51 and 52 show the distribution of particulate organic nitrogen (PON) for the January, March, and May cruise periods. The distribution of PON essentially mimics the POC distribution just described. The seasonal cycle of mean PON concentrations is shown in Figure 53.

130. The lowest PON concentrations (~39 µg/l) were observed in January in which the spatial distribution was very nearly uniform (Figures 51 a,b; 52 a,d). PON concentrations were slightly elevated at the western end of the sampling area (Figure 52 a).

131. By March, PON had increased to about 100 µg/l and the spatial distribution was characterized by a strong concentration gradient increasing toward the west and, for many stations, decreasing with depth (Figures 51 c,d; 52 b).

132. The highest PON concentrations (~80-240 µg/l) were observed in May. However, during this period PON's were very patchy throughout the sampling area (Figure 51 e,f).

133. Chlorophyll a. The horizontal and vertical distributions of chlorophyll a concentrations for the January, March, and May sampling periods are presented in Figures 54 and 55. The seasonal cycle of mean chlorophyll a concentrations is given in Figure 56.

134. During the January period, chlorophyll a concentrations observed at all stations and depths were uniformly low, ~ 2 $mg/m^3$ (Figures 54 a,b; 55 a,d).

135. In March, chlorophyll a concentrations increased to 10-24 $mg/m^3$ in which the highest concentrations were observed at stations nearest the north shore of Long Island at the western end of the sampling area (Figure 54 c,d). Concentrations decreased with depth at all stations during the March

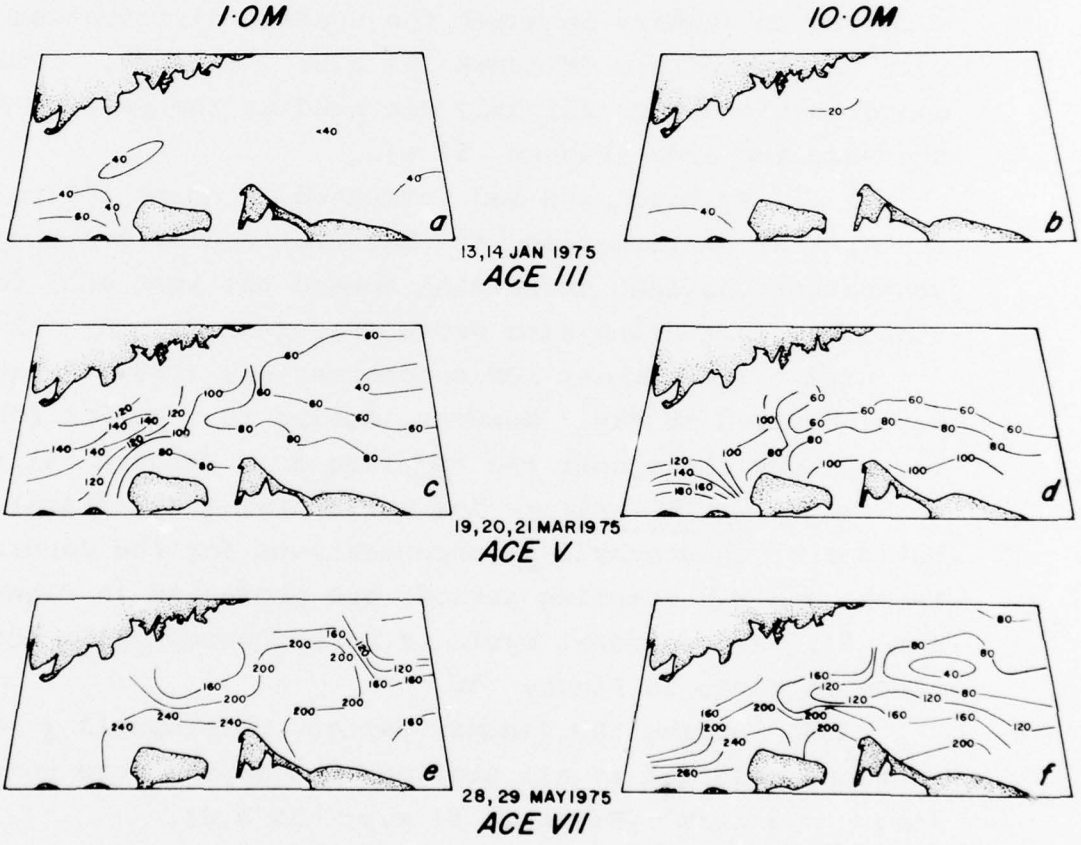



Figure 51. Horizontal distribution of particulate nitrogen concentration (µg/l).

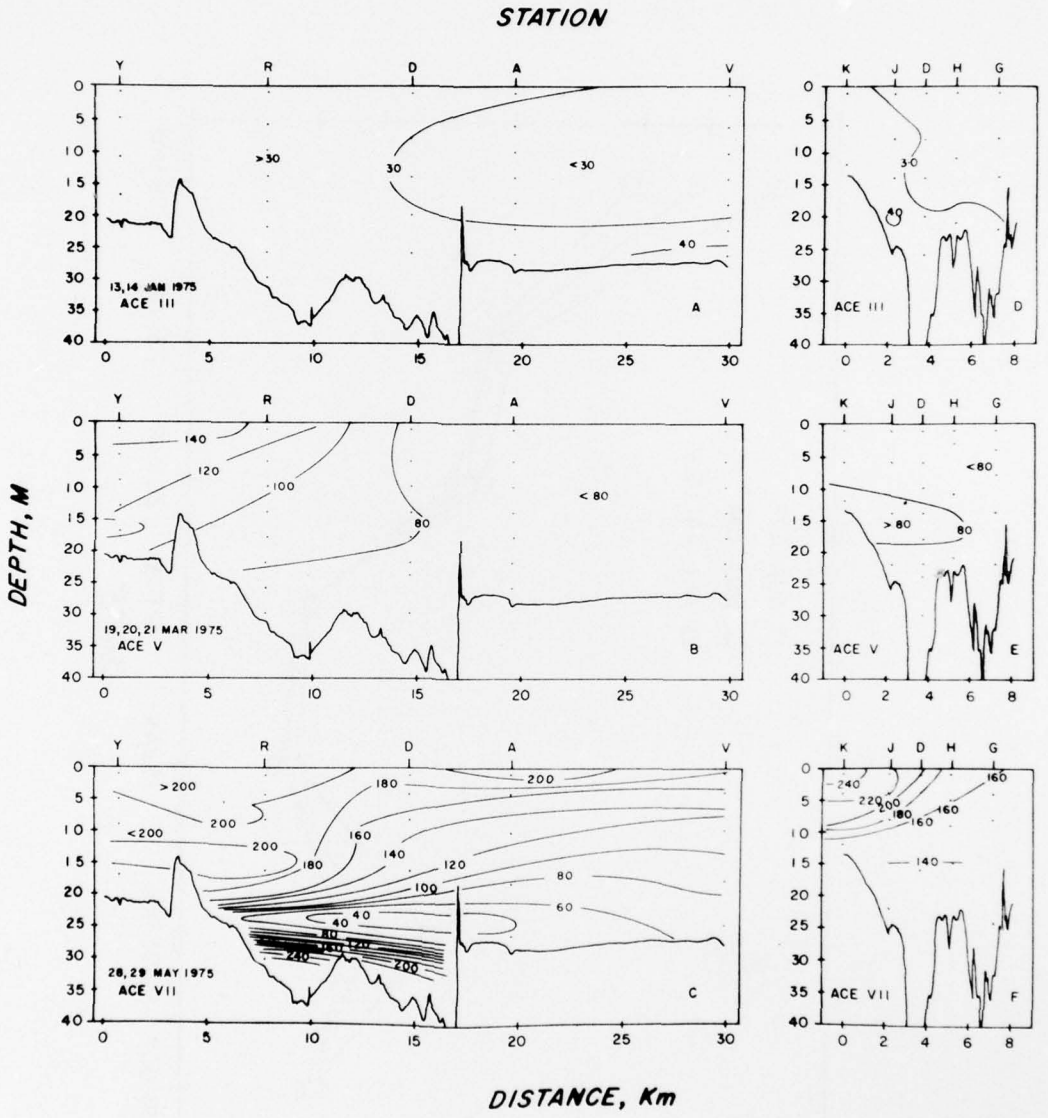



Figure 52. Vertical section of particulate nitrogen concentration (µg/l).

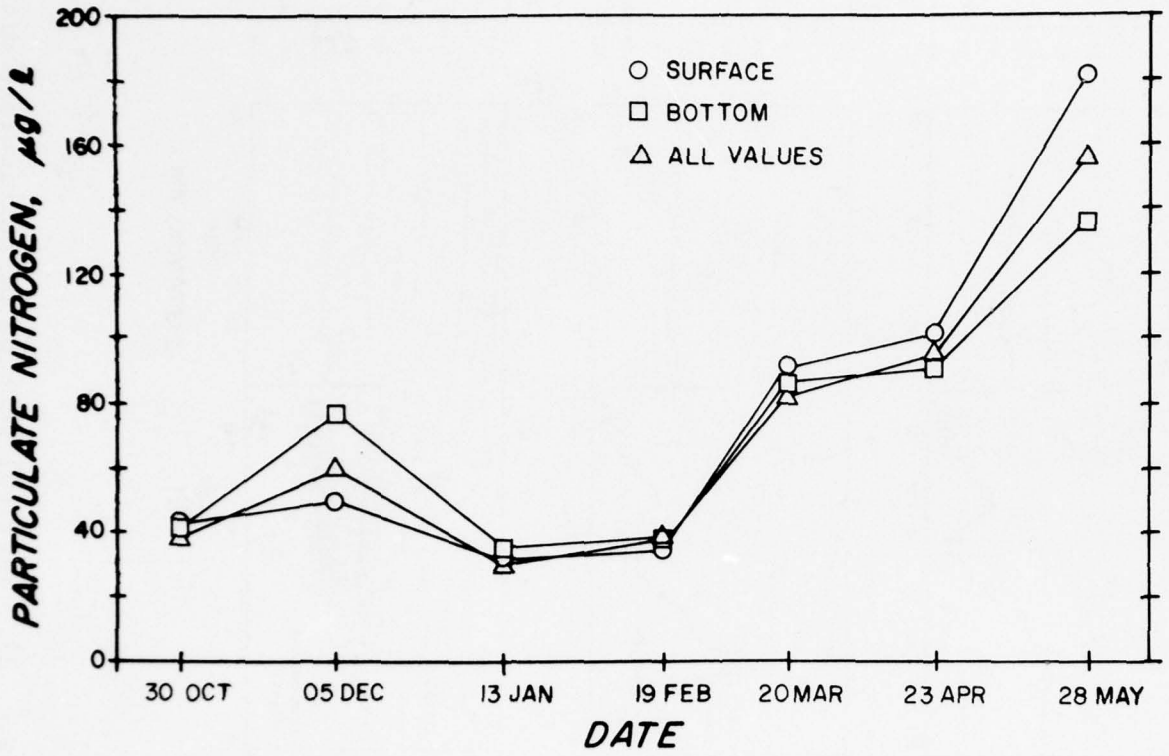



Figure 53. Seasonal variation of particulate nitrogen concentration.

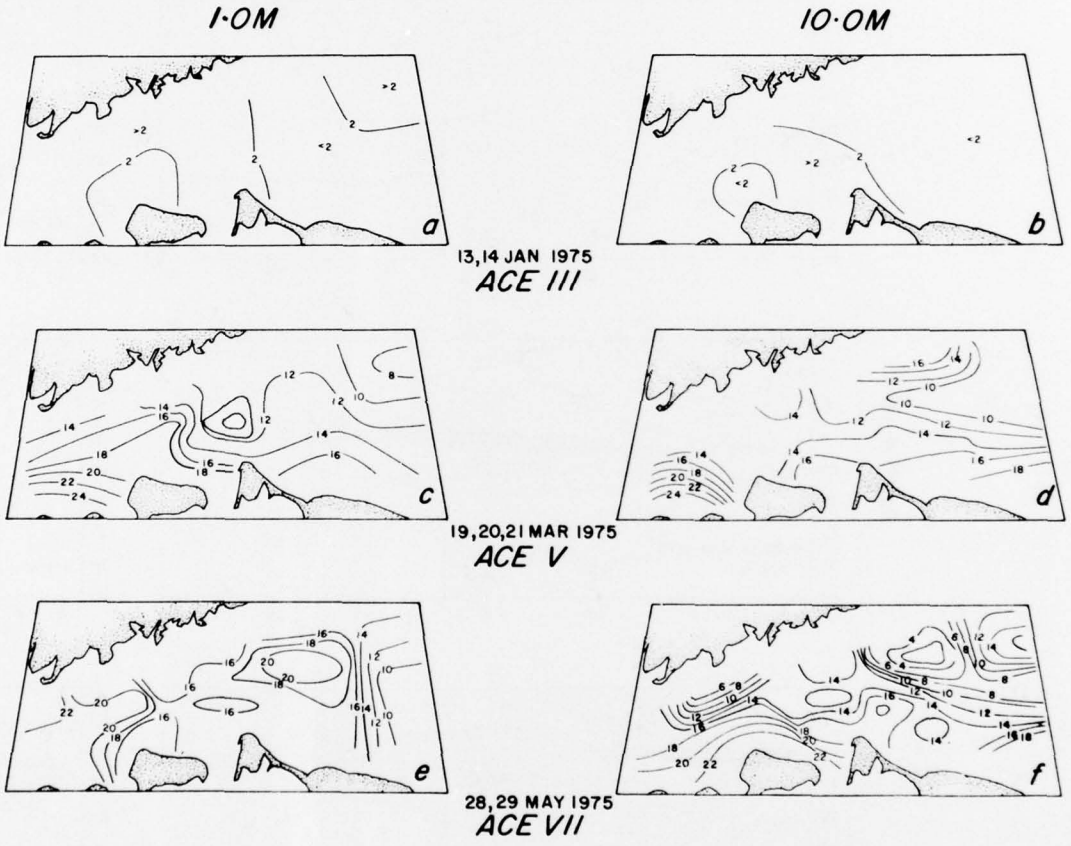



Figure 54. Horizontal distribution of chlorophyll a concentration ($mg/m^3$).

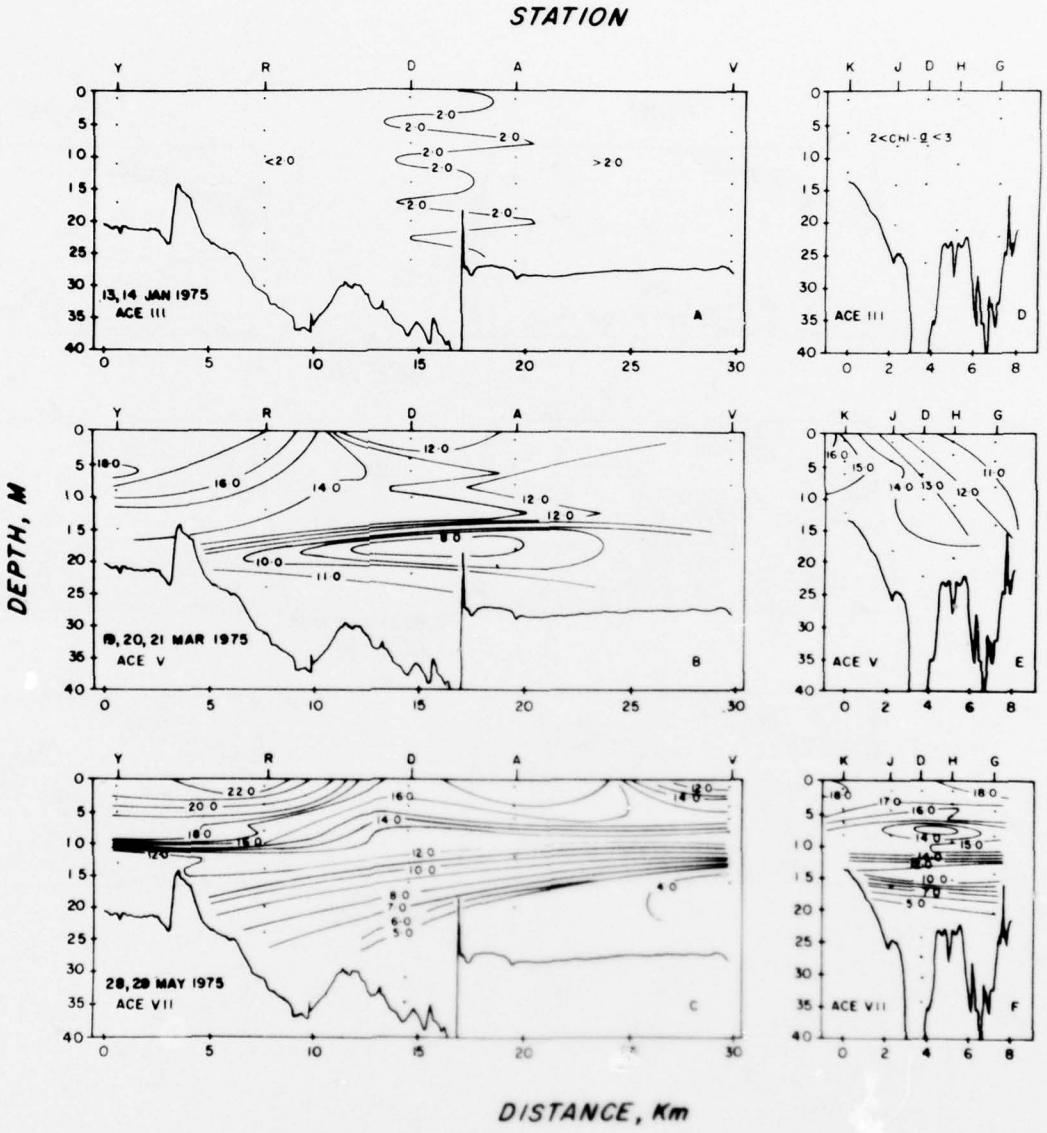



Figure 55. Vertical section of chlorophyll a concentration ($mg/m^3$).

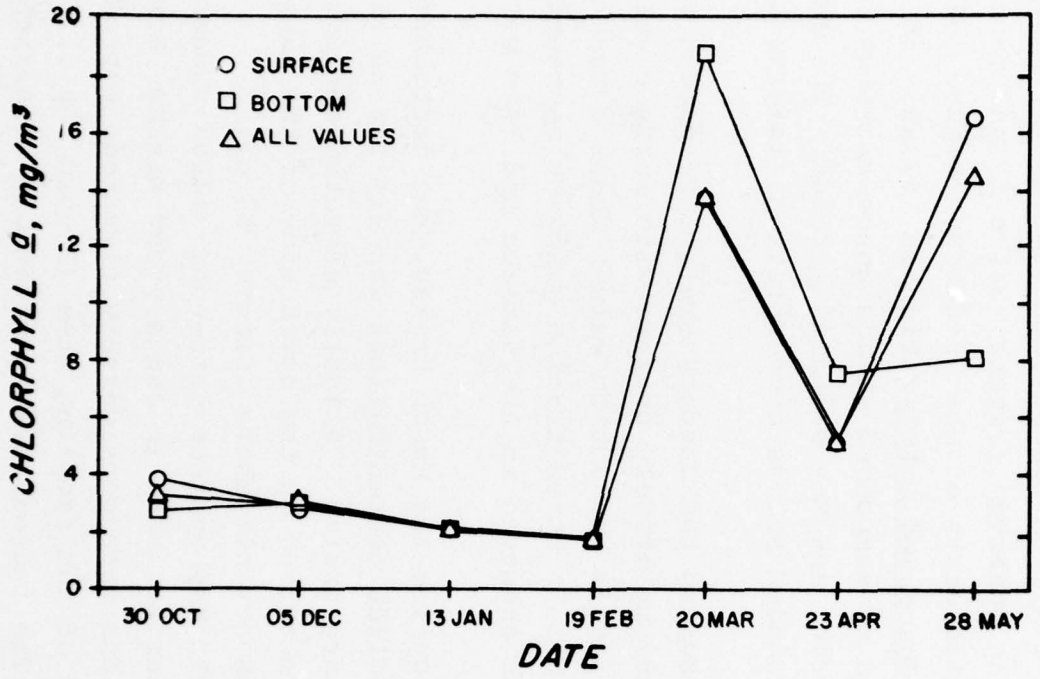



Figure 56. Seasonal variation of chlorophyll a concentration.

sampling period (Figure 55 b,e).

136. During the May sampling period, surface and 10-m chlorophyll a concentration levels occasionally exceeded 20 $mg/m^3$ (Figure 54 e,f) and the distributions were patchy. The higher chlorophyll a concentrations seem to be associated with shoreward stations on both sides of the sound (Figure 54 e,f). A concentration gradient, decreasing toward the east, was observed (Figure 54, e,f) and concentrations decreased with depth at most stations (Figure 54 c,f).

137. Suspended solids. Figures 57 and 58 show the distribution of suspended solids concentrations for the January, March, and May sampling periods. The seasonal cycle of mean suspended solids concentrations is presented in Figure 59.

138. During the January cruise, suspended solids concentrations were relatively uniform with surface values in the ~2-4 mg/l range and bottom values about 5 mg/l (Figures 57 a; 58 a). A concentration gradient increasing towards the west was observed in the surface and 10-m waters (Figure 57 a,b).

139. During the March cruise, the distribution of suspended solids concentrations was similar to that observed in the January cruise. Slightly elevated surface concentrations were observed on the north side of the sampling area near the Connecticut shore (Figure 57 c).

140. In May, surface suspended solids concentrations were again similar to those in January and March. However, bottom concentrations were considerably elevated, especially at the western end of the sampling area (Figure 58 c).

141. The increased concentrations of suspended solids observed in the December cruise (Figure 59) was due to sediment resuspension by a storm that passed through the area.[59]

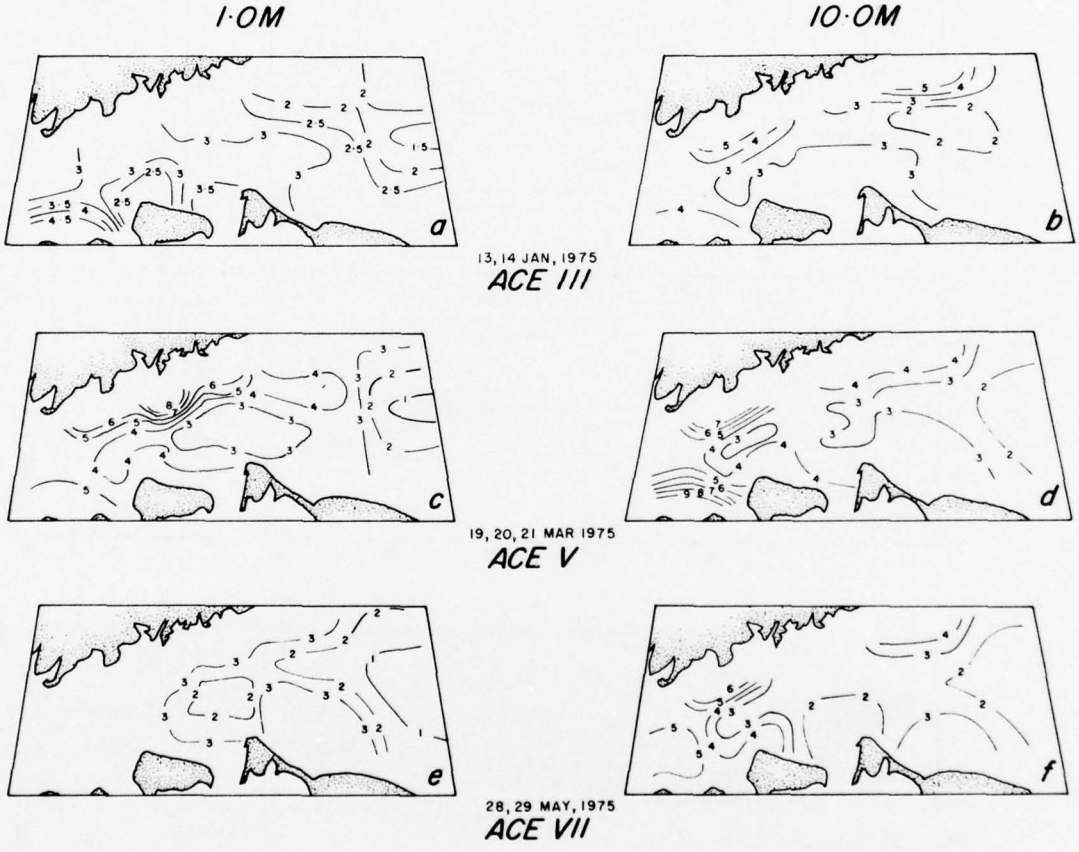



Figure 57. Horizontal distribution of suspended solids concentration (mg/l).

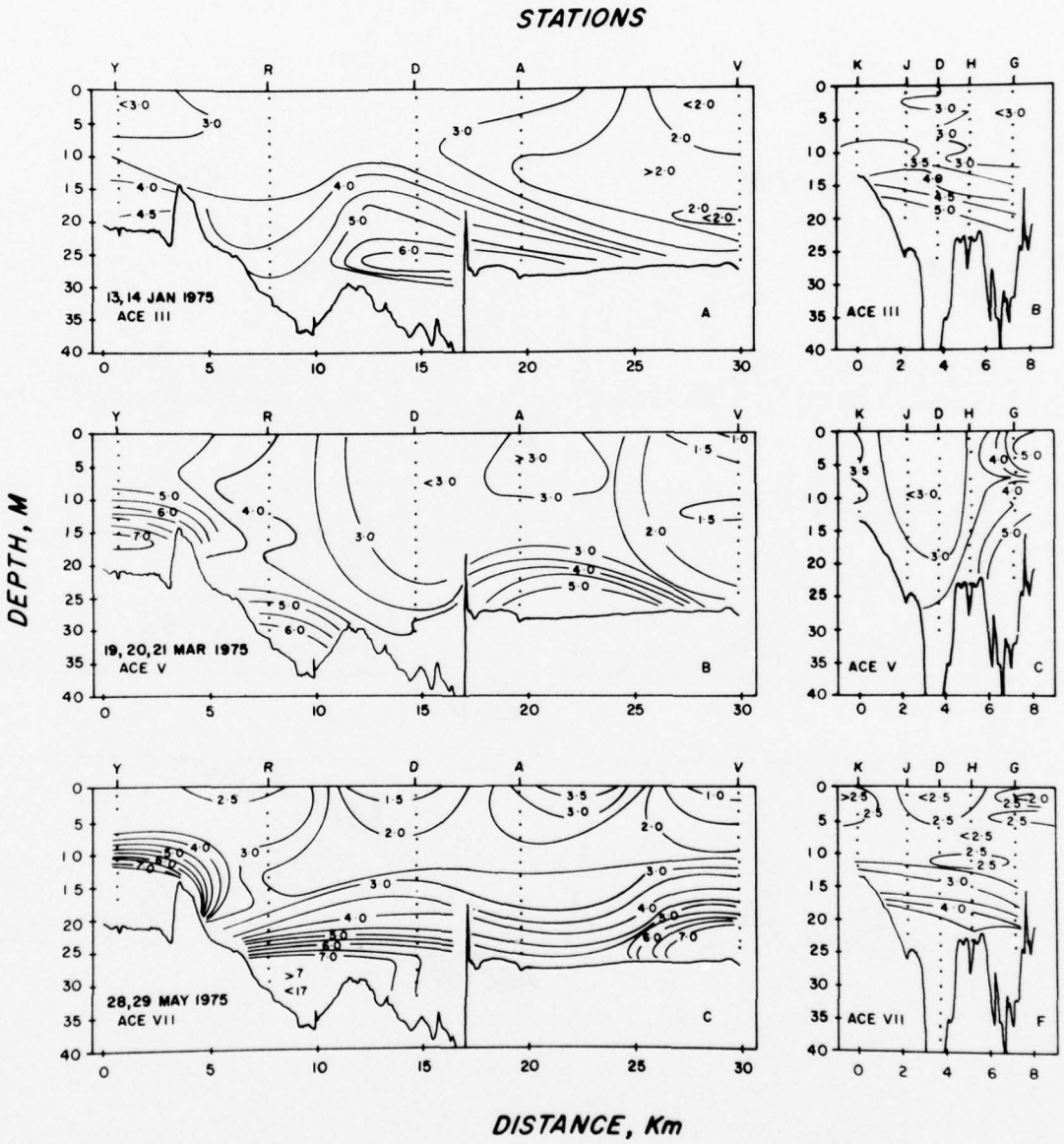



Figure 58. Vertical section of suspended solids concentration (mg/l).

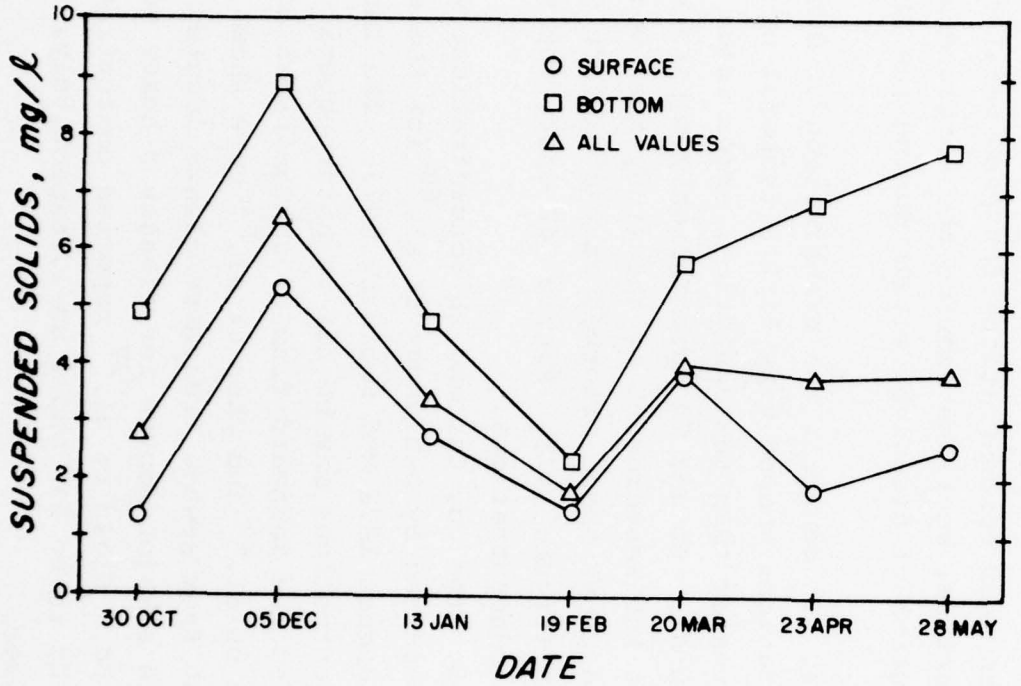



Figure 59. Seasonal variation of suspended solids concentration.

Figure 60 shows the typical size distribution of the suspended solids collected at selected stations in the sampling area.

142. Dissolved metals. The concentrations (µg/l) of dissolved Cd, Cu, Fe, Mn, Ni, Pb, and Zn were determined in approximately 165 samples and dissolved Hg in 28 samples.

143. Mean concentrations ranged from 0.6 µg/l for Cd to a high of 8.5 µg/l for Fe. Table 7 summarizes the low, high, and mean concentrations for each metal and Figure 61 shows vertical sections showing the longitudinal (east-west) distribution of dissolved metals during the January sampling period.

144. In general, the distribution of dissolved metal concentrations showed very little temporal or spatial variation greater than the analytical error which is given in Appendix A'. Pb and Cd were the only metals whose concentrations at the western end of the study area were slightly elevated above those observed at the eastern end of the transect (Figure 61). Figure 62 shows the seasonal cycle of mean concentrations.

145. The Cd, Cu, and Pb concentrations were about twice those reported by Dehlinger et al.[60] for the eastern sound during August 1972 and February 1973. The increased Pb and Cd concentrations may be due to anthropogenic inputs to the East River and the downward flux of contaminated aerosols. Mytelka et al.[26] and Chen et al.[61] have shown that discharged effluent from sewage treatment plants located on the East River is a major source for dissolved heavy metals, such as Pb and Cd. Klein et al.[27] reported concentrations of dissolved Pb and Cd to be 530 and 3 ug/l,respectively, for the lower East River.

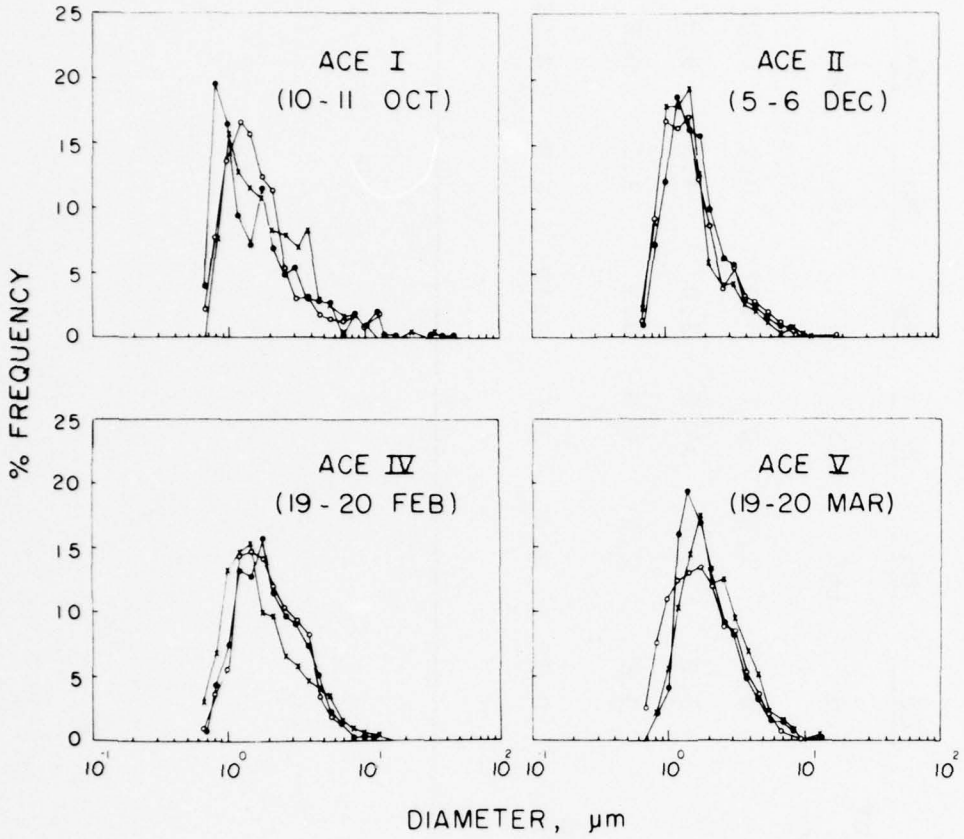



Figure 60. Size frequency of suspended solids.

Table 7

Dissolved Metal Concentrations (ug/l)

| | Cd | Cu | Fe | Hg | Mn | Pb | Zn |
|---|---|---|---|---|---|---|---|
| Number of samples analyzed | 165 | 166 | 165 | 28 | 165 | 165 | 166 |
| Low | 0.02 | 1.5 | 0.1 | 0.01 | 0.1 | 0.02 | 1.0 |
| High | 3.2 | 5.6 | 33.6 | 2.0 | 7.8 | 9.3 | 54.1 |
| Mean | 0.6 | 2.5 | 8.5 | 0.7 | 2.1 | 0.8 | 5.4 |
| Standard Deviation | 0.32 | 0.4 | 3.1 | 0.43 | 0.9 | 0.56 | 2.8 |

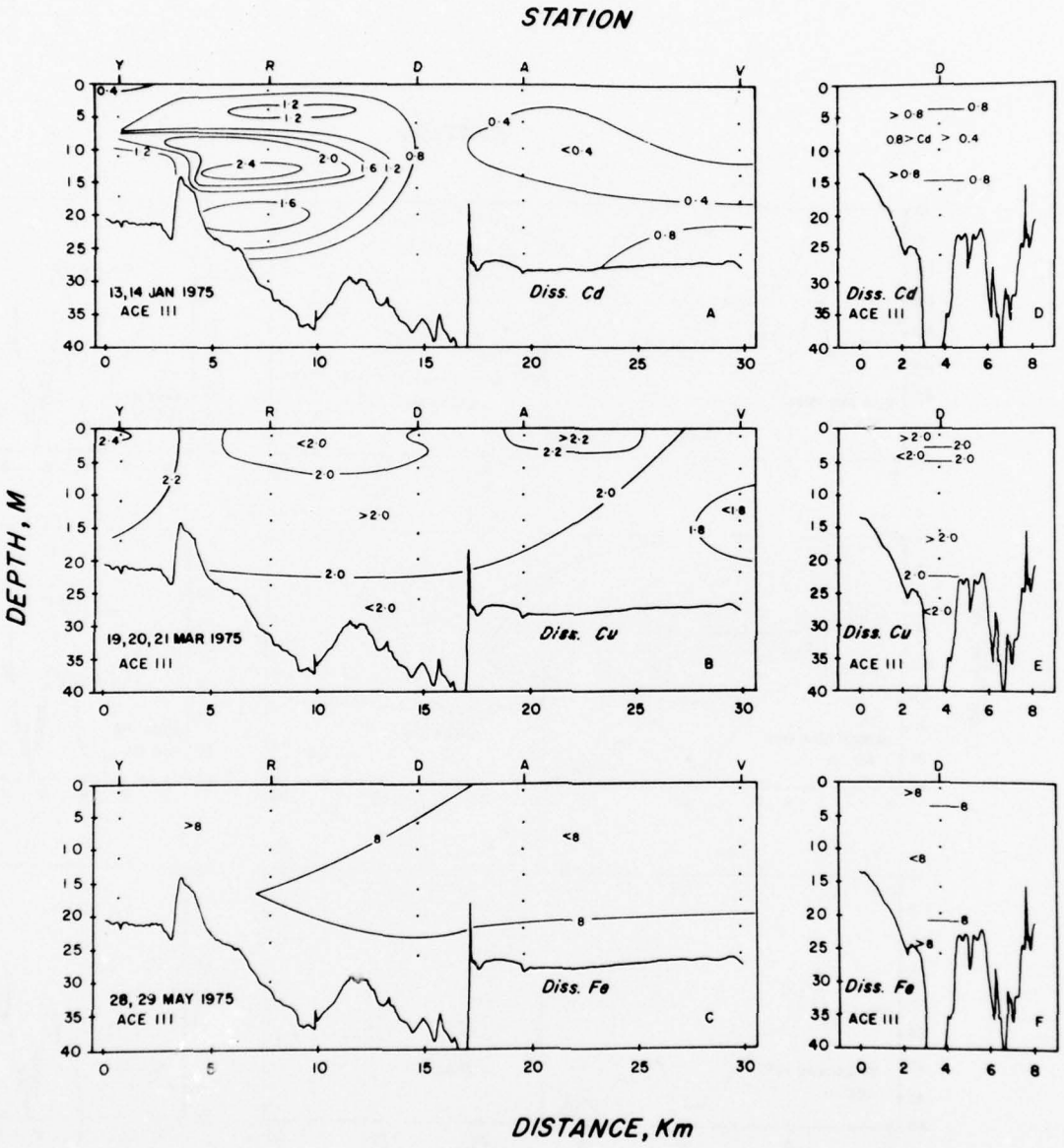



Figure 61. Vertical section of dissolved metals concentration (µg/l), 13-14 Jan. 1975.

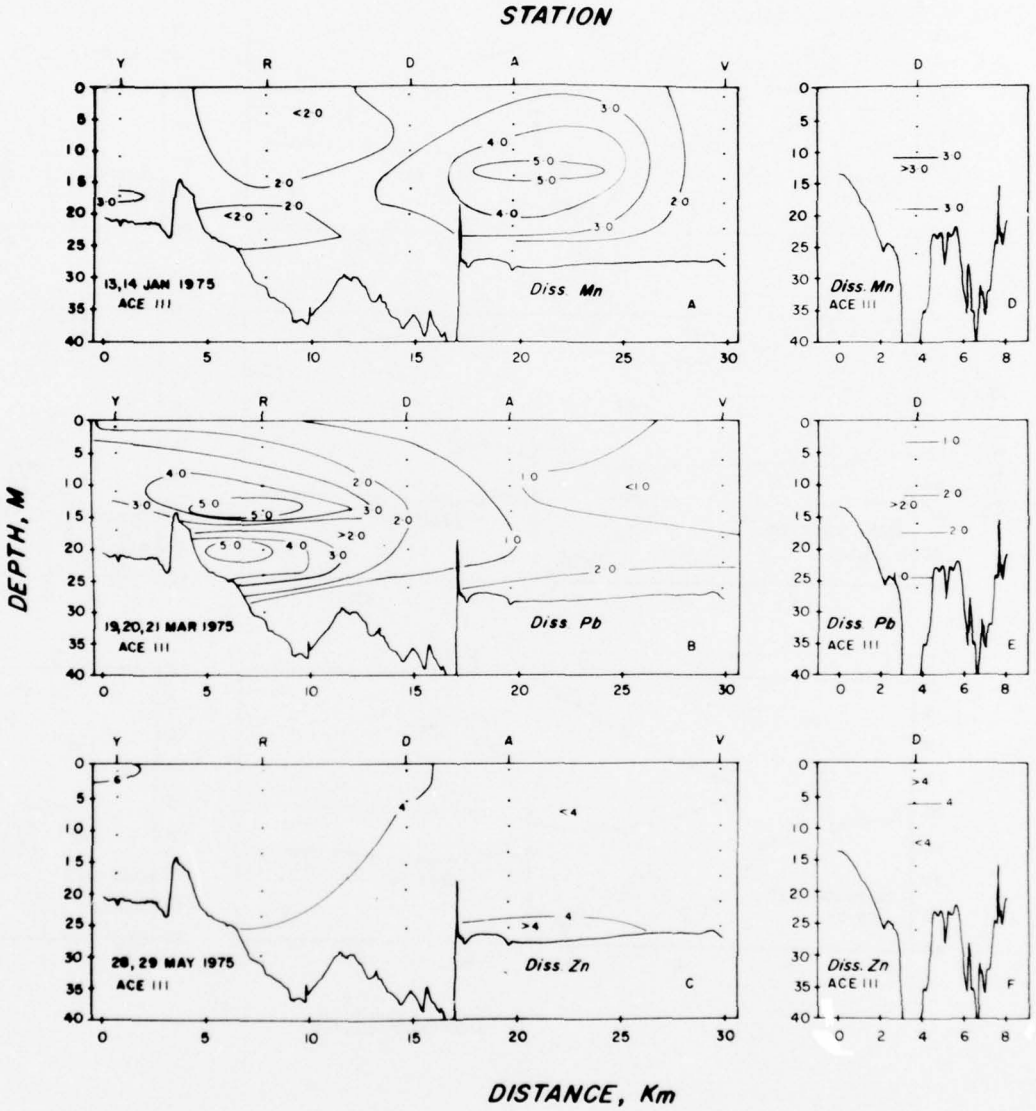



Figure 61. (continued)

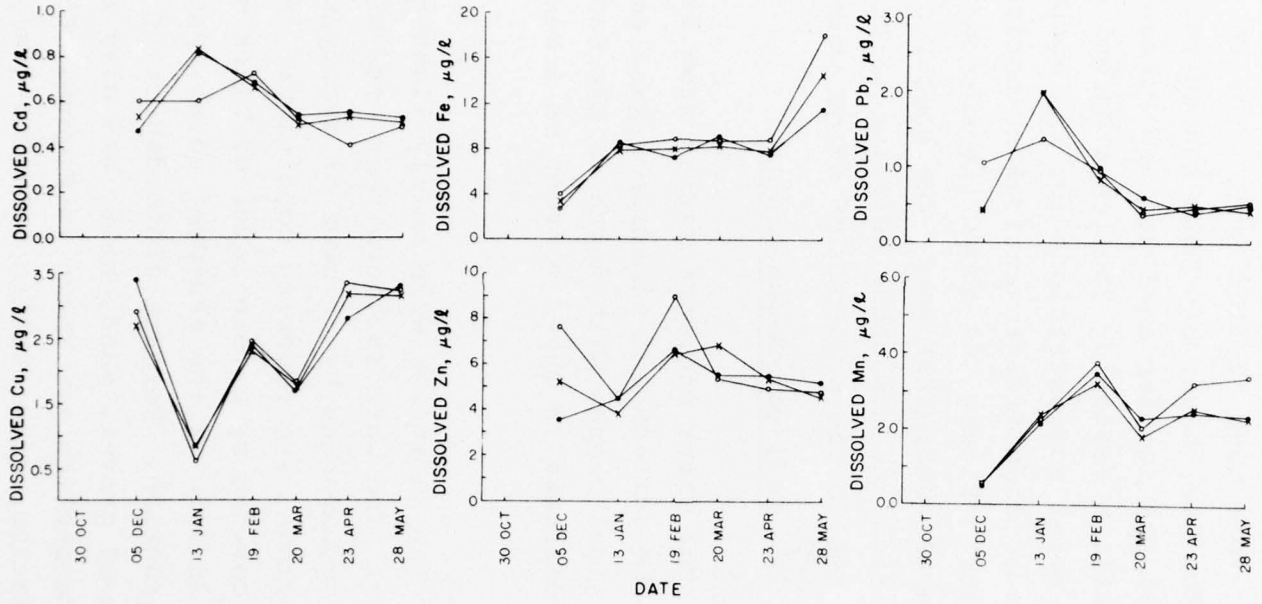



Figure 62. Seasonal variation of dissolved metal concentration.

146. Suspended metals. The concentrations (µg/l) of Ag, Cd, Cr, Cu, Fe, Hg, Mn, Pb, and Zn were determined in 164 to 192 samples. Mean concentrations ranged from a low of 0.010 µg/l to a high of 1330 µg/l for Fe. Table 8 summarizes the low, high, and mean concentrations of suspended metals in all the samples analyzed and Figure 63 shows vertical sections depicting the longitudinal distribution of particulate metal concentrations for the January cruise. The figure shows no significant vertical or horizontal concentration gradients. Figure 64 shows the seasonal cycle of suspended metal concentrations. The higher concentration of particulate iron and manganese relative to the other metals is probably due to the presence of oxide phases.[62]

## Sediment Geochemistry

### Water content

147. The water contents varied from 10.9 to 76.3 percent by mass in the surface and subsurface samples. The most obvious physical change with depth in the sediments was a systematic decrease in water content as a result of sediment compaction.

### Texture

148. The sediments were mainly light-gray to black clayey silts. The core sections that were black in color were invariably accompanied by an odor of hydrogen sulfide, thus reflecting prevailing reducing conditions. Many sediment cores were covered by a thin layer of black organic-rich muddy material. In some of the sediment cores, sand was the dominant size fraction. Ternary plots depicting the relative proportions of gravel, sand, silt, and clay fractions present in each core section are shown in Figures 65- 70. The station designation, core section interval (cm), cruise number, and sediment type for each core are also given.

Table 8

Particulate Metal Concentrations (ug/l)

In Water Colum Samples

| | Ag | Cd | Cr | Cu | Fe | Hg | Mn | Pb | Zn |
|---|---|---|---|---|---|---|---|---|---|
| Number of samples analyzed | 190 | 164 | 192 | 192 | 192 | 192 | 192 | 190 | 178 |
| Low | 0.0024 | 0.0024 | 0.076 | 0.088 | 8.0 | 0.0032 | 4.8 | 0.16 | 0.016 |
| High | 0.095 | 0.061 | 4.7 | 9.2 | 1330 | 0.074 | 240 | 4.2 | 120 |
| Mean | 0.020 | 0.010 | 0.71 | 0.88 | 115 | 0.019 | 17.8 | 0.66 | 3.9 |
| Standard Deviation | 0.0098 | 0.0087 | 0.54 | 0.66 | 74 | 0.010 | 11.6 | 0.34 | 7.1 |

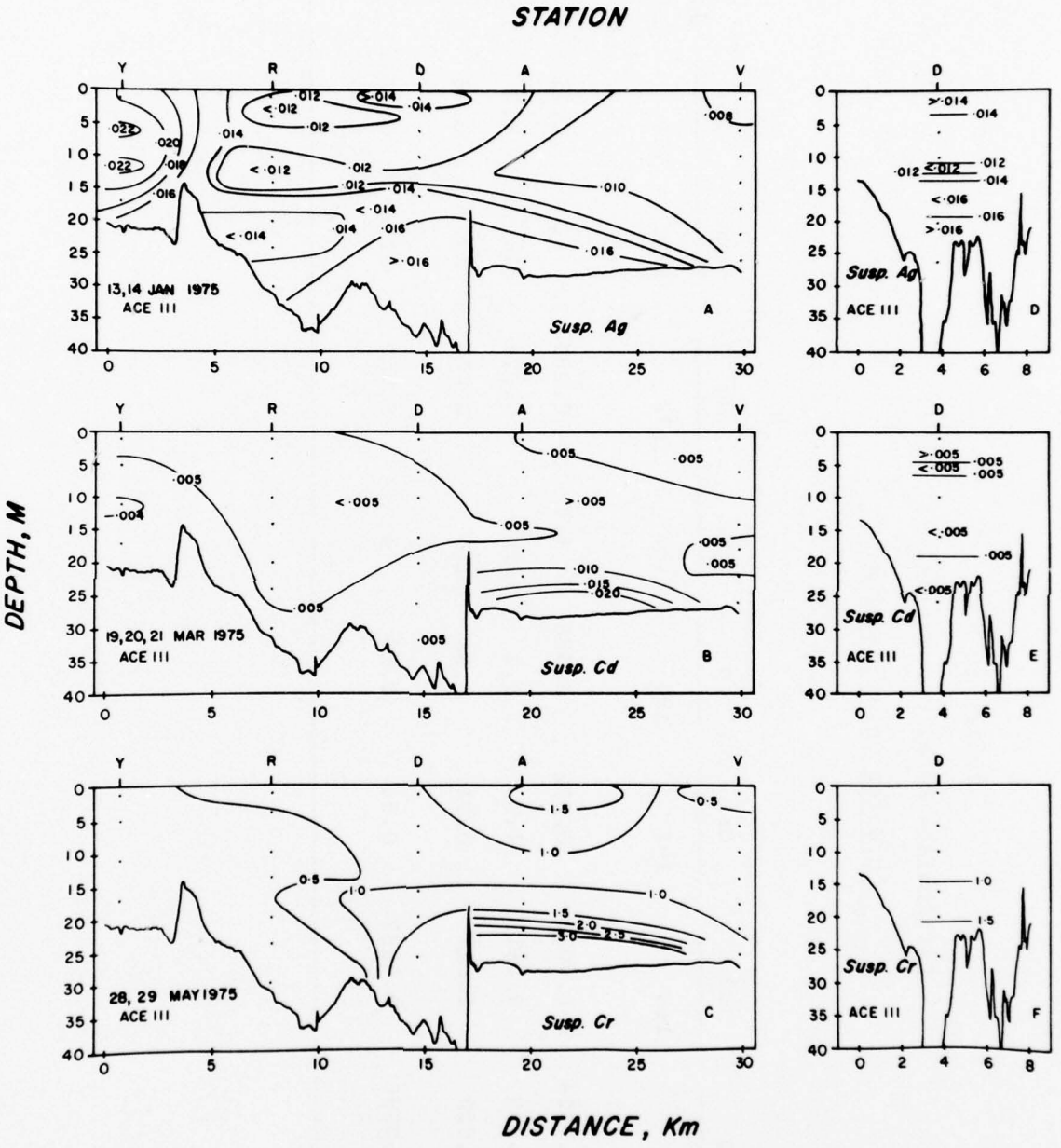



Figure 63. Vertical sections of suspended metals concentration (µg/l), 13-14 Jan. 1975.

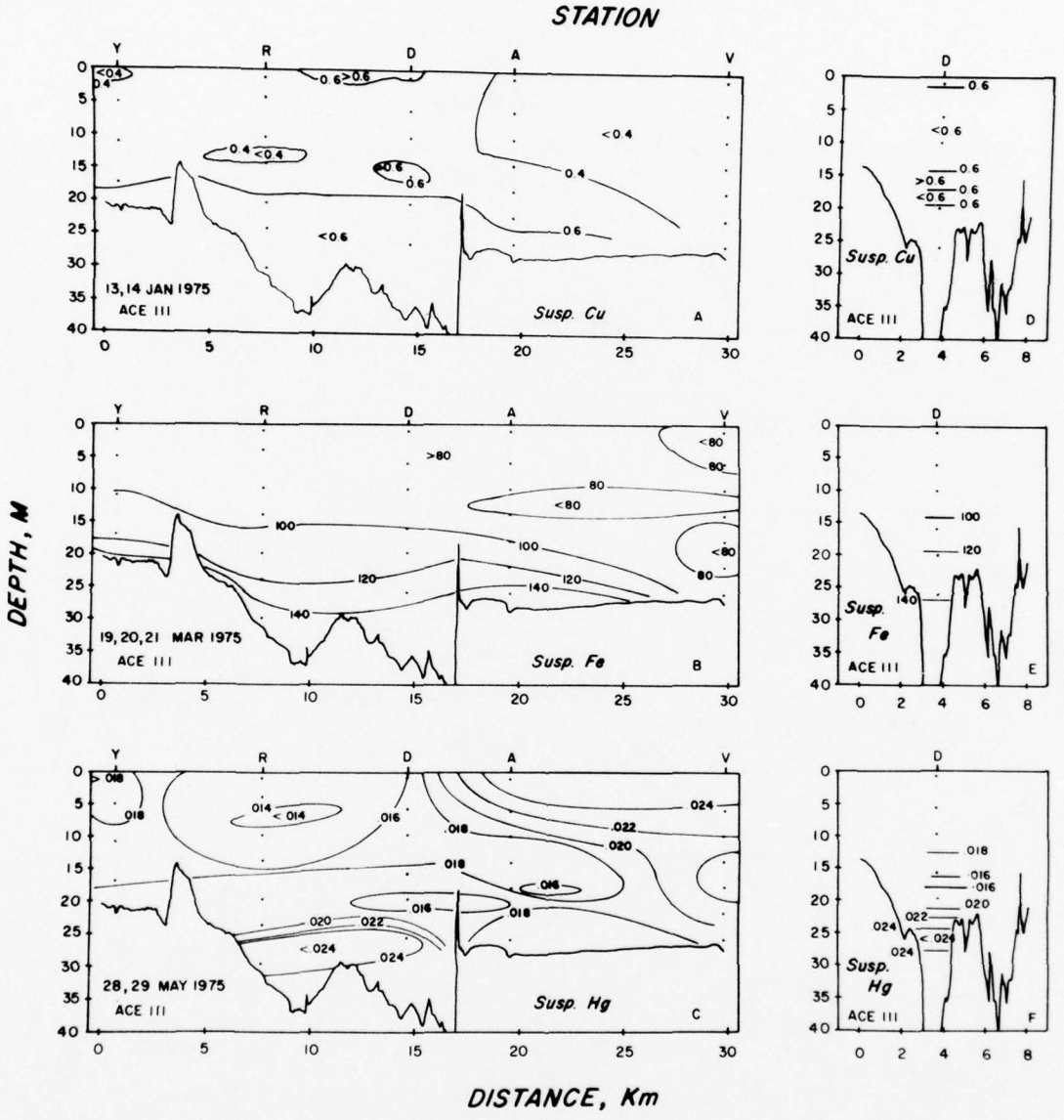



Figure 63. (continued)

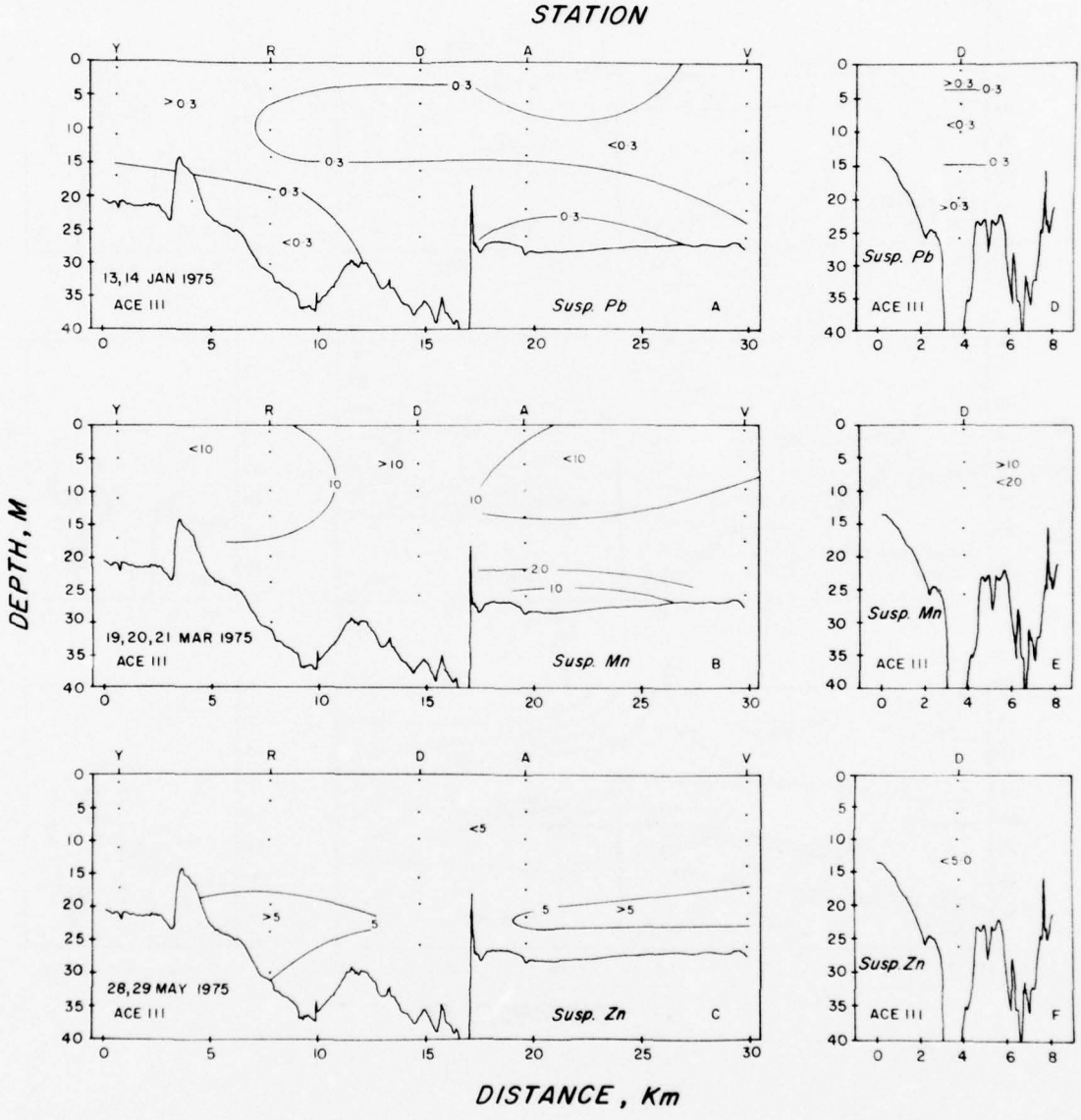



Figure 63. (continued)

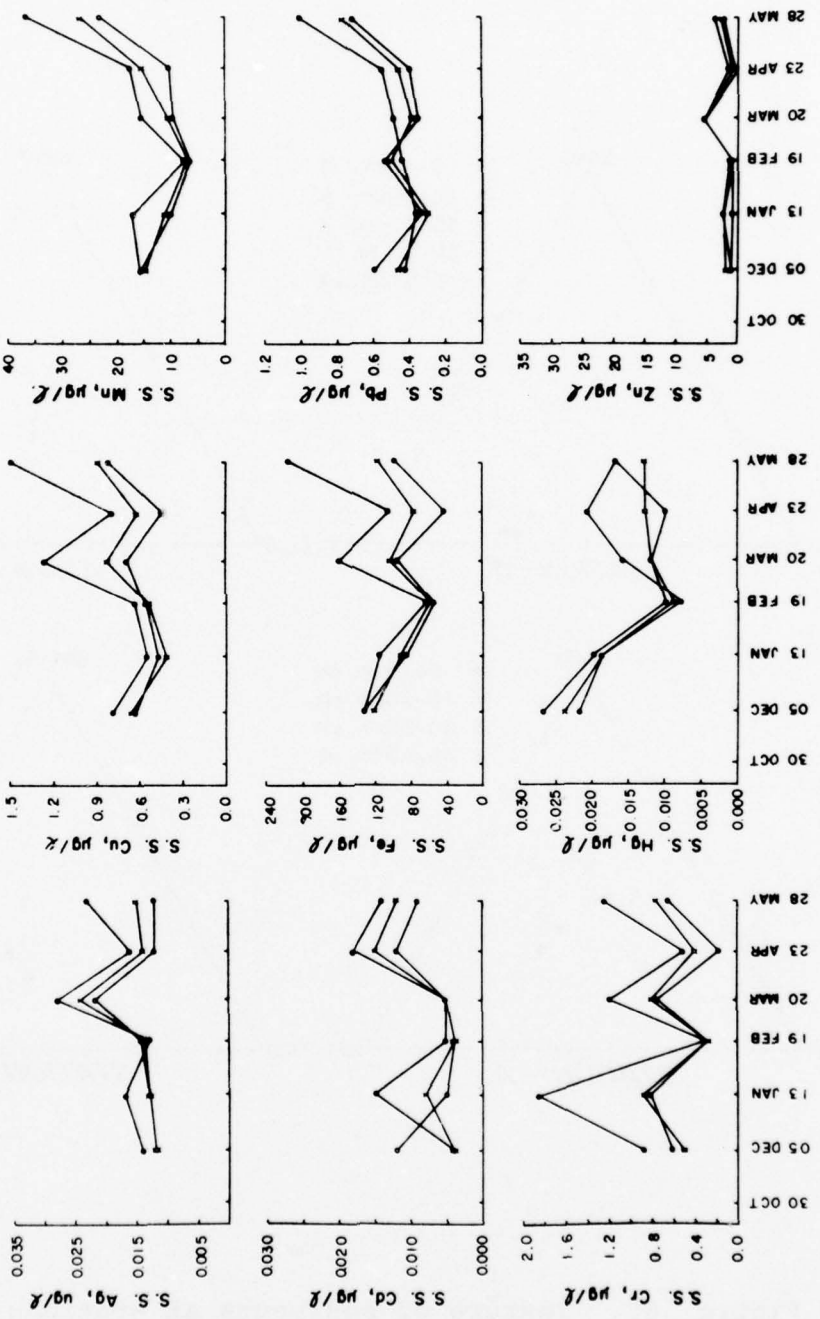



Figure 64. Seasonal variation of suspended solids concentration.

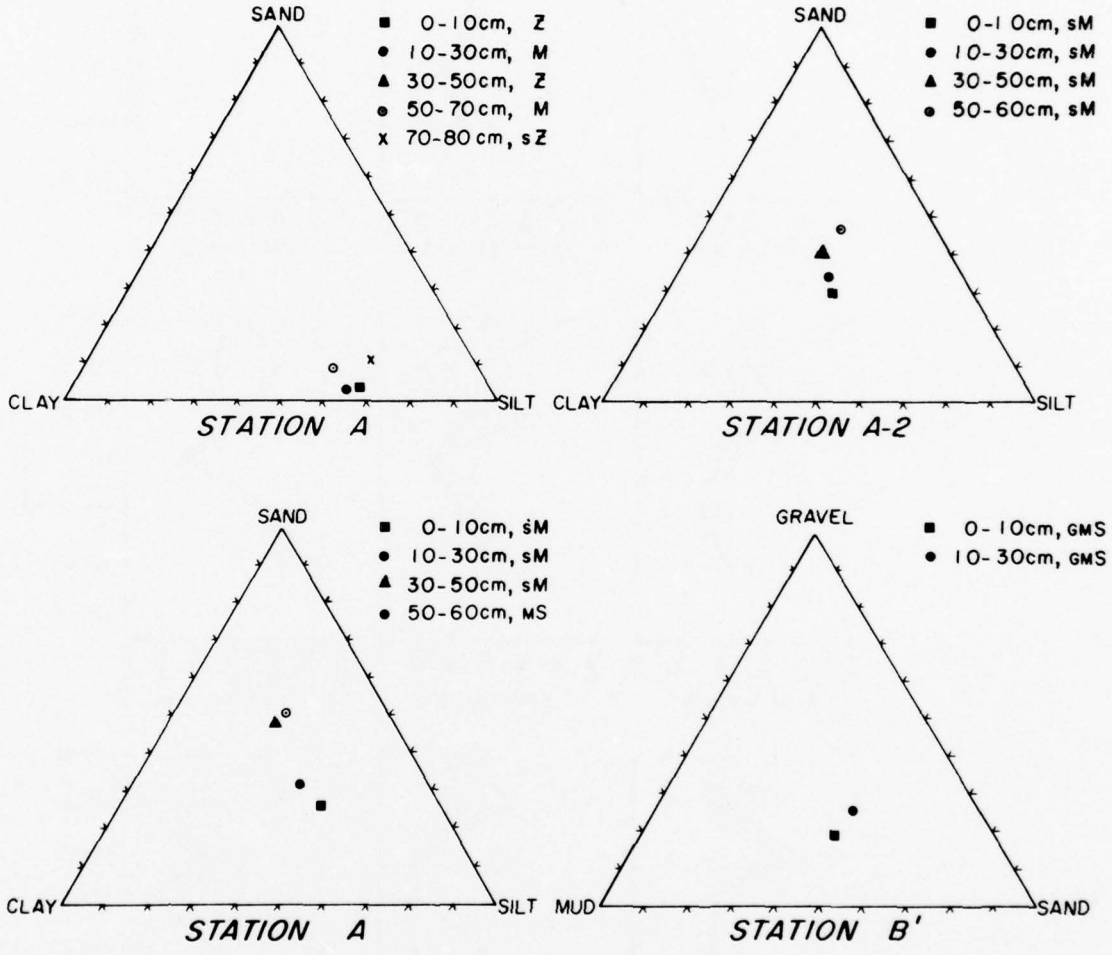



Figure 65. Texture of sediments at stations A and B.

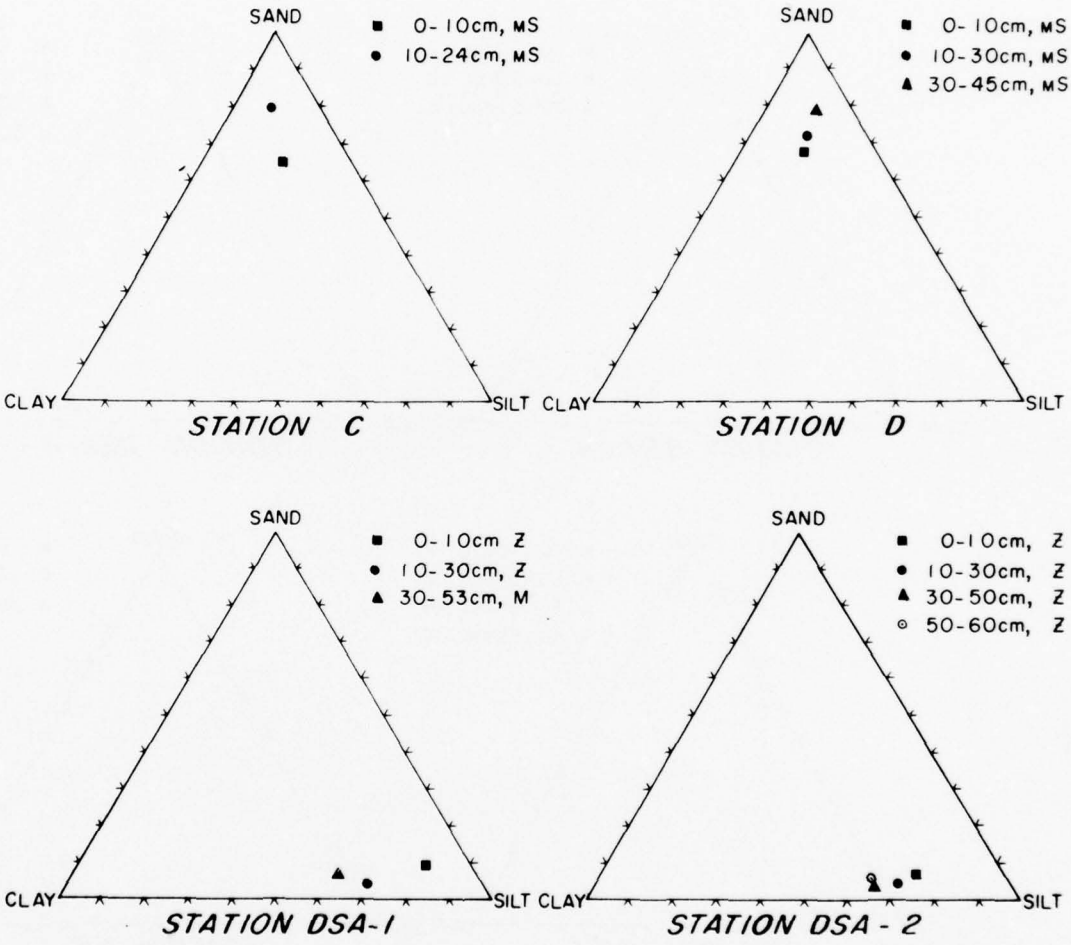



Figure 66. Texture of sediments at stations C, D, DSA-1, and DSA-2.

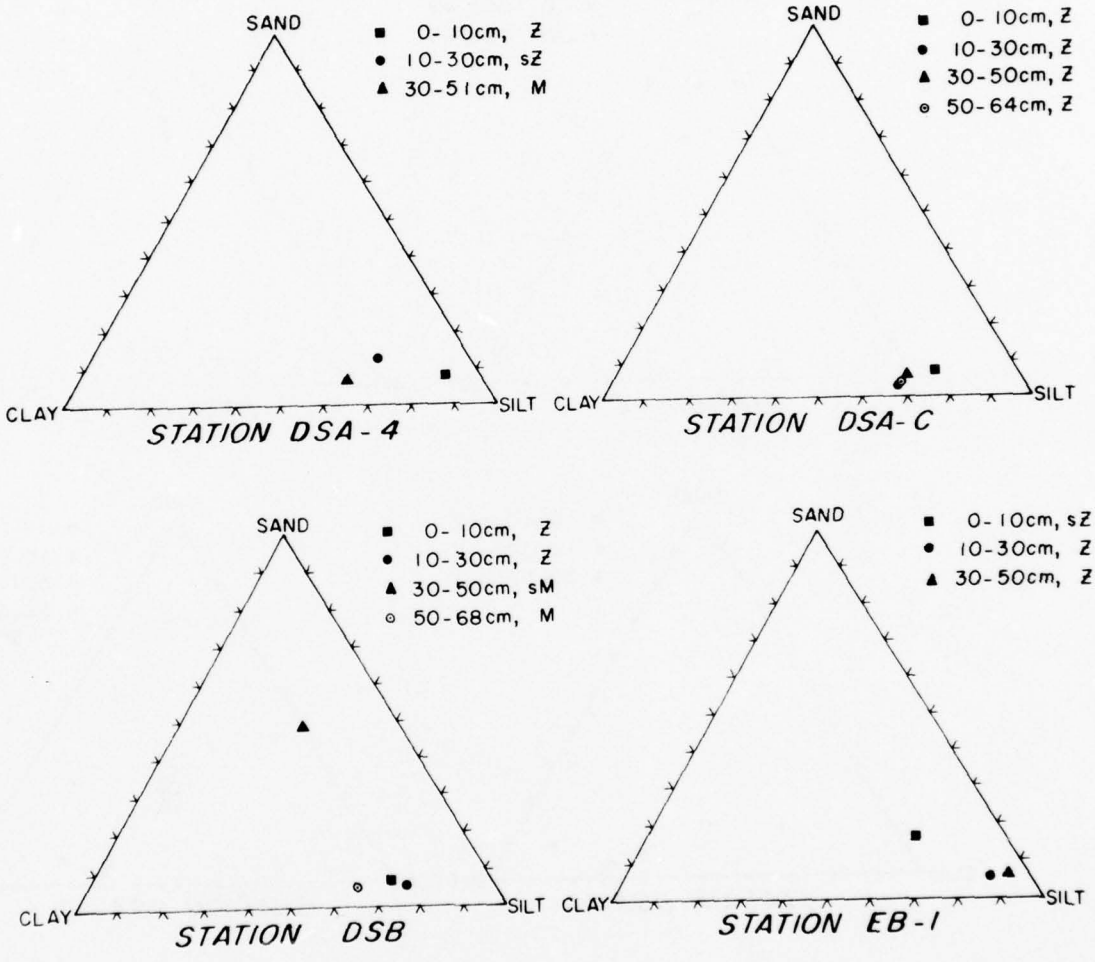



Figure 67. Texture of sediments at station DSA-4, DSA-C, DSB, and EB-1.

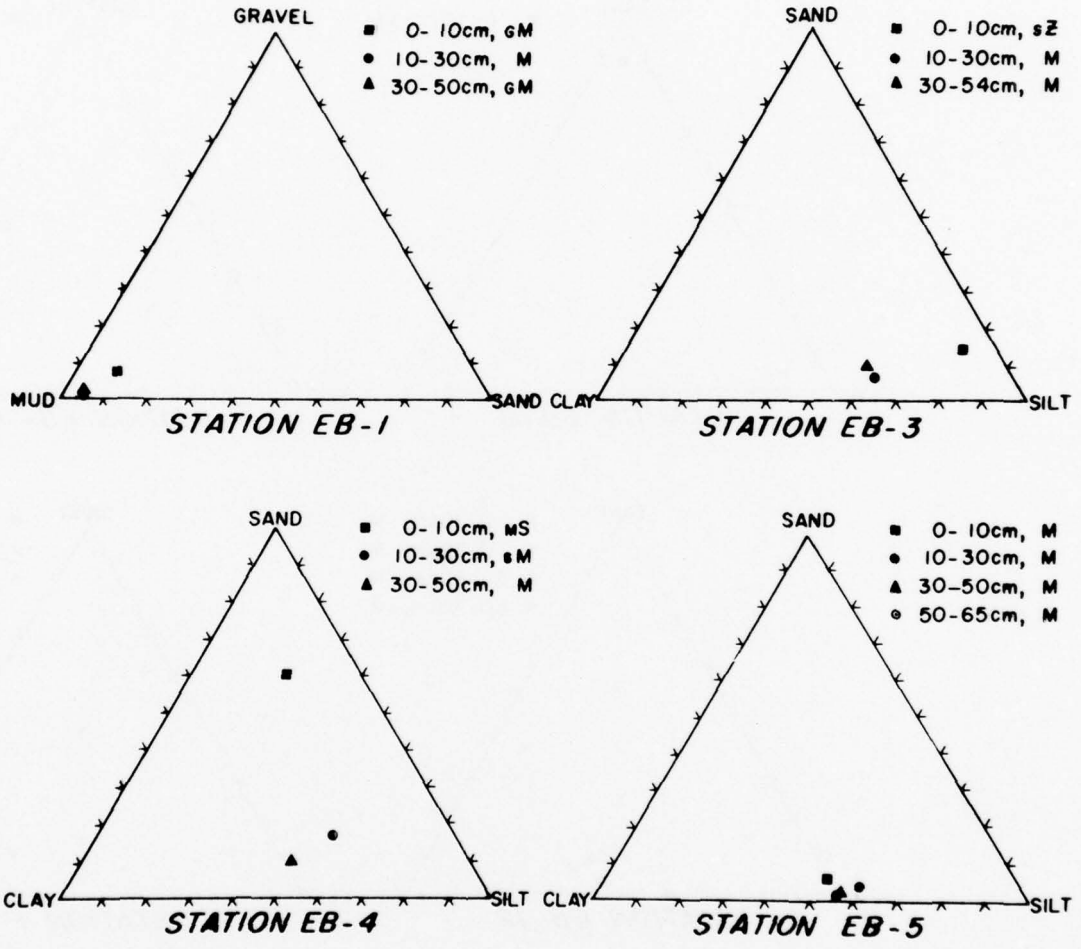



Figure 68. Texture of sediments at stations EB-1, EB-3, EB-4, and EB-5.

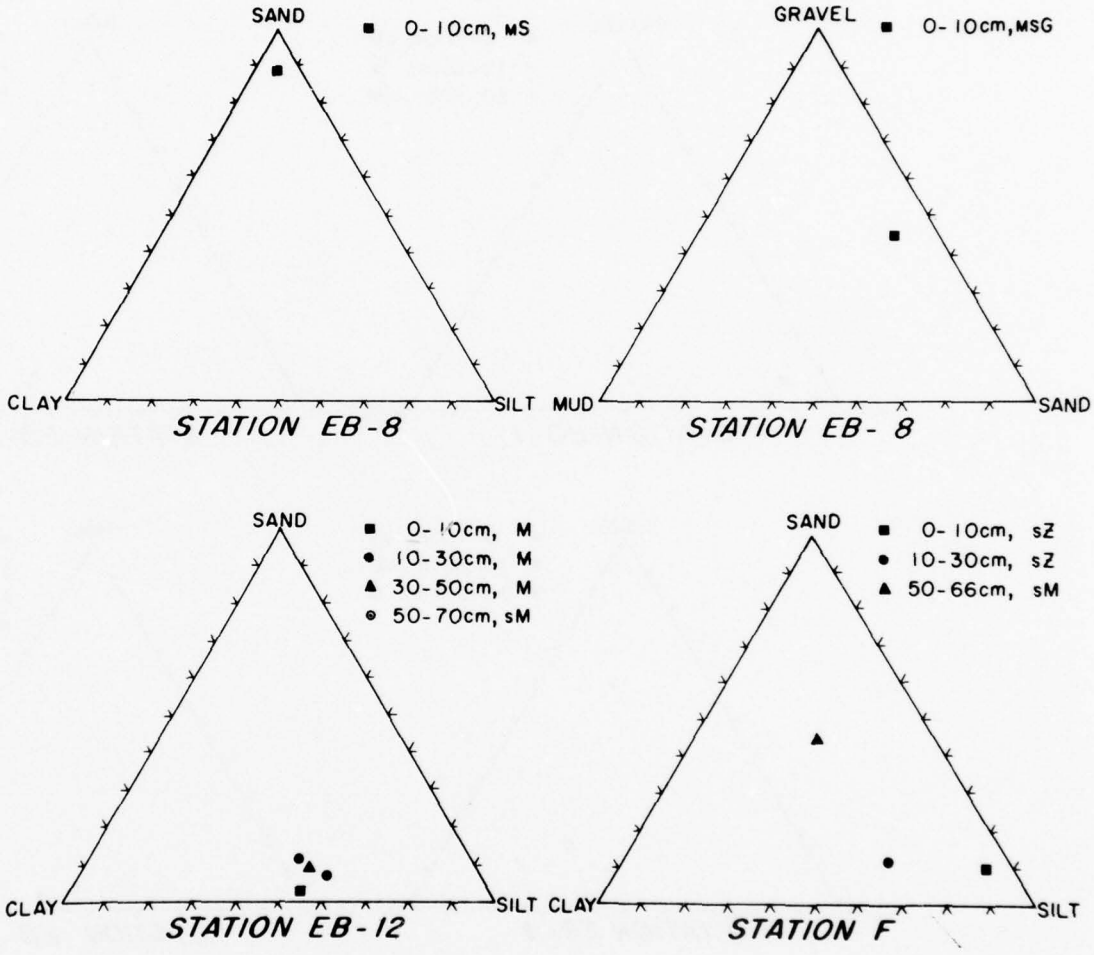



Figure 69. Texture of sediments at stations EB-8, EB-12, and F.

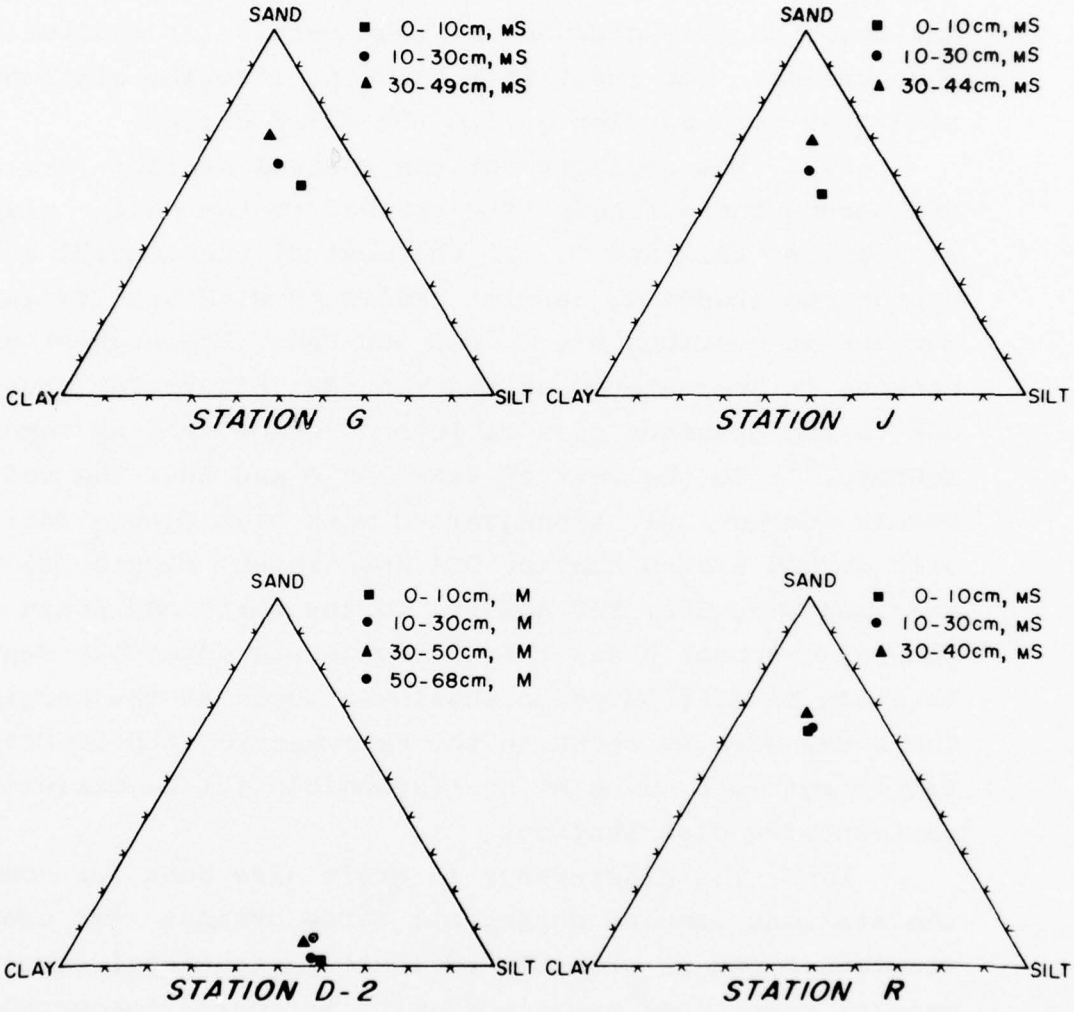



Figure 70. Texture of sediments at stations G, J, D-2, and R.

149. The relative distribution of gravel, sand, silt, and clay fractions in near-surface sediments in the area of study are shown in Figures 71- 74. Values given at each station correspond to the top sections of cores collected during the first, second and third cruises. Hyphen (-) indicates no core obtained at that particular station for that cruise. The inset is a blow-up of coring stations around DSA3 that were sampled during the third cruise.

150. The sediments at the control station are sandy and become increasingly fine-grained to the east - clayey silt at stations EB12 and O. To the west of the control site, the bottom mud grades to sandier sediments with significant gravel content at stations B', C, EB8 and EB4. The highest gravel content is encountered at station EB8 (Figure 70) presumably due to the presence of a cable and anchor reef as reported by McCrone.[63] To the west of stations D and EB4, the sediments become increasingly fine-grained with high concentrations of silt at and around station DSA (see inset, Figure 72) and stations EB5, EB1, EB3 and F. To the north and south of the general disposal area, the sediments are generally sandy. This can be attributed to shallower depth at the margins of the study area as shown in the bathymetric map in Figure 1. Bottom currents may also be responsible for maintaining this pattern size distribution.

151. The discrepancy in grain size data for some of the stations sampled during all three cruises (for example, stations A and D) probably reflects navigational error and general patchiness associated with irregular topography in the area of study.

pH-Eh

152. The pH readings indicated slightly alkaline to acidic conditions in the core sections that were examined.

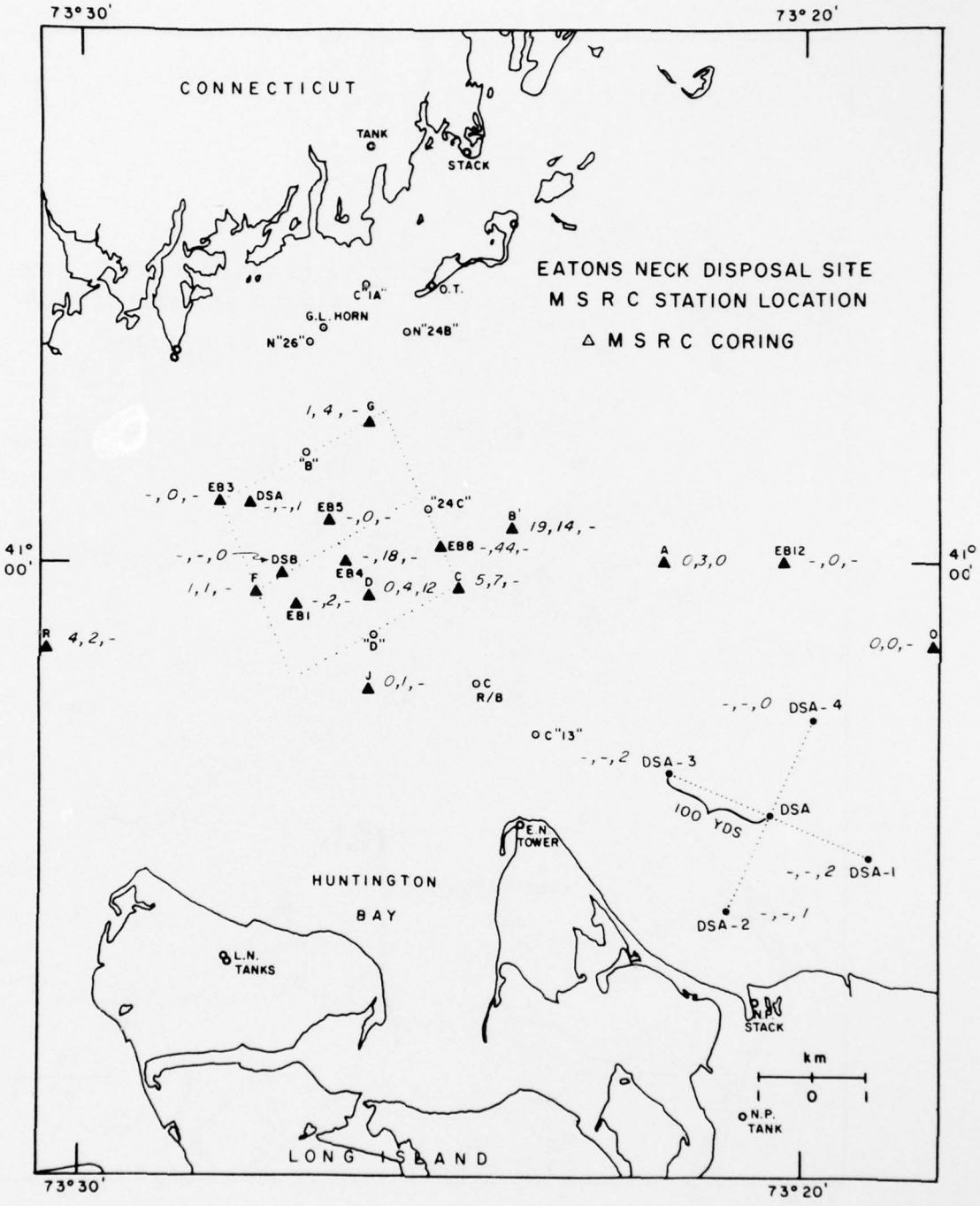



Figure 71. Weight percent gravel in near-surface sediments in the study area.

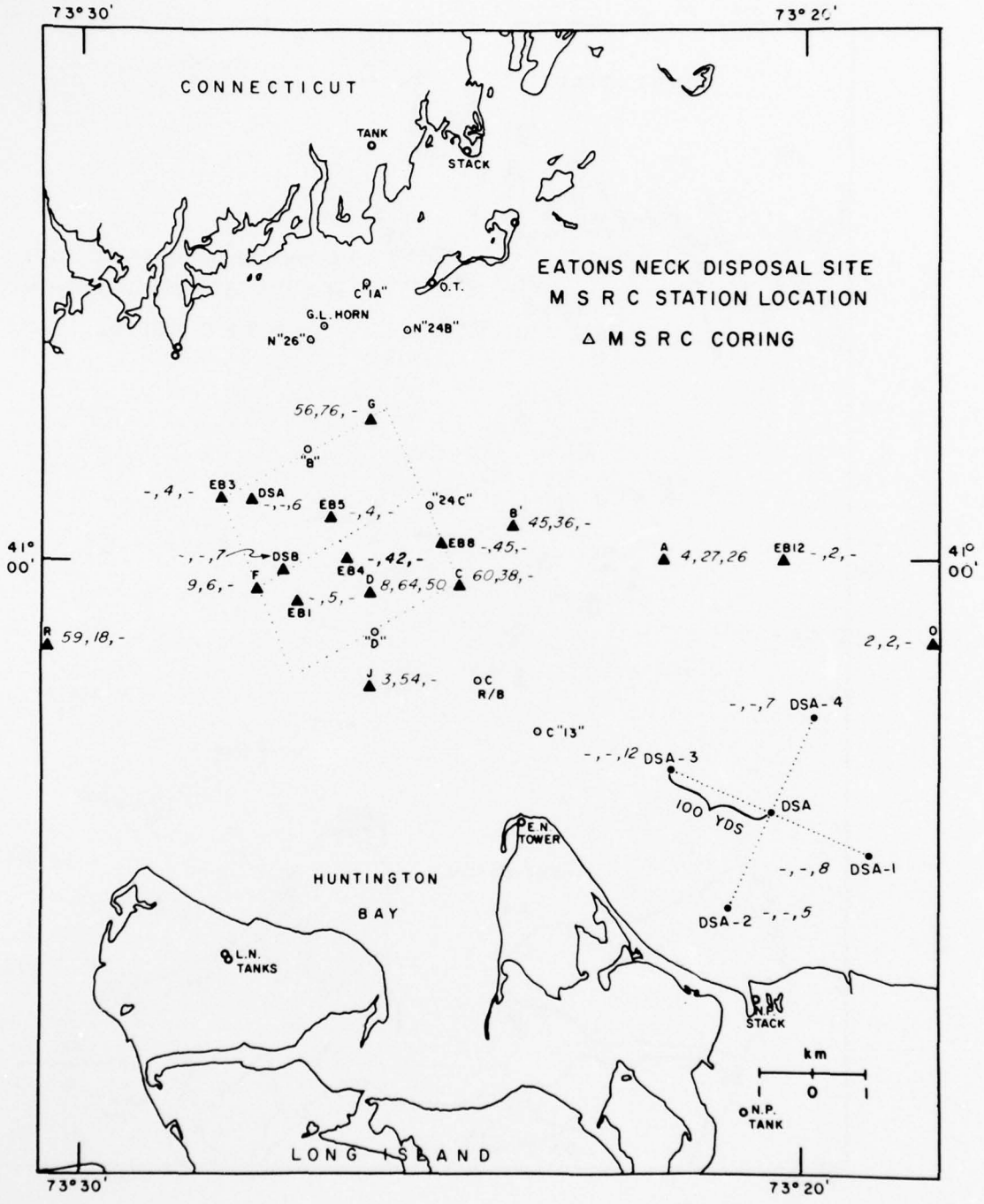



Figure 72. Weight percent sand in near-surface sediments in study area.

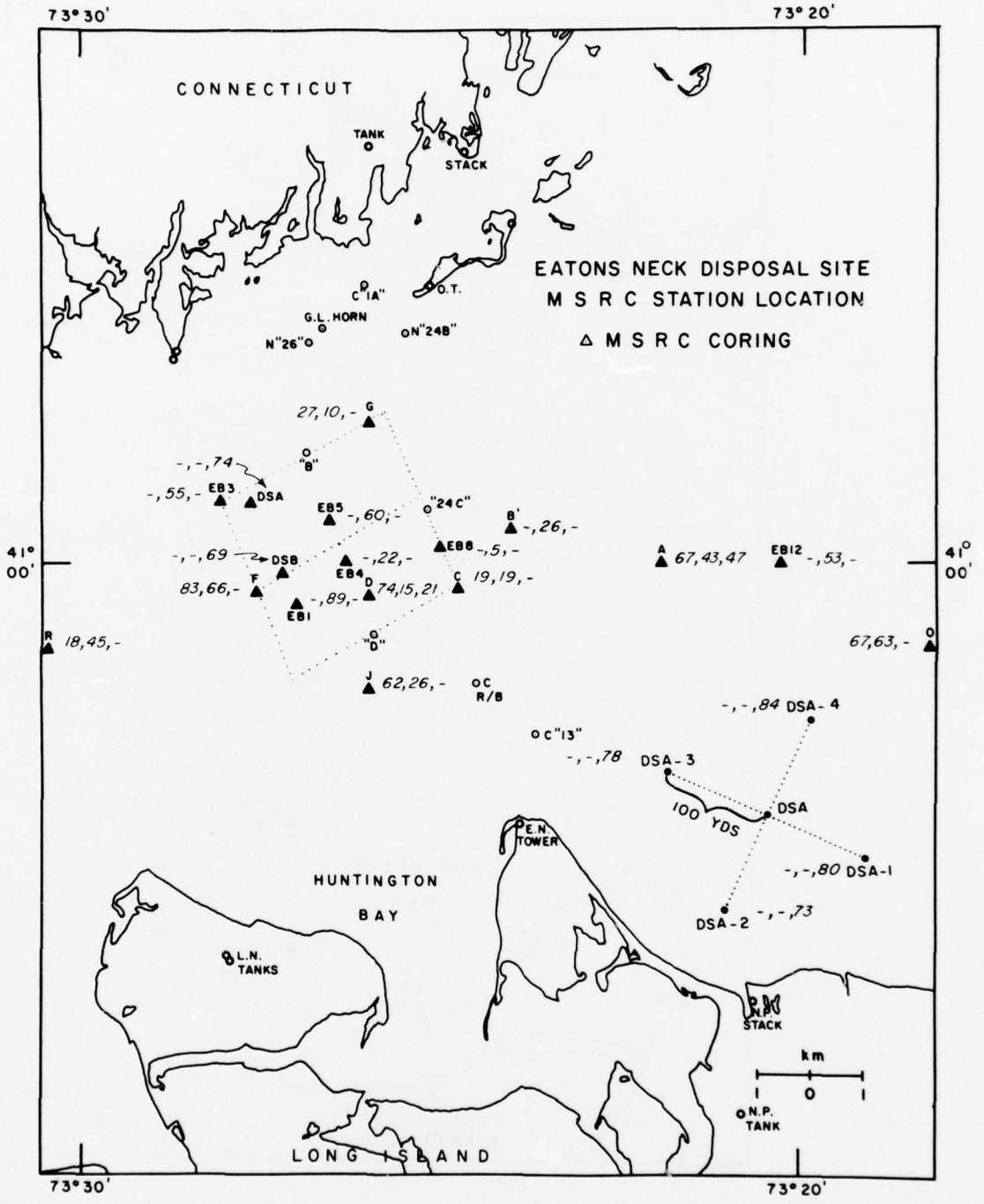



Figure 73. Weight percent silt in near-surface sediments in study area.

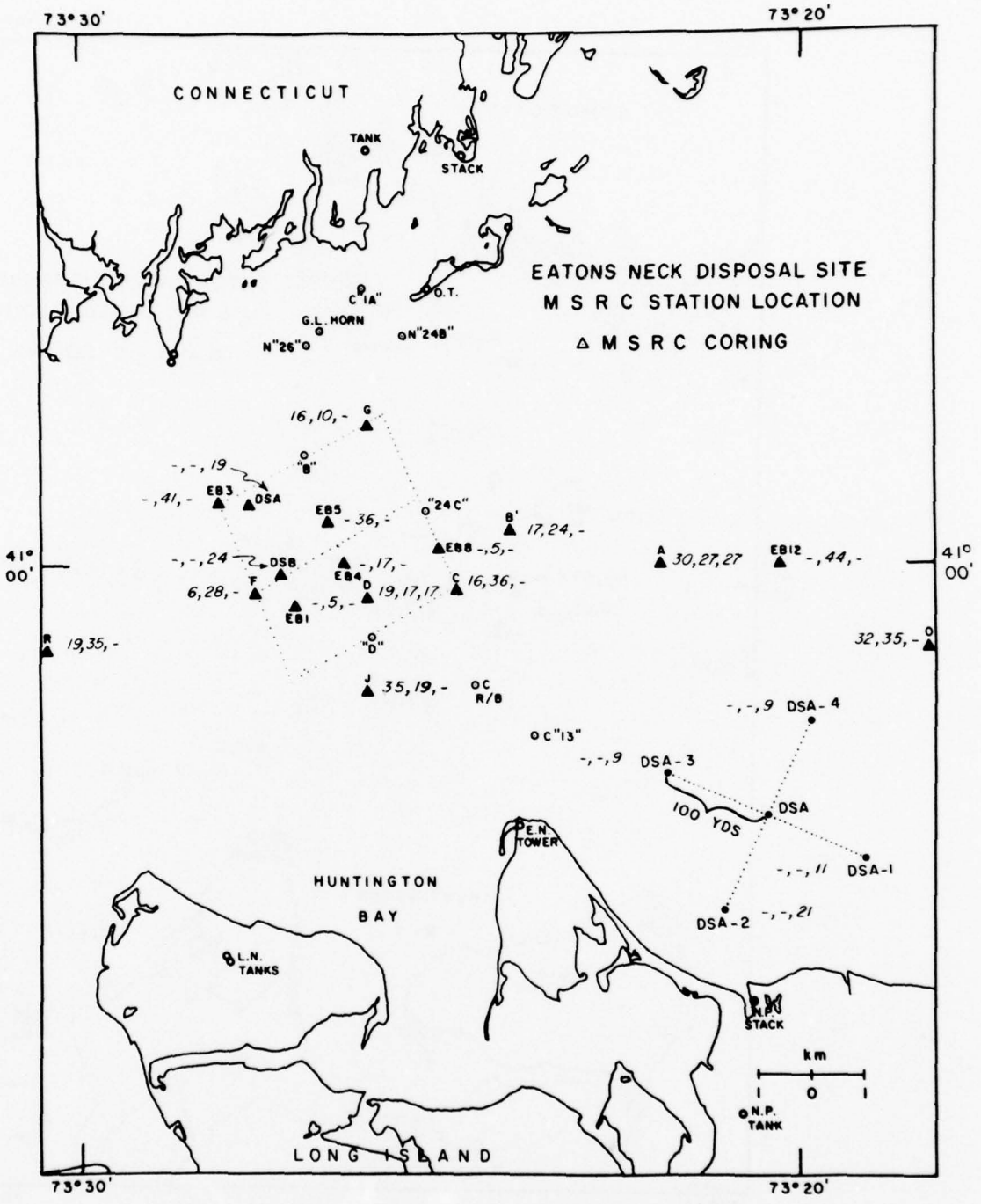



Figure 74. Weight percent clay in near-surface sediments in study area.

Although Eh measurements were not made, the presence of hydrogen sulfide odor in most core sections indicated reducing conditions.

Mineralogy

153. The top 10-cm sections of 10 selected cores were analyzed for bulk mineralogy by x-ray diffraction. Soluble salts were removed by washing the finely ground powder with distilled water. Random mounts of the samples were scanned from 1° to 60°2θ at 2°/min. The diffractograms showed that the bulk samples were composed principally of quartz and feldspars with only minor amounts of amphiboles and clay minerals. Since the bulk mineralogy data were based on x-ray diffraction analysis, trace amounts of other minerals present could not be detected. Microscopic analyses of bottom sediments from western Long Island Sound reported by McCrone[63] revealed the presence of other minerals, such as aragonite, calcite, muscovite, biotite, augite, kyanite, dolomite, garnet, magnetite, hematite, and zircon.

154. The clay fraction was composed mainly of chlorite, illite, kaolinite, and mixed-layer montmorillonite, with traces of quartz, orthoclase, and plagioclase. The chlorite present was of the Fe-rich type as indicated by strong second- and fourth-order basal reflections. Glycolation and heating tests indicate that the mixed layer component was of the illite-chlorite type.

155. Kaolinite was present in appreciable amounts in all sediment samples. It is known to be present in Connecticut soils and must be transported into the sound by the Housatonic and Connecticut Rivers. McCrone[63] reported the absence of kaolinite basal reflections on the diffractograms of clay samples heated at 550°. According to Carroll,[53] kaolinite is converted to amorphous metakaolin when heated to 550-600°C.

However, disordered kaolinite becomes amorphous at lower temperatures. In this study, the (002) kaolinite reflection at 3.58 Å could always be distinguished from the (004) chlorite reflection at 3.54 Å on a slow scan diffractogram. No heat treatment of the samples was required. Quantitative estimates of clay mineralogical composition did not reveal any significant trends from one station to another. The relative distribution of montmorillonite, illite, kaolinite, and chlorite in the surface sediments of the study area are shown in Figures 75- 78. The following range of variation was encountered: montmorillonite plus mixed layer clay, 3-15 percent; chlorite,13-28 percent; kaolinite, 13-30 percent; and illite, 38-61 percent. The values for montmorillonite plus mixed layer component are not too reliable due to the uncertainty in the measurement at low 2θ angles.

156. At stations A, D, and F, the subsurface samples were also analyzed. X-ray diffraction patterns indicated that the clay mineralogy of the cores is essentially uniform from top to bottom, thus implying that no structural transformation occurs during early diagenesis. The clay mineral data for surface and subsurface samples at stations A, D, and F are presented on ternary plots shown in Figures 79- 81. It should be mentioned that kaolinite and chlorite together represent one end component. At station A, a slight variation in clay mineralogy with depth is observed. The top section of the core exhibits about 20 percent enrichment in illite at the expense of 7 Å components relative to subsurface samples.

Particulate nitrogen and carbon

157. The nitrogenous part of organic matter deposited in the bottom sediments varied from 0.01 to 0.46 percent by dry weight for surface and subsurface samples. At many

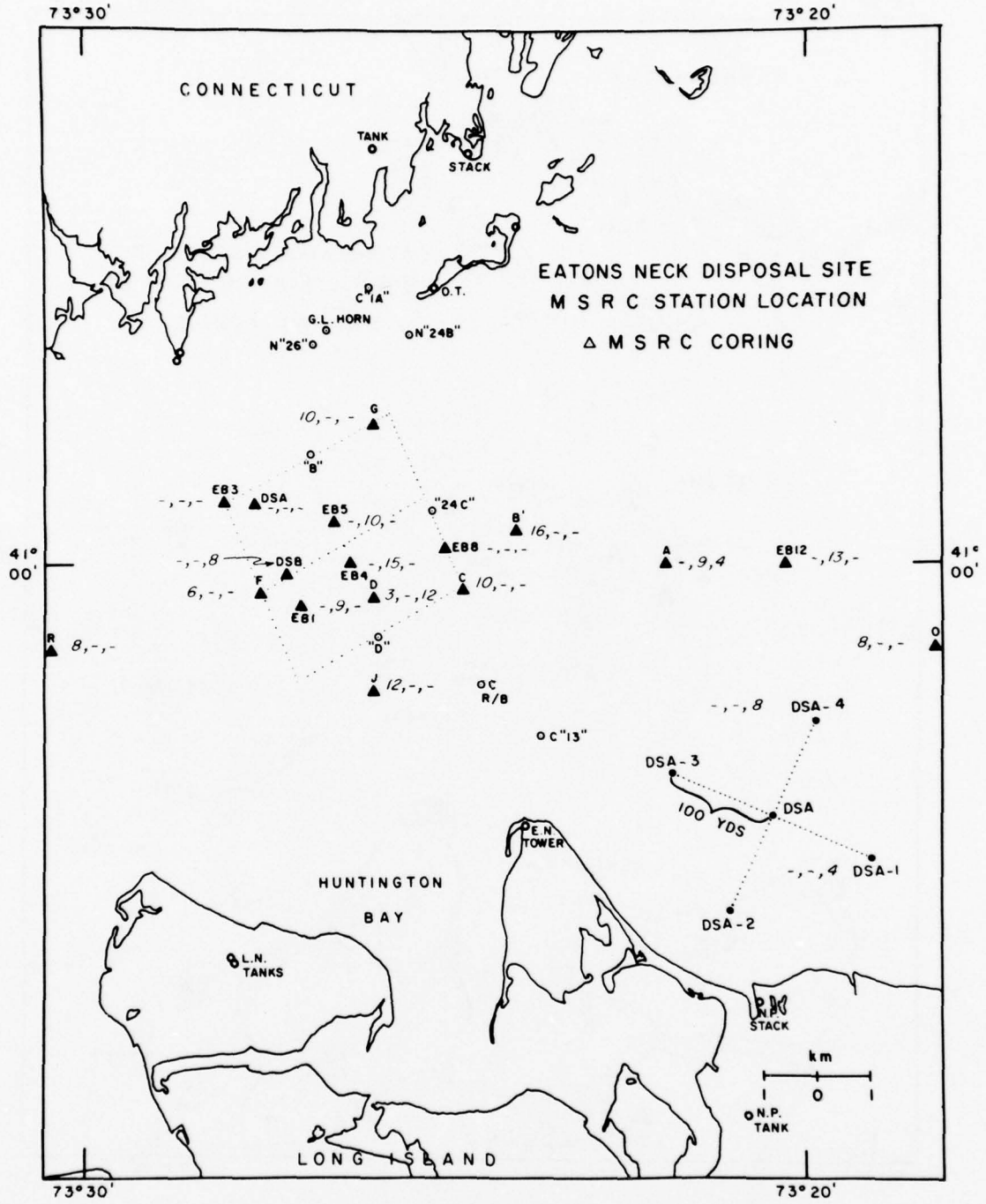



Figure 75. Weight percent montmorillonite in near-surface sediments in study area.

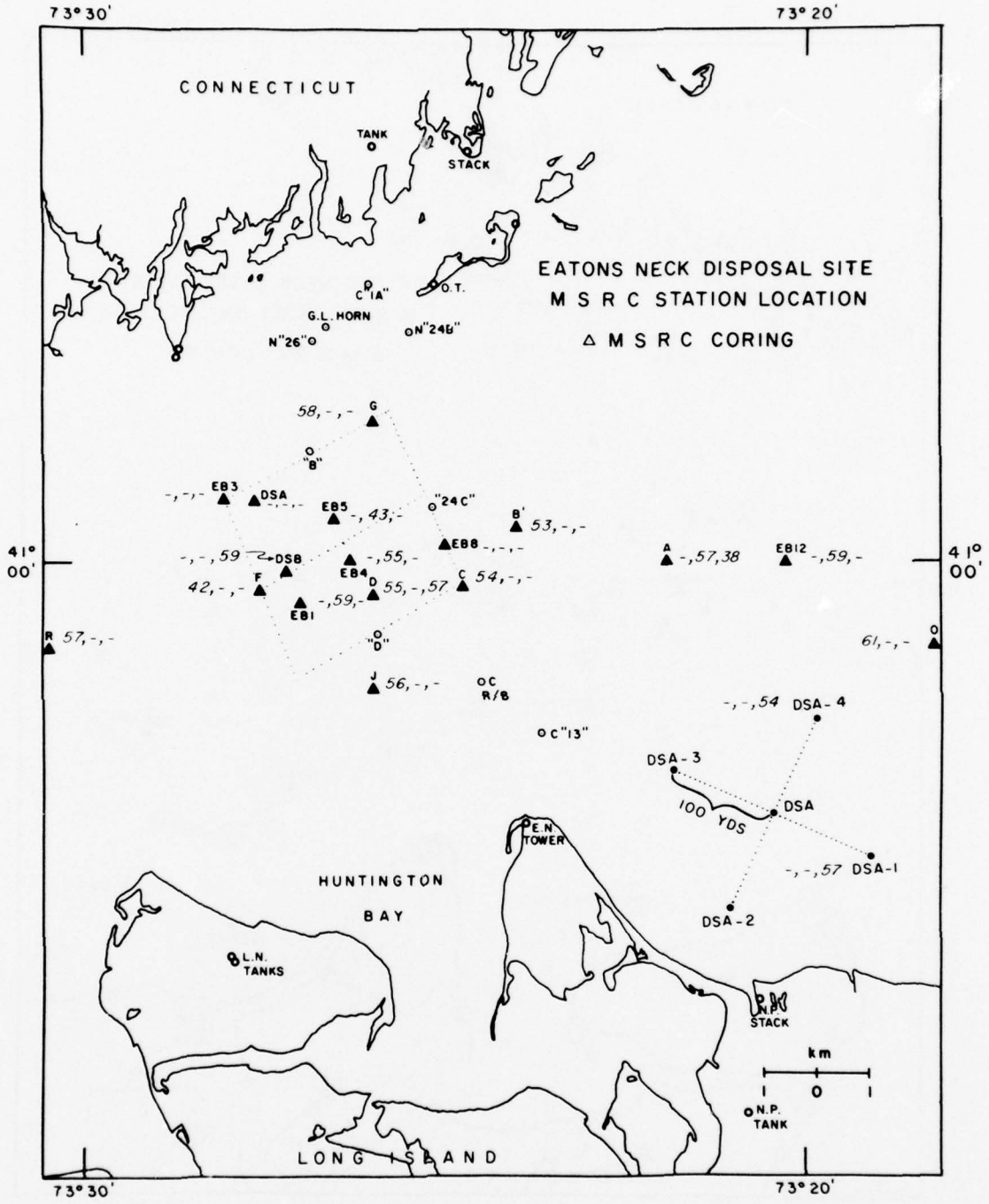



Figure 76. Weight percent illite in near-surface sediments in study area.

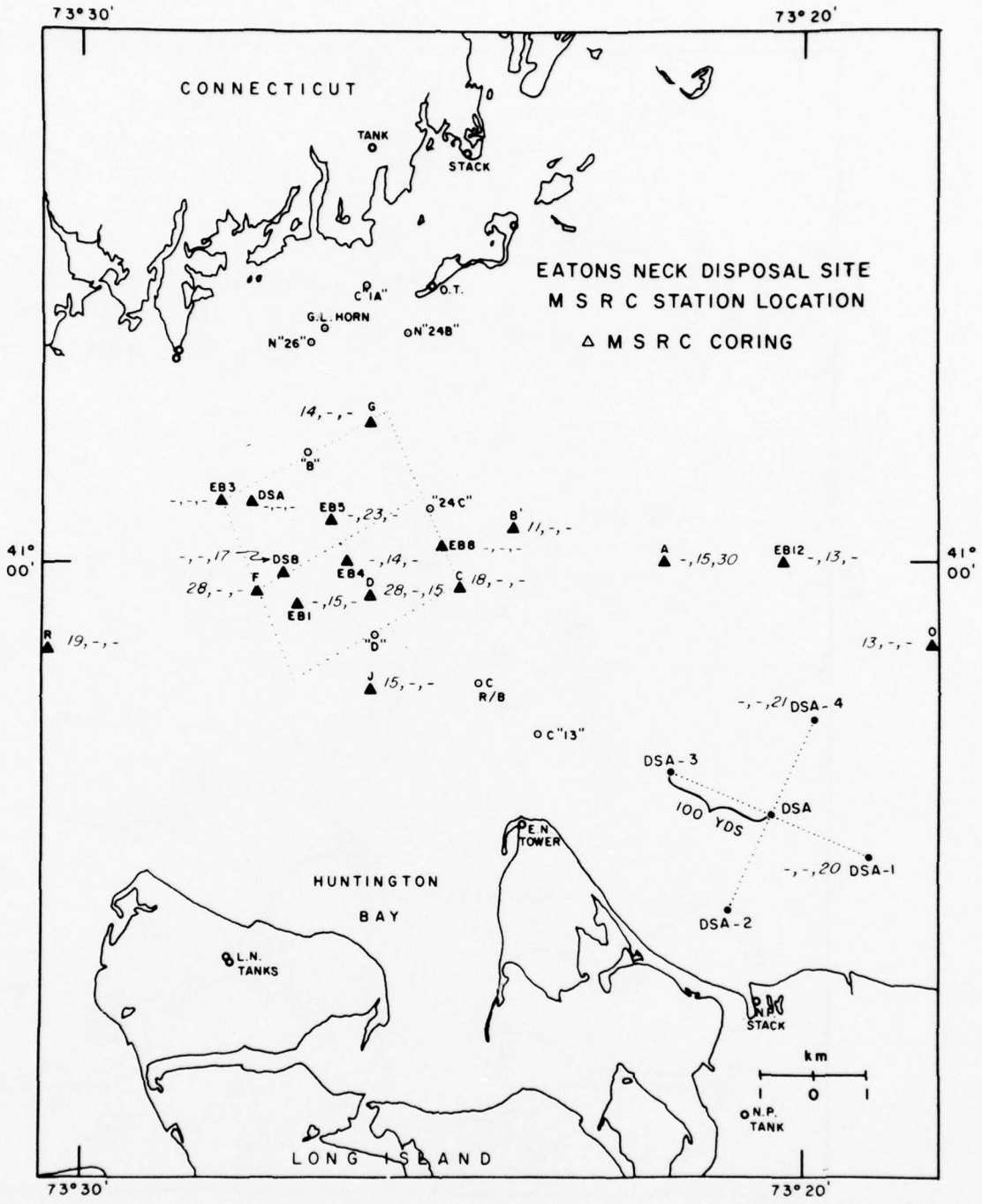



Figure 77. Weight percent kaolinite in near-surface sediments in study area.

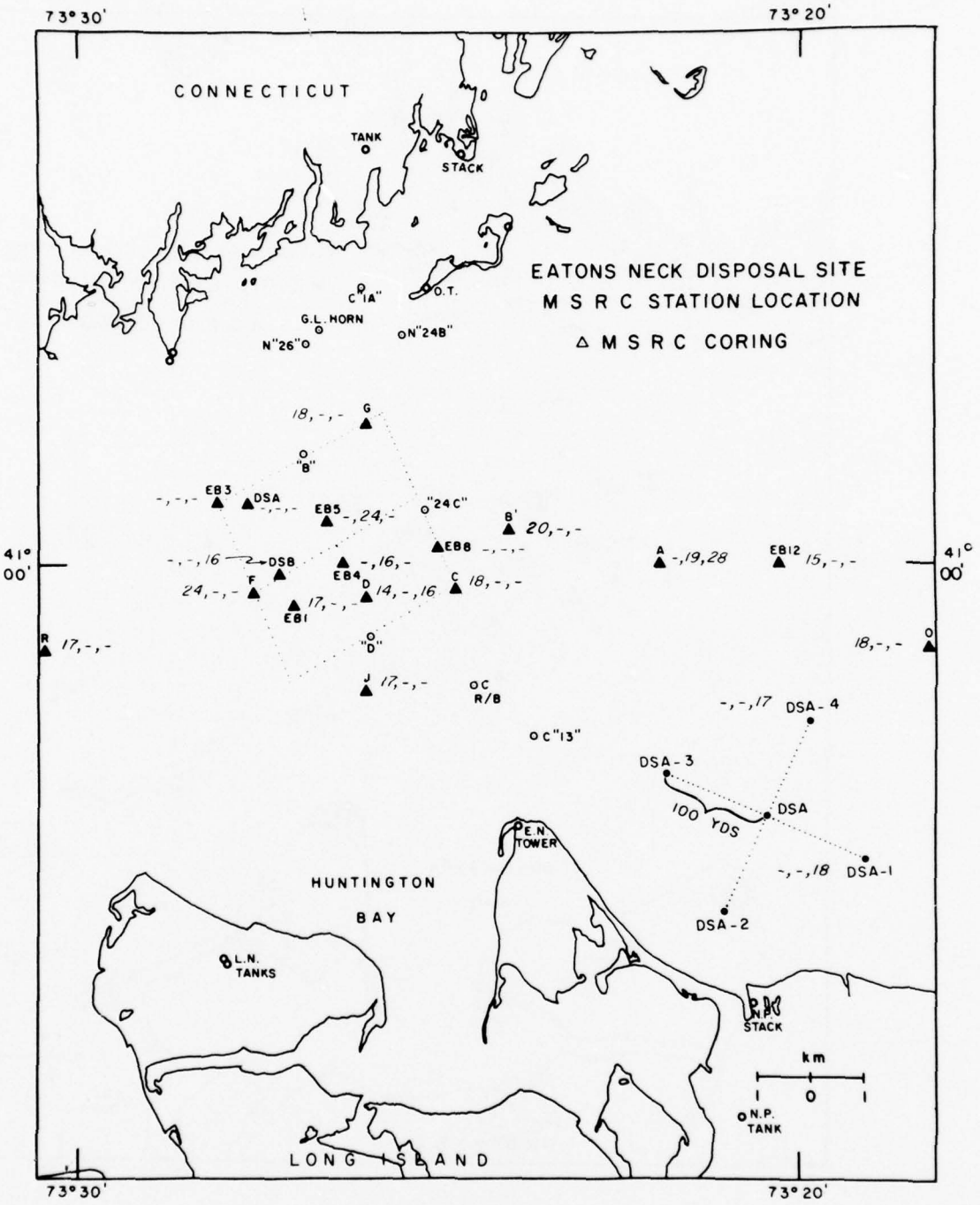



Figure 78. Weight percent chlorite in near-surface sediments in study area.

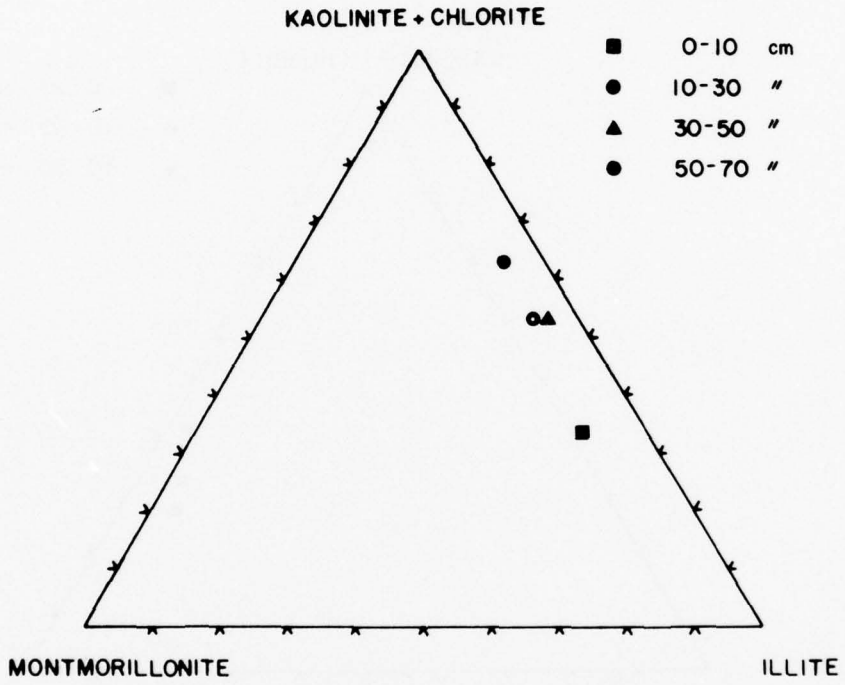



Figure 79. Ternary plot depicting the clay mineralogical composition in sediment core at station A.

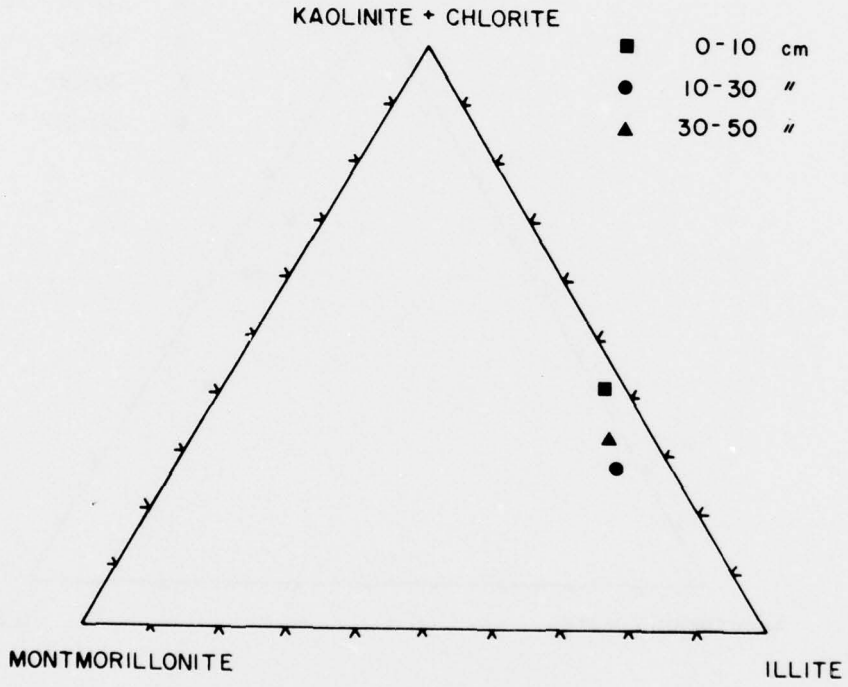



Figure 80. Ternary plot depicting the clay mineralogical composition in sediment core at station D.

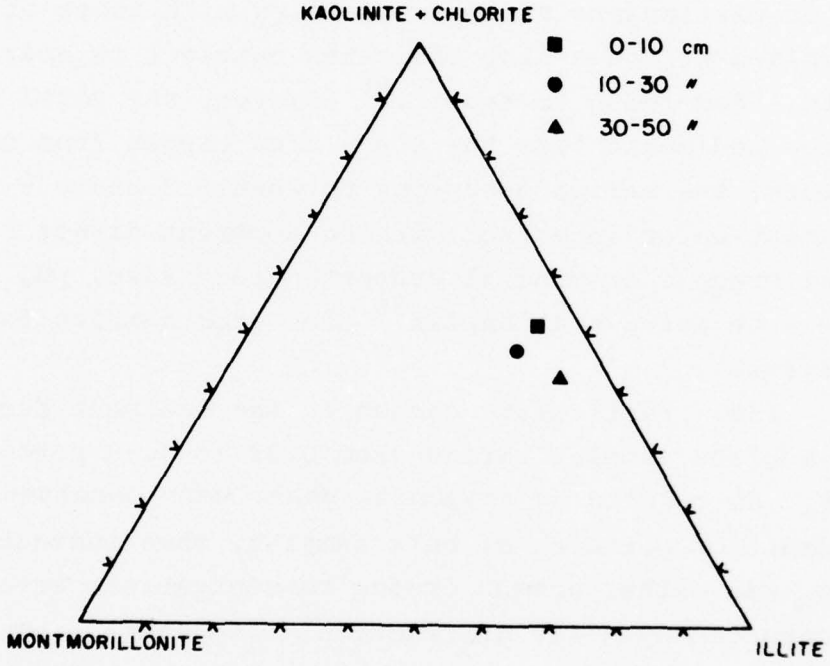



Figure 81. Ternary plot depicting the clay mineralogical composition in sediment core at station F.

stations there was a general decrease in nitrogenous matter with depth. The concentration-depth profiles for cores collected during the April coring cruise are shown in Figures 82- 90. In addition, C/N ratio-depth profiles are also included in the figures. The C/N values range from 5 to 12. This low range is similar to that reported[64,65] for sediments in the sludge dump site in the New York Bight. The decrease in nitrogen content as a function of increasing depth implies that much of it is decomposed, reforming nutrients. Comparison of particulate nitrogen profiles with those of total dissolved nitrogen also indicates nutrient regeneration at depth. According to Kaplin,[66] however, the total nitrogen in the sediments from the study area ranges from 0.01 to 0.17 percent, the maxima occurring between 0.3 and 0.6 m below the sediment/water interface with no apparent direct relation to total organic or mineral content, grain size, pH, or Eh. It should be noted that Kaplin[66] took grab samples for the analyses.

158. Particulate carbon in the sediment surface and sub-surface samples varied from 0.32 to 4.60 percent by dry mass. No calcite or aragonite peaks were observed on the diffraction patterns of bulk samples, thus indicating that $CaCO_3$ was either absent or the concentrations were too low to be detected by x-ray diffraction. In general, the surface samples showed marked enrichment relative to the subsurface samples. The concentration-depth profiles are shown in Figures 82-90. At most stations, the carbon content decreases with increasing depth. Methane and carbon dioxide are known to form during early diagenesis of sediments. Reeburgh[67] has shown that in the pore waters of sediments from Chesapeake Bay, methane is produced so rapidly that it reaches supersaturation and escapes across the sediment-water

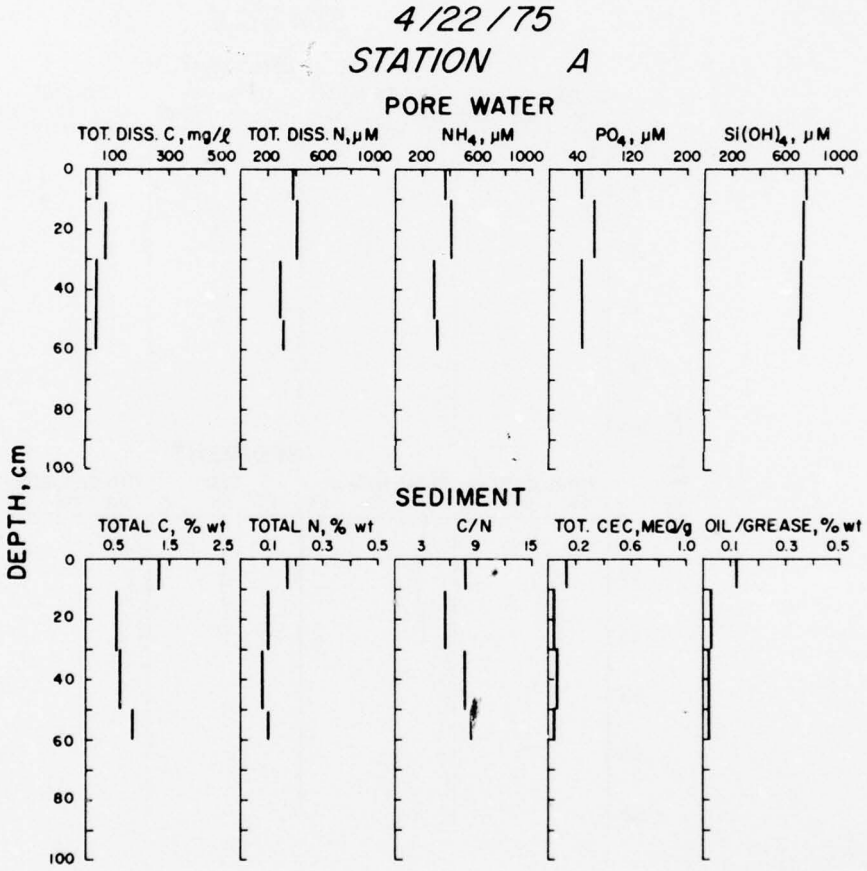



Figure 82. Sediment properties as a function of depth in core at station A.

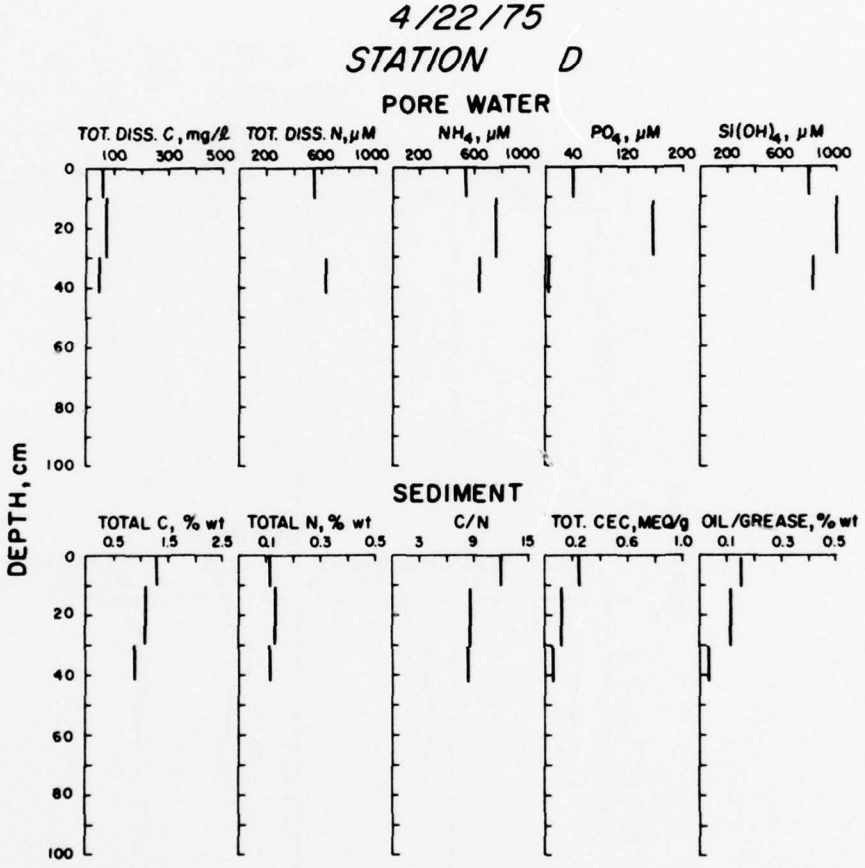



Figure 83. Sediment properties as a function of depth in core at station D.

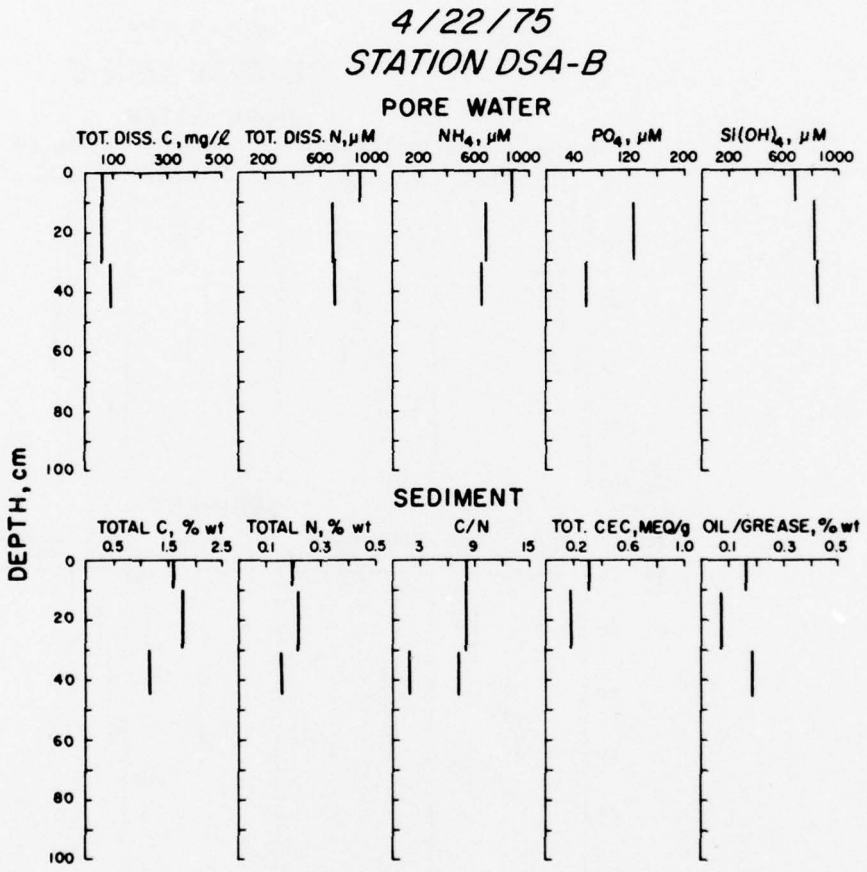



Figure 84. Sediment properties as a function of depth in core at station DSA-B.

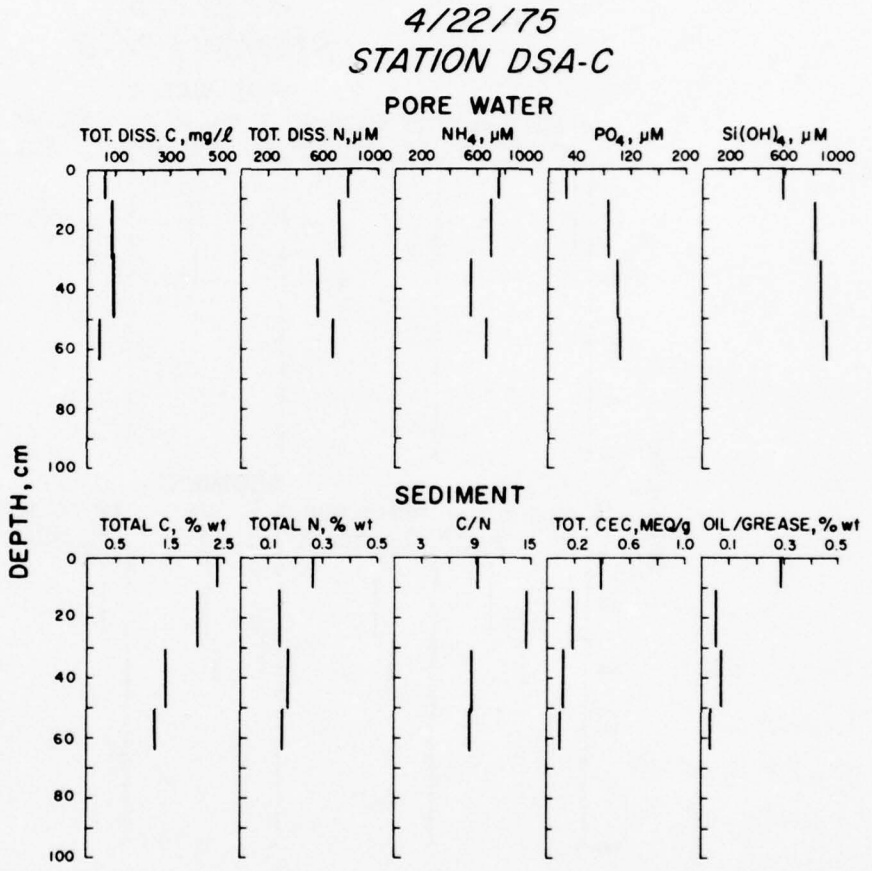



Figure 85. Sediment properties as a function of depth in core at station DSA-C.

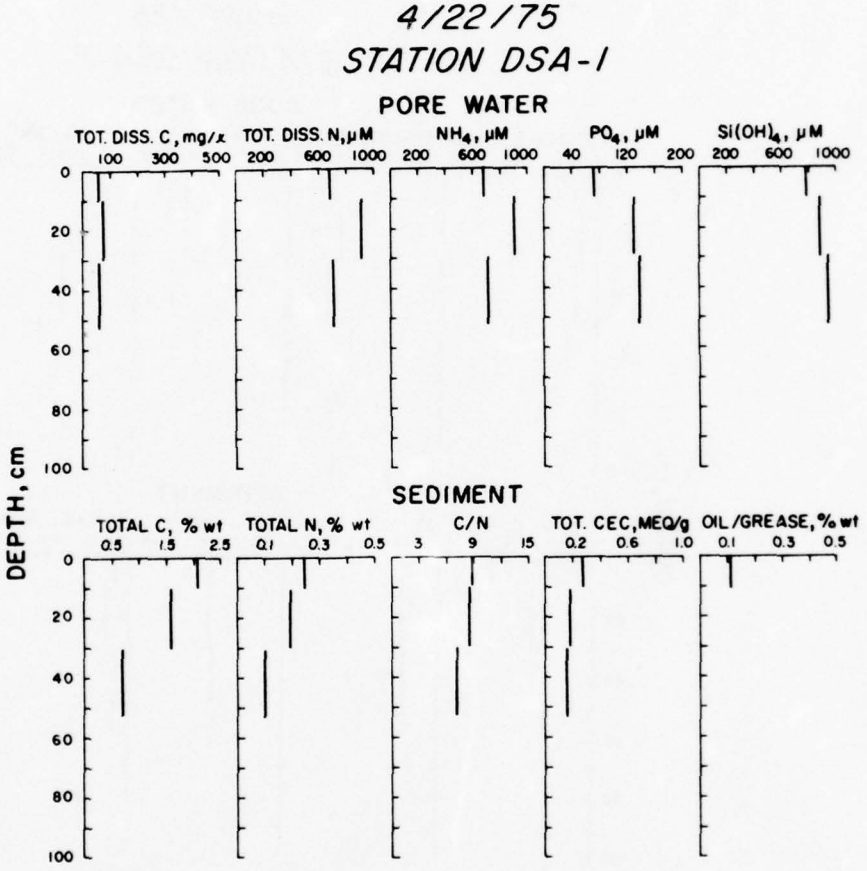



Figure 86. Sediment properties as a function of depth in core at station DSA-1.

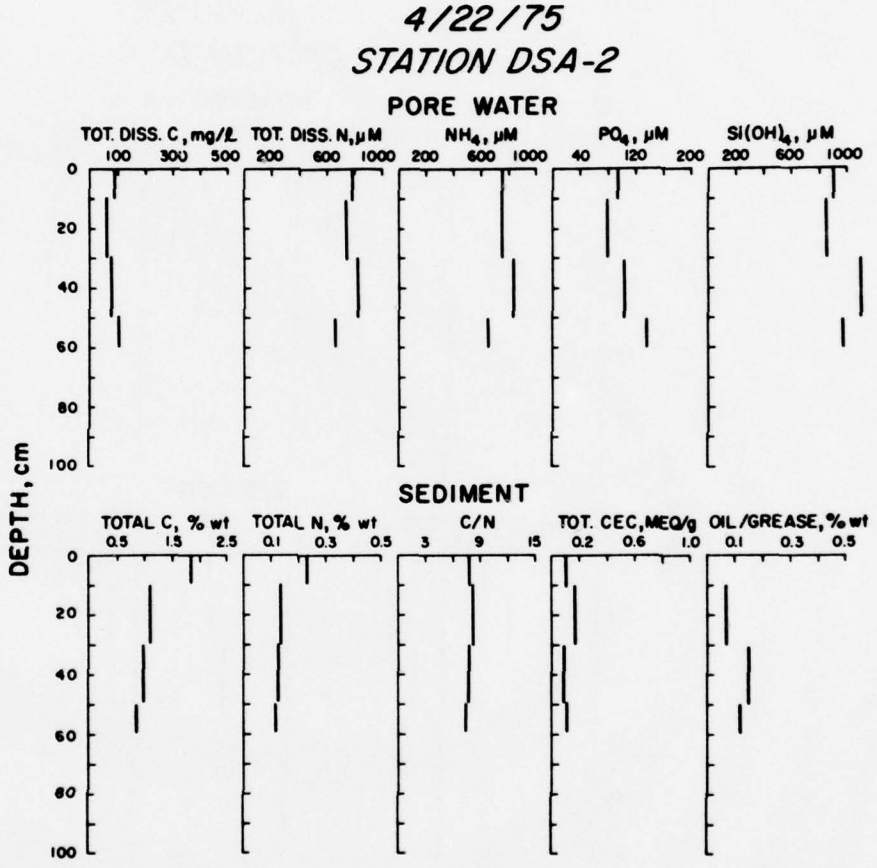



Figure 87. Sediment properties as a function of depth in core at station DSA-2.

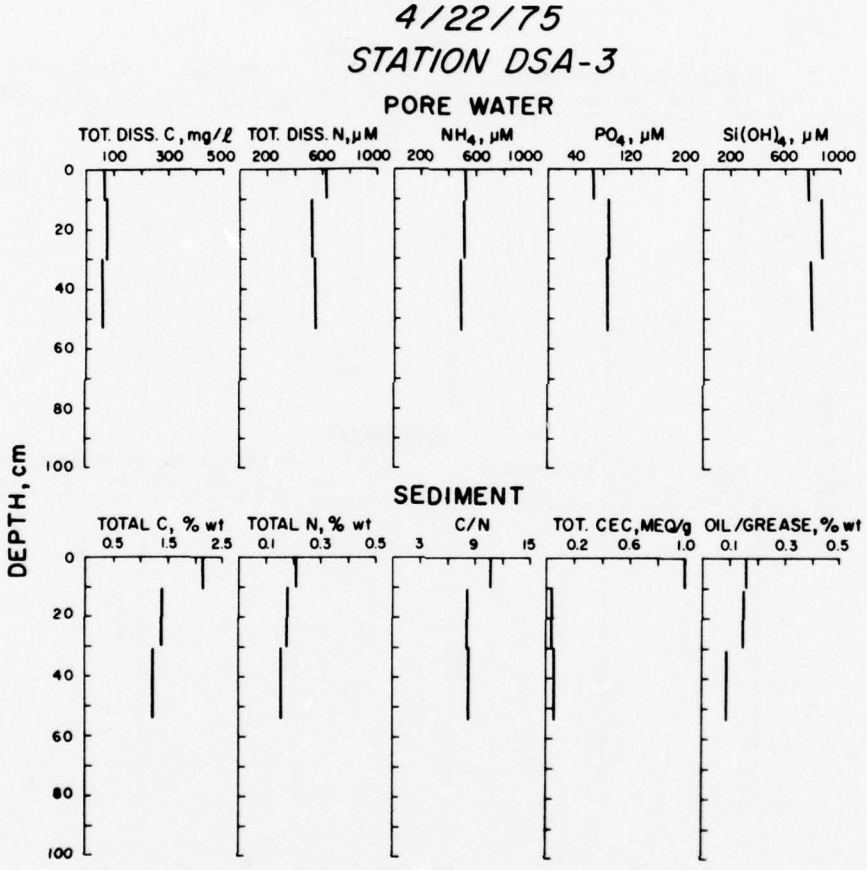



Figure 88. Sediment properties as a function of depth in core at station DSA-3.

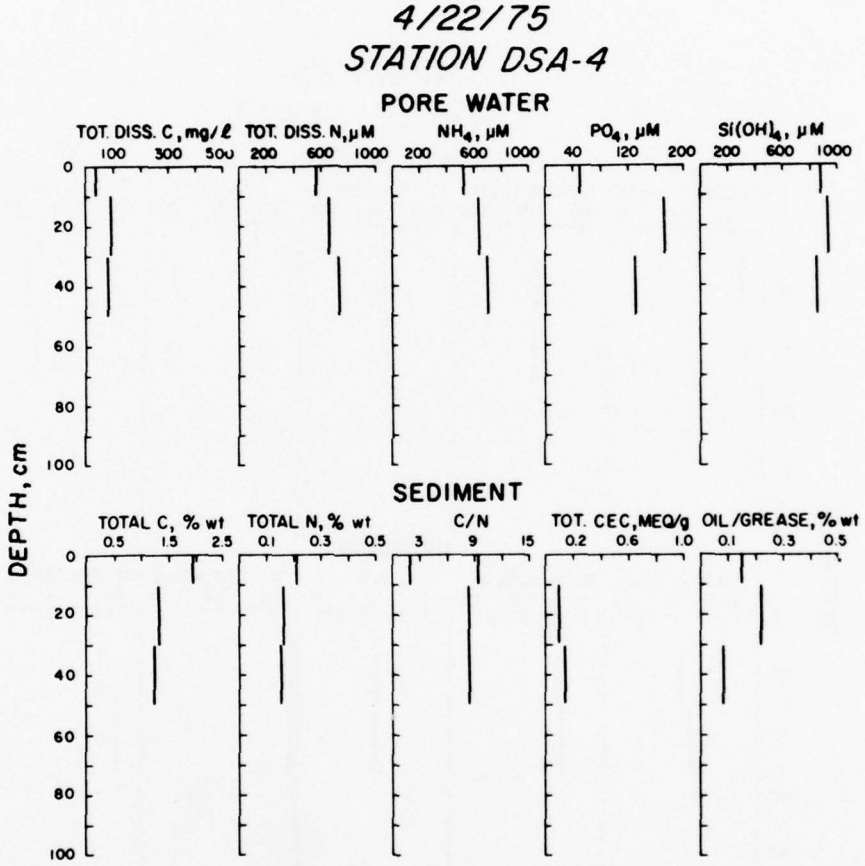



Figure 89. Sediment properties as a function of depth in core at station DSA-4.

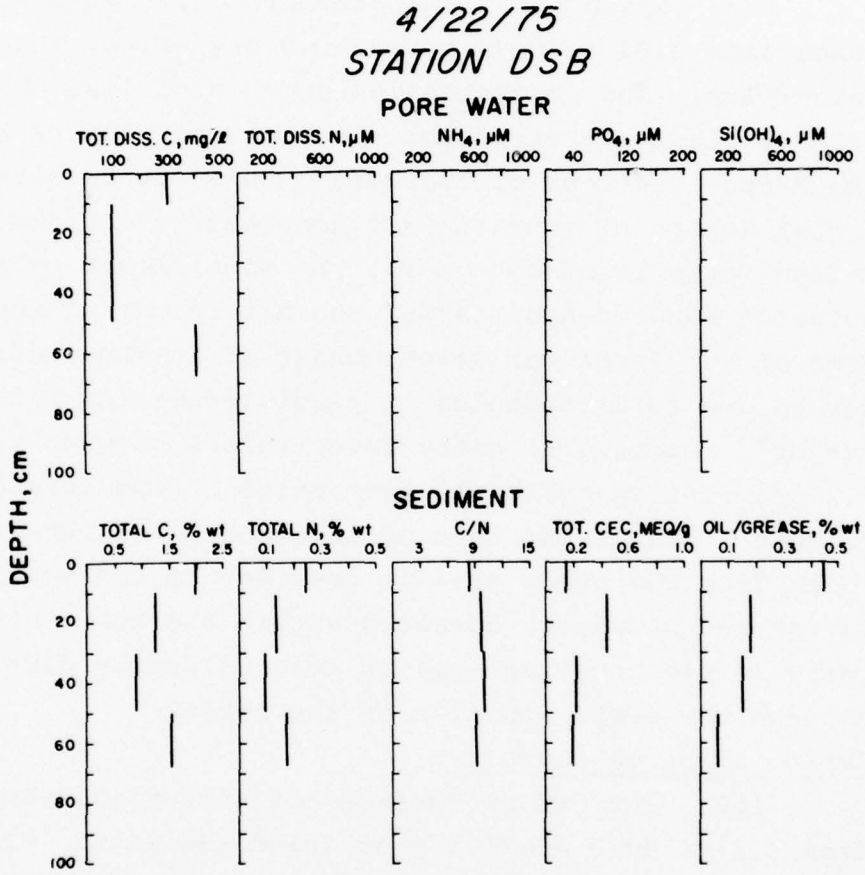



Figure 90. Sediment properties as a function of depth in core at station DSB.

interface in the form of bubbles. The relatively high organic carbon content in the sediments may indicate man's impact on the environment as marked increases in organic carbon content have been registered in the top core sections.

Oil and grease

159. Hydrocarbon extracts from sediments were found to range from 0.01 to 0.44 percent by dry weight in surface and subsamples. The concentration-depth profiles, shown in Figure 82- 90, indicate enrichment in the upper layers relative to the deeper sections of the core. This can be attributed to higher inputs of aromatic and nonaromatic compounds to Long Island Sound in recent years. No significant relation was detected between hydrocarbon and mineralogy of the cores. Some of the large variations observed in the surficial samples may be due to differences in particle-size distribution. Danker[68] reported slightly lower values ranging from 0.006 to 0.25 percent in sediments from western Long Island Sound. McCrone[63] also found that organic content in the sediment cores from the study area is greatest in the topmost sediment layers and decreases downward within the top foot of most cores before becoming more or less uniformly distributed through the deeper portion of the cores.

Cation exchange capacity

160. The CEC of surface and subsurface samples varies from 0.1 to 99.6 meq/100 g of dried sediment. Plots of CEC versus depth in the sediment cores are given in Figures 82- 90. For several sediment cores, the figures reveal a general trend of decreasing CEC with increasing depth. This pattern can not be attributed to grain-size distribution and fine-fraction mineralogy because the changes in these parameters with depth are not significant (Figures 65- 70, 79). At several stations, the exchangeable Ca decreases with increasing depth.

It seems that the decrease in total CEC with depth is related to the exchangeable Ca pattern in sediment cores. It is probable that Ca fixation occurs in the expandable component of the clay fraction with increasing depth of sediment burial. Some sediment samples having extremely low CEC consist of a much coarser gravelly type of sediment. Organic matter may also account for the observed variations in the CEC values. CEC values range in the order of 30 to 40 meq/100 g for surface sediments in the Hudson River Estuary (McCrone[69]). McCrone[69] found that clay-size organic matter, rather than clay minerals, account for the largest fraction of this capacity.[64]

Total and dissolved metals

161. Sediment. The acid-leaching technique used in this study for the determination of total metal concentration is similar to that used by Thomas et al. (in Turekian[37]). These authors have shown that 1 N $HNO_3$-leached samples release 85-90 percent of the total concentration of the metals present in totally dissolved samples.

162. The metal concentrations in sediments showed large variations from one station to another. The range of metal concentrations found in surface and subsurface samples were Cu, 6-230 mg/l; Pb, 4-145 mg/l; Zn, 19-278 mg/l; Cd, 300-3100 µg/l; Hg, 5-1420 µg/l; Ni, 6-33 mg/l; Mn, 124-1628 mg/l; and Fe, 7000-38000 mg/l. In most cases, the highest concentrations of Cu, Pb, Zn, Cd, and Hg were typically found near the surface. Fe, Mn, and Ni exhibited a somewhat erratic distribution pattern. The total metal and interstitial metal concentration-depth profiles for the sediment cores collected during the three coring cruises are given in Figures 91- 125. The cruise date is given on each figure. The vertical bar represents the metal concentration and its size is the length

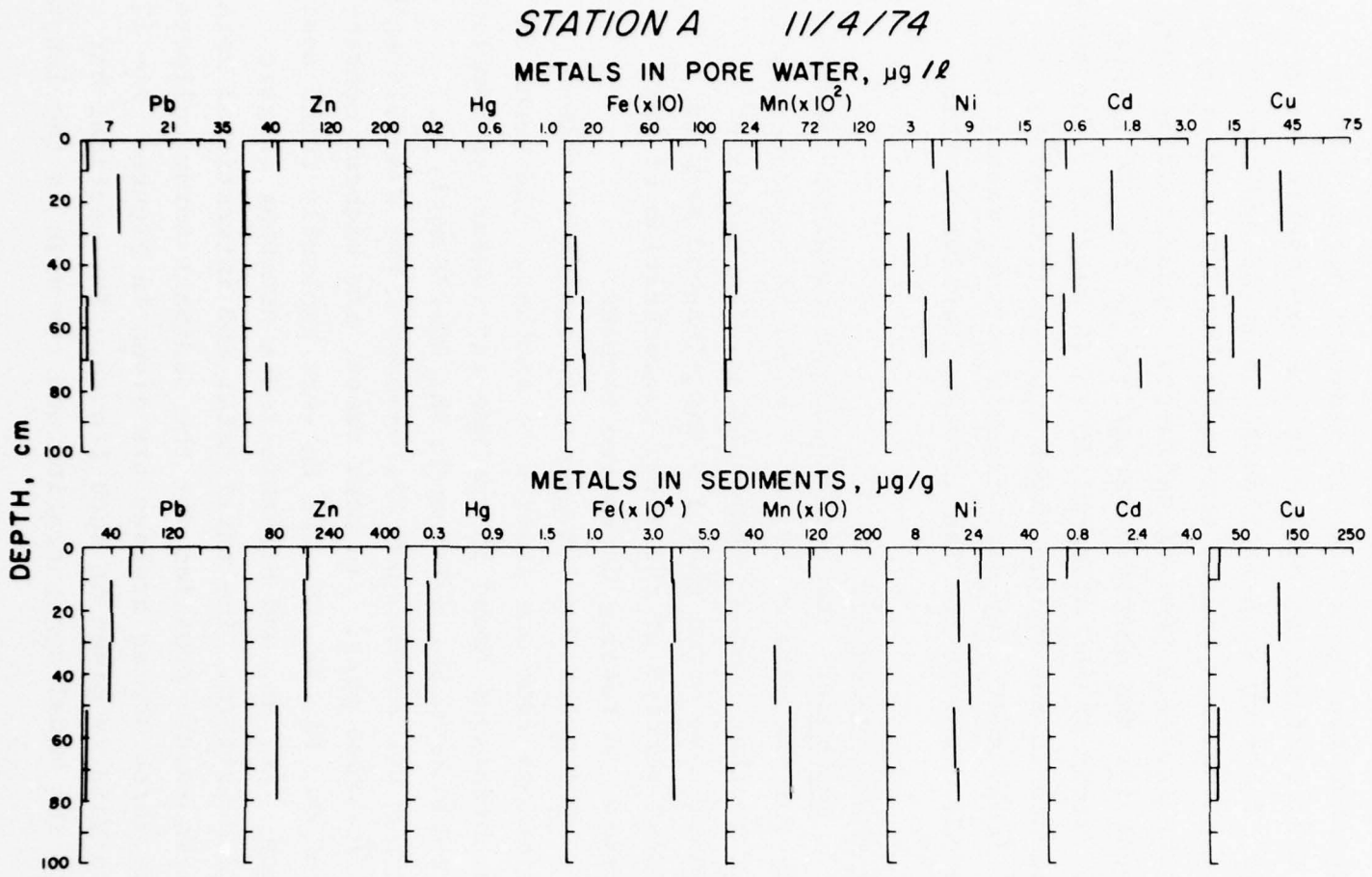



Figure 91. Total and dissolved metal concentration - depth profiles for core at station A.

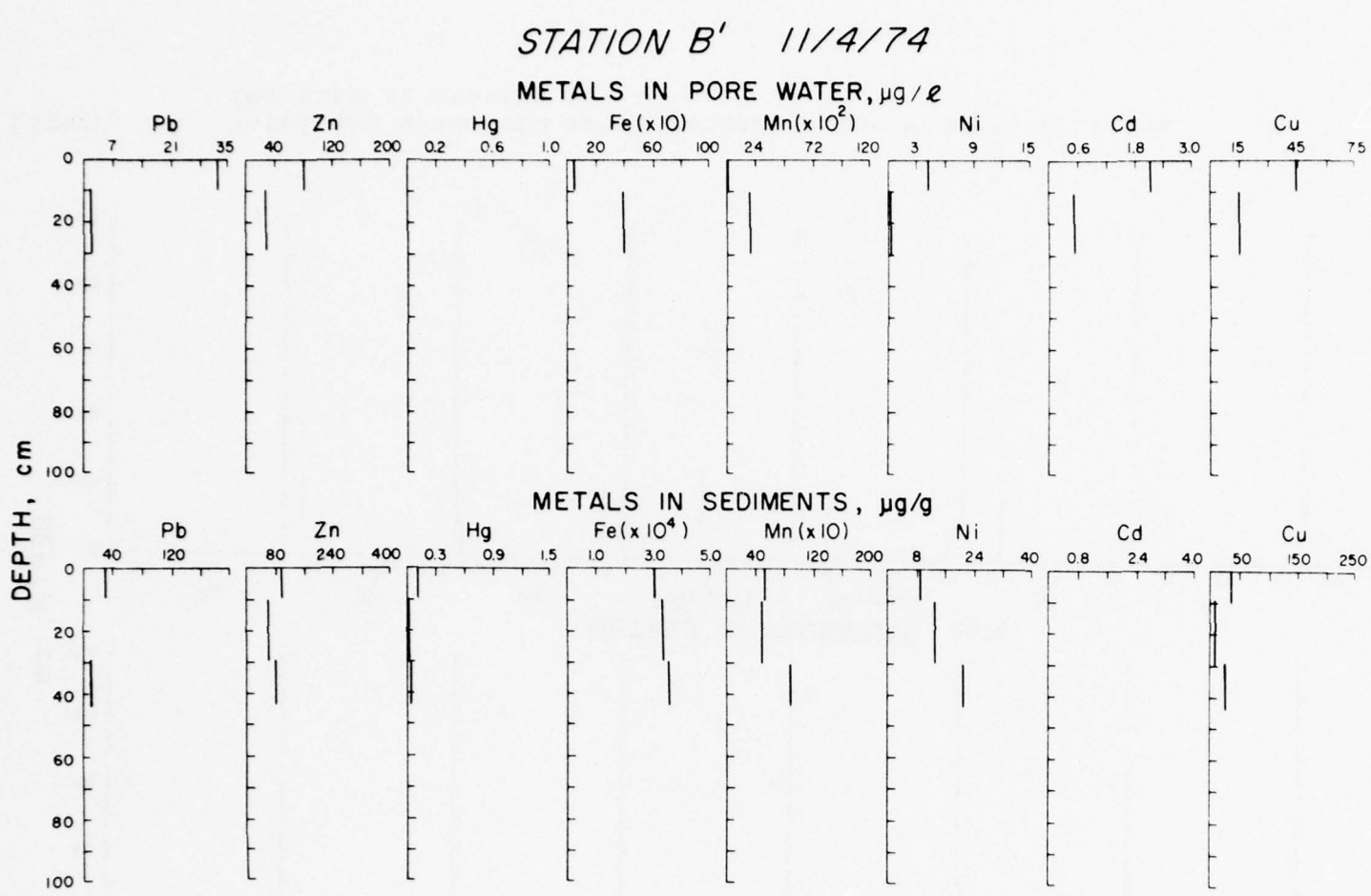



Figure 92. Total and dissolved metal concentration - depth profiles for core at station B'.

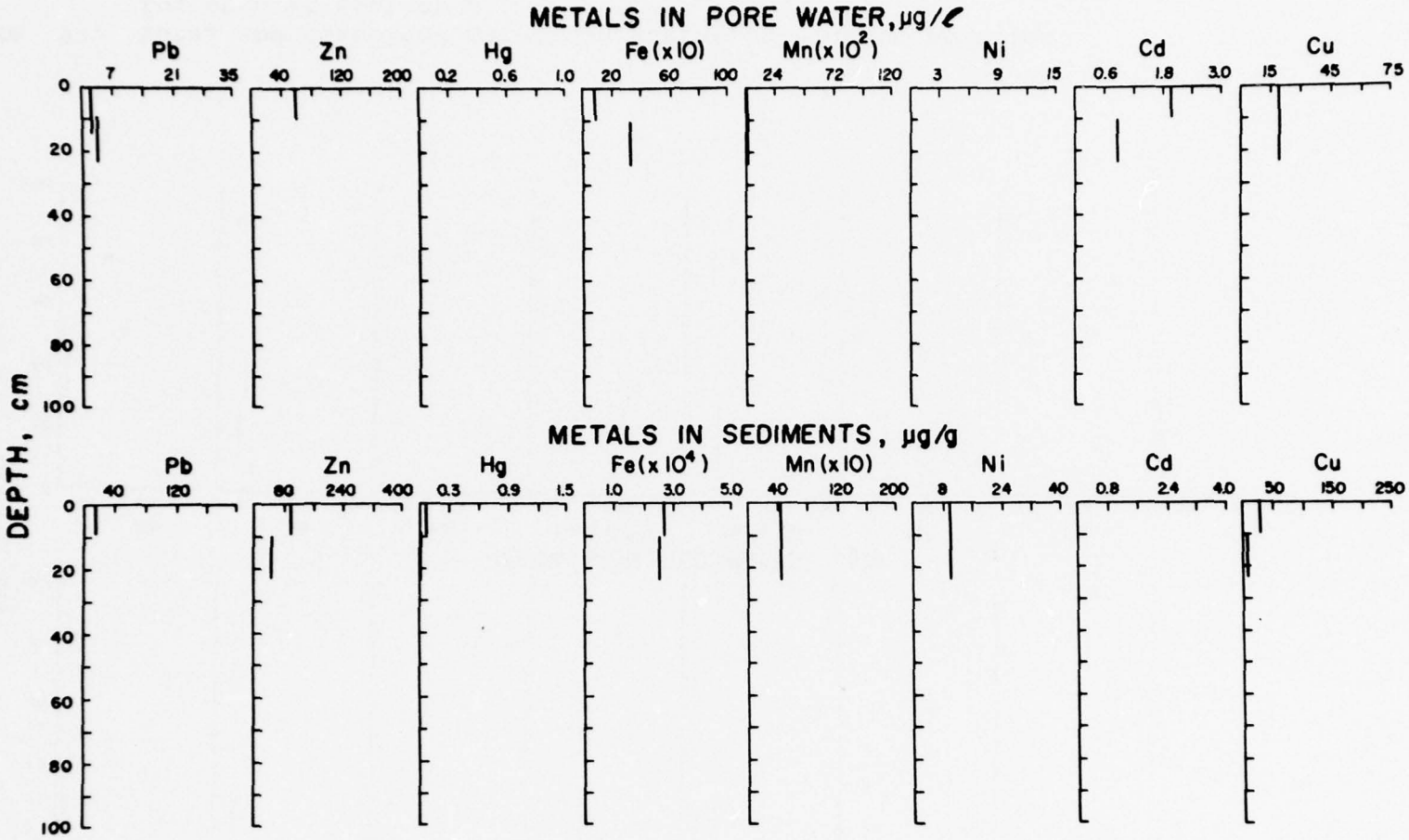



Figure 93. Total and dissolved metal concentration - depth profiles for core at station C.

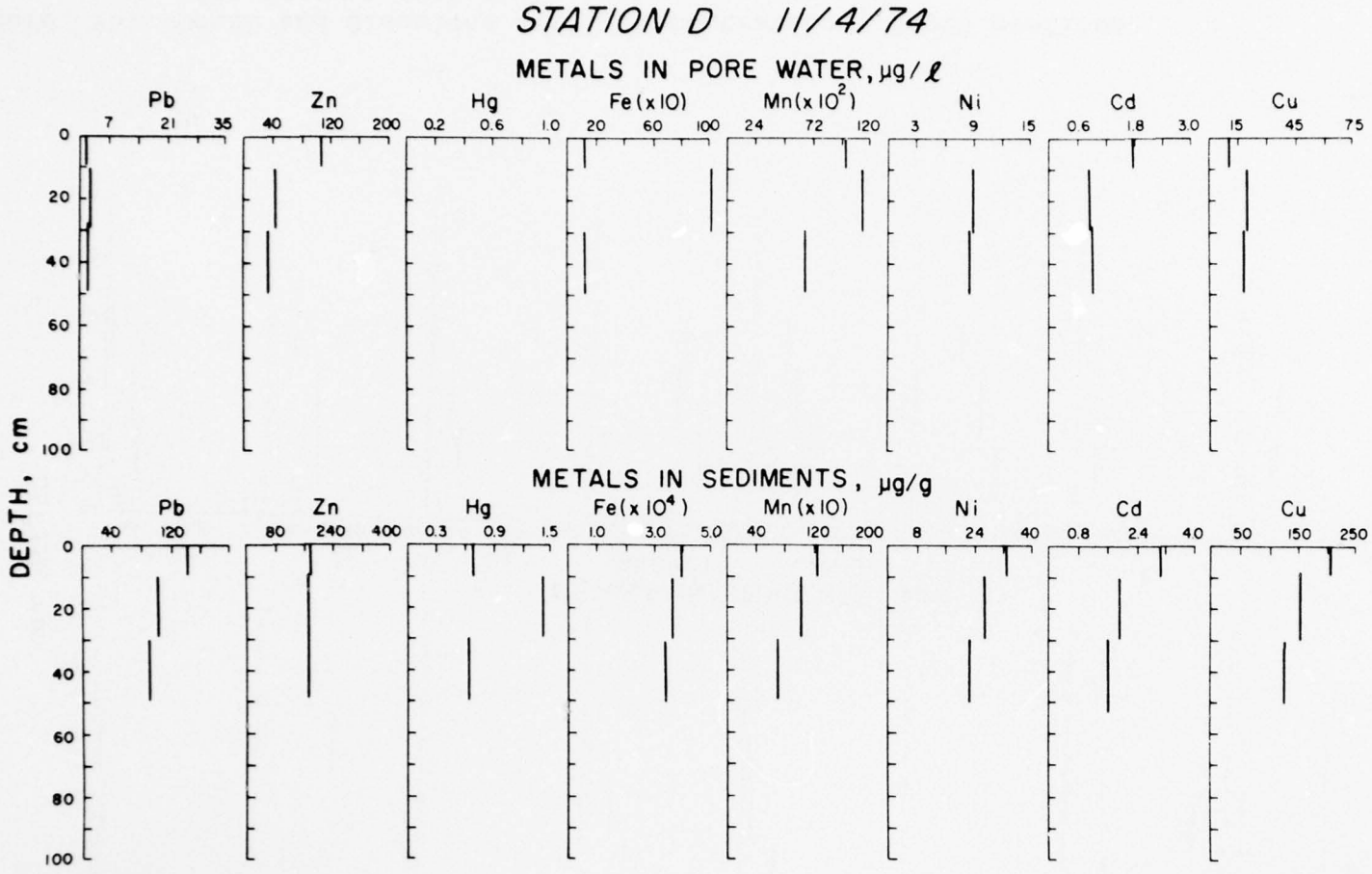



Figure 94. Total and dissolved metal concentration - depth profiles for core at station D.

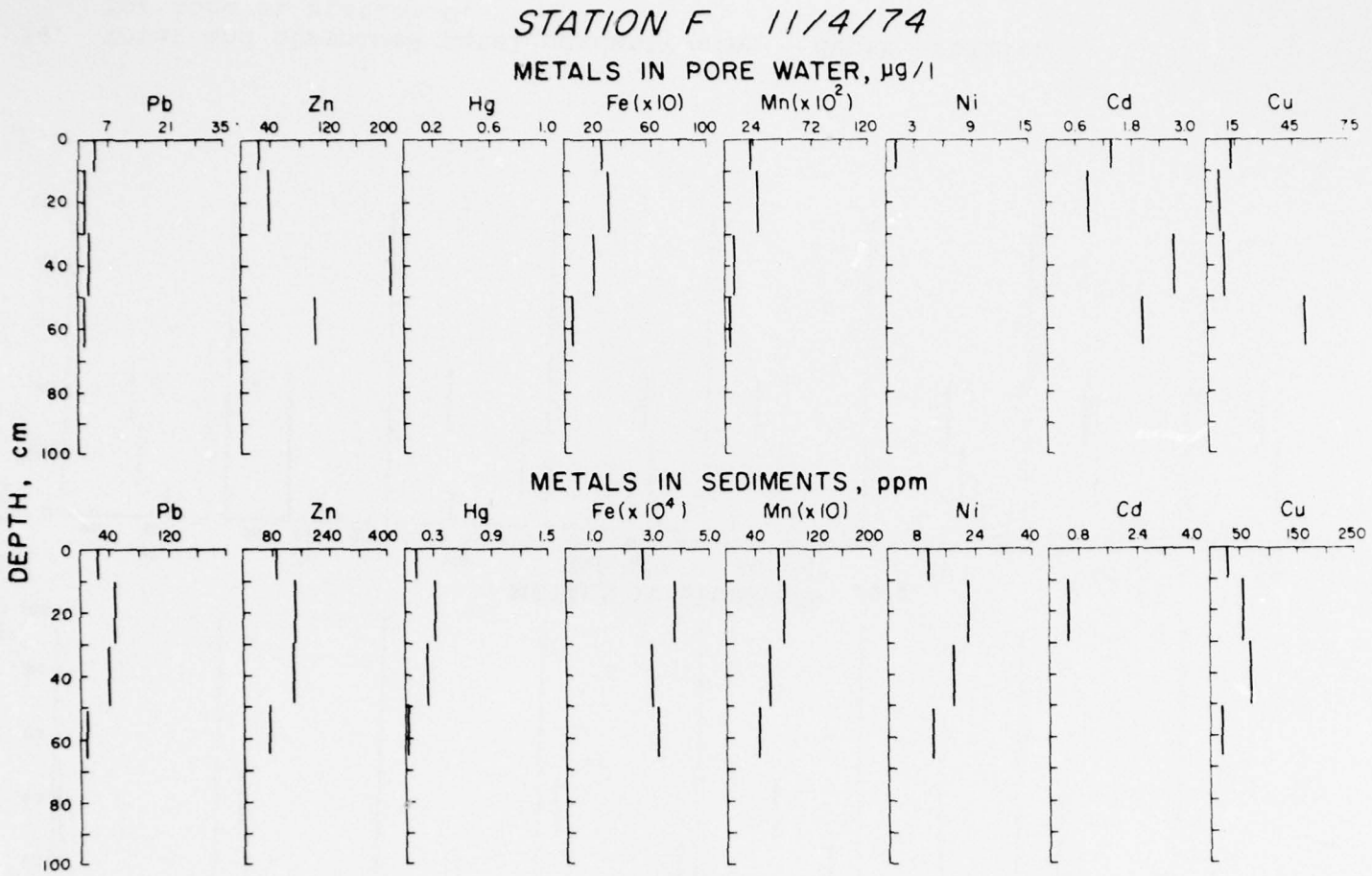



Figure 95. Total and dissolved metal concentration - depth profiles for core at station F.

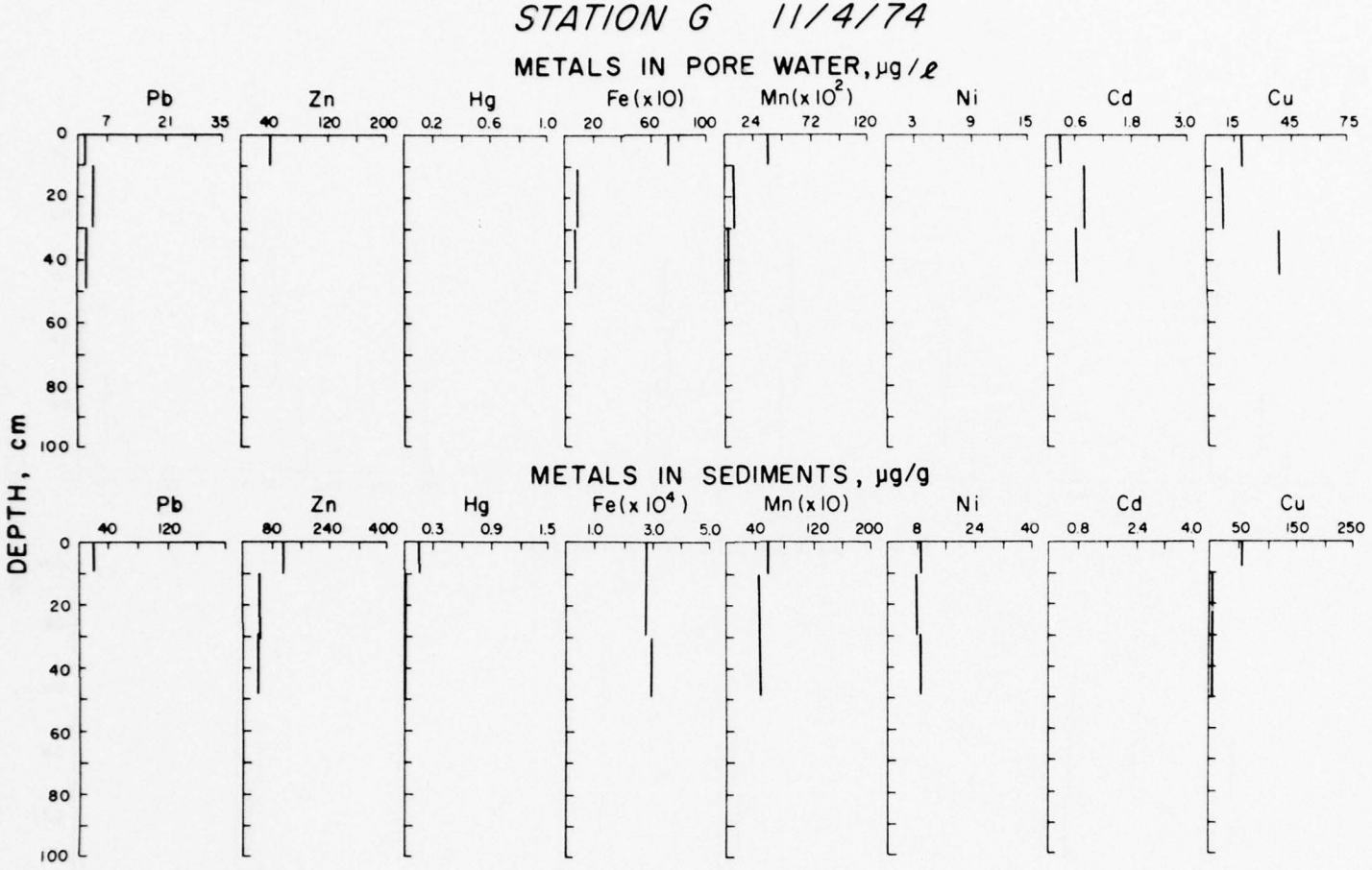



Figure 96. Total and dissolved metal concentration - depth profiles for core at station G.

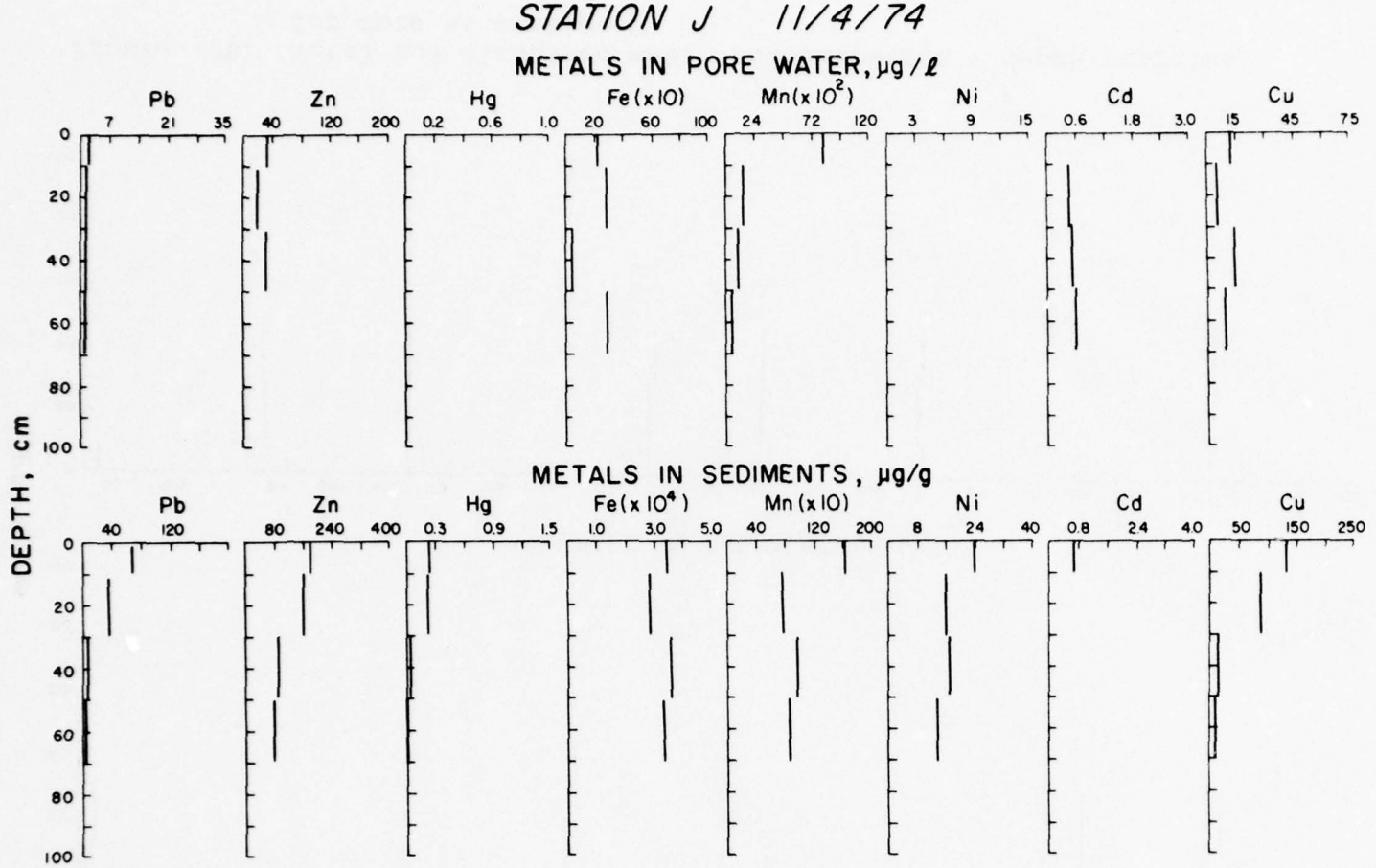



Figure 97. Total and dissolved metal concentration - depth profiles for core at station J.

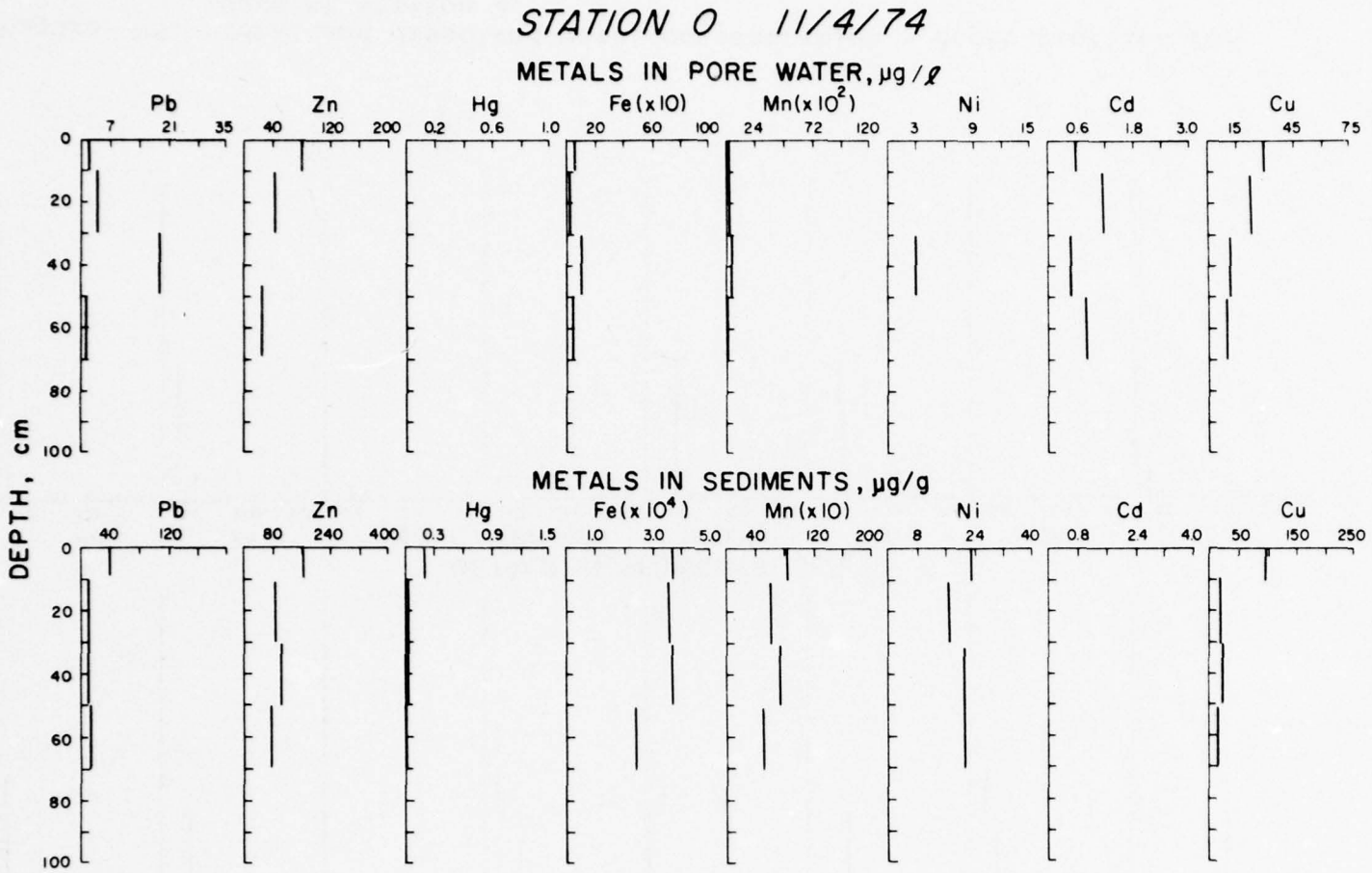



Figure 98. Total and dissolved metal concentration - depth profiles for core at station 0.

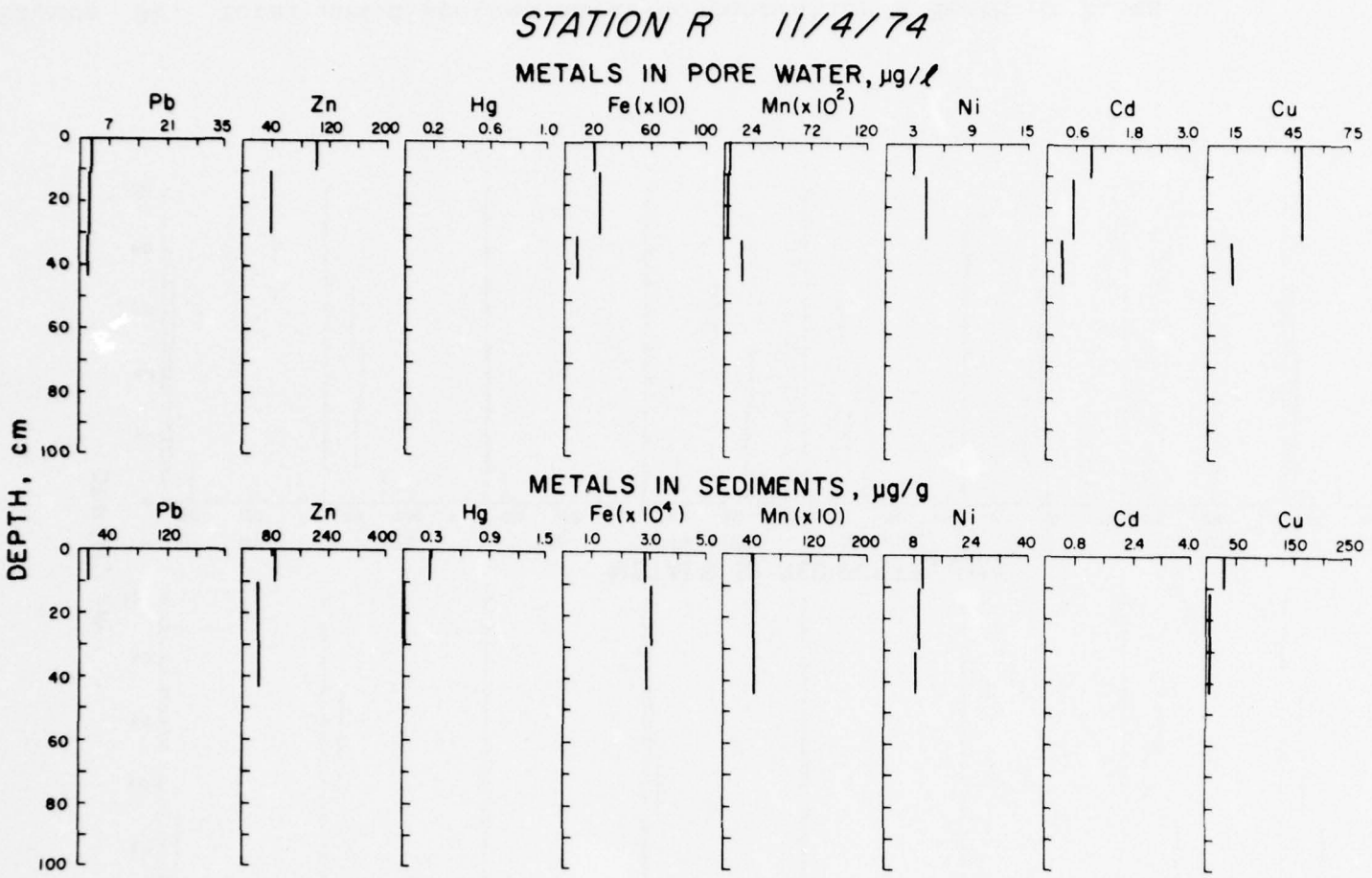



Figure 99. Total and dissolved metal concentration - depth profiles for core at station R.

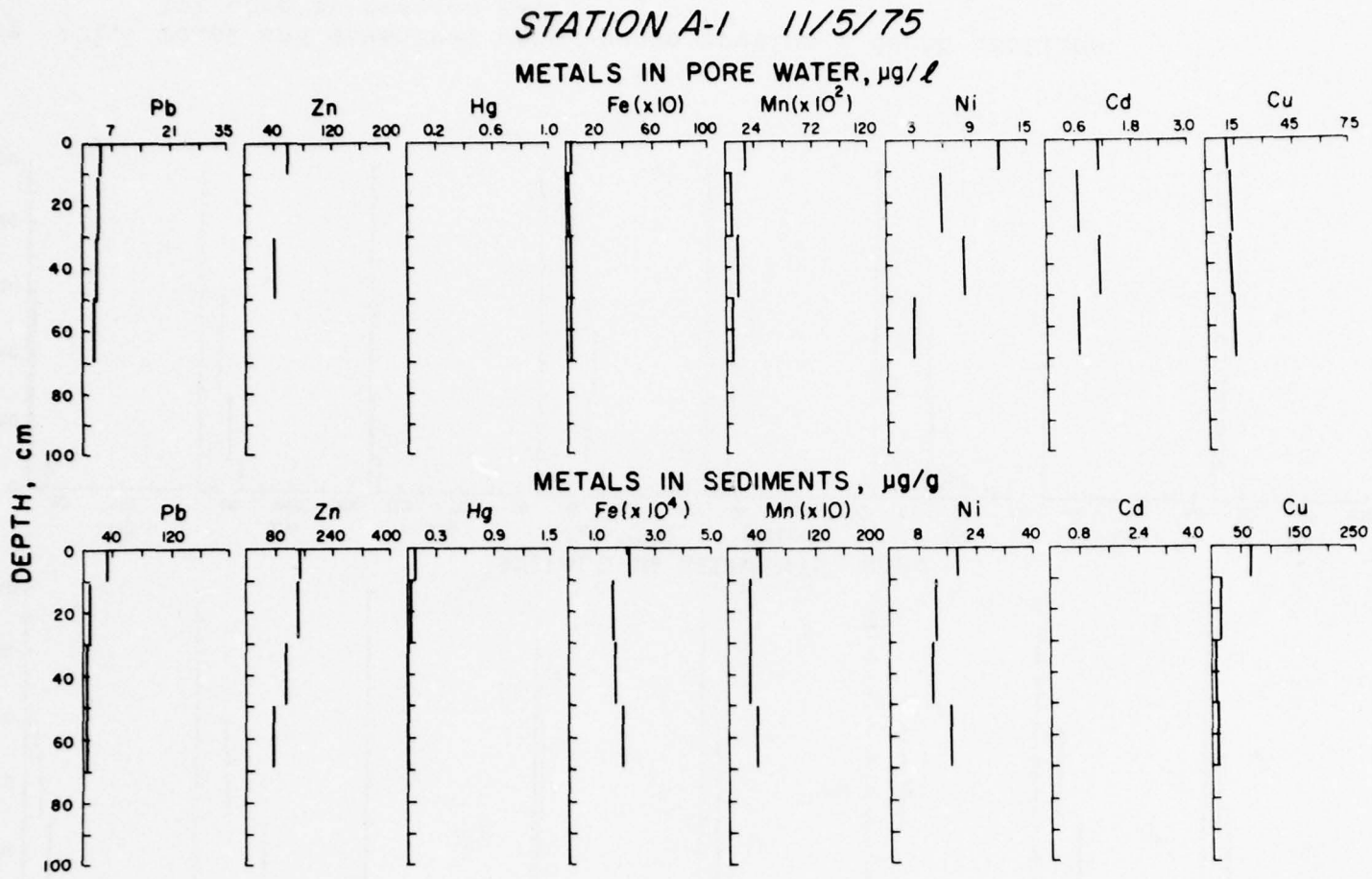



Figure 100. Total and dissolved metal concentration - depth profiles for core at station A1.

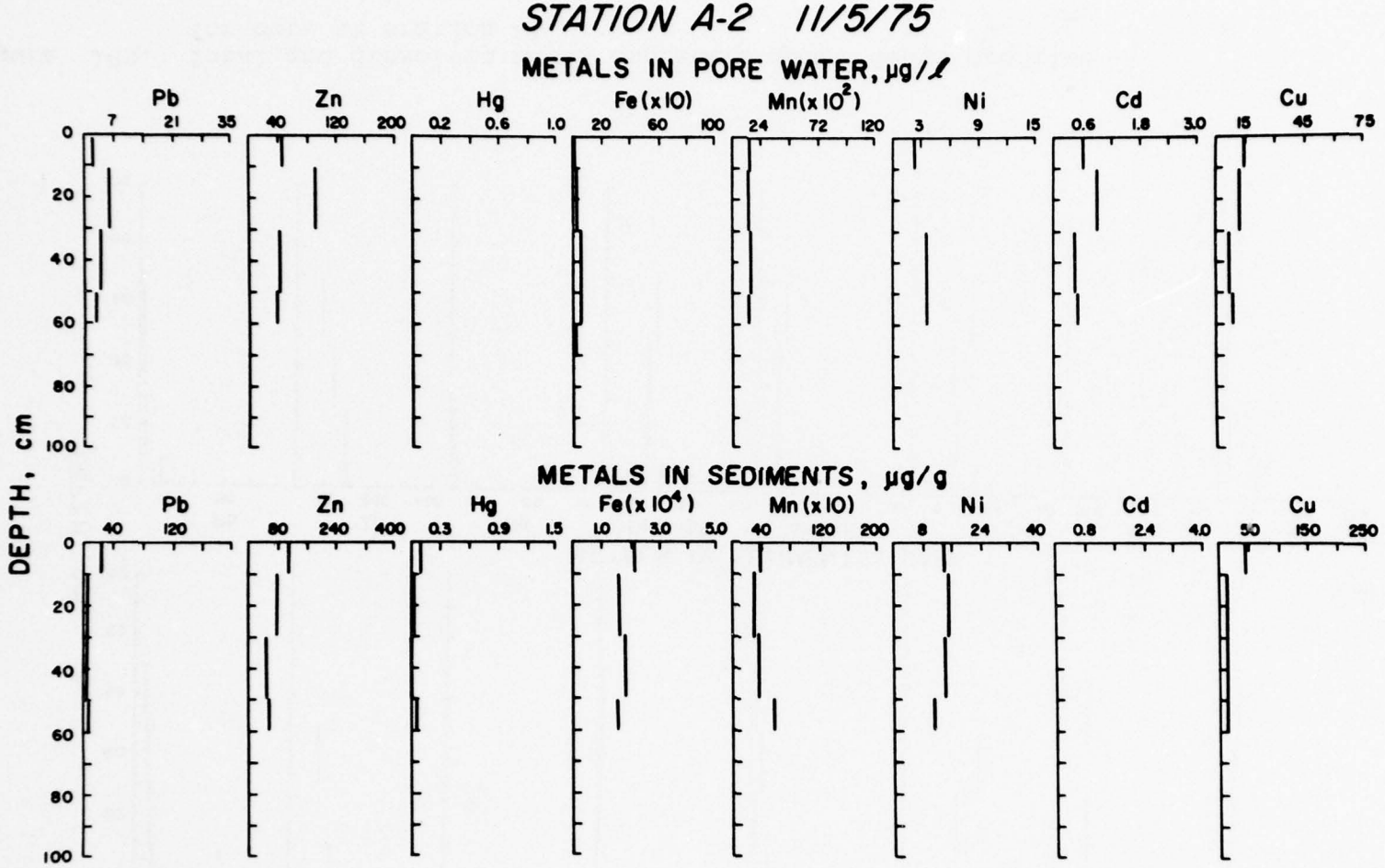



Figure 101. Total and dissolved metal concentration - depth profiles for core at station A2.

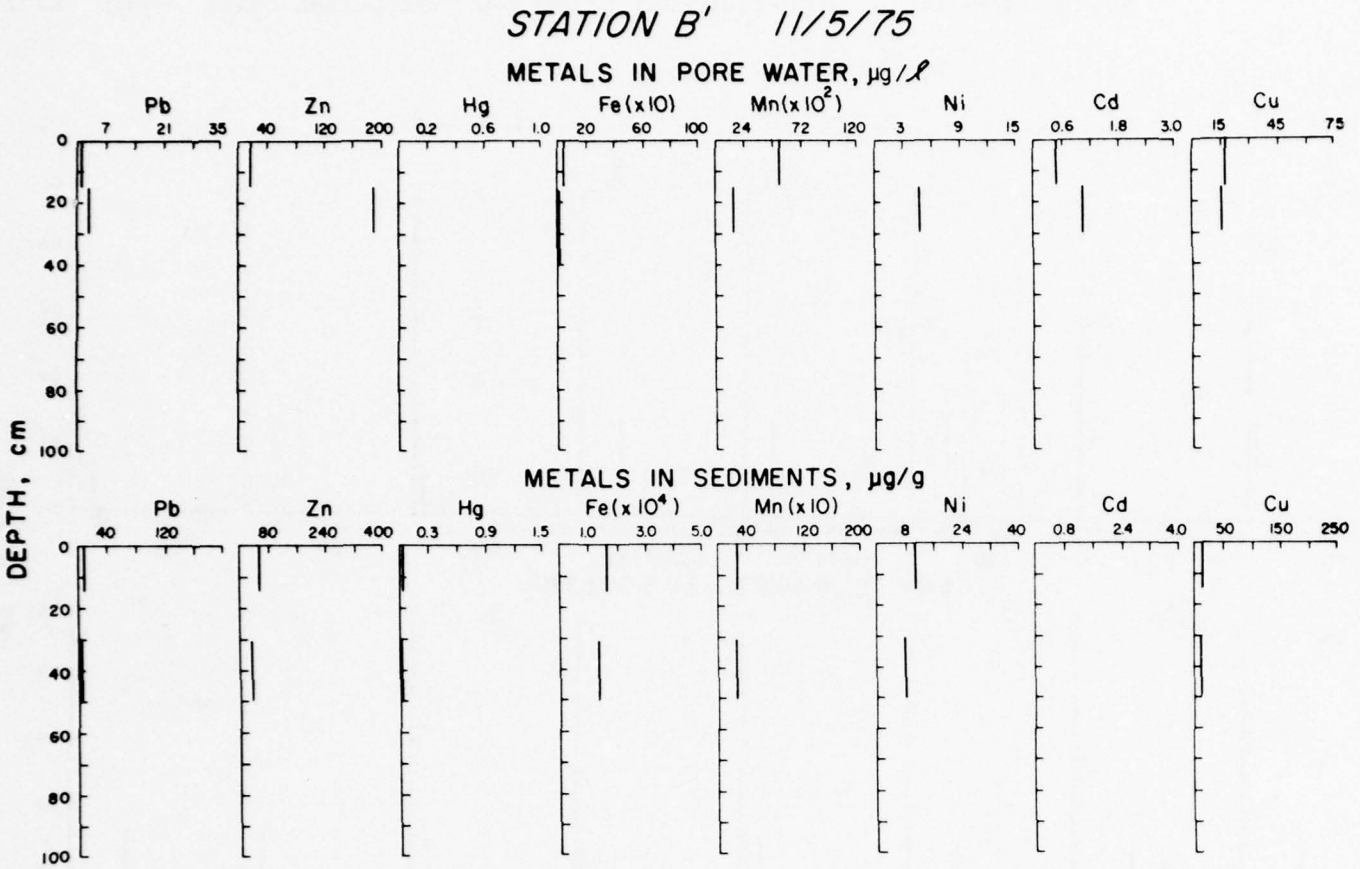



Figure 102. Total and dissolved metal concentration - depth profiles for core at station B'.

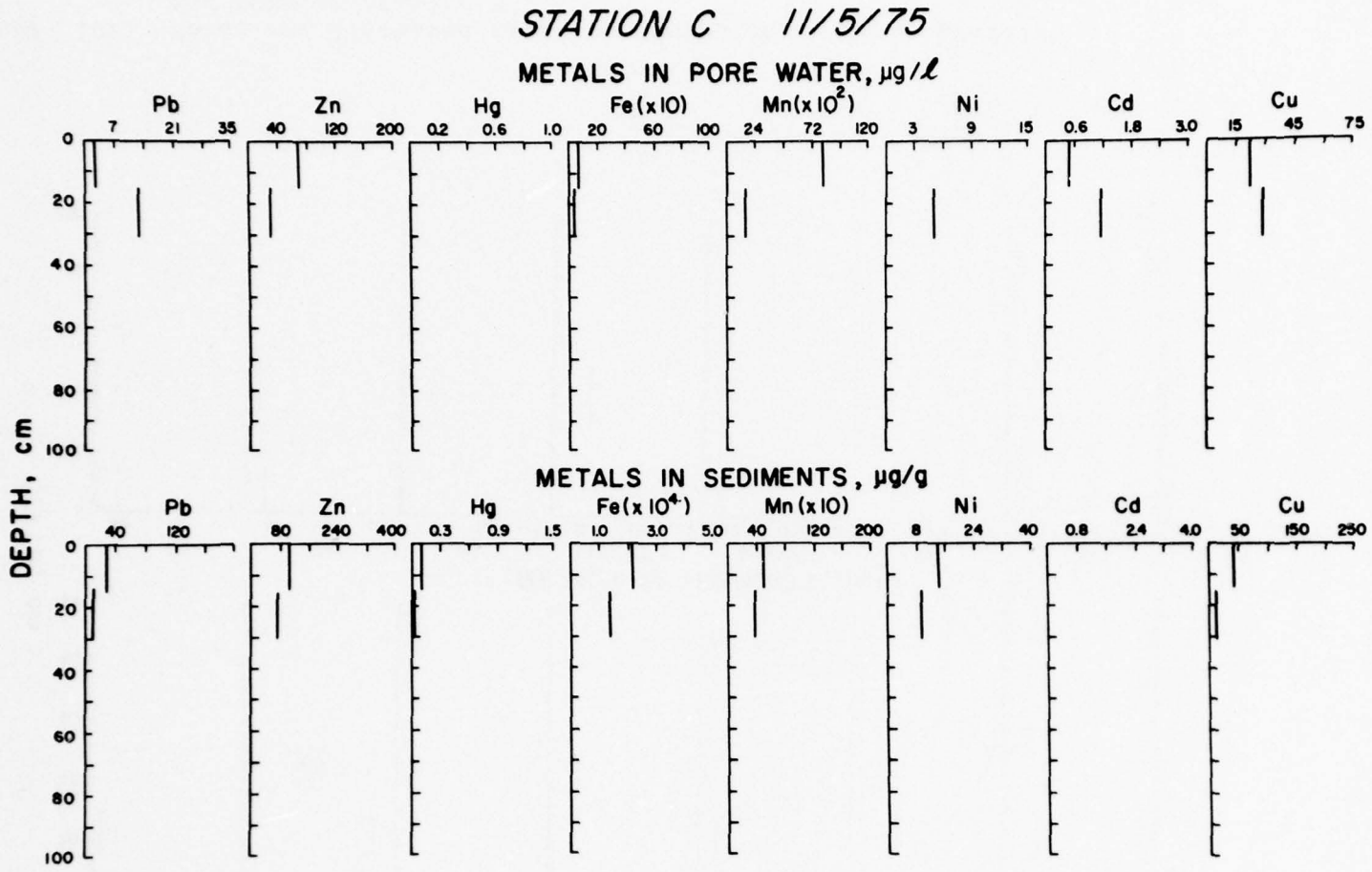



Figure 103. Total and dissolved metal concentration - depth profiles for core at station C.

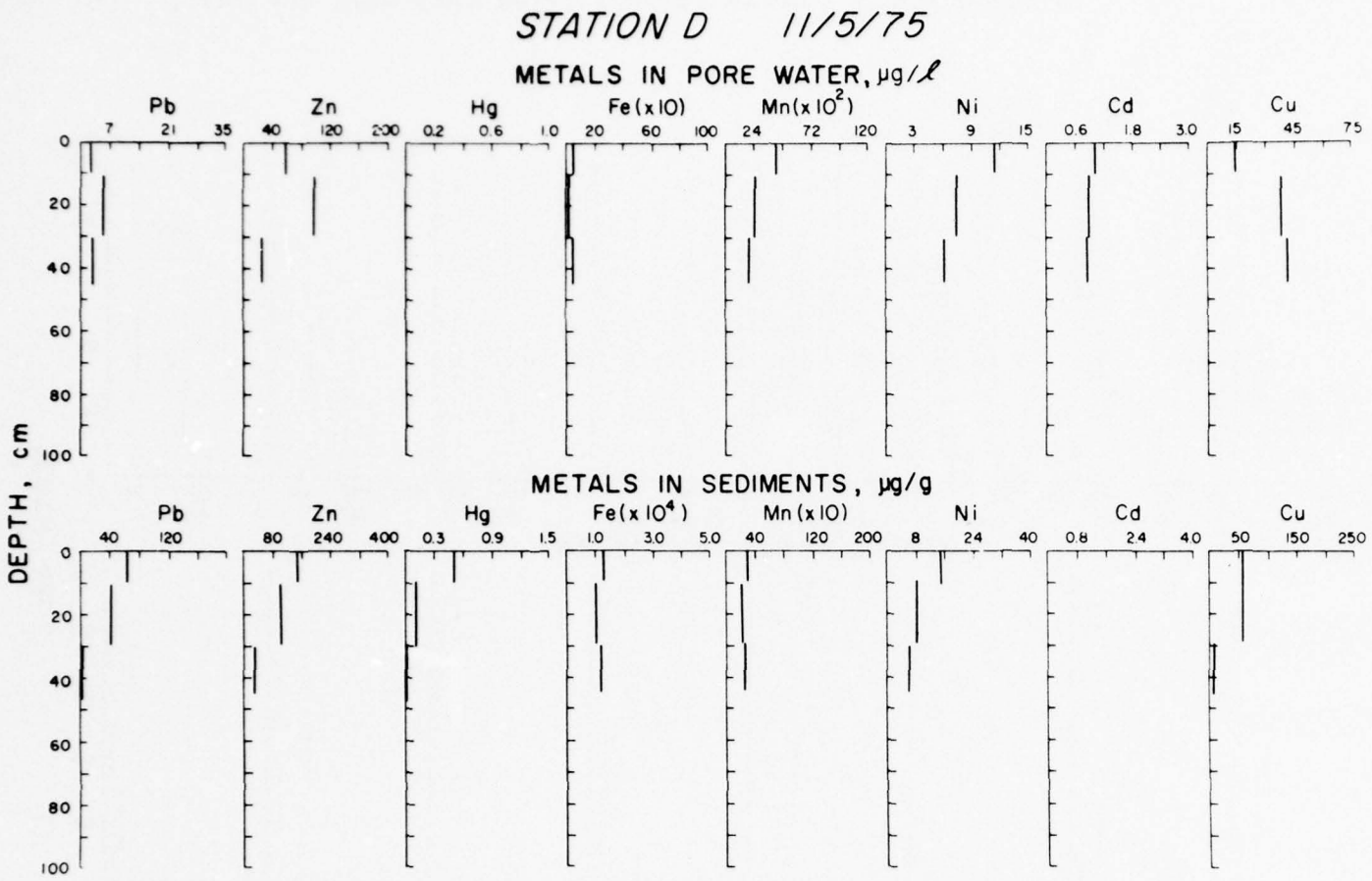



Figure 104. Total and dissolved metal concentration - depth profiles for core at station D.

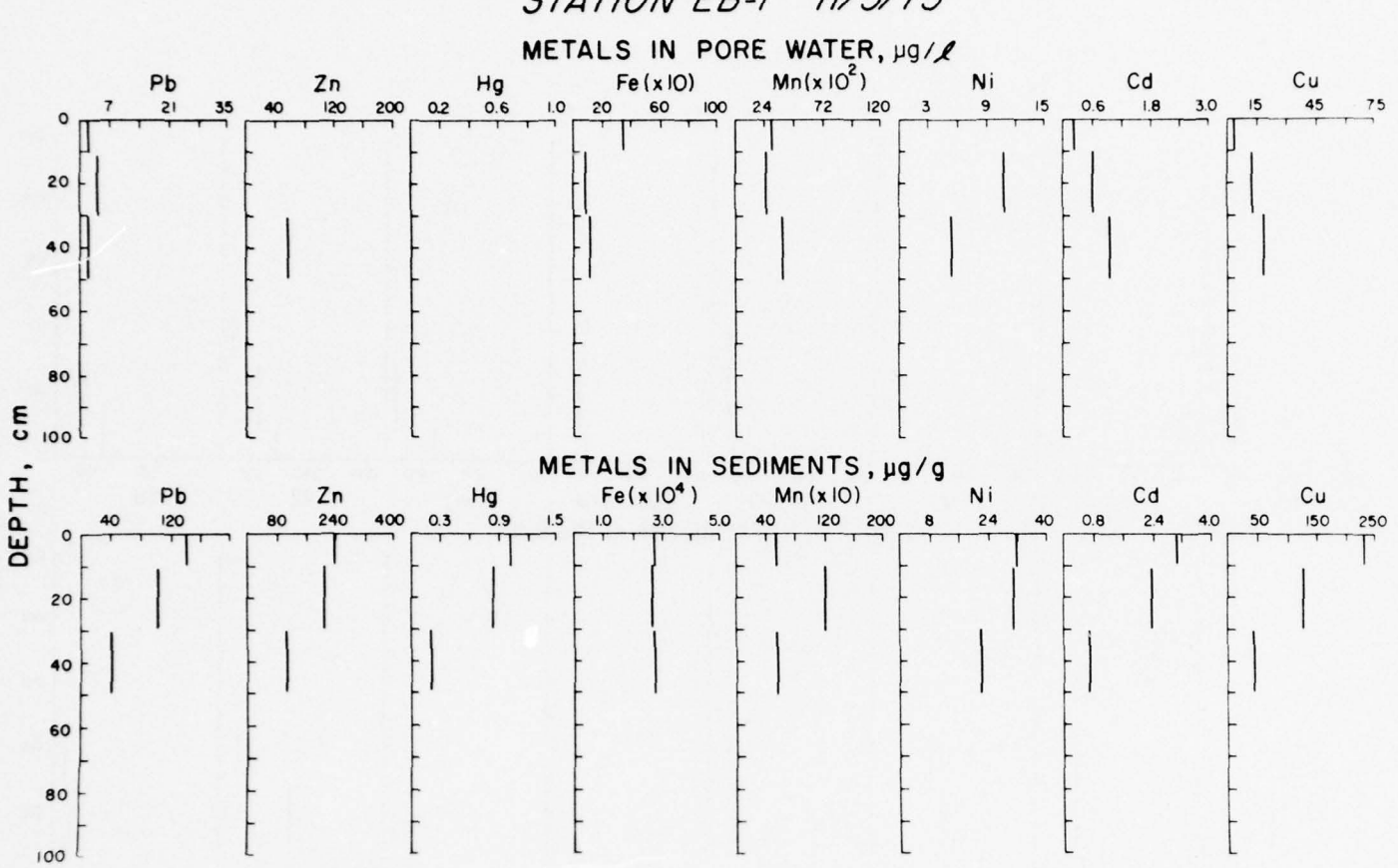



Figure 105. Total and dissolved metal concentration - depth profiles for core at station EB-1.

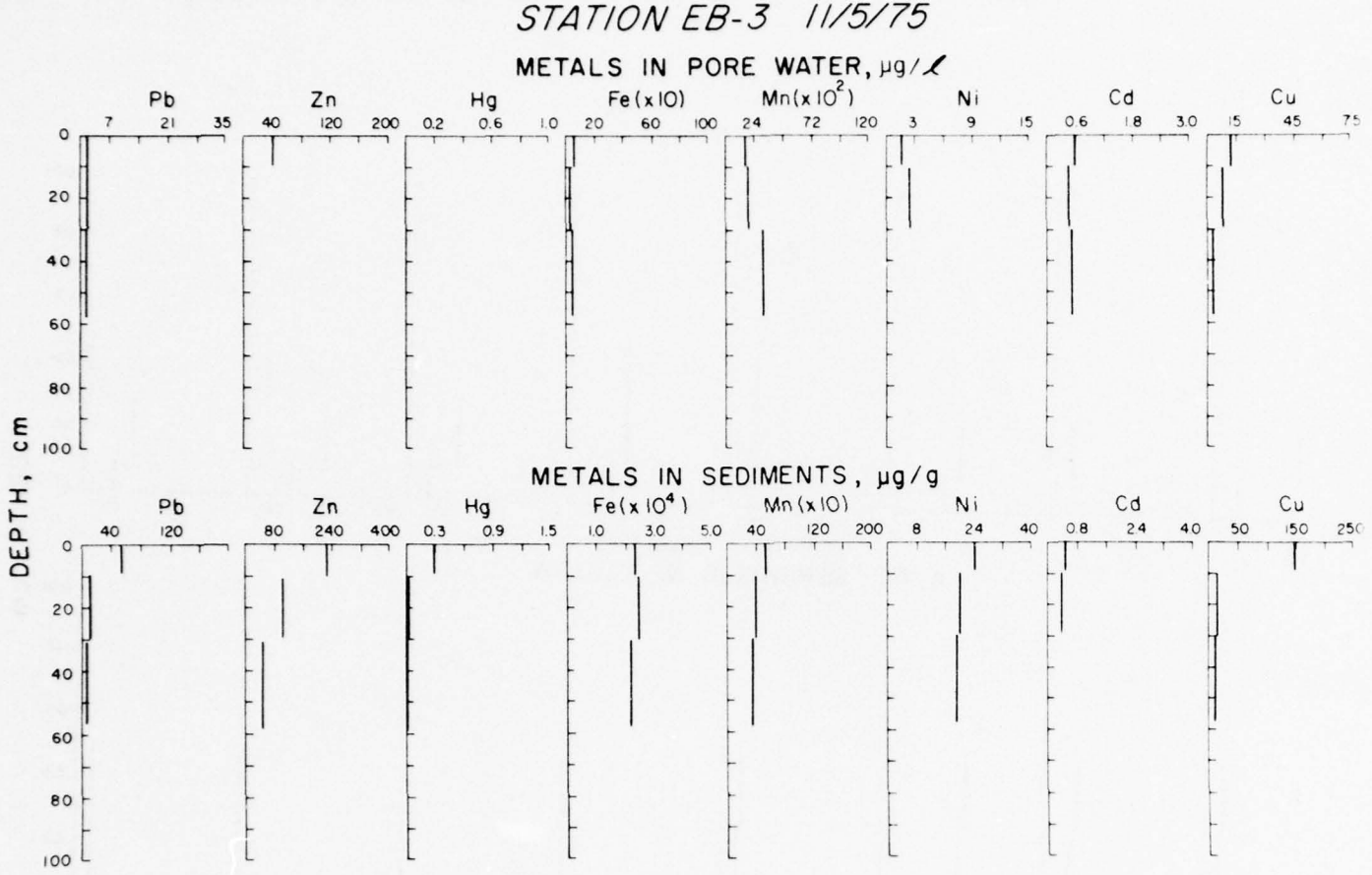



Figure 106. Total and dissolved metal concentration - depth profiles for core at station EB-3.

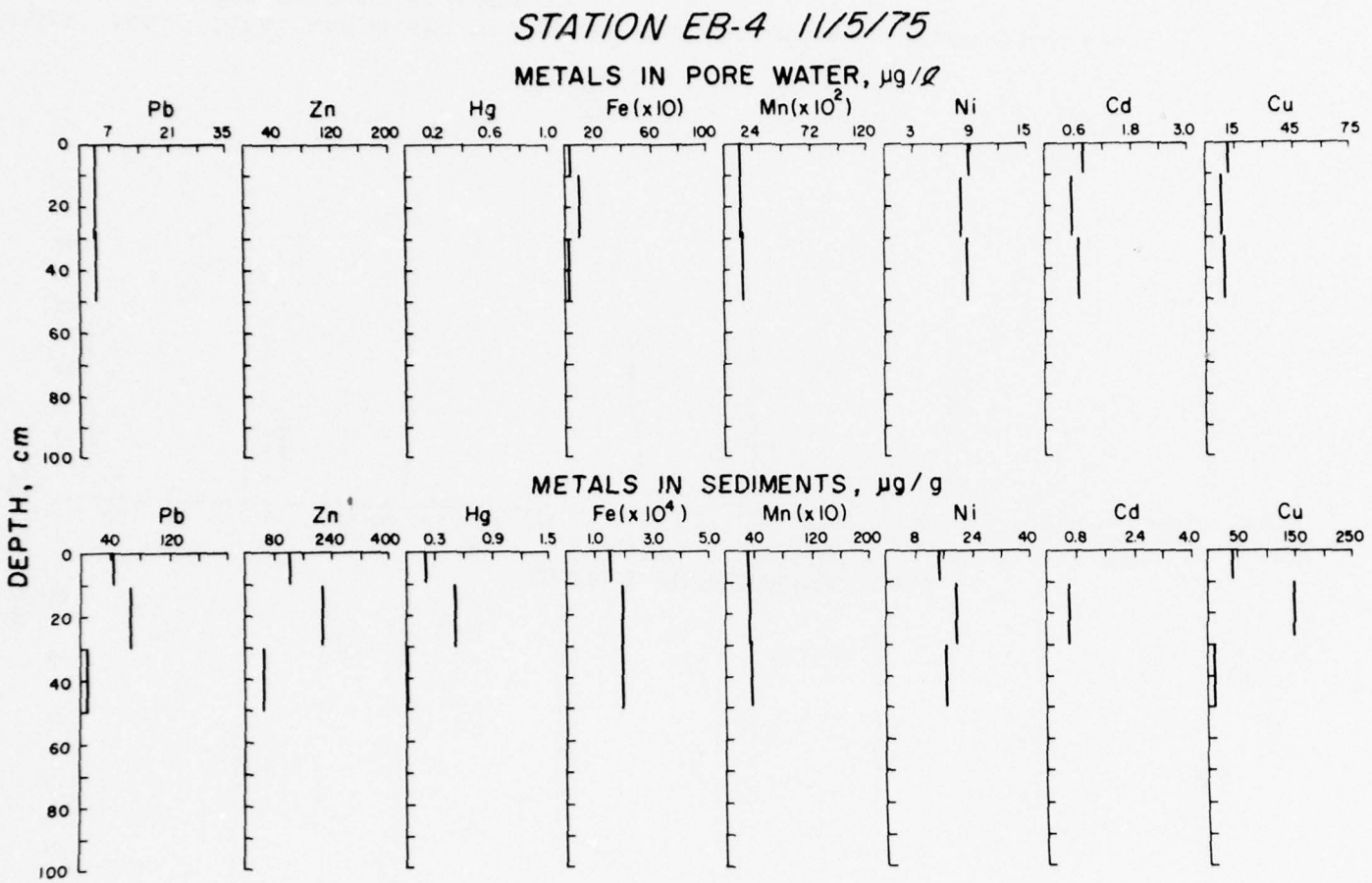



Figure 107. Total and dissolved metal concentration - depth profiles for core at station EB-4.

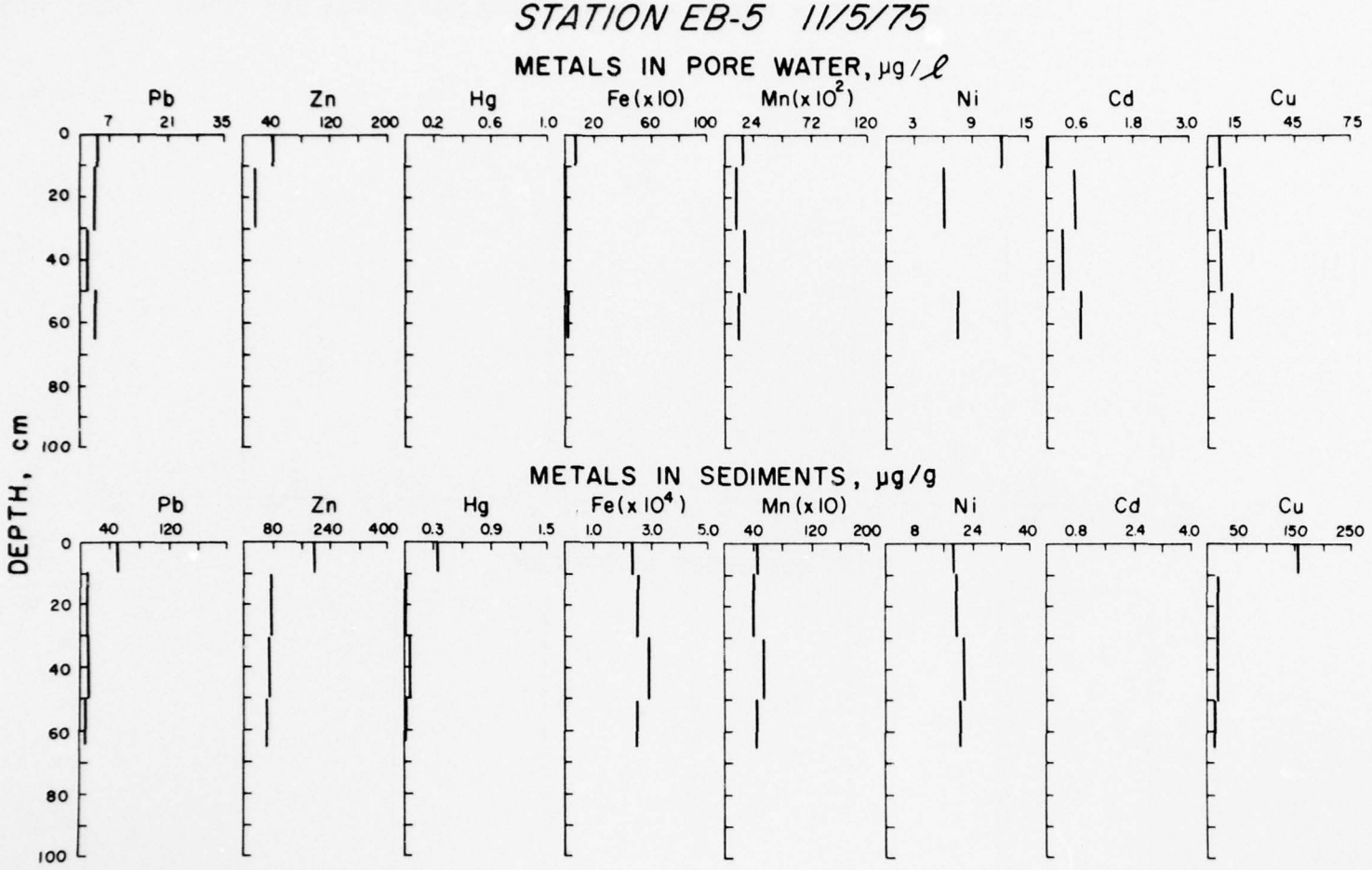



Figure 108. Total and dissolved metal concentration - depth profiles for core at station EB-5.

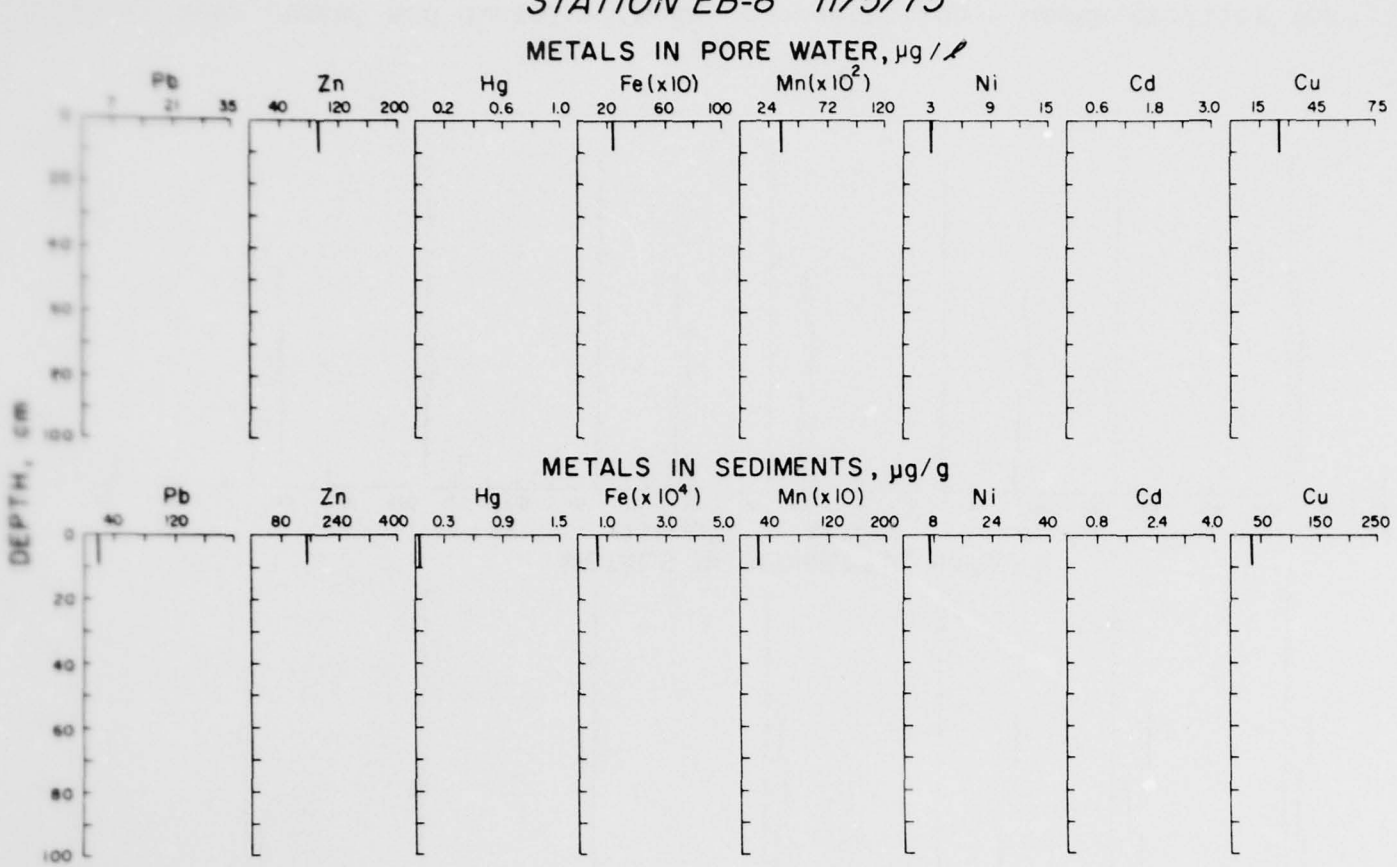



Figure 109. Total and dissolved metal concentration - depth profiles for core at station EB-8.

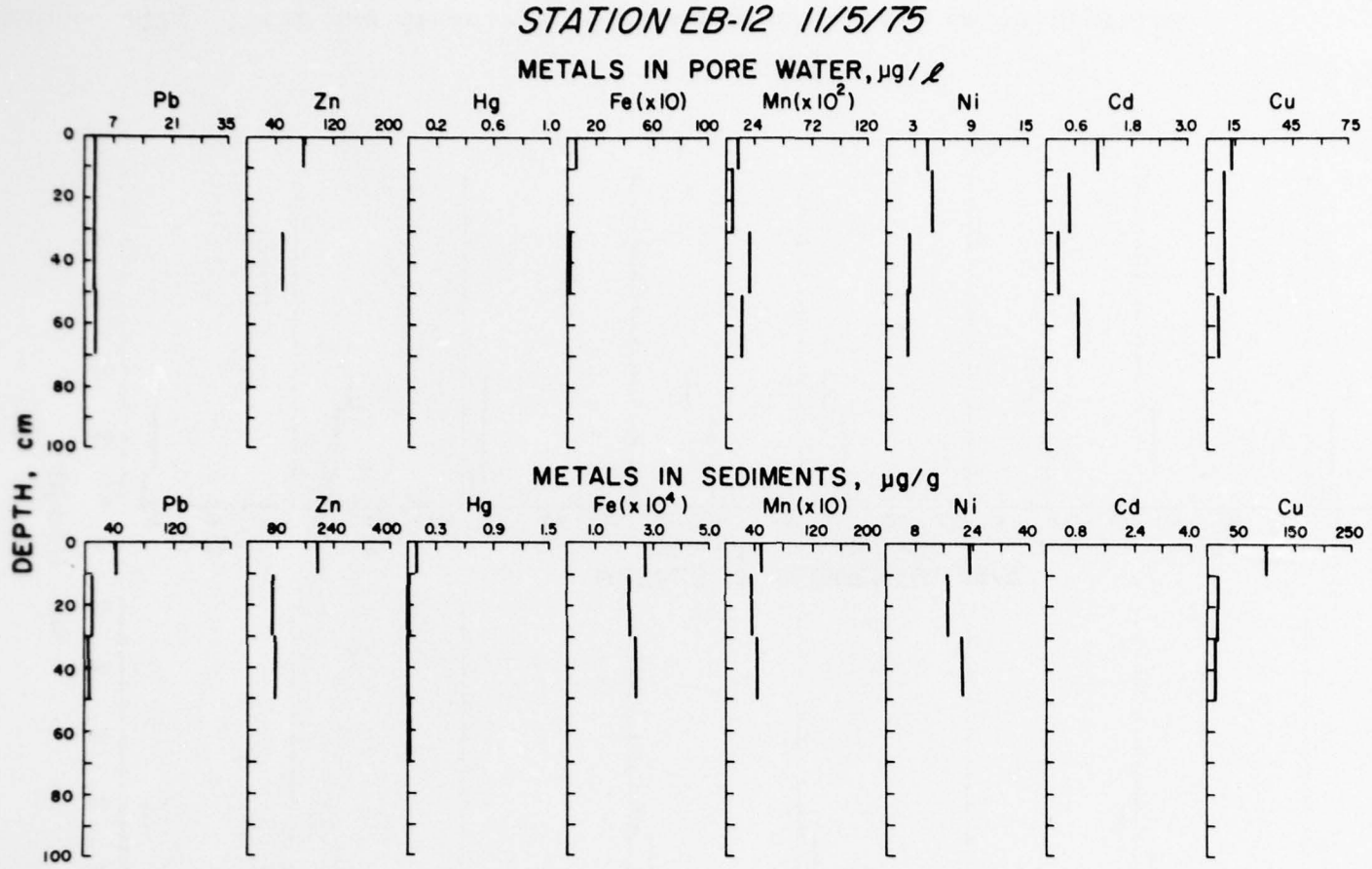



Figure 110. Total and dissolved metal concentration - depth profiles for core at station EB-12.

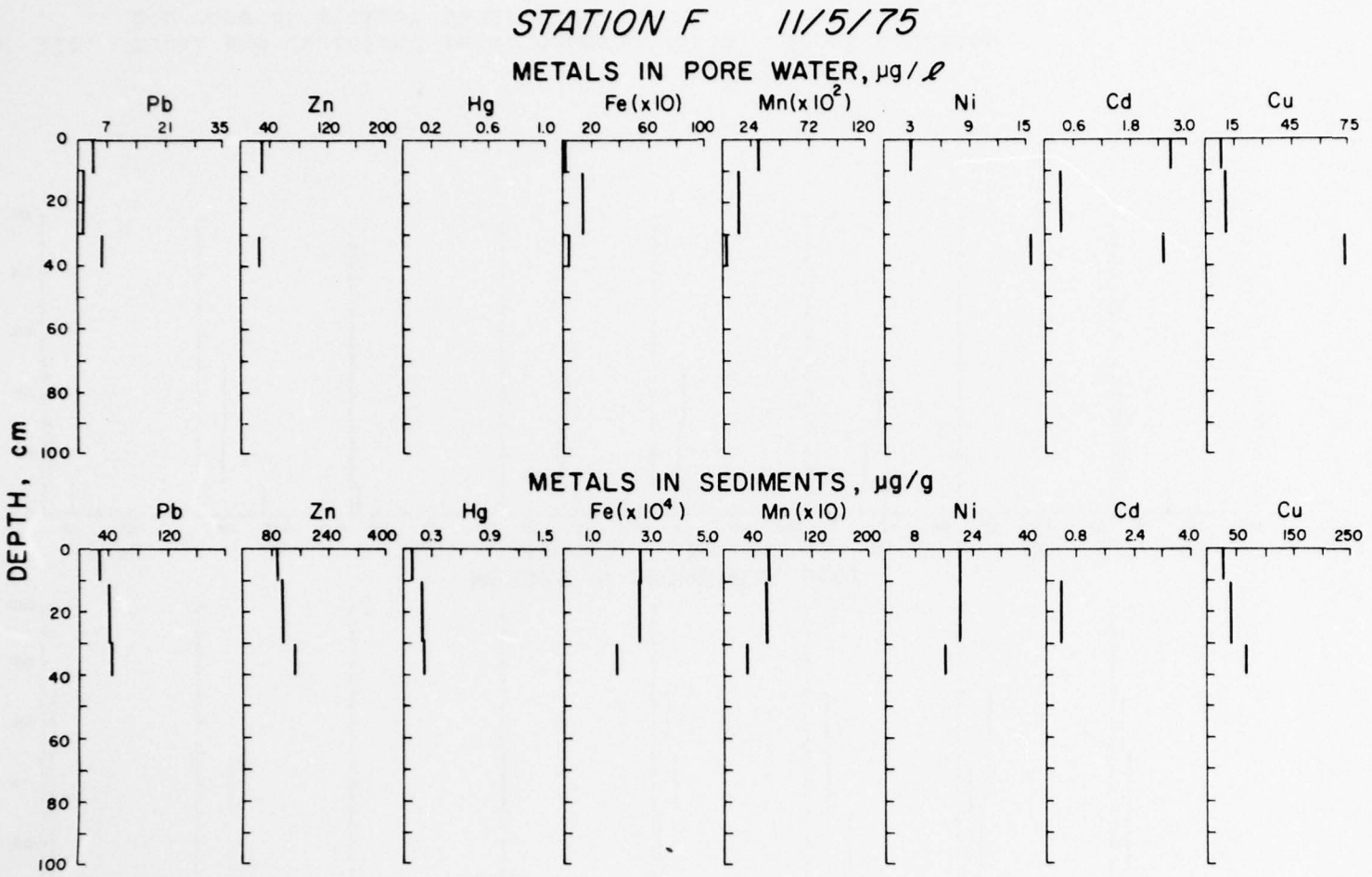



Figure 111. Total and dissolved metal concentration - depth profiles for core at station F.

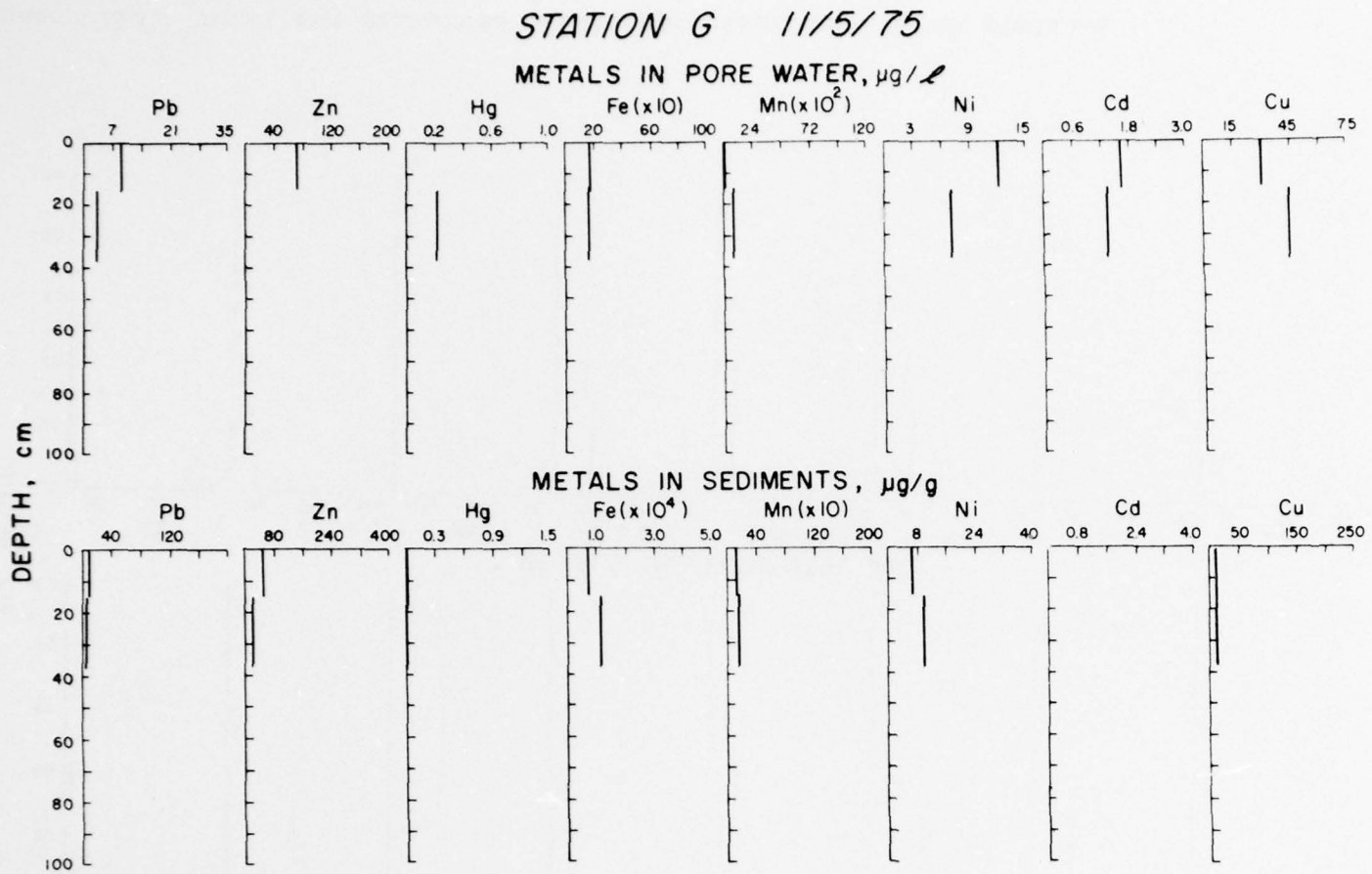



Figure 112. Total and dissolved metal concentration - depth profiles for core at station G.

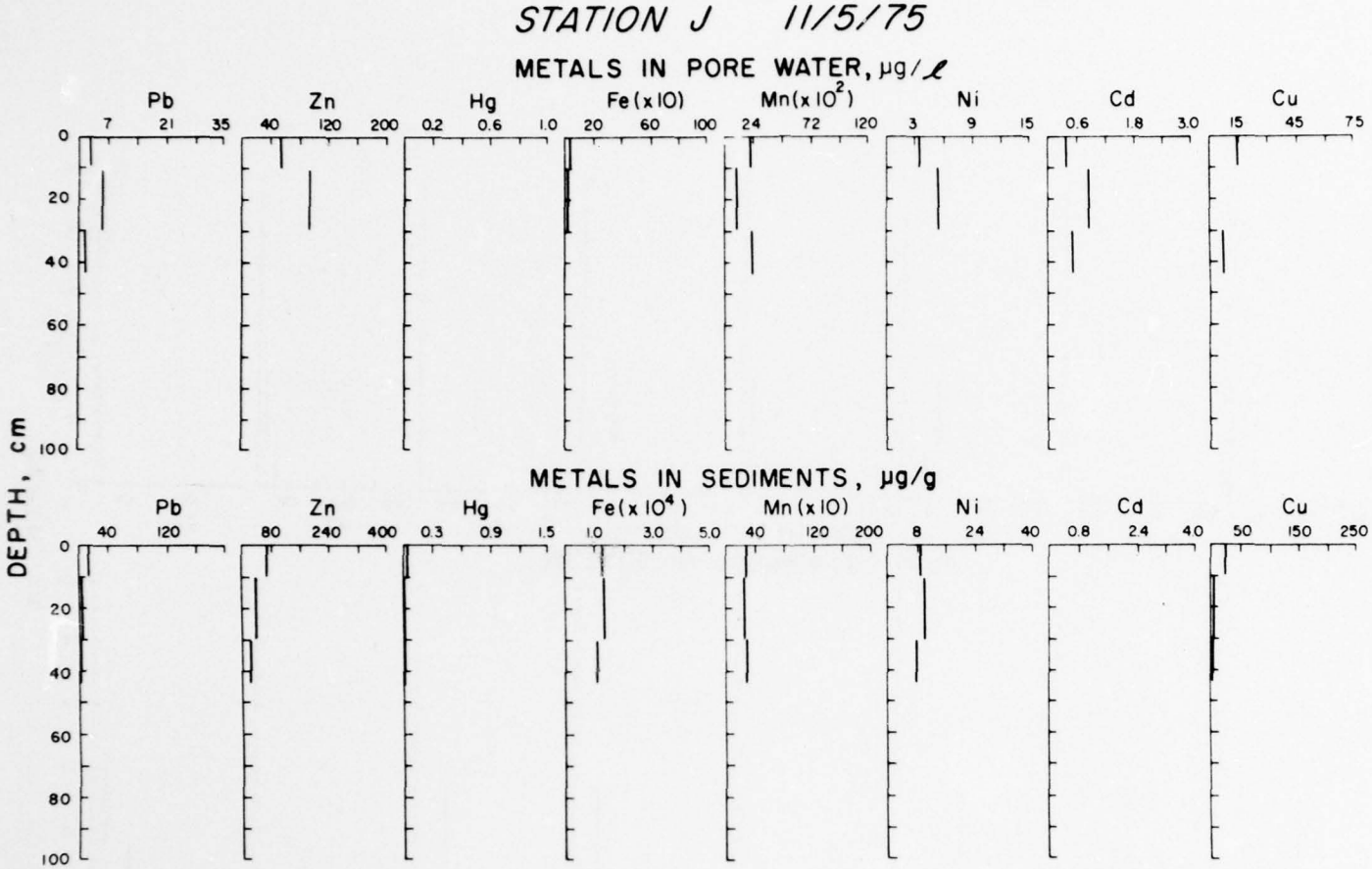



Figure 113. Total and dissolved metal concentration - depth profiles for core at station J.

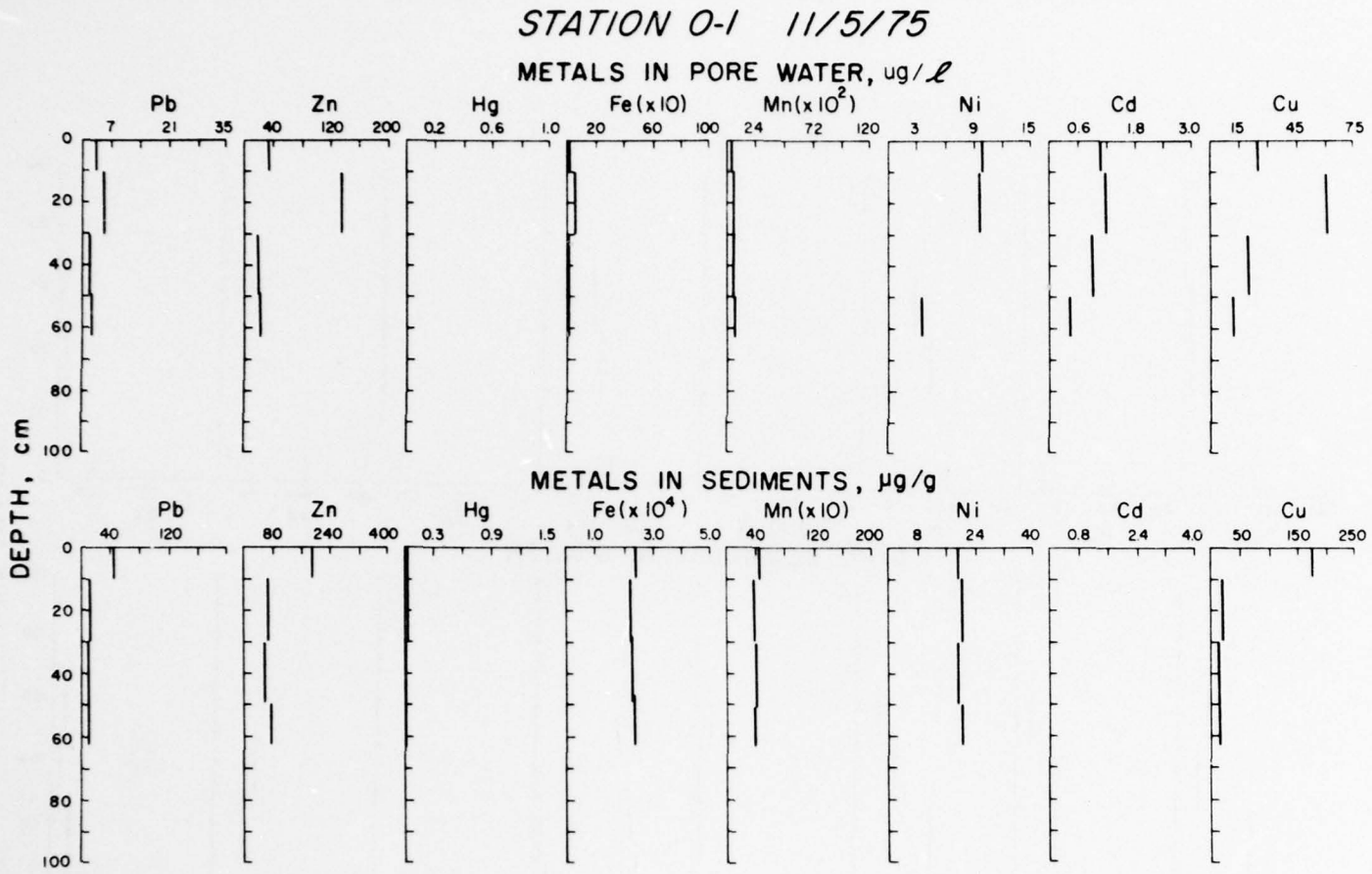



Figure 114. Total and dissolved metal concentration - depth profiles for core at station O-1.

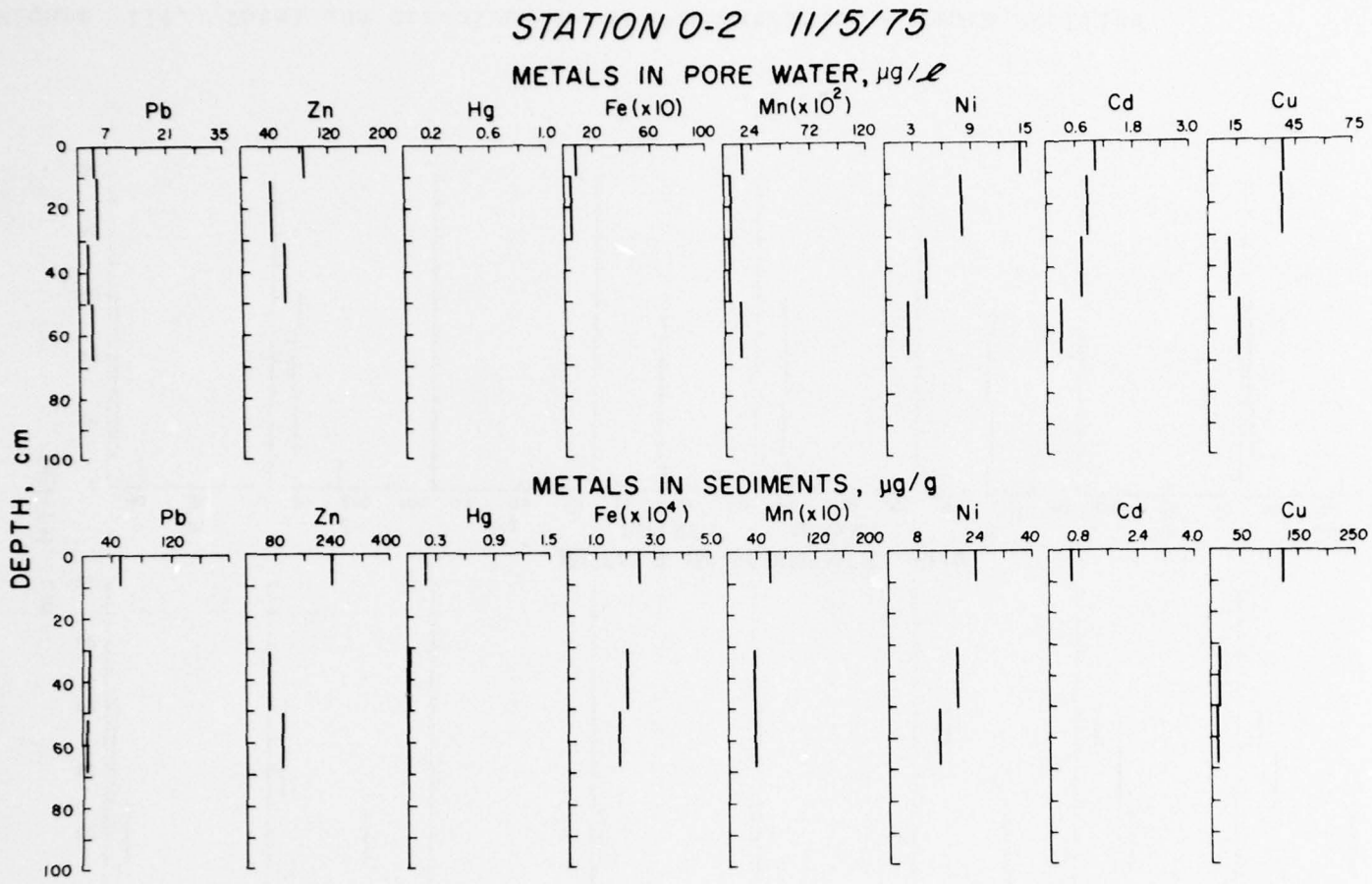



Figure 115. Total and dissolved metal concentration - depth profiles for core at station O-2.

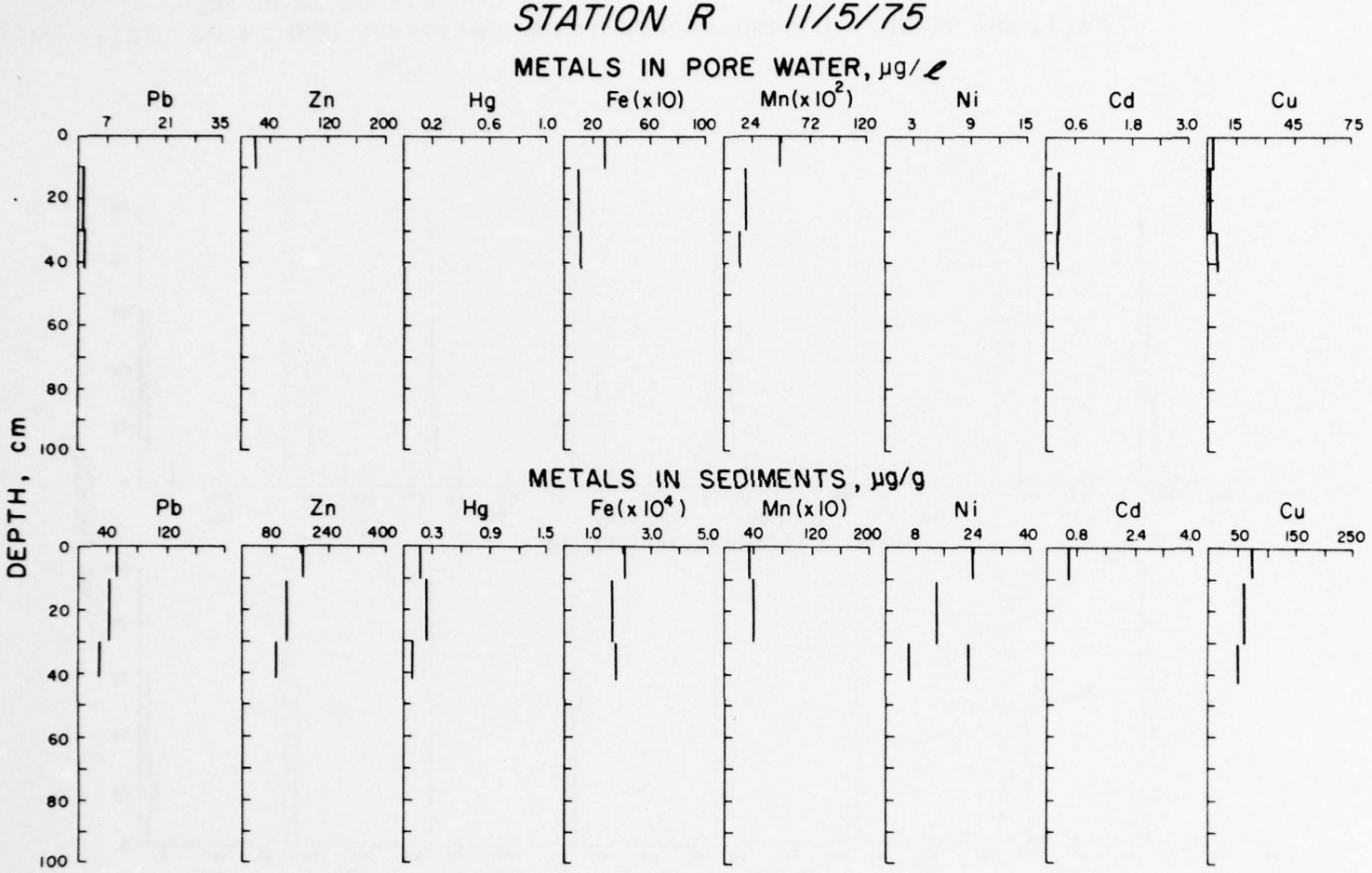



Figure 116. Total and dissolved metal concentration - depth profiles for core at station R.

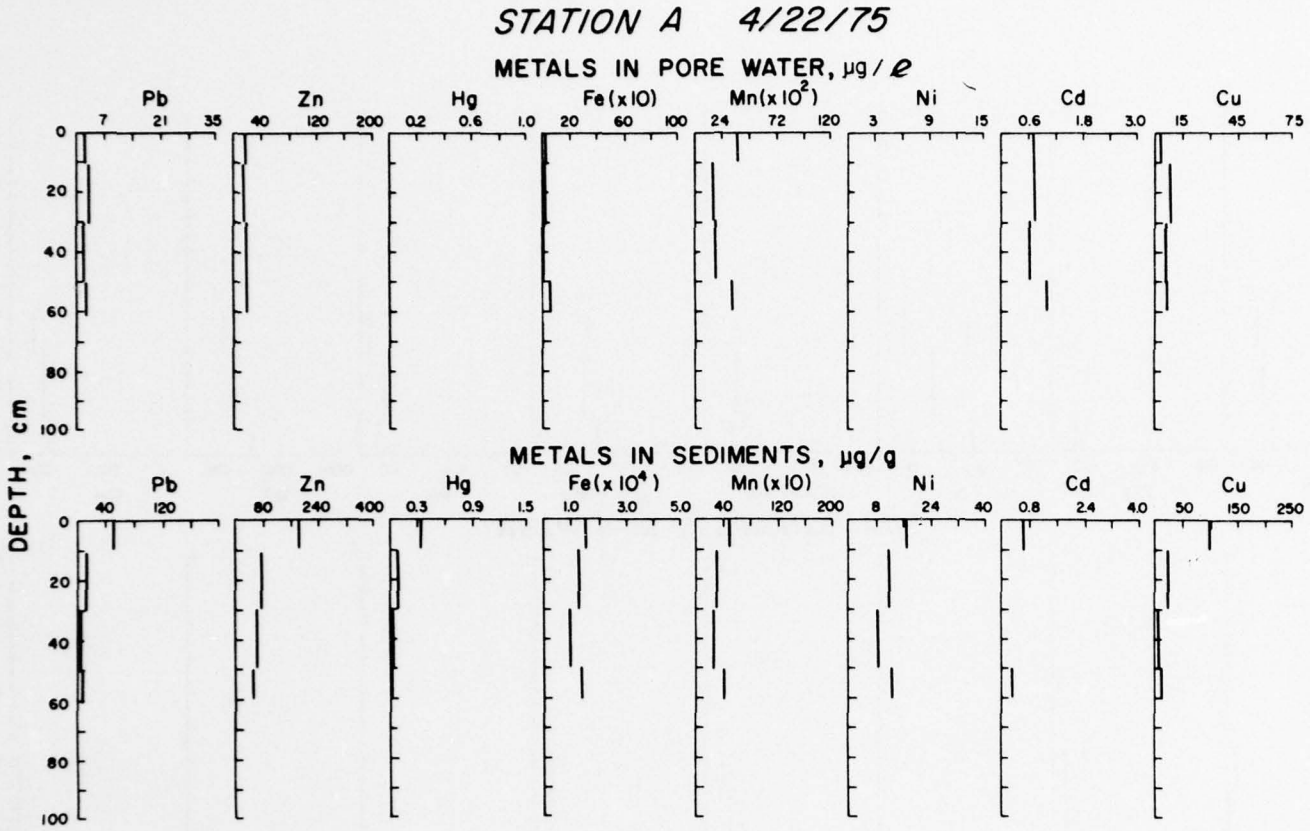



Figure 117. Total and dissolved metal concentration - depth profiles for core at station A.

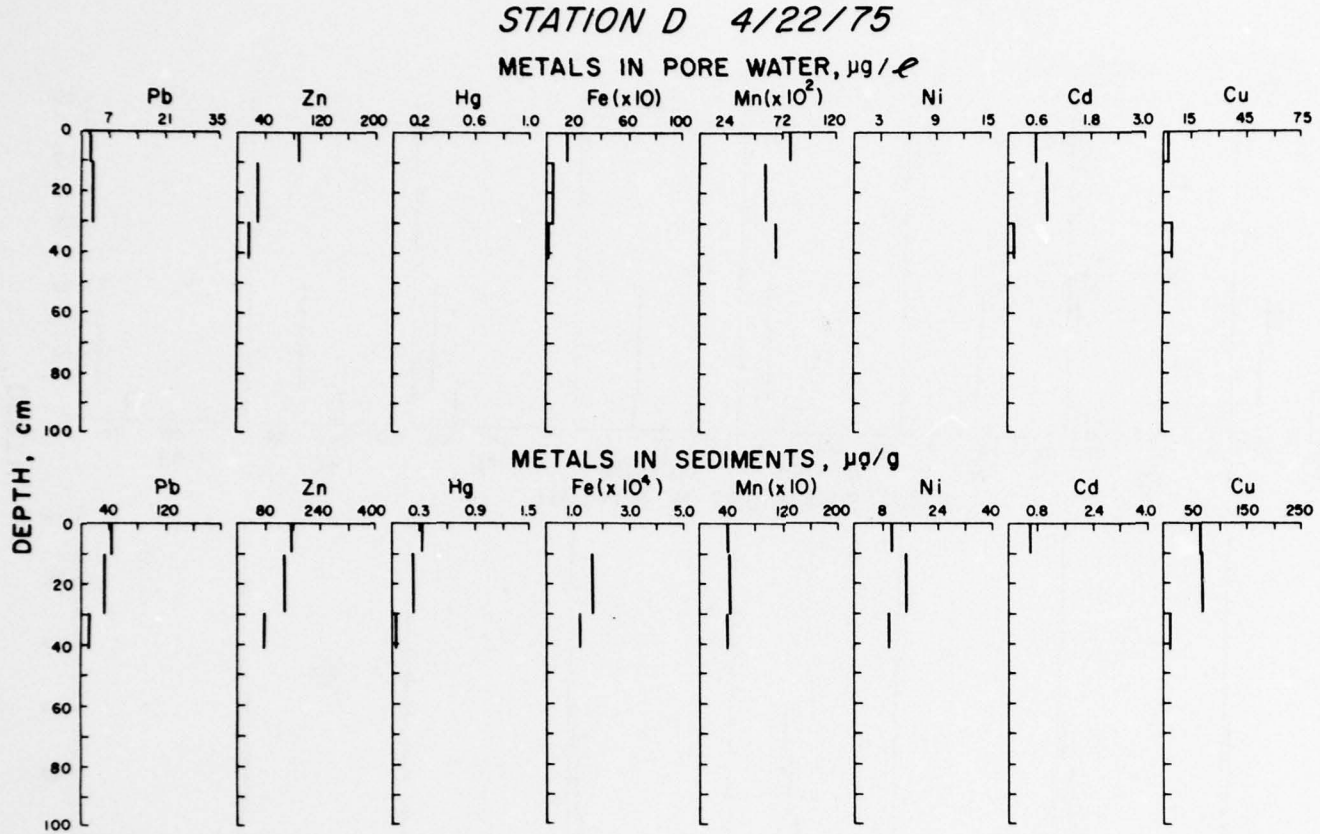



Figure 118. Total and dissolved metal concentration - depth profiles for core at station D.

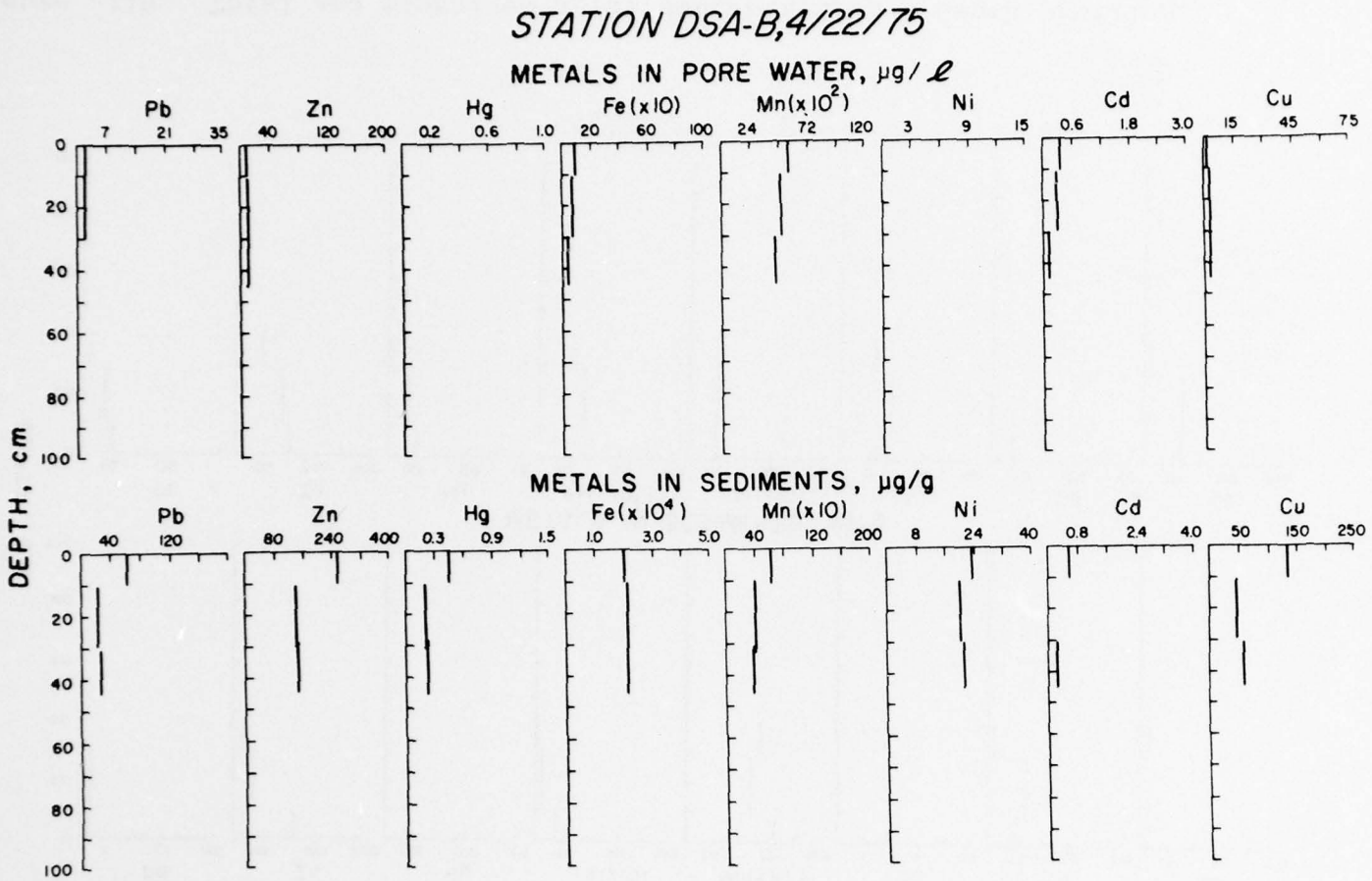



Figure 119. Total and dissolved metal concentration - depth profiles for core at station DSA-B.

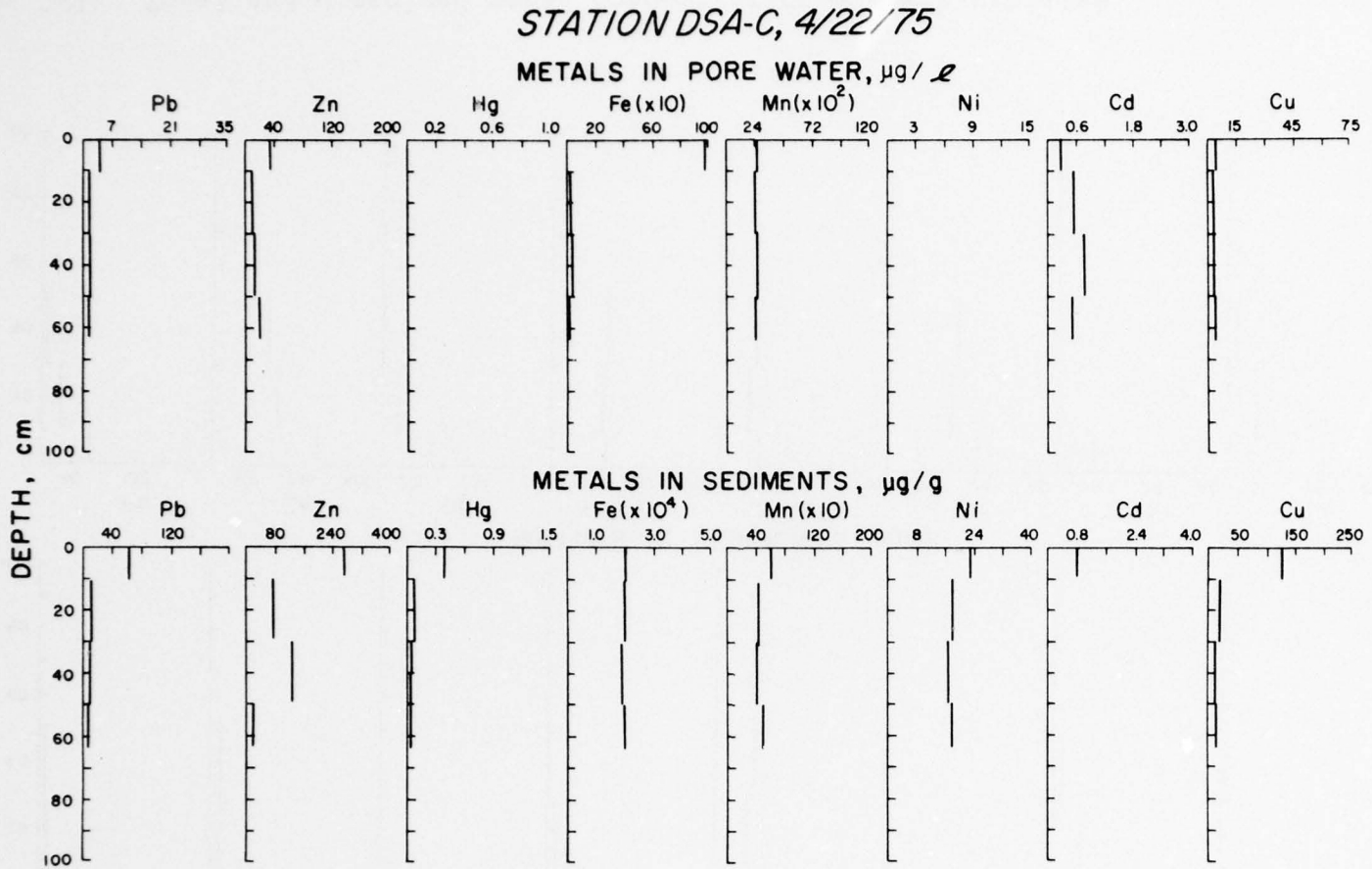



Figure 120. Total and dissolved metal concentration - depth profiles for core at station DSA-C.

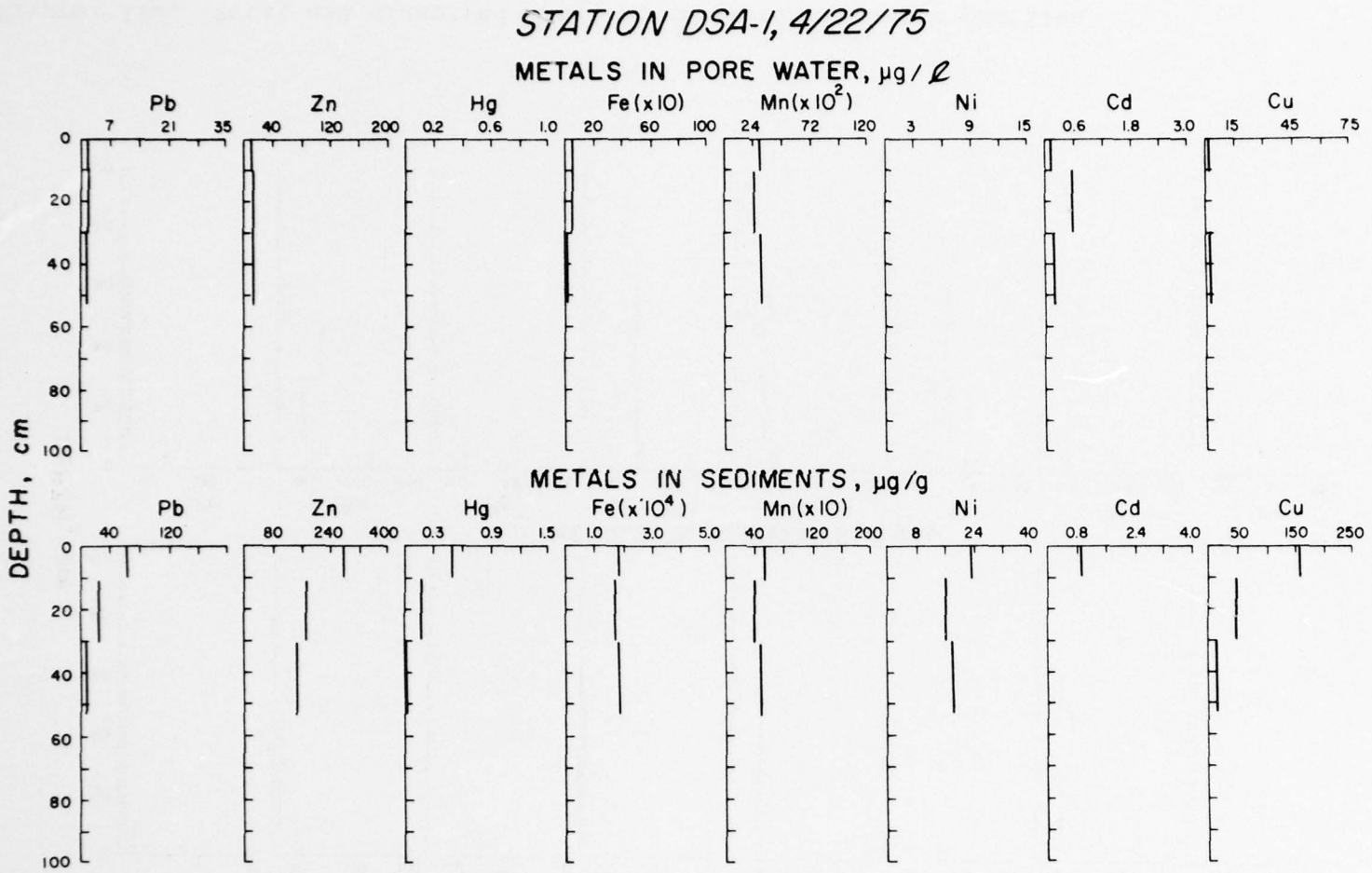



Figure 121. Total and dissolved metal concentration - depth profiles for core at station DSA-1.

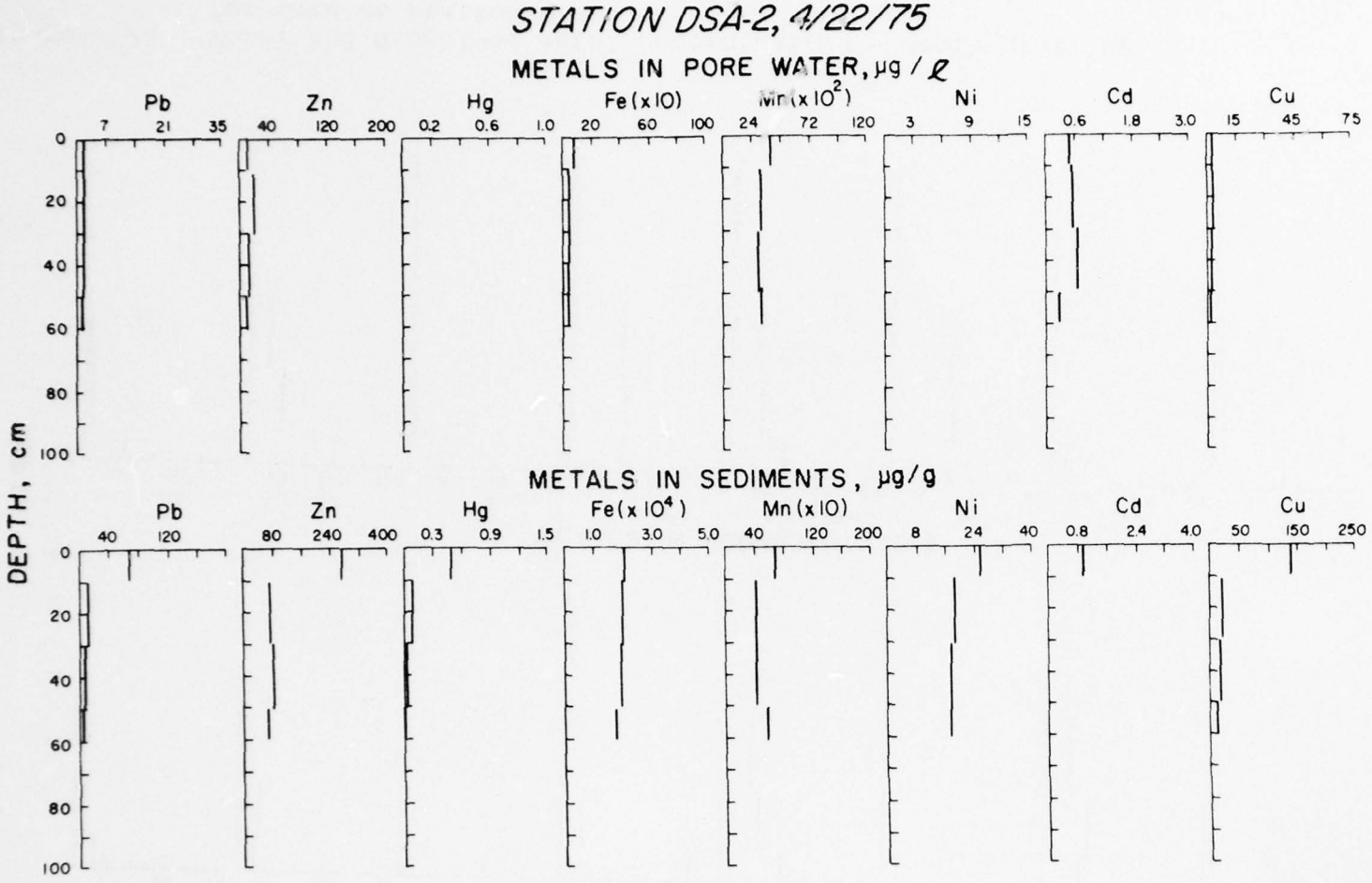



Figure 122. Total and dissolved metal concentration - depth profiles for core at station DSA-2.

AD-A053 427 STATE UNIV OF NEW YORK AT STONY BROOK MARINE SCIENCES--ETC F/G 13/2
AQUATIC DISPOSAL FIELD INVESTIGATIONS, EATONS NECK DISPOSAL SIT--ETC(U)
JAN 78 DACW51-75-C-0016

UNCLASSIFIED WES-TR-D-77-6-APP-B NL

3 OF 5
AD A053427



05342

1.0
1.1
1.25
1.4
1.6
2.8
3.2
3.6
4.0
2.5
2.2
2.0
1.8

MICROCOPY RESOLUTION TEST CHART
NATIONAL BUREAU OF STANDARDS-1963-A

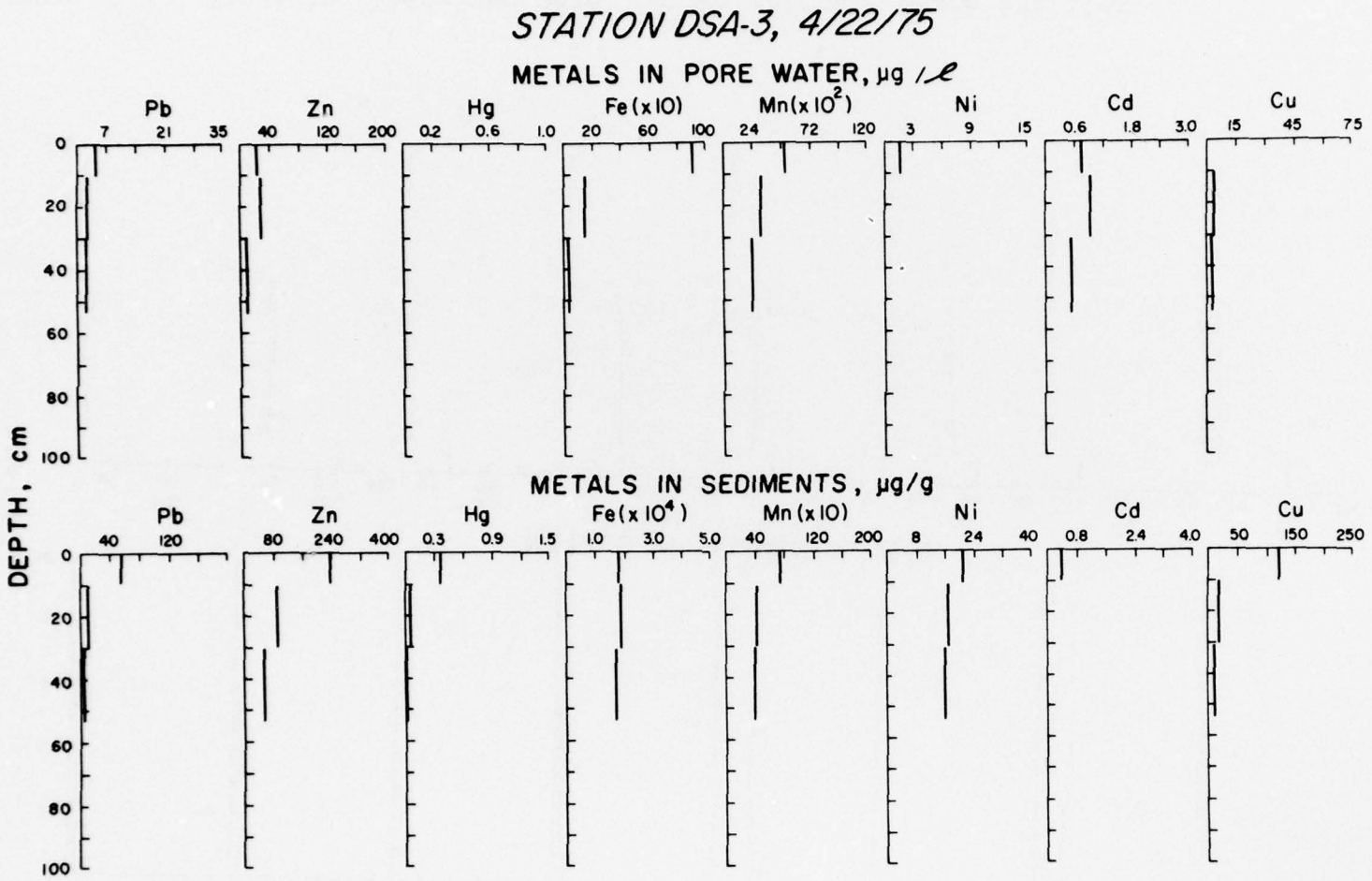



Figure 123. Total and dissolved metal concentration - depth profiles for core at station DSA-3.

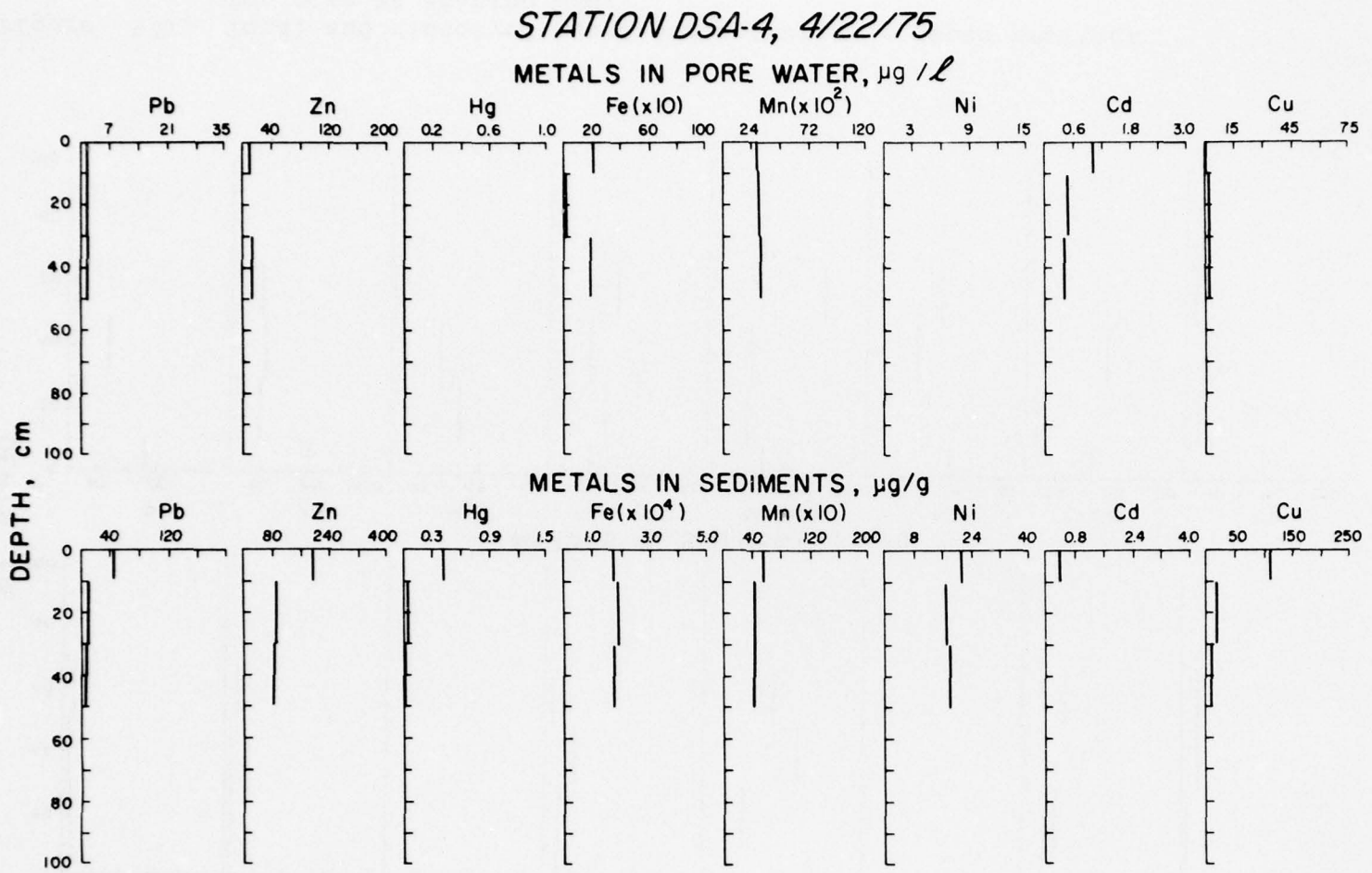



Figure 124. Total and dissolved metal concentration - depth profiles for core at station DSA-4.

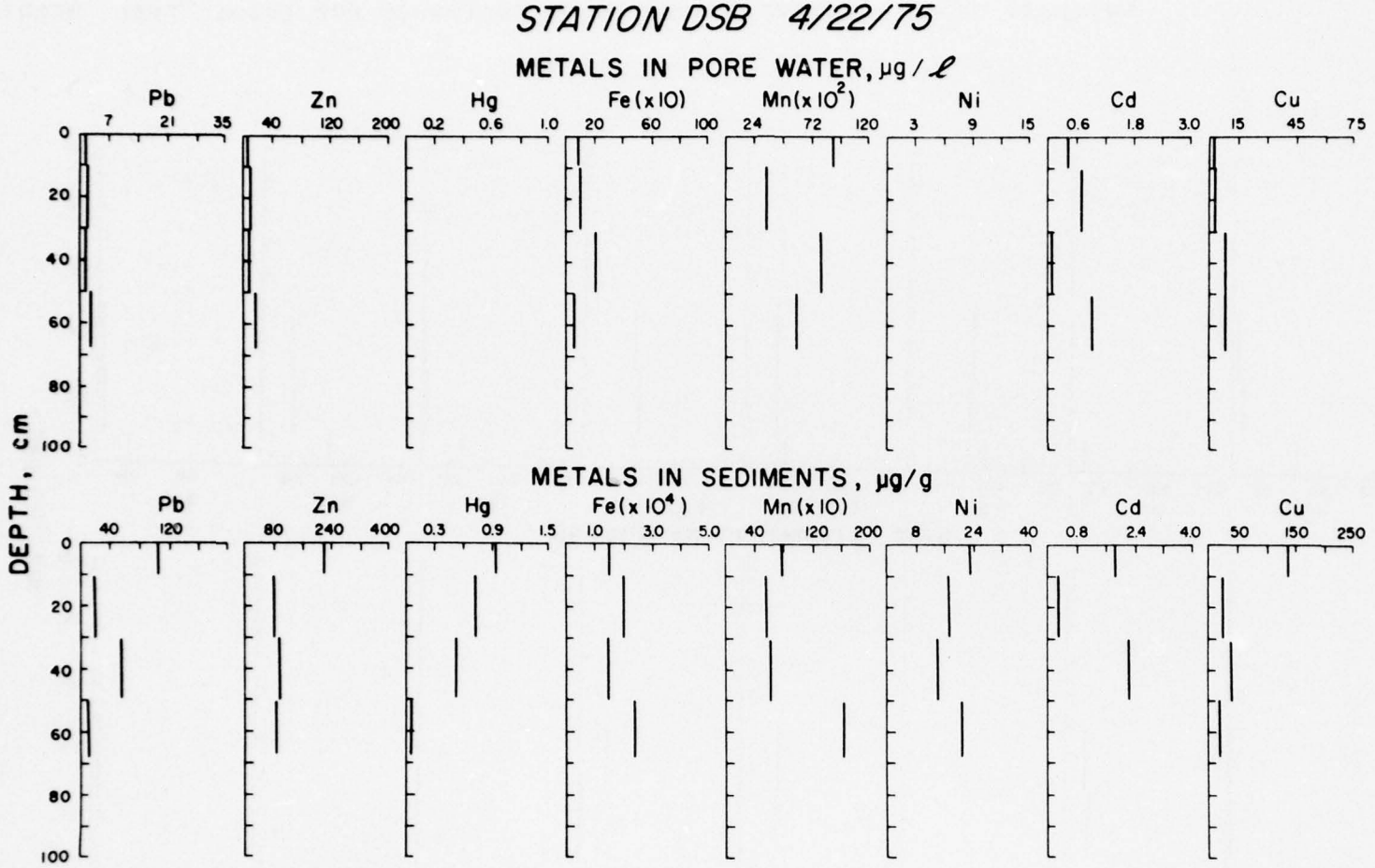



Figure 125. Total and dissolved metal concentration - depth profiles for core at station DSB.

of the core section. The absolute concentrations of the dissolved metals in sediment pore waters reported here (shown in Figures 91- 125) are generally greater than those found in the overlying water column. This is in general agreement with the observations made by several other workers (Presley et al.;[70] Brooks et al.;[71] Duchart et al.[72]). The dissolved metal concentrations exhibit a rather wide range of variation: Zn, 2-269 µg/l; Pb, 0.9-32.2 µg/l; Cd, 0.03-2.68 µg/l; Cu, 1.6-92.2 µg/l; Ni, 0.3-15.3 µg/l; Mn, 80-11250 µg/l; and Fe, 11-968 µg/l. For some of the samples, the pore water metal concentrations were below the limits of detection. Interstitial Hg in sediments was not determined because the analytical method was not developed to detect low concentration levels. At a few stations, some metals show no variations with depth. Most of the metals exhibit irregular vertical variations. Too few data points are available to interpret the dissolved metal concentration profiles.

163. In many cores, a pattern of decreasing total metal concentration with increasing depth of sediment burial is observed for Pb, Zn, Cu, and Hg. Since the mineralogy and grain-size distribution do not show any significant trend with depth in the cores, these parameters can not account for the observed metal concentration profiles. Turekian[37] observed a similar distribution in a core from the central Long Island Sound for Cu, Zn, Pb, and Hg and reported that, for reducing sediments, the concentration of sulphide ions in sediment pore waters determines the mobility of metals. Table 9, adapted from Skinner and Turekian,[73] gives the solubility product constants of metal sulphides for a sulphide ion activity of $10^{-9}$ moles/litre at 25°C. Therefore, the metals whose solubility product constants are exceeded will form authigenic sulphide phases and be trapped in the sediment

Table 9

Expected Equilibrium Concentrations for Some Metals in Pore Waters of Sediments Having a Sulphide Ion Activity of $10^{-9}$ Moles/Litre at 25°C (Adapted From Skinner and Turekian[73])

| Metal | Log concentration (moles/litre) |
|---|---|
| Nickel | - 10.7 |
| Iron | - 6.4 |
| Manganese | - 2.6 |
| Copper | - 26.0 |
| Zinc | - 14.1 |
| Cadmium | - 16.2 |
| Mercury | - 43.7 |
| Lead | - 16.6 |

column. On the other hand, metals that do not precipitate as metal sulphides at concentrations encountered in pore waters of reducing sediments are mobile within the sediment.

164. Using the Pb-210 method to determine an average rate of sedimentation of 0.45 cm/yr in central Long Island Sound, Turekian[37] estimated the time when the rate of metal fluxes to Long Island Sound changed drastically as a result of man's activity. Assuming the top of the core to be zero age, they found that the major change in the metal supply to Long Island Sound took place about 100 yr ago with a sharp increase about 70 yr ago.

165. In this study, the observed interstitial metal data showed that the concentration levels of Cu, Zn, Cd, Pb, and Ni are much higher than those expected from control by precipitation of their respective metal sulphides. This presumably means that these metals are present as organic complexes or are controlled by other precipitation-dissolution reactions. It is probable that these metals are associated with the humic-acid fraction of organic matter or oil and grease component of the sediment because the upper sediment layers have relatively higher carbon content than deeper sections of the core. Lindberg and Harris[74] found that the sediments from the Florida Everglades and Mobile Bay estuary exhibit strong associations between sediment Hg and sediment organic matter and between dissolved interstitial Hg and dissolved organic carbon.

166. Mn and Fe, on the other hand, may be present as sulphides because the observed interstitial concentrations of these metals are below the equilibrium solubility of their respective sulphide phases. The black color of many $H_2S$ - smelling samples is also indicative of the presence of Fe sulphide phases. Berner[75] has reported that in recent

sulphide-rich sediments, black iron sulfides are common. The principal mineralogical phases present are mackinawite (tetragonal $Fe_{1+x}S$) and greigite (cubic $Fe_3S_4$). An inspection of the sediment metal data indicates that the total Fe is much more abundant than total Mn in the sediments. However, the concentration of dissolved Fe is much less than that of dissolved Mn. The lower concentration of dissolved Fe can be attributed to the much greater ease for formation and stability of Fe sulphide compared with Mn sulphide. The correlation between the dissolved metal concentration and total metal concentration for other metals is not so clear cut.

167. While other metals show marked enrichment in the more recently deposited sediments, Fe, Mn, and Ni exhibit a somewhat erratic distribution pattern and no elevated concentrations in the top layers were observed. It seems that the other metals Pb, Cu, Zn, Hg, and Cd are being introduced anthropogenically at rates greater than the natural ones; whereas Fe, Mn, and Ni have natural deposition rates much greater than the rate of man-induced fluxes of these metals. The total metal content of the sediments is not associated with the clay fraction, thus implying that the metals are not bound to surfaces and edges of the fine-grained component of sediment. Ni, however, exhibits a covariant relationship with the clay content. The association of Ni with clay minerals is well known. Chester and Messiha-Hanna[76] found that most of the Ni in nearshore North Atlantic sediments is lithogenous. According to Chester and Hughes,[77,78] the lithogenous fraction of Ni is present within the lattice of clay minerals. Bruland et al.[79] reported that Ni, present in inner basin sediments off the coast of southern California, appears to be introduced solely from detrital mineral particles.

Interstitial nutrient concentrations

168. The importance of sediments in the control of nutrients has been recognized for the following reasons: (1) nutrients are incorporated into the sediments in particulate form and subsequently escape to the overlying water in dissolved forms; (2) the top few metres of the sediment column is the site of major transformation between solid and dissolved phases and speciation of dissolved forms (Berner[80]); and (3) the sediments can act as a reservoir and source of dissolved nutrients (Sholkovitz,[81] Rittenberg et al.[82]).

169. Previous nutrient studies in Long Island Sound have mainly been concerned with transport and recycling processes occurring within the water column (Riley,[7] Harris[21]). Little attention has been given to processes in the sediment column and at the sediment-water interface and how they may affect the nutrient composition of the overlying water column. Biogeochemical and physical processes taking place in the top few metres of the sediment column and at the sediment-water interface may play an important part in maintaining the nutrient composition of the overlying water column in Long Island Sound because (1) certain parts of the sound are known to contain reducing sediments enriched in organic carbon and nitrogen (Martens and Berner[38]); (2) the sound is relatively shallow; and (3) bioturbation is reported to be an active process in certain parts of the sound (Goldhaber et al.[83]).

170. The concentration-depth profiles of dissolved $NH_4^+$, $PO_4^{3-}$, $Si(OH)_4$, and total dissolved nitrogen present in sediment cores collected during the April cruise are given in Figures 82- 90. The interstitial $NH_4^+$ concentrations in sediment cores vary from 280 to 2100 µM. Relative to the overlying bottom waters, the sediments are enriched by two to three orders of magnitude in terms of dissolved $NH_4^+$. The sharp concentration gradient at the sediment-water

interface implies that the bottom sediments may be a potential source of nutrients. However, the interface was not studied in detail and further interpretation is not justified. The interstitial $NH_4^+$ concentration profiles often show a strong maximum at about 15 to 20 cm for the top of the core. The maximum in the $NH_4^+$ distribution may be attributed to increased input of organic detritus since the last 70-100 yr, assuming a sedimentation rate of 0.5 cm/year. The removal of $NH_4^+$ in the upper 10 cm may be due to diffusion, bioturbation, or a combination of both.

171. Interstitial silica concentrations also show a considerable enrichment compared to the overlying waters. The interstitial $Si(OH)_4$ concentrations vary from 600 to 1470 μM. In most of the cores, the $Si(OH)_4$ values show saturation at depth. Since these values are higher than the equilibrium solubility of quartz and common clay minerals, the interstitial silica concentration must be regulated by the solubility of biogenic opal contained in the sediments as reported by Siever and Woodford,[84] Fanning and Schink,[85] and Hurd.[86] The shape of the interstitial concentration profiles indicate that $Si(OH)_4$ is lost by diffusive processes to the overlying waters.

172. The concentration-depth profiles of interstitial $PO_4^{3-}$ in sediment cores are given in Figures 82- 90. The $PO_4^{3-}$ concentrations range from 5 to 1287 μM. Some of the $PO_4^{3-}$ concentrations are similar to those observed for $NH_4^+$ and total dissolved nitrogen. This suggests that the processes operative for $PO_4^{3-}$ regeneration at depth and loss to the overlying waters may be similar to those for $NH_4^+$. Since the Long Island Sound sediments are depleted in calcium carbonate, authigenic formation of apatite would not be expected and extensive supersaturation relative to apatite can be maintained. Berner[87] reported concentrations of interstitial phosphate exceeding 10 μM in the polluted surface sediment from New Haven Harbor, Long Island Sound.

## PART IV: SUMMARY OF RESULTS

### Seasonal and Depth Distribution of the Important Water Column Data

173. The averaged water column data collected on all cruises for temperature, salinity, $\sigma_t$, $NH_4^+$, $NO_3^-$, $PO_4^{3-}$, $Si(OH)_4$, chlorophyll *a*, particulate carbon, and particulate nitrogen are summarized in Figure 126. Data were averaged for all stations sampled on each cruise for a given depth interval. The averaged data were plotted with depth for each cruise and were contoured. The figures show the temporal changes in these variables for the sampled depths. A similar plot of mean water column stability is also presented.

174. Figure 126a illustrates seasonal water column cooling that progressed through March. On the average, the water column was uniform, with respect to temperature, on each cruise until 23 April, when the spring warming was evident in the surface layer of about 10 m depth. By 28 May, the water column showed considerable thermal stratification, ranging from less than 11°C below 16 m depth to above 15°C near the surface.

175. Figure 126b illustrates the temporal changes in the depth distribution of $S°/_{oo}$ and $\sigma_t$. [$\sigma_t$ = (density-1) x 1000.] Salinity averages were relatively uniformly distributed with depth on each cruise. Variations of $0.5°/_{oo}$ or less were encountered until May when a stronger halocline was observed. A weak pycnocline was observed, beginning in January, probably due to the small depth variation in mean salinity, the water column temperature average being nearly uniform. By May, both the slightly increased halocline and much intensified thermocline combined to produce a higher degree of density stratification.

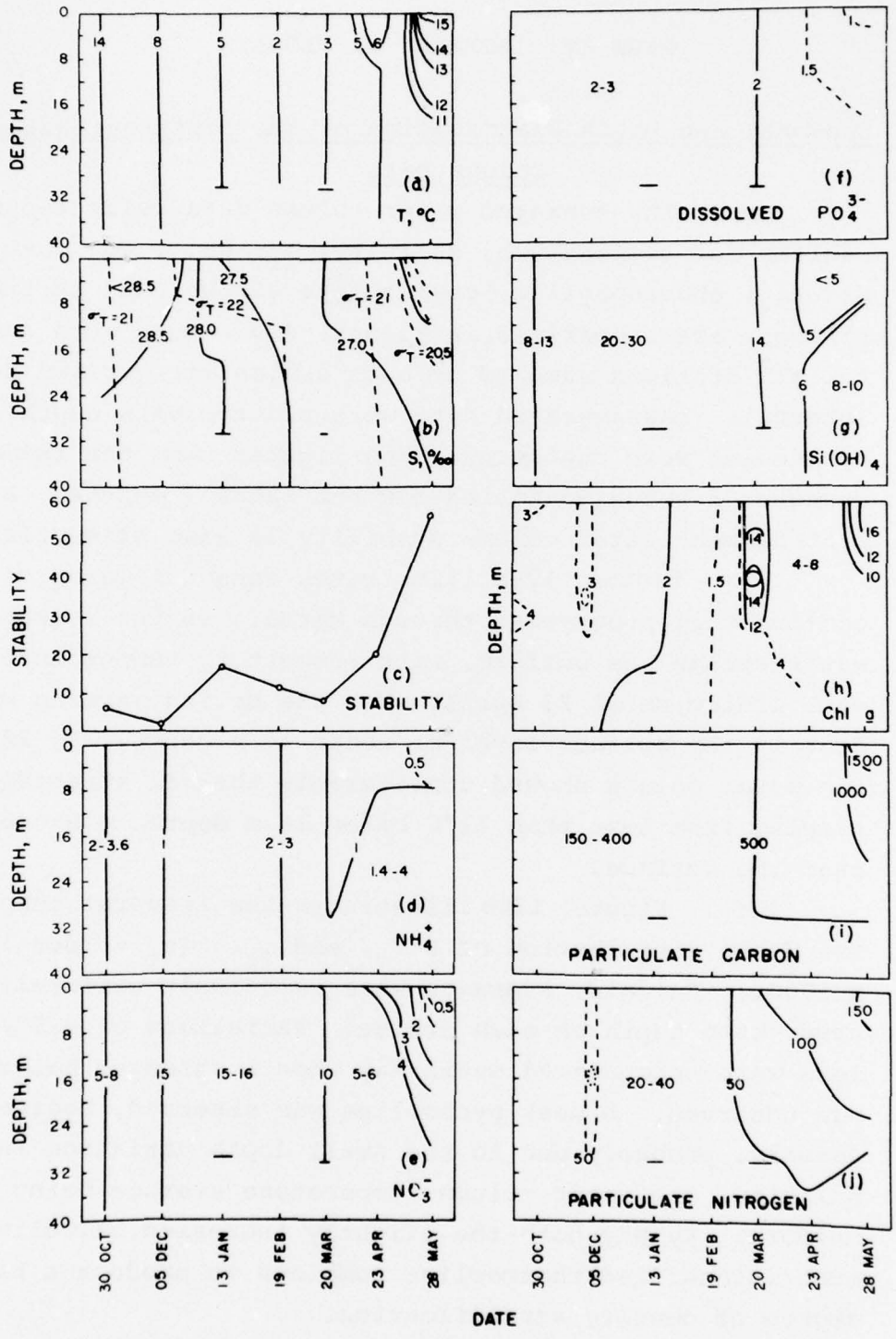



Figure 126. Seasonal water column averages.

176. Figure 126c shows the seasonal distribution of water column stability, calculated as the station average of

$$\text{Stability} = \frac{[\sigma_t \text{ surface} - \sigma_t \text{ bottom}] \times 1000}{\text{water column depth}}$$

for each cruise.

177. Figure 126d through g illustrate the seasonal depth distribution for $NH_4^+$, $NO_3^-$, $PO_4^{3-}$, and $Si(OH)_4$, respectively. Relatively high, but uniform, water column mean nutrient concentrations were observed on each cruise until April and May, when concentrations in the surface layer were observed to have decreased. By 20 May, both the average water column $NO_3^-$ and $NH_4^+$ concentrations had fallen to below 0.5 µM in the surface layer at ~4 m depth. $Si(OH)_4$ declined to values below 5 µM in the surface layer during this period.

178. The observed decline in mean nutrient concentrations was accompanied by observations of increased water column stability and increasing mean water column concentrations of chlorophyll *a* (Figure 126h). Two blooms of algae were observed, one on 20 March and one on 28 May.

179. Particulate carbon and particulate nitrogen (Figure 126i and j) mean concentrations increased from low values during the winter period to much higher concentrations during the period corresponding to that of increased water column stability, declining nutrient concentrations, and increasing chlorophyll *a* levels.

180. Taken together, the averaged water column data represent the late fall to spring portion of the annual cycle of water column stability and nutrient and phytoplankton concentrations observed previously by Riley[5,6] and others for

temperate latitudes. The expected increase in phytoplankton stock was in response to the seasonal increase in intensity and duration of solar illumination. The decline in the observed average nutrient concentration was likely due in large measure to phytoplankton utilization.

181. One of the most significant results in the distribution of dissolved metals was the increased concentrations observed at the western end of the sampling area. These findings are summarized in Figure 127, which shows the seasonal variation in water column averages for stations Y and V (Figure 2), the westward and eastward stations, respectively. For the 13 January cruise, the average dissolved Pb concentration at station Y was about three times greater than the value for station V. Concentrations of dissolved Cu, Mn, and Zn were also greater at station Y during this period. A similar pattern was observed during the 19 February cruise, but with concentrations of Cd and Fe now greater at the western end. During the 20 March cruise, the period of intense phytoplankton blooming, the differences between the concentrations at stations Y and V were essentially zero.

182. The increased concentrations of dissolved metals at the western end of the sampling area during the January and February periods are probably due to heavy metal input[26,27] from the East River-Western Long Island Sound system. The decreased concentrations at station Y during the bloom period suggest that biological processes at the western end may be important in the removal of metals from the water column. That organisms may be incorporating dissolved metals in their biomass is shown in a comparison of the seasonal variation of suspended metals (Figure 128) with chlorophyll *a* and particulate carbon and nitrogen (Figure 129). The 20 March and 28 April cruises occurred during periods of peak chlorophyll *a* concentration; likewise maximum concentrations

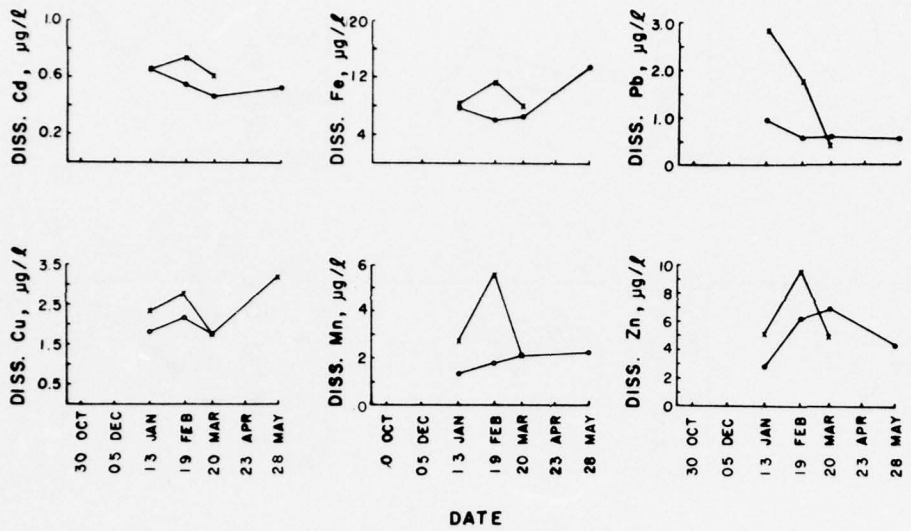



Figure 127. Seasonal variation in the mean concentration of dissolved metals at westward station Y (x symbol) and V (∘ symbol).

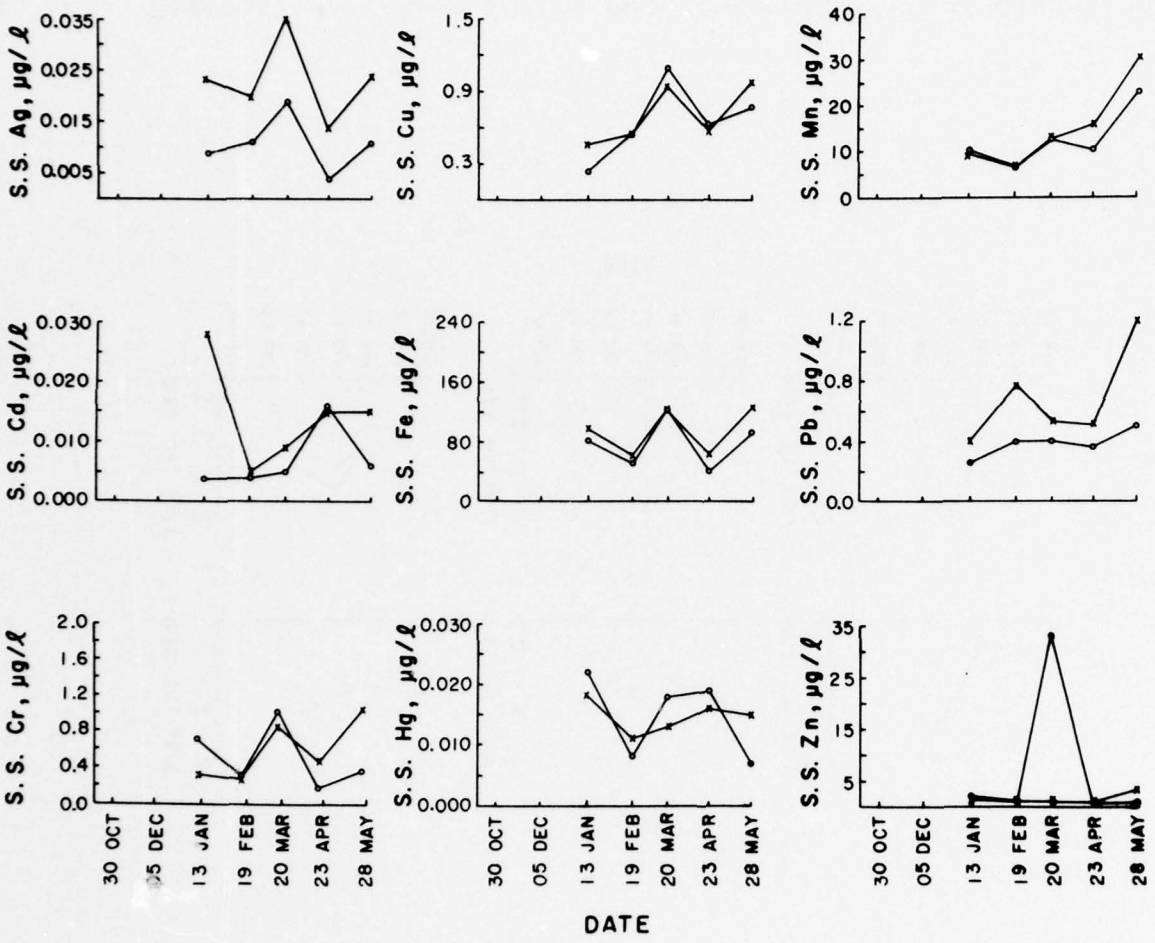



Figure 128. Seasonal variation in the mean concentration of particulate metals at stations Y (x symbol) and V (o symbol).

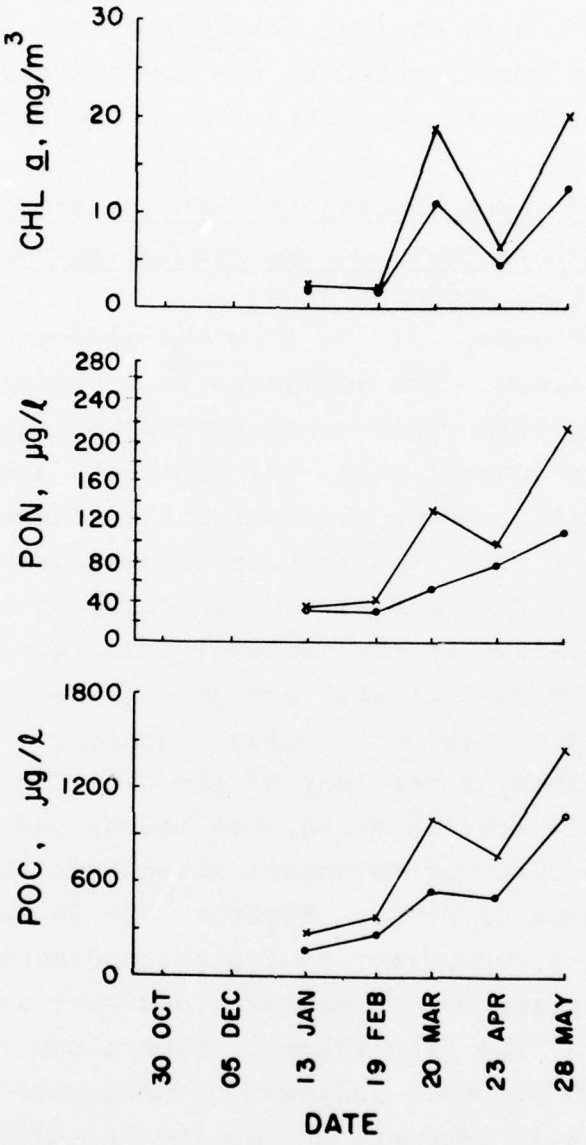



Figure 129. Seasonal variation in the mean concentration of chlorophyll a, particulate nitrogen, and particulate carbon at stations Y (x symbol and V (o symbol).

of suspended Ag, Cu, Cr, and Fe were also observed during these periods. Concentrations of suspended Pb and Mn, however, showed a more or less steady increase from 13 January to 28 May and corresponded to the approximately steady seasonal increase in concentrations of particulate carbon and nitrogen.

## Evaluation of Proposed Disposal Site Relative to the Control Site in Terms of Sediment Properties

### Sediment texture and mineralogy

183. Figures 71- 74 show the sediment distribution in the area of study. The sediments in the disposal area are mainly silty, with minor concentration of clay followed by sand. At the control site, the sediments are sandy mud, with the silt fraction being the dominant component. To the east of the control site, the textural distribution grades to clayey silt or fine mud with practically no sand fraction present. Relative to the disposal area, the sediments in the region of the control site are more fine-grained with relatively higher concentrations of clay fraction.

184. X-ray mineralogy of the clay fraction shows the presence of illite, chlorite, kaolinite, and montmorillonite with minor amounts of feldspars and quartz in the sediments within the area of study. Figures 75- 78 show the distribution of illite, chlorite, kaolinite, and montmorillonite in the clay fraction of near-surface sediment samples. At the disposal site, the fine-fraction mineralogy is dominated by illite - 43-59 percent, followed by kaolinite - 14-28 percent, chlorite - 14-18 percent, and montmorillonite - 3-15 percent. At the control site, the relative percentage of clay minerals does not differ significantly from that at the disposal site.

### Chemistry

185. Most of the cores obtained from the disposal area had a hydrogen sulphide odor. The total carbon and nitrogen

content of the near-surface sediments are similar in both areas.

186 . Figures 130-137 show the concentration distribution of total Zn, Pb, Hg, Cu, Mn, Ni, Cr, and Fe present in near-surface sediments within the area of study. The distributions of metals in surface sediments however, do not reveal any significant difference in the concentration pattern in the areas of interest.

Summarized Interpretation of Sediment Geochemistry Data Based on Correlation Coefficient Matrix

187 . The correlation coefficient matrix for sediment data is given in Table 13. The plus (+) and minus (-) signs correspond to statistically significant positive and negative correlation, respectively. The positive and negative numerical r values are given where the relationship is highly significant. The n (number of points) values are also given below these r values.

188 . Zn, Pb, Cu, Cd, and Hg show a negative relationship with sample depth in most sediment cores. In particular Zn, Pb, and Cu exhibit a strong negative correlation (r=0.5, n=112) with increasing sediment depth. Fe, Mn, and Ni do not reveal any significant trend with depth in core, thus indicating that no elevated concentrations above baseline levels are encountered for these metals. Table 13 indicates that all metals are strongly associated statistically with the organic fraction of sediment, with r values ranging from 0.5 to 0.8 for n greater than 100. All metals, with the exception of Cd and Hg, show positive correlation with the total iron content of sediment.

189 . Of particular interest is the strong association of metals with each other. A positive relationship exists between the metals, excluding Cd, and total CEC of sediment.

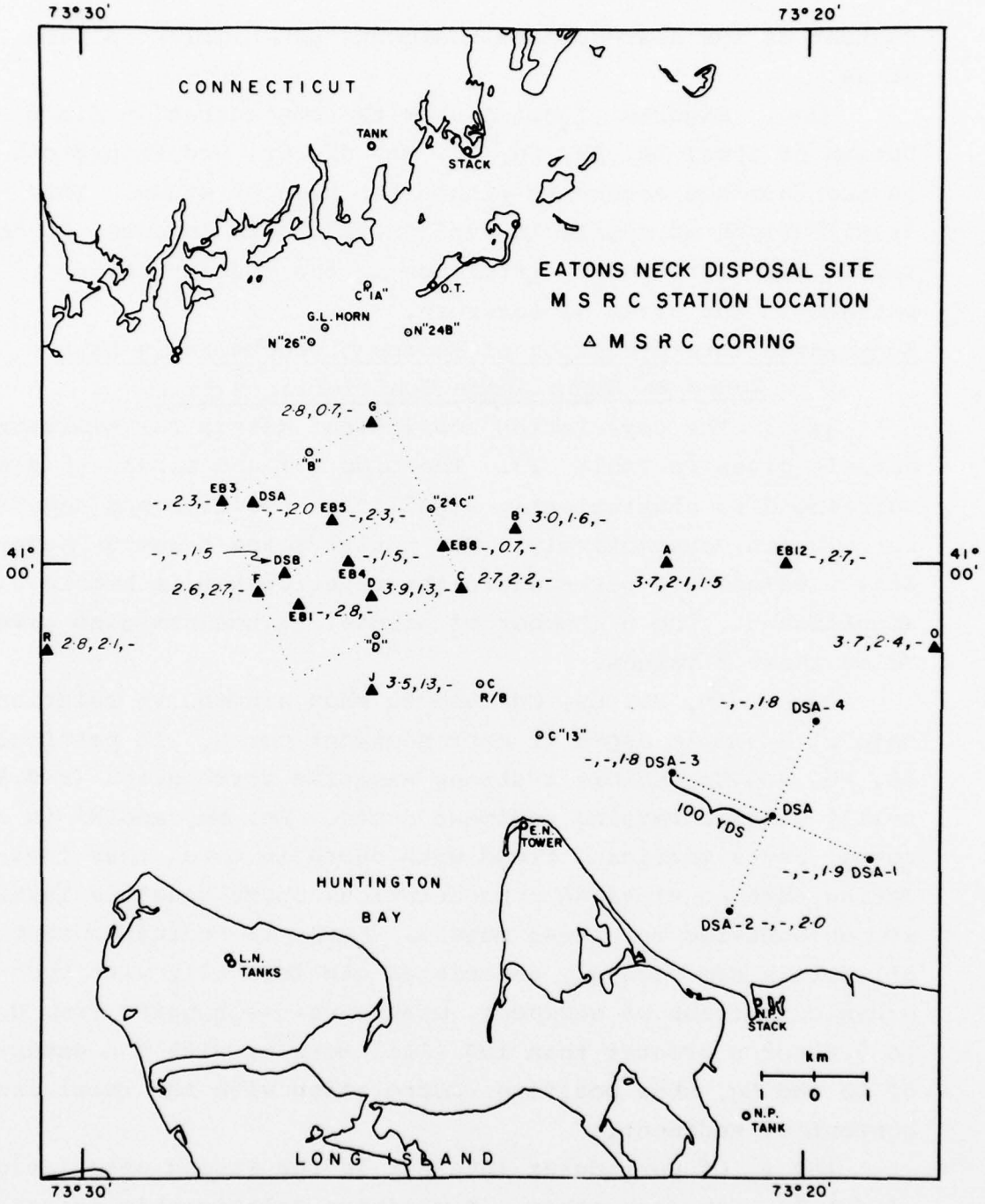



Figure 130. Weight percent total iron in near-surface sediments in study area.

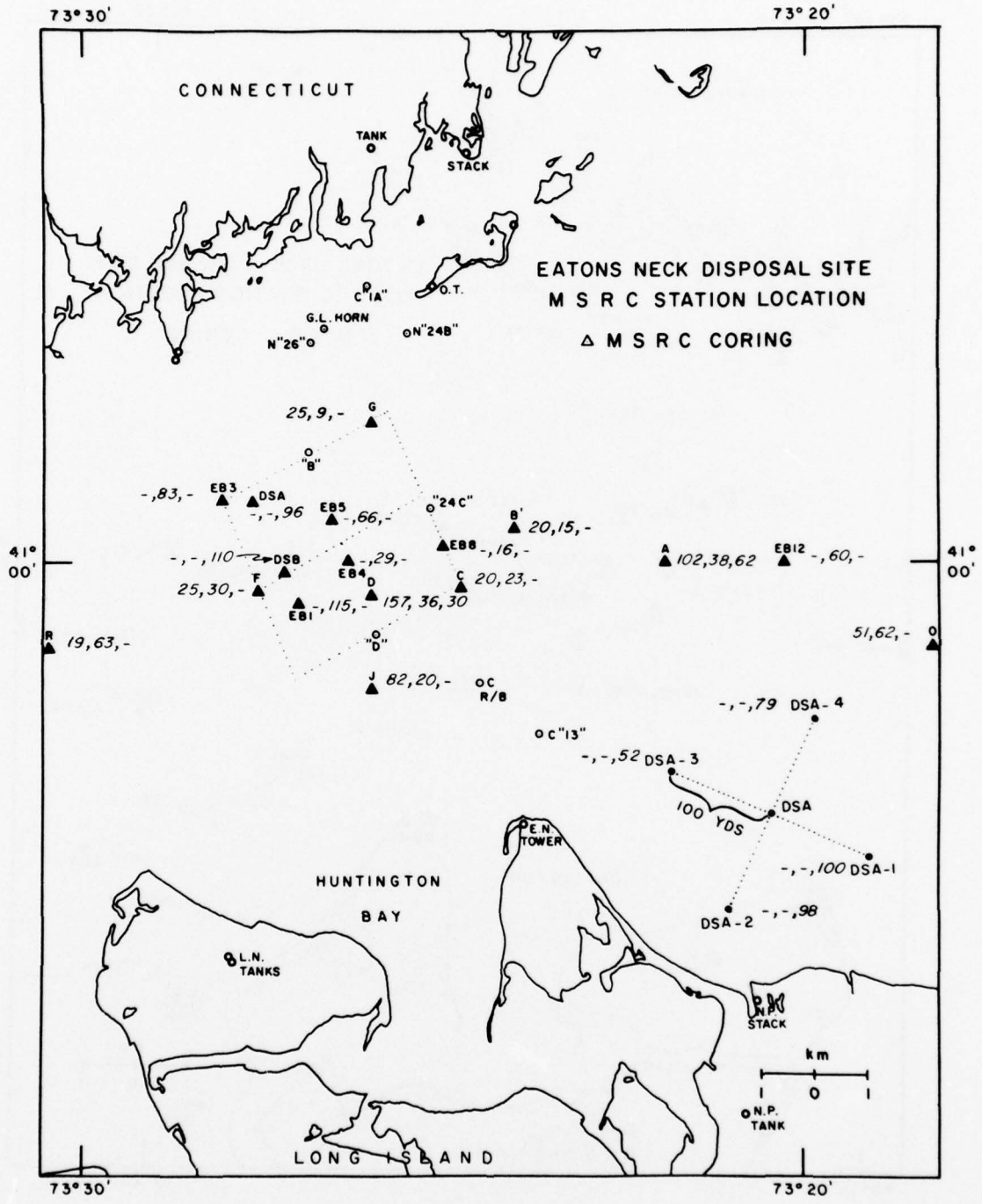



Figure 131. Total chromium (µg/g) in near-surface sediments in the study area.

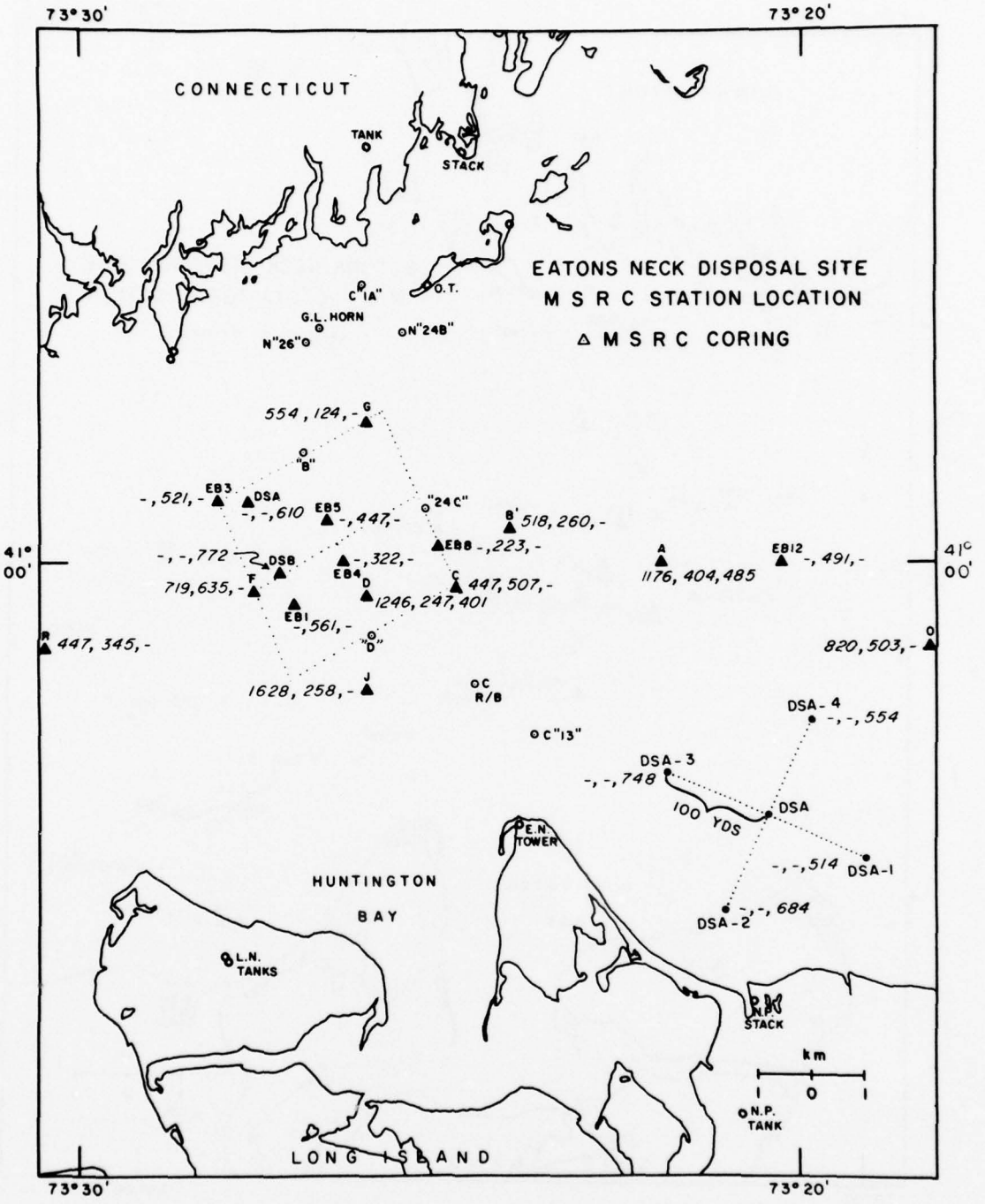



Figure 132. Total manganese (µg/g) in near-surface sediments in study area.

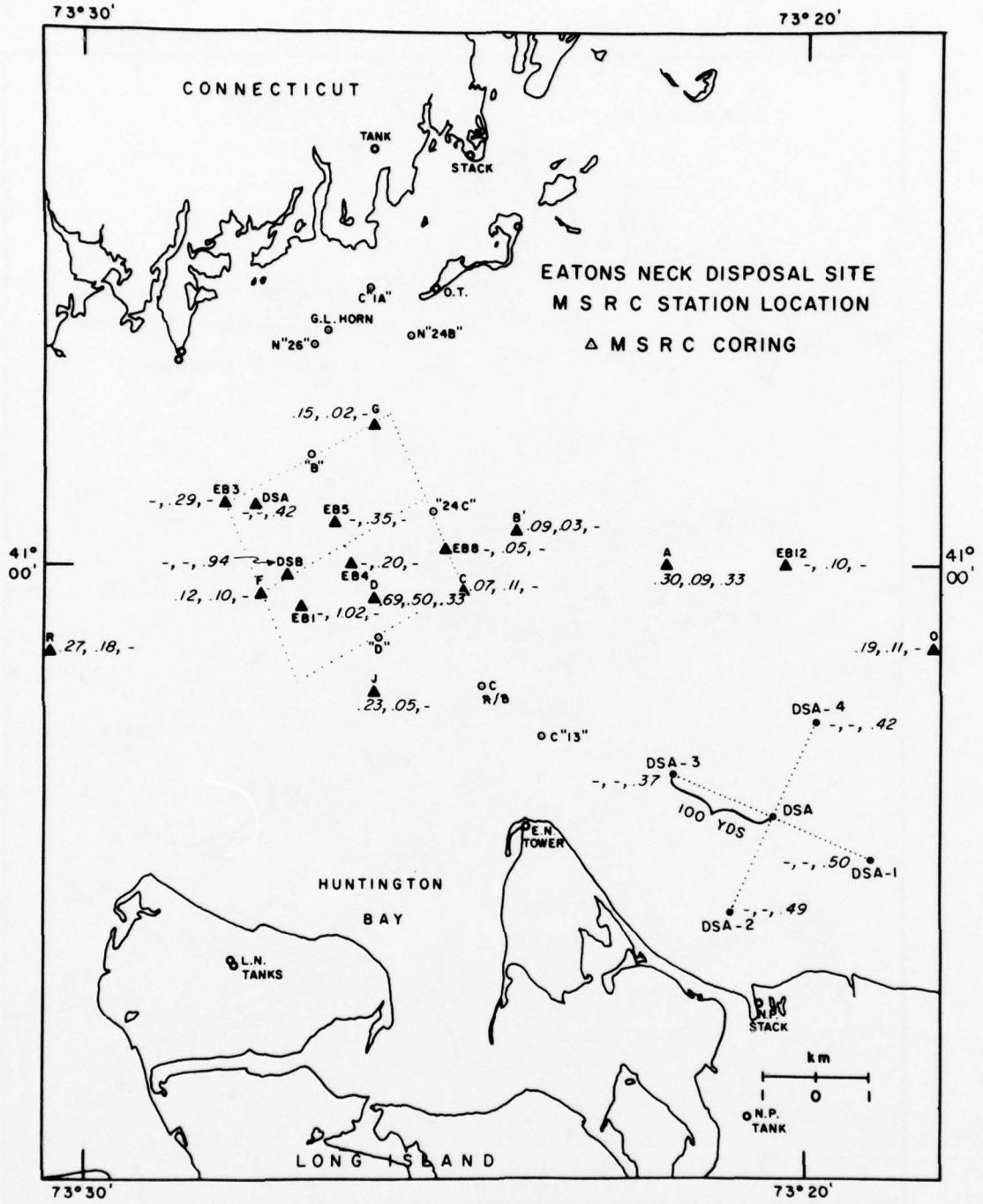



Figure 133. Total mercury (µg/g) in near-surface sediments in study area.

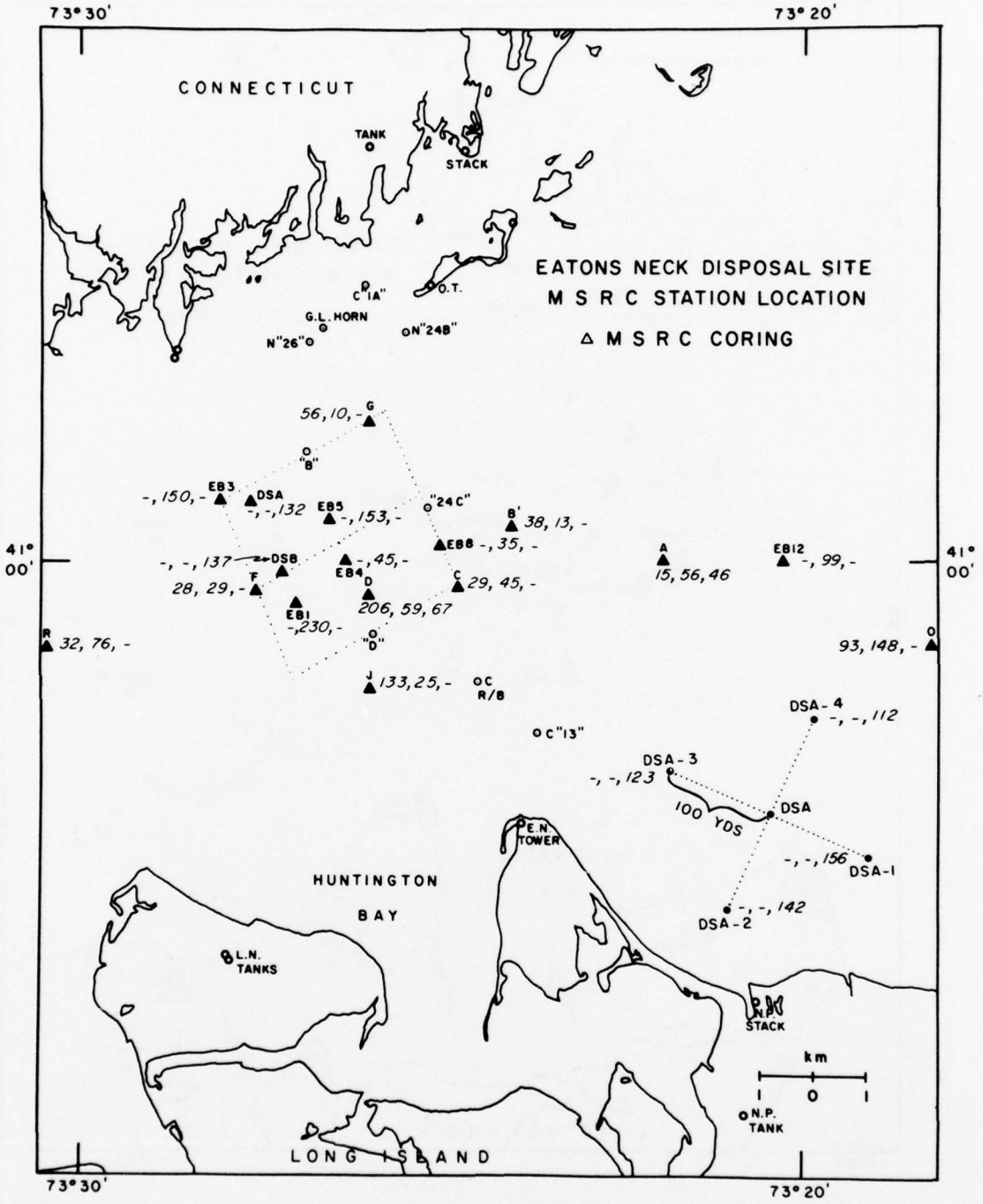



Figure 134. Total copper (µg/g) in near-surface sediments in study area.

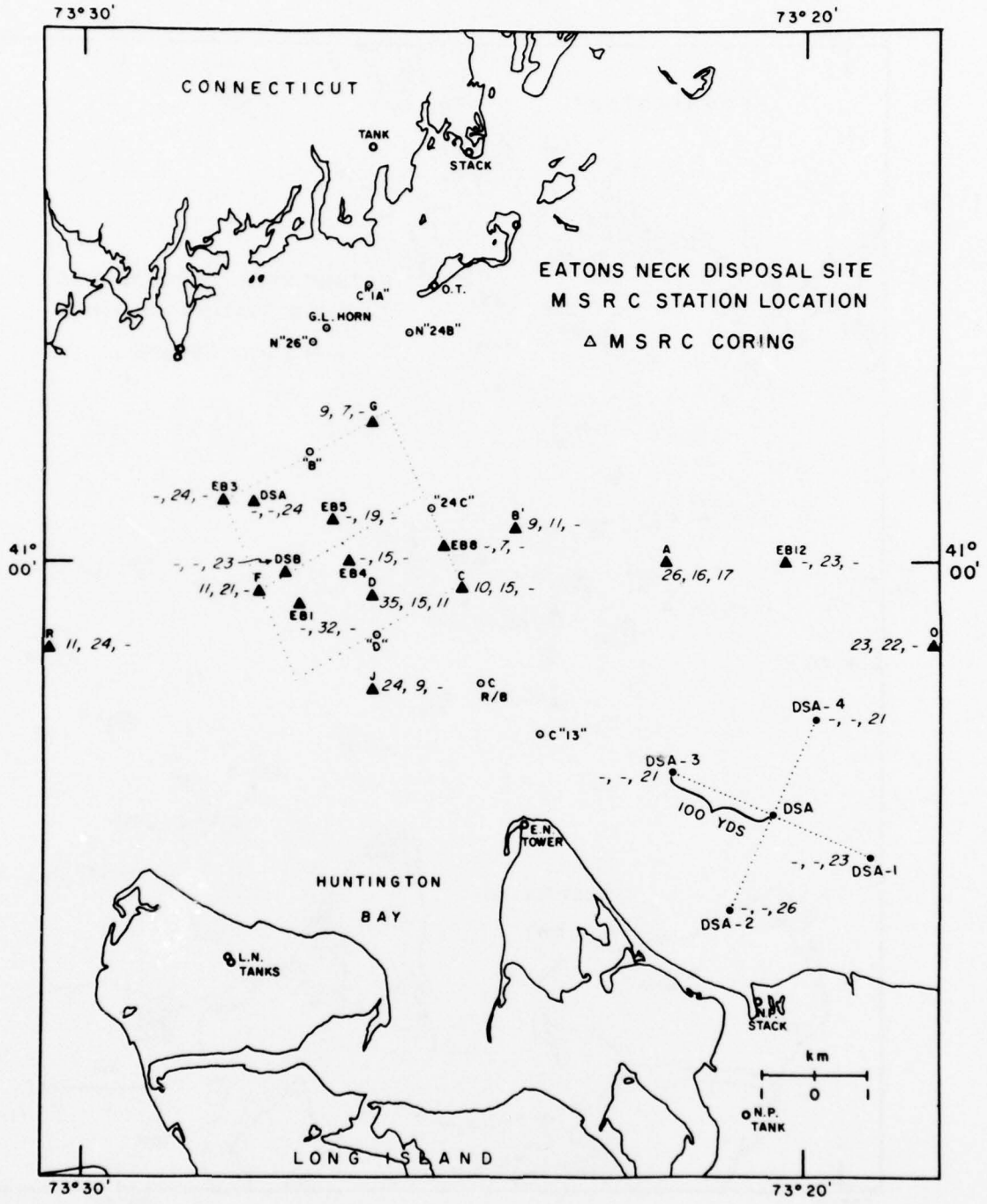



Figure 135. Total nickel (µg/g) in near-surface sediments in the study area.

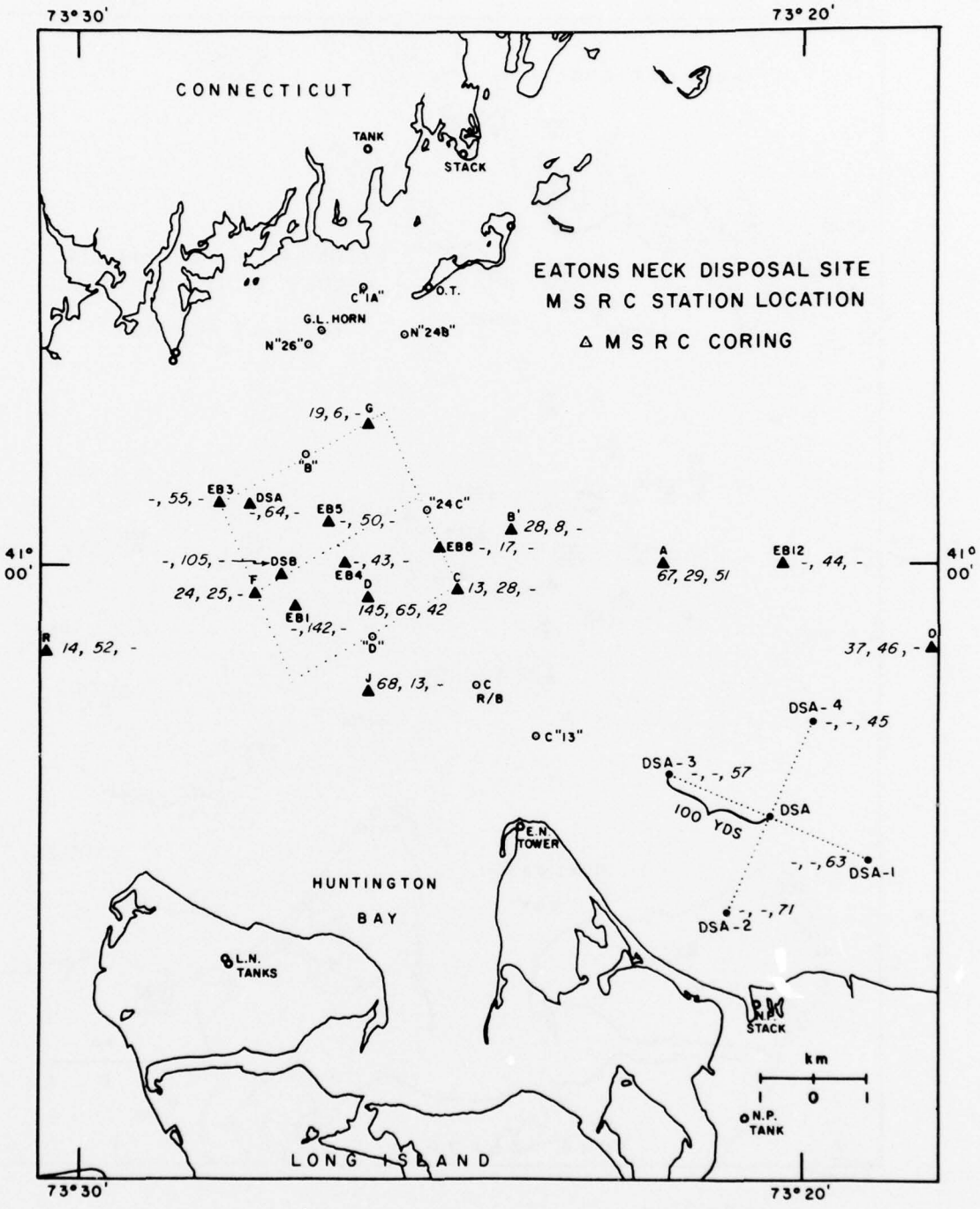



Figure 136. Total lead (µg/g) in near-surface sediments in study area.

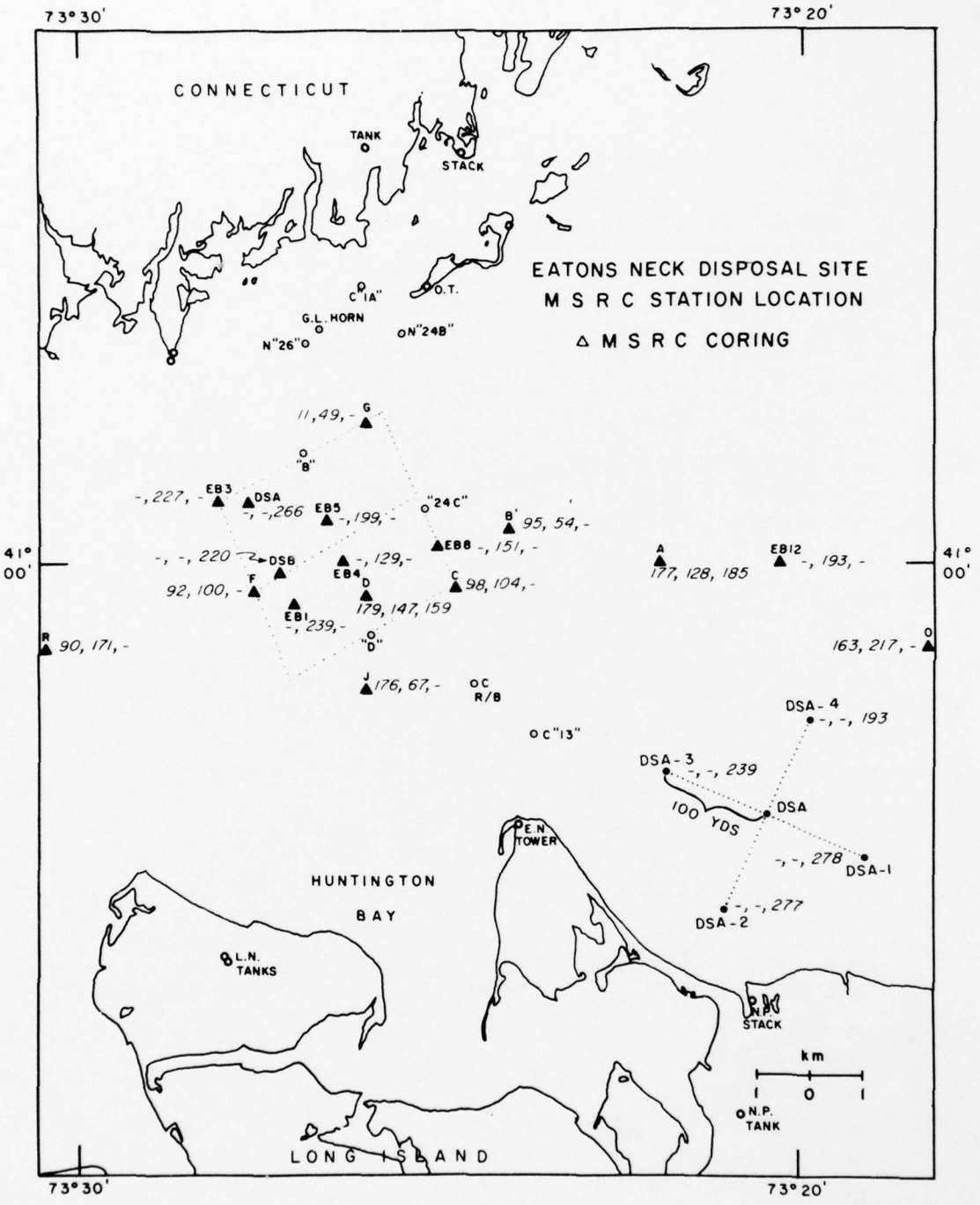



Figure 137. Total zinc (µg/g) in near-surface sediments in study area.

# Table 13

## Correlation Coefficient Matrix for Sediment Data

| | Segment depth | $H_2O$ | TOC | TON | Fe | Mn | Ni | Co | Cr | Zn | Cd | Hg | Pb | Cu | Ca ex. | Mg ex. | Na ex. | K ex. | CEC | Oil + Grease | Gravel | Sand | Mud | Silt | Clay | Fe (I) | Mn (I) | Ni (I) | Cu (I) | Zn (I) | Cd (I) | Pb (I) | |
|---|---|---|---|---|---|---|---|---|---|---|---|---|---|---|---|---|---|---|---|---|---|---|---|---|---|---|---|---|---|---|---|---|---|
| Segment depth | 1 | 0 | - | - | 0 | 0 | 0 | 0 | - | -0.5<br>112 | 0 | - | -0.5<br>104 | -0.5<br>110 | - | 0 | 0 | 0 | - | - | 0 | 0 | 0 | 0 | + | - | - | 0 | 0 | - | 0 | 0 | Segment depth |
| $H_2O$ | | 1 | 0.5<br>100 | 0.5<br>99 | 0 | 0 | 0.6<br>101 | 0.5<br>101 | + | + | 0 | + | + | + | 0 | + | + | 0.5<br>99 | 0 | 0 | -0.5<br>104 | -0.7<br>104 | 0.7<br>104 | 0.7<br>104 | 0.5<br>104 | 0 | 0 | 0 | 0 | - | 0 | - | $H_2O$ |
| TOC | | | 1 | 0.9<br>108 | 0.5<br>108 | 0.5<br>107 | 0.7<br>109 | 0.5<br>108 | 0.7<br>109 | 0.6<br>109 | 0 | + | 0.6<br>102 | 0.6<br>108 | + | + | + | 0 | + | + | 0 | -0.6<br>105 | 0.6<br>105 | 0.6<br>105 | + | + | + | 0 | 0 | 0 | 0 | 0 | TOC |
| TON | | | | 1 | 0.5<br>107 | 0.6<br>106 | 0.8<br>108 | 0.6<br>107 | 0.7<br>107 | 0.6<br>108 | 0 | + | 0.6<br>101 | 0.6<br>106 | + | 0.5<br>104 | + | 0 | 0.5<br>103 | + | 0 | -0.6<br>104 | 0.6<br>104 | 0.6<br>104 | + | + | + | 0 | + | 0 | 0 | 0 | TON |
| Fe | | | | | 1 | 0.7<br>109 | 0.5<br>111 | 0.5<br>110 | + | + | 0 | 0 | + | + | + | + | + | - | + | + | 0 | - | + | + | 0 | + | 0 | 0 | 0 | 0 | 0 | 0 | Fe |
| Mn | | | | | | 1 | 0.6<br>110 | + | 0.5<br>109 | + | 0 | + | + | + | + | + | 0 | - | 0.5<br>103 | + | 0 | - | + | 0.5<br>104 | 0 | + | + | 0 | 0 | 0 | 0 | 0 | Mn |
| Ni | | | | | | | 1 | 0.8<br>111 | 0.8<br>111 | 0.6<br>112 | 0.6<br>28 | 0.5<br>108 | 0.6<br>104 | 0.6<br>110 | + | 0.5<br>106 | + | + | + | + | 0 | -0.8<br>106 | 0.7<br>106 | 0.8<br>106 | + | 0 | + | 0 | 0 | 0 | 0 | 0 | Ni |
| Co | | | | | | | | 1 | + | + | 0 | 0 | 0 | + | 0 | 0.7<br>106 | + | + | + | 0 | 0 | -0.8<br>106 | 0.8<br>106 | 0.7<br>106 | 0.6<br>106 | 0 | 0 | 0 | 0 | 0 | 0 | 0 | Co |
| Cr | | | | | | | | | 1 | 0.9<br>111 | 0.5<br>27 | 0.8<br>107 | 0.9<br>104 | 0.9<br>110 | + | + | 0 | 0 | + | 0.6<br>102 | 0 | -0.5<br>105 | + | 0.6<br>105 | 0 | + | + | + | 0 | 0 | 0 | 0 | Cr |
| Zn | | | | | | | | | | 1 | 0 | 0.7<br>108 | 0.8<br>104 | 0.9<br>110 | + | 0 | 0 | 0 | + | 0.5<br>102 | 0 | - | + | 0.5<br>106 | 0 | + | + | + | 0 | 0 | 0 | 0 | Zn |
| Cd | | | | | | | | | | | 1 | 0.8<br>27 | 0.8<br>26 | 0 | 0 | 0 | 0 | 0 | 0 | + | 0 | 0 | 0 | 0 | 0 | 0 | 0 | 0 | 0 | 0 | 0 | 0 | Cd |
| Hg | | | | | | | | | | | | 1 | 0.9<br>101 | 0.7<br>106 | + | 0 | 0 | 0 | + | 0.6<br>101 | 0 | 0 | 0 | + | - | + | + | + | 0 | 0 | 0 | 0 | Hg |
| Pb | | | | | | | | | | | | | 1 | 0.9<br>104 | + | 0 | 0 | 0 | + | 0.5<br>96 | 0 | 0 | 0 | + | - | + | 0.5<br>97 | + | 0 | 0 | 0 | 0 | Pb |
| Cu | | | | | | | | | | | | | | 1 | + | 0 | 0 | 0 | + | 0.5<br>101 | 0 | - | + | + | 0 | + | + | + | 0 | 0 | 0 | 0 | Cu |
| Ca ex. | | | | | | | | | | | | | | | 1 | 0 | 0 | 0 | 0.9<br>106 | + | 0 | - | 0 | + | - | + | + | 0 | 0 | 0 | 0 | 0 | Ca ex. |
| Mg ex. | | | | | | | | | | | | | | | | 1 | 0.5<br>108 | + | + | 0 | 0 | -0.6<br>104 | 0.6<br>104 | 0.5<br>104 | 0.5<br>104 | 0 | 0 | 0 | 0 | 0 | 0 | 0 | Mg ex. |
| Na ex. | | | | | | | | | | | | | | | | | 1 | + | + | 0 | 0 | -0.5<br>104 | 0.5<br>104 | + | 0.5<br>104 | 0 | - | 0 | 0 | 0 | 0 | 0 | Na ex. |
| K ex. | | | | | | | | | | | | | | | | | | 1 | + | 0 | - | - | + | + | 0.5<br>104 | - | 0 | 0 | - | - | 0 | 0 | K ex. |
| CEC | | | | | | | | | | | | | | | | | | | 1 | + | 0 | - | + | 0.5<br>103 | 0 | + | + | 0 | 0 | 0 | 0 | 0 | CEC |
| Oil + Grease | | | | | | | | | | | | | | | | | | | | 1 | 0 | - | + | + | - | + | + | 0 | - | 0 | 0 | 0 | Oil + Grease |
| Gravel | | | | | | | | | | | | | | | | | | | | | 1 | + | - | - | - | + | + | 0 | 0 | 0 | 0 | 0 | Gravel |
| Sand | | | | | | | | | | | | | | | | | | | | | | 1 | -0.9<br>109 | -0.9<br>109 | -0.6<br>109 | 0 | 0 | 0 | 0 | + | 0 | 0 | Sand |
| Mud | | | | | | | | | | | | | | | | | | | | | | | 1 | 0.9<br>109 | 0.6<br>109 | 0 | 0 | 0 | 0 | - | 0 | - | Mud |
| Silt | | | | | | | | | | | | | | | | | | | | | | | | 1 | + | 0 | 0 | 0 | 0 | - | 0 | - | Silt |
| Clay | | | | | | | | | | | | | | | | | | | | | | | | | 1 | - | - | 0 | 0 | 0 | 0 | 0 | Clay |
| Fe (I) | | | | | | | | | | | | | | | | | | | | | | | | | | 1 | + | 0 | 0 | 0 | 0 | 0 | Fe (I) |
| Mn (I) | | | | | | | | | | | | | | | | | | | | | | | | | | | 1 | 0 | - | 0 | - | - | Mn (I) |
| Ni (I) | | | | | | | | | | | | | | | | | | | | | | | | | | | | 1 | 0 | 0 | 0 | 0 | Ni (I) |
| Cu (I) | | | | | | | | | | | | | | | | | | | | | | | | | | | | | 1 | + | + | + | Cu (I) |
| Zn (I) | | | | | | | | | | | | | | | | | | | | | | | | | | | | | | 1 | + | + | Zn (I) |
| Cd (I) | | | | | | | | | | | | | | | | | | | | | | | | | | | | | | | 1 | + | Cd (I) |
| Pb (I) | | | | | | | | | | | | | | | | | | | | | | | | | | | | | | | | 1 | Pb (I) |

It should be mentioned, here, that a major fraction of the exchange capacity is attributable to exchangeable $Ca^{2+}$. The metals also show association with the oil and grease content of sediment.

190. The correlation coefficient matrix shown in Table 13 also indicates that most of the organic matter, including oil and grease, is concentrated in the mud fraction, especially silt, as evident from high r values for n greater than 100. The association of organic matter with mud fraction also explains the positive relationship between metal content and mud fraction.

191. Interstitial metal concentrations exhibit some correlation mutually and with other sediment parameters, but no systematic trends were detected. None of the dissolved metals seem to be associated with the dissolved organic carbon content. The interstitial nutrient concentrations exhibit some trends with depth in core. This has been discussed earlier in the text. Total dissolved nitrogen concentration profiles are similar to those of dissolved $NH_4^+$, thus indicating that the major component of dissolved nitrogen in sediment pore waters is dissolved $NH_4^+$. Since the $PO_4^{3-}$ and $NH_4^+$ concentrations are strongly dependent on Eh conditions, a close similarity is observed between the interstitial $NH_4^+$ and $PO_4^{3-}$ concentration profiles. The control of dissolved $PO_4^{3-}$ by precipitation of vivianite [$Fe_3(PO_4)_2 \cdot 8H_2O$] is unlikely in this case because the phosphate profiles do not show any relationship with dissolved iron distribution.

## APPENDIX A': SAMPLING AND ANALYTICAL PROCEDURES USED FOR THE DETERMINATION OF TRACE HEAVY METALS

I. Dissolved and particulate metals in the water column

A. Decontamination of the apparatus used for sampling dissolved and particulate metals in the water column.

1. Water sampler: General Oceanics' Niskin "top-drop" bottles of 10-l capacity. These bottles are constructed from polyvinylchloride. Prior to each cruise they were cleaned by leaching with 1 N HCl for 48 hr followed by a rinsing with Super-Q.

2. At-sea sample container: Narrow-mouth Nalgene$^{R}$ polypropylene bottles of 500-ml capacity. New bottles were cleaned by rinsing with concentrated HCl followed by Super-Q and then calibrated to contain 500 ml. One week prior to sampling, the bottles were filled with 1 percent (V/V) concentrated $HNO_3$. Before use at sea, the bottles were emptied and rinsed with Super-Q. Just prior to filling at sea, each bottle was rinsed with about 100 ml of the filtered seawater sample.

3. At-sea filter holders: Millipore$^{R}$ Swinnex filter holders (polypropylene) of 25-mm diameter. These holders were cleaned by soaking in HCl and rinsing with Super-Q.

4. Filters: Type A gelman glass fiber filters (25-mm diameter). According to the manufacturer's description (Arthus H. Thomas Catalog, 1974, p. 628), the pore size is such

that the filter will "retain 99.7% or more of particles larger than 0.3 micron and over 98% of particles as small as 0.05 micron." However, according to Cranston and Buckley,[88] (p. 12) the experimental pore diameter is 2 microns; where "...the experimental pore diameter...is defined as that size of sphere [latex bead] that is 90% effectively removed from 1 liter of a 1 mg $l^{-1}$ suspension [of latex beads]."

5. Filter storage containers: 47-mm plastic petri dishes (Millipore$^{R}$). These dishes were cleaned by soaking in 1 N HCl followed by a rinsing with Super-Q.

6. At-sea sample bottle for dissolved Hg: 125-ml Pyrex$^{R}$ glass reagent bottles with ground glass stoppers. The bottles were cleaned by rinsing with concentrated $HNO_3$ followed by rinsing with Super-Q; each bottle was calibrated to contain 106 ml. The bottles were stored filled with a solution of 5 percent (V/V) concentrated $HNO_3$ + 0.1 percent (W/V) $K_2Cr_2O_7$. Just prior to going to sea, each bottle was drained and rinsed with Super-Q.

7. Preserving solution for dissolved Hg samples: The composition of this solution is 0.177 g $K_2Cr_2O_7$ in 100 ml of concentrated $HNO_3$ (Feldman[89]). Six ml of this solution was added to each Hg sample bottle, just prior to going to sea.

B. Sampling and preservation methods used for the determination of dissolved and particulate metals in the water column.

1. Water sampling: The Niskin bottles were attached to the stainless steel hydrowire which was weighted by a lead weight enclosed in a polyethylene bag. The Niskin bottles were lowered to the appropriate sampling depths and then triggered by dropping a stainless steel messenger. At least 10 sec were allowed for the top-drop to fall to the bottom. The bottles were brought to the deck and secured to a specially constructed PVC-lined wall cabinet located inside the ship's wet-lab.

2. Niskin pressure manifold and sampling from the Niskin bottles: Tygon tubing and plastic swagelok fittings were used to connect the Niskin bottles to a tank of UHP $N_2$ (see Figure A1). The swinnex-glass fiber filter assemblies were attached to the Niskin outflow valves and the bottles were pressurized to 20 psi maximum to force seawater through the swinnex filter assembly. This arrangement permitted (1) a measure of the total volume of seawater passing through the filter; (2) the glass fiber filter to be washed without contaminating samples taken for dissolved metals; and (3) rinsing of the sample bottle with the filtered seawater sample prior to filling.

When the filter clogged, or after 1, 1.5, or 2 l of seawater had passed through the filter, the swinnex assembly was disconnected from each Niskin bottle. Seawater remaining

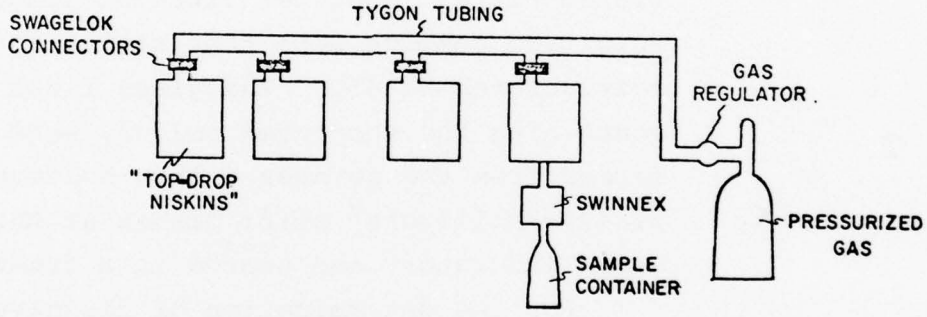



Figure A1. Niskin pressure manifold

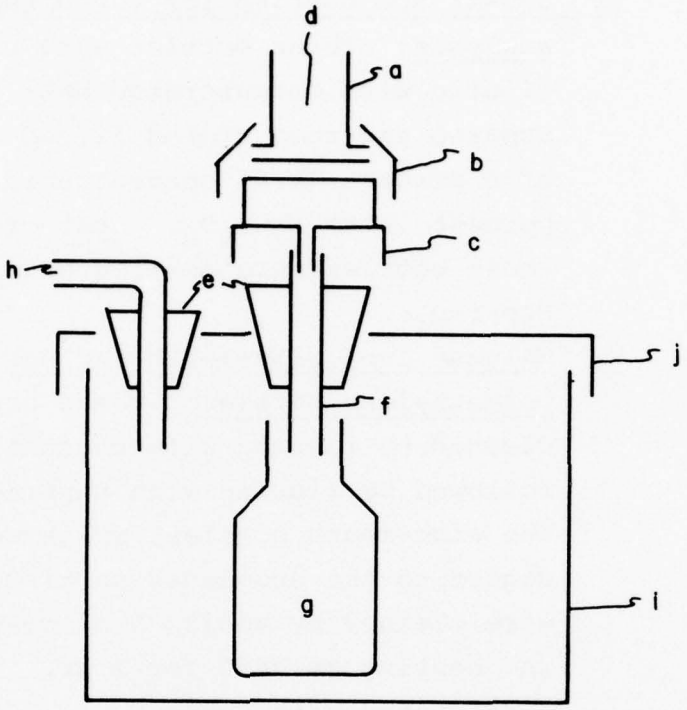
in the swinnex assembly was forced through the filter, using a plastic syringe, and discarded. A second set of unfiltered samples, collected through the shipboard Plunket system (Hulse[44]) and later filtered through Nuclepore[R] filters, provided a calibration for the concentration of suspended solids (mg/l) obtained on the glass fiber filters.

3. Preservation of the dissolved and particulate metals samples: After returning to the land-based laboratory (usually in about 14 hr), the pH of the dissolved metals samples was lowered to less than 2 using 3 ml of concentrated Ultrex[R] $HNO_3$ per litre of sample. The acidified samples were then stores in a refrigerator at 4°C. The glass fiber filters, containing the suspended solids, were transferred from the swinnex filter holders to plastic Millipore[R] petri dishes at the land-based laboratory and stored in a freezer.

   For the determination of dissolved Hg, separate 100-ml aliquots of filtered seawater were collected in the calibrated 125-ml Pyrex[R] reagent bottles which contained 6 ml of Hg preserving solution. (See section I-A-7 or Feldman[89]). These preserved Hg samples were frozen until analysis could be performed. Dissolved Hg samples were collected during the December 1974 cruise only.

C. Decontamination of the apparatus used for the analysis of dissolved and particulate metals samples.

1. 300-ml BOD bottles for the dissolved Hg analysis: These bottles were cleaned by rinsing with concentrated $HNO_3$ followed by Super-Q and then stored filled with a solution of 5 percent (V/V) concentrated $HNO_3$ + 0.1 percent (W/V) $K_2Cr_2O_7$. Just prior to analysis these bottles were emptied and rinsed with Super-Q.
2. Nalgene 1-oz wide-mouth and narrow-mouth polyethylene bottles: These bottles were cleaned by rinsing with concentrated HCl followed by rinsing with Super-Q. In addition, the wide-mouth bottles, which were used for digesting the suspended particulates filters, were cleaned by adding 5 ml concentrated $HNO_3$ and heating at 80°C for 2 hr. These bottles were rinsed with Super-Q.
3. 125-ml Pyrex$^R$ glass separatory funnels (with plastic stoppers and Teflon stopcocks) for the dissolved metals analysis: These funnels were cleaned by rinsing with concentrated HCl followed by rinsing with Super-Q, concentrated $HNO_3$, and Super-Q. Each funnel was completely filled with Super-Q to displace acid vapors. The funnels were calibrated to contain both 25 ml and 100 ml. Just prior to the actual extraction of the samples, the separatory funnels were pre-extracted according to the extraction procedure.
4. Small volume plastic filtration apparatus: This apparatus was used for filtering the digest solutions of the suspended particulates filters. (See Figure A2).




a. Sawed-off top of a 25-mm plastic Gelman$^{R}$ filtering apparatus.

b. Sawed-off top of a 25-mm plastic swinnex filter holder.

c. Bottom of a 25-mm plastic swinnex filter holder.

d. Gelman$^{R}$ glass fiber filter type A, 25-mm diameter (pore size: see section I-A-4).

e. Rubber stoppers.

f. Plastic tubing.

g. Narrow-mouth 1-oz polyethylene bottle.

h. Glass tubing to water aspirator.

i. Glass jar.

j. Plastic jar lid.

Figure A2. Small volume plastic filtration apparatus

The filtering apparatus shown in Figure A2 was cleaned by aspirating concentrated $HNO_3$ through the filter followed by Super-Q.

D. Analytical procedures used for the determination of dissolved and particulate metals in the water column samples.

1. Analytical procedure for the determination of dissolved metals in seawater: The filtered seawater samples were analyzed for dissolved trace heavy metals within 9 months after collection using the extraction procedure of Duchart et al.[72]

The preserved seawater samples taken during any particular cruise (approximately 40 samples) were removed from refrigerated storage and allowed to come to room temperature (20°C). A 100-ml aliquot was poured into a calibrated 125-ml separatory funnel. A group of 100-ml aliquots of Super-Q served as reagent blanks. Atomic absorption standards were prepared by the method of additions; minute quantities of mixed standard were added to four 100-ml aliquots of a seawater sample. The four resulting seawater plus standard solutions contained an additional 1, 2, 4, and 8 µg/l of metal, respectively.

The pH of the samples and standards was adjusted to 2 with $NH_4OH$. Four ml of a 20 percent (W/V) sodium potassium tartrate solution was added and, after shaking, the samples were allowed to stand for 15 min. The pH was adjusted to 6 with $NH_4OH$ after which 4 ml of a 20 percent (W/V) sodium diethyl dithiocarbamate

solution was added. Five ml of 4 methyl pentan-2-ol (methyl isobutyl carbinol) were added and the funnels shaken mechanically for 15 min. The organic and aqueous phases were allowed to separate for 20 min. The aqueous layer was then drained and the organic layer collected in a 1-oz wide-mouth polyethylene bottle.

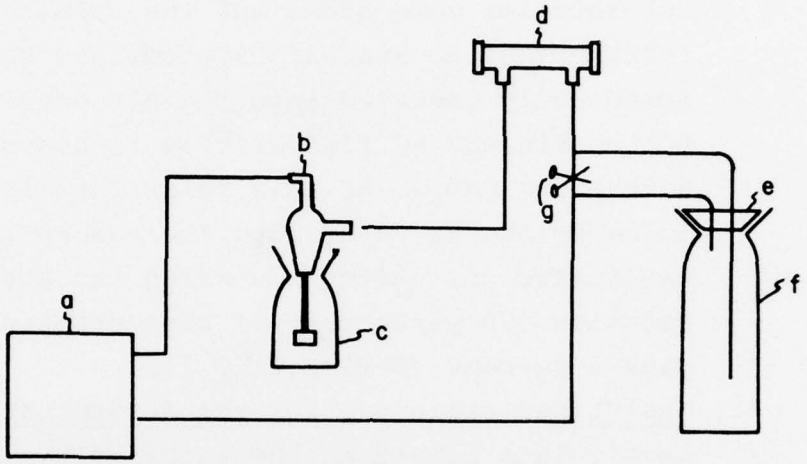
The AA measurements were performed on the organic extract in the order of increasing stability of the metal chelate complex. Mn, Zn, Fe, and Cu were determined by aspirating the extract into an air-$C_2H_2$ flame. Ag, Cd, Pb, Ni, and Co were determined by injecting the extract into a Heated Graphite Atomizer (flameless AA) equipped with a grooved graphite furnace tube.

2. Analytical procedure for the determination of dissolved Hg in seawater: The preserved Hg samples (100 ml seawater + 6 ml preservative) were removed from frozen storage and, after thawing, they were transferred from the reagent bottles to 300-ml BOD bottles. Standards were prepared by adding 100 ml of a Hg standard solution (0.5, 1, 2, 3, 4, and 5 µg/l Hg in Super-Q) plus 6 ml of preservative to a 300-ml BOD bottle. The reagent blanks were prepared by adding 100 ml of Super-Q plus 6 ml of a preservative to each of several 300-ml BOD bottles.

To each solution (blank, standard, and sample), 1 ml of 5 percent (W/V) $KMnO_4$ solution

was added. All solutions were then warmed on a sand-bed hot plate at 60°C for 1 hr. Next, to each BOD bottle individually, 5 ml of a 10 percent (W/V) $SnCl_2$ plus 1 percent (V/V) concentrated HCl solution were added and the bubbler of the Perkin-Elmer Hg analysis system (see Figure A3) immediately inserted into the BOD bottle. The BOD bottle was swirled briefly to dissolve the dark-brown $MnO_2$. At this point the air flow to sweep the Hg vapor into the absorption tube was turned on. After recording the absorbance solution [50 percent (V/V) concentrated $HNO_3$ plus 5 percent (W/V) $K_2Cr_2O_7$].

3. Analytical procedure for the determination of particulate metals in the water column: The glass fiber filters containing the suspended particulates were dried at 30°C for 48 hr. Each filter was transferred from the Millipore$^R$ petri dish to a Nalgene$^R$, 1-oz wide-mouth polyethylene bottle. Five ml concentrated $HNO_3$ were added to the bottle which was then tightly capped and shaken to shred the glass fiber filter. The bottle was placed on a sand-bed hot plate and heated at 80°C for 2 hr. After the digestion period, the solution was filtered through the small volume plastic filtration apparatus (see Figure A2). The filtrate was collected in a Nalgene$^R$, 1-oz narrow-mouth polyethylene bottle. The digesting bottle and the filtering apparatus were washed with four 5-ml aliquots of Super-Q; each wash was added to the filtrate for a total volume of filtrate plus




a. Air pump

b. Bubbler

c. 300-ml glass BOD bottle

d. Hg optical absorption tube

e. Rubber stopper

f. Hg vapor absorbing trap

g. Pinch clamp

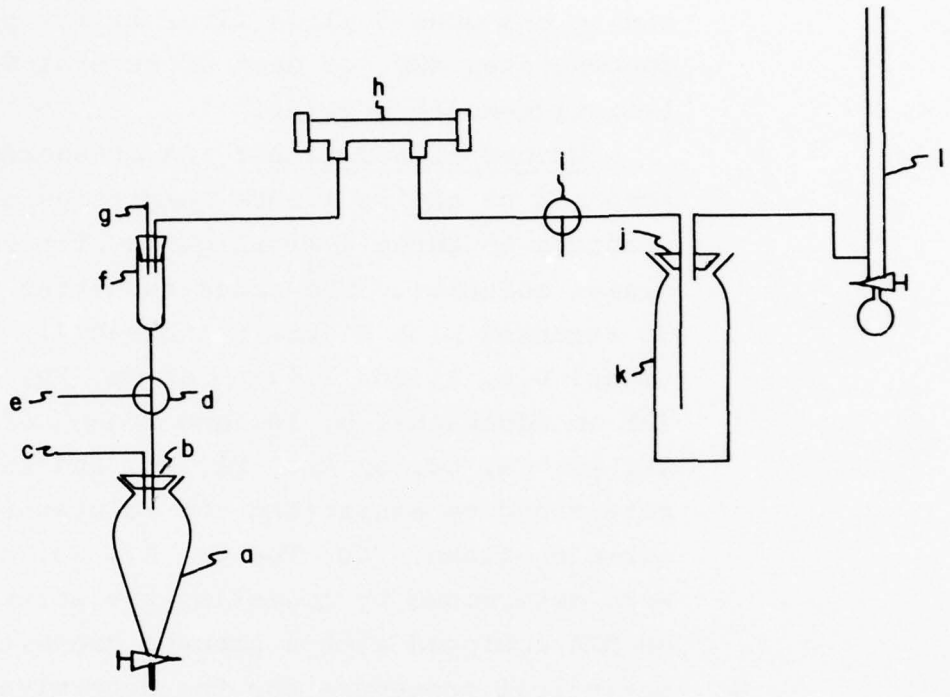
Figure A3. Perkin-Elmer cold vapor Hg analysis system

wash = 25 ml. Reagent blanks were obtained by adding one unused glass fiber filter plus 5 ml concentrated $HNO_3$ to each of several Nalgene$^R$, 1-oz wide-mouth bottles.

Method of additions: AA standards were prepared by adding minute quantities of mixed standard to three 4-ml aliquots of a sample digest solution. The three resulting solutions of standard plus digest contained (1) an additional 0.5, 1, and 1.5 mg/l of Mn, Zn, and Fe or (2) an additional 5, 10, and 20 µg/l of Cu, Pb, Cr, Ag, Co, Cd, or Ni. Fe, Mn, and Zn were determined by aspirating the solutions into an air-$C_2H_2$ flame. Cu, Pb, Cr, Ag, Co, and Ni were determined by injecting the solutions into an HGA equipped with a grooved graphite tube.

4. Analytical procedure for the determination of particulate Hg in the water column: To determine Hg, 3 ml of the reducing solution [1 percent (W/V) $SnCl_2$ + 1 percent (V/V) concentrated HCl] was injected into the small volume Hg apparatus (see Figure A4) adapted from Hawley and Ingle.[90] After the air flow purged Hg contamination from the $SnCl_2$-HCl solution, 10 ml of a filter digest was injected into the small volume Hg apparatus. The peak absorbance was recorded. This procedure was repeated for 10 ml of each Hg standard [0.5, 1, 2, and 3 µg/l Hg in 5 percent (V/V) concentrated $HNO_3$ plus 0.01 percent (W/V) $KMnO_4$].

II. Trace heavy metals associated with bottom sediment and interstitial water.




a. 250-ml Pyrex$^{R}$ separatory funnel
b. Rubber stopper
c. Tubing to water aspirator
d. 3-way valve
e. Tubing to the Perkin-Elmer AA burner control box: source of compressed air
f. Medium porosity sintered glass filter funnel with rubber stopper
g. Rubber septum inserted into a glass tube
h. Hg optical absorption tube
i. 3-way valve
j. Rubber stopper
k. Hg vapor absorbing trap
l. Bubble burette

Figure A4. Small volume Hg apparatus

A. Decontamination of the apparatus used for sampling bottom sediment and interstitial water. (Described in Part II of main report)

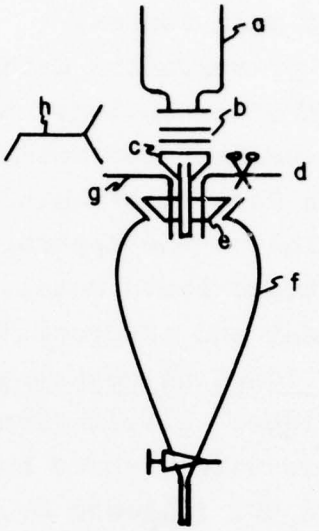
B. Sampling and preservation methods used for the determination of trace heavy metals associated with bottom sediment and interstitial water. (Described in Part II of main report)

C. Decontamination of the apparatus used for the analysis of trace heavy metals associated with bottom sediment and interstitial water.

1. Sediment leaching container: Four-oz narrow-mouth Nalgene$^{R}$ polyethylene bottles. These containers were cleaned by rinsing with concentrated HCl followed by Super-Q. Ten ml of concentrated $HNO_3$ was added to each bottle; the bottles were capped tightly and then placed on a sand-bed hot plate at 80°C for 2 hr. The bottles were rinsed with Super-Q.

2. Containers for collecting the organic phase during solvent extraction: One-oz wide-mouth Nalgene$^{R}$ polyethylene bottles. These bottles were cleaned by rinsing with concentrated HCl followed by Super-Q. The bottles were stored filled with Super-Q.

3. Millipore$^{R}$ filtering assembly (see Figure A5): A Millipore$^{R}$ filtering apparatus was mounted on a 500-ml glass separatory funnel having a Teflon stopcock. Gelman$^{R}$ glass fiber filters, Type A, 47-mm diameter, were used in the Millipore$^{R}$ filtering apparatus (see section I-A-4 for the filter pore size). The filters, filter holder, and separatory funnel were




a. Top half of a 47 mm diameter glass Millipore$^{R}$ filtering apparatus.
b. Two 47-mm diameter Gelman$^{R}$ glass fiber Type A filters.
c. Bottom half of a 47-mm diameter glass Millipore$^{R}$ filtering apparatus.
d. 90° glass elbow connected to a plastic tube which serves as a vacuum release valve.
e. Rubber stopper.
f. 500-ml Pyrex$^{R}$ separatory funnel.
g. 90° glass elbow connected to a water aspirator.
h. Millipore$^{R}$ clamp for holding together the top and bottom halves of the Millipore$^{R}$ filtering apparatus.

Figure A5. Millipore filtering assembly

cleaned by filtering concentrated $HNO_3$ through the complete assembly. After draining the concentrated $HNO_3$ from the separatory funnel, the assembly was rinsed with Super-Q.

4. Pyrex$^R$ glass volumetric flasks used to make dilutions for atomic absorption analysis (Class A; 50-, 25-, and 10-ml capacity): These flasks were cleaned by rinsing with concentrated $HNO_3$ followed by Super-Q.
5. Glass 300-ml BOD bottles used for the analysis of Hg associated with bottom sediment: They were cleaned by rinsing with concentrated $HNO_3$ followed by Super-Q and calibrated to contain 100 ml. Each bottle was filled with a solution of 5 percent (V/V) concentrated $HNO_3$ + 1 percent (W/V) $K_2Cr_2O_7$ (Feldman[89]). Prior to analysis, the $HNO_3$-$K_2Cr_2O_7$ soaking solution was removed and the bottle rinsed with Super-Q.
6. Pyrex$^R$ 125-ml glass separatory funnels: (See section I-C-3 for description and cleaning procedures).

D. Analytical procedures used for the determination of trace heavy metals associated with bottom sediment and interstitial water.

1. Analytical procedure used for the determination of trace heavy metals associated with bottom sediment: Approximately 2.5 g of ground sediment, weighed to the nearest 0.001 g, was transferred to a 4-oz Nalgene$^R$ polyethylene narrow-mouth bottle. Ten ml concentrated $HNO_3$ was added. The tightly capped bottle was placed on a sand-bed hot plate at 80°C for 2 hr. After the 2-hr

period, the digest was filtered through two Gelman$^{R}$ glass fiber type A filters using the Millipore$^{R}$ filtering assembly (see Figure A5). The filtrate was collected in a 50-ml Pyrex$^{R}$ volumetric flask. The plastic digest bottle and the filtering apparatus were washed with Super-Q and the washes added to the filtrate. The solution was diluted to 50 ml and then shaken. Processing 10 ml of concentrated $HNO_3$ as a sample provided a reagent blank.

Method of additions: AA standards were prepared by adding minute quantities of mixed standard to three 10-ml aliquots of a digest solution. The three resulting digest plus standard solutions contained an additional 0.5, 1, and 1.5 mg/l metals, respectively. The solutions were aspirated into an air-$C_2H_2$ flame. Absorbances of the samples and standards were recorded. When required, the samples were diluted with Super-Q to keep absorbance readings within the linear range of the AA.

2. Analytical procedure used for the determination of Hg in bottom sediment: Approximately 1.0 g of ground sediment, weighed to the nearest 0.001 g, was transferred to a 300-ml glass BOD bottle. Ten ml concentrated $HNO_3$ was added. The bottle was stoppered and the $HNO_3$-sediment mixture allowed to digest at room temperature for 24 hr, with occasional swirling. Ten ml concentrated $HNO_3$ in a stoppered BOD bottle served as a reagent blank. To each BOD bottle, 25 ml of a 5 percent (W/V) $KMnO_4$ solution was added.

The stoppered BOD bottles were placed on a sand-bed hot plate at 60°C for 1 hr, after which the samples were diluted to 100 ml with Super-Q. The standards were prepared by adding 100 ml of a Hg standard solution [0.5, 1, 2, 3, 5, 10, and 20 µg/l Hg in 5 percent (V/V) concentrated $HNO_3$ plus 0.01 percent (W/V) $KMnO_4$] to a BOD bottle.

Next, each BOD bottle was treated individually as follows. Twenty ml of a 1.5 percent (W/V) $NH_2OH \cdot HCl$ solution was added and the solution swirled briefly while the brown $MnO_2$ dissolved. Five ml of a 10 percent (W/V) $SnCl_2$ plus 1 percent (V/V) HCl solution was added and the bubbler of the Perkin-Elmer Hg analysis system (See Figure A3) immediately inserted into the BOD bottle. After briefly swirling the contents of the BOD bottle, an air pump was turned on which cycled the Hg vapor through the absorption cell. The absorbance was recorded while the Hg vapor from each sample circulated through the cell.

3. Analytical procedure used for the determination of trace heavy metals in interstitial water: Mn and Zn concentrations were determined directly by aspirating the interstitial water into an air-$C_2H_2$ flame.

Method of additions: AA standards (+0.5, +1, +2, +3, and +10 mg/l metal) were prepared by adding minute quantities of mixed standard to 100-ml aliquots of seawater. The metal concentrations were recorded directly by using

the concentration mode and curve straightening capabilities of the AA.

Cu and Fe were determined directly by injecting the interstitial water into the HGA (flameless AA).

Method of additions: AA standards, in concentrations ranging from +1 to +500 µg/l, were prepared by adding minute quantities of mixed standards to 10-ml aliquots of seawater.

Pb, Cd, Ni, Co, and Ag were extracted from interstitial water samples according to the extraction procedure of Duchart et al.[72] A 25-ml aliquot of interstitial water was poured into a calibrated 125-ml separatory funnel. Twenty-five-ml aliquots of Super-Q served as reagent blanks.

Method of additions: AA standards (+1, +2, +4, and +8 µg/l) were prepared by adding minute quantities of mixed standard to 25-ml aliquots of seawater. The pH of the solutions was adjusted to 2 with $NH_4OH$. Two ml of a 10 percent (W/V) sodium potassium tartrate solution were added to each separatory funnel. After shaking, the funnels were allowed to stand for 15 min. The pH was then raised to 6 with $NH_4OH$. Two ml of a 10 percent (W/V) sodium diethyl dithiocarbamate solution was added to each funnel followed by the addition of 5 ml of 4 methyl pentan-2-ol (methyl isobutyl carbinol). The funnels were mechanically shaken for 15 min after which the organic layers were allowed to separate for 20 min. The aqueous

layer was drained and the organic layer collected in a 1-oz wide-mouth polyethylene bottle. Ag, Cd, Pb, Ni, and Co were determined by injecting the extract into an HGA equipped with a grooved graphite furnace tube.

4. Analytical procedure used for the determination of Hg in interstitial water: Immediately after squeezing the core segment, 10 ml of interstitial water were placed in a 25-ml glass volumetric flask. One ml of concentrated $HNO_3$ and 1 ml of a 5 percent (W/V) $KMnO_4$ solution were added to the flask. The flask was stoppered and then heated on a sand-bed hot plate at 60°C for 1 hr. Standards were prepared by adding 10 ml of a Hg standard solution (0.5, 1, 2, and 3 µg/l Hg in Super-Q) plus 1 ml concentrated $HNO_3$ plus 1 ml of a 5 percent $KMnO_4$ solution to a 25-ml volumetric flask. Super-Q reagent blanks were prepared in a similar manner.

Three ml of reducing solution [1 percent (W/V) $SnCl_2$ + 1 percent (V/V) concentrated HCl] was injected into the small volume Hg apparatus (see Figure A4) adapted from Hawley and Ingle.[90] While the air flow purged Hg contamination from the reducing solution, 0.5 ml of a 1.5 percent (W/V) $NH_2OH \cdot HCl$ solution was added to one of the 25-ml volumetric flasks. After briefly swirling to dissolve the $MnO_2$, the contents of the flask were transferred to the small volume Hg apparatus and the peak absorbance recorded.

III. Instrumentation and data reduction.

A. Instrumentation.

1. Spectrometer and associated equipment for

metal analyses:

a. Perkin-Elmer Model 403 Atomic Absorption Spectrometer.

b. Perkin-Elmer HGA 70 (Heated Graphite Atomizer) with modifications for gas interrupt and variable charring temperature (Segar and Gonzalez;[91] Kahn and Slavin[92]). The purge gas selected was 0.5 percent methane in Ar (UHP).

c. Perkin-Elmer Deuterium Arc Background Absorption Corrector (Kahn[93]).

d. Perkin-Elmer single element hollow cathode lamps.

e. Hewlett-Packard Model 7100 B strip chart recorder.

f. Perkin-Elmer cold vapor Hg analysis system (see Figure A3).

g. Small volume Hg apparatus adapted from Hawley and Ingle[90] (see Figure A4).

2. Instrumental settings: Recommended in the 1971 Perkin-Elmer handbook entitled "Analytical Methods for Atomic Absorption Spectrophotometry", were used with the exception that the Pb 2170 Å line was used rather than the recommended Pb 2833 Å line.

B. Data Reduction

A Hewlett-Packard Model 9830A Programmable calculator/plotter was used to perform all calculations. A polynominal regression program calculated and plotted the slope and intercept of the concentration vs. absorbance standard curves. The program also calculated the concentrations of metals in the samples according to the following

formulas:

1. Seawater and interstitial water: The metals concentration $[M_n]$ was calculated from:

$$[M_n] = \frac{\text{nanograms dissolved metal}}{\text{ml of water sample}} \quad (\mu g/l)$$

$$= (\text{absorbance of the sample} - \text{absorbance of the blank}) \times (\text{slope of the standard curve})$$

where the slope of the standard curve has units of ng/ml/absorbance.

2. Sediment: The metals concentration $[M_s]$ is calculated from:

$$[M_s] = \frac{\text{micrograms metal}}{\text{gram of sediment sample}} \quad (\mu g/g)$$

$$= (\text{absorbance of the sample} - \text{absorbance of the blank}) \times (\text{slope of the standard curve}) \times \frac{(\text{volume of the sample digest solution: 50 ml})}{(\text{weight of sample, grams})} \times (\text{dilution factor})$$

where the slope of the standard curve has units of µg/ml/absorbance.

3. Suspended particulates: The metals concentration

$$[M_{sp}] = \frac{\text{micrograms metal}}{\text{liters of seawater filtered through glass fiber filter}} \quad (\mu g/l)$$

$$= (\text{absorbance of the sample} - \text{absrobance of the blank}) \times (\text{slope of the standard curve, µg/ml/absorbance}) \times (\text{volume of the sample digest solution: 25 ml}) \div (\text{volume of seawater filtered, liters})$$

IV. Detection limits and precision and detection limits tables.

A. Definitions of the terms used in the precision and detection limits tables.

1. Smallest Measurable Difference (SMD): Calculate the SMD by substituting the smallest measurable difference in absorbance into the equations for calculating the concentration of metal in the sample. The units are concentration.

2. Instrumental Uncertainty or Atomic Absorption Noise (AA Noise): AA Noise was defined as 0.5 the width of the recorder pen baseline. The units are $\pm$ absorbance. When substituted into the formulas for calculating the concentration of metals in the samples, the $\pm$ absorbance becomes the uncertainty in the concentration of a sample (e.g. $\pm$mg/l) due to instrument noise.

3. Detection Limit (DL): The DL was defined as twice the uncertainty in the concentration of a sample due to instrument noise (as defined above). For example, if the instrument noise produces an uncertainty of $\pm$ Xmg/l, (as defined above), then the DL concentration is defined as 2X mg/l. This implies a minimum uncertainty of at least $\pm$ 50 percent for concentrations near the DL:

$$\frac{\pm \text{ X mg/l}}{\text{2X mg/l}} \times 100 = \pm 50\%$$

In general, the magnitudes of the AA Noise, SMD, and DL will vary with different instrumental conditions, different metals, and

different sample types.

4. Range of Sample Concentrations:

n is defined as the number of samples for which the concentration of a specific trace heavy metal has been determined.

low designates the lowest concentration value in the set of n concentration values obtained by analyzing n samples for a specific trace heavy metal.

high designates the highest concentration value in the set of n concentration values obtained by analyzing n samples for a specific trace heavy metal.

avg designates the average concentration value for the set of n concentration values obtained by analyzing n samples for a specific trace heavy metal.

$\sigma$ designates the standard deviation for the set of n concentration values obtained by analyzing n samples for a specific trace heavy metal.

5. Precision of the AA Instrument: The HGA instrumental precision was calculated by dividing the standard deviation ($\sigma_{AA}$) of a series of absorbance measurements ($n_{AA}$) by the average ($\bar{X}_{AA}$) of the series: $\sigma_{AA}/\bar{X}_{AA}$, where

$$\bar{X}_{AA} = \sum_{i=1}^{i=n_{AA}} X_i/n_{AA} \ .$$

The series of absorbance measurements was obtained by repeated injection of one sample solution into the HGA furnace tube.

The flame instrumental precision was calculated by dividing the AA Noise by the concentration of the sample:

$$\text{AA Noise}/X_j \text{ where } j = \begin{Bmatrix} \text{low} \\ \text{high} \\ \text{avg.} \end{Bmatrix}.$$

6. Precision of the Analytical Procedure: The precision of the analytical procedure was obtained by taking several aliquots ($n_{analysis}$) of one sample through the entire analytical process of sample preparation and instrumental analysis. The precision was calculated by dividing the standard deviation ($\sigma_{analysis}$) for the ($n_{analysis}$) aliquot values by the average value ($\bar{X}_{analysis}$) obtained from $n_{analysis}$ aliquots: $\sigma_{analysis}/\bar{X}_{analysis}$

$$\text{where } \bar{X}_{analysis} = \sum_{i=1}^{i=n_{analysis}} X_i/n_{analysis}.$$

7. Precision of the Sampling Procedure: The precision of the sampling procedure was determined by taking several independent samples ($n_{sampling}$) from one sampling location through the entire analytical process of sample preparation and instrumental analysis. The precision was calculated by dividing the standard deviation ($\sigma_{sampling}$) by the average ($\bar{X}_{sampling}$) of the $n_{sampling}$ replicates: $\sigma_{sampling}/\bar{X}$ sampling,

$$\text{where } \bar{X}_{sampling} = \sum_{i=1}^{i=n_{sampling}} X_i/n_{sampling}.$$

B. Tables A1, A2, A3, and A4 summarize the precision and DL of the methods for trace heavy metal analysis.

V. Reagents and standards

A. Reagents

All reagents and standards used were American Chemical Society quality or ultra pure.

1. Water: Super-Q, Millipore$^{R}$ ultrapure water system composed of a 0.5-μ prefilter, an organic contaminant exchange column, an ionic exchange column, and a 0.22-μ final filter. Super-Q System$^{R}$ water quality specifications:[94]

| | |
|---|---|
| Dissolved inorganics mg/l $CaCO_3$ | 0.025 |
| Dissolved Organics mg/l | <1. |
| Specific resistance megohm·cm @ 25°C | 18. |
| Particles and microorganisms | <0.22 micron dia. |

2. ACS HCl (J. T. Baker Chemical Co.): 37.3 percent by weight.

3. ACS $HNO_3$ (J. T. Baker Chemical Co.): 70.3 percent by weight.

4. Ultrex$^{R}$ $HNO_3$ (J. T. Baker Chemical Co.): 70.2 percent by weight.

5. $NH_4OH$ (Fisher Scientific Co.) minimum concentration 28 percent by weight.

6. 4 methyl pentan-2-ol (methyl isobutyl carbinol, MIBC): (Eastman Co.)

7. 20 percent (W/V) sodium diethyl dithiocarbamate (NaDDC): (Fisher Scientific Co.) 20 g NaDDC

Table A1

Precision and Detection Limits: Dissolved Metals in Seawater

(See Appendix Section IV—A for the definitions of the terms in this table.)

| | Ag | Cd | Co | Cr*** | Cu | Fe | Hg | Mn | Ni | Pb | Zn |
|---|---|---|---|---|---|---|---|---|---|---|---|
| Average SMD (µg/l) | 0.03 | 0.02 | 0.2 | | 0.1 | 0.3 | 0.03 | 0.1 | 0.2 | 0.03 | 0.3 |
| Average AA Noise (± µg/l) | 0.03 | 0.04 | 0.4 | | 0.1 | 0.5 | 0.03 | 0.3 | 0.6 | 0.05 | 0.3 |
| Average DL (µg/l) | 0.06 | 0.08 | 0.7 | | 0.3 | 1 | 0.05 | 0.5 | 1 | 0.1 | 0.5 |
| Range of Sample Concentrations (µg/l) | | | | | | | | | | | |
| n | | 165 | | | 166 | 165 | 28 | 165 | | 160 | 166 |
| low | | 0.02 | | | 1.5 | 0.1 | 0.01 | 0.1 | | 0.02 | 1 |
| high | | 3.24 | | | 5.6 | 33.6 | 2.01 | 7.8 | | 9.31 | 54.1 |
| avg. | | 0.6 | | | 2.5 | 8.5 | 0.7 | 2.1 | | 0.81 | 5.4 |
| σ | | 0.32 | | | 0.4 | 3.1 | 0.43 | 0.9 | | 0.56 | 2.8 |
| Precision of the AA Instrument: | | | | | | | | | | | |
| $n_{AA}$ | | 6 | | | 9 | NA* | NA | NA | | 6 | NA |
| σ AA | | 0.06 | | | 0.7 | AA Noise | AA Noise | AA Noise | | 0.04 | AA Noise |
| At low conc. range | | 3 | | | 0.47 | 5 | 3 | 3 | | 2 | 3 |
| At high conc. range | | 0.02 | | | 0.13 | 0.01 | 0.01 | 0.04 | | 0.004 | 0.006 |
| At average conc. range | | 0.1 | | | 0.28 | 0.06 | 0.04 | 0.14 | | 0.05 | 0.06 |
| Precision of the Analytical Procedure: | | | | | | | | | | | |
| n analysis | | 3 | | | 3 | 3 | | 3 | | 3 | 3 |
| σ analysis | | 1.4 | | | 0.06 | 0.1 | | 0.2 | | 1.11 | 0.1 |
| At low conc. range | | 70 | | | 0.04 | 1 | | 2 | | 55.5 | 0.1 |
| At high conc. range | | 0.43 | | | 0.01 | 0.003 | | 0.03 | | 0.12 | 0.002 |
| At average conc. range | | 2.33 | | | 0.02 | 0.01 | | 0.1 | | 1.37 | 0.02 |
| Precision of the Sampling Procedure: | | | | | | | | | | | |
| $n_{sampling}$ | | 5(x2) | | | 5(x2) | 5(x2) | | 5(x2) | | 5(x2) | 5(x2) |
| $\sigma_{sampling}$ | | <.16>** | | | <.29> | <3.7> | | <.33> | | <.11> | <1.4> |
| At low conc. range | | 8 | | | 0.19 | 37 | | 3.3 | | 5.5 | 1.4 |
| At high conc. range | | 0.05 | | | 0.05 | 0.11 | | 0.04 | | 0.01 | 0.03 |
| At average conc. range | | 0.27 | | | 0.12 | 0.44 | | 0.16 | | 0.14 | 0.26 |

* NA = Not Applicable

** <Average>

***Dissolved Cr was not determined in the sea water samples.

Table A2

Precision and Detection Limits: Pore Water Metals*

(See Appendix Section IV-A for the definitions of the terms in this table.)

| | (HGA, Cd MIBC)** | (Direct Flame; HGA) Cu MIBC) | | (Direct Fe HGA)*** | (Direct Mn Flame)**** | (HGA, Ni MIBC) | (HGA, Pb MIBC) | (Flame, Zn Direct) |
|---|---|---|---|---|---|---|---|---|
| Average SMD (µg/l) | 0.02 | 1 | 0.1 | 4 | 0.04 | 0.3 | 0.06 | 0.008 |
| Average AA Noise (± µg/l) | 0.04 | 1 | 0.1 | 4 | 0.04 | 1.0 | 0.12 | 0.008 |
| Average DL (µg/l) | 0.07 | 2 | 0.2 | 8 | 0.08 | 2.0 | 0.24 | 0.016 |
| Range of Sample Concentrations (µg/l): | | | | | | | | |
| n | 133 | 85 | 46 | 108 | 113 | 53 | | 86 |
| low | 0.03 | 1.8 | 1.6 | 11 | 80 | 0.3 | 0.9 | 7 |
| high | 4.68 | 92 | 8 | 997 | 11250 | 15.3 | 32.2 | 269 |
| average | 0.80 | 20 | 4 | 137 | 2551 | 5.5 | 2.0 | 46 |
| σ | 0.60 | 15 | 2 | 175 | 2108 | 3.3 | 3 | 37 |
| Precision of the AA Instrument: | | | | | | | | |
| $n_{AA}$ | 5 | 4 | 9 | 4 | NA* | | 5 | NA* |
| $\sigma_{AA}$ | 0.06 | 1.29 | 0.7 | 11.4 | AA Noise | | 0.19 | AA Noise |
| low conc. range | 2 | 0.72 | 0.47 | 1.04 | 0.5 | | 0.21 | 1.14 |
| high conc. range | 0.013 | 0.01 | 0.10 | 0.01 | 0.004 | | 0.006 | 0.03 |
| average conc. range | 0.08 | 0.06 | 0.18 | 0.08 | 0.02 | | 0.04 | 0.17 |
| Precision of the Analytical Procedure: | | | | | | | | |
| $n_{Analysis}$ | 3 | NA | 3 | NA* | NA* | | 3 | NA* |
| $\sigma_{Analysis}$ | 1.4 | NA | 0.06 | NA | NA | | 1.11 | NA |
| low conc. range | 70 | NA | 0.04 | NA | NA | | 55.5 | NA |
| At high conc. range | 0.43 | NA | 0.01 | NA | NA | | 0.12 | NA |
| average conc. range | 2.33 | NA | 0.02 | NA | NA | | 0.38 | NA |
| Precision of the Sampling Procedure: | | | | | | | | |
| $n_{sampling}$ | 4x2 | 4x2 | | 4x2 | 4x2 | | 4x2 | 4x2 |
| $\sigma_{sampling}$ | 0.14 | 0.96 | | 21 | 1272 | | 0.58 | 9 |
| low conc. range | 4.67 | 0.53 | | 1.91 | 16 | | 0.64 | 1.29 |
| At high conc. range | 0.03 | 0.01 | | 0.02 | 0.11 | | 0.02 | 0.03 |
| average conc. range | 0.18 | 0.05 | | 0.15 | 0.50 | | 0.20 | 0.20 |

* Not Applicable

** Analysis performed using HGA furnace and MIBC.

*** Analysis performed using direct injection of sample into HGA furnace.

**** Analysis performed using direct aspiration of sample into flame.

Table A3

Precision and Detection Limits: Trace Heavy Metals in Sediment

(See Appendix Section IV-A for the definitions of the terms in this table.)

| | Ag | Cd | Co | Cr | Cu | Fe | Hg | Mn | Ni | Pb | Zn |
|---|---|---|---|---|---|---|---|---|---|---|---|
| Average SMD (µg/g) | 0.23 | 0.15 | 0.78 | 0.64 | 0.29 | 320 | 0.008 | 22 | 0.54 | 0.76 | 8 |
| Average AA Noise (± µg/g) | 0.22 | 0.1 | 1 | 1 | 0.3 | 300 | 0.01 | 22 | 1 | 1 | 12 |
| Average DL (µg/g) | 0.45 | 0.3 | 2 | 2 | 0.6 | 600 | 0.03 | 45 | 2 | 2 | 25 |
| Range of Sample Concentrations (µg/g): | | | | | | | | | | | |
| n | | | 111 | 112 | 112 | 111 | 110 | 111 | 112 | 106 | 112 |
| low | | | 4 | 7.1 | 4.7 | $0.67 \times 10^3$ | 0.005 | 124 | 6 | 2 | 19 |
| high | | | 15 | 157 | 230 | $3.9 \times 10^3$ | 1.42 | 2555 | 33 | 145 | 278 |
| average | | | 9.33 | 38 | 49.3 | $2.33 \times 10^3$ | 0.183 | 557 | 17 | 30 | 116 |
| σ | | | 2 | 29 | 51.2 | 0.44 | 0.246 | 291 | 6 | 30 | 61 |
| Precision of the AA Instrument: | | | | | | | | | | | |
| $n_{AA}$ = Not Applicable | | | NA* | NA | NA | NA | NA | NA | NA | NA | NA |
| $\sigma_{AA}$ = AA Noise | | | AA Noise | AA Noise | AA Noise | AA Noise | AA Noise | AA Noise | AA Noise | AA Noise | AA Noise |
| low conc. range | | | 0.25 | 0.14 | 0.06 | 0.45 | 2 | 0.18 | 0.17 | 0.5 | 0.63 |
| At high conc. range | | | 0.07 | 0.01 | 0.01 | 0.08 | 0.01 | 0.01 | 0.03 | 0.01 | 0.04 |
| average conc. range | | | 0.11 | 0.03 | 0.01 | 0.13 | 0.05 | 0.04 | 0.06 | 0.03 | 0.10 |
| Precision of the Analytical Procedure: | | | | | | | | | | | |
| $n_{Analysis}$ | | | 4x2 | 4x2 | 4x2 | 4x2 | 4x2 | 4x2 | 4x2 | | 4x2 |
| $\sigma_{Analysis}$ | | | <.9>** | <.9> | <12> | $<.09 \times 10^3>$ | <.335> | <67> | <1.8> | | <10> |
| low conc. range | | | 0.23 | 0.13 | 2.5 | 0.13 | 67 | 0.54 | 0.3 | | 0.53 |
| At high conc. range | | | 0.06 | 0.01 | 0.05 | 0.02 | 0.24 | 0.03 | 0.05 | | 0.04 |
| average conc. range | | | 0.10 | 0.02 | 0.24 | 0.04 | 1.83 | 0.12 | 0.11 | | 0.09 |
| Precision of the Sampling Procedure: | | | | | | | | | | | |
| $n_{sampling}$ | | | 2x2 | 2x2 | 2x2 | 2x2 | 2x2 | 2x2 | 2x2 | 2x2 | 2x2 |
| $\sigma_{sampling}$ | | | <.4> | <12> | <13> | $<.09 \times 10^3>$ | <.087> | <17> | <1.6> | <5.7> | <91> |
| low conc. range | | | 0.1 | 1.69 | 2.8 | 0.13 | 17.4 | 0.14 | 0.27 | 2.85 | 4.8 |
| At high conc. range | | | 0.03 | 0.08 | 0.06 | 0.02 | 0.06 | 0.01 | 0.05 | 0.04 | 0.33 |
| average conc. range | | | 0.04 | 0.32 | 0.26 | 0.04 | 0.48 | 0.03 | 0.09 | 0.19 | 0.78 |

* Not Applicable

** <Average>

Table A4

Precision and Detection Limits: Particulate Metals in the Water Column

(See Appendix Section IV-A for the definitions of the terms in this table.)

| | Ag | Cd | Co | Cr | Cu | Fe | Hg | Mn | Ni | Pb | Zn |
|---|---|---|---|---|---|---|---|---|---|---|---|
| **Average** SMD (mg/l) | 0.14 | 0.09 | 2 | 6 | 5 | $0.22 \times 10^3$ | 0.38 | $0.07 \times 10^3$ | 3.2 | 6 | $0.03 \times 10^3$ |
| Average AA (± mg/l) | 0.16 | 0.17 | 4 | 5 | 5 | $0.22 \times 10^3$ | 0.38 | $0.07 \times 10^3$ | 7 | 7 | $0.03 \times 10^3$ |
| Average DL (mg/l) | 0.33 | 0.35 | 8 | 9 | 10 | $0.44 \times 10^3$ | 0.76 | $0.14 \times 10^3$ | 13 | 13 | $0.06 \times 10^3$ |
| Range of Sample Concentrations (mg/l): | | | | | | | | | | | |
| n | 190 | 164 | | 192 | 192 | 192 | 192 | 192 | | 190 | 178 |
| low | 0.60 | 0.06 | | 19 | 22 | $2 \times 10^3$ | 0.81 | $1.2 \times 10^3$ | | 40 | $0.004 \times 10^3$ |
| high | 23.66 | 15.32 | | 1179 | 2297 | $333.5 \times 10^3$ | 18.49 | $59.9 \times 10^3$ | | 1043 | $29.9 \times 10^3$ |
| average | 5.03 | 2.52 | | 177 | 220 | $28.7 \times 10^3$ | 4.68 | 4.47 | | 165 | $0.980 \times 10^3$ |
| σ | 2.46 | 2.17 | | 136 | 166 | $18.4 \times 10^3$ | 2.62 | $2.89 \times 10^3$ | | 84 | $1.77 \times 10^3$ |
| Precision of the AA Instrument: | | | | | | | | | | | |
| $n_{AA}$ | 5 | 8 | | (10,5) | (4,4,6) | NA* | NA | NA | | 6 | NA |
| σ AA | 1.02 | 0.39 | | <24> | <53> | Noise | Noise | Noise | | 5 | Noise |
| low conc. range | 1.7 | 6.5 | | 1.26 | 2.4 | 0.11 | 0.46 | 0.06 | | 0.13 | 7.5 |
| At high conc. range | 0.04 | 0.03 | | 0.02 | 0.02 | 0.001 | 0.02 | 0.001 | | 0.005 | 0.001 |
| average conc. range | 0.20 | 0.15 | | 0.14 | 0.24 | 0.01 | 0.08 | 0.02 | | 0.03 | 0.03 |
| Precision of the Analytical Procedure: | | | | | | | | | | | |
| $n_{Analysis}$ | NA* | NA | NA | NA | NA | NA | NA | NA | NA | NA | NA |
| $\sigma_{Analysis}$ | NA | NA | NA | NA | NA | NA | NA | NA | NA | NA | NA |
| low conc. range | NA | NA | NA | NA | NA | NA | NA | NA | NA | NA | NA |
| avg. conc. range | NA | NA | NA | NA | NA | NA | NA | NA | NA | NA | NA |
| Precision of the Sampling Procedure: | | | | | | | | | | | |
| $n_{sampling}$ | **<5>(x5) | <5>(x5) | | <5>(x5) | <5>(x5) | <5>(x5) | <5> (x5) | <5>(x5) | | <5>(x5) | <5>(x5) |
| $\sigma_{sampling}$ | <1.2> | <1.89> | | <58> | <60> | <4> | <1.61> | <0.4> | | <21.4> | <5.7> |
| low conc. range | 2 | 31.5 | | 3.05 | 2.7 | 2 | 1.99 | 0.33 | | 0.54 | 1425 |
| At high conc. range | 0.05 | 0.12 | | 0.05 | 0.03 | 0.01 | 0.09 | 0.01 | | 0.02 | 0.19 |
| average conc. range | 0.24 | 0.75 | | 0.33 | 0.27 | 0.14 | 0.34 | 0.09 | | 0.13 | 5.8 |

*Not Applicable (Because 1 filter cannot be carried through the analysis 5 times, i.e. more than once)

** <Average>

diluted to 100 ml with Super-Q. Filter and extract the solution with MIBC to remove trace heavy metals.

8. 20 percent (W/V) sodium potassium tartrate (NaKT): (Fisher Scientific Co.) 20 g NaKT + 0.5 g NaDDC diluted to 100 ml with Super-Q. Filter and extract the solution with MIBC to remove trace heavy metals.
9. Hg preserving solution: 0.177 g $K_2Cr_2O_7$ (Fisher Scientific Co.) diluted to 100 ml with concentrated $HNO_3$.
10. 5 percent (V/V) concentrated $HNO_3$ + 0.1 percent (W/V) $K_2CR_2O_7$: 5 ml concentrated $HNO_3$ + 0.1 g $K_2CR_2O_7$ diluted to 100 ml with Super-Q.
11. 5 percent (W/V) $KMnO_4$: 5 g $KMnO_4$ (Fisher Scientific Co.) diluted to 100 ml with Super-Q.
12. 1.5 percent (W/V) $NH_2OH \cdot HCl$: (Fisher Scientific Co.) 1.5 g hydroxyl ammine hydrochloride diluted to 100 ml with Super-Q.
13. 10 percent (W/V) $SnCl_2$ + 1 percent (V/V) concentrated HCl: 10 g $SnCl_2$ (Fisher Scientific Co.) + 1 ml concentrated HCl diluted to 100 ml with Super-Q.

B. Standards

One of the following metals or metal salts (Table A5) was added to a 100-ml class A volumetric flask and dissolved in 10 ml of a 50 percent (V/V) concentrated $HNO_3$ solution. The resulting solution was diluted to 100 ml with Super-Q.

Table A5

Concentrations of Standards*

| Metal or Salt | Weight g | Metal Concentration mg/l | Supplier |
|---|---|---|---|
| $Co(NO_3)_2.6H_2O$ | 0.49368 | 998.6 | JMC |
| $K_2CrO_4$ | 0.37430 | 1001.9 | Fisher |
| $MnSO_4.H_2O$ | 0.30881 | 983.7 | Allied Chemical |
| $Pb(NO_3)_2$ | 0.16608 | 1037.8 | Alfa-Ventron |
| Cd | 0.15006 | 1500.6 | Alfa-Ventron |
| Cu | 0.09273 | 927.3 | Baker |
| Fe | 0.10400 | 1040.0 | Baker |
| Ni | 0.10028 | 1002.8 | Alpha-Ventron |
| Zn | 0.17720 | 708.8 | Alpha-Ventron |
| $AgNO_3$ | 0.15957 | 1013.3 | Fisher |

*Hg standard: 0.1380 g $HgCl_2$ + 50 ml concentrated $HNO_3$ + 0.1 g $K_2Cr_2O_7$ diluted to 1 ℓ with Super-Q for a Hg standard of 102.2 mg/l Hg.

## APPENDIX B': WATER COLUMN OBSERVATIONS DURING CRUISES ACE II, ACE III, ACE IV, ACE V, ACE VI, AND ACE VII


| Figures | Variable | Pages |
|---|---|---|
| B1-B6 | Temperature | 241-246 |
| B7-B12 | Dissolved oxygen concentration | 247-252 |
| B13-B18 | Ammonium concentration | 253-258 |
| B19-B24 | Nitrite concentrations | 259-264 |
| B25-B30 | Nitrate concentrations | 265-270 |
| B31-B36 | Silicic acid concentration | 271-276 |
| B37-B42 | Dissolved phosphate concentration | 277-282 |
| B43-B48 | Total phosphorus concentration | 283-288 |
| B49-B54 | Particulate nitrogen concentration | 289-294 |
| B55-B60 | Particulate carbon concentration | 295-300 |
| B61-B66 | Chlorophyll-*a* concentration | 301-306 |
| B67-B72 | Suspended solids concentrations | 307-312 |

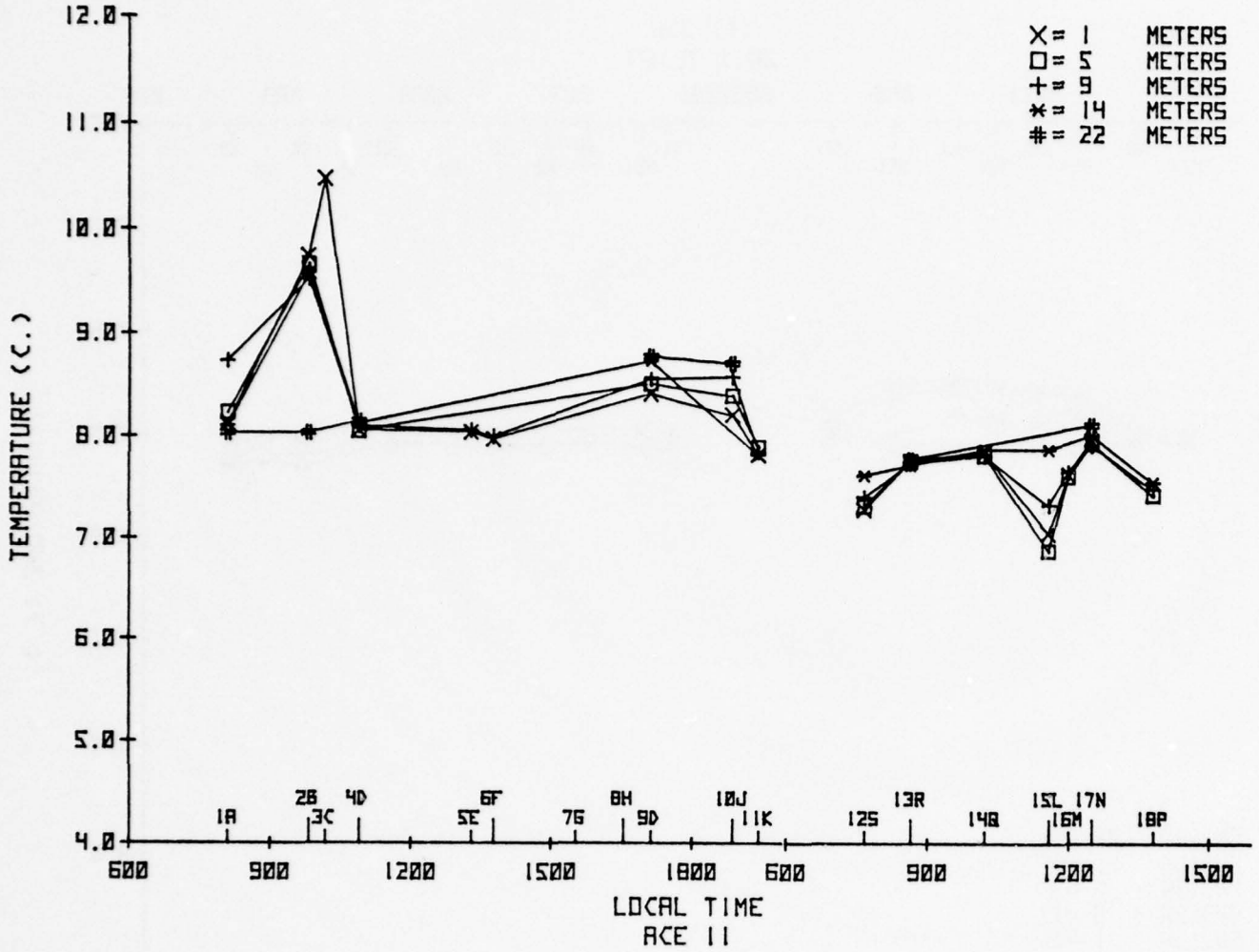



Figure B1. Temperature observations during 5-6 December 1974.

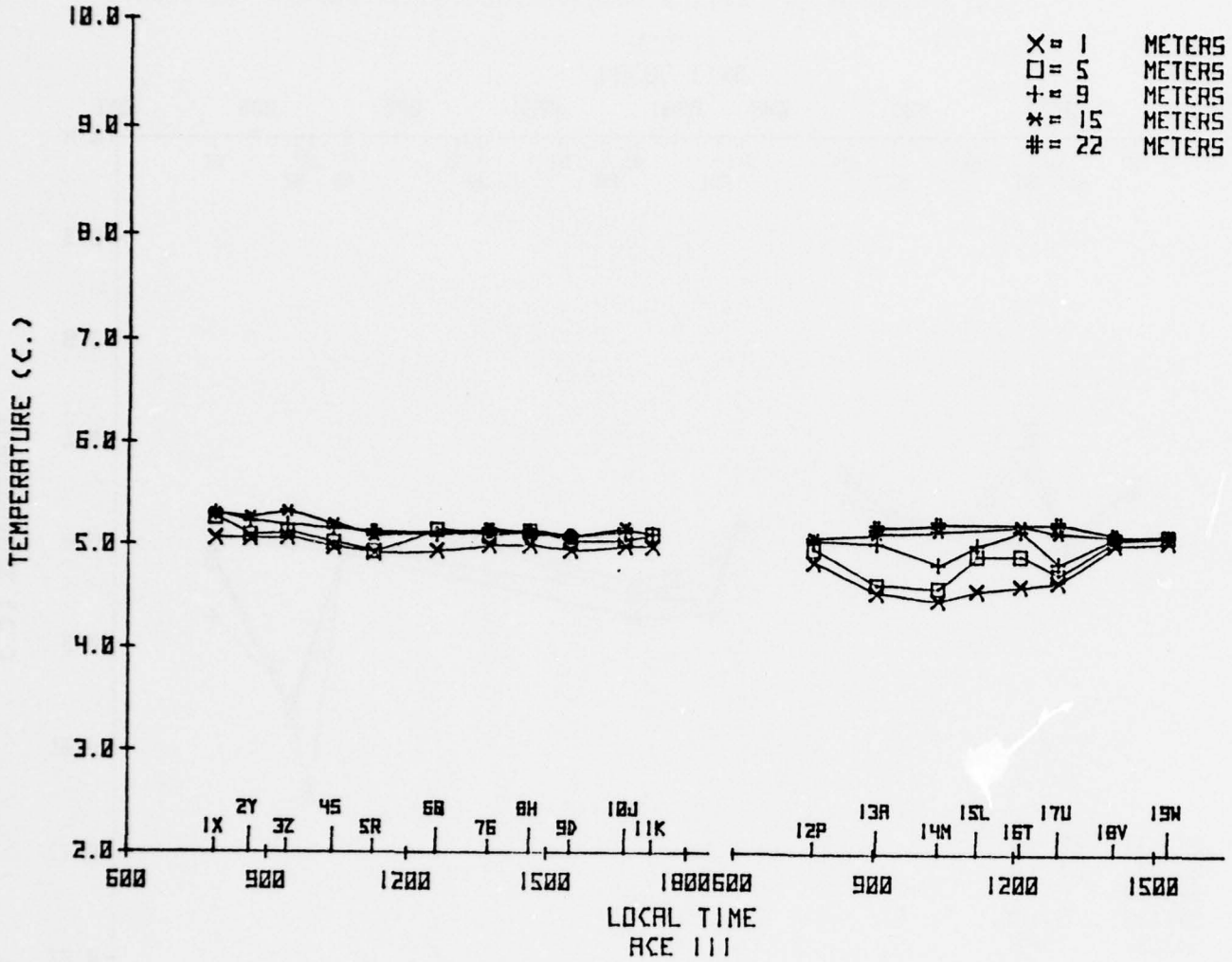



Figure B2. Temperature observations during 13-14 January 1975.

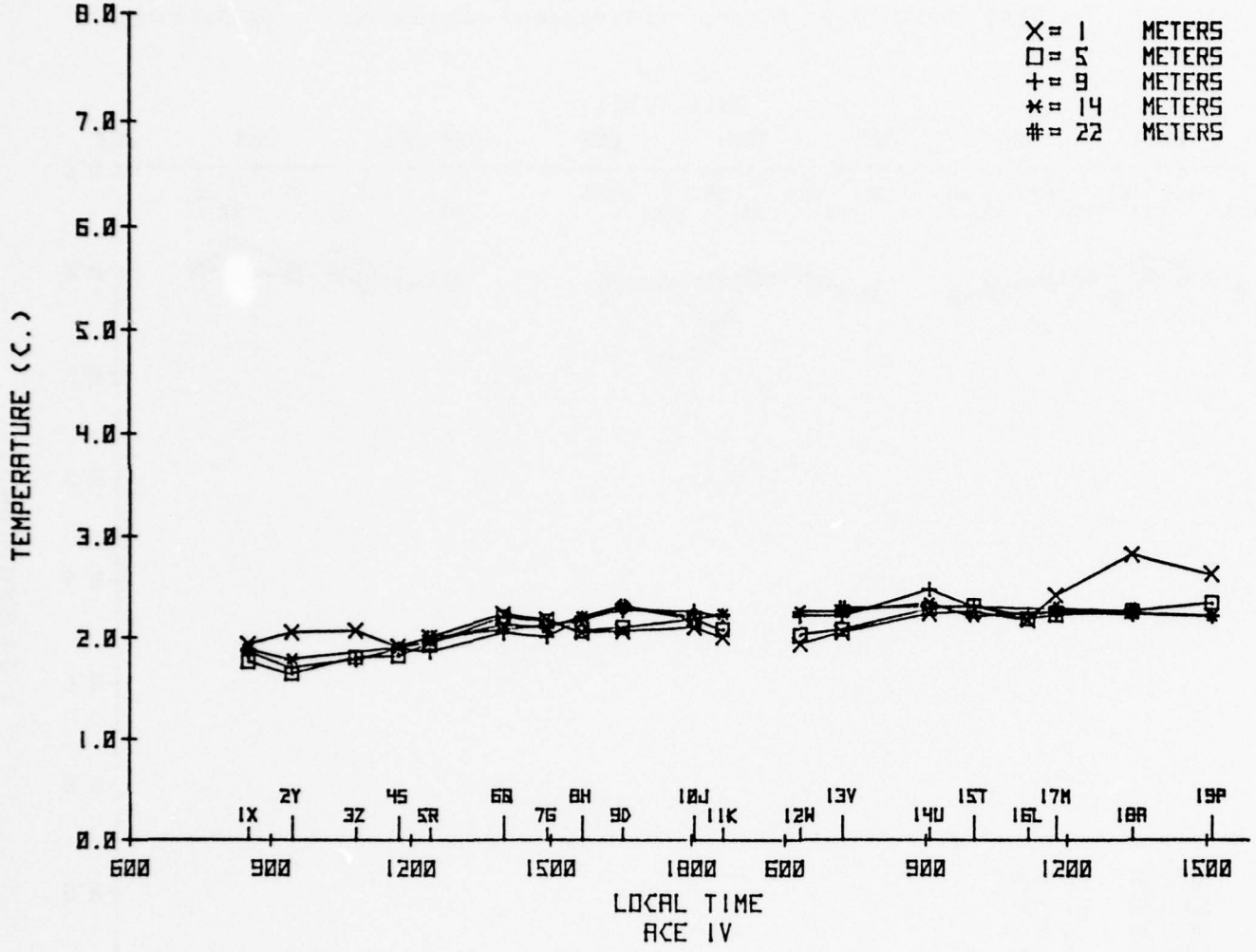
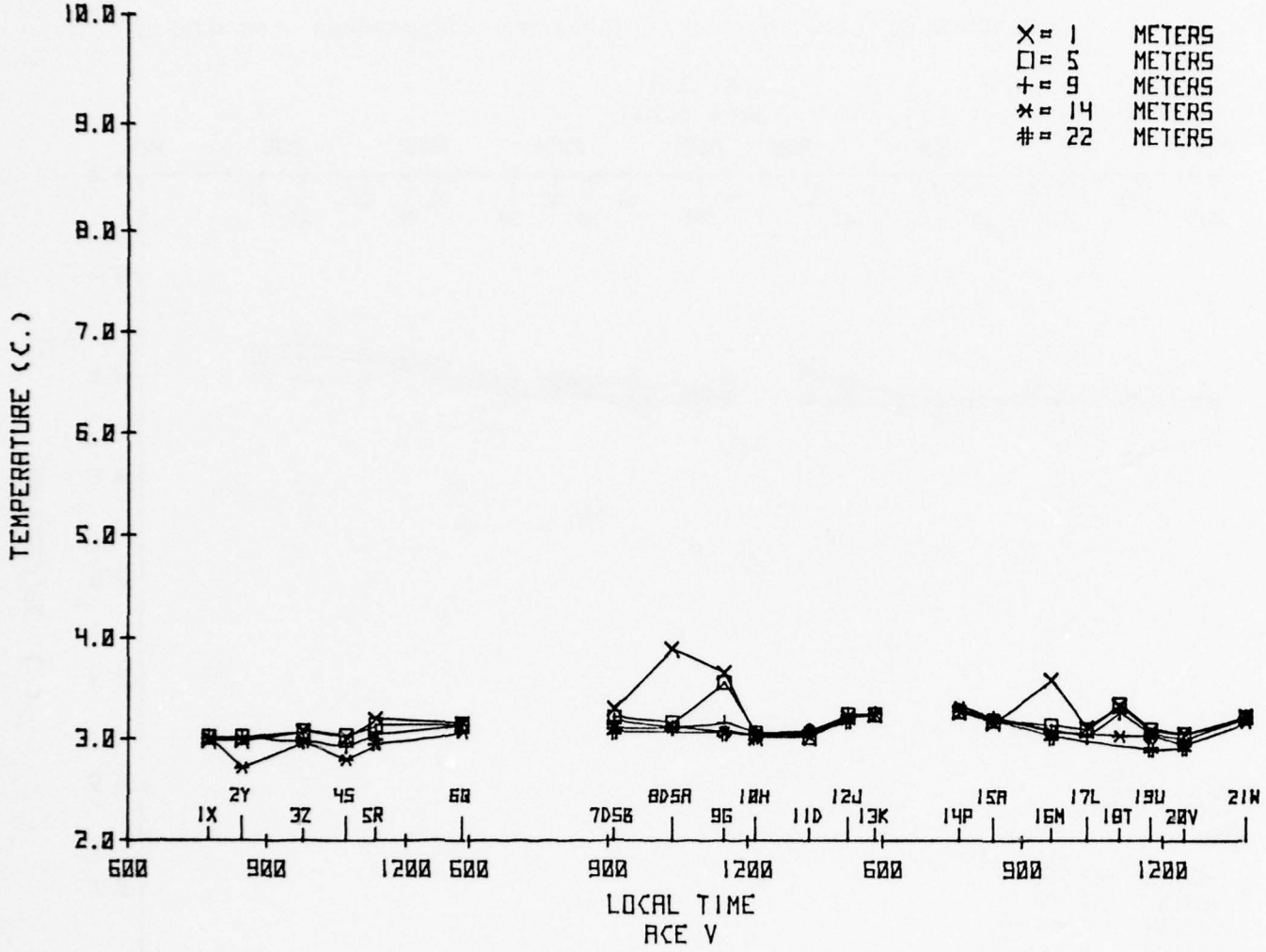



Figure B3. Temperature observations during 19-20 February 1975.




February B4. Temperature observations during 19-21 March 1975.

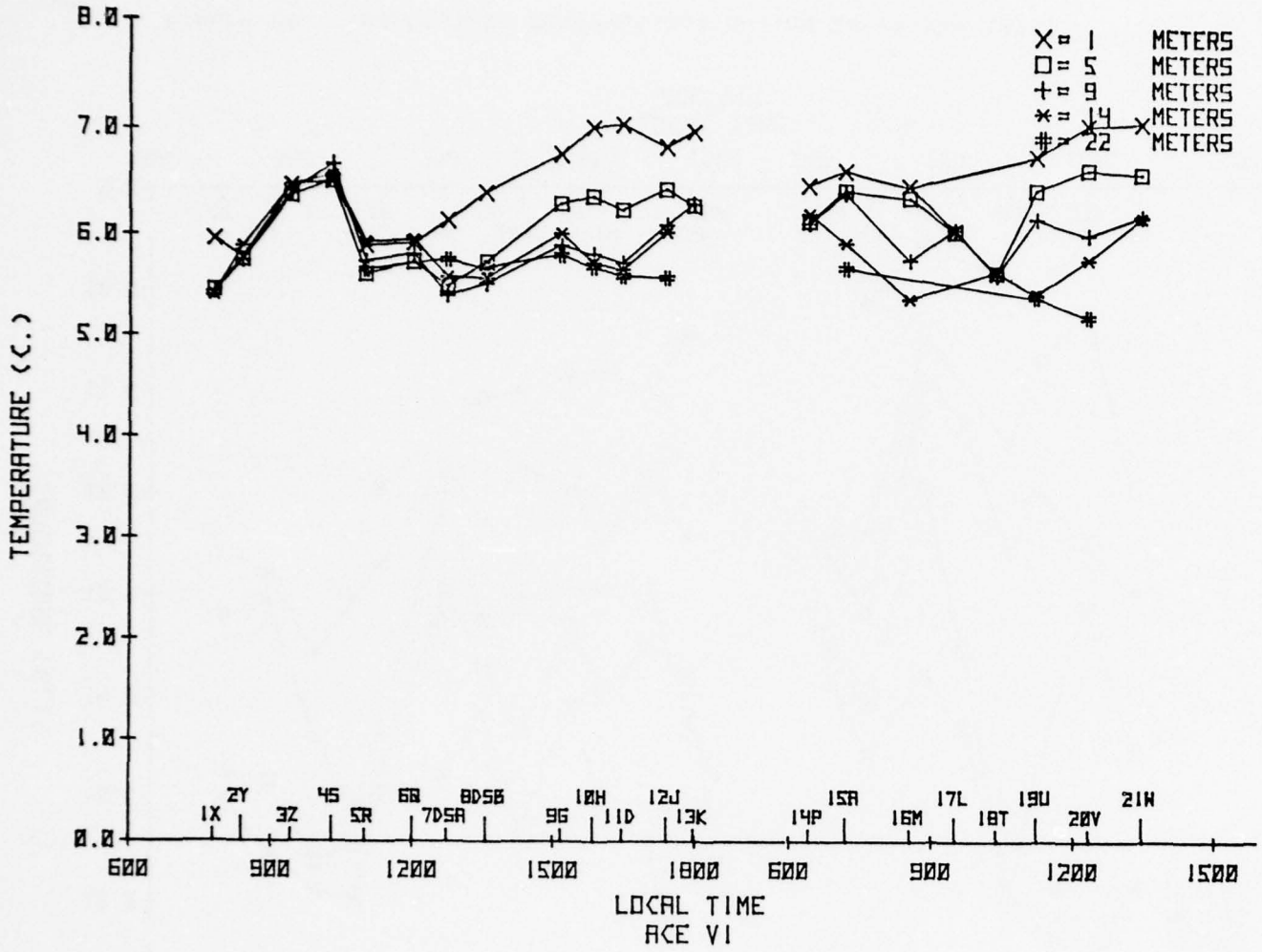



Figure B5. Temperature observations during 23-24 April 1975.

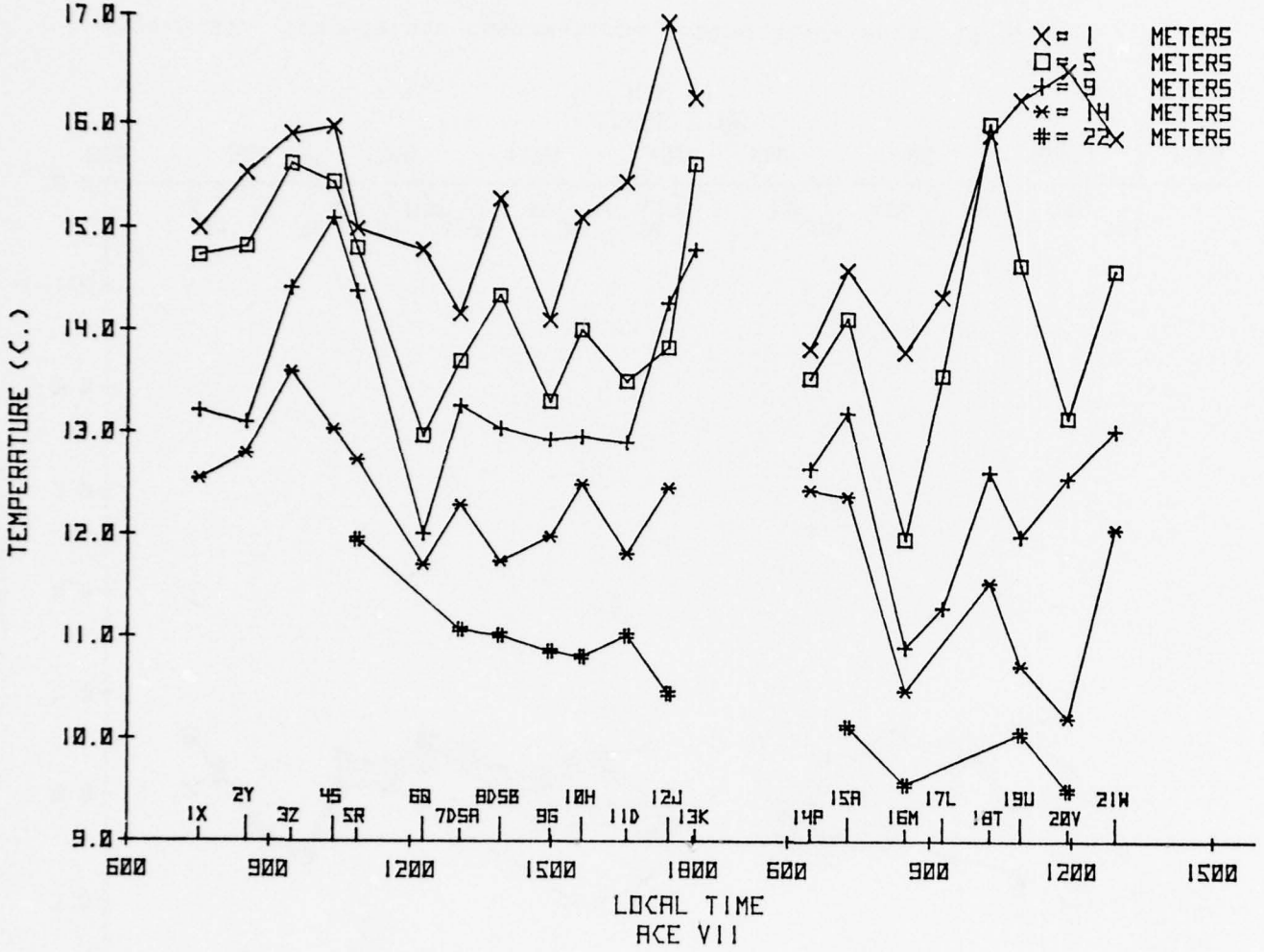



Figure B6. Temperature observations during 28-29 May 1975.

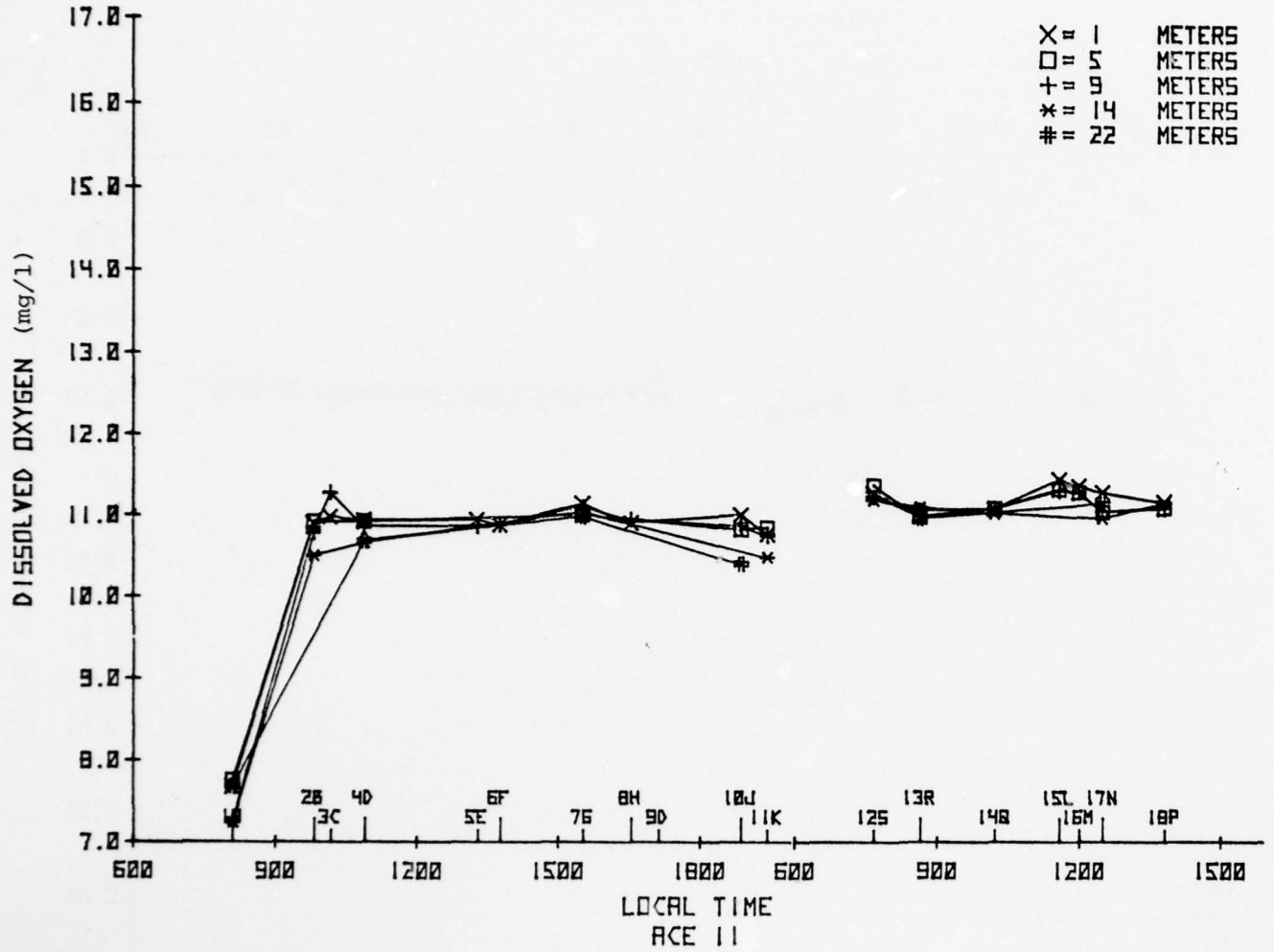



Figure B7. Dissolved oxygen concentrations during 5-6 December 1974.

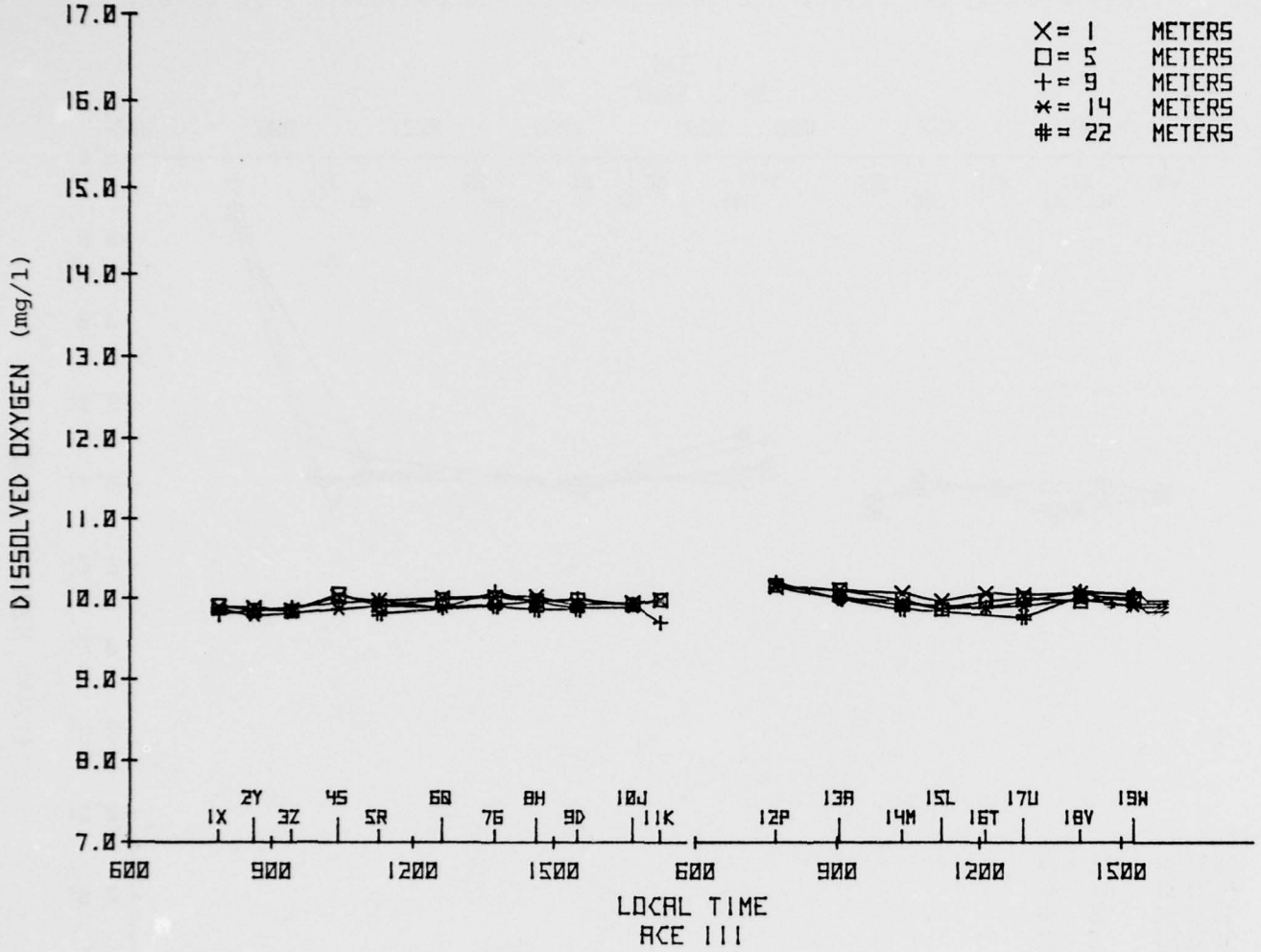



Figure B8. Dissolved oxygen concentrations during 13-14 January 1975.

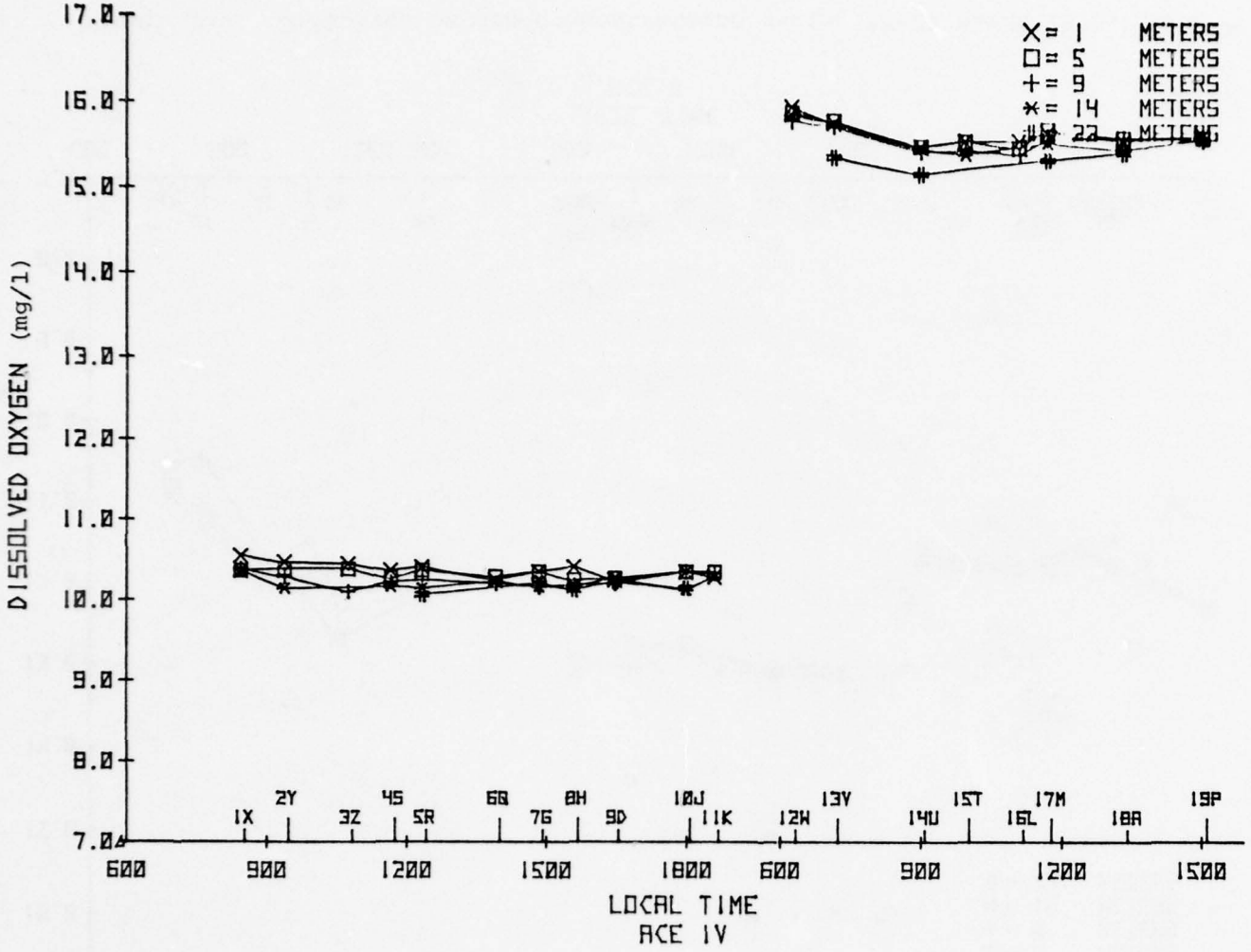



Figure B9. Dissolved oxygen concentrations during 19-20 February 1975.

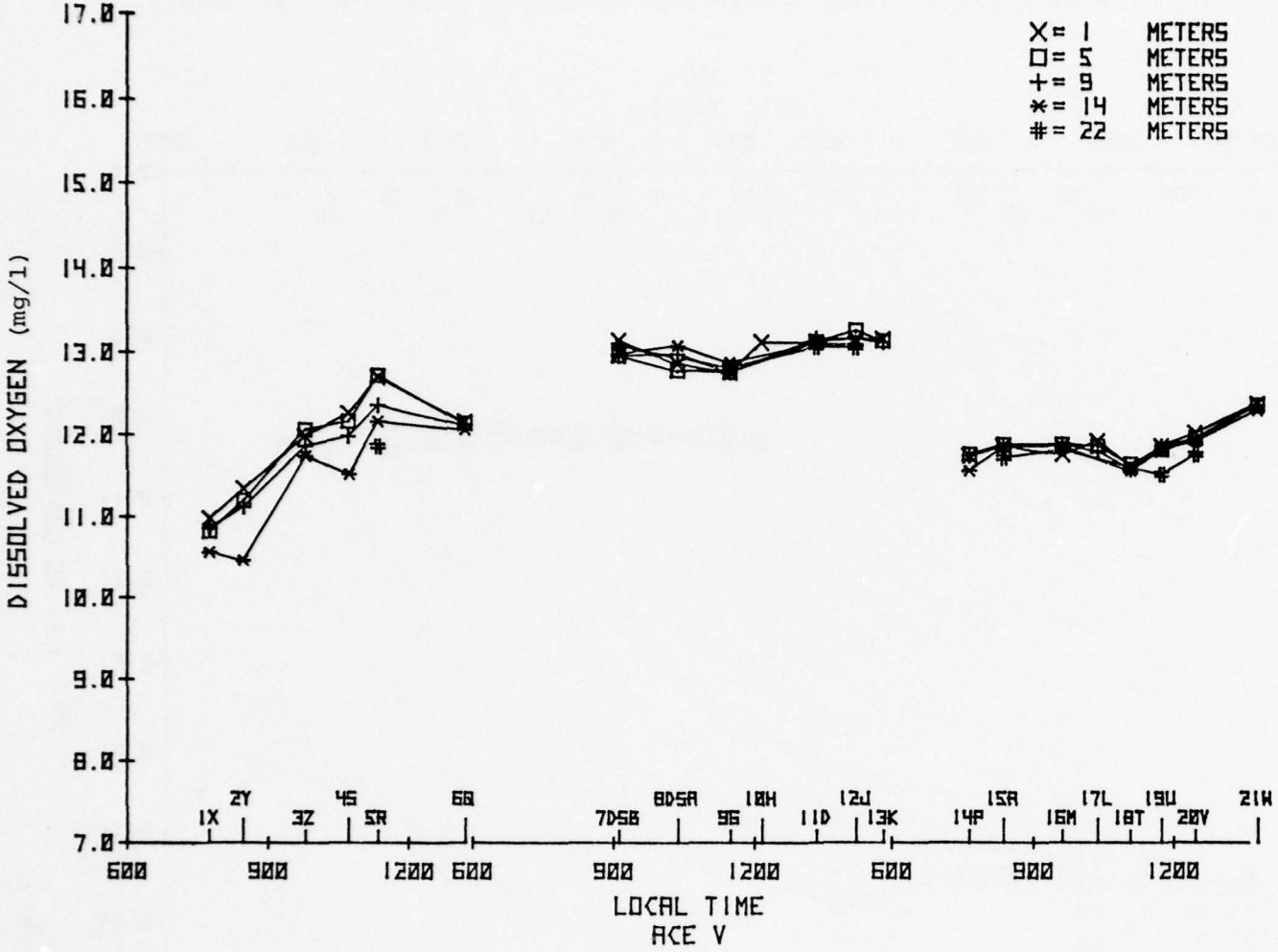



Figure B10. Dissolved oxygen concentrations during 19-21 March 1975.

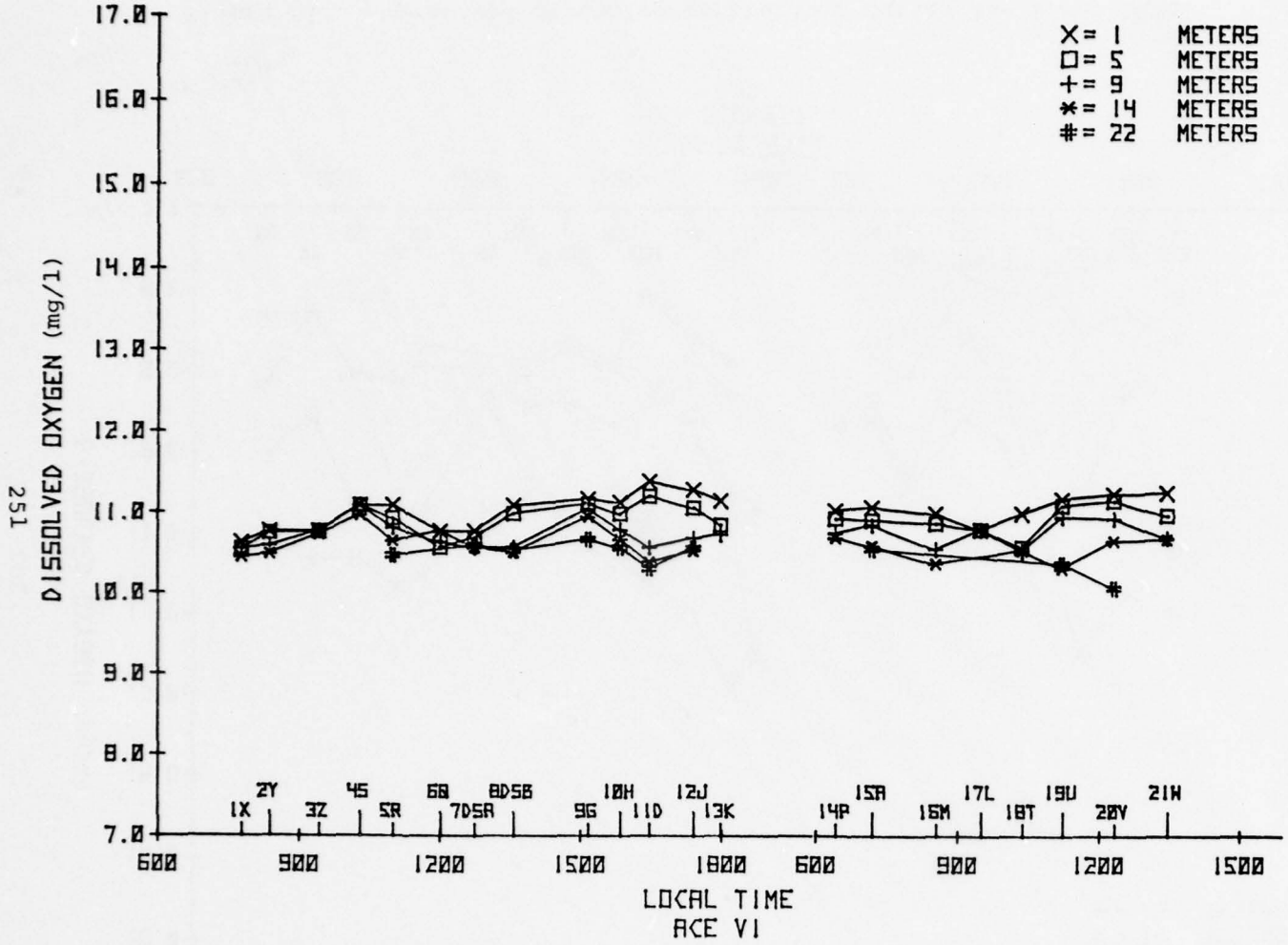



Figure B11. Dissolved oxygen concentrations during 23-24 April 1975.

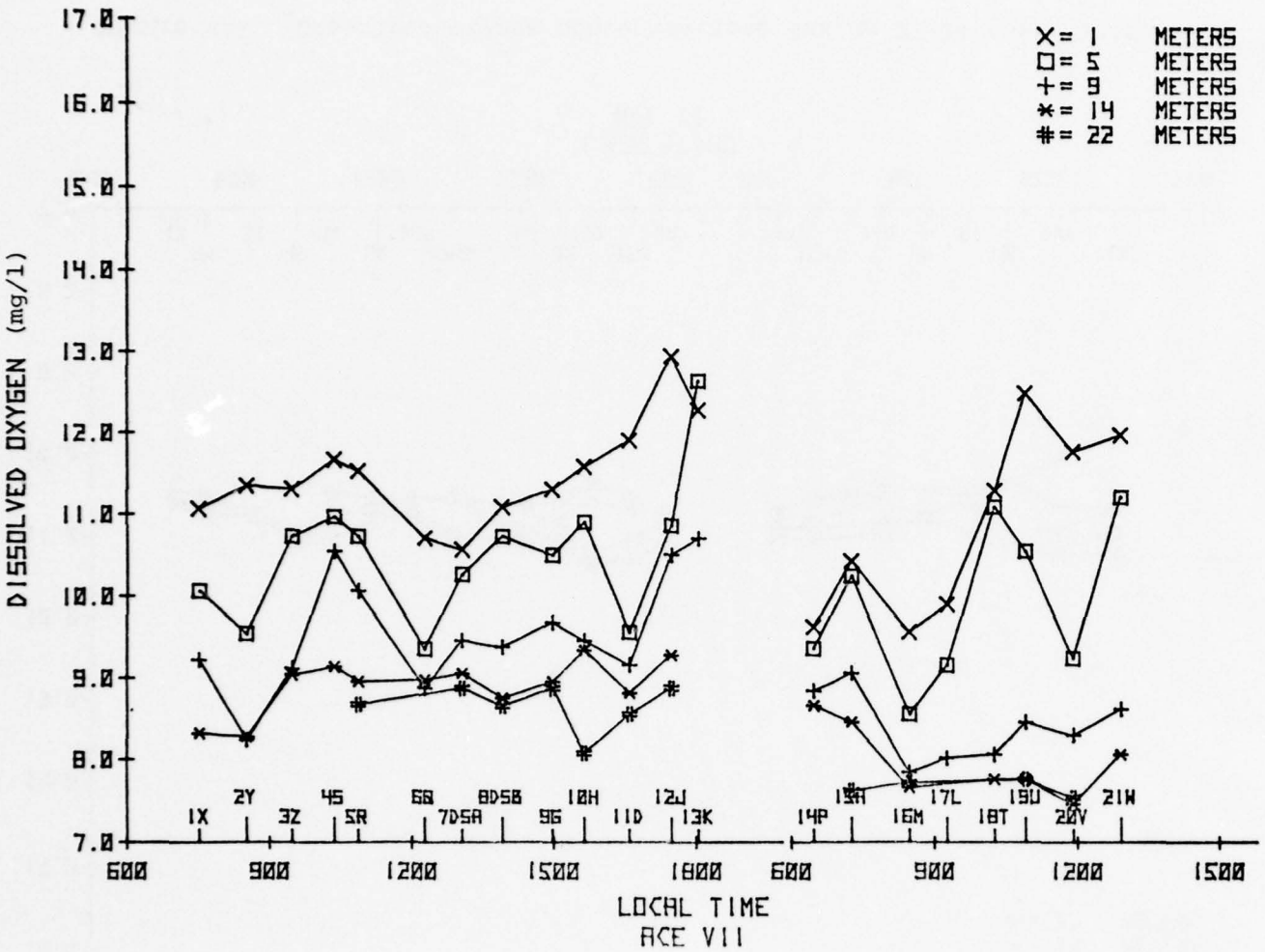



Figure B12. Dissolved oxygen concentrations during 28-29 May 1975.

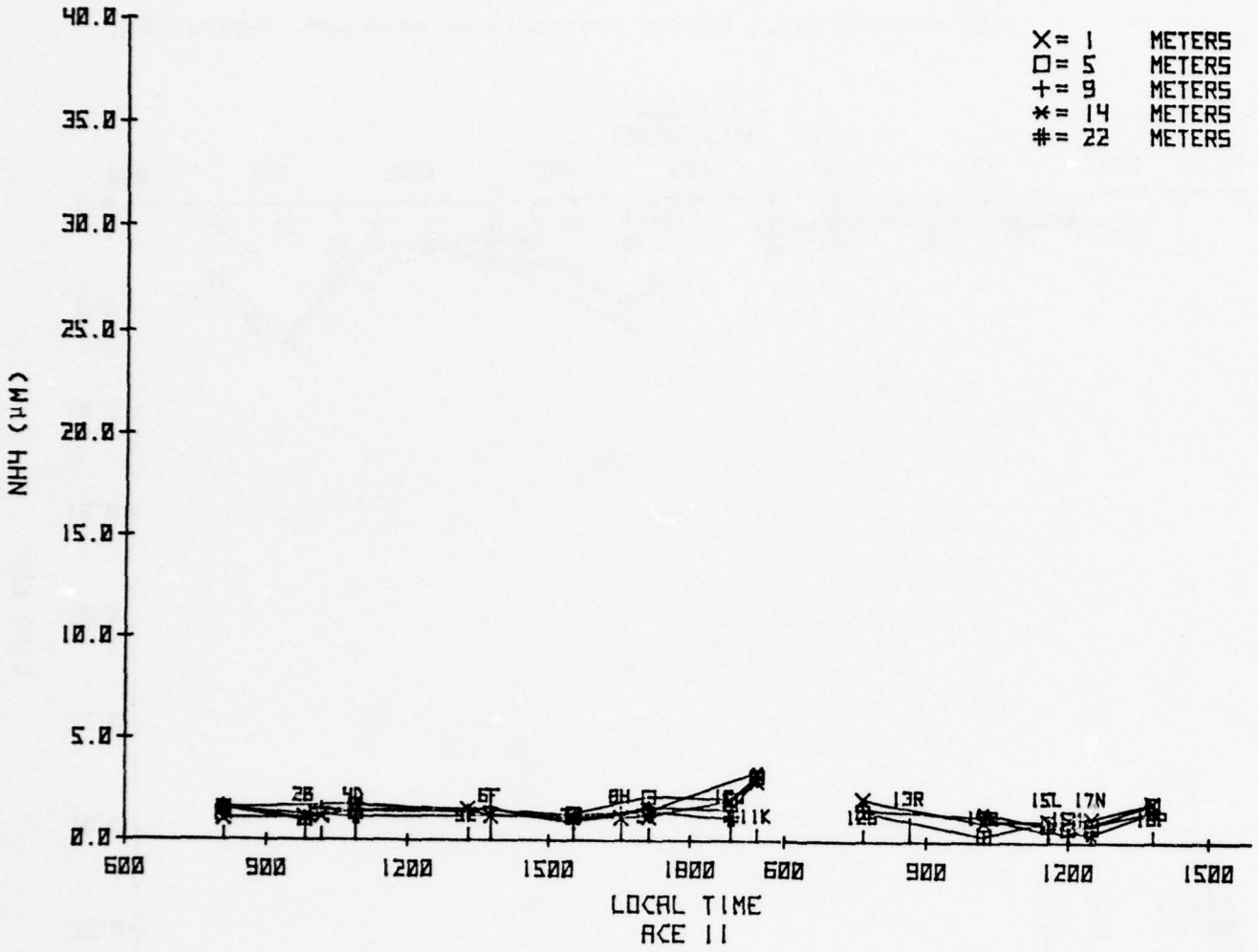



Figure B13. Ammonium observations during 5-6 December 1974.

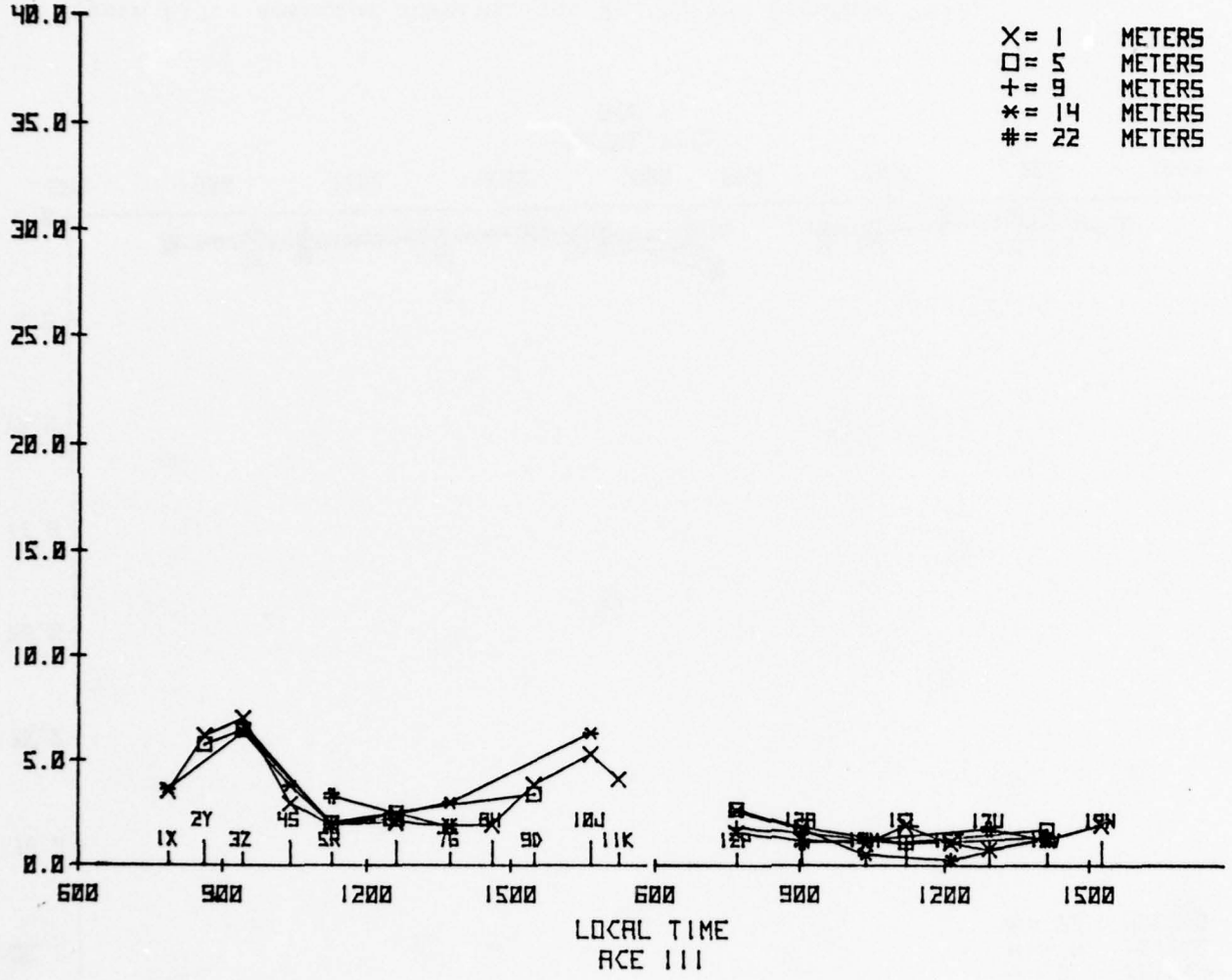



Figure B14. Ammonium observations during 13-14 January 1975

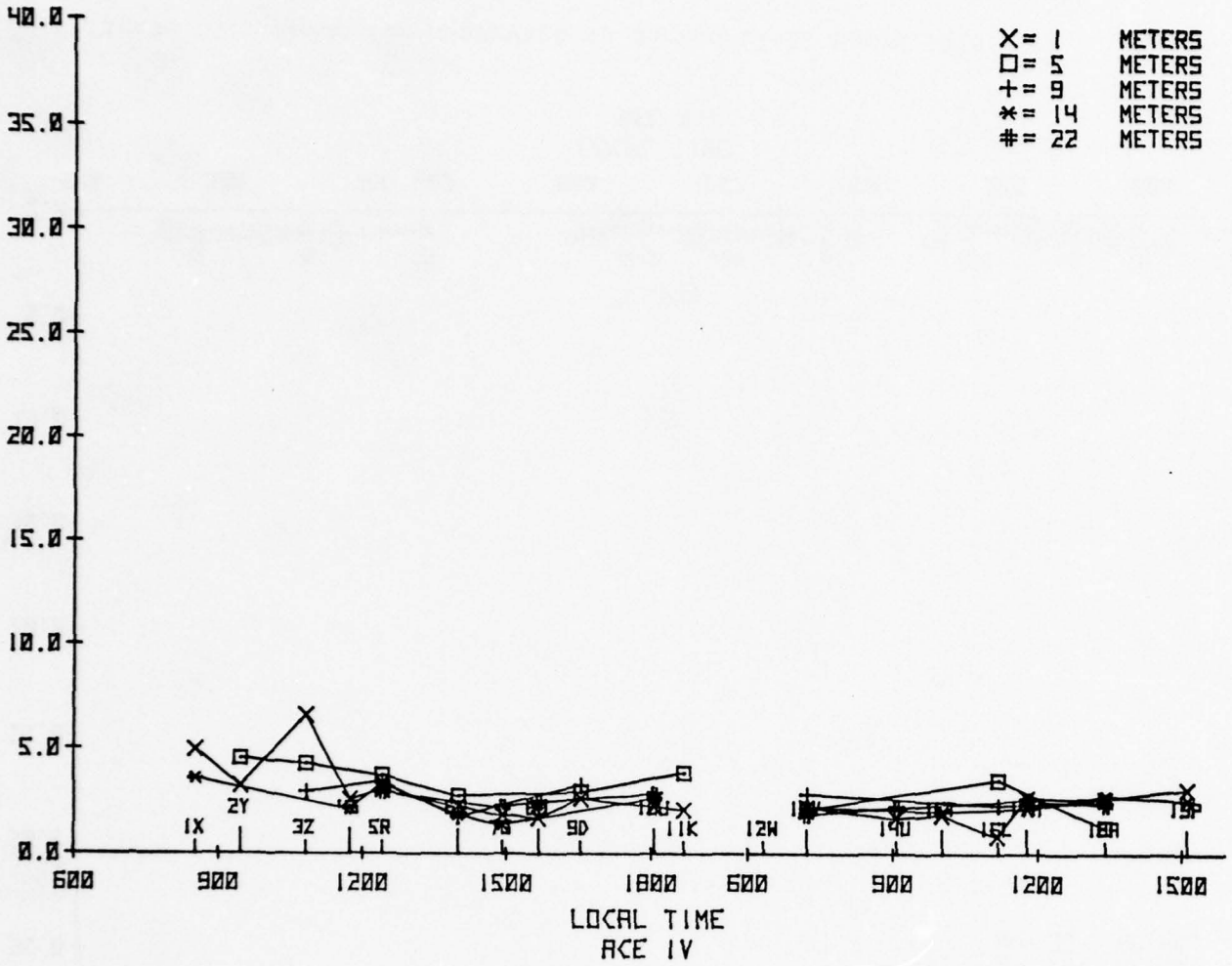



Figure B15. Ammonium observations during 19-20 February 1975.

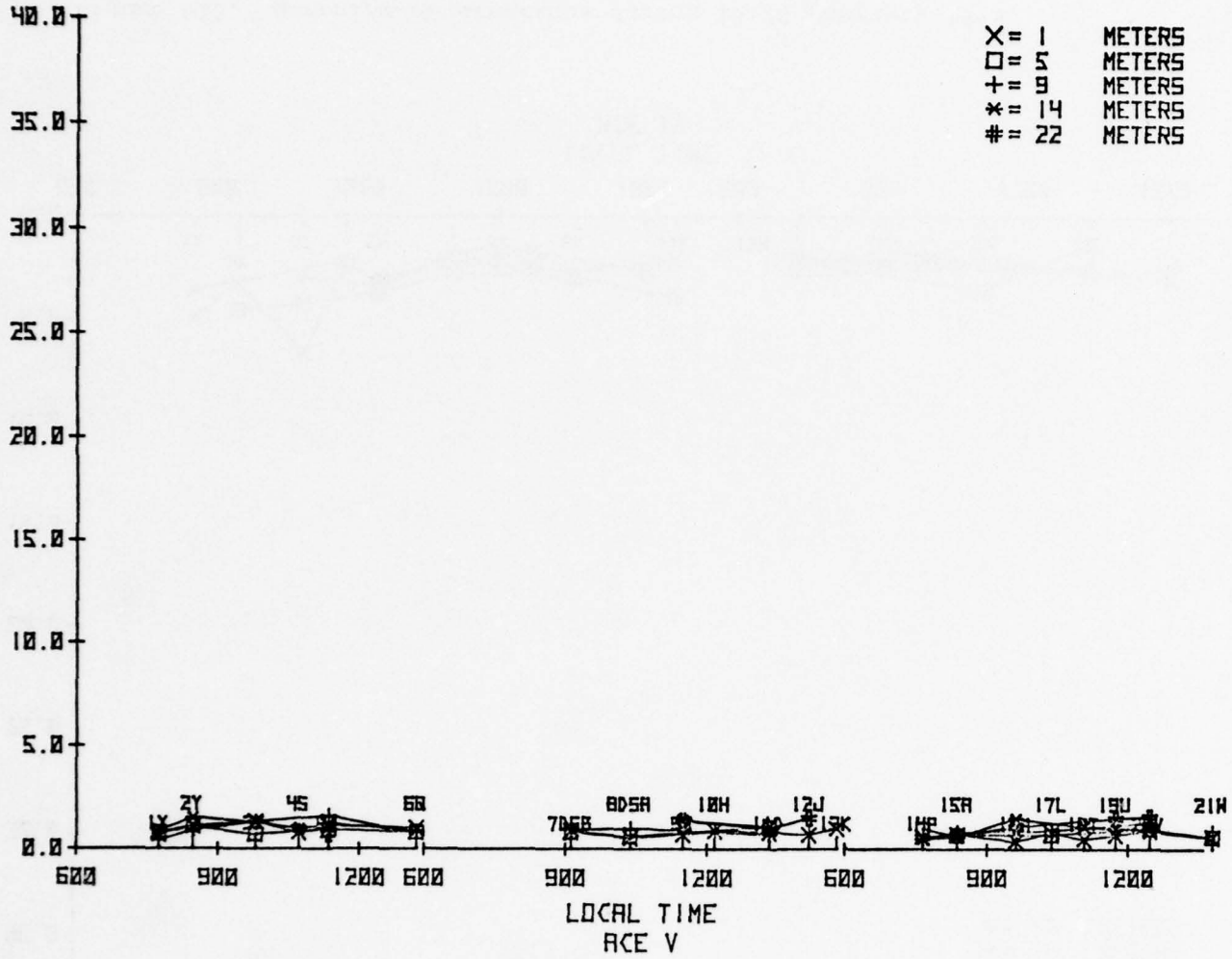



Figure B16. Ammonium observations during 19-21 March 1975.

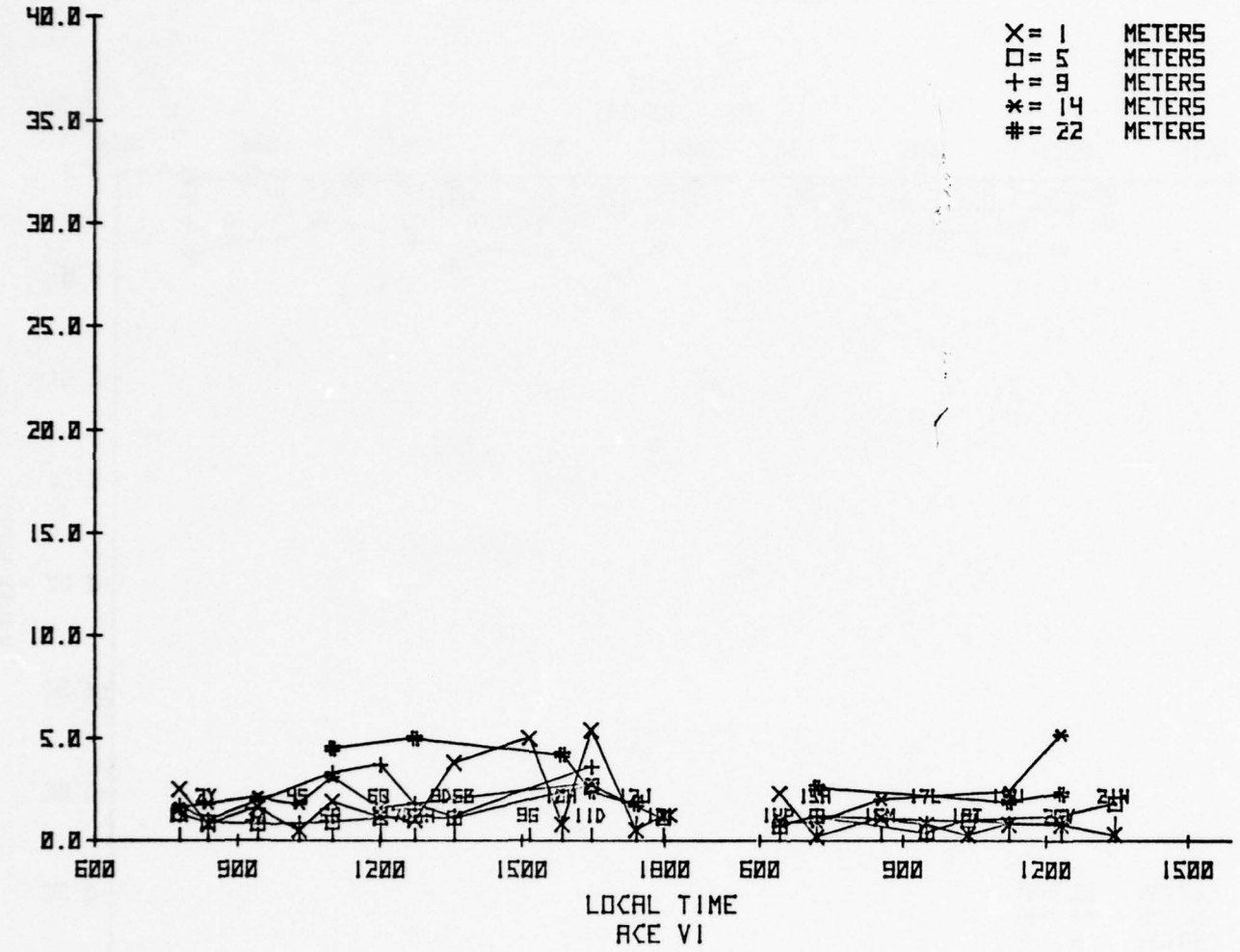



Figure B17. Ammonium observations during 23-24 April 1975.

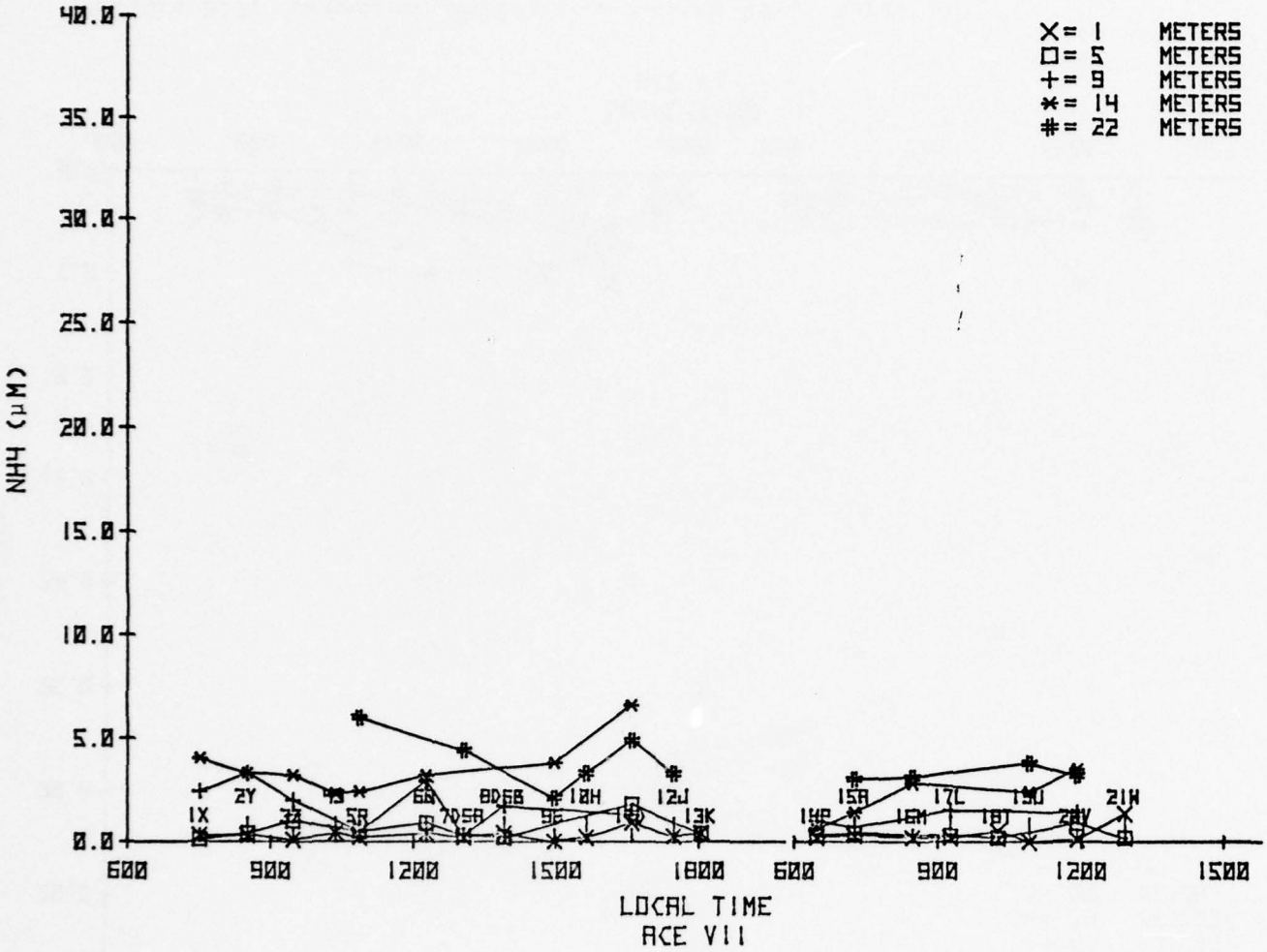



Figure B18. Ammonium observations during 28-29 May 1975.

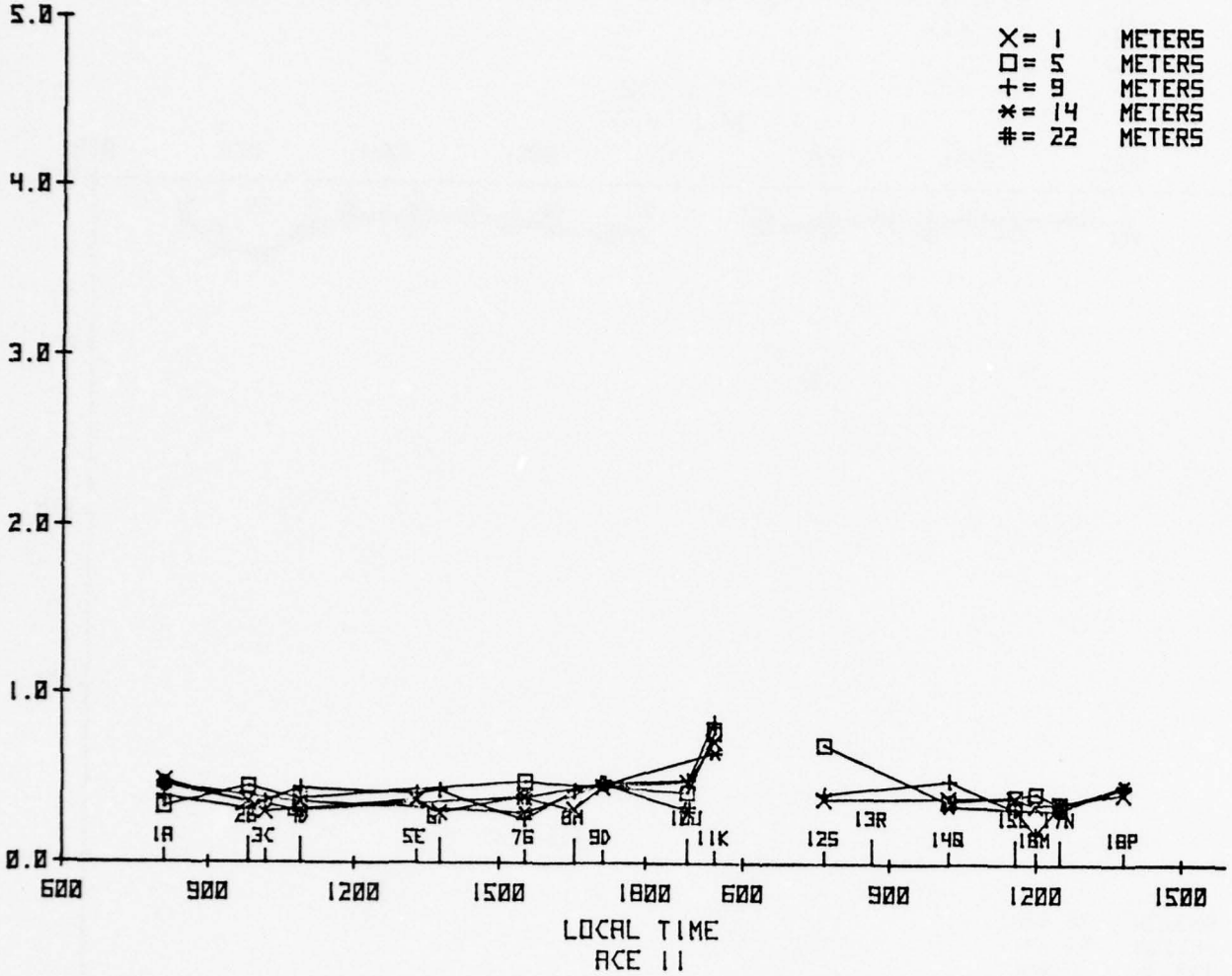



Figure B19. Nitrite observations during 5-6 December 1974.

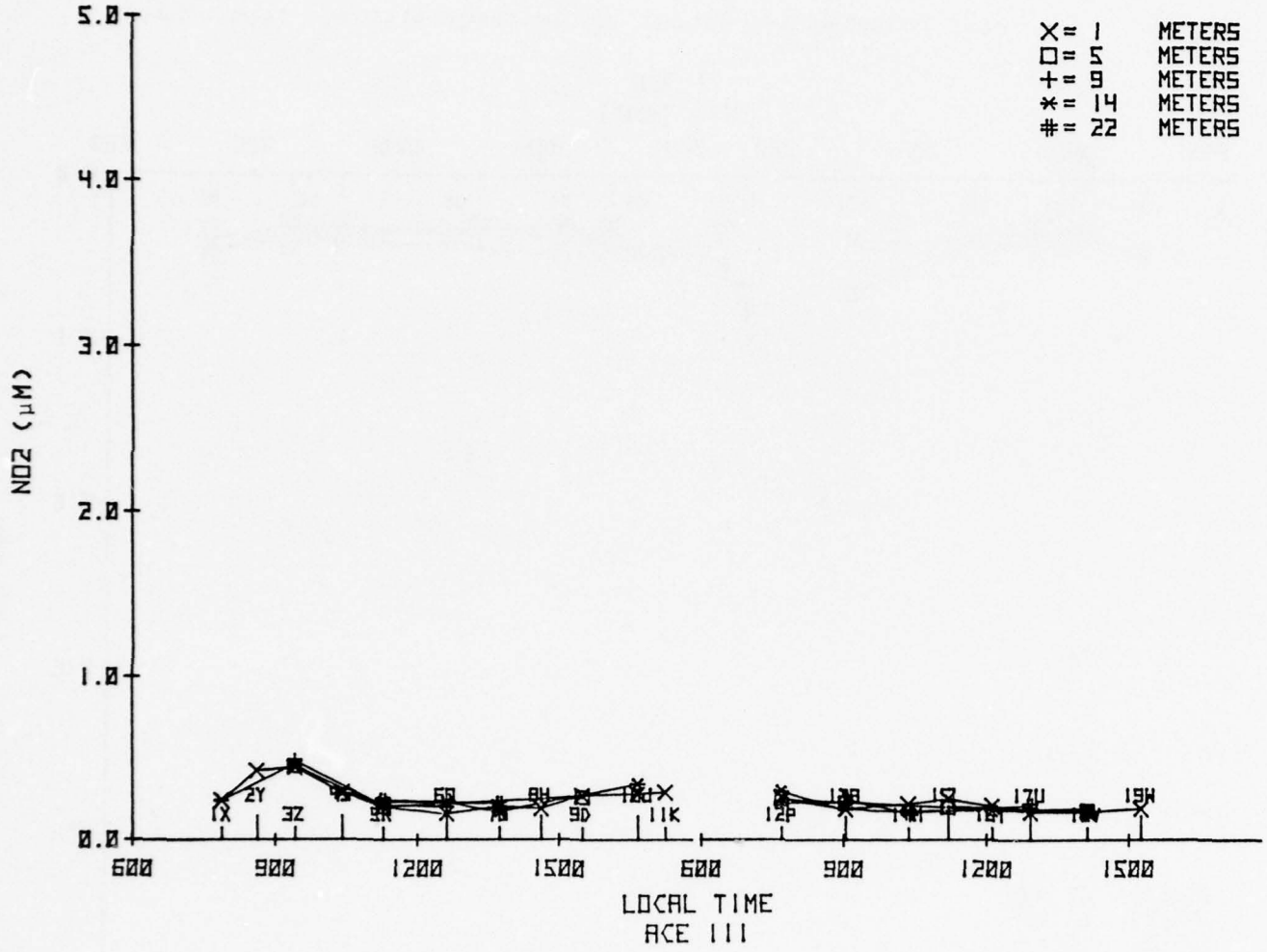



Figure B20. Nitrite observations during 13-14 January 1975.

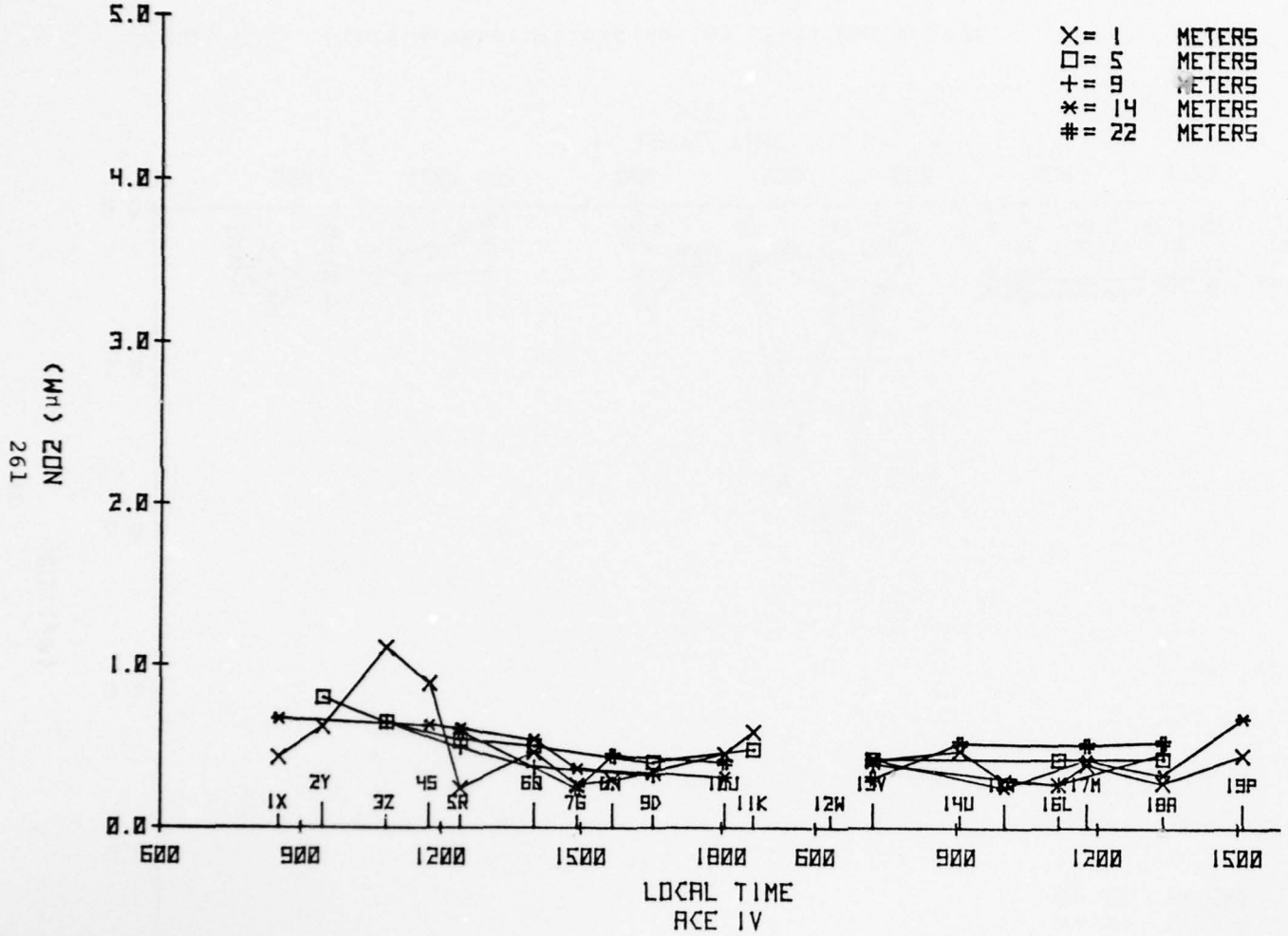



Figure B21. Nitrite observations during 19-20 February 1975.

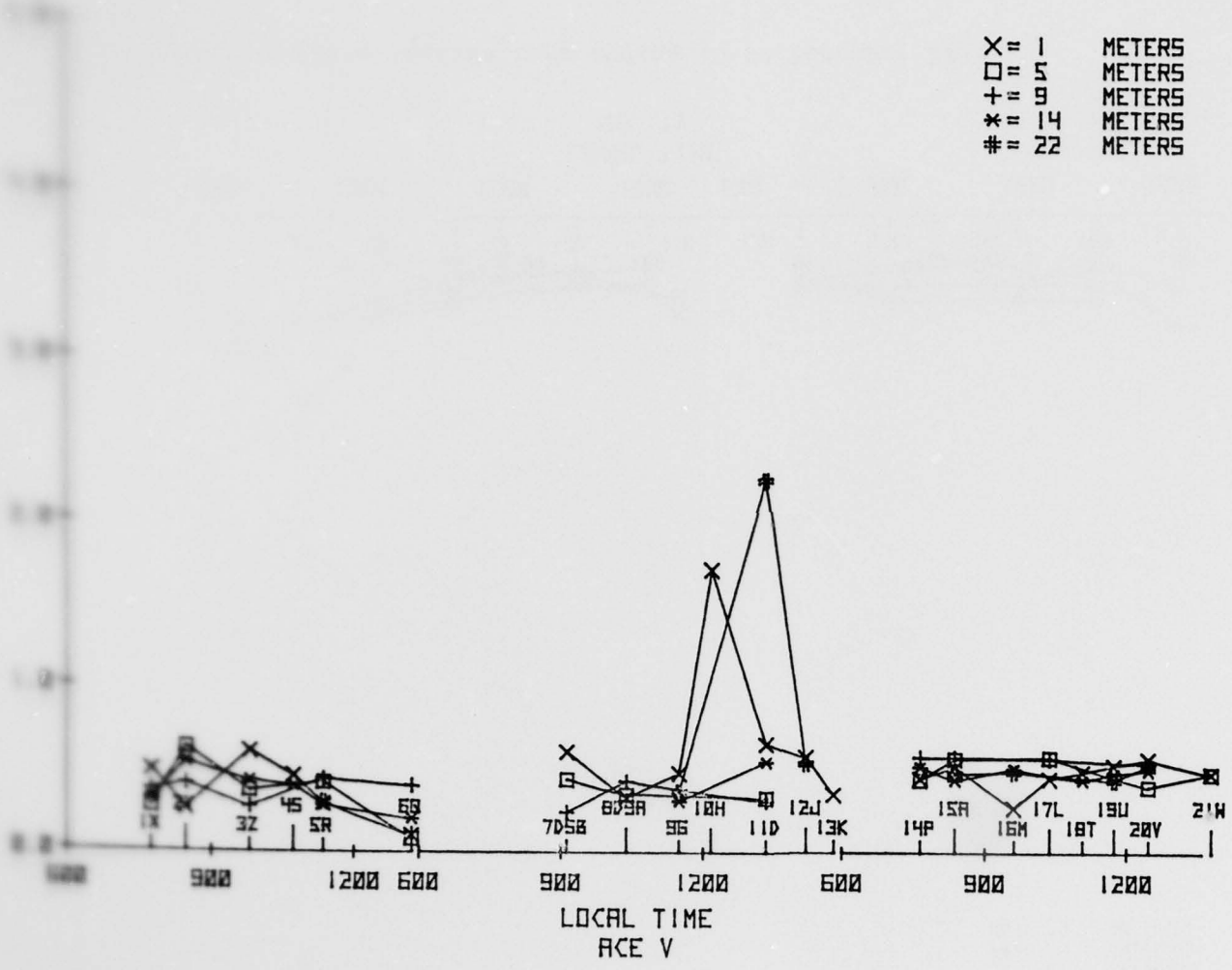



Figure B22. Nitrite observations during 19-21 March 1975.

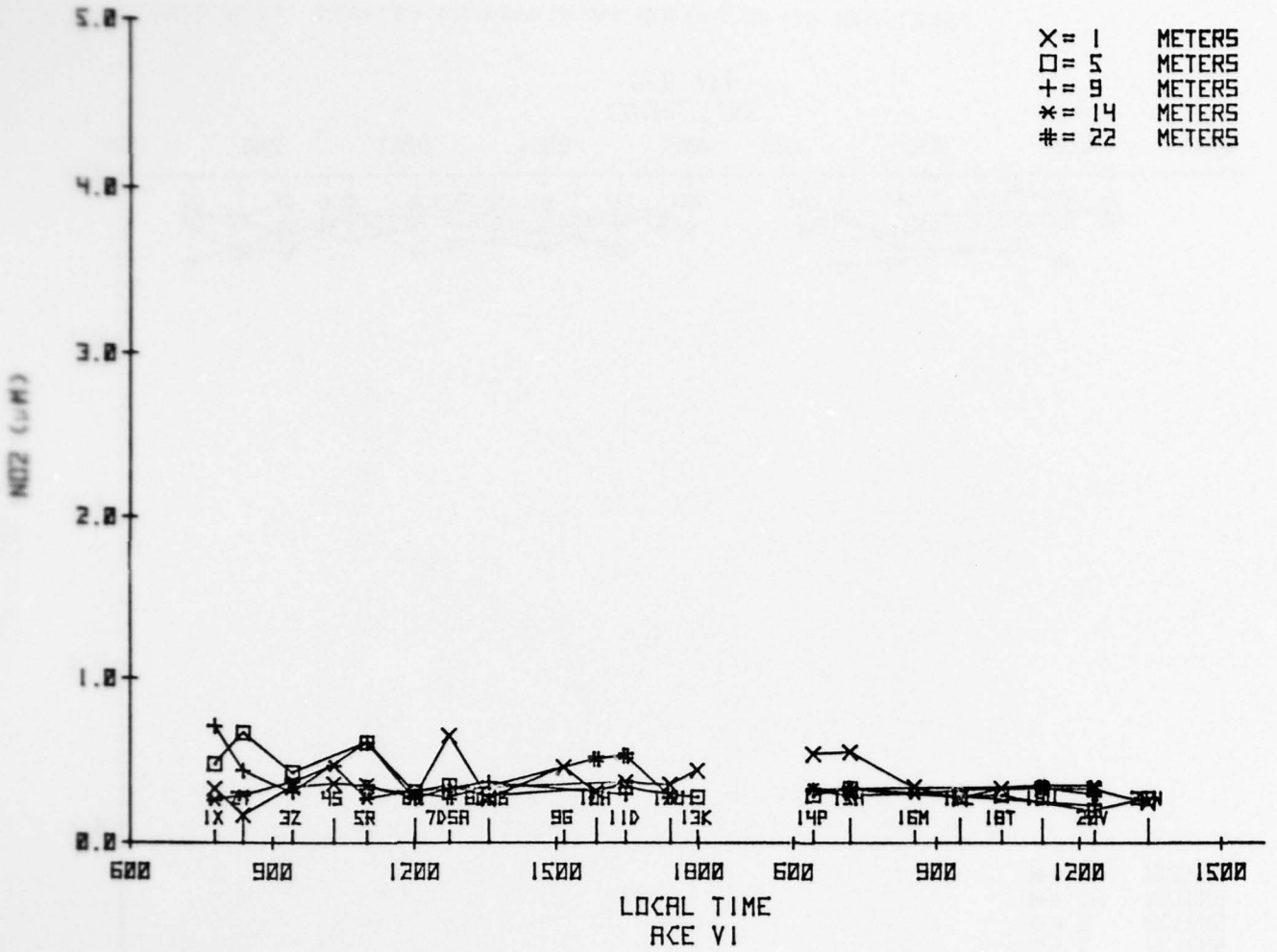



Figure B23. Nitrite observations during 23-24 April 1975.

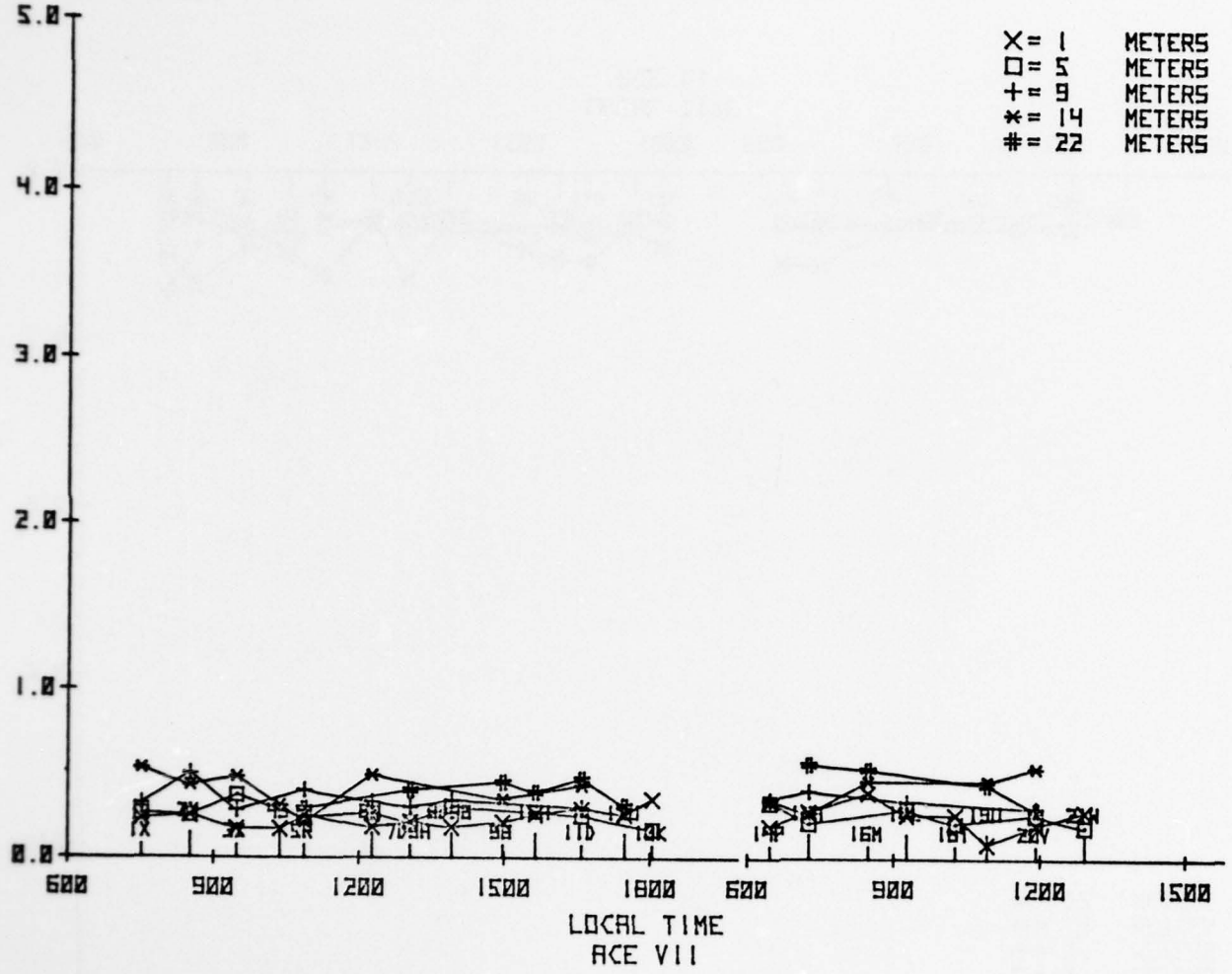



Figure B24. Nitrite observations during 28-29 May 1975.

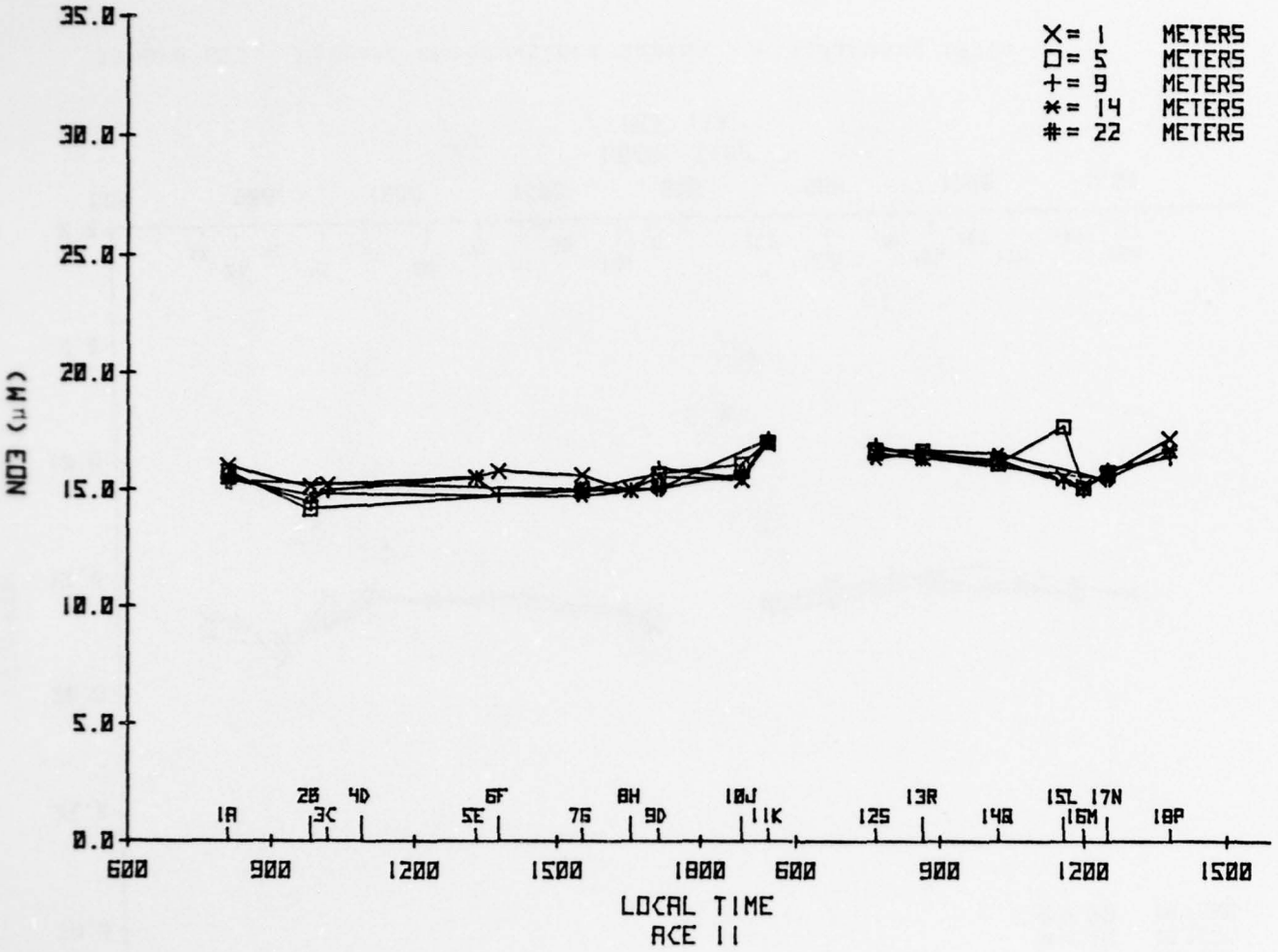



Figure B25. Nitrate observations during 5-6 December 1974.

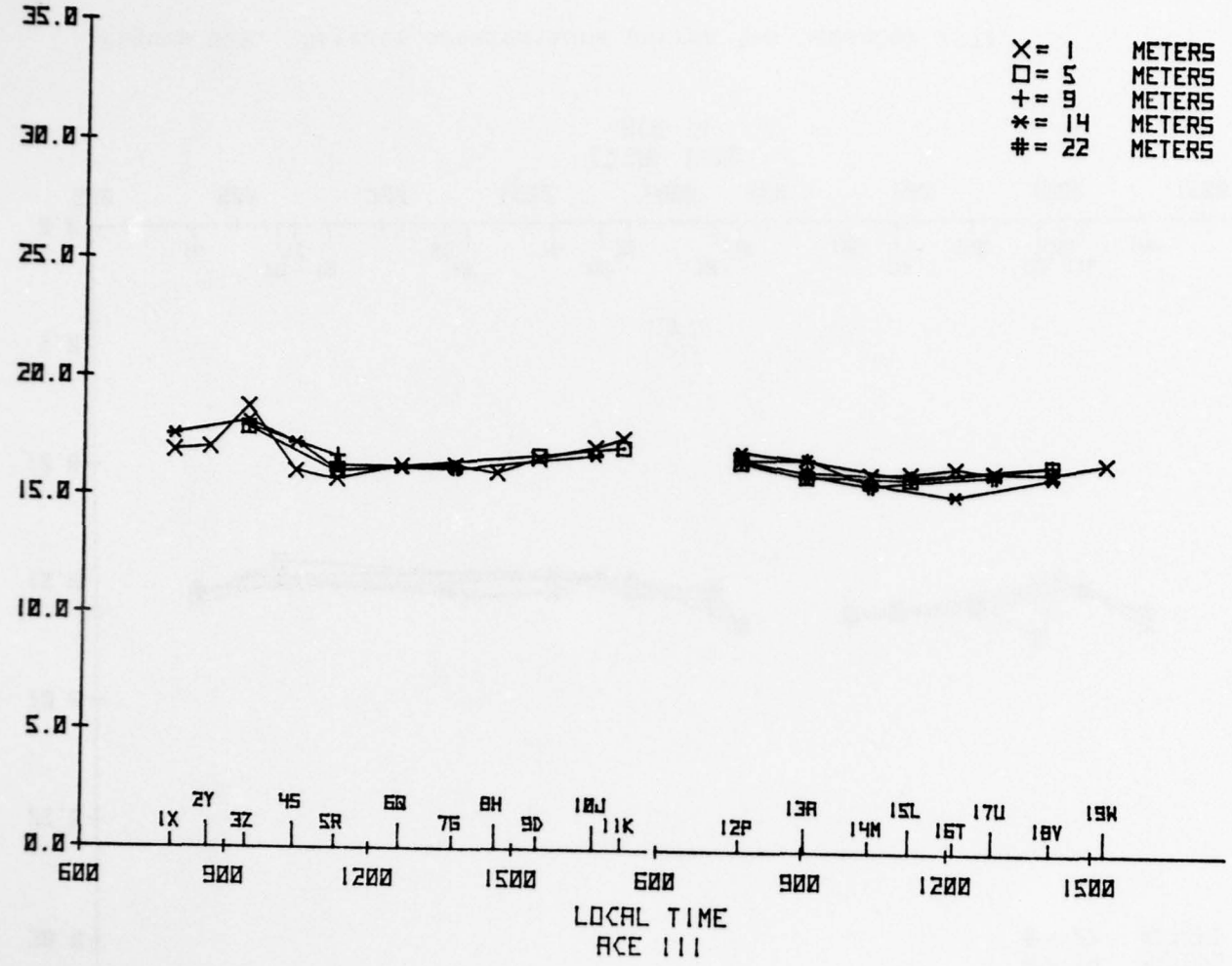



Figure B26. Nitrate observations during 13-14 January 1975.

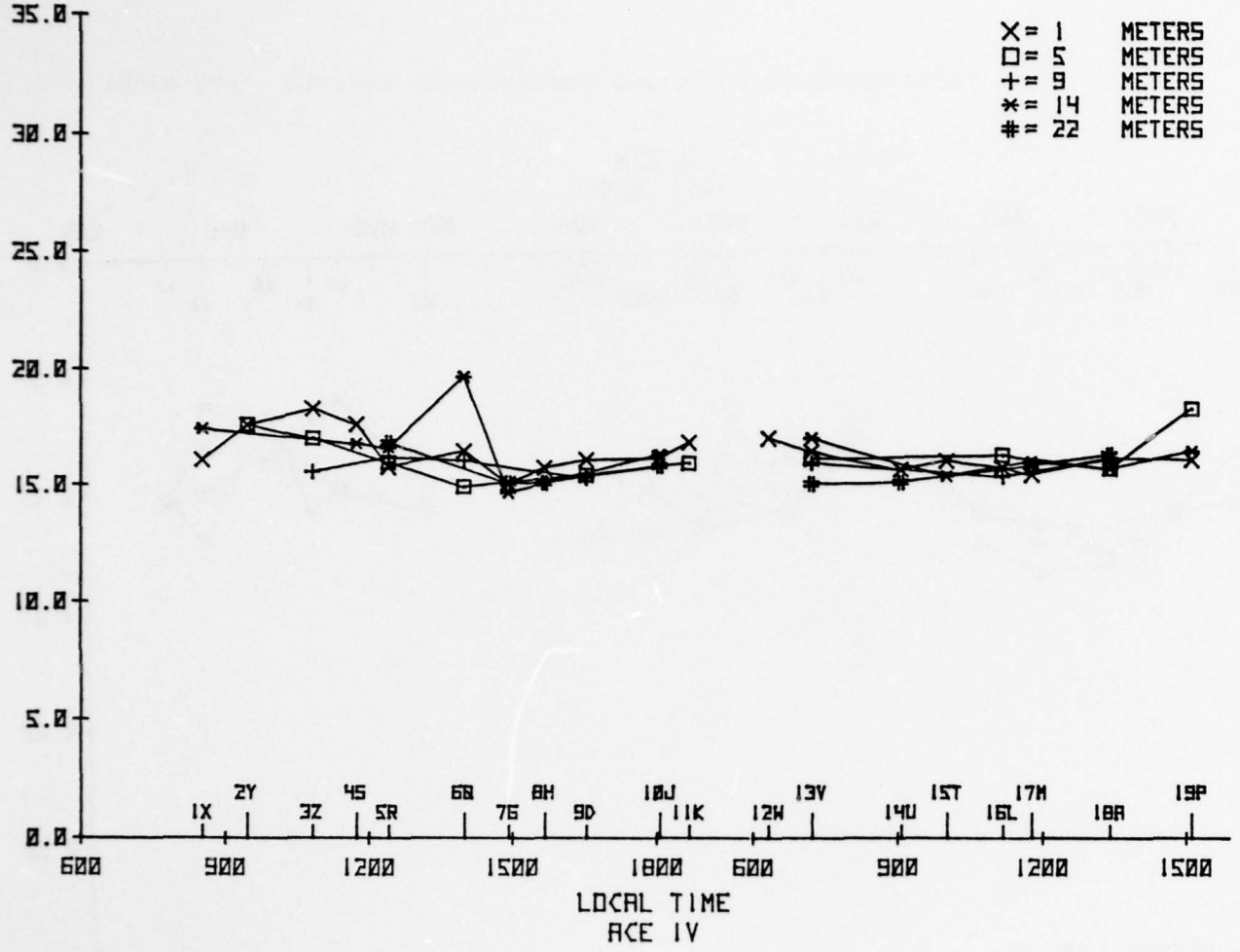



Figure B27. Nitrate observations during 19-20 February 1975.

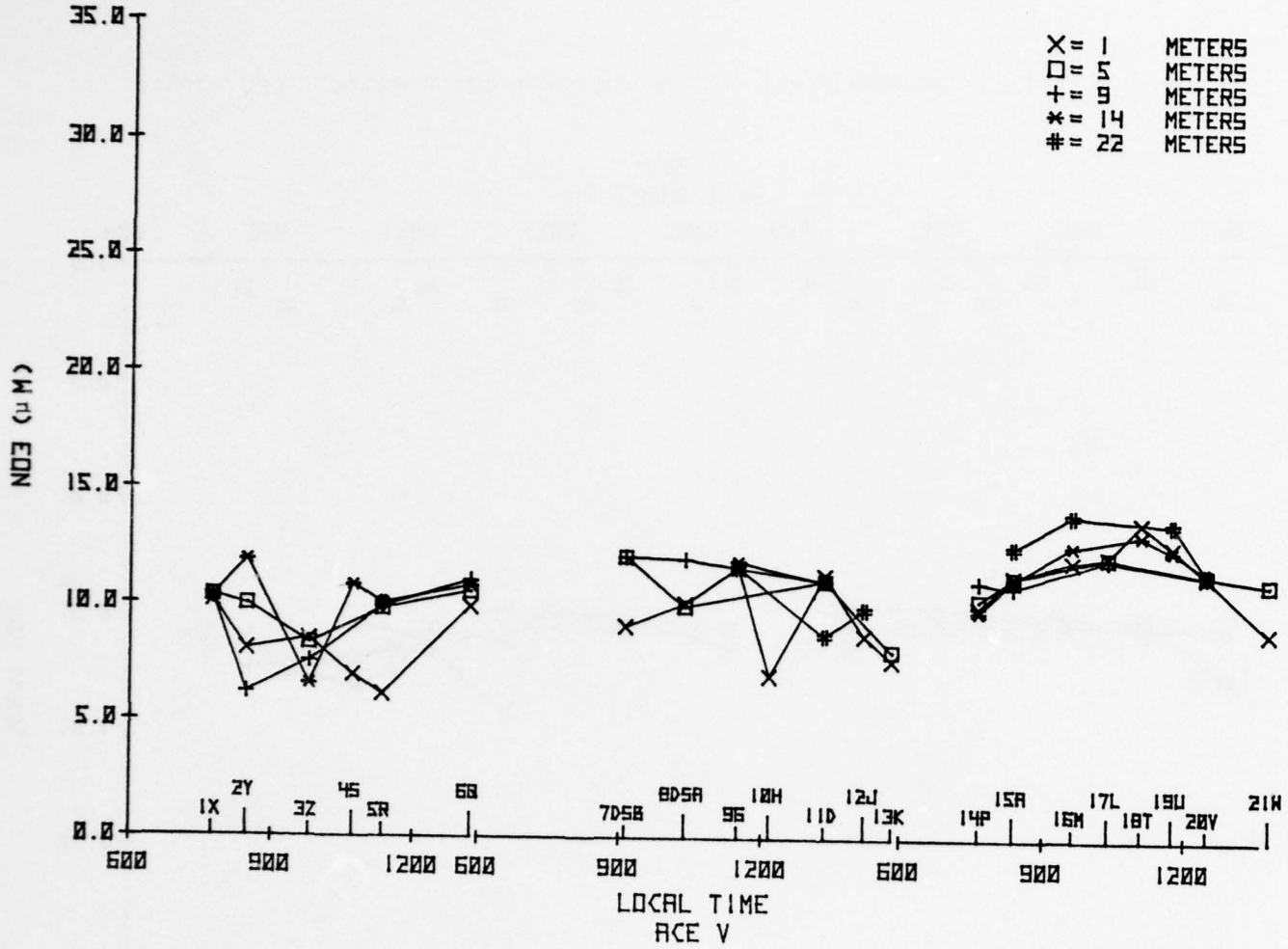



Figure B28. Nitrate observations during 19-21 March 1975.

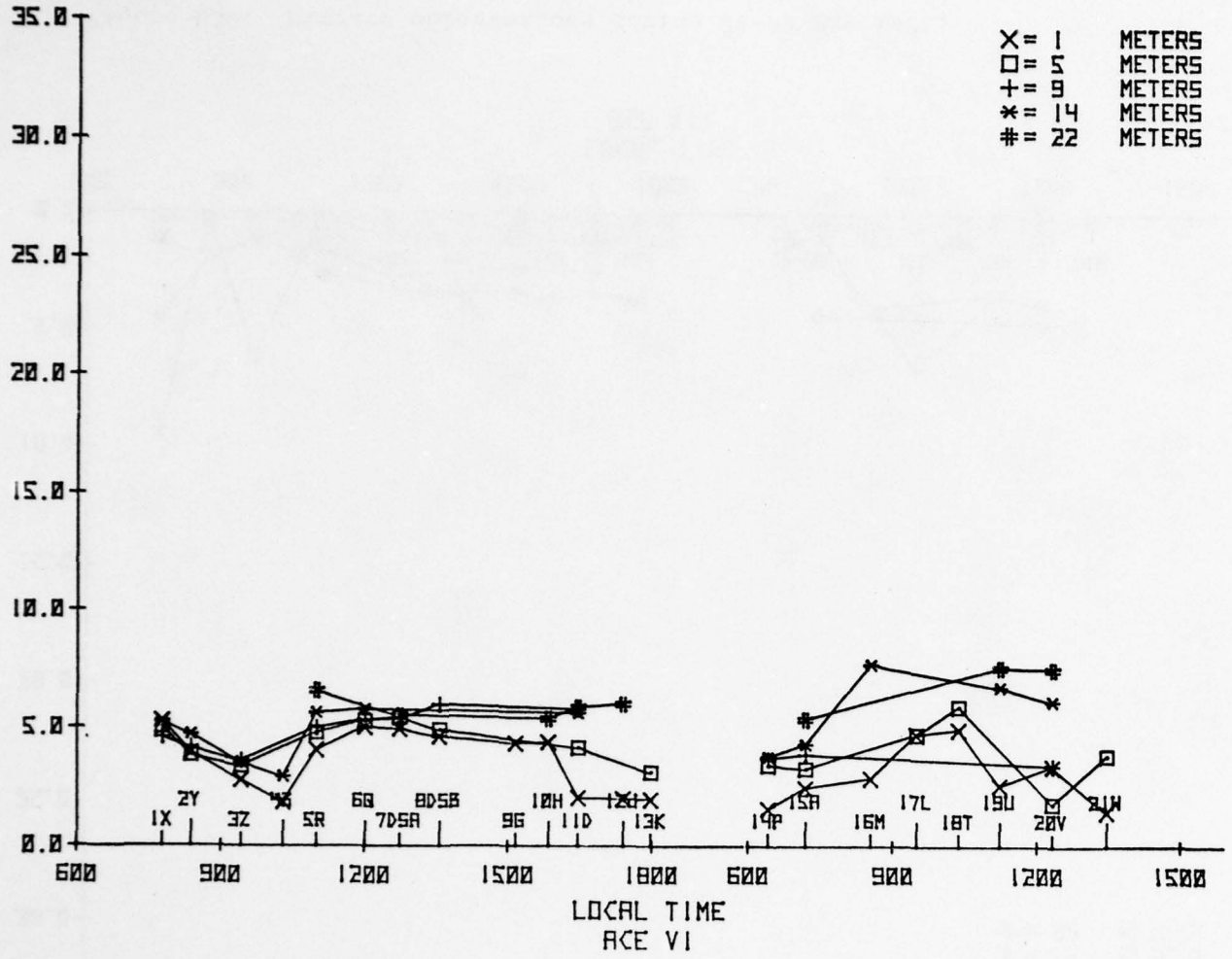



Figure B29. Nitrate observations during 23-24 April 1975.

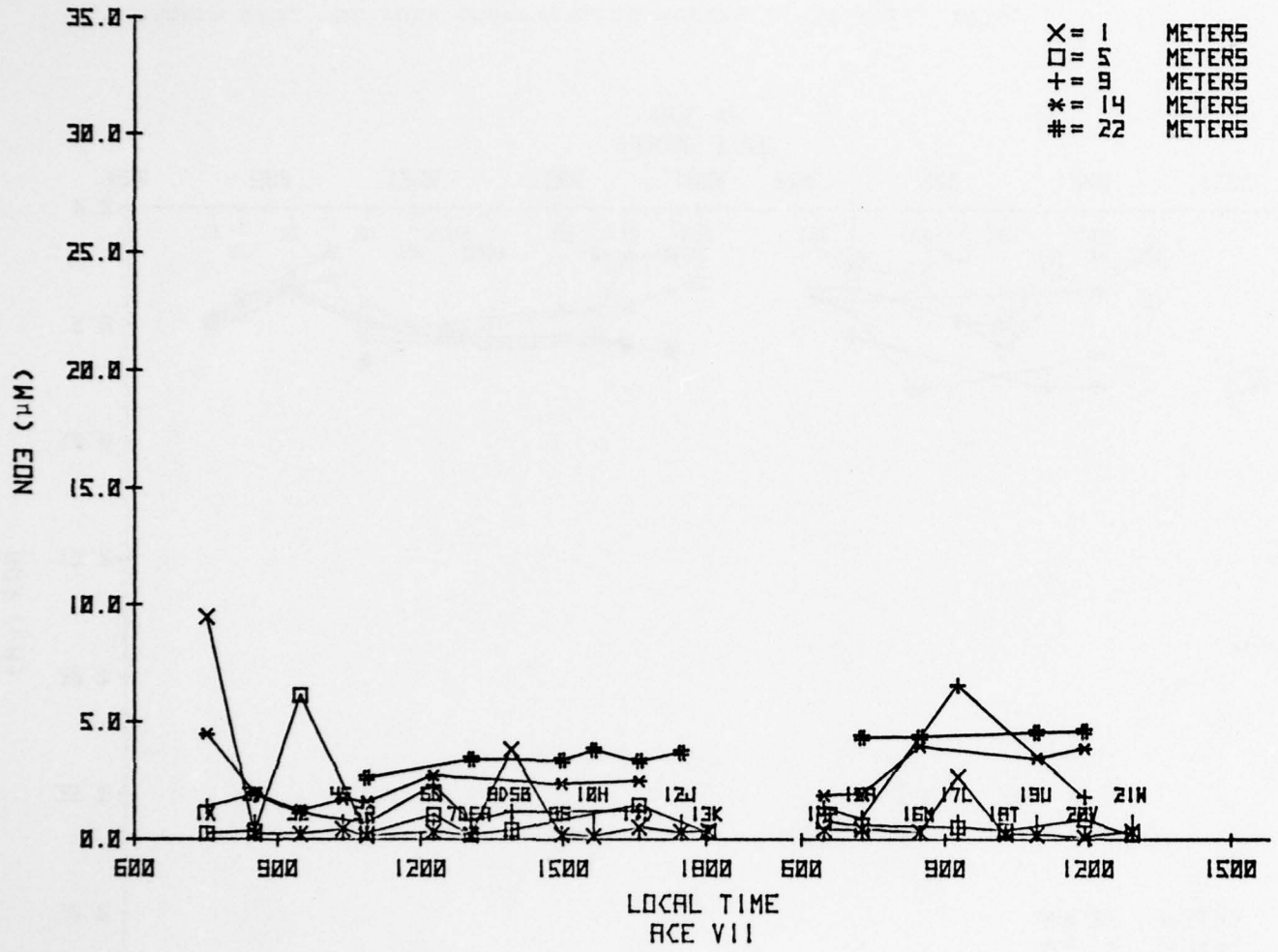



Figure B30. Nitrate observations during 28-29 May 1975.

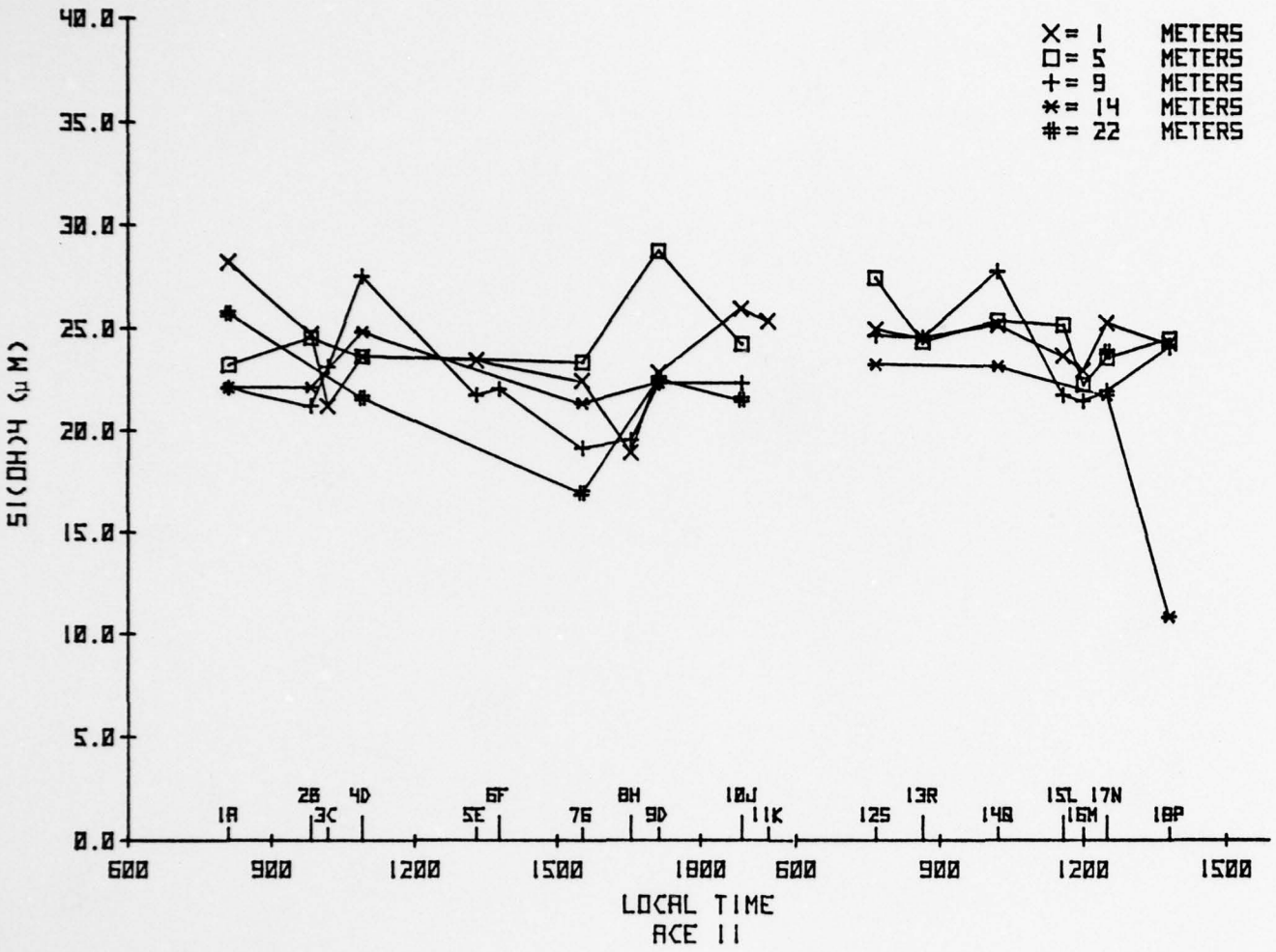



Figure B31. Silicic acid observations during 5-6 December 1974.

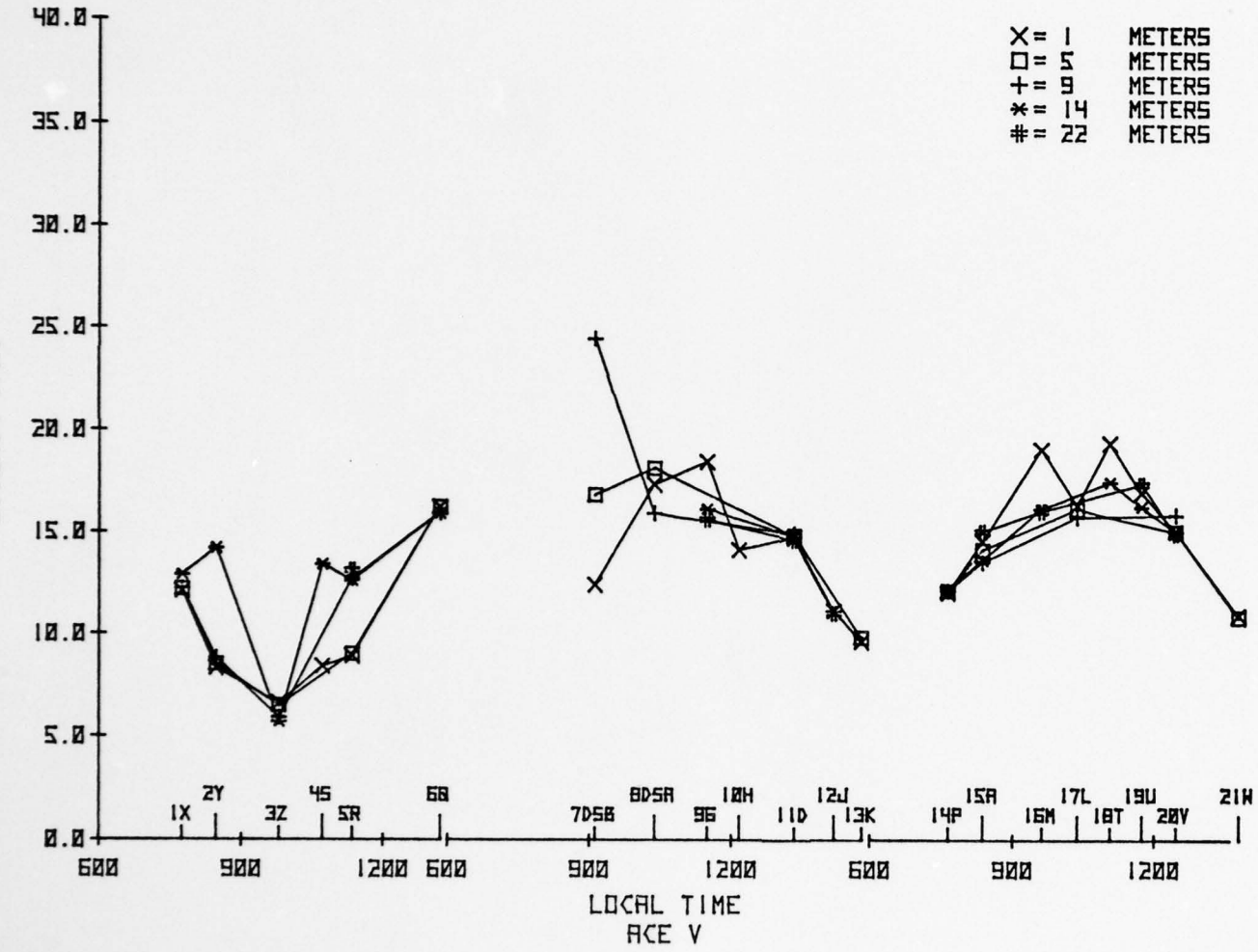



Figure B34. Silicic acid observations during 19-21 March 1975.

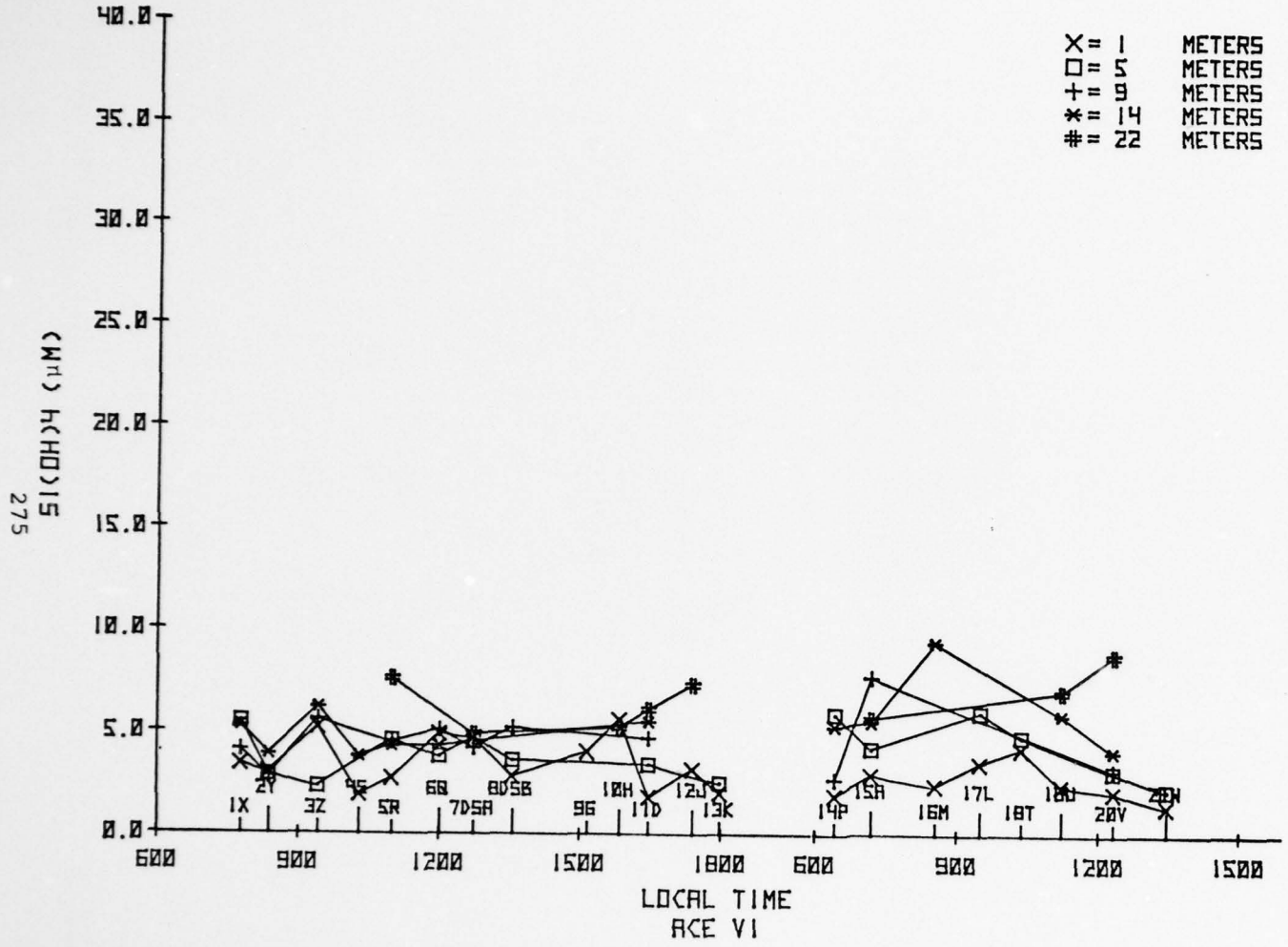



Figure B35. Silicic acid observations during 23-24 April 1975.

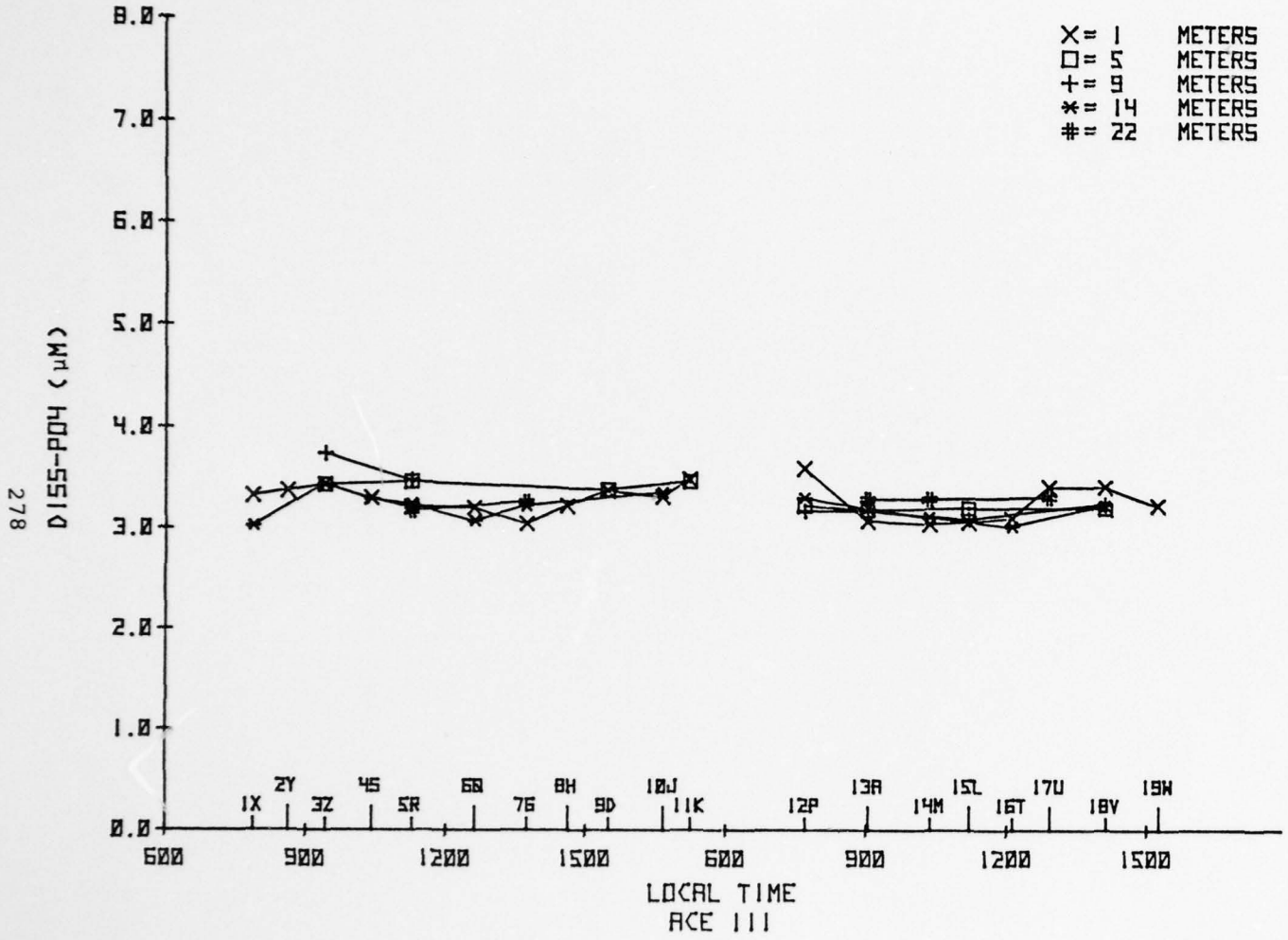



Figure B38. Dissolved phosphate observations during 13-14 January 1975.

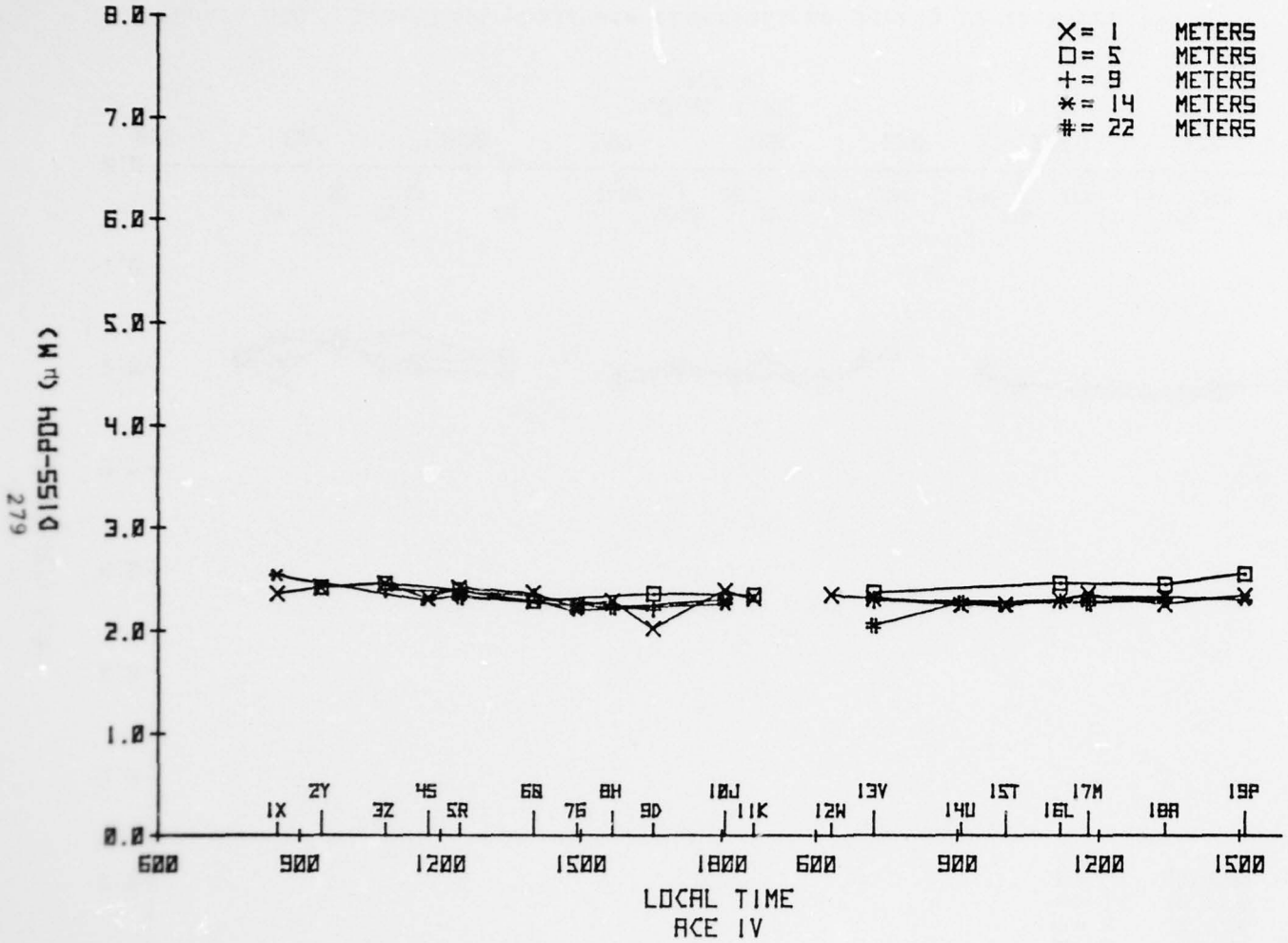



Figure B39. Dissolved phosphate observations during 19-20 February 1975.

AD-A053 427 STATE UNIV OF NEW YORK AT STONY BROOK MARINE SCIENCES--ETC F/G 13/2
AQUATIC DISPOSAL FIELD INVESTIGATIONS, EATONS NECK DISPOSAL SIT--ETC(U)
JAN 78 DACW51-75-C-0016

UNCLASSIFIED WES-TR-D-77-6-APP-B NL

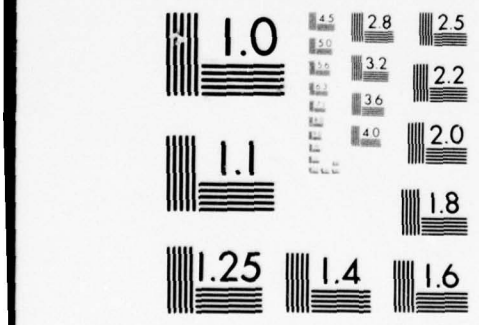
4 OF 5
AD A053427



END
DATE FILMED
6 -78
DDC

CONT.

05342




MICROCOPY RESOLUTION TEST CHART
NATIONAL BUREAU OF STANDARDS-1963-A

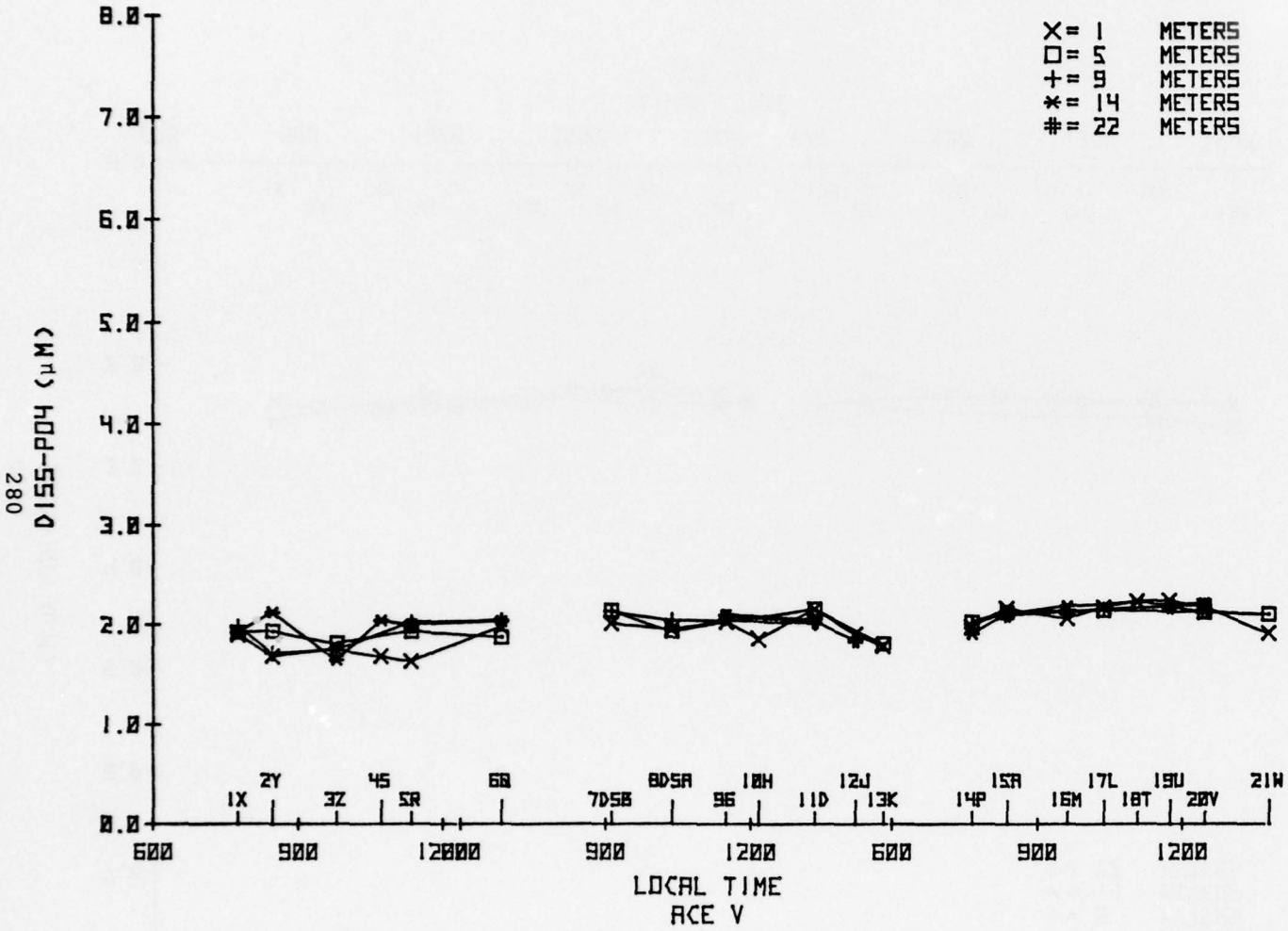



Figure B40. Dissolved phosphate observations during 19-21 March 1975.

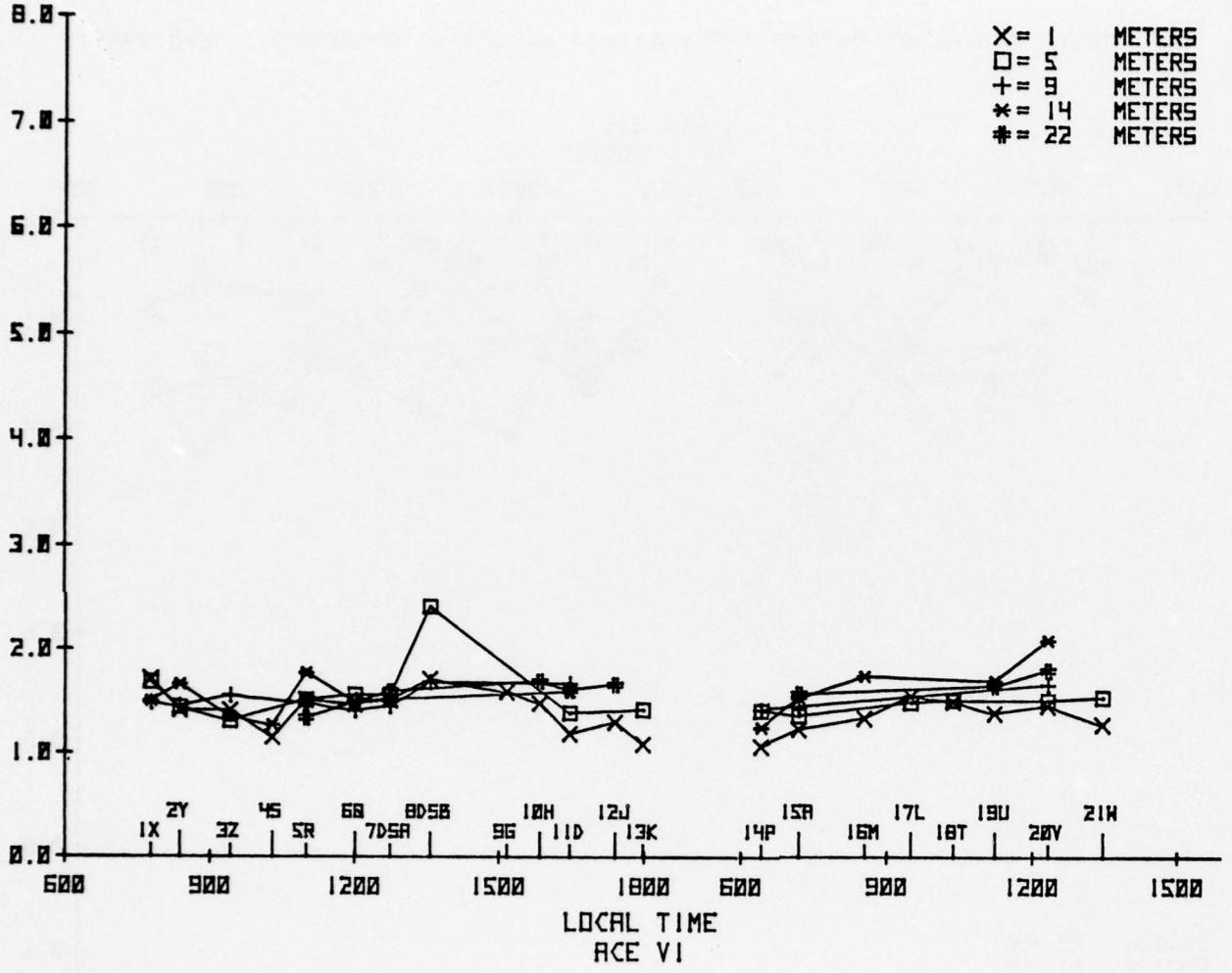



Figure B41. Dissolved phosphate observations during 23-24 April 1975.

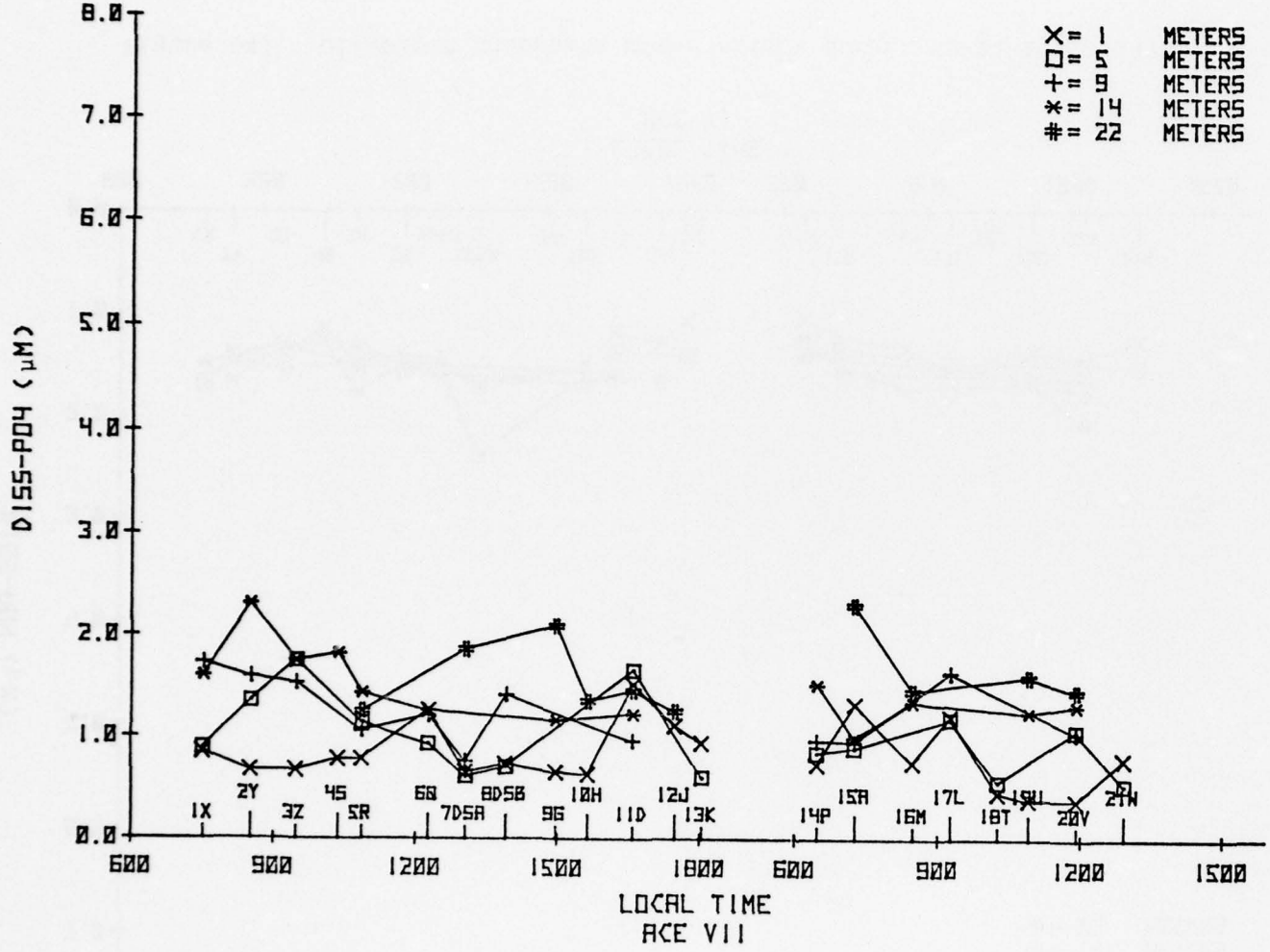



Figure B42. Dissolved phosphate observations during 28-29 May 1975.

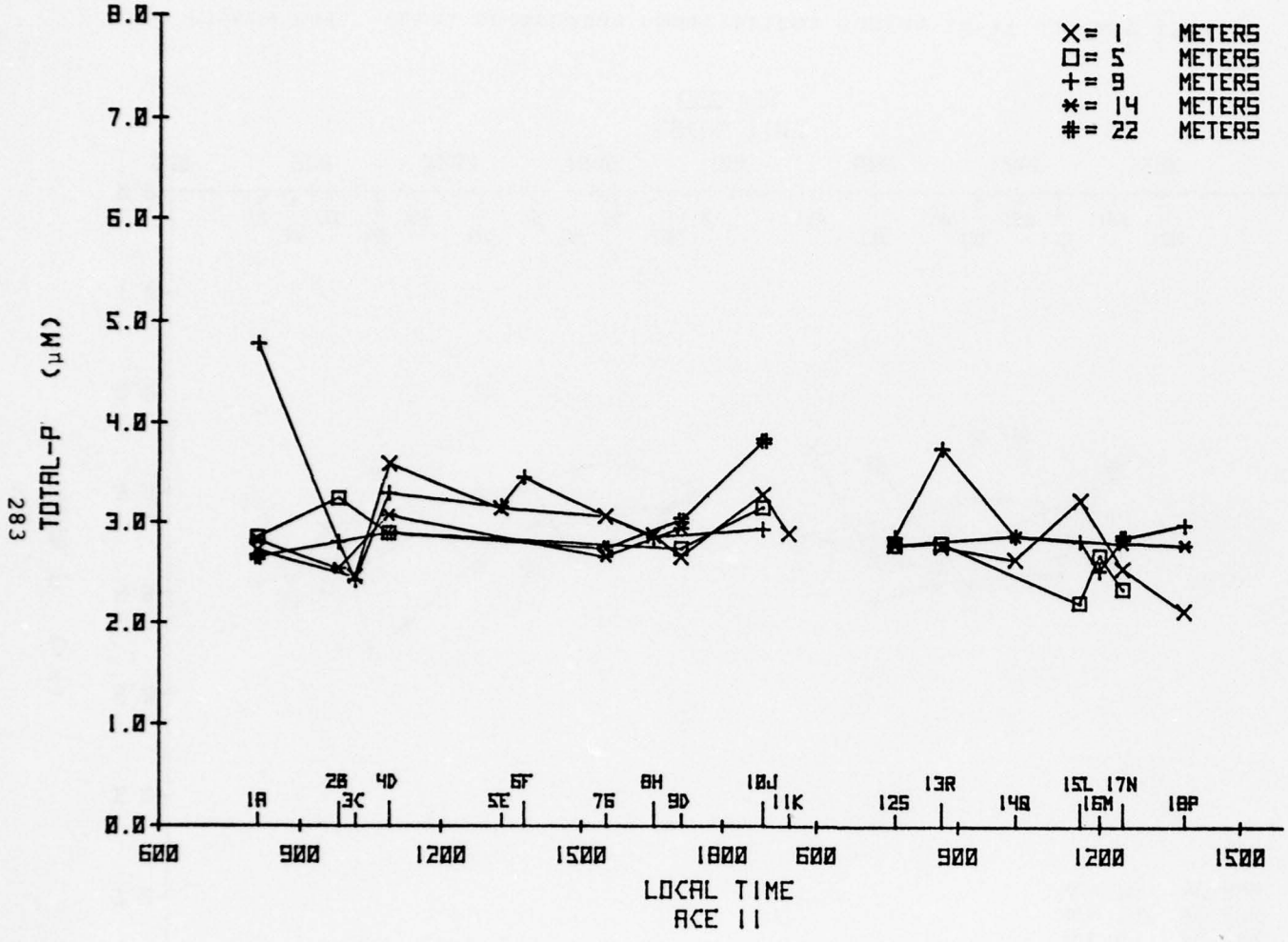



Figure B43. Total phosphorus observations during 5-6 December 1974.

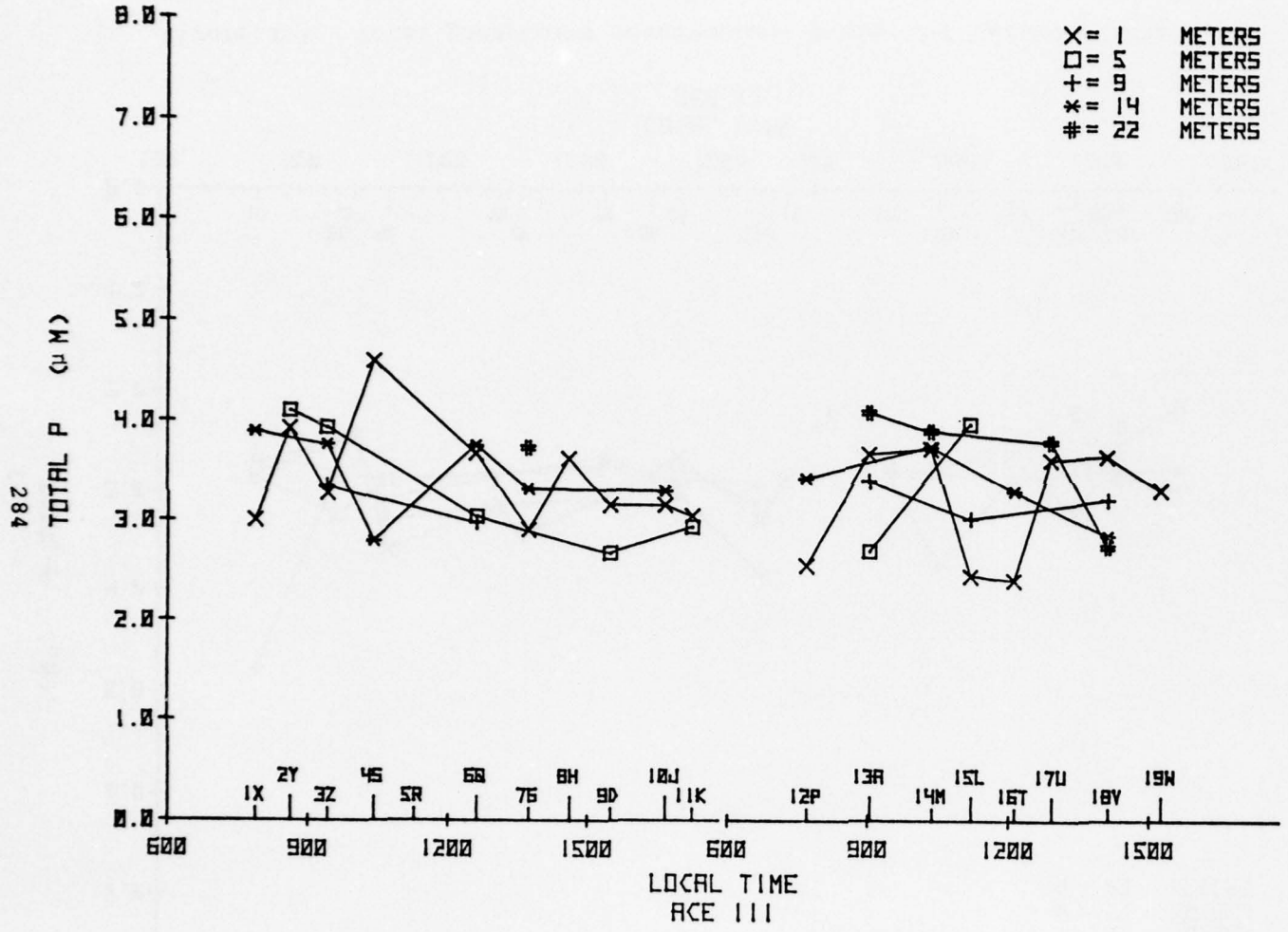



Figure B44. Total phosphorus observations during 13-14 January 1975.

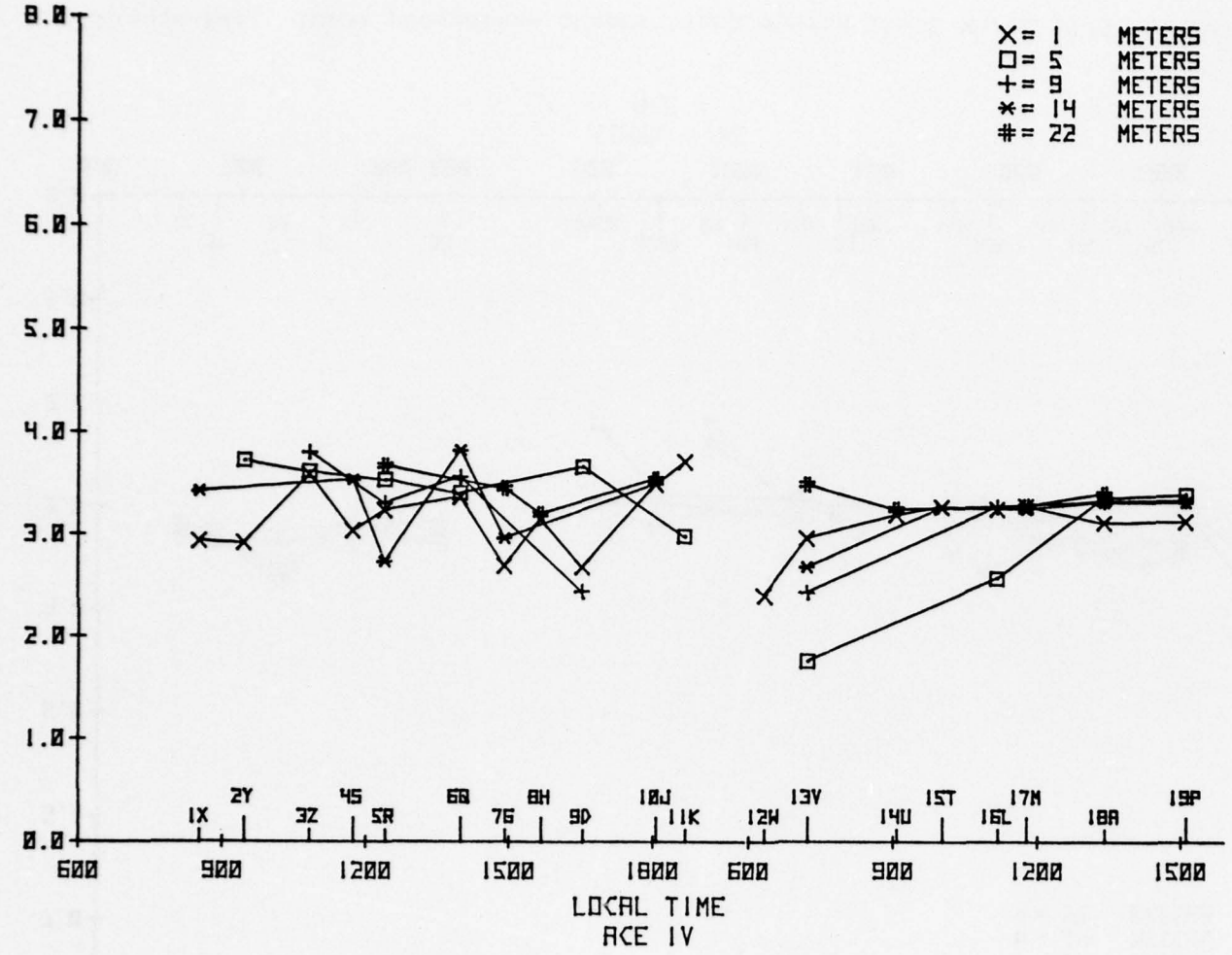



Figure B45. Total phosphorus observations during 19-20 February 1975.

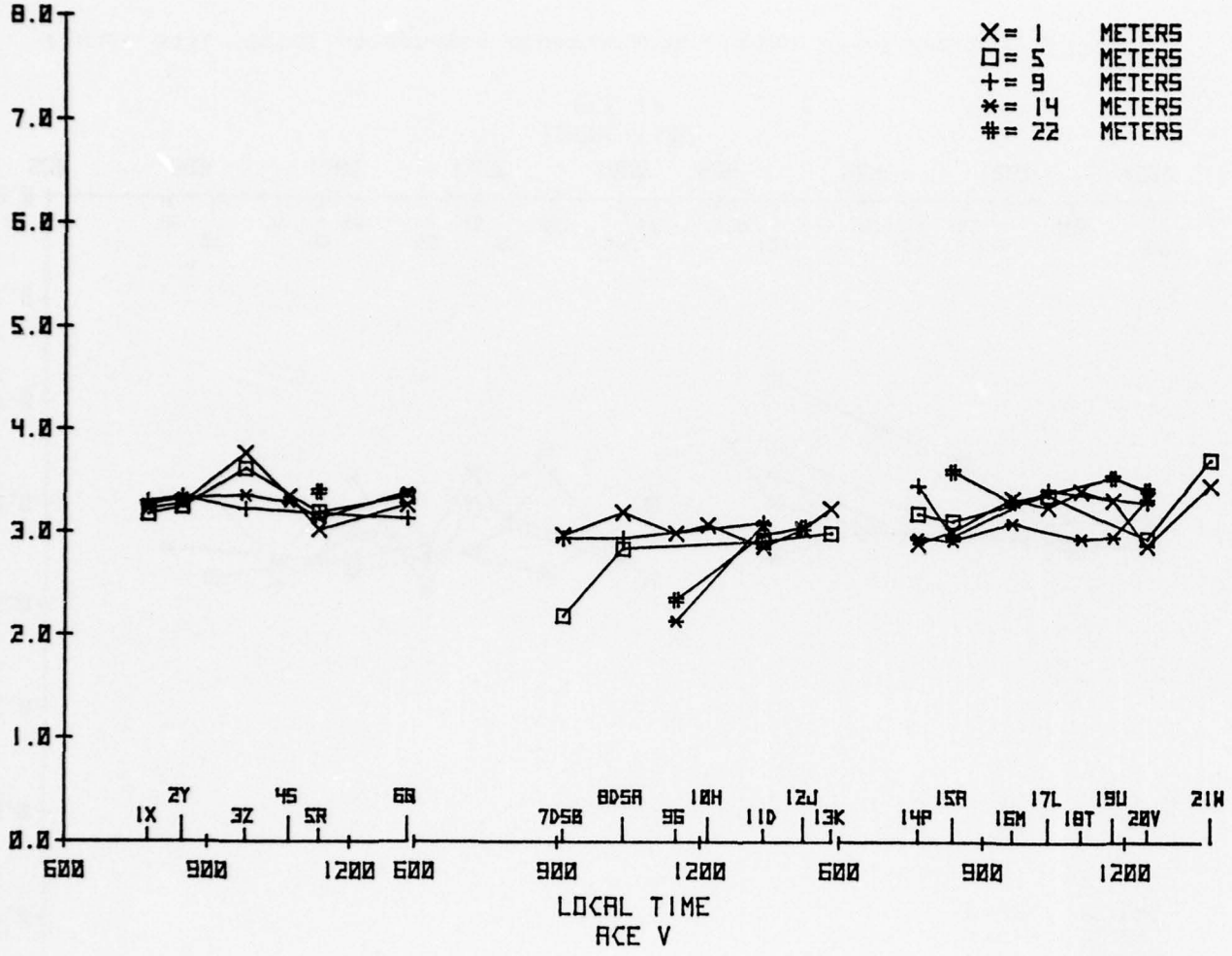



Figure B46. Total phosphorus observations during 19-21 March 1975.

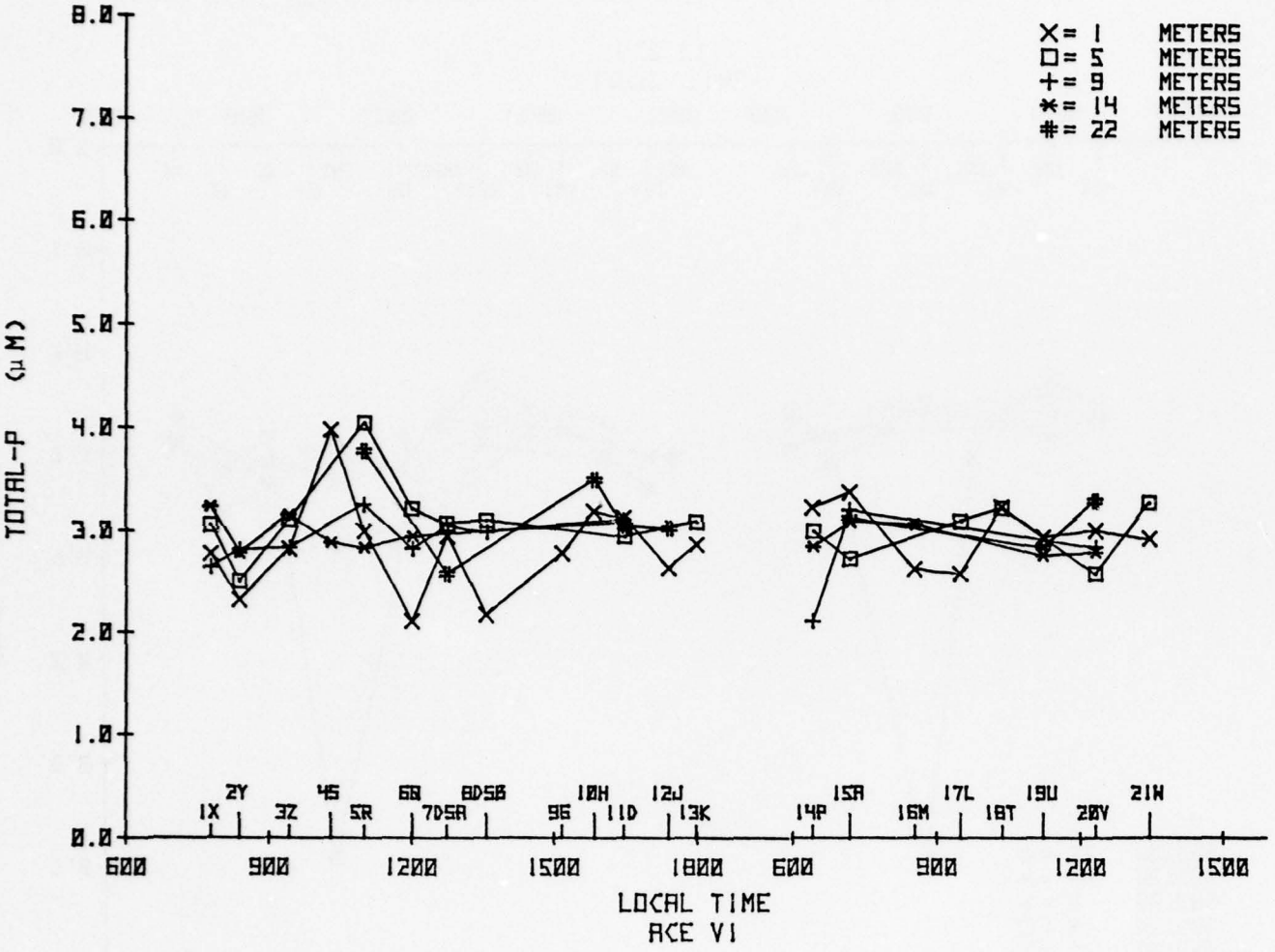



Figure B47. Total phosphorus observations during 23-24 April 1975.

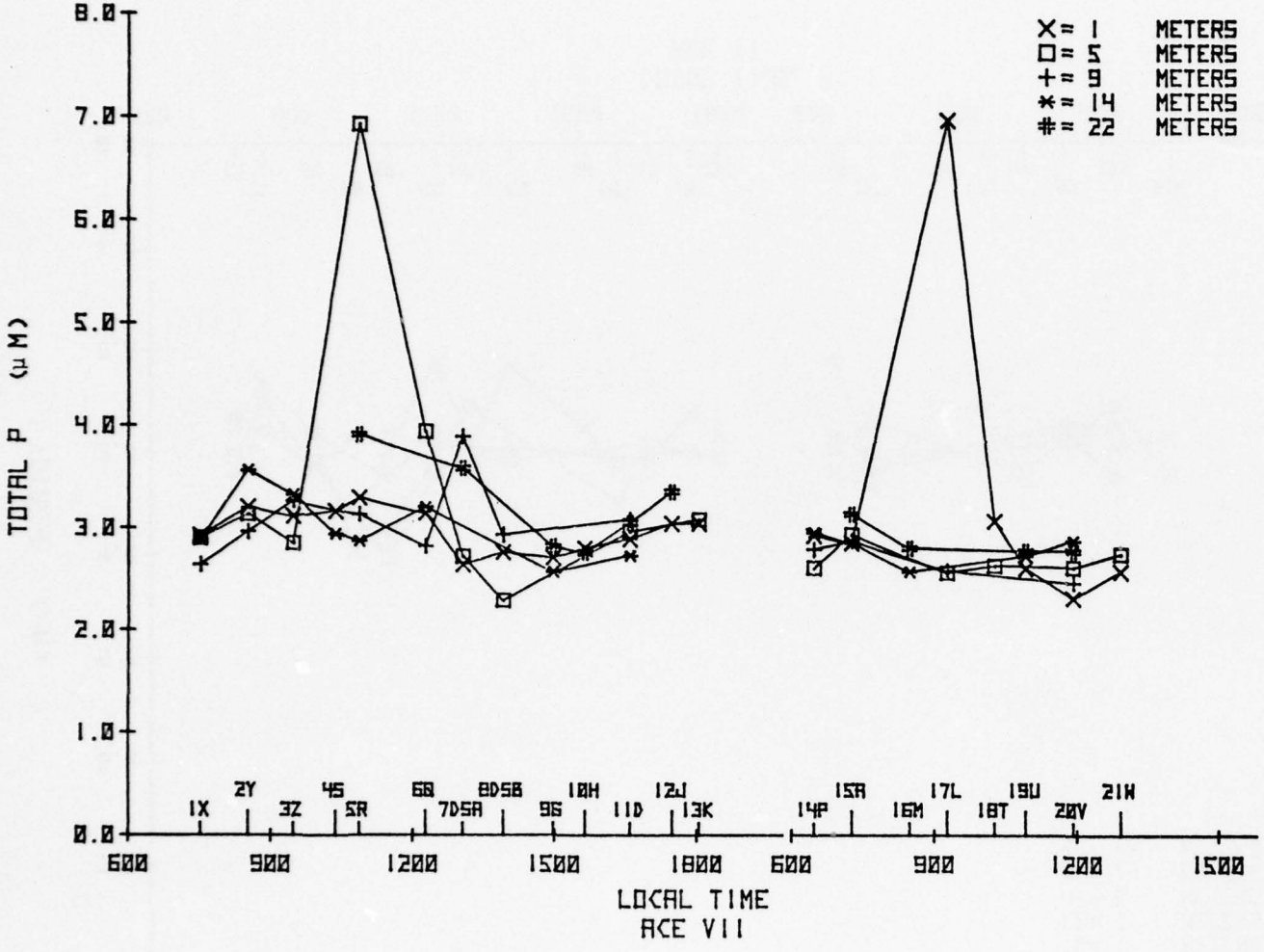



Figure B48. Total phosphorus observations during 28-29 May 1975.

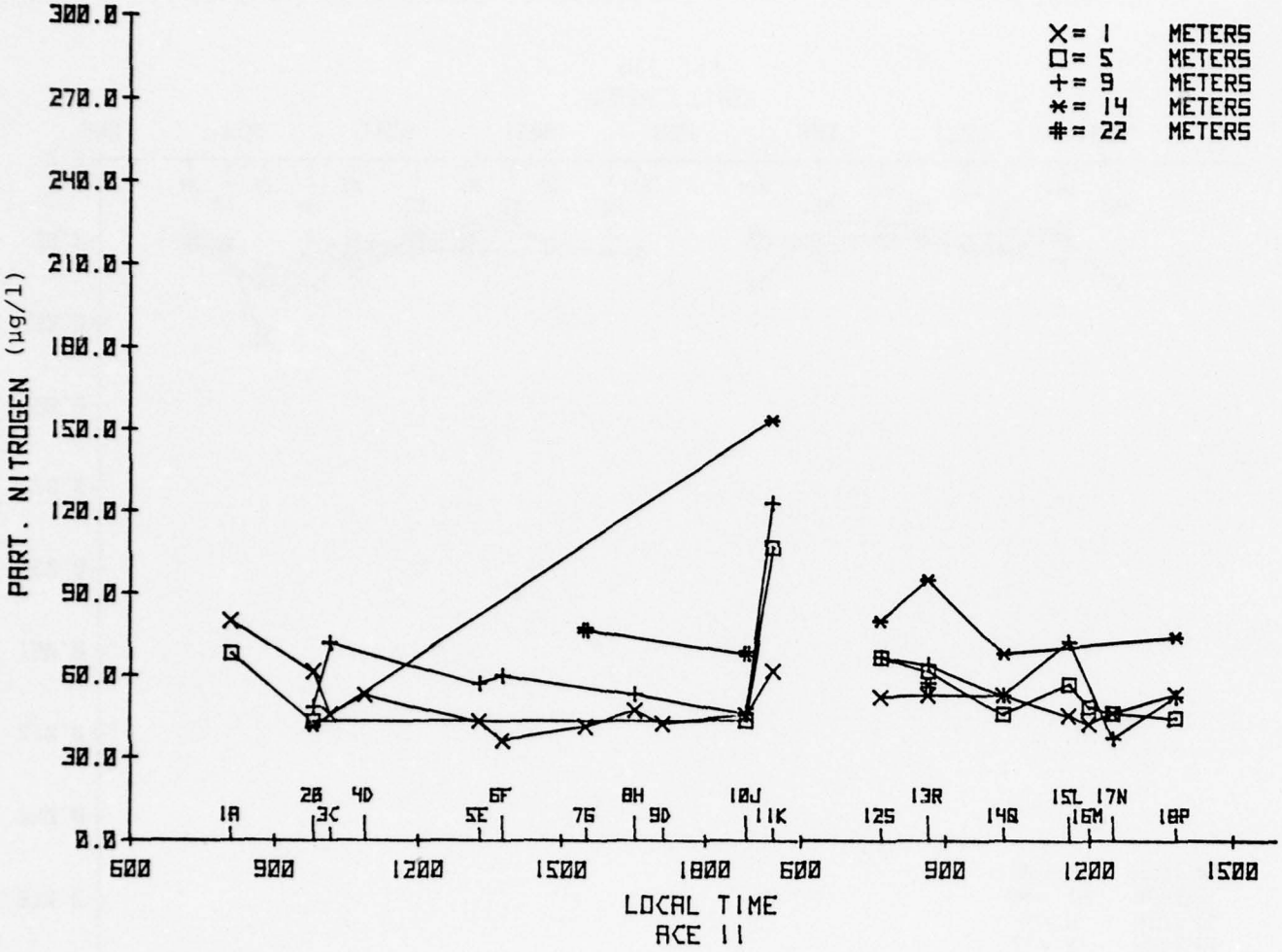



Figure B49. Particulate nitrogen observations during 5-6 December 1974.

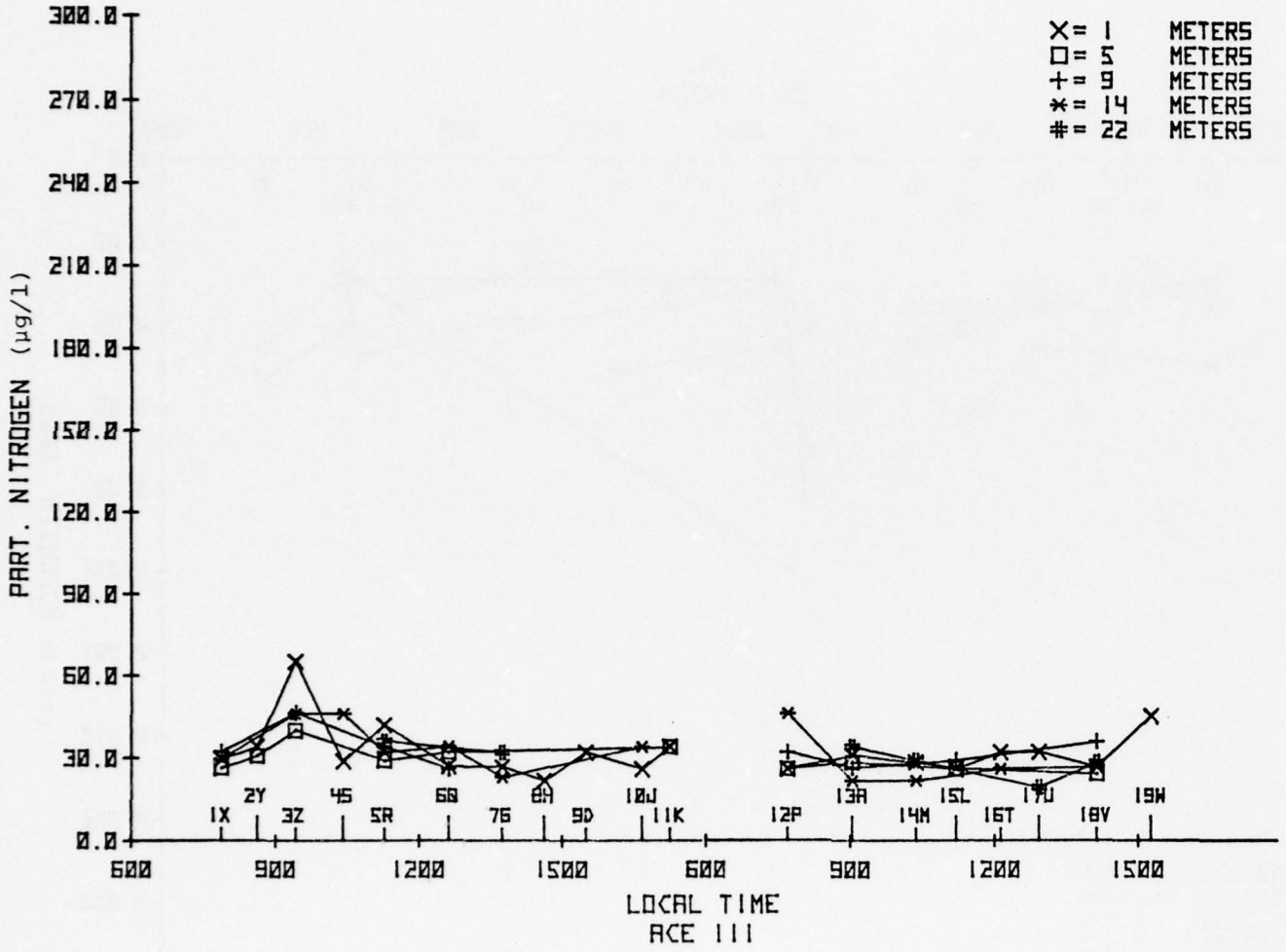



Figure B50. Particulate nitrogen observations during 13-14 January 1975.

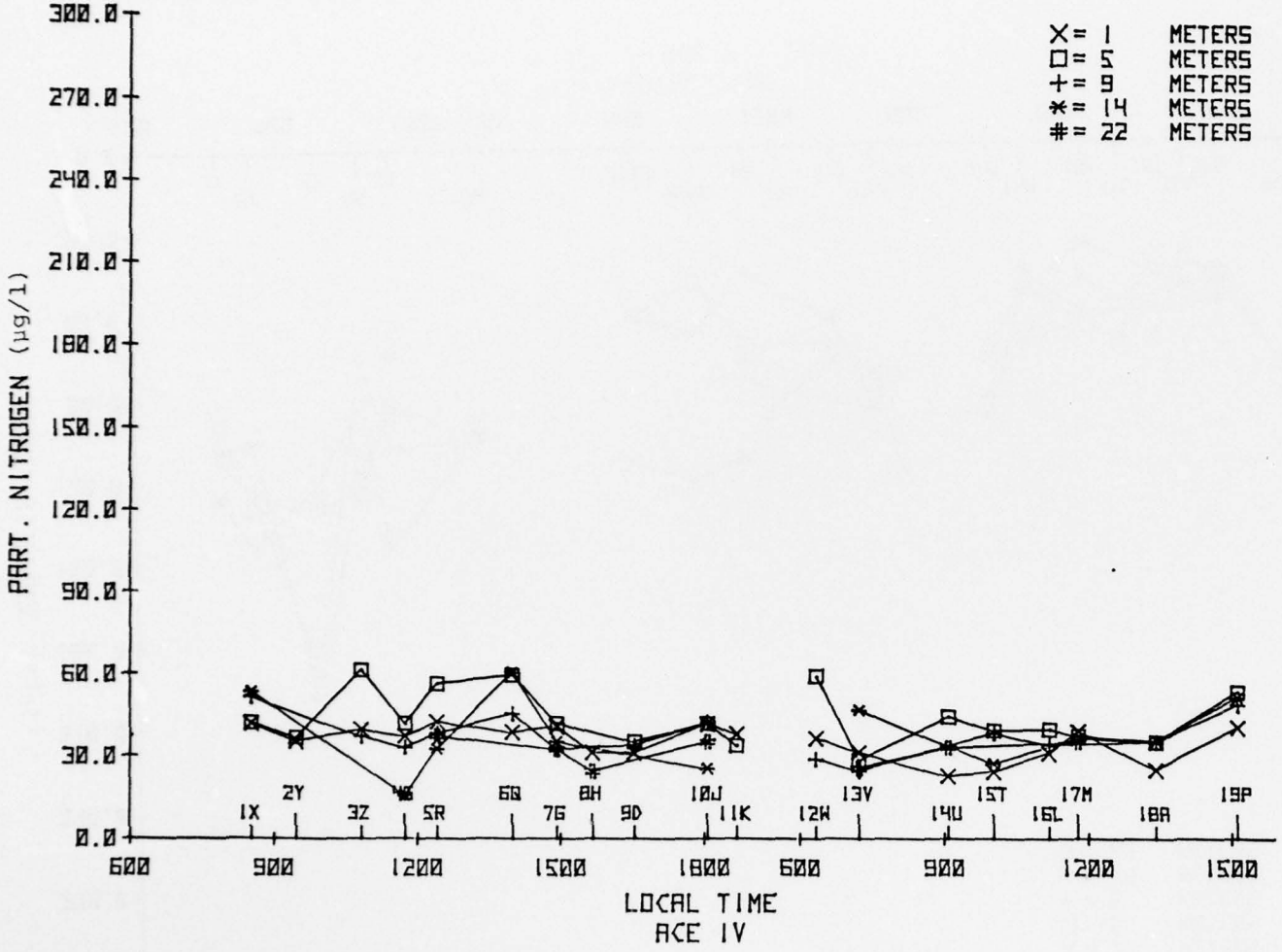



Figure B51. Particulate nitrogen observations during 19-20 February 1975.

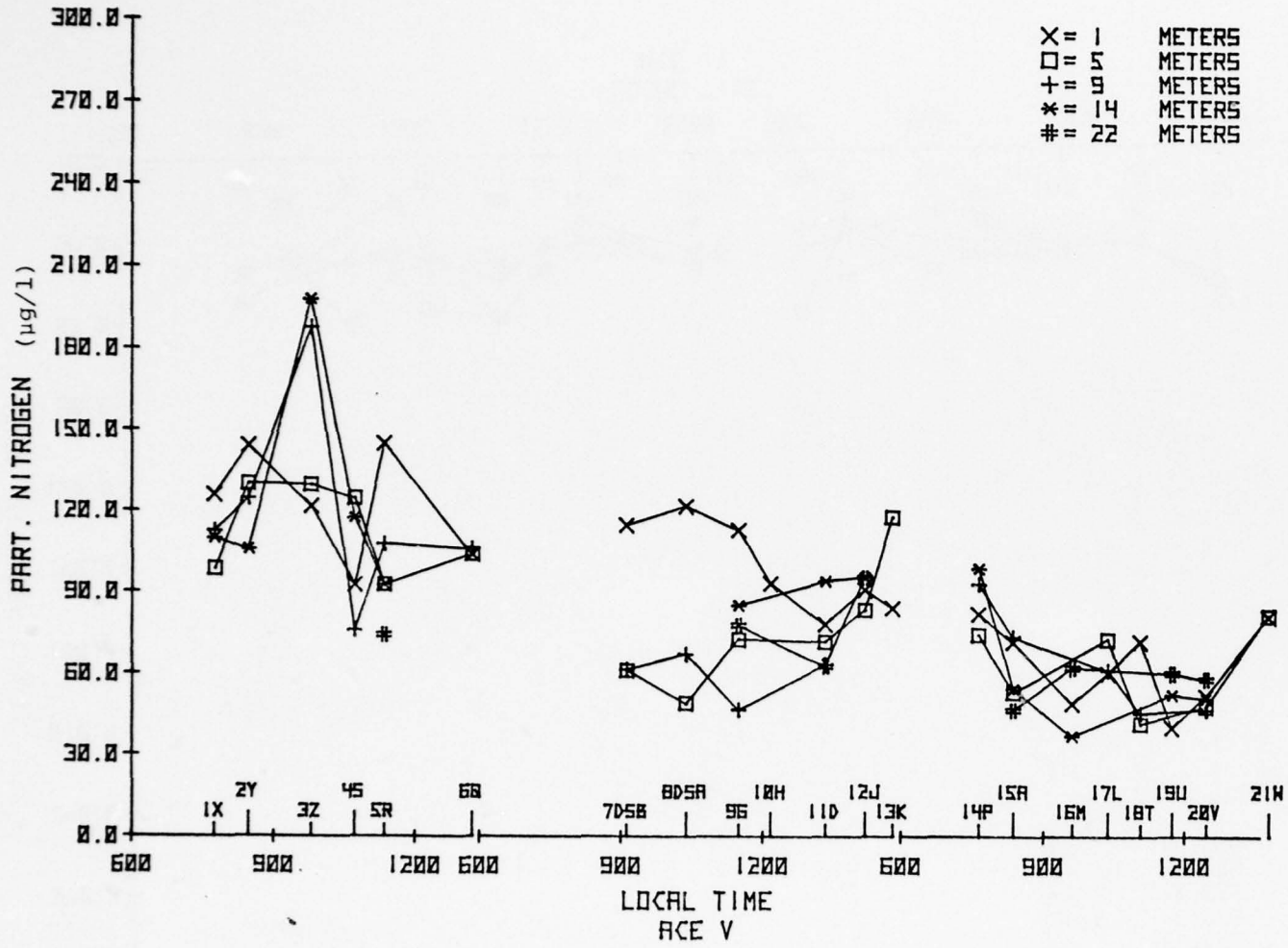



Figure B52. Particulate nitrogen observations during 19-21 March 1975.

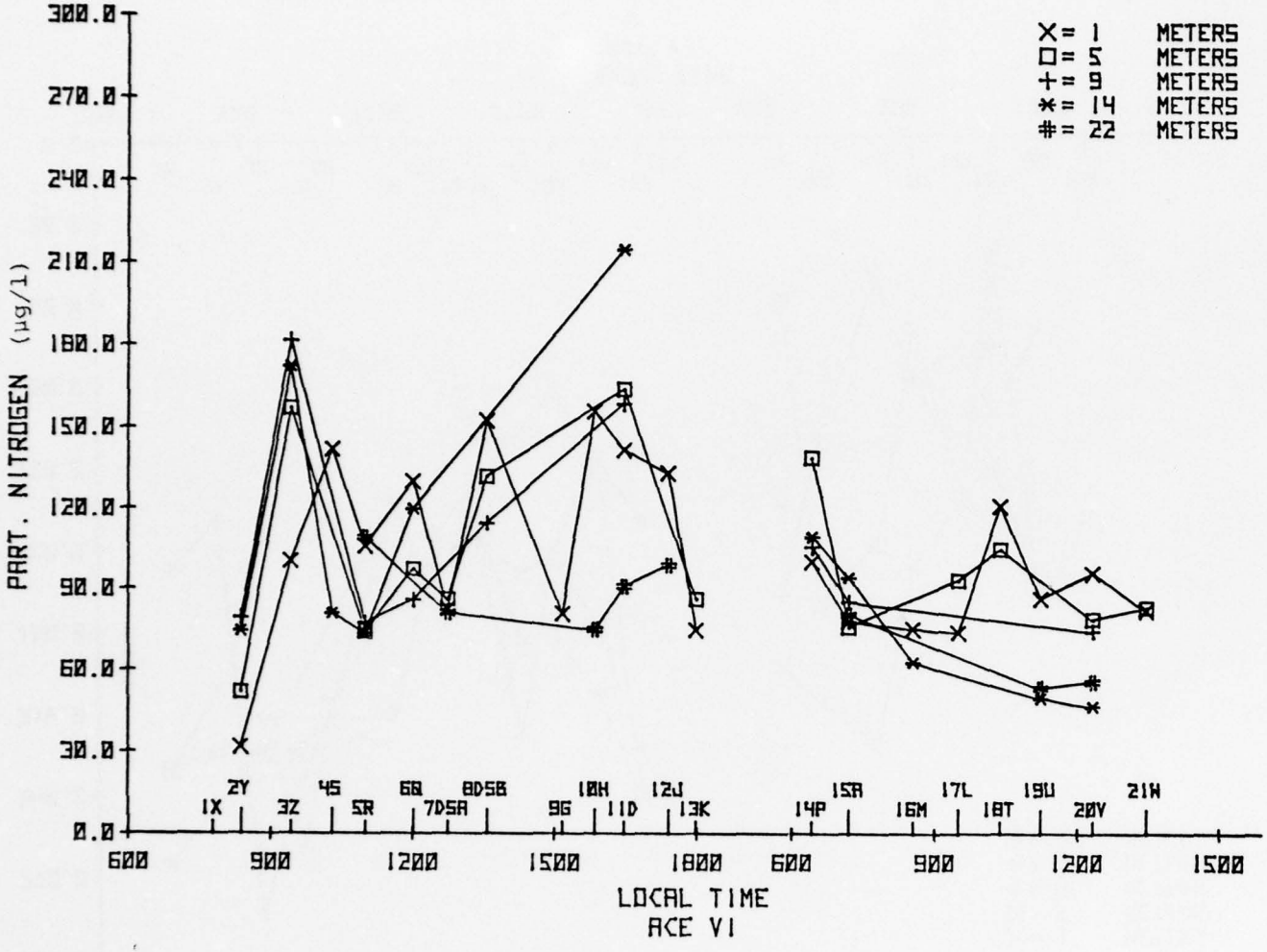



Figure B53. Particulate nitrogen observations during 23-24 April 1975.

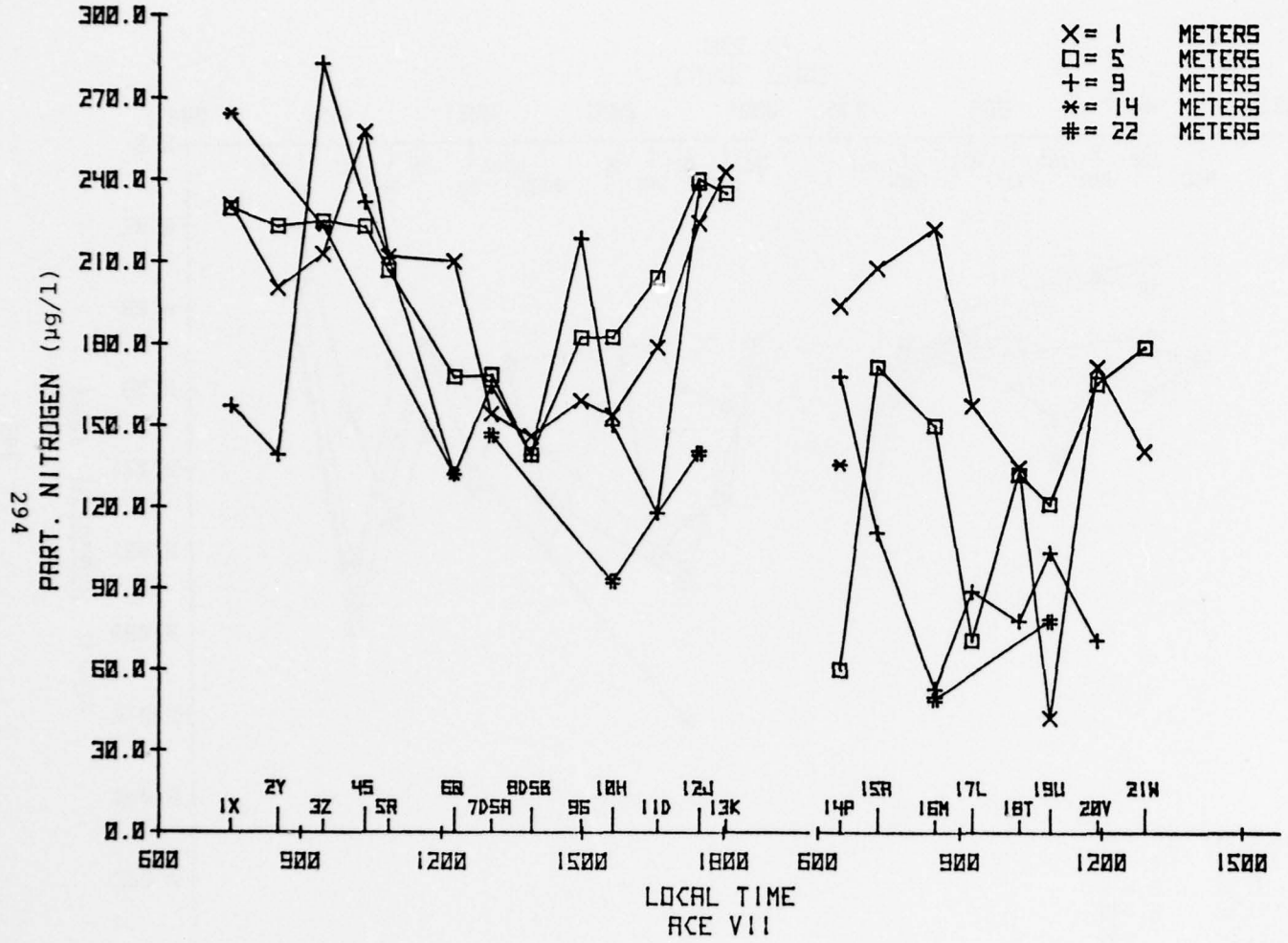



Figure B54. Particulate nitrogen observations during 28-29 May 1975.

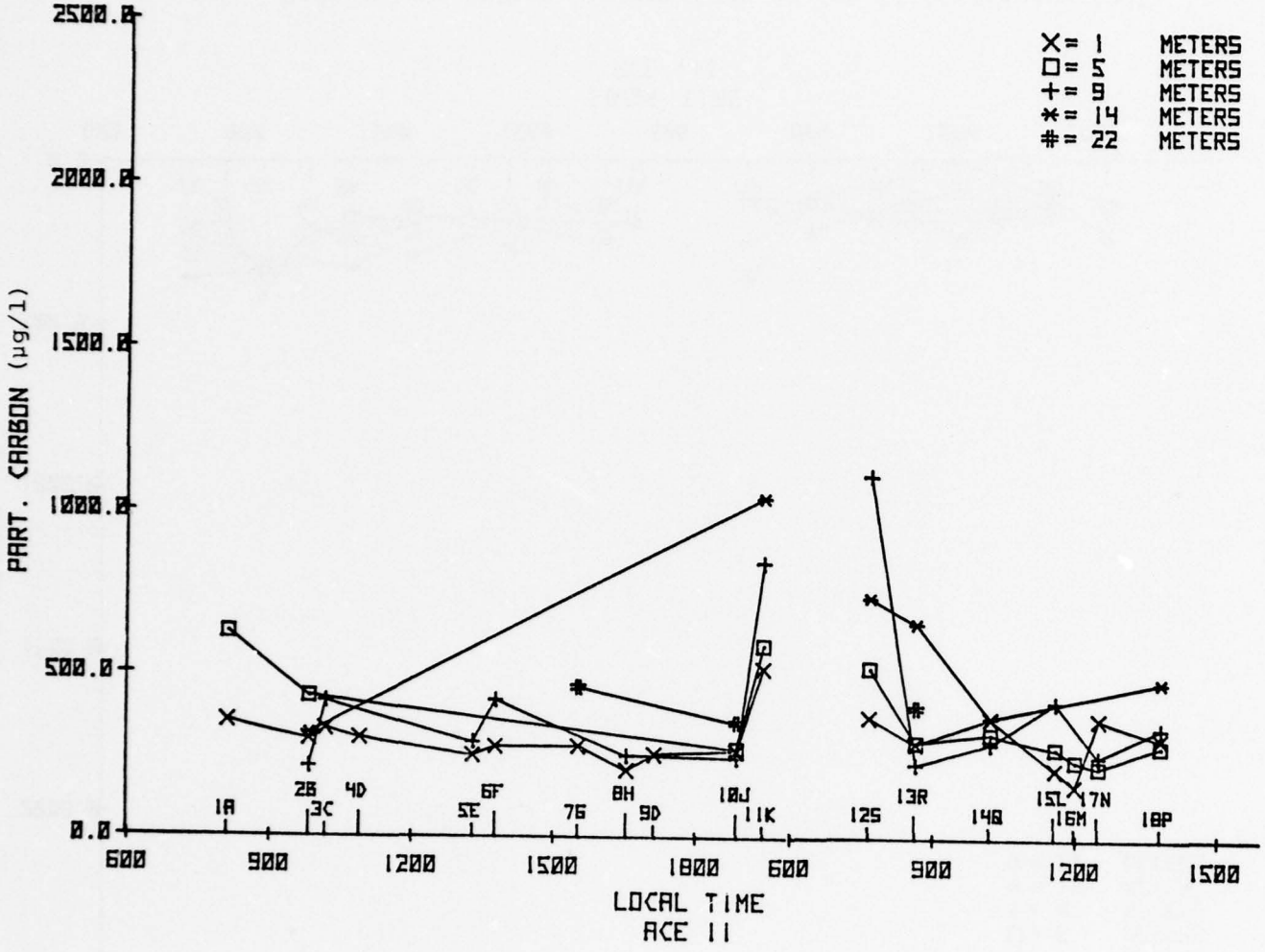



Figure B55. Particulate carbon observations during 5-6 December 1974.

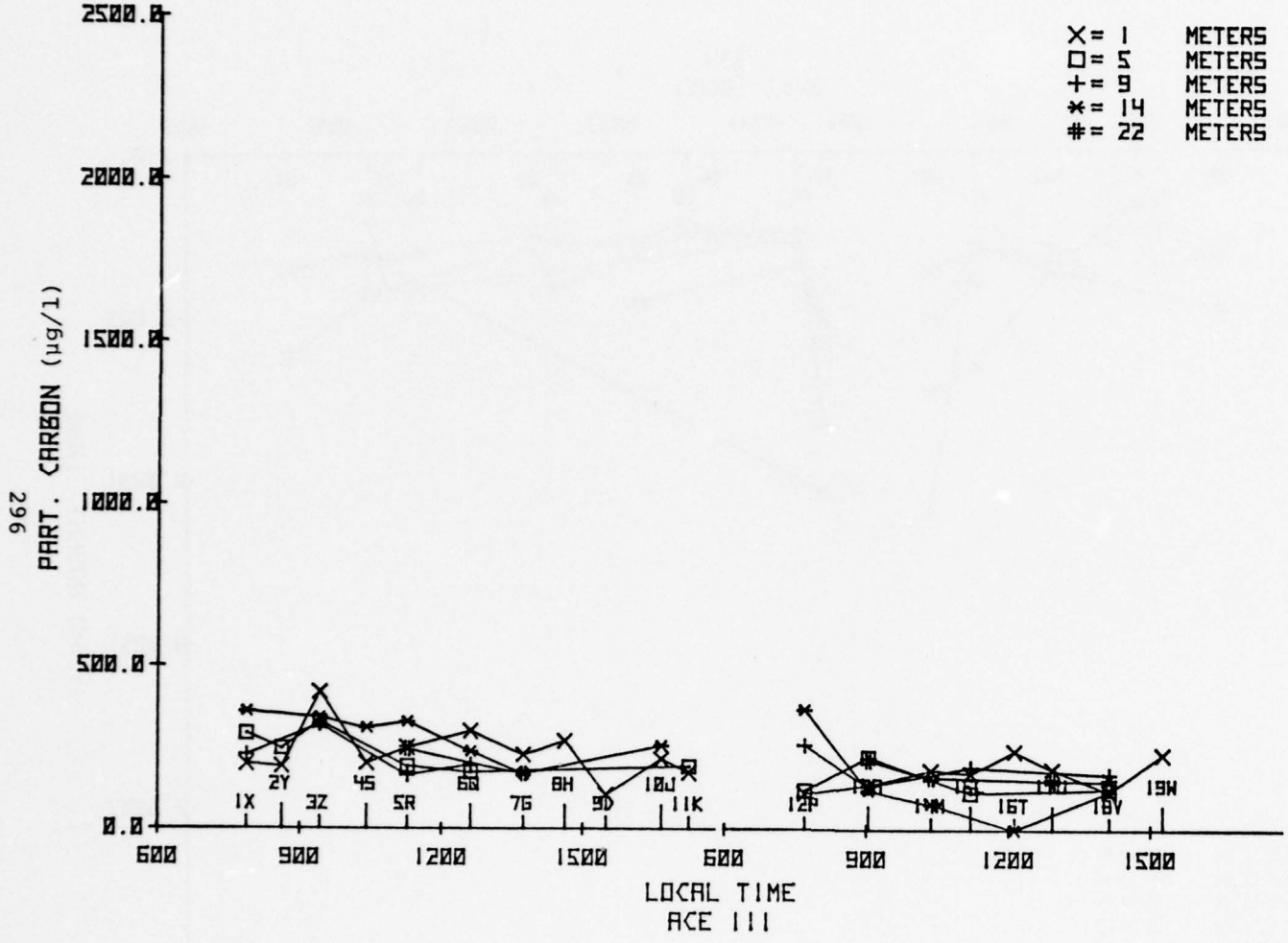



Figure B56. Particulate carbon observations during 13-14 January 1975.

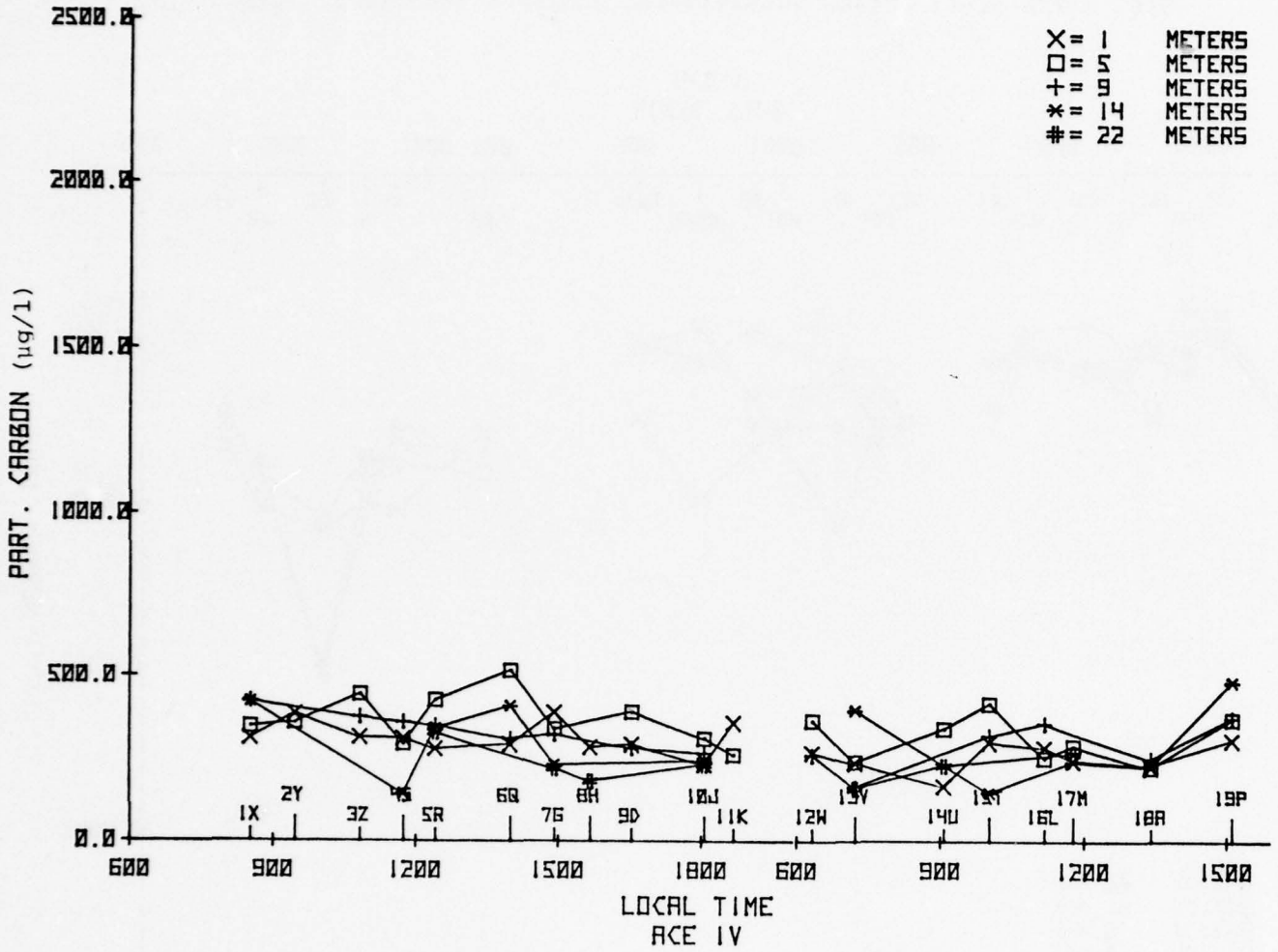



Figure B57. Particulate carbon observations during 19-20 February 1975.

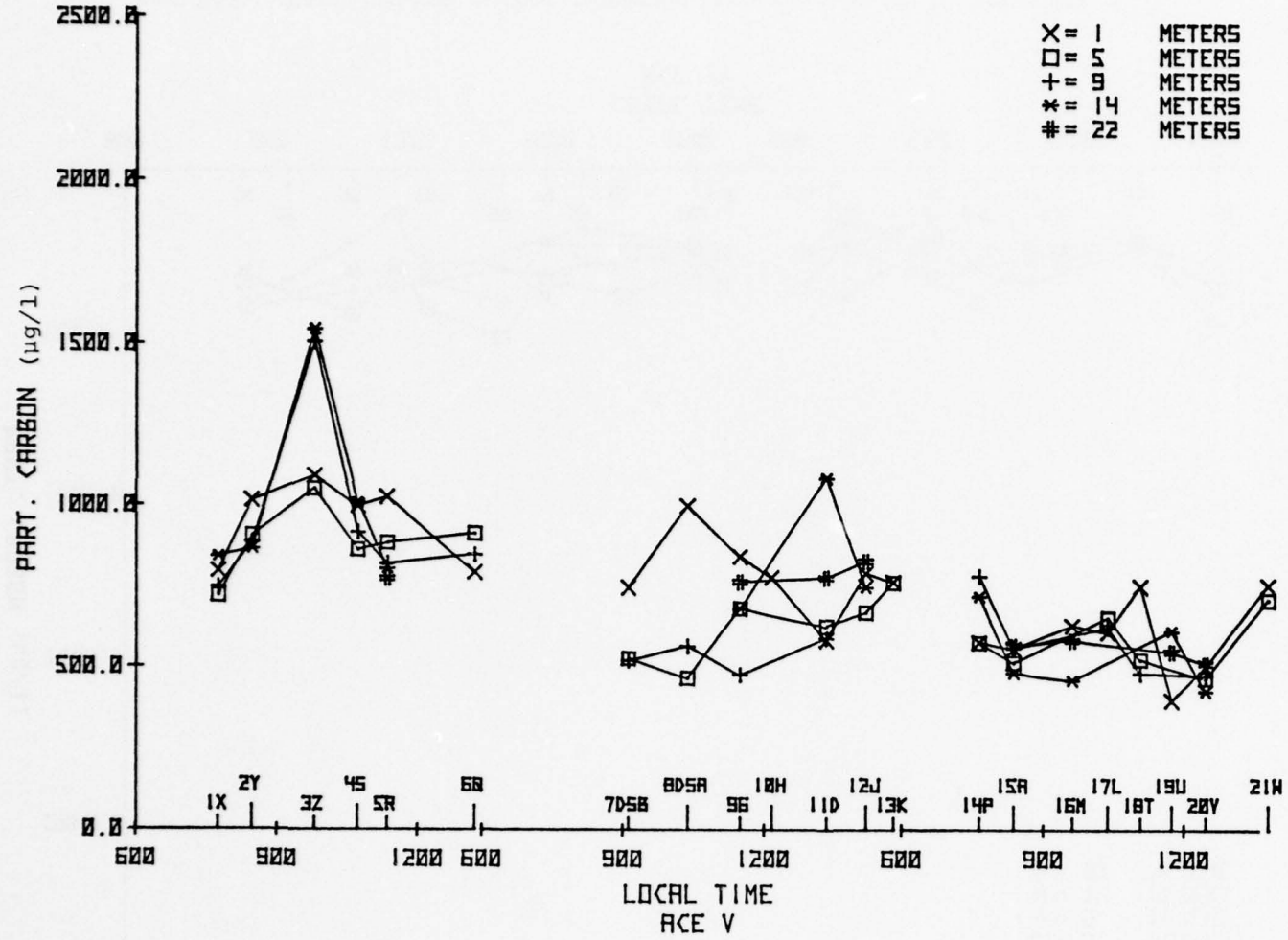



Figure B58. Particulate carbon observations during 19-21 March 1975.

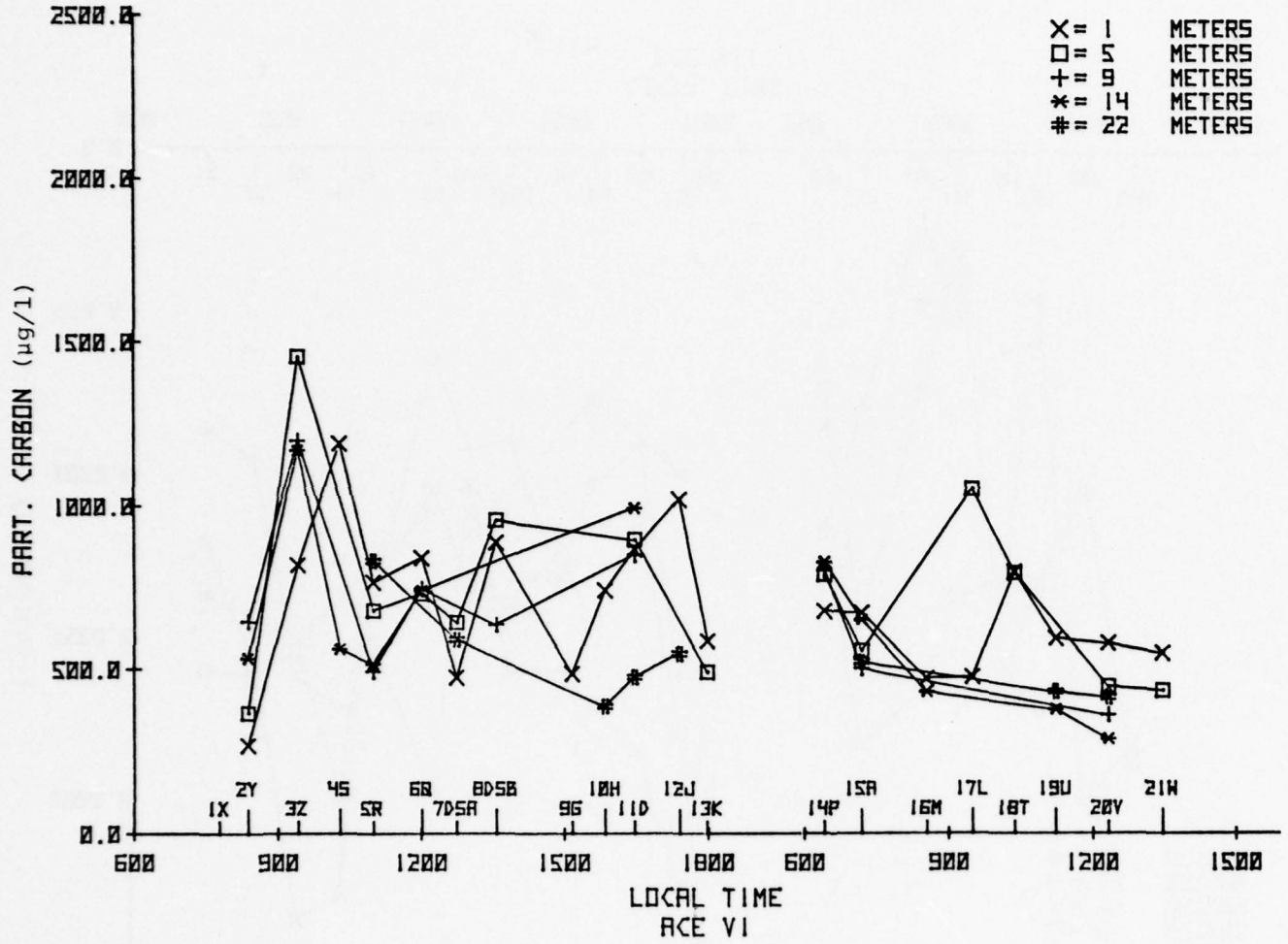



Figure B59. Particulate carbon observations during 23-24 April 1975.

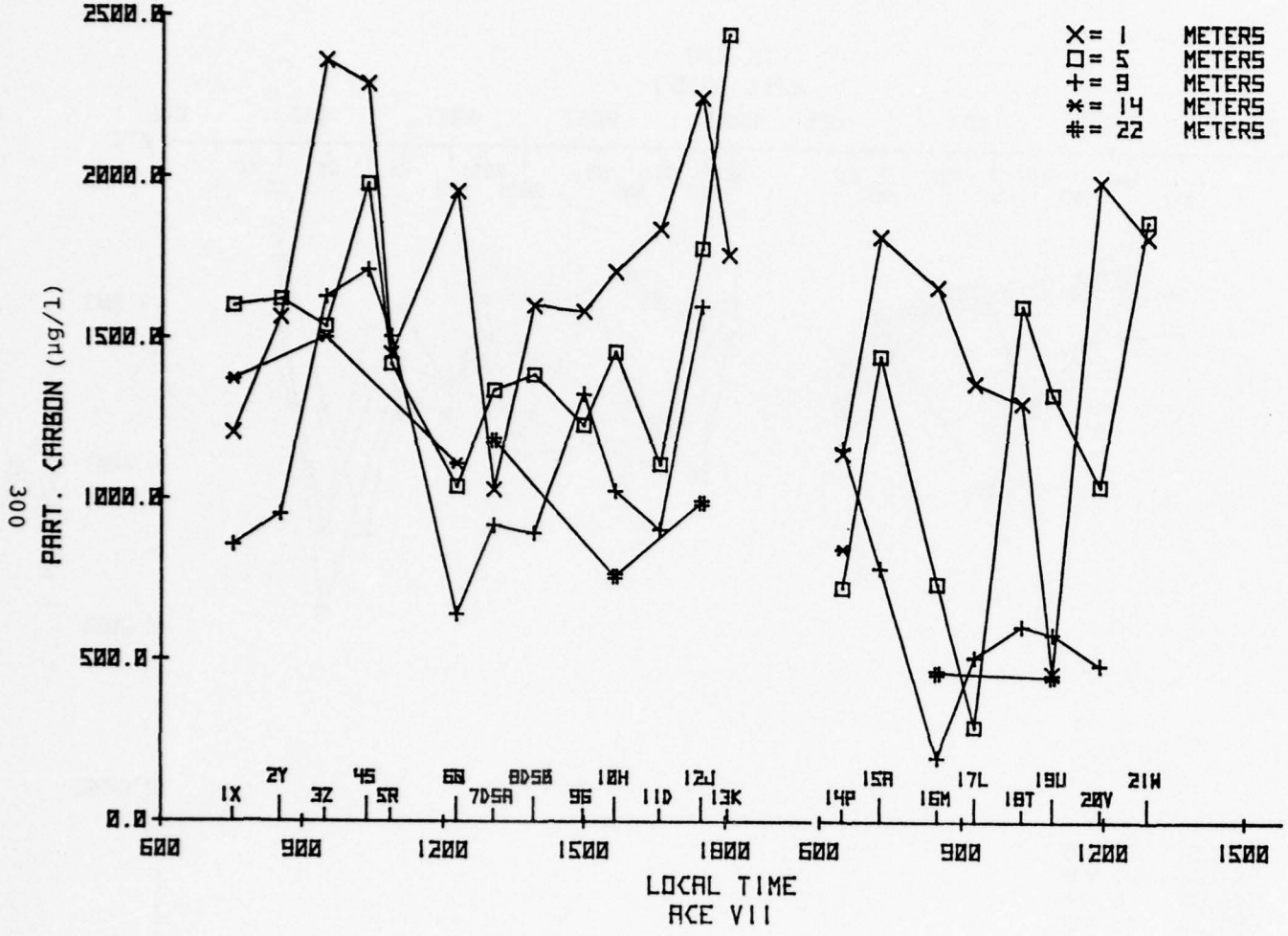



Figure B60. Particulate carbon observations during 28-29 May 1975.

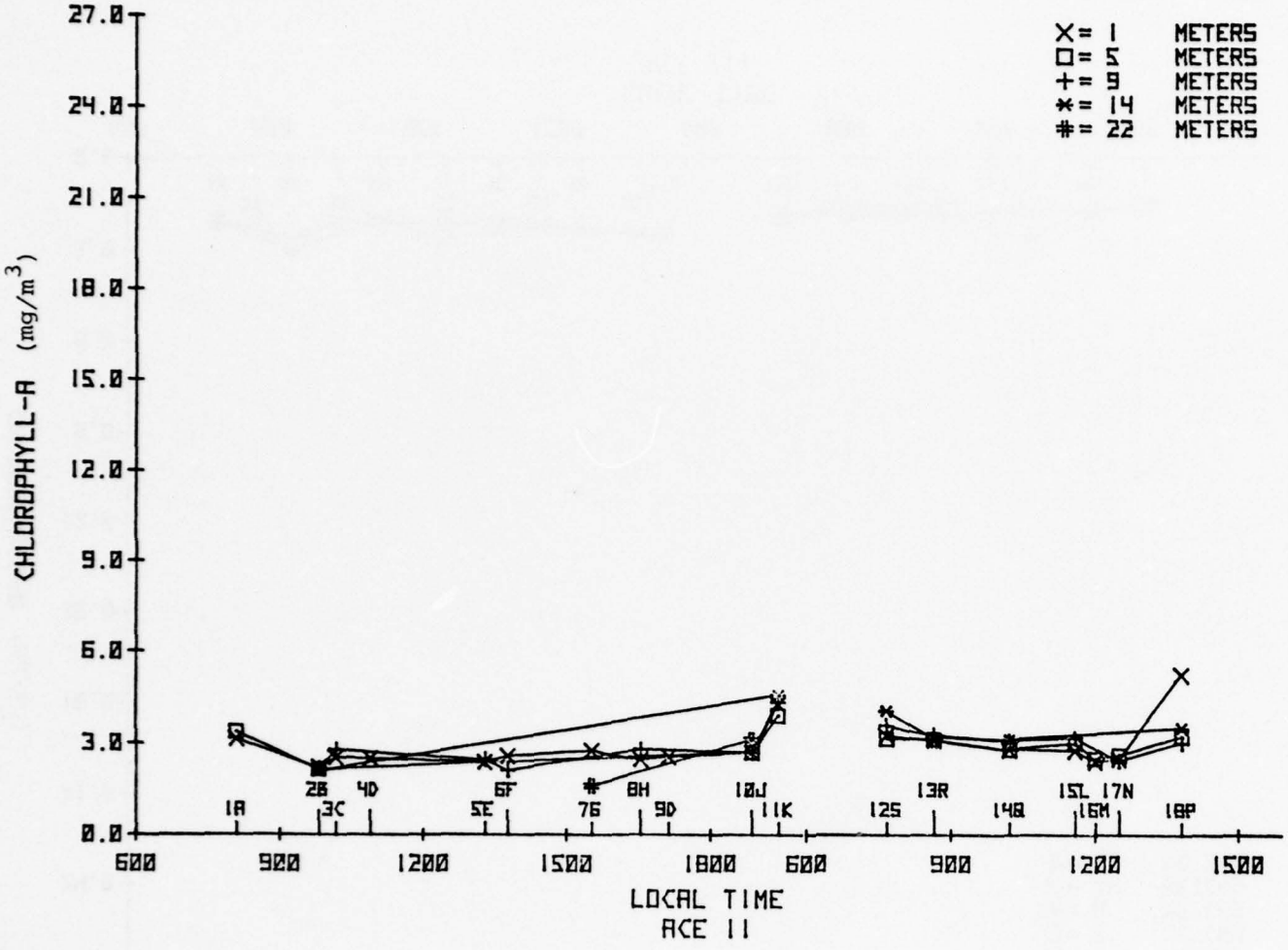



Figure B61. Chlorophyll-a observations during 5-6 December 1974.

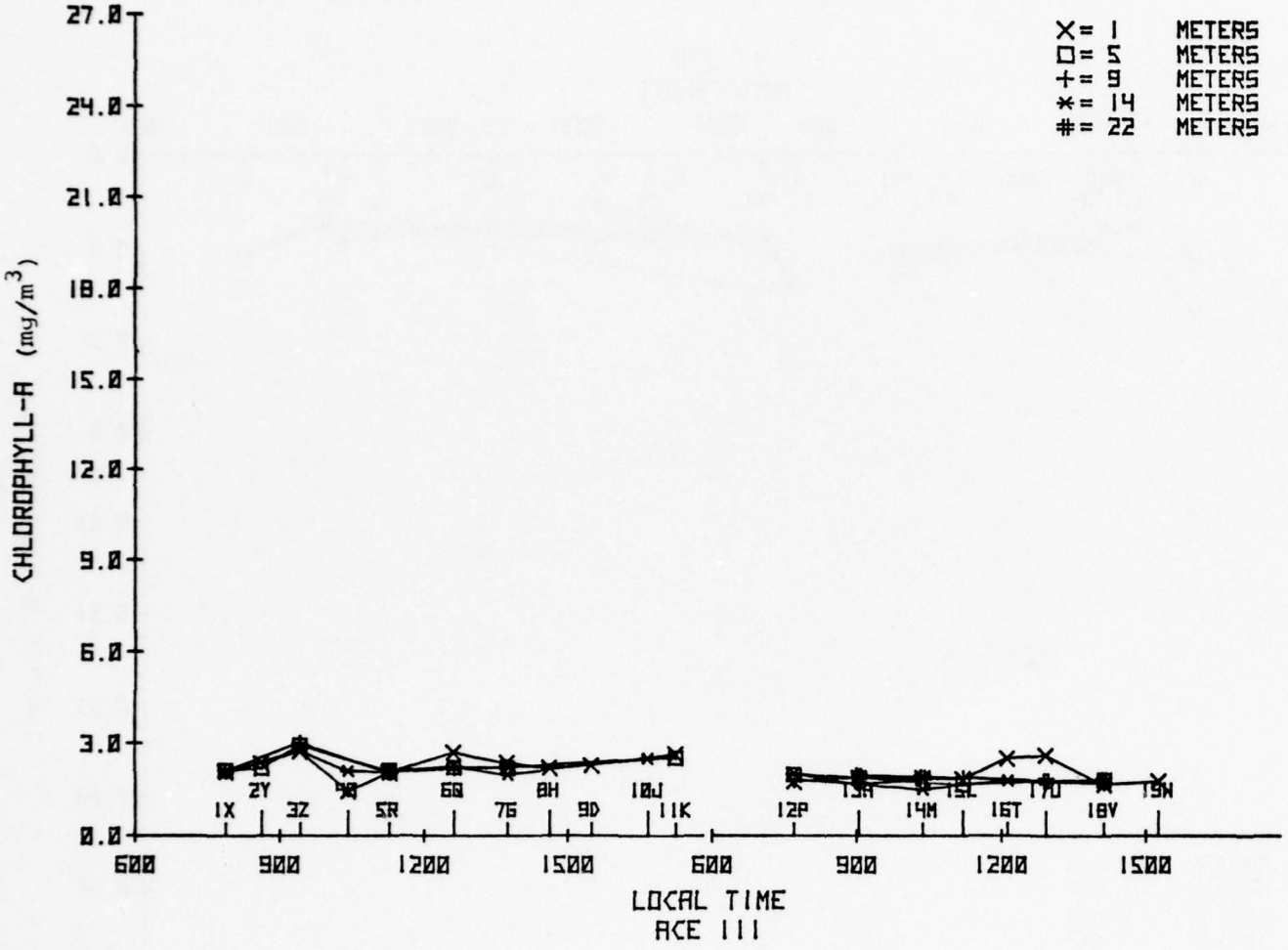



Figure B62. Chlorophyll-a observations during 13-14 January 1975.

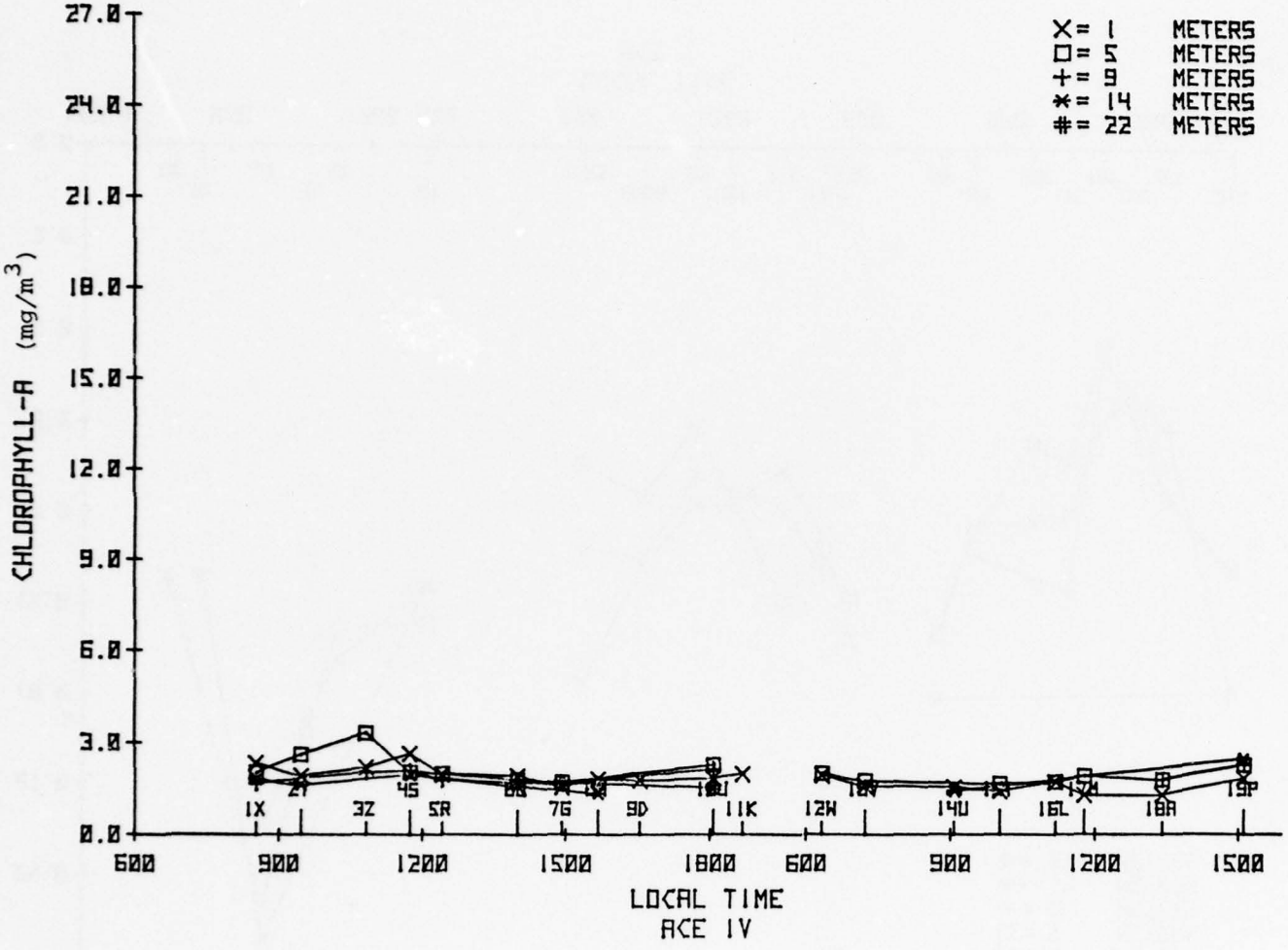



Figure B63. Chlorophyll-a observations during 19-20 February 1975.

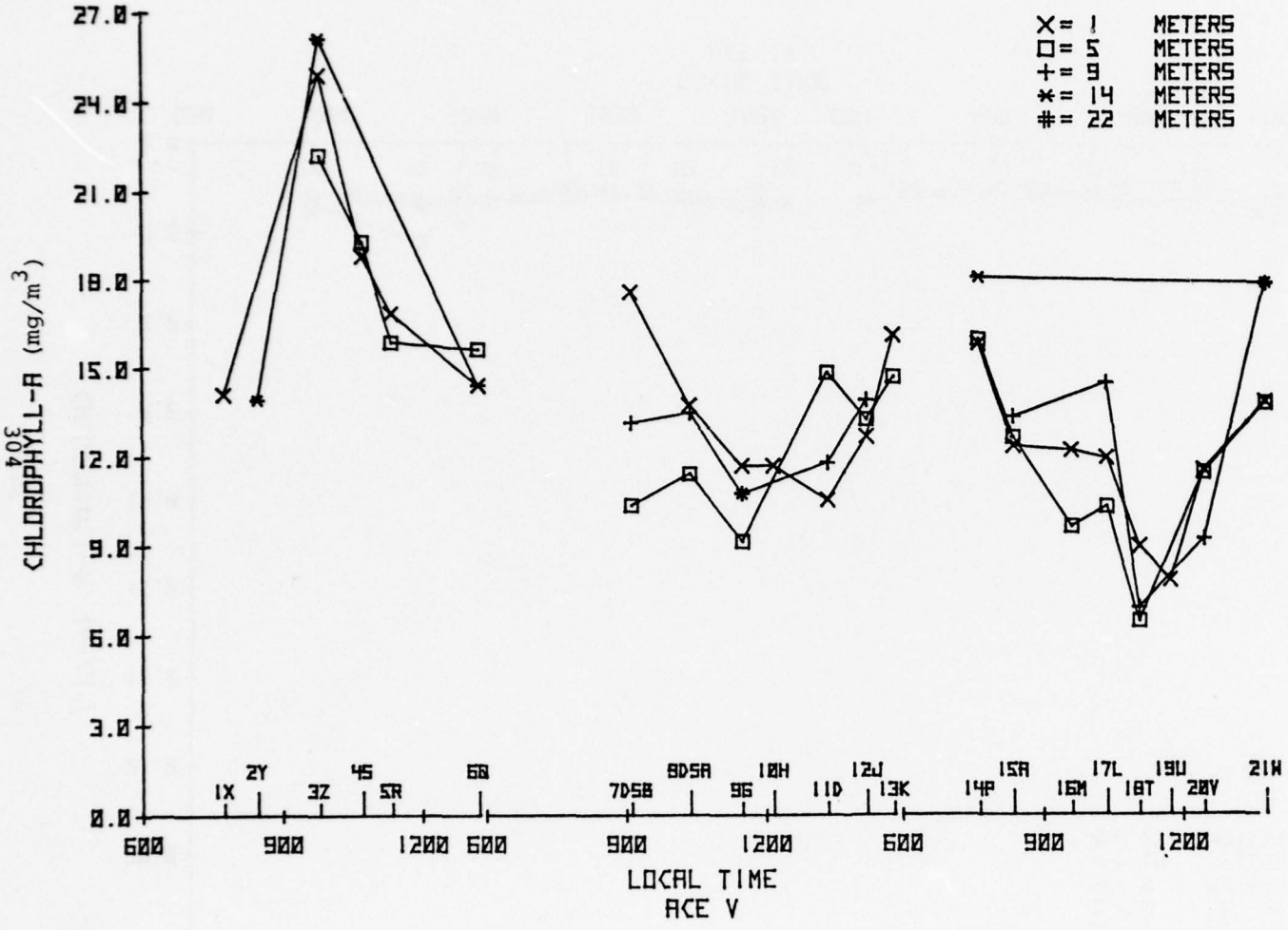



Figure B64. Chlorophyll-a observations during 19-21 March 1975.

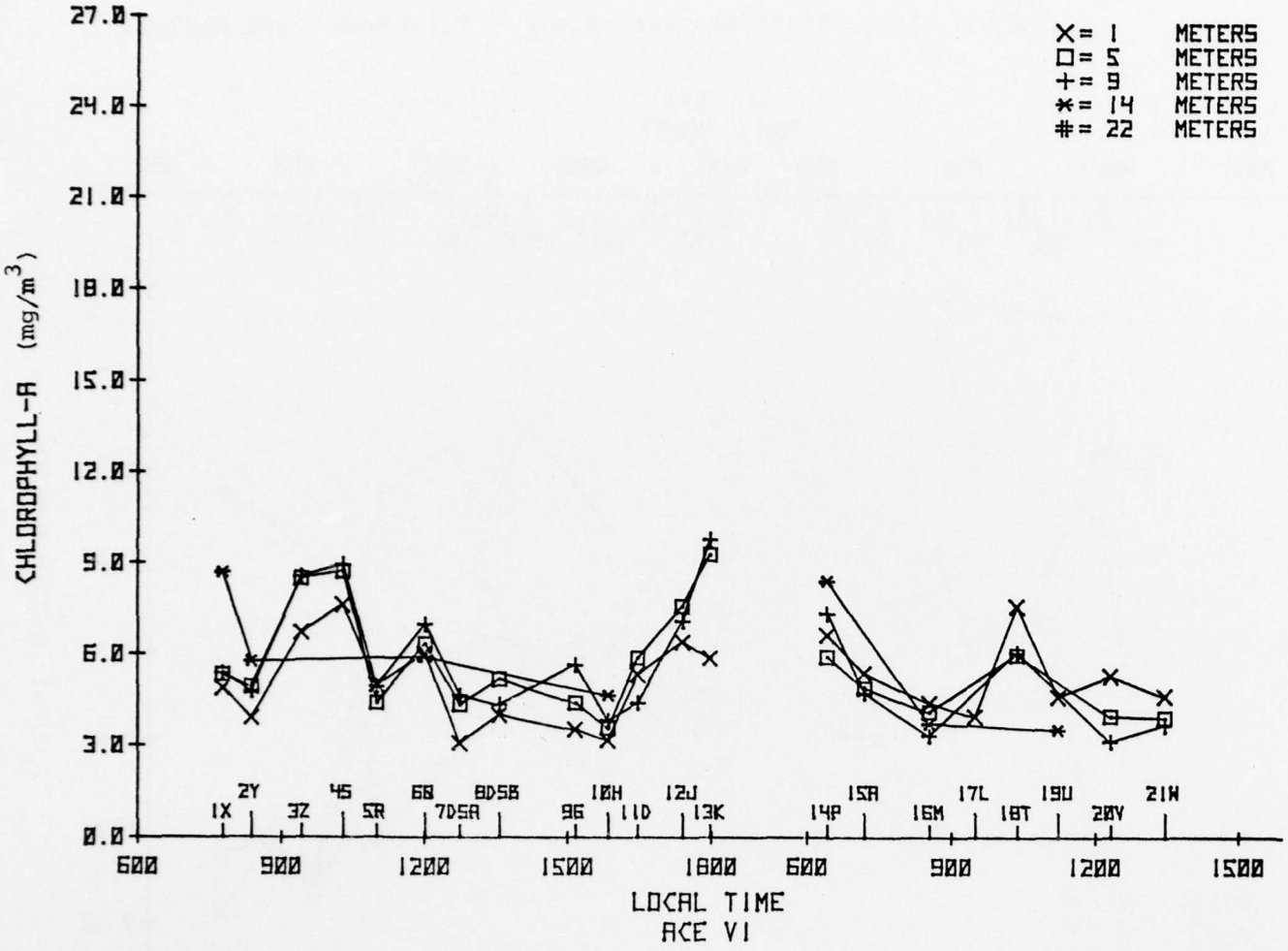



Figure B65. Chlorophyll-a observations during 23-24 April 1975.

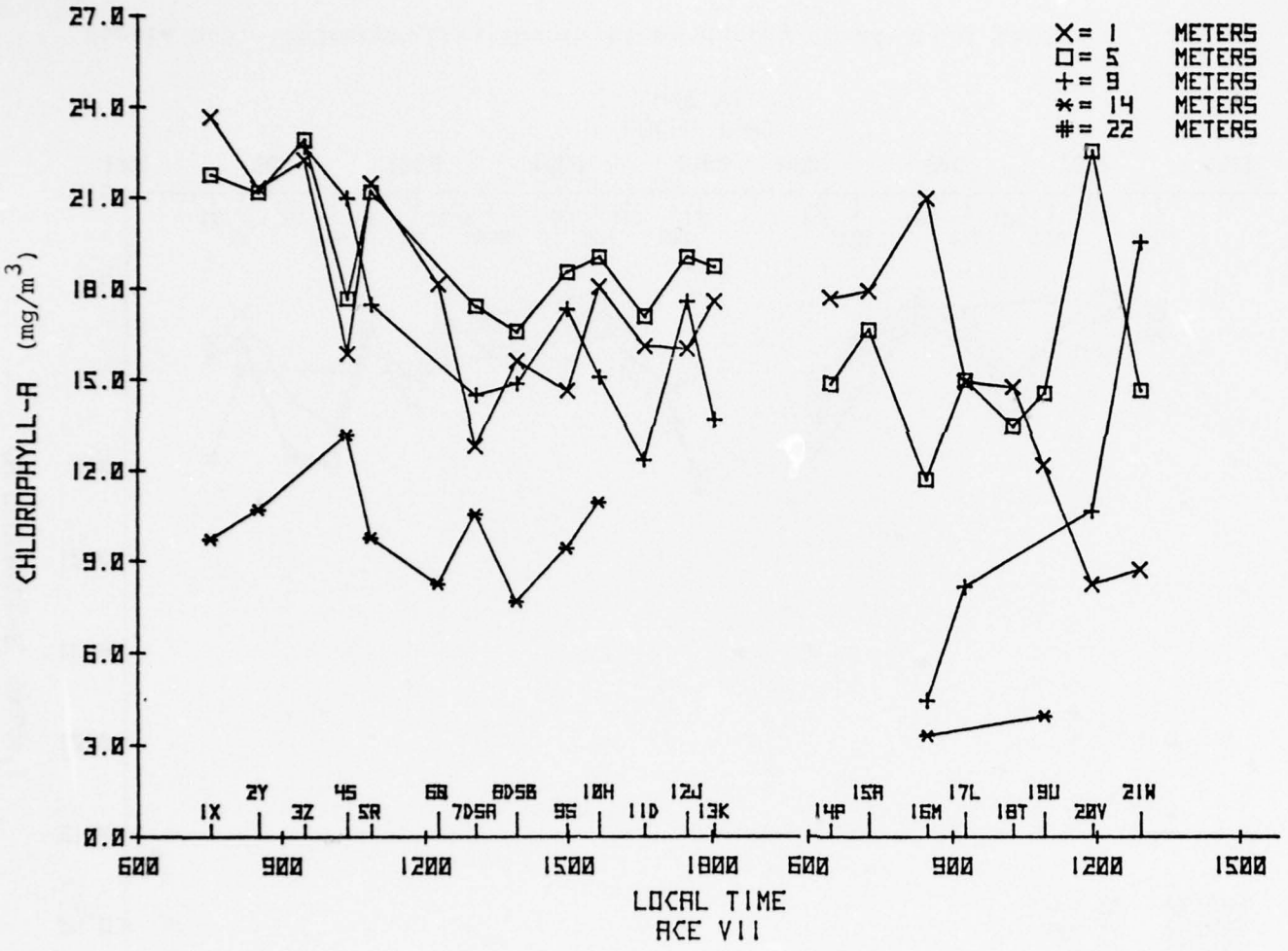



Figure B66. Chlorophyll-a observations during 28-29 May 1975.

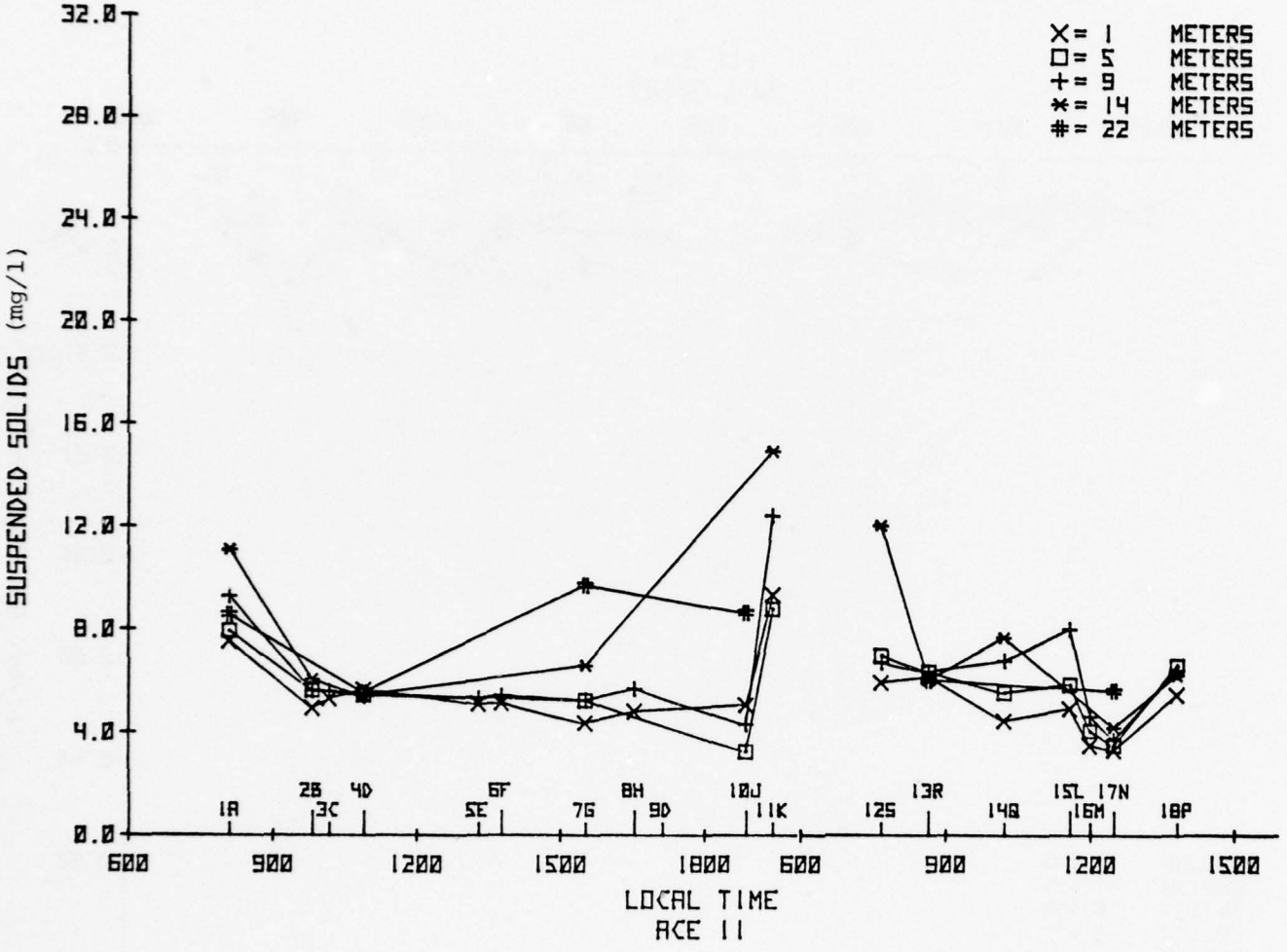



Figure B67. Suspended solids observations during 5-6 December 1974.

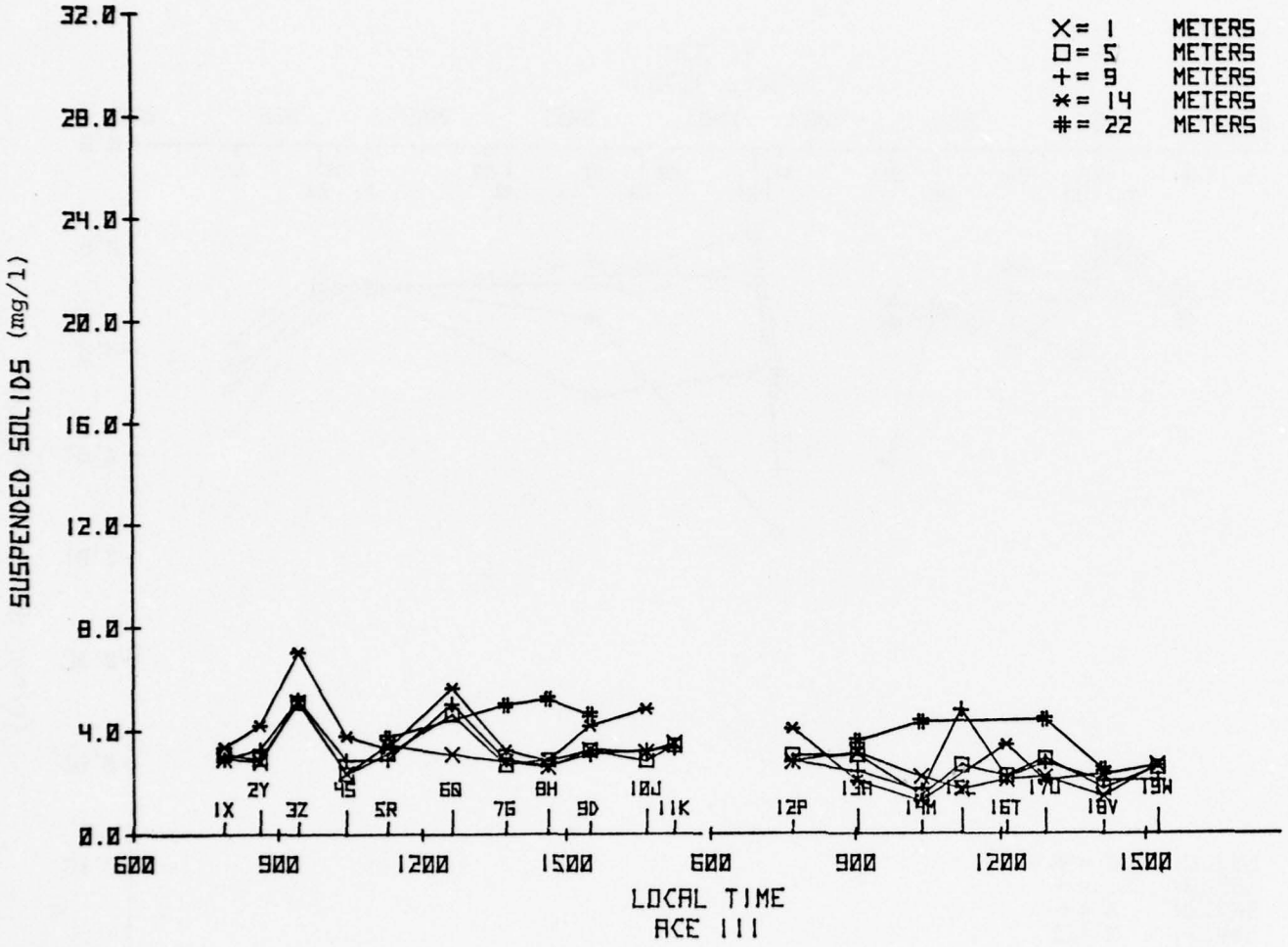



Figure B68. Suspended solids observations during 13-14 January 1975.

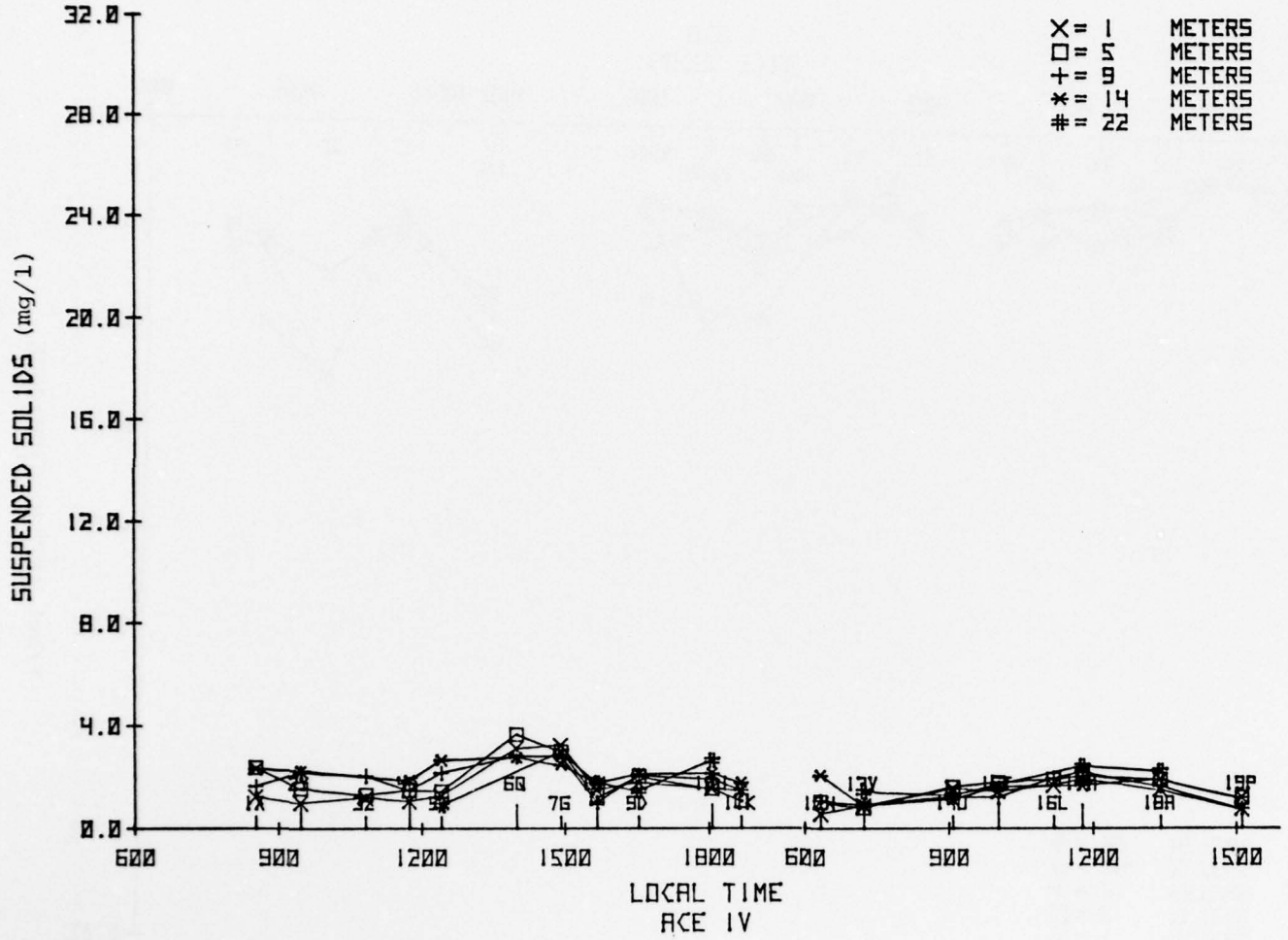



Figure B69. Suspended solids observations during 19-20 February 1975.

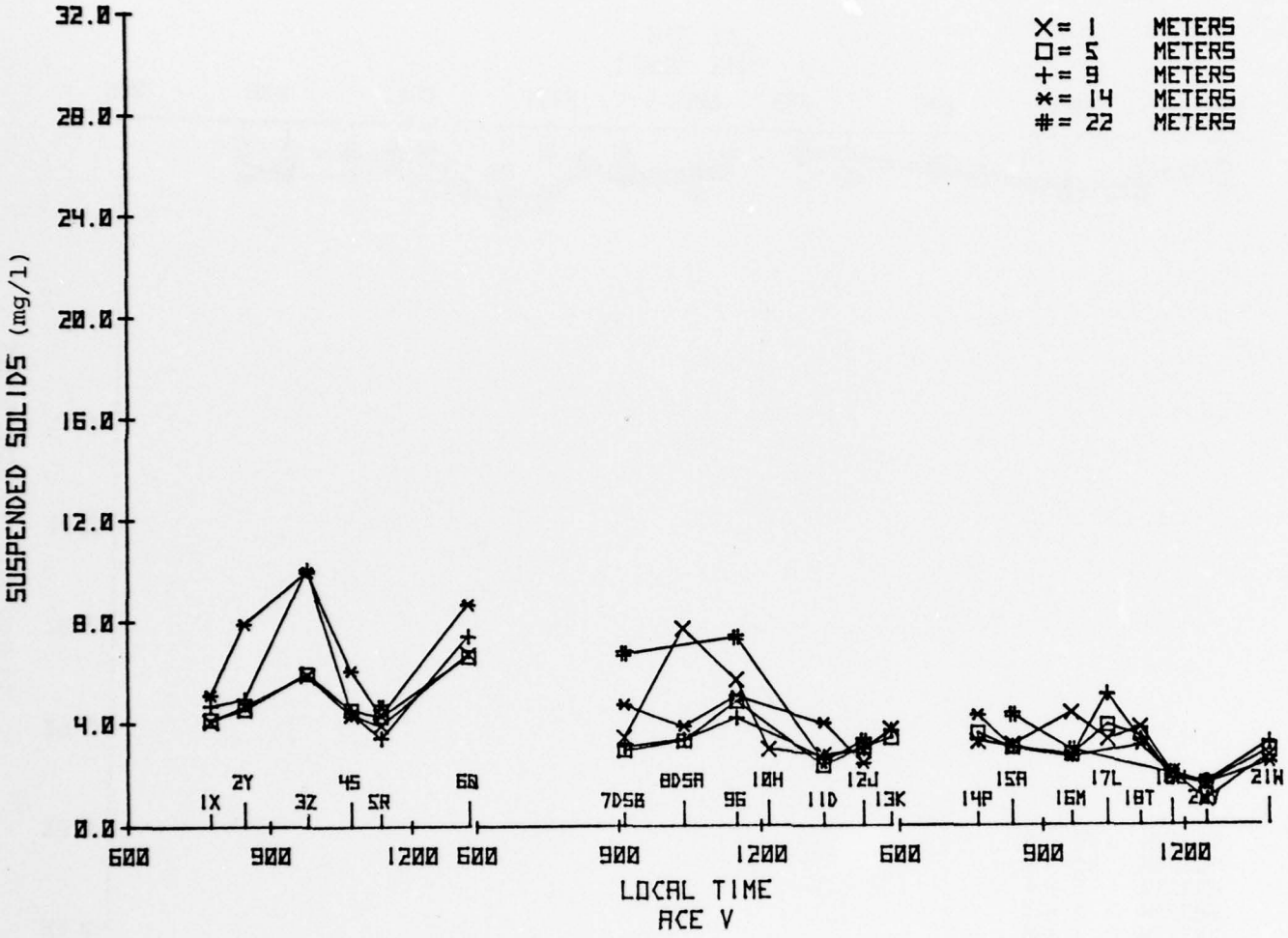



Figure B70. Suspended solids observations during 19-21 March 1975.

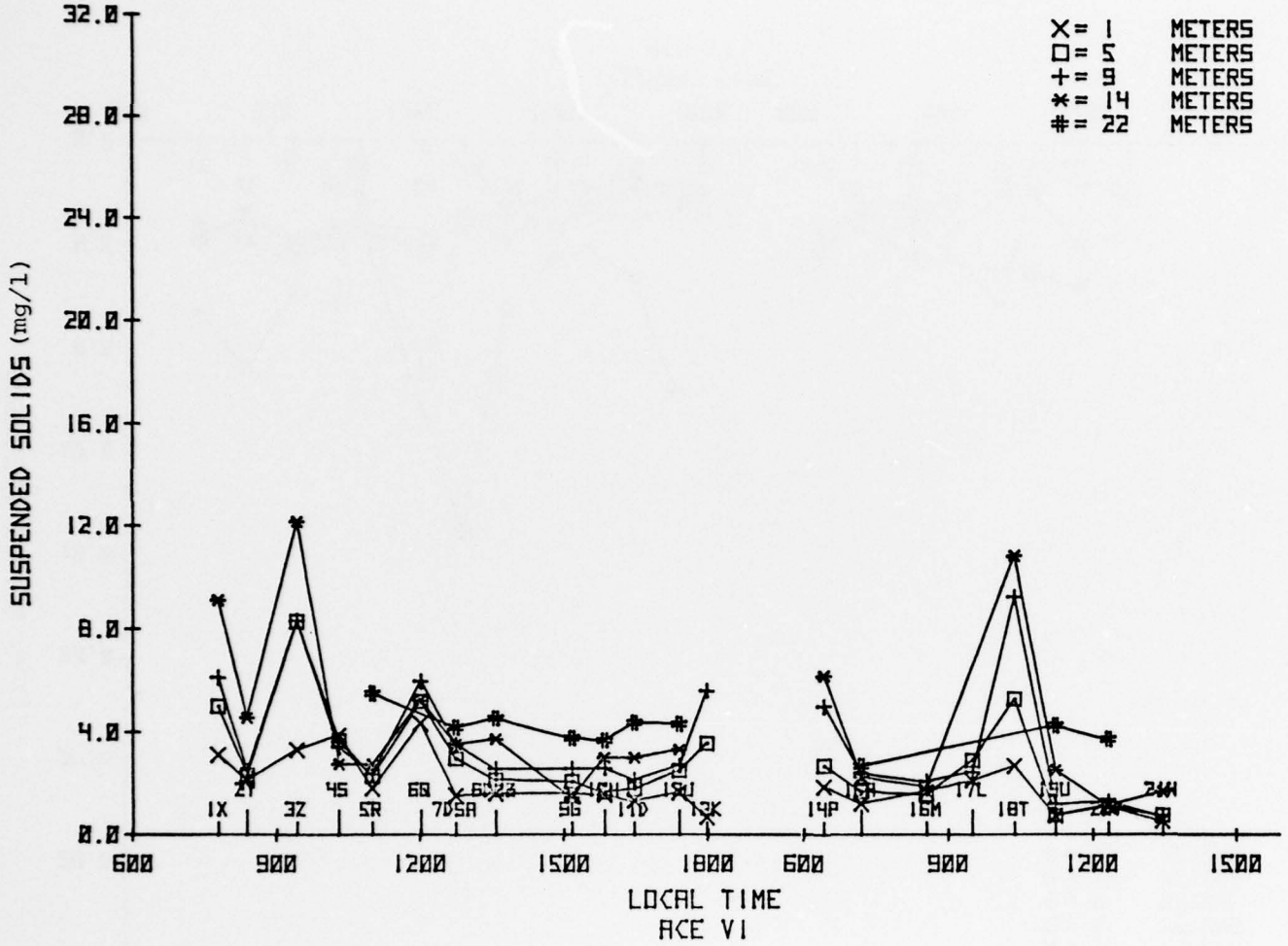



Figure B71. Suspended solids observations during 23-24 April 1975.

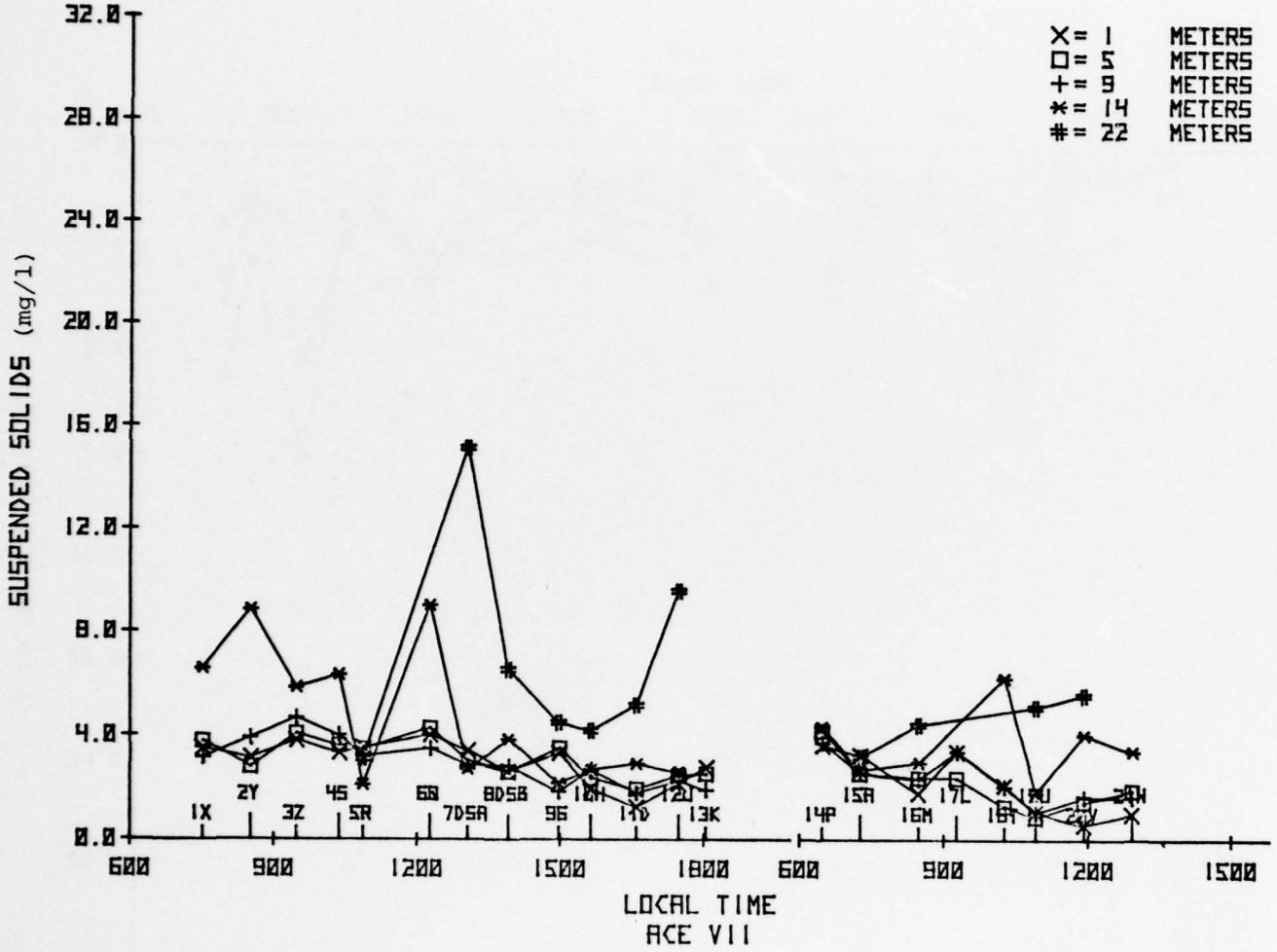



Figure B72. Suspended solids observations during 28-29 May 1975.

## REFERENCES


1. LeLacheur, E. A. and Sammons, J. C., "Tides and Currents in Long Island and Block Island Sounds," Special Publication 174, U. S. Coast and Geod. Surv., 1973, Washington, D. C.

2. Riley, G. A., "Hydrography of Long Island and Block Island Sounds," Bull. Bingham Oceanogr. Coll., Vol. 13, 1952, pp 5-39.

3. Prytherch, H. F., "Investigation of the Physical Conditions Controlling Spawning of Oysters and the Occurrence, Distribution, and Settling of Oyster Larvae in Milford Harbor, Connecticut," Bull. U. S. Bur. Fish., Vol. 44, 1929, pp 429-503.

4. Suttie, R. H., "Report on the Water Resources of Connecticut," Bull. Conn. Geolo. Nat. Hist. Surv., Vol. 44, 1928, pp 1-168.

5. Riley, G. A., "Oceanography of Long Island Sound, 1952-1954. II. Physical Oceanography," Bull. Bingham Oceanogr. Coll., Vol. 15, 1956a, pp 15-46.

6. Riley, G. A., "Oceanography of Long Island Sound 1954-1955," Bull. Bingham Oceanogr. Coll., Vol. No. 1, 1959, pp 9-30.

7. Riley, G. A., "Review of the Oceanography of Long Island Sound," Papers in Marine Biology, Supplement to Volume 3 of Deep Sea Research, 1956b, pp 224-238.

8. Hardy, C. D., "Hydrographic Data Report: Long Island Sound, 1969," Technical Report No. 4, Marine Sciences Research Center, State University of New York, Stony Brook, 1970, 44 p.

9. Hardy, C. D. and Weyl, P. K., "Hydrographic Data Report: Long Island Sound, Part I," Technical Report No. 6, Marine Sciences Research Center, State University of New York, Stony Brook, 1970, 50 p.

10. Hardy, C. D., "Movement and Quality of Long Island Sound Waters," Technical Report No. 17, Marine Sciences Research Center, State University of New York, 1971, 66 p.

11. Gross, M. G. and Bumpus, D., "Residual Drift of Near Bottom Waters in Long Island Sound," Limnol. Oceanogr., Vol. 17, 1972, pp 636-638.

12. Paskausky, D. F. and D. L. Murphy, "Seasonal Variation of Residual Drift in Long Island Sound," Est. Coast. Mar. Sci. Vol. 4, 1976, pp 513-522.

13. Wilson, R. E., "Gravitational Circulation in Long Island Sound," Est. Coast. Mar. Sci., in press, 1976.

14. Swanson, R. L., "Some Aspects of Currents in Long Island Sound," Ph.D. Thesis, Oregon State University, Corvallis, Oregon, 1971, 149 p.

15. Gordon, R. B. and Pilbeam, C. C., "Circulation in Central Long Island Sound," J. Geophys. Res., Vol. 80, 1975, pp 414-422.

16. Weyl, P. K., "The Water," Chapter 4 In: The Urban Sea: Long Island Sound by Koppelman, L. E., Weyl,, Gross, M. G., and Davis, D. S., Praeger Special Studies, Design/Environmental Planning Series, 1976, 223 p.

17. Riley, G. A. and Conover, S. A. M., "Oceanography of Long Island Sound. III. Chemical Oceanography," Bull. Bingham Oceanogr. Coll., Vol. 15, 1956, pp 47-61.

18. Riley, G. A., "Oceanography of Long Island Sound, 1952-1954. IX. Production and Utilization of Organic Matter," Bull. Bingham Oceanogr. Coll., Vol. 15, 1956, pp 324-344.

19. Harris, E. and Riley, G. A., "Oceanography of Long Island Sound, 1952-1954. VIII. Chemical Composition of the Plankton," Bull. Bingham Oceanogr. Coll., Vol. 15, 1956, pp 315-323.

20. Riley, G. A., "Note on Particulate Matter in Long Island Sound," Bull. Bingham Oceanogr. Coll., Vol. 17, 1959, pp 83-85.

21. Harris, E., "The Nitrogen Cycle in Long Island Sound," Bull. Bingham Oceanogr. Coll., Vol. 17, 1959, pp 31-65.

22. Hardy, C. D., "Nitrogen in Long Island Marine Waters, Conference Proceedings of Nitrogen in Long Island Water Systems," The Environmental Improvement Committee, American Chemical Society, Nassau-Suffolk Subsection, 1973, pp 92-126.

23. Bowman, M. J., "Nutrient Distributions and Transport in Long Island Sound," Est. Coastal Mar. Sci., (In press).

24. Hardy, C. D. and Weyl, P. K., "Distribution of Dissolved Oxygen in the Waters of Western Long Island Sound," Technical Report No. 11, Marine Sciences Research Center, State University of New York, Stony Brook, 1971, 37 p.

25. Turekian, K. K., "Rivers, Tributaries, and Estuaries," In: Impingement of Man on the Oceans, (ed., D. Hook) John Wiley and Sons, New York, 1971, pp 9-73.

26. Mytelka, A. I., Czachor, J. S., Guggino, W. B., and Golub, H., "Heavy Metals in Wastewater and Treatment Plant Effluent. J. Water Poll. Control Fed., Vol. 45, 1973, pp 1859-1864.

27. Klein, L. A., Lang, M., Nash, N., and Kirschner, S. L., "Source of Metals in New York City Wastewater," J. Water Poll. Control Fed., Vol. 46, 1974, pp 2653-2662.

28. Interstate Sanitation Commission, "1974 Annual Report of the Interstate Sanitation Commission," Interstate Sanitation Commission, 10 Columbus Circle, New York, 1974, 63 p.

29. Gross, M. G., Black, J. A., Kalin, R. J., Schramel, J. R., and Smith, R. N. "Survey of Marine Waste Deposits, New York Metropolitan Region," Technical Report No. 8, Marine Sciences Research Center, State University of New York, Stony,Brook, N.Y., 1971.

30. Kharkar, D. P., Turekian, K. K., and Bertine, K. K., "Stream supply of dissolved silver, molydenum, antimony, selenlum, chromium, cobalt, rubidium, and cesium to the oceans," Geochim. Cosmochim. Acta, Vol. 32, 1968, pp 285-298.

31. Fitzgerald, W. F., Szechtman, R. J., and Hunt, C. D., "A preliminary Budget for Cu and Zn in Long Island Sound," in: Investigations on Concentrations, Distributions, and Fates of Heavy Metal Wastes in Parts of Long Island Sound by Dehlinger, P. et al., Final Report, dated October 1974, and submitted to Office of Sea Grant Programs, National Oceanic and ATmospheric Administration, Rockville, Md., 1974.

32. McCrone, A. W., Ellis, B. F., and Charmatz, R., "Preliminary Observations on Long Island Sound Sediments," New York Acad. Sci. Trans., Vol. 24, 1961, pp 119-129.

33. Buzas, M. A., "The Distribution and Abundance of Foraminifera in Long Island Sound," Smithsonian Misc. Colls. 4604, Vol. 149, 1965, pp 1-89.

34. McCrone, A. W., "Sediments from Long Island Sound (New York): Physical and Chemical Properties Reviewed," J. Sed. Petrol., Vol. 35, 1965, pp 234-236.

35. Bokuniewicz, H. J., Gerbert, J., and Gordon, R. B., "Sediment Mass Balance of a Large Estuary, Long Island Sound," Est. Coastal Mar. Sci., Vol. 4, 1976, pp 523-536.

36. Akpati, B. N., "Mineral Composition and Sediments in Eastern Long Island Sound, New York," Maritime Sediments, Vol. 10, 1974, pp 19-30.

37. Turekian, K. K., "Trace Elements in Natural Waters," Annual Progress Report (July 1, 1973 to June 30, 1974 grant period) to Atomic Energy Commission for Grant AT (11-1)-3573. Date Submitted: April 1, 1974.

38. Martens, C. S. and Berner, R. A., "Methane Production in the Interstitial Waters of Sulphate-Depleted Marine Sediments," Science, Vol. 185, 1974, 1167-1169.

39. Aller, R. C. and Cochran, K., "$^{234}Th/^{238}U$ Disequilibrium in Nearshore Sediment: Particle Reworking and Diagenetic Time Scales," Earth Planet. Sci. Leh., Vol. 29, 1976, pp 37-50.

40. Gross, M. G., "New York Metropolitan Region -- A Major Sediment Source," Water Resources Res., Vol. 6, 1971, pp 927-031.

41. Gross, M. G., Black, J. A., Kalin, R. J., Schramel, J. R., and Smith, R. N., "Survey of Marine Waste Deposits, New York Metropolitan Region," Technical Report No. 8, Marine Sciences Research Center, State University of New York, Stony Brook, New York, 1971, 72 p.

42. O'Connors, J. S., "Dredging and Spoiling on Long Island," Technical Report No. 19, Marine Sciences Research Center, State University of New York, Stony Brook, New York, 1973, 34 p.

43. Gordon, R. B., "Dispersion of Dredge Spoil Dumped in Near-Shore Waters," Est. Coast. Mar. Sci., Vol. 2, 1974, pp 349-358.

44. Hulse, G. L., "The Plunket: A Shipboard Water Qaulity Monitoring System," Technical Report No. 22, Marine Sciences Research Center, Stony Brook, New York, 1975, 124 p.

45. Whitfield, M., "The Hydrolysis of Ammonium Ions in Sea Water - A theoretical Study," J. Mar. Biol. Ass. U. K., Vol. 54, 1974, pp 565-580.

46. Strickland, J. D. H. and Parsons, R. R., "A Manual of Sea Water Analysis," Fish. Res. Bd. of Canada, Bull. No. 125 (second edition, revised), 1972.

47. McCarthy, J. J., "A Urease Method for Urea in Seawater," Limnol. Oceanogr., Vol. 15, 1970, pp 309-313.

48. Reeburgh, W. S., "An Improved Interstitial Water Sampler," Limnol. Oceanogr., Vol. 12, 1967, pp 163-165.

49. Folk, R. L., Petrology of Sedimentary Rocks, Hemphill's, Austin, Texas, 1968, 170 p.

50. Folk, R. L., "The Distinction Between Grain Size and Mineral Composition in Sedimentary Rock Nomenclature," J. Geol., Vol. 62, 1954, pp 344-359.

51. Gibbs, R. J., "Error Due to Segregation in Quantitative Clay Mineral X-ray Diffraction Mounting Techniques," Amer. Mineral., Vol. 50, 1965, pp 741-751.

52. Carlton, R. W., "An Inexpensive Plate Holder for the Suction-on-Ceramic-Plate Method of Mounting Clay Minerals for Semi-Quantitative Analysis," J. Sed. Petrol., Vol. 45, 1975, pp 543-545.

53. Carroll, D., "Clay Minerals: A Guide to Their X-ray Identification," Geol. Soc. Amer. Special Paper 126, 1970, 180 p.

54. Biscaye, P. E., "Distinction Between Kaolinite and Chlorite in Recent Sediments by X-ray Diffraction," Amer. Mineral., Vol. 49, 1964, pp 1281-1289.

55. El Wakeel, S. K. and Riley, J. P., "Chemical and Mineralogical Studies of Deep-Sea Sediments," Geochim. Cosmochim. Acta, Vol. 25, 1961, pp 110-146.

56. Stevenson, F. J., Methods of Soil Analysis, Pt. II, 1965, pp 1409-1414.

57. Solkal, R. R. and Rohlf, F. J., Biometry, W. H. Freeman, 1969, p. 776.

58. U. S. Geological Survey, "Water Resources Data for Connecticut Water Year 1975," Water Resources Division, 135 High St., Hartford, Conn., 1976, p. 366.

59. U. S. Department of Commerce, "1974-75 Local Climatological Data," National Climatic Center, Federal Bldg., Asheville, N. C.

60. Dehlinger, P., Fitzgerald, W. F., Feng, S. Y., Paskausky, D. F., Garvine, R. W. and Bohlen, W. F., "A Determination of Budgets of Heavy Metal Wastes in Long Island Sound," First Annual Report (Parts I and II), The University of Connecticut, Marine Sciences Institute, Groton, Connecticut, submitted to Office of Sea Grant Programs, National Oceanic Atmospheric Administration, Rockville, Maryland, June, 1973.

61. Chen, M., Canelli, and Fuhs, G. W., "Effects of Salinity on Nitrification in the East River," J. Water Poll. Control Fed., Vol. 47, 1975, pp 2474-2481.

62. Stumm, W. and Morgan, J. J., Aquatic Chemistry, Wiley-Interscience, New York, 1970, 583 p.

63. McCrone, A. W., "Sediments from Long Island Sound (New York): Physical and Chemical Properties Reviewed," J. Sed. Petrol., Vol. 35, 1965, pp 234-236.

64. Duedall, I. W., O'Connors, H. B., and Irwin, B., "Fate of Wastewater Sludge in the New York Bight Apex," J. Water Poll. Control Fed., Vol. 47, 1975, pp 2702-2706.

65. Oakley, S. A. and Duedall, I. W., Report on Carbon and Nitrogen in Sediment Cores from the New York Bight Apex," Unpublished Reprot, dated 25 October 1976, submitted to Marine Ecosystems Analysis (MESA), National Oceanic and Atmospheric Administration, Stony Brook, New York, 1976, 7p.

66. Kaplin, S., "Chemical and Oxidation-Reduction Potential Studies of the Long Island Sound Sediments," Unpublished Masters Thesis, New York University, 1961.

67. Reeburgh, W. S., "Measurement of Gases in Sediments," Ph.D. Thesis, Johns Hopkins University, 1967, 93 p.

68. Danker, J. A., "A Micro-Environmental Study of the Hydrocarbons of the Long Island Sound Sediments," Unpublished Master's Thesis, 1963.

69. McCrone, A. W., "The Hudson River Estuary: Sedimentary and Geochemical Properties Between Kingston and Haverstraw, New York," J. Sed. Petrol, Vol. 37, 1967, pp 475-456.

70. Presley, B. J., Brooks, R. R., and Kaplan, I. R., "Manganese and Related Elements in the Interstitial Waters of Marine Sediments," Science, Vol. 158, 1967, pp 906-910.

71. Brooks, R. R., Presley, B. J., and Kaplan, I. R., "Trace Elements in the Interstitial Waters of Marine Sediments," Geochim. Cosmochim. Acta, Vol. 32, 1968, pp 397-414.

72. Duchart, P., Calvert, S. E., and Prince, N. B. "Distribution of Trace Metals in the Pore Waters of Shallow Marine Sediments," Limnol. Oceanogr., Vol. 18, 1973, pp 605-610.

73. Skinner, B. J. and Turekian, K. K., Man and the Ocean, Prentice-Hall Inc., Englewood Cliffs, New Jersey, 1973, 149 p.

74. Lindberg, S. E. and Harris, R. C., "Mercury-organic Matter Associations in Estuarine Sediments and Interstitial Water," Environ. Sci. Tech., Vol. 8, 1974, pp 459-462.

75. Berner, R. A., Principles of Chemical Sedimentology, McGraw Hill, Inc., New York, 1971, 240 p.

76. Chester, R. and Messiha-Hanna, R. G., "Trace Element Partition Patterns in North Atlantic Deep-Sea Sediments," Geochim. et Cosmochim. Acta, Vol. 34, 1970, pp 1121-1128.

77. Chester, R. and Hughes, M. J., "The Distribution of Manganese, Iron and Nickel in a North Pacific Deep-Sea Clay Core," Deep-Sea Res., Vol. 13, 1966, pp 627-634.

78. Chester, R. and Hughes, M. J., "The Trace Element Geochemistry of a North Pacific Pelagic Clay Core," Deep-Sea Res., Vol. 16, 1969, pp 639-654.

79. Bruland, K. W., Bertine, K., Loide, M., and Goldberg, E. D., "History of Metal Pollution in Southern California Coastal Zone," Environ. Sc. and Tech., Vol. 8, 1974, pp 425-432.

80. Berner, R. A., "Kinetic Models for the Early Diagenesis of Nitrogen, Sulphur, Phosphorus, and Silicon in Anoxic Marine Sediments," In: E. D. Goldberg, Ed., The Sea, Vol. V, New York, John Wiley and Sons, 1974, pp 427-450.

81. Sholkovitz, E., "Interstitial Water Chemistry of the Santa Barbara Basin Sediments," Geochim. Cosmochim. Acta, Vol. 37, 1973, pp 2043-2073.

82. Rittenberg, S. C., Emery, K. O. and Orr, W. L., "Regeneration of Nutrients in Sediments of Marine Basins," Deep-Sea Res., Vol. 3, 1955, pp 23-45.

83. Goldhaber, M., Berner, R. A., Aller, R. C., and Cochran, J. K., "Sulphate Reduction, Diffusion and Bioturbation in Long Island Sound," Spec. Symp. on Marine Chemistry in the Coastal Environment, Philadelphia, Pennsylvania, April 8-10 (abstract), 1975.

84. Siever, R. and Woodford, N., "Sorption of Silica by Clay Minerals," Geochim. Cosmochim. Acta, Vol. 37, 1973, pp. 1851-1880.

85. Fanning, K. A. and Schink, D. R., "Interaction of Marine Sediments with Dissolved Silica," Limnol. and Oceanogr., Vol. 14, 1969, pp. 59-68.

86. Hurd, D. C., "Interactions of Biogenic Opal, Sediment, and Seawater in the Central Equatorial Pacific." Unpublished Thesis, Hawaii Institute of Geophysics, University of Hawaii, 1973, 82 p.

87. Berner, R. A., "Kinetic Models for the Early Diagenesis of Nitrogen, Sulfur, Phosphorus, and Silicon in Anoxic Marine Sediments," In: The Sea (E. D. Goldberg, Ed.), Wiley-Interscience, New York, 1974, 895 p.

88. Cranston, R. E. and Buckley, D. E., "The Application and Performance of Microfilters in Analyses of Suspended Particulate Matter," (unpublished manuscript), Bedford Institute, Table VII, 1972, p 12.

89. Feldman, C., "Preservation of Dilute Mercury Solutions," Analytical Chemistry, Vol. 46, 1974, pp 99-102.

90. Hawley, J. E. and Ingle, Jr., J. D., "Improvements in Cold Vapor Atomic Absorption Determination of Mercury," Analytical Chemistry, Vol. 47, 1975, pp 719-723.

91. Segar, D. A. and Gonzalez, I. G., "Evaluation of Atomic Absorption with a Heated Graphite Atomizer for the Direct Determination of Trace Transition Metals in Sea Water," Analytica Chimica Acta, Vol. 58, 1972, pp 7-14.

92. Kahn, H. L. and Slavin, S., "Static Method of Analysis with Graphite Furnace (HGA-70)," Atomic Absorption Newsletter, Vol. 10, 1971, p 125.

93. Kahn, H. C., "A Background Compensation System for Atomic Absorption," Atomic Absorption Newsletter, Vol. 7, 1968, pp 40-43.

94. Milli-Q™ Systems for High Purity Water, Bulletin MB414, Millipore Corporation, Nov. 1973, p 15.

**In accordance with letter from DAEN-RDC, DAEN-ASI dated 22 July 1977, Subject: Facsimile Catalog Cards for Laboratory Technical Publications, a facsimile catalog card in Library of Congress MARC format is reproduced below.**

New York (State). State University at Stony Brook. Marine Sciences Research Center.
Aquatic disposal field investigations, Eatons Neck disposal site, Long Island Sound; Appendix B: Water-quality parameters and physicochemical sediment parameters / by Marine Sciences Research Center, State University of New York, Stony Brook, New York. Vicksburg, Miss. : U. S. Waterways Experiment Station ; Springfield, Va. : available from National Technical Information Service, 1978.
vi, 322 p. : ill. ; 27 cm. (Technical report - U. S. Army Engineer Waterways Experiment Station ; D-77-6, Appendix B)
Prepared for Office, Chief of Engineers, U. S. Army, Washington, D. C., under Contract No. DACW51-75-C-0016 (DMRP Work Unit No. 1A06B)
References: p. 313-322.

1. Dredged material disposal. 2. Eatons Neck Disposal Site. 3. Field investigations. 4. Long Island Sound. 5. Sediment sampling. 6. Water quality. I. United States. Army. Corps of Engineers. II. Series: United States. Waterways Experiment Station, Vicksburg, Miss. Technical report ; D-77-6, Appendix B.
TA7.W34 Appendix B

AD-A053 427 STATE UNIV OF NEW YORK AT STONY BROOK MARINE SCIENCES--ETC F/G 13/2
AQUATIC DISPOSAL FIELD INVESTIGATIONS, EATONS NECK DISPOSAL SIT--ETC(U)
JAN 78 DACW51-75-C-0016

UNCLASSIFIED WES-TR-D-77-6-APP-B NL

5 OF 5
ADA
053427




END
DATE
FILMED
12-78
DDC


DA
534

# SUPPLEMENTARY

# INFORMATION

DEPARTMENT OF THE ARMY
WATERWAYS EXPERIMENT STATION, CORPS OF ENGINEERS
P. O. BOX 631
VICKSBURG, MISSISSIPPI 39180

IN REPLY REFER TO: WESYV

26 June 1978

AD-A053 427

Errata Sheet

No. 1

AQUATIC DISPOSAL FIELD INVESTIGATIONS, EATONS NECK DISPOSAL SITE, LONG ISLAND SOUND; APPENDIX B: WATER-QUALITY PARAMETERS AND PHYSICOCHEMICAL SEDIMENT PARAMETERS

Technical Report D-77-6

January 1978

1. Page i, third paragraph, first part of first sentence should read:

The following Marine Sciences Research Center personnel assisted in all phases of the research project: